ISSN 1019-5149 - E ISSN 2651-5032 - NLM ID 9423821

Turkish Neurosurgery

Official Journal of the Turkish Neurosurgical Society

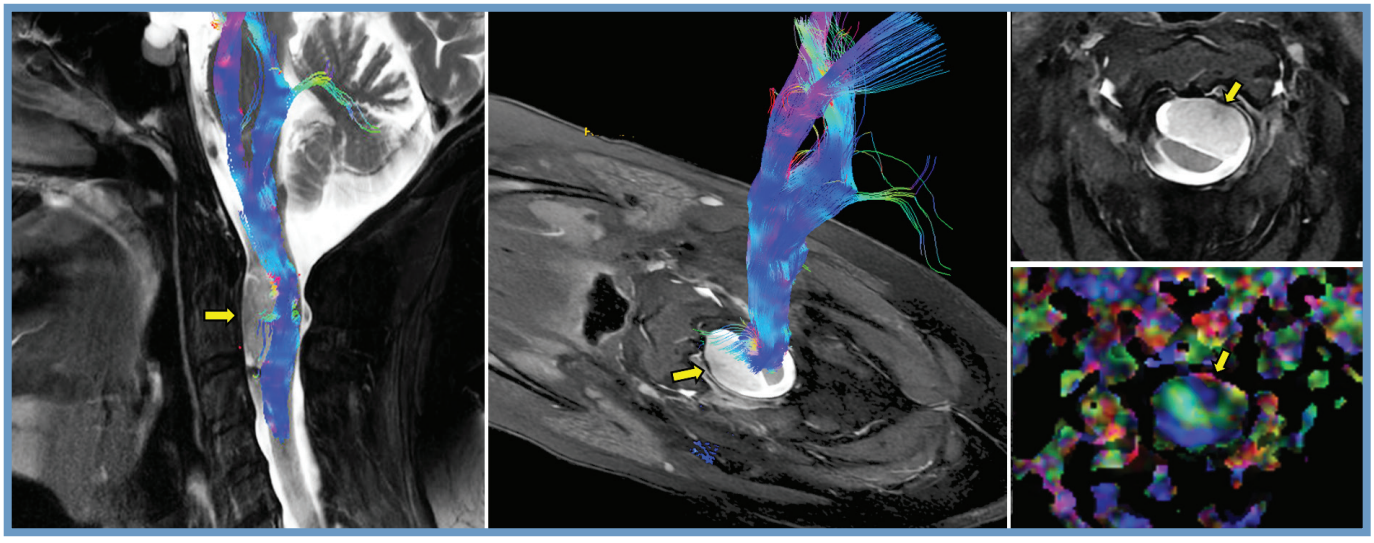

Volume 36 • Number 1 • January 2026

Turkish Neurosurgery

Official Journal of the Turkish Neurosurgical Society

ISSN: 1019-5149,
E-ISSN: 2651-5032
NLM ID: 9423821

TURKISH NEUROSURGICAL SOCIETY

Volume: 36 Number: 1 Year: 2026

www.turkishneurosurgery.org.tr

Turkish Neurosurgery has been accepted for indexing in: SCIENCE CITATION INDEX EXPANDED, INDEX MEDICUS, MEDLINE, PubMed, EBSCO, Scopus, TR Index, Islamic World Science Citation Center (ISC)

Impact Factor* : 0.8
5yr-Impact Factor*: 0.8
Journal Citation Indicator*TM: 0.34

*ISI Web of Knowledge℠, Journal Citation Reports®, 2024 JCR Science Edition

Turkish
Neurosurgery

Volume: 36 Number: 1 Year: 2026

Official Journal of the Turkish Neurosurgical Society

Turkish Neurosurgery is published six times per year (bimonthly) by the Turkish Neurosurgical Society
(January, March, May, July, September, and November)

Owned and controlled by the Turkish Neurosurgical Society

Publishing Manager:
İlker SOLMAZ

Key title: Turkish Neurosurgery
Abbreviated key title: Turk Neurosurg
www.turkishneurosurgery.org.tr

ISSN: 1019-5149, **E-ISSN:** 2651-5032
NLM ID: 9423821

Turkish Neurosurgery is an open access and totally free journal.
All electronic materials can be found on internet without any charge. Please visit: http://www.turkishneurosurgery.org.tr/
2026 Subscription Rates for Printed Materials:
Within Türkiye 5000 TL (shipping costs not included); Outside Türkiye 100 € (shipping costs not included)
For further information and questions; please contact: bulus@bulustasarim.com.tr

Page layout and publishing services
BULUŞ DESIGN AND PRINTING SERVICES COMPANY
Mebusevleri Mah. Turgut Reis Cad. 11/1 Çankaya, Ankara, Türkiye
Phone: +90 312 222 44 06
E-mail: bulus@bulustasarim.com.tr

Advertisement: editor@turkishneurosurgery.org.tr

Publishing Date: 30.01.2026

Cover picture: Fırat Z, pp. 99

Turkish Neurosurgical Society
Taşkent Caddesi 13/4 06500 Bahçelievler, Ankara/TÜRKİYE
Phone: +90 312 212 64 08 Fax : +90 312 215 46 26
E-mail: info@turknorosirurji.org.tr
www.turknorosirurji.org.tr www.turkishneurosurgery.org.tr

Yayın Türü: Yaygın süreli yayın
Yayın Sahibi: Türk Nöroşirürji Derneği adına Hüseyin Hayri KERTMEN
Sorumlu Yazı İşleri Müdürü: İlker SOLMAZ

5187 Sayılı Basın Yasasının 7. maddesi uyarınca dergi künyesinin Türkçesi belirtilmiştir.

Review of the articles in the journal to make sure they conform to publishing standards, typesetting, getting the journal ready for publication and finally the publishing process has been the responsibility of Buluş Design and Printing Services Company.

The paper used to print this journal conforms to ISO 9706: 1994 standard (Requirements for Permanence).
The National Library of Medicine suggests that biomedical publications be printed on acid-free paper (alkaline paper).

22
PAP

ENVIRONMENTAL INFORMATION

The company that manufactures the paper used in this journal has an ISO 14001 environmental management certificate. The company obtains all wood fiber in a sustainable manner. The forests and plantations of the company are certified. The water used in production is purified and used after recovery.

Heavy metals or film are not used for the publication of this journal. The fluids used for developing the aluminum printing templates are purified. The templates are recycled. The inks used for printing do not contain toxic heavy metals.

This journal can be recycled. Please dispose of it in recycling containers.

INSTRUCTION TO THE AUTHORS

Journal Description

Turkish Neurosurgery is a peer-reviewed, multidisciplinary, open access journal directed at an audience of neurosurgery physicians and scientists. The official language of the journal is *English*. The journal publishes original articles in the form of clinical and basic research. *Turkish Neurosurgery* will only publish studies that have institutional review board (IRB) approval and have strictly observed an acceptable follow-up period. With the exception of reference presentation, *Turkish Neurosurgery* requires that all manuscripts be prepared in accordance with the *Uniform Requirements for Manuscripts Submitted to Biomedical Journals*.

Turkish Neurosurgery periodically publishes the following papers: Research (Original Investigation, Clinical and Experimental Studies), Review Article, Case Report, Letter to Editor, Technical Note and Turkish Neuro-Excursion.

Our mission is providing a scientific forum relevant to neurosurgeons and health care providers.

Open Access Policy

As the Turkish Neurosurgery Journal, we believe science is a common denominator of the humanity which should be publicly available and free. Since its establishment in 1989, all our effort and workforce were based on volunteers and their efforts.

Definition of Open Access Publication[1]

An Open Access Publication [A] is one that meets the following two conditions:

1. The author(s) and copyright holder(s) grant(s) to all users a free, irrevocable, worldwide, perpetual right of access to, and a license to copy, use, distribute, transmit and display the work publicly and to make and distribute derivative works, in any digital medium for any responsible purpose, subject to proper attribution of authorship [B], as well as the right to make small numbers of printed copies for their personal use.

2. Complete version of the work and all supplemental materials, including a copy of the permission as stated above, in a suitable standard electronic format is deposited immediately upon initial publication in at least one online repository that is supported by an academic institution, scholarly society, government agency, or other well-established organization that seeks to enable open access, unrestricted distribution, interoperability, and long-term archiving (for the biomedical sciences, PubMed Central is such a repository).

Notes:

A. Open access is a property of individual works, not necessarily journals or publishers.

B. Community standards, rather than copyright law, will continue to provide the mechanism for enforcement of proper attribution and responsible use of the published work, as they do now.

[1] https://dash.harvard.edu/bitstream/handle/1/4725199/Suber_bethesda.htm#note1

Digital Archiving

Bulus Tasarim and the "Turkish Neurosurgery" journal provide for long-term digital preservation through Portico.

Portico is a leading digital preservation service worldwide. The content is preserved as an archival version and is not publically accessible via Portico, but is provided when required under specific conditions, such as discontinuation of the collection or catastrophic failure of the website.

Manuscript Submission

Authors are to submit their manuscripts through the web based tracking system at http://www.turkishneurosurgery.org.tr. The site contains instructions and advice on how to submit manuscripts, guidance on the creation / scanning and saving of electronic art and supporting documentation. **ORCID** identifier (ID) is required for **ALL** authors during the submission process. **ORCID ID** can be obtained free of charge at http://orcid.org. **E-mail address of all authors** should also be provided during the submission process. In addition to allowing authors to submit manuscripts on the web, the site allows authors to follow the progression of their manuscript through the peer review process. Authors who submit their manuscripts through the web-based tracking system are asked **not** to send hard copies of the manuscript to the editorial office. Please address all inquiries regarding manuscripts not yet accepted or published to the Journal's editorial office. The editorial office will acknowledge receipt of your manuscript and will send you a manuscript number for reference.

Before submission please ensure that:

One author has been designated as the correspondent with full contact details including e-mail address, postal address and phone number. In any case of editorial board could not contact with the corresponding author, Turkish Neurosurgery journal have the right to decide what is appropriate.

Submission Checklist;

1) Your title page is in .doc or .docx format, includes title of your manuscript, author names, affiliations and ORCID numbers; name and full contact information of corresponding author, running title, keywords, and authorship contribution statements-the latter can be found on the Copyright transfer and authorship contribution statement Form. Please be sure that authorship contribution statements are presented in the form as well as in the title page. Of note, authors should indicate conflicts of interest relating to their research-if any.

The Journal is not responsible for published misspelled names due to author error and the title page **must be uploaded as a separate file**. Running Head in the title page should be no more than three to five words from the title, and should NOT include the authors' names.

2) Your main document is in .doc or .docx format includes **structured abstract, key words, abbreviation list, structured main text, disclosure and conflicts of interest, references and figure legends** sections in this order. Structured main text should be organized as **Introduction, Material and Methods, Results, Discussion, and Conclusion.** Do not add any information about institution names. Also do not add figures and tables in the main document. **Be sure your main document is written in Calibri or Times New Roman, line gap set to double spaced and justified on both sides.** Journal's official language is English. Refer to drugs and therapeutic agents by their accepted generic or chemical names, and do not abbreviate them. Use code numbers only when a generic name is not yet available. In that case, supply the chemical name and a figure giving the chemical structure of the drug. Capitalize the trade names of drugs and place them in parentheses after the generic names. To comply with trademark law, include the name and location (city and country) of the manufacturer of any drug, supply, or equipment mentioned in the manuscript. Use the metric system to express the units of measure and degrees Celsius to express temperatures, and SI units rather than conventional units. Define abbreviations at first mention in text and in each table and figure. If a brand name is cited, supply the manufacturer's name and address (city and state/country).

3) All your figures are in **TIFF** format. Color figures should have a resolution of at least **300 dpi**, black and white figures should have a resolution of at least **600 dpi**. Turkish Neurosurgery does not demand any color figure fee.

4) All your video files are in .mpeg and .mp4 format, not longer than 10 minutes, and not bigger than 40 MB. Video files should include an embedded audio narration and subtitles in English.

5) All your tables are in .doc or .docx format, created using the table creating and editing feature of the word processing software. Do not use Excel or comparable software. Upload a single text file which includes **ALL the tables in separate pages.** Cite tables consecutively in the text, and number them in that order. Key each on a separate sheet, include the table title, appropriate column heads, and explanatory legends (including definitions of any **abbreviations** used). Do not embed tables within the main text.

If your manuscript does not meet these requirements, manuscript **WILL BE RETURNED** to the corresponding author for technical revision before undergoing peer review.

Submission Steps

1. Upload signed copyright form by the corresponding author which is available at http://neurosurgery.dergisi.org/submit/Copyright_transfer_form.pdf. Choose your manuscript type and click continue.
2. Add names of institutions of all authors. If one or more author has affiliation with more institutions, specify it in the title page. Then click continue.
3. Write last name and first name of all authors. Add their institution numbers, e-mails and ORCID numbers. Standard page appears with spaces enough for 8 author names. If your paper has more authors, please fill all the first 8 authors names and affiliations then click add author. Without filling all required fields, you cannot add more authors. Do not use abbreviations in the author names. Then click continue.
4. Write the title of the manuscript. If the title contains special characters use the left below table. You can copy-paste the title from your title page. Then click continue.
5. Write the abstract of your manuscript to the field**.** Abstracts should be structured including Aim, Material and Methods, Results and Conclusion. **Abstracts should not exceed 300 words. There is no need of Turkish abstract.** Then click continue.
6. Write the keywords separated by commas. Please use keywords from https://meshb.nlm.nih.gov/search. Then click continue.
7. Click the appropriate answer stating if your manuscript has not been published and / or is not being considered for publication elsewhere or your manuscript was presented in the congress indicated below and was published in abstract form in the proceedings of the congress. Then write your cover letter to the editor to the field. Then click continue.
8. Upload your manuscript files. Be sure your files are main document (manuscript), figure(s), video(s), title page, and table(s). For every file, write the description of your file and click upload button. The names of the files you have submitted should not resemble the names or institutions of the authors. Be sure all your text files are in .doc or .docx format. When you are sure you uploaded all your files click continue.
9. When you complete all the submission process click approve for all the files you want to submit and click **Submit your Manuscript** button.

Revised Submission

Author's comments to the reviewers are required for revised submissions. Authors must address all the reviewer's concerns/suggestions and whether the change was made or not. Authors must also highlight the changes made within the text. Do not track the additions or deletions to the manuscript. If the authors do not want to revise the manuscript within a period of **two months**, the manuscript will be declined.

Ethics, patient anonymity and informed consent:

This journal adheres to the ethical standards described by the Committee on Publication Ethics (https://publicationethics.org/) and the International Committee of Medical Journal Editors (https://www.icmje.org/). Authors are expected to adhere to these standards.

It is the author's responsibility to ensure that a patient's anonymity is carefully protected and to verify that any experimental investigation with human subjects reported in the manuscript was performed with informed consent and followed all the guidelines for experimental studies with human subjects required by the institution(s) with which all the authors are affiliated. Authors should mask patients' eyes, private parts and remove patients' names from all figures. Editorial board of the Turkish Neurosurgery

have the right to demand ethical committee forms or informed consent forms **at any stage of the submission and publication.** All animal experiments should comply with the ARRIVE guidelines https://www.nc3rs.org.uk/arrive-guidelines. Also, Editorial board of the Turkish Neurosurgery have the right to withdraw any paper, even it is accepted, if there is any ethical issue.

Authorship should be limited to those who have made a significant contribution to the conception, design, execution, or interpretation of the reported study. The authors should ensure that they have written entirely original works, and if the authors have used the work and/or words of others, that this has been appropriately cited or quoted. Editorial board of the Turkish Neurosurgery have the right to withdraw any paper if there is any plagiarism. All submissions must include disclosure of all relationships that could be viewed as presenting a potential conflict of interest. All authors must disclose any financial and personal relationships with other people or organizations that could inappropriately influence (bias) their work. Examples of potential competing interests include employment, consultancies, stock ownership, honoraria, paid expert testimony, patent applications/registrations, and grants or other funding. Authors must disclose any interests in the disclosure and conflicts of interest section of the main document.

Authorship Change

Authors are expected to consider carefully the list and order of authors before submitting their manuscript and provide the definitive list of authors at the time of the original submission. Any addition, deletion or rearrangement of author names in the authorship list after submitting the paper is **inappropriate and prohibited**. Authors should **withdraw** their paper if there is a need for authorship change.

Types of Manuscripts

Turkish Neuro-Excursion: The editor will invite experts for these special types of papers which may cover a broad spectrum in various fields of medicine, science, art, history, law as well as any important theme on actuality other than core neurosurgery. The number of words, figures, tables and references are not restricted.

Research (Original Investigation, Clinical and Experimental Studies): The main text should not exceed 4500 words **excluding the** references, tables, and figure legends for original articles, including randomized controlled trials, observational (cohort, case-control or cross-sectional) studies, diagnostic accuracy studies, nonrandomized behavioral and public health intervention trials, experimental animal trials and any other retrospective or prospective clinical or experimental studies. The number of figures, tables, videos and references are not restricted. The specifications for figures and video files are given.

Review Article: All review articles should be systematic reviews and meta-analyses. A systematic review protocol describes the rationale, hypothesis, and planned methods of the review. It should be prepared before a review is started and used as a guide to carry out the review. Turkish Neurosurgery no more accept papers as "Case Report and Review of the Literature". All systematic reviews and meta-analyses SHOULD COMPLY with **PRISMA** guidelines http://www.prisma-statement.org/. Systematic reviews and meta analyses SHOULD INCLUDE a **CONSORT** Flow Diagram http://www.consort-statement.org/consort-statement/flow-diagram. Any systematic review and meta-analysis without a CONSORT Flow Diagram will be rejected.

Case Report: Turkish Neurosurgery values **demonstrative and unique case reports** with **high quality figures**. A case report should be so clear and easy to understand that the reader could replicate the case in his/her daily practice. Word count must not exceed 1500 (excluding references, tables, and figure legends). Case reports cannot have more than 15 references, and 6 figures or tables. Turkish Neurosurgery **does not accept** papers as **"Case Report and Review of the Literature"** anymore.

Technical Note: Turkish Neurosurgery values **demonstrative technical notes** with **high quality figures**. Technical notes reinforced with high-quality anatomical studies are welcome. A technical note should be so clear and easy to understand that the reader could replicate the technique in the operating room or on cadaveric specimen. The number of words must not exceed 2000, and there should not be more than 20 references. The number of figures and tables are not restricted.

Letter to the Editor: Letters should refer to the title and authors of a recent Turkish Neurosurgery article. The letter should be no longer than 300 words with no more than 3 references. Unpublished data should not be used Letters to the Editor are sent to the article authors for response. The Editor-in-Chief makes the final decision on whether letters to the editor and the responses are published.

References

The authors are responsible for the accuracy of the references. Key the references (double-spaced) at the end of the manuscript. Cite references in the text in alphabetical order within parentheses. Do not link the references to the text. Cite unpublished data, such as papers submitted but not yet accepted for publication or personal communications, in parentheses in the text (please be sure that such have a DOI number to be presented). **Do not use "et al." in the references.** List all the authors of the reference. Refer to the List of Journals Indexed in Index Medicus for abbreviations of journal names, or access the list at "http://www.nlm.nih.gov/tsd/serials/lji.html. The DOI numbers are mandatory in accordance with the library indexes; please be sure to present the DOI numbers for each reference at the end of its sentence. The reference styles for Zotero and EndNote are available on the journal's home page.

Sample references are given below:

A. Journal article

Umeoka K, Mizunari T, Murai Y, Kobayashi S, Morita A: Occlusion of the ascending pharyngeal artery during carotid artery surgery: Importance and technique. Turk Neurosurg 24: 546-548, 2014. https://doi.org/10.5137/1019-5149.JTN.9527-13.0

B. Book chapter

Martin A: Literacies for the digital age. In: Martin A, Madigan D (eds), Digital literacies for learning. Facet, 2006:3-25. DOI: https://doi.org/10.29085/9781856049870.003

C. Entire book

Smith T, Williams BM, Streefkerk R: The citation manual for students: A quick guide (2nd ed). Wiley, 2020. https://doi.org/10.1000/182

D. Example of thesis

Kanpolat Y: Experimental percutaneous access to the trigeminal ganglion and the histopathological evaluation of radiofrequency thermic lesion (Unpublished dissertation), Ankara: Ankara University, 1978:1- 52

E. Software

Epi Info [computer program]. Version 6. Atlanta: Centers for Disease Control and Prevention, 1994

F. Online journals

Friedman SA. Preeclampsia: A review of the role of prostaglandins. Obstet Gynecol [serial online]. January 1988;71:22-37. Available from: BRS Information Technologies, McLean, VA. Accessed December 15, 1990

G. Database

CANCERNET-PDQ [database online]. Bethesda, MD: National Cancer Institute, 1996. Updated March 29, 1996

H. World Wide Web

Gostin LO. Drug use and HIV/AIDS [JAMA HIV/AIDS web site]. June 1, 1996. Available at: http://www.ama-assn.org/ special/ hiv/ ethics. Accessed June 26, 1997

ARTIFICIAL INTELLIGENCE USAGE POLICY

Permitted Uses of Artificial Use (AI) Tools: Authors may use generative AI tools (e.g. ChatGPT, Bing Chat, Bard, etc.) to assist with certain aspects of manuscript preparation – for example, to improve grammar and readability, to brainstorm research questions, or to summarize background literature – provided that these tools are used responsibly and with human oversight. AI can be a helpful aid for editing and idea generation, but it must not replace the authors' own critical analysis and writing.

Authorship and Accountability: AI tools cannot be listed as an author or co-author under any circumstances. All authors listed on the paper must be human and must meet the International Committee of Medical Journal Editors (ICMJE) authorship criteria (having made substantial contributions, written or revised the text, and able to take responsibility for the work). The human authors take full responsibility for all content of the manuscript, including any portions that may have been AI-assisted. If errors, biases, or plagiarism are found in the content – even if introduced by an AI – the authors will be held accountable.

Mandatory Disclosure of AI Usage: Authors are required to disclose any use of AI in the creation of their manuscript. During submission, the corresponding author will need to answer a checkbox/question about AI use (e.g. "Did you use any generative AI or AI-assisted tools during the writing or preparation of this manuscript?"). If the answer is "Yes," the author must provide a brief description of how and where AI was used.

Location of Disclosure in Manuscript: In addition to the submission form, authors must insert an "AI Assistance Statement" in the manuscript itself. This should be placed at the end of the manuscript (just before the References) under a separate heading, for example: "Declaration of Generative AI Use."

Content of the Disclosure: The disclosure statement should identify the AI tool and version, and describe the specific purpose and section of the manuscript for which it was used. For instance: "Declaration of Generative AI Use: During the preparation of this article, the authors used ChatGPT (GPT-4, OpenAI, September 2025) to refine the English language in the Introduction and Discussion sections. The AI was not used to generate any scientific conclusions or new content, but only to improve readability. After using this tool, the authors thoroughly reviewed and edited the text to ensure accuracy and originality, and take full responsibility for the content of this manuscript."*.

This example can be adapted as needed. The key is to include which tool, for what purpose/section, and a confirmation of author oversight (i.e., that the authors reviewed and approve the AI-influenced content). Minor uses of software for spell-checking or reference formatting do not need to be declared.

Limitations on AI Use: Authors should not use AI tools to generate original scientific content or to circumvent the scholarly work. In particular:

No Generative AI for Data Analysis without Disclosure: If an AI or algorithm is part of the research (for example, analyzing images or data sets), this should be described in the Methods like any other tool.

No AI-Generated Figures or Images: Do not use AI image generators to create figures, diagrams, or any visual element of the paper, unless this is part of the study itself and is explicitly described in the Methods. Any inadvertent AI modifications to images (beyond standard brightness/contrast adjustments) are not allowed. Editors may request original image data to verify integrity.

No Undisclosed AI Text: All text must be either written by the authors or, if AI-assisted, disclosed as described. Do not submit a manuscript composed wholly by an AI – this is not acceptable and would be treated as academic misconduct (similar to plagiarism).

Confidentiality and Ethics: Do not feed sensitive or confidential information (such as unpublished data, patient details, or identifiable personal information) into any AI service unless it's in accordance with privacy laws and ethical guidelines. Many AI tools may store or reuse input data, so use them with caution regarding confidential content.

Enforcement: Submissions will be checked for compliance. Omission of a required AI disclosure or false statements about AI use will be treated seriously. It could lead to rejection of the manuscript or, if discovered later, a correction or retraction, as it violates publication ethics. Conversely, transparent disclosure of AI assistance will not negatively impact the editorial decision; it will simply be noted in the final publication to inform readers. Our journal's stance is that honesty about the use of new tools is always the best policy.

Continual Policy Updates: Finally, this is an evolving area. The journal will regularly review and update these AI usage guidelines in line with COPE recommendations and industry best practices. Any future changes will be communicated to authors via updated instructions for authors.

Conclusion

In summary, our neurosurgery journal will permit the limited use of AI tools in manuscript writing only with proper disclosure and human oversight. Authors must state explicitly if and how AI was used in preparing their paper, and they remain fully responsible for the integrity of their work. Under no circumstances can an AI be an author, or can AI-generated material be presented as original human work. This policy follows the lead of major journals like Nature and World Neurosurgery, which similarly require authors to report AI assistance and forbid AI authorship. By implementing

these guidelines, we aim to embrace beneficial innovations while upholding the rigor, ethics, and transparency expected in scientific publishing. Of note, The Editorial Board have the right to request revisions or withdraw any paper if there is any misuse of AI.

Biswas, SS. ChatGPT-for-Research-and-Publication-A-Step-by-Step Guide. (https://meridian.allenpress.com/jppt/article/28/6/576/496601/ChatGPT-for-Research-and-Publication-A-Step-by)(https://doi.org/10.5863/1551-6776-28.6.576)

Ramoni D, Sgura C, Liberale L, Montecucco F, Ioannidis JPA, Carbone F. Artificial intelligence in scientific medical writing: Legitimate and deceptive uses and ethical concerns. European Journal of Internal Medicine, Volume 127, 31 - 35

PEER REVIEW PROCESS

This journal uses double-blind review, which means that both the reviewer and author identities are concealed from the reviewers, and vice versa, throughout the review process.

1. Manuscript Submission

The corresponding or submitting author submits the paper to the journal through http://turkishneurosurgery.org.tr/.

2. Assessment of the Paper for Journal Requirements

The editorial office checks the paper's composition and arrangement against the journal's Author Guidelines - Instruction to the Authors (http://turkishneurosurgery.org.tr/static.php?id=7) - to make sure it includes the required sections and stylizations.

3. Evaluation by the Editor-in-Chief (EIC)

The EIC checks the paper's scientifical appropriateness for the journal, its originality and actuality. If not, the paper may be rejected without being reviewed any further.

4. EIC Assigns a Section Editor (SE)

Section Editors handle the peer review process. All manuscripts that reach this step will go through a double-blind peer-review process. In order to ensure an unbiased evaluation process, each submission will be reviewed by at least two external, independent peer reviewers who are experts in the field.

5. Invitation to Reviewers

The SE sends invitations to individuals he or she believes would be appropriate reviewers. As responses are received, further invitations are issued, if necessary, until the required number of acceptances is obtained.

6. Response to Invitations

Potential reviewers consider the invitation against their own expertise, conflicts of interest and availability. They then accept or decline.

7. Review is Conducted

The reviewer sets time aside to read the paper several times. The first read is used to form an initial impression of the work. If major problems are found at this stage, the reviewer may feel comfortable rejecting the paper without further work. Otherwise they will read the paper several more times, taking notes so as to build a detailed point-by-point review. The review is then submitted to the journal, with a recommendation to accept or reject it – or else with a request for revision (either major or minor) before it is reconsidered.

8. Journal Evaluates the Reviews

The SE considers all the returned reviews before making an overall decision. If the reviews differ widely, the editor may invite an additional reviewer so as to get an extra opinion before making a decision.

9. The Decision is Communicated

The EIC is the final authority in the decision-making process for all submissions. He or She sends a decision e-mail to the author including any relevant reviewer comments.

AFTER ACCEPTANCE

Online Proof Correction

Corresponding authors will receive an e-mail including final PDF version of their manuscript. Authors are obligated to proofreading their manuscript in 72 hours.

Turkish Neurosurgery workflow processes to get your article published quickly and accurately. Please use this proof only for checking the typesetting, editing, completeness and correctness of the text, tables and figures. Significant changes to the article as accepted for publication will only be considered at this stage with permission from the Editor. It is important to ensure that all corrections are sent back to us in one communication. Please check carefully before replying, as inclusion of any subsequent corrections cannot be guaranteed. Proofreading is solely your responsibility. **Authorship change is not accepted during proofreading and is prohibited.**

Rapid Publication Option

In accordance with the Turkish Neurosurgical Society's Board Decision on August 5, 2023, "Turkish Neurosurgery" journal is starting to publish articles with a rapid publication option (RPO). This type of publication choice will have no effect on the peer review process or acceptance of the submission since it will be requested by the authors after acceptance of the article.

What is RPO?: The RPO ensures the accepted article will be immediately prepared in electronic format (e-pdf), and it will be printed in one of the upcoming issues of the journal. This service has a publication fee that needs to be met by the authors, their institutions, or the research funders for each article that is published in a timely manner. The decision for RPO will be made by the authors, and they will only be charged upon their requests and if their paper is accepted. As there is a limited space for such option in each publishable issue, this process will be granted on a first-come, first-served basis, and the Turkish Neurosurgical Society is responsible for organizing the demands and informing the Editorial Board as well as the Publisher.

Why RPO?: There is a waiting list, and the number of articles per issue is constant and limited. It generally takes 6–14 months for a research paper to be published in a printed journal. This service allows immediate publication of the article in both electronic and printed formats. Of note, the printed article will be published in one of the upcoming issues of the journal.

Please be sure to use the RPO service and contact the society, even if you are in early need of an e-pdf manuscript.

Benefits of RPO: Here, it's important to make sure that articles are published as soon as possible, are subject to the proper quality controls, and are extensively read. By using RPO, the authors are able to publish their ideas faster, receive credit for the idea and the manuscript, get ready to strengthen their enrollment for future applications and grants, and last but not least, have increased visibility in a quick-paced setting.[1]

[1] https://www.editage.com/insights/publish-faster-progress-faster-the-basics-of-rapid-publication

RPO Price and Communication Details: The RPO charge for the journal is EUR 1000/article, including taxes.

This service is carried out by Turkish Neurosurgical Society. Please contact with: Turkish Neurosurgical Society, Taskent Caddesi 13/4 06500 Bahcelievler, Ankara/TÜRKİYE

E-mail: info@turknorosirurji.org.tr

Reprints

Reprint requests should be faxed or e-mailed with the corrected proofs by the corresponding author, if needed. Reprints are normally shipped 6 to 8 weeks after publication of the issue in which the item appears.

Contact with the Publisher: Bulus Tasarim, Mebusevleri Mah. Turgut Reis Cad. 11/1, Çankaya, Ankara, TÜRKİYE.

E-mail: bulus@bulustasarim.com.tr

The price for 2 sets of hardcopy journal*:

Within Türkiye 1500 TL (shipping costs not included);
Outside Türkiye 40 € (shipping costs not included)

**Depend on shipping cost. Please contact Bulus Tasarim.*

Manuscript Checklist (before submission. For author reference only)

1. ORCID identifier (ID) is required for all authors during the submission process. ORCID ID can be obtained free of charge at http://orcid.org	☐
2. E-mail address of all authors should be provided during the submission process.	☐
3. Title page	
Title (brief, definite, didactic)	☐
Corresponding author designated, and full mailing address included on title page	☐
E-mail address of corresponding author included on title page	☐
Running head	☐
Approval of Institutional Review Board (Decision No/Date) and/or signed patient consent forms	☐
Permission to reproduce copyrighted material	☐
Acknowledgements listed for grants, technical support, and corporate support on title page	☐
4. Structured abstract with key words (300 words)	☐
5. Manuscript text with page numbers [Microsoft Word (.doc)] (without author names and affiliations)	☐
6. Figure legends	☐
7. Tables (Word, Wordperfect)	☐
8. Figures (TIFF)	☐
9. Videos (avi, mpeg, mp4) with narration and/or subtitles	☐
10. References double-spaced and cited in alphabetical order	☐

CONTENTS

Turkish Neurosurgery

Volume: 36 Number: 1 Year: 2026

HISTORY OF NEUROSURGERY

ORIGINAL INVESTIGATIONS

■ Neurotrauma

■ Cerebrovascular-Endovascular

■ Spine and Peripheral Nerves

CASE REPORT

LETTER TO EDITOR

CORRIGENDUM

EDITORIAL

Turkish Neurosurgery

Volume: 36 Number: 1 Year: 2026

As we start a new year, we are delighted to once again come together with the continuity of science and the power of collaborative effort.

As the Turkish Neurosurgery Journal, we sincerely congratulate all our academic community, who contribute to the field of neurosurgery in the entire world, on the new year. In the year 2025, we have witnessed a significant surge in scientific production, multi-center collaborations, and high-quality academic contributions.

We would like to express our sincerest thanks to all the authors who submitted their works to our journal, to our reviewers who contributed with outstanding dedication to the scientific evaluation process, and to our editors who worked at every stage of the publication process.

These voluntary and meticulous contributions, which form the basis of academic publishing, are advancing the scientific quality and prestige of our journal day by day. With the new year, we are entering a period focused on renewal and development in our journal. With our updated approach in many areas, from our visual identity to our publication processes, as well as our scientific content, we will continue to support current, original, and high-quality studies in the field of neurosurgery. We will be pleased to see all scientific outputs that will contribute to our field, including clinical research, experimental studies, reviews, and case presentations in our journal.

We hope that 2026 will be a year in which productivity, collaboration, and academic solidarity are further strengthened in the light of science, and we wish all our academic community a year full of health, success, and well-being.

Sincerely,

The Editorial Board of Turkish Neurosurgery

Turk Neurosurg 36(1):1-5, 2026
DOI: 10.5137/1019-5149.JTN.49096-25.1

History of Neurosurgery

Received: 07.05.2025
Accepted: 27.07.2025
Published Online: 16.01.2026

Ernst von Bergmann and the First Neurotraumatology Book

Ersin HACIYAKUPOGLU[1], Uygur ER[2,3], Sait NADERI[4]

[1]Heinrich-Braun Klinikum Zwickau, Department of Neurosurgery, Zwickau, Germany
[2]Near East University, Neurosurgery Clinics, Nicosia, Turkish Republic of Northern Cyprus (TRNC)
[3]Ankara Acibadem Hospital, Department of Neurosurgery, Ankara, Türkiye
[4]Umraniye Training and Research Hospital, Neurosurgery Clinics, Istanbul, Türkiye

Corresponding author: Uygur ER ✉ uygurer@gmail.com

ABSTRACT

We aimed to introduce Ernst von Bergman, who contributed greatly to the establishment of modern neurosurgery and introduced antisepsis practices to routine use in surgery, and his important work, which is the first book on neurotrauma.

The world's first book dedicated to neurotrauma, Lehre von Kopfverletzungen, written in 1880, is examined and presented together with the author's academic career.

Bergmann was the first surgeon to use surgical instrument sterilization and played a pioneering role in the establishment of the antiseptic method. In addition to his valuable studies and important results on intracranial pressure changes in head trauma, the innovations and principles he brought to wound care are very important.

Surgical sterilization, head trauma and the resulting increase in intracranial pressure, and his standardization of wound care make Ernst von Bergmann an important figure in the establishment of modern neurosurgery. Bergmann is the author of the first book on neurotrauma, which places him in a distinguished place in the history of neurosurgery.

KEYWORDS: Ernst von Bergmann, History of Neurosurgery, Neurotrauma, Incraised intracranial pressure

INTRODUCTION

Ernst von Bergmann (1836-1907) served as a professor of surgery in Würzburg and Berlin (Figure 1), and he also held roles as a military surgeon and neurosurgeon. His service practiced as a medical officer included participation in the Austro-Prussian war (1866), Franco-Prussian war (1870-1871) and Russo-Turkish war (1877-1878), through which he gained extensive experience of neurotrauma in the battlefield. He is known as a pioneer of aseptic surgery, introduced heat sterilization of surgical instruments and aseptic dressing. Most importantly, he was one of the founders of some neurosurgical applications, and author of the first neuro-traumatology book and one of the first neurosurgery books. The aim of this study is to review his medical life, and his contributions to neurosurgery.

LIFE and EDUCATION

Ernst Gustav Benjamin von Bergmann was born on 16 December 1836 in Riga, Livonia Governorate (now Latvia) within the borders of the Russian Empire. He received his doctorate from the University of Dorpat now known as University of Tartu (Estonia) at the age of 24 between 1854 and 1860. While working in Dorpat, he visited Albrecht Werner's clinic in Königsberg and made observations on hygiene measures that were very advanced for their time. In addition, he visited the clinic of Franz Schuh in Vienna, who performed the first pericardial puncture and used ether anesthesia. It is known that he also visited the clinics of Virchow and Langenbeck as an observer. He followed the work of Weber and Billroth and conducted research on human infections. He gained surgical experience to participate voluntarily in the army in the Austro-Prussian War in 1866 (4).

He started his assistantship at the surgery clinic of Prof. Georg von Adelmann and Prof. Georg von Oettingen. He completed his surgical training in 1864 at the age of 28. He published 3 important papers in 1868. In between 1870 and 71, he volunteered once again for the Franco-Prussian war.

Ersin HACIYAKUPOGLU : 0000-0002-9712-9913 Uygur ER : 0000-0002-6641-0075 Sait NADERI : 0000-0002-6784-4270

Figure 1: Portrait of Ernst von Bergmann, circa 1890.

He was the director in Lazarett Seilerbahn and carried out an outstanding job there. In 1871 he was appointed professor in Dorpat and worked there for 7 years. The Russo-Turkish War (1877-78) was the last war he participated in. He introduced new antiseptic wound treatment methods and immobilization of the extremities before searching for bullets, saving many lives and preventing amputations (14).

In 1878 he was accepted as a professor in Würzburg and after working for 4 years he was appointed to succeed Prof. Bernhard von Langenbeck in Berlin in 1888. His Clinic in Ziegelstresse Berlin was one of the best at his time. He used sublimate for disinfection. He published this work in 1880, which made him known as one of the most successful pioneers of the antisepsis concept (15). One of her assistants in Berlin was Curt Theodor Schimmelbusch (16 November 1860 – 2 August 1895), who invented the mechanical method of sterilizing surgical instruments and designed the Schimmelbusch -mask, which ensures the safety of the patient while she is under anesthesia (8). His other important pupil was Friedrich Gustav von Bramann (25 September 1854 – 21 April 1913).

Ernst von Bergmann was one of the most important surgeons of his time. In addition to his contributions to antiseptics and wound management, he was one of the pioneers in German surgery and neurosurgery. His clinic in Berlin was one of the best in the world and accepted patients from all over the world (12). He conducted research on the relationship between brain injury and intracranial pressure (ICP). In 1880, he wrote "Lehre von Kopfverletzungen", the first neurotraumatology book in history (11). In addition, in 1889, he wrote a second neurosurgery book, "Chirurgische Behandlung von Hirnkrankheiten" (10).

Bergmann died in Wiesbaden on 25 March 1907 at the age of 70, due to pencreas necrosis and peritonitis, even though he diagnosed himself as colon carcinoma 5 years before (3).

CONTRIBUTIONS

Bergmann's most important contribution to medicine and surgery was his ability to sterilize surgical instruments, thereby significantly reducing the rate of surgical infection. Bergmann's other notable contribution to infection reduction was his introduction of steam-sterilized surgical dressings and his demonstration that they were superior to chemical sterilization in dealing with infection. Bergmann was one of the first users and advocates of the knee-length white coat in medicine. As a military medic on the battlefield, he took a special interest in gunshot wounds, with an increased interest in cranial injuries (9).

As a general surgeon, he played a leading role in surgeries for hydrocele and esophageal diverticulum and contributed to appendectomy (7).

Bergmann left behind many medical works. The most important of these is "Die Lehre von den Kopfverletzungen" (The theory of head injuries), which deals with head trauma, published in 1880. His other important book in terms of brain surgery is "Die Chirurgische Behandlung der Hirnkrankheiten" (The surgical treatment of brain diseases), published in 1888. He also published a journal with his two colleagues called "Zeitschrift für ärztliche Fortbildung" (Journal for continuing medical education), which was about medical education, in 1904.

LEHRE VON KOPFVERLETZUNGEN

Lehre von Kopfverletzungen, was first published in 1880 (Figure 2). This book was a special part of Deutsche Chirurgie issued by Prof. Dr. Billroth and Prof. Dr. Luecke.

Lehre von den Kopfverletzungen consists of 560 pages. The book mainly contains 2 parts, and 6 sections. The part one contains 2 sections and 21 chapters. Part 2 contains 4 sections and 20 chapters (Table I). There are 2 lithographed plates and 55 illustrations (33 figures in part I, and 22 figures in part 2) demonstrating the fracture types, brain injury types, and ICP (Intracranial pressure) images.

All illustrations in this book are hand drawings and he explains the injury mechanism of that patient (Figure 3).

Part 1 is on bony and soft tissue injuries of head. It is divided into three sections and 21 chapters. Section 1 is on the intrauterin head injuries and birth injuries. Section 2 is on soft tissue injuries of the head, and section 3 is on skull injuries.

In chapters 8-21, the author classified skull fractures as impression fractures, split fractures, depression fractures, isolated fractures, and diastasis of sutures, He reviewed trans-

port, care, antisepsis and surgical treatment of fractures. He focused on skull base and craniovertebral junction fractures in separated chapters and discussed indications of trepanation in skull fractures. In chapter 15 the author explains trepanation techniques after skull fractures.

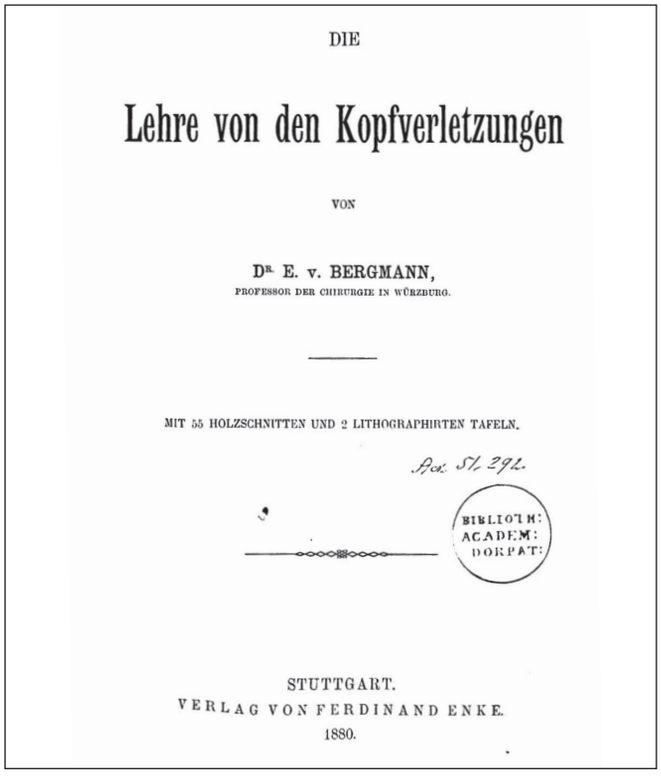
DIE

Lehre von den Kopfverletzungen

VON

Dr. E. v. BERGMANN,
PROFESSOR DER CHIRURGIE IN WÜRZBURG.

MIT 55 HOLZSCHNITTEN UND 2 LITHOGRAPHIRTEN TAFELN.

Acc. St. 292.

BIBLIOTH: ACADEM: DORPAT:

STUTTGART.
VERLAG VON FERDINAND ENKE.
1880.

Figure 2: Title page of "Die Lehre von den Kopfverletzungen". Verlag von Ferdinand Enke, Stuttgart, 1880.

Part 2 is on brain injuries and consists of 4 sections and 20 chapters. In the first section of part 2, the author gives sufficient information about anatomy, role of cerebrospinal fluid

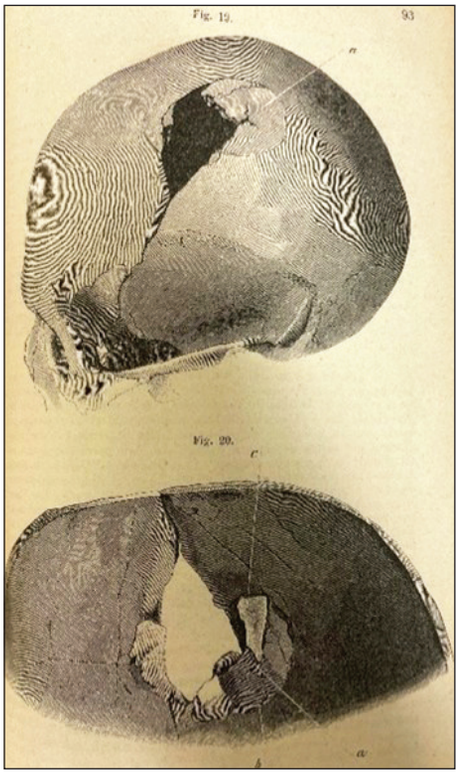

Figure 3: This drawing was made to show a gunshot wound in Karlsruhe, causing brain injury and arterial bleeding due to middle meningeal artery laceration from page 93 of the book, figure 19.

Table I: Summary of Contents of Each Part, Section and Chapter of the Lehre von den Kopfverletzungen

Part I	
Section 1 Chapter 1-2	Cranial injuries before or suring birth
Section 2 Chapters 3-7: covering scalp	Scalp injury of soft tissues
Section 2 Chapter 8-21	Cranial bone fracture
Part II	
Section 1 Chapter 1-5	Etiology, diagnosis and teratment of cerebral injuries. Classifications of cerebral injuries
Section 2 Chapter 6-8	Intracranial fossae and nerve injuries
Section 3 Chapter 9-18	Cerebral contusion, foreign body, postraumatic epilepsy, bainstem injuries, traumatic diabetes, teratment of fresh brain injury, tarumatic brain abscess, cerebral herniation, tarumatic psychose
Section 4 Chapter 19-20	Surgical teratment, indications, trepanation technique

(CSF), capacity of skull volume and its relationship with brain tissue, blood and CSF. Chapter 1-5 contains general aspects of cerebral injuries, their etiology, diagnosis and treatment, including the role of operative craniectomy and trepanation in neural injuries. The author classified cerebral injuries as commotio cerebri and compressio cerebri. Chapter 6-8 contains epidural and subdural hematomas, traumatic pachymeningitis, intrameningeal bleeding, injuries of cranial nerves, dural sinuses, and intracranial arteries, as well as arteriovenous fistulas (AVFs).

Chapter 9-18 contains cerebral contusion, foreign body, posttraumatic epilepsy, brainstem injuries, traumatic diabetes, traumatic brain abscesses, cerebral herniation, and traumatic psychoses (Figure 4). Chapter 19-20 contains surgical treatment, indications, and technique of trepanation in neural injuries.

WOUND MANAGEMENT

He was a strong advocate of antisepsis in surgical practice, and particularly in craniocerebral injuries. For the management of cranial wounds, other than bandage, he advised cold/ice application. There were various types of cold bandages. Ernst von Bergmann used the one that was invented by Goldschmidt, which was a compression bandage to reduce ICP that could be connected to a water pipe system to cool the head (Figure 5).

INTRACRANIAL PRESSURE AND INTRACRANIAL HYPERTENSION

Special emphasis is given to posttraumatic raised ICP and possible mechanisms of intracranial hypertension (ICH) in this book. In the book, three different hypotheses are put forward to explain the development mechanism of posttraumatic ICH. He attributed posttraumatic ICH to bleeding from brain vessels, impression fractures or foreign bodies, and infections. He also mentioned that the first two of those reasons are directly due to trauma, but infections are chronic complications of trauma. He measured ICP with a manometer and examined the circumstances resulting intracranial hypertension (Figure 6).

He stated that intracranial lesions increase the ICP and, as a result, decrease cerebral circulation. Reaction of cardiovascular system to raised ICP in patients and in experiments with dogs were well examined and shown in the book.

He recommended non-operative techniques such as venous drainage, cooling, other than surgical methods for treatment of intracranial hypertension.

DISCUSSION

Long-lasting, painless surgery without or with less risk of infection started in the 19th century. In 1846, ether anesthesia and in 1847 chloroform anesthesia were introduced and allowed for long lasting surgeries. Joseph Lister, British surgeon, defined principles of antisepsis, which reduced the risk of infection-related morbidity and mortality (6). Thus, reducing infection deaths drew attention to these new methods. During

Figure 4: Drawing of a Russion soldier with brain prolaps after a shotwound at the head on 18.07.1877. He saw this patient during his treatment by Dr. Kusmin in Sistowa at 50.th Feldnazareth, from page 533, figure 55.

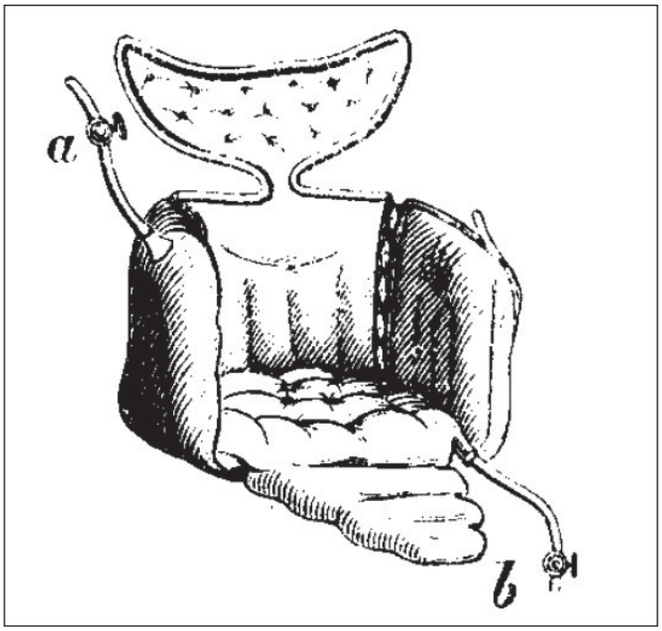

Figure 5: Water pipe system to cool the head in craniocerebral injuries. The letter a shows the pipe connected to the water pipe, and b is the drainage pipe of water, from page 53, figure 10.

Figure 6: Manometer diagram showing raised ICP after compression of neck, from page 324, figure 45.

his professional work, Bergmann understood the importance of antisepsis, visited the clinics of prominent surgeons in this field, developed what he learned and put it into practice. He also passed on his knowledge to future generations by writing down the principles he developed. It is very significant that he gave the principles of antisepsis and wound care in a work in which he wrote about trauma diseases that are most susceptible to infection. His work is the first neurosurgery book written solely about head traumas. Furthermore, Bergmann not only applied antisepsis, but he also introduced steam (heat) sterilization of surgical instruments and dressings in 1886. Surgical instrument sterilization, which is a common and essential practice today, was met with skepticism in Bergmann's time and received numerous objections from his colleagues.

Bergmann's other important contribution was in the field of military surgery. It is noteworthy that the organized military health service was started in the second half of the 18th century by Dominique Jean Larrey (1766-1842) and Pierre-François Percy (1757-1825) during the wars of Napoleon I (13). A school was opened in Algeria between 1840 and 1850, which served as a military health school for French surgeons. A similar one was used for the training of German surgeons during the Schleswig War (1848-1851) (5). Bergmann was also a pioneer in the application of antisepsis in German organized military health institutions. He stated that

'Like cholera, every gunshot wound becomes a source of poison for the organism that receives this wound. The body then becomes a workshop for this frightful poison or germ that is then able to spread itself throughout the entire organism' (2).

By the war of 1870, Bergmann was aware of the concept of cerebral localization and knew that brain lesions could cause contralateral symptoms (1). However, the mortality rate of his trepanations was around 75%, leading her to think that there might be some problems related to increased ICP. He demonstrated cardiovascular results of raised ICP in 1873, which was later defined as "Cushing's reflex" in 1901 by Harvey Cushing.

CONCLUSION

This study revealed that Ernst von Bergmann is one of the most important surgeons of the 19th century. His contributions are not limited to the establishment of antisepsis in surgery and wound management. He was also a pioneer in ICP concept in head traumas and organized military health services.

ACKNOWLEDGEMENTS

We thank the Turkish Neurosurgical Society for their assistance with English editing.

Declarations

Funding: This research did not receive any specific grant from funding agencies in the public, commercial, or not-for-profit sectors.

Availability of data and materials: Figures in the text are in public domain. No material that would give rise to copyright was used in the article.

Disclosure: The authors declare no competing interests.

AUTHORSHIP CONTRIBUTION

Study conception and design: UE, SN, EH
Data collection: SN, EH
Analysis and interpretation of results: UE, SN, EH
Draft manuscript preparation: UE, EH
Critical revision of the article: UE, SN, EH
All authors (EH, UE, SN) reviewed the results and approved the final version of the manuscript.

REFERENCES

1. Blair JSG: "Ernst Von Bergmann". J Royal Army Med Corps 152:108-119, 2006. https://doi.org/10.1136/jramc-152-02-09
2. Buchholtz A: Ernst von Bergmann: mit Bergmanns Kriegsbriefen von 1866, 1870/71 und 1877. Leipzig, Vogel, 1911.
3. Czymek R, Düsel W: On the centennial of Ernst von Bergmann's death. Der Chirurg; Zeitschrift für Alle Gebiete der Operativen Medizen 78:265-272, 2007. https://doi.org/10.1007/s00104-006-1299-8
4. Hanigan WC, Ragen W, Ludgera M: Neurological surgery in the nineteenth century: the principles and techniques of Ernst von Bergmann. Neurosurgery 30:750-757, 1992. https://doi.org/10.1227/00006123-199205000-00017
5. Legouest L: Traité de Chirurgie d'Armée. Paris, J.B. Baillière, 1872.
6. Lister J: Illustrations of the antiseptic system of treatment in surgery. Lancet 2:668-669, 1867. https://doi.org/10.1016/S0140-6736(02)58116-2
7. Luther B, Wirth I: The development of surgery by Ernst von Bergmann. Zentralblatt für Chirurgie 111:1389-1397, 1986.
8. Pawlow W: Die wissenschaftlichen Leistungen des Chirurgen Ernst von Bergmann (1836-1907) für die Entwicklung der Medizin im Spiegel seiner Korrespondez in den Jahren 1877 bis 1878. Beitr Orthop Traumatol 37:349-352, 1990
9. Salcman M: Ernst von Bergmann performs a brain operation - by Franz Skarbina. Neurosurgery 38:1254-1255, 1996. https://doi.org/10.1227/00006123-199606000-00046
10. Von Bergmann E: Die Chirurgische Behandlung von Hirnkrankheiten. Berlin, Hirschwald, 1889.
11. Von Bergmann E: Lehre von den Kopfverletzungen, Stuttgart, Verlag von Ferdinandenke, 1880
12. Von Bruns V: Die chirurgischen Krankheiten und Verletzungen des Gehirns und seiner Umhüllungen. German: Tübingen Laupp, 1854
13. Walusinski O: Neurology and Neurologists during the Franco-Prussian War (1870–1871). Front Neurol Neurosci 38:77-92, 2016. https://doi.org/10.1159/000442595
14. Zimmermann M: Life and work of the surgeon Ernst von Bergmann (1836–1907), long-term editor of the Zentralblatt für Chirurgie. Zentralblatt für Chirurgie 125:552-560, 2000
15. Zülch KJ: Ernst von Bergmann and the beginning of neurosurgery in Berlin. In: Wenker H, Klinger M, Brock M, Reute F (eds). Advances in Neurosurgery, Vol. 14. Berlin: Springer-Verlag Heidelberg, 1986:6-7. https://doi.org/10.1007/978-3-642-71108-4_2

Turk Neurosurg 36(1):6-15, 2026
DOI: 10.5137/1019-5149.JTN.49125-25.1

Original Investigation
Neurotrauma

Received: 18.05.2025
Accepted: 23.07.2025
Published Online: 16.01.2026

Integration of a Hybrid Operating Room for the Management of Severe Traumatic Brain Injury: A Combined Approach with Real-Time Xper-CT Imaging and Neurointervention

Hong Suk AHN, Hong Jun JEON, Byung Moon CHO, Se Hyuck PARK

Hallym University College of Medicine, Kangdong Sacred Heart Hospital, Department of Neurosurgery, 150 Seongan-ro, Gangdong-gu, Seoul 134-701, Republic of Korea

Corresponding author: Hong Jun JEON ✉ homeoman@hanmail.net

ABSTRACT

AIM: To evaluate the safety and efficacy of the hybrid operating room (HOR) approach in the management of severe traumatic brain injury (sTBI) using Xper-computed tomography (CT)-guided imaging and neurointerventional techniques

MATERIAL and METHODS: A retrospective analysis was conducted on 154 patients with TBI treated surgically between February 2020 and December 2023. Among these, 26 patients with sTBI were managed in an HOR equipped with an Allura Xper FD 20® system. Intraoperative interventions included Xper-CT confirmation, real-time imaging-guided hematoma aspiration or catheter placement, and combined neurointerventional procedures. Clinical outcomes were assessed using the Glasgow Outcome Scale-Extended (GOS-E) at 6 months, and procedural morbidity and mortality rates were documented.

RESULTS: The 26 patients with sTBI had a mean age of 45.3 ± 12.0 years, with 60.4% being male. Xper-CT was used in all cases (mean: 1.7 scans/patient) for confirmation and in 11 cases (42.3%) for real-time guidance, enabling precise interventions such as parenchymal hematoma aspiration (30.8%) and external ventricular drainage (11.5%). Vascular injuries were managed with N-butyl cyanoacrylate glue or polyvinyl alcohol particle embolization (15.4%) and endovascular coiling for pseudoaneurysms (11.5%), with intraoperative angiography performed in 7.7% of cases. No HOR-related complications or reoperations were noted. Favorable outcomes (GOS-E≥4) were observed in 42.3% of patients at 6 months, whereas the 28-day mortality rate was 19.2%, primarily owing to initial trauma (n=3) and pneumonia or sepsis (n=2).

CONCLUSION: The HOR approach represents a significant advancement in the management of sTBI and potentially improves the overall quality of emergency neurosurgical care.

KEYWORDS: Cerebrovascular trauma, Craniocerebral trauma, Subdural hematoma, Traumatic brain injury

ABBREVIATIONS: CT: Computed tomography, **ED:** Emergency department, **EDH:** Epidural, **EVD:** External ventricular drainage, **GCS:** Glasgow Coma Scale, **GOS-E:** Glasgow Outcome Scale-Extended, **HOR:** Hybrid operating room, **ICP:** Increased intracranial pressure, **SDH:** Subdural hemorrhage, **sTBI:** Severe traumatic brain injury, **T-ICH:** Traumatic intracerebral hemorrhage

INTRODUCTION

Traumatic brain injury (TBI) is a global health burden and one of the leading causes of death and disability worldwide (11). TBI is characterized by an abrupt disruption in brain function owing to external mechanical forces and presents considerable clinical challenges, especially in the context of emergency neurosurgery (7). Long-term studies of patients with TBI have revealed that more than half of them have some

Hong Suk AHN : 0000-0002-5589-6022
Hong Jun JEON : 0000-0001-7370-1324
Byung Moon CHO : 0000-0001-9906-8125
Se Hyuck PARK : 0009-0007-4518-2919

form of disability and a high mortality rate (24,28). The presence of complex hemorrhages, multiple fractures, and rapid evolution of symptoms often necessitate immediate and precise interventions (27).

The traditional neurosurgical management of TBI typically involves sequential procedures across various settings, requiring separate stages for imaging, neurointervention, and surgical treatment. In cases with cerebrovascular injury, the diagnostic and treatment procedures can become even more complex (3,26). This segmented approach can lead to delays in care, which may affect patient outcomes (12,27,33). The advent of hybrid operating rooms (HORs) offers a promising solution for streamlining TBI management. HORs are specially designed surgical suites that integrate advanced imaging capabilities, such as Xper computed tomography (CT), with interventional and surgical tools in a single environment (8,21,22). This setup enables real-time imaging and allows surgeons to perform both diagnostic and therapeutic procedures without relocating the patient, thereby reducing treatment delays and enhancing procedural accuracy.

By examining patient outcomes in cases of severe traumatic brain injury (sTBI) treated using HORs, we aimed to determine their potential to improve the efficiency and quality of emergency neurosurgical care.

MATERIAL and METHODS

Patient Selection

All procedures involving human participants were conducted in accordance with institutional and national ethical standards, as well as the 1964 Declaration of Helsinki and its later amendments. This study followed the STrengthening the Reporting of Observational Studies in Epidemiology (STROBE) guidelines. This retrospective study was approved by the local institutional review board (Approval number: 2025-01-013, Approval date: 05 Feb 2025).

This study retrospectively analyzed patients who underwent surgical management for TBI between February 2020 and December 2023. Of the 154 patients treated surgically for TBI, 26 (16.9%) were specifically classified as having sTBI and managed within an HOR. sTBI was classified based on institutional standards and specific clinical indicators, including the Glasgow Coma Scale (GCS) score, acute neurological and systemic signs, and neuroimaging findings (35).

The criteria for defining sTBI in this study included:

1. **Glasgow Coma Scale:** An initial GCS score of 8 or less within the first 24 h post-injury was used to identify severe impairment (36). Persistent scores of 8 or less beyond the acute phase indicated prolonged sTBI, necessitating intensive monitoring and management
2. **Acute neurological and systemic signs:** Indicators such as non-reactive pupils, hemiparesis, abnormal posturing, and irregular vital signs suggestive of brainstem dysfunction (e.g., Cushing's reflex) were considered significant markers.
3. **Neuroimaging findings:** Evidence of substantial structural brain damage on imaging, such as intracranial hemorrhages (subdural, epidural, or intraparenchymal), diffuse axonal injury, traumatic intracerebral hemorrhage (T-ICH), or significant brain edema, was a critical component of classification. Additionally, detection of blunt cerebrovascular injury using imaging modalities such as CT angiography or magnetic resonance angiography was included (26,32). Common blunt cerebrovascular injury findings encompassed arterial dissections, pseudoaneurysms, and vessel occlusions, which informed the need for targeted surgical or interventional management.

HOR

The HOR was equipped with the Allura Xper FD 20® system (Philips, Best, The Netherlands), a ceiling-mounted monoplane flat-panel detector seamlessly integrated with a three-dimensional rotational angiography workstation. This system enabled intraoperative imaging modalities such as Xper-CT® and three-dimensional rotational angiography without requiring patient movement or repositioning, ensuring efficient workflow. Although the flat panel CT resolution for brain tissue is inferior to that of standard CT, the system provides critical advantages for managing sTBI, including real-time imaging confirmation, guided interventions, and the integration of endovascular and open surgical techniques. Based on these capabilities, we utilized it for accurate intraoperative decision-making and effective planning of strategic interventions, implementing three primary approaches for sTBI management in the HOR.

1. **Xper-CT confirmation:** Intraoperative Xper-CT imaging was used to confirm the successful evacuation of intracranial hemorrhages and to monitor the development of new lesions. This imaging approach was crucial for ensuring complete removal of hematomas and maintaining real-time surveillance of the intracranial status, thereby reducing the risk of postoperative complications.
2. **Xper-CT guidance:** Xper-CT provided real-time imaging guidance for targeted interventions, such as hematoma aspiration and external ventricular drainage (EVD) placement. Using a 240° scan trajectory, the system captured 600 frames over a 20 s period at a rate of 30 frames/s, enabling high-resolution visualization. The 30×40 cm detector format allowed for detailed imaging of critical anatomical landmarks. The acquired source images were transferred to a workstation where a volumetric dataset was reconstructed within 1 min. This rapid feedback facilitated precise procedural execution and enhanced the accuracy of interventions within the hybrid setting.
3. **Combined neurointervention:** This approach incorporated neurointerventional techniques, including glue embolization, and angiography, primarily aimed at stabilizing and controlling vascular injuries associated with TBI. By achieving immediate hemostasis, these procedures minimized intraoperative bleeding risks and improved patient safety, especially in complex cases requiring both surgical and endovascular management.

Clinical Outcomes

Clinical outcomes were evaluated to assess the effectiveness and safety of the HOR treatments. Functional outcomes were measured using the Glasgow Outcome Scale-Extended (GOS-E) 6 months post-injury, categorizing the results into unfavorable outcomes (scores 1–3: death, vegetative state, or severe disability) and favorable outcomes (scores 4–8: moderate to low disability or good recovery). Assessments were conducted through neurosurgical evaluations of hospitalized patients, reviews of referral documents for transferred patients, and structured telephone interviews of discharged patients. Procedural outcomes included procedure-related morbidity and complications directly linked to systematically recorded HOR interventions. Mortality rates at 28 days and 6 months post-injury were documented, with the causes analyzed and attributed to the initial trauma, increased intracranial pressure (ICP), or other factors. Additionally, reoperation rates were tracked to assess the need for subsequent surgical interventions after the initial procedures in the HOR.

Statistical Analysis

All statistical analyses were performed using IBM SPSS version 28.0 (IBM Corp, Armonk, NY). All categorical variables are presented as percentages and 95% confidence intervals. All continuous variables are presented as means ± standard deviations.

RESULTS

A total of 26 patients with sTBI were treated at our HOR (Table I). This cohort included 16 men (60.4%) and 10 women (39.6%) with a mean age of 45.3 ± 12.0 years. The primary trauma causes included falls (n=14, 53.8%), car accidents (n=5, 19.2%), bicycle accidents (n=4, 15.4%), pedestrian injuries (n=2, 7.7%), and motorcycle accidents (n=1, 3.8%). Skull fractures were identified in all patients, including depressed (n=6; 23.1%), basilar (n=5; 19.2%), compound (n=11; 42.3%), and linear (n=4; 15.4%) fractures. Radiographic findings revealed epidural hemorrhage (EDH) in two (7.7%) patients, EDH with subdural hemorrhage (SDH) and traumatic intracerebral hemorrhage (T-ICH) in four (15.4%) patients, SDH with T-ICH in 12 (46.2%) patients, and SDH with T-ICH and intraventricular hemorrhage and traumatic subarachnoid hemorrhage in eight (30.8%) patients.

Table II presents the types of surgical procedures, applications of the HOR, and clinical outcomes in our cohort. The initial surgical approach was determined based on preoperative imaging and clinical status. Most patients underwent decompressive craniectomy and hematoma evacuation (n=23, 88.5%). In cases where the extent of injury allowed for a less invasive approach, craniotomy and hematoma evacuation were performed in three patients (11.5%). However, intraoperative Xper-CT, performed at an average of 7.5 ± 4 minutes (min) after the initial operation, identified additional findings in 10 patients (38.4%), necessitating immediate surgical modifications. Among these, contralateral craniectomy and hematoma evacuation were performed in five patients (19.2%) owing to newly detected hematoma expansion, whereas in three patients (11.5%), contralateral craniotomy and hematoma evacuation were required to address developing mass effects on the opposite side. Additionally, ipsilateral extended craniectomy was performed in two patients (7.7%) to manage rapid brain swelling requiring further decompression. All patients underwent intraoperative Xper-CT confirmation at an average of 1.7 times per patient. The mean interval from neurointervention to surgery was 14.5 ± 7 min. Xper-CT guidance was used in 11 patients (42.3%), primarily for hematoma evacuation and EVD placement. Among the surgical interventions, parenchymal hematoma aspiration was performed in eight patients (30.8%), whereas EVD placement for ICP control and monitoring was conducted in three patients (11.5%). For hemostatic control in patients with basilar skull fractures, N-butyl cyanoacrylate was used in three patients (11.5%) and polyvinyl alcohol particles in one patient (3.8%). Additionally, coil embolization was performed in three patients (11.5%) to treat pseudoaneurysms associated with traumatic vascular injuries, and intraoperative angiography was conducted in two

Table I: Demographics of the 26 Patients with Severe TBI Treated in the Hybrid Operating Room

Characteristic	Value
Age, mean ± SD (range), years	45.3 ± 12.0 (21–78)
Gender	**n (%)**
Male	16 (61.5)
Female	10 (38.5)
Trauma Cause	**n (%)**
Fall	14 (53.8)
Car	5 (19.2)
Bicycle	4 (15.4)
Pedestrian	2 (7.7)
Motorcycle	1 (3.8)
Initial GCS (mean)	6 (3.8)
Type of Skull Fracture	**n (%)**
Depressed	6 (23.1)
Basilar	5 (19.2)
Compound	11 (42.3)
Linear	4 (15.4)
Classification of Hemorrhage	**n (%)**
EDH	2 (7.7)
EDH + SDH + T-ICH	4 (15.4)
SDH + T-ICH	12 (46.2)
SDH + T-ICH + IVH + T-SAH	8 (30.8)

EDH: *Epidural hemorrhage,* ***GCS:*** *Glasgow Coma Scale,* ***IVH:*** *Intraventricular hemorrhage,* ***SDH:*** *Subdural hemorrhage,* ***TBI:*** *Traumatic brain injury,* ***T-ICH:*** *Traumatic intracerebral hemorrhage,* ***T-SAH:*** *Traumatic subarachnoid hemorrhage.*

Table II: Surgical Procedures and Outcomes via Hybrid Operating Room

Surgical Procedures and Outcomes	n (%)
Decompressive craniectomy and hematoma evacuation	23 (88.5)
Craniotomy and hematoma evacuation	3 (11.5)
Type of application	
Xper CT confirmations	26 (100.0)
Contralateral craniectomy & hematoma evacuation	5 (19.2)
Contralateral craniotomy & hematoma evacuation	3 (11.5)
Ipsilateral extended craniectomy	2 (7.7)
Xper CT guidance	11 (42.3)
Aspiration of parenchymal hemorrhage	8 (30.8)
EVD	3 (11.5)
Combined with neurointervention	9 (34.6)
Embolization with nBCA or PVA	4 (15.4)
Coil embolization for traumatic pseudo-aneurysm	3 (11.5)
Angiography for evaluation of vessel injury	2 (7.7)
Time interval from operation to Xper CT (minutes)	7.5 ± 4
Time interval from intervention to operation (mean ± SD) (minutes)	14.5 ± 7
Re-operation after use of HOR	0 (0.0)
GOS-E at 6 months	
Good recovery	11 (42.3)
Moderate disability	9 (34.6)
Severe disability/vegetative state/death	6 (23.0)
Mean ICU stay / total hospitalization (mean ± SD) (days)	22.5±3.5 / 35.7±4.6
HOR-related morbidity	0 (0.0)
Mortality at 28 days	4 (15.4%; 95% CI, 6.2–33.5%)

CT: *Computed tomography,* ***EVD:*** *External ventricular drainage,* ***GOS-E:*** *Glasgow Outcome Scale-Extended,* ***HOR:*** *Hybrid operating room,* ***ICU:*** *Intensive care unit,* ***nBCA:*** *N-butyl cyanoacrylate,* ***PVA:*** *Polyvinyl alcohol,* ***95% CI:*** *95% confidence interval.*

patients (7.7%) to evaluate arterial and venous injuries. Notably, none of the 26 patients required immediate reoperation after HOR-assisted treatment. Furthermore, no HOR-related morbidities, such as surgical site infections, femoral puncture site complications, procedural rebleeding, cerebral infarction, or acute hydrocephalus requiring additional intervention, were observed. At discharge, favorable GOS-E was observed in nine patients (34.6%); however, 17 (65.4%) had unfavorable outcomes. By 6 months post-injury, the proportion of patients with good recovery, defined as a GOS-E score between 4 and 8, increased to 11 (42.3%), with moderate disability reported in nine patients (34.6%) and severe disability, vegetative state, or death occurring in six (23.0%). The mean intensive care unit stay was 22.5 ± 3.5 days, and the mean total hospitalization duration was 35.7 ± 4.6 days, reflecting the intensive care needs and prolonged recovery period in sTBI management. The 28-day mortality rate was four (15.4%), with one death (7.7%) attributed to the initial traumatic injury, two (7.7%) to increased ICP, and one (3.8%) from secondary complications, such as sepsis and pneumonia.

Illustrative Cases

Case 1 (Figure 1)

A 37-year-old male construction worker was admitted to the emergency department (ED) with altered mental status (initial GCS score: 7) following a fall from a height at a construction site. The initial brain CT revealed a sagittal skull fracture with extensive EDH, SDH, and T-ICH in the frontal lobe. The patient underwent emergency bilateral decompressive craniectomy with hematoma evacuation in the HOR. Intraoper-

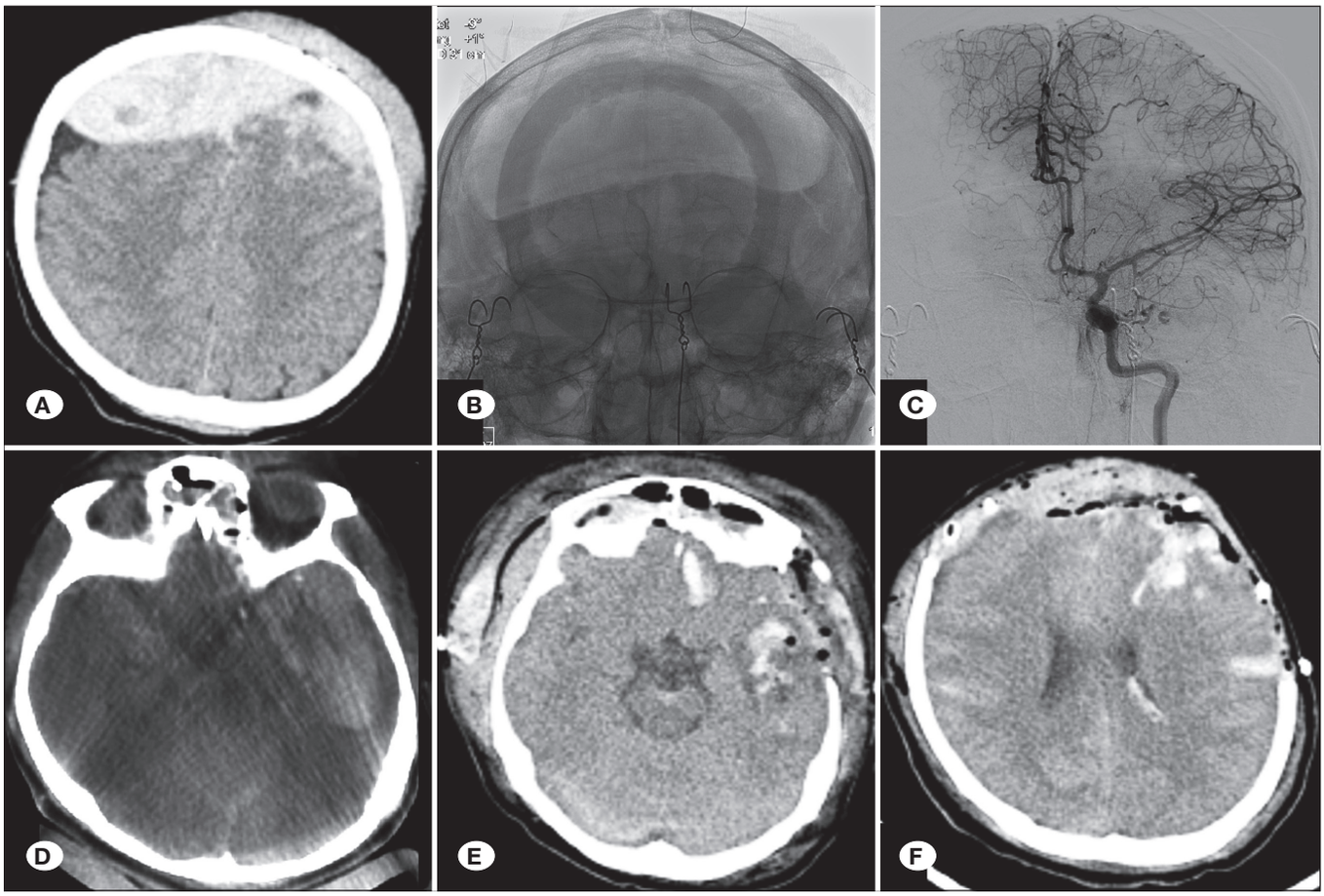

Figure 1: Illustrative case 1. **A)** Brain CT showing an epidural hematoma and subdural hematoma. **B)** Intraoperative fluoroscopic image demonstrating the extent of bifrontal decompressive craniectomy. **C)** Displaced bone fragment causing injury to the sagittal sinus and underlying dura, with cerebral angiography performed to evaluate for additional vascular injury. **D)** Intraoperative Xper CT showing a left temporal traumatic intracerebral hemorrhage. **E, F)** Postoperative CT scans showing complete evacuation of the primary hematoma and secondary evolved lesions. **CT:** computed tomography.

ative exploration revealed a sagittal sinus laceration caused by displaced bone fragments, leading to further evaluation via cerebral angiography for associated vascular injuries. Intraoperative Xper-CT revealed newly increased T-ICH levels in the left frontal and temporal regions, likely secondary to evolving parenchymal damage and venous congestion, necessitating additional hematoma evacuation. Postoperative CT confirmed the complete clearance of all traumatic hematomas. During the subsequent 2-week neurocritical care course, the patient demonstrated rapid neurological improvement, including ICP normalization, improved consciousness, and resolution of focal deficits. He was discharged for home-based rehabilitation with a GOS-E score of 7, indicating good recovery with minor neurological sequelae.

Case 2 (Figure 2)

A 36-year-old male construction worker was brought to the ED in a semi-comatose state following blunt head trauma from falling construction material and a concurrent fall of approximately 3 m. He had severe maxillofacial crush injuries and emergency decompressive craniectomy with hematoma evacuation was performed in the HOR. Intraoperative Xper-CT revealed diffuse cerebral edema without new hemorrhage but with persistent ICP elevation, indicating secondary brain injury. To manage the acute-phase ICP, EVD was performed under Xper-CT guidance to ensure accurate ventricular targeting and real-time monitoring. With aggressive neurocritical care, including ICP control and sedation, the patient's condition gradually stabilized. The patient was weaned off mechanical ventilation on postoperative day 14 and underwent tracheostomy decannulation at week 4. Eight weeks after the injury, the patient was discharged to a neurorehabilitation facility with a GOS-E score of 4, indicating moderate disability.

Case 3 (Figure 3)

A 20-year-old male was brought to the ED with altered consciousness, left-sided mydriasis, and active oral and nasal bleeding after a motorcycle accident. Brain CT revealed a large EDH, along with facial bone and basal skull fractures. Urgent glue embolization of the external carotid artery branches at the active bleeding site was performed, followed by evacuation of the EDH. The patient recovered rapidly postoperatively

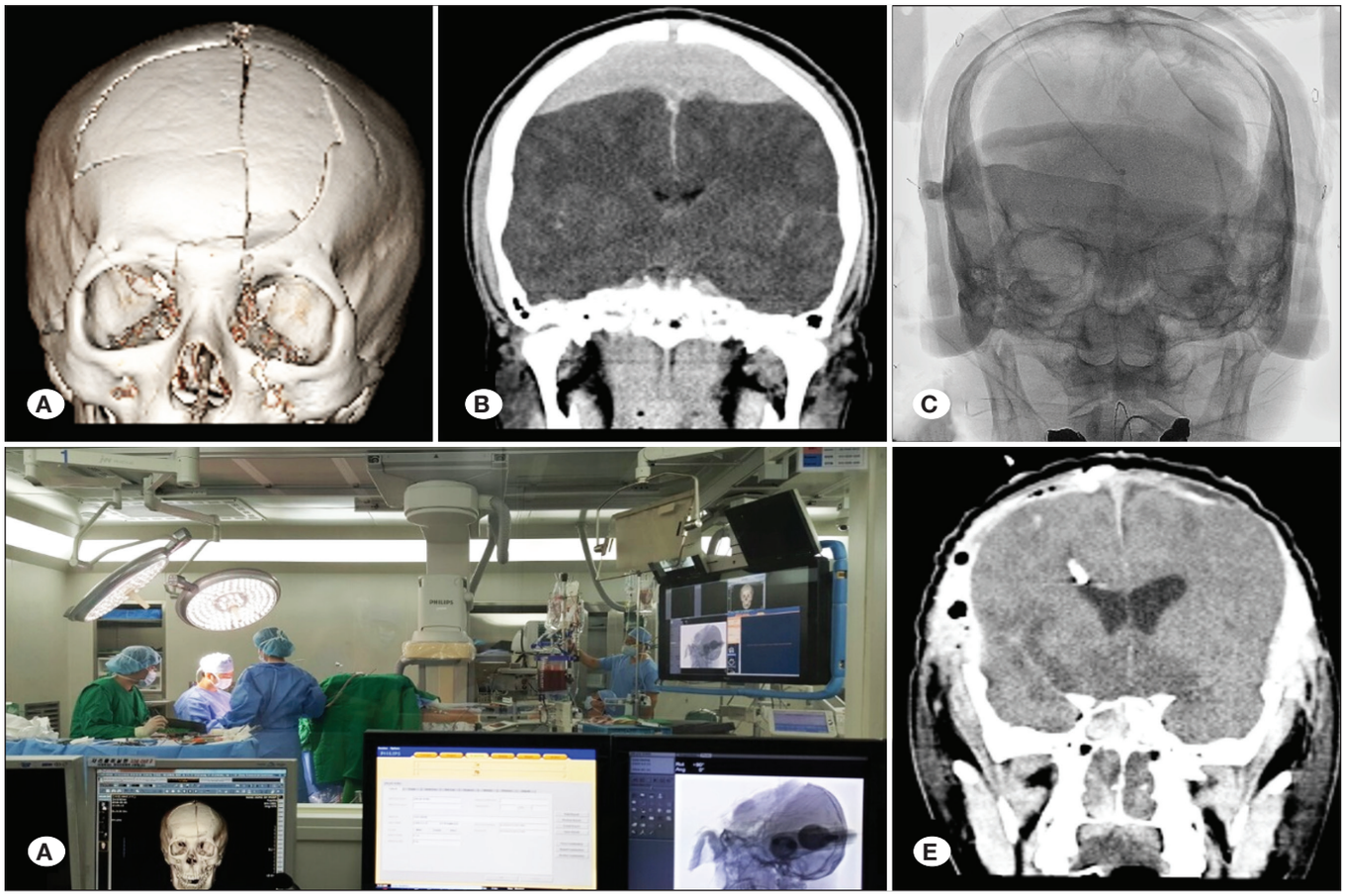

Figure 2: Illustrative case 2. **A)** 3D reconstructed CT showing a large depressed fracture of the frontal bone with a diastatic fracture along the sagittal suture. **B)** Brain CT demonstrating a subdural hematoma at the vertex and signs of IICP. **C)** Intraoperative fluoroscopic image showing the extent of bifrontal decompressive craniectomy and Xper CT-guided EVD insertion for IICP control. Intraoperative photograph in the hybrid operating room showing the actual setup, including positions of anesthesiology staff and imaging equipment. **D)** Intraoperative view of hybrid operating room. **E)** Postoperative CT showing the evacuated hematoma, inserted EVD, and ischemic injury in the basal area caused by IICP. **CT:** Computed tomography; **IICP:** Increased intracranial pressure; **EVD:** External ventricular drainage.

without complications and was discharged on postoperative day 28 without neurological deficits.

DISCUSSION

The management of sTBI requires a rapid, multidisciplinary approach to minimize secondary injuries and improve outcomes. Traditional neurosurgical workflows often involve staged interventions that require multiple imaging sessions, reoperation for delayed hemorrhage, and separate neurovascular procedures. Frequent patient transfers between the CT suite, operating room, and neurointerventional suite delay treatment and increase the risk of secondary ischemia and transport-related complications, which can worsen patient outcomes (2,18,19,23). The HOR enhances workflow efficiency by integrating intraoperative imaging, Xper-CT guided hematoma evacuation or cerebrospinal fluid drainage, and real-time neurovascular interventions within a single setting. This setup eliminates unnecessary patient transfers, enables immediate reassessment of evolving hemorrhages, and facilitates timely intervention without workflow disruptions.

Expedited management is a key determinant of TBI outcomes as delays in hematoma evacuation and neurovascular stabilization are directly linked to increased mortality (12,33). Prior studies have shown that conventional hospital workflows result in an average delay of 45 ± 12 min for initial imaging and 65 ± 18 min for neurointervention (2,12,33). In contrast, intraoperative Xper-CT in the HOR reduced these delays by 60% and 57%, respectively, enabling immediate confirmation of hematoma clearance and vessel integrity (8,22). Furthermore, the time from admission to definitive surgical intervention improved by 38%, decreasing from 120 ± 30 min to 75 ± 15 min, which is significant given that each 30-min delay in TBI intervention increases mortality risk by 20–25% (12,33). In our HOR setting, intraoperative imaging to confirm surgical results required an average of 7.5 ± 4 min, and the interval between neurointervention procedures and craniotomy was approxi-

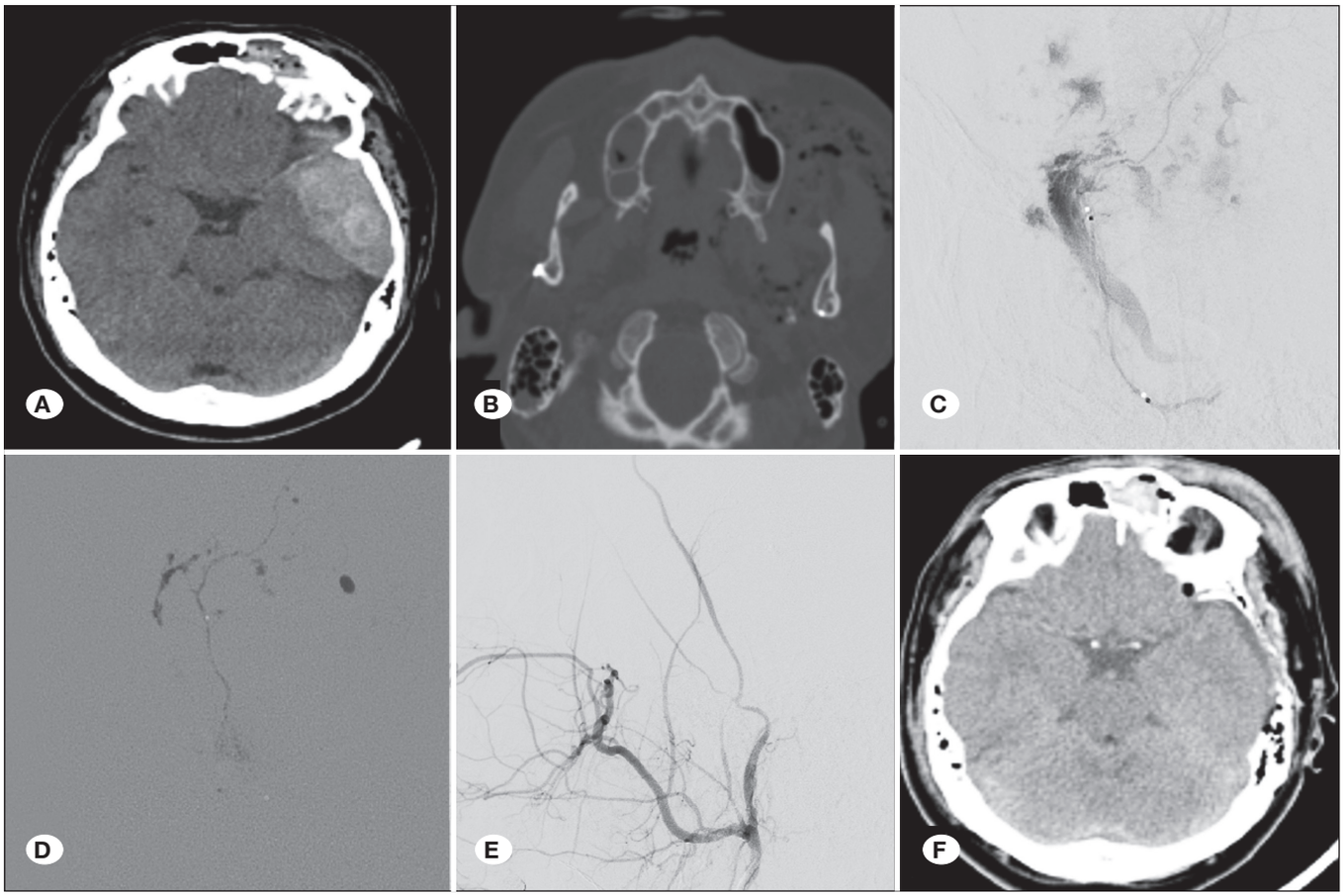

Figure 3: Illustrative case 3. **A)** Brain CT after a motorcycle accident showing an epidural hematoma and skull fracture. **B)** Facial bone CT demonstrating a large hematoma around the left maxillary and mandibular areas caused by active bleeding. **C)** n-BCA embolization of actively bleeding branches of the left external carotid artery performed in the HOR. **D, E)** Additional embolization of the left middle meningeal artery using n-BCA glue for further bleeding control. **F)** Postoperative CT scans showing complete evacuation of the primary hematoma and successful control of active bleeding. **CT:** Computed tomography; n-BCA, N-butyl cyanoacrylate glue; **HOR:** Hybrid operating room.

mately 14.5 ± 7 min, ensuring a highly efficient workflow while minimizing the risk of secondary brain injury.

Postoperative hemorrhagic progression remains a major concern in the management of sTBI, with conventional treatment protocols reporting progression rates of 15–25% (1,4,9,29). Traditional surgical workflows often fail to detect delayed intraoperative hematoma expansion, necessitating reoperation in up to 18.5% of cases because of unrecognized residual or new hemorrhages (13,40). In our study, Xper-CT was utilized intraoperatively in 100% of patients, providing immediate post-evacuation assessment and facilitating early detection of any persistent or new hemorrhagic foci. This real-time imaging modality enables prompt surgical correction and prevents delayed hematoma expansion, which may only have been detected postoperatively. Previous studies have demonstrated that the implementation of intraoperative CT may provide a nearly 60% chance of changing the surgical plan from hematoma removal to surgical decompression (5). Our findings further substantiate this trend, as none of the patients (0%) in our cohort required reoperation for postoperative hemorrhage, reinforcing the critical role of intraoperative imaging in optimizing surgical outcomes and minimizing the need for secondary interventions (4,29).

Beyond hemorrhage control, ICP elevation remains a significant secondary complication of sTBI, occurring in 23.2% of patients treated with conventional management (25,34). Delayed recognition of cerebral edema, progressive mass effect, or midline shift frequently necessitate secondary decompressive craniectomy, which has been associated with poor neurological outcomes (37). In our study, intraoperative evaluation using Xper-CT allowed immediate surgical decision-making. Postoperative Xper-CT confirmed that patients exhibiting severe ICP elevation underwent extended decompressive craniectomy and EVD without delay, demonstrating effective ICP reduction and adequate decompression. No patient required postoperative secondary decompressive craniectomy, indicating that integrating intraoperative imaging and aggressive surgical intervention within the HOR effectively mitigated

the need for additional procedures. These findings align with those of previous studies emphasizing the role of real-time intraoperative ICP monitoring and hemorrhage control in reducing the need for secondary decompression and improving overall neurological outcomes (13,34,40).

The integration of the Xper-CT guidance system within the HOR significantly enhanced procedural precision in sTBI, particularly in cases that required hematoma aspiration and EVD placement (10). Given that conventional EVD placement is associated with a 21–30% misplacement rate owing to anatomical distortion following sTBI, optimizing accuracy is critical for improving patient outcomes (4,10,38). In our study, not a single misplacement occurred when Xper-CT-guided EVD placement was used, demonstrating the system's real-time trajectory visualization and immediate intraoperative feedback capability. This approach minimizes procedural errors by ensuring precise catheter placement and reducing reliance on anatomical approximations, which is particularly crucial in cases of significant cerebral edema or midline shifts (37-40). Furthermore, the incorporation of real-time X-ray flow navigation facilitated the dynamic assessment of needle trajectories and catheter depth, ensuring safer and minimally invasive interventions (25,34). Importantly, Xper-CT navigation significantly reduced the risk of inadvertent cortical injury, reinforcing its role in reducing neurotrauma surgical workflows and improving procedural safety (5,29).

Another notable benefit of the HOR is the integration of endovascular techniques, such as embolization, into the neurosurgical workflow, providing an effective approach for managing complex TBIs, particularly in cases involving extensive base of skull fractures with active hemorrhage (14,31). By enabling concurrent endovascular embolization and surgical hematoma evacuation, the HOR ensures rapid hemostasis, significantly reducing intraoperative blood loss and enhancing hemodynamic stability (17,30). Techniques such as polyvinyl alcohol particle or N-butyl cyanoacrylate glue embolization of the meningeal branches beneath the foramen spinosum or sphenopalatine branches provide precise, targeted occlusion at the hemorrhage source, effectively halting active bleeding. Additionally, in cases of traumatic pseudoaneurysms causing persistent bleeding from major arteries, such as the vertebral artery and the posterior inferior cerebellar artery, endovascular coiling offers a minimally invasive approach that not only ensures rapid hemorrhage control but also preserves the integrity of the surrounding vasculature (20). This direct endovascular approach mitigates the risk of hemorrhagic shock and minimizes the need for secondary surgical intervention, thereby ensuring effective hemorrhage control in complex neurotrauma.

Beyond hemostasis, the HOR setup facilitates the real-time identification and management of major vessel injuries, including dissection of the carotid or vertebral artery and dural sinus tears (15,16). These neurovascular complications, often difficult to address using conventional open surgical techniques alone, can be effectively managed within the hybrid environment through a synergistic approach that integrates endovascular and microsurgical interventions (6,31). The immediate availability of endovascular modalities within the HOR facilitates rapid and efficient interventions for complex neurovascular injuries, minimizing morbidity, optimizing surgical outcomes, and enhancing long-term prognoses in patients with sTBI (17,31).

Despite the promising results of the present study, a few limitations must be acknowledged. First, this was a single-center retrospective analysis, which limits the generalizability of our findings to broader populations. Although our results suggest that the HOR approach improves workflow efficiency and clinical outcomes, larger multicenter prospective studies are necessary to validate these findings across diverse institutional settings. Second, although intraoperative Xper-CT demonstrated significant advantages in real-time decision making, its resolution remains inferior to that of standard multidetector CT scanners. Consequently, small-volume hemorrhages or subtle ischemic changes may be underrecognized, potentially influencing postoperative management strategies. Third, this study focused on patients with sTBI, and the findings may not be directly applicable to mild-to-moderate TBI cases, which may require different treatment approaches. Additionally, our cohort included a relatively small sample size, which may have limited the statistical power of our outcome assessments, particularly in evaluating long-term neurological recovery. Fourth, although the HOR facilitates the integration of neurosurgical and neurointerventional techniques, it requires significant institutional investment and multidisciplinary coordination which may not be feasible in resource-limited settings. The availability of clinical staff trained in neurointerventions, dedicated hybrid surgical teams, and the financial burden of maintaining an advanced HOR infrastructure must be carefully considered when adopting this model in clinical practice.

CONCLUSION

The integration of the HOR in the management of sTBI represents a significant advancement in neurotrauma care, offering a unified platform that combines real-time imaging, neurointervention, and surgical treatment. By optimizing procedural workflows and minimizing treatment delays, the HOR approach enhances surgical precision and facilitates immediate intraoperative decision making, which may improve patient outcomes. As neurosurgical technology continues to evolve, a hybrid approach is likely to become an essential component of neurotrauma management, particularly in complex cases requiring rapid multidisciplinary intervention. However, further large-scale multicenter studies are required to validate the long-term efficacy of this approach, optimize patient selection criteria, and refine standardized protocols for broader implementation in emergency neurosurgical care.

Declarations

Funding: This work was supported by the Kangdong Sacred Heart Hospital Fund (grant no. 2025-04).

Availability of data and materials: The datasets generated and/or analyzed during the current study are available from the corresponding author by reasonable request.

Disclosure: The authors declare no competing interests.

AUTHORSHIP CONTRIBUTION

Study conception and design: HSA, HJJ, SHP
Data collection: HSA, HJJ
Analysis and interpretation of results: HSA, BMC
Draft manuscript preparation: HSA, HJJ, SHP
Critical revision of the article: HSA, HJJ
All authors (HSA, BMC, HJJ, SHP) reviewed the results and approved the final version of the manuscript.

REFERENCES

1. Adatia K, Newcombe VFJ, Menon DK: Contusion progression following traumatic brain injury: A review of clinical and radiological predictors, and influence on outcome. Neurocrit Care 34:312-324, 2021. https://doi.org/10.1007/s12028-020-00994-4
2. Braman SS, Dunn SM, Amico CA, Millman RP: Complications of intrahospital transport in critically ill patients. Ann Intern Med 107:469-473, 1987. https://doi.org/10.7326/0003-4819-107-4-469
3. Bromberg WJ, Collier BC, Diebel LN, Dwyer KM, Holevar MR, Jacobs DG, Kurek SJ, Schreiber MA, Shapiro ML, Vogel TR: Blunt cerebrovascular injury practice management guidelines: The Eastern Association for the Surgery of Trauma. J Trauma 68: 471-477, 2010. https://doi.org/10.1097/TA.0b013e3181cb43da
4. Bumberger A, Braunsteiner T, Leitgeb J, Haider T: Intracranial pressure monitoring following traumatic brain injury: Evaluation of indications, complications, and significance of follow-up imaging-an exploratory, retrospective study of consecutive patients at a level I trauma center. Eur J Trauma Emerg Surg 48:863-870, 2022. https://doi.org/10.1007/s00068-020-01570-3
5. Chen KT, Lee ST, Wu CT: The clinical value of intraoperative mobile computed tomography in managing high-risk surgical patients with traumatic brain injury-a single tertiary trauma center experience. World Neurosurg 98:727-733, 2017. https://doi.org/10.1016/j.wneu.2016.11.090
6. Das AS, Vicenty-Padilla JC, Chua MMJ, Jeelani Y, Snider SB, Regenhardt RW, Al-Mufti F, Du R, Izzy S: Cerebrovascular injuries in traumatic brain injury. Clin Neurol Neurosurg 223: 107479, 2022. https://doi.org/10.1016/j.clineuro.2022.107479
7. Dixon KJ: Pathophysiology of traumatic brain injury. Phys Med Rehabil Clin N Am 28:215-225, 2017. https://doi.org/10.1016/j.pmr.2016.12.001
8. Drevets P, Chung JM, Schampaert S, Schroeder C: Hybrid operating room: One-stop-shop for diagnosis, staging, and treatment. Innovations 14:463-467, 2019. https://doi.org/10.1177/1556984519863800
9. Flint AC, Manley GT, Gean AD, Hemphill JC 3rd, Rosenthal G: Post-operative expansion of hemorrhagic contusions after unilateral decompressive hemicraniectomy in severe traumatic brain injury. J Neurotrauma 25:503-512, 2008. https://doi.org/10.1089/neu.2007.0442
10. Gautschi OP, Smoll NR, Kotowski M, Schatlo B, Tosic M, Stimec B, Fasel J, Schaller K, Bijlenga P: Non-assisted versus neuro-navigated and XperCT-guided external ventricular catheter placement: A comparative cadaver study. Acta Neurochir 156:777-785, 2014. https://doi.org/10.1007/s00701-014-2026-8
11. Ghajar J: Traumatic brain injury. Lancet 356:923-929, 2000. https://doi.org/10.1016/S0140-6736(00)02689-1
12. Gupta S, Khajanchi M, Kumar V, Raykar NP, Alkire BC, Roy N, Park KB: Third delay in traumatic brain injury: Time to management as a predictor of mortality. J Neurosurg 132: 289-295, 2020. https://doi.org/10.3171/2018.8.JNS182182
13. He J, Chen J, Wu T, Zhang C, Yang L, Shi ZH, Wang YH: The value of managing severe traumatic brain injury during the perioperative period using intracranial pressure monitoring. J Craniofac Surg 30: 2217-2223, 2019. https://doi.org/10.1097/SCS.0000000000005861
14. Hemphill JC 3rd, Gress DR, Halbach VV: Endovascular therapy of traumatic injuries of the intracranial cerebral arteries. Crit Care Clin 15:811-829, 1999. https://doi.org/10.1016/s0749-0704(05)70089-0
15. Jin H, Liu J: Application of the hybrid operating room in surgery: A systematic review. J Invest Surg 35:378-389, 2022. https://doi.org/10.1080/08941939.2020.1838004
16. Jin H, Lu LG, Liu JW, Cui M: A systematic review on the application of the hybrid operating room in surgery: Experiences and challenges. Updates Surg 74:403-415, 2022. https://doi.org/10.1007/s13304-021-00989-6
17. Kim DH, Lee JY, Jeon HJ, Cho BM, Park SH, Oh SM: Intraoperative endovascular embolization of middle meningeal artery and a pseudoaneurysm by using N-butyl 2-cyanoacrylate for hemostasis during operation of acute epidural hemorrhage. Korean J Neurotrauma 11:167-169, 2015. https://doi.org/10.13004/kjnt.2015.11.2.167
18. Knight PH, Maheshwari N, Hussain J, Scholl M, Hughes M, Papadimos TJ, Guo WA, Cipolla J, Stawicki SP, Latchana N: Complications during intrahospital transport of critically ill patients: Focus on risk identification and prevention. Int J Crit Illn Inj Sci 5:256-264, 2015. https://doi.org/10.4103/2229-5151.170840
19. Lahner D, Nikolic A, Marhofer P, Koinig H, Germann P, Weinstabl C, Krenn CG: Incidence of complications in intrahospital transport of critically ill patients--experience in an Austrian university hospital. Wien Klin Wochenschr 119:412-416, 2007. https://doi.org/10.1007/s00508-007-0813-4
20. Larson PS, Reisner A, Morassutti DJ, Abdulhadi B, Harpring JE: Traumatic intracranial aneurysms. Neurosurg Focus 8:e4, 2000. https://doi.org/10.3171/foc.2000.8.1.1829
21. Leng S, Li W, Cai Y, Zhang Y: The endovascular treatment strategies of cerebrovascular injuries in traumatic brain injury. Chin J Traumatol 28:81-90, 2025. https://doi.org/10.1016/j.cjtee.2025.01.001
22. Loftus TJ, Croft CA, Rosenthal MD, Mohr AM, Efron PA, Moore FA, Upchurch GR Jr, Smith RS: Clinical impact of a dedicated trauma hybrid operating room. J Am Coll Surg 232:560-570, 2021. https://doi.org/10.1016/j.jamcollsurg.2020.11.008

23. Lovell MA, Mudaliar MY, Klineberg PL: Intrahospital transport of critically ill patients: Complications and difficulties. Anaesth Intensive Care 29:400-405, 2001. https://doi.org/10.1177/0310057X0102900412
24. McMillan TM, Teasdale GM, Stewart E: Disability in young people and adults after head injury: 12-14 year follow-up of a prospective cohort. J Neurol Neurosurg Psychiatry 83:1086-1091, 2012. https://doi.org/10.1136/jnnp-2012-302746
25. Meyfroidt G, Bouzat P, Casaer MP, Chesnut R, Hamada SR, Helbok R, Hutchinson P, Maas AIR, Manley G, Menon DK, Newcombe VFJ, Oddo M, Robba C, Shutter L, Smith M, Steyerberg EW, Stocchetti N, Taccone FS, Wilson L, Zanier ER, Citerio G: Management of moderate to severe traumatic brain injury: An update for the intensivist. Intensive Care Med 48:649-666, 2022. https://doi.org/10.1007/s00134-022-06702-4
26. Miller PR, Fabian TC, Bee TK, Timmons S, Chamsuddin A, Finkle R, Croce MA: Blunt cerebrovascular injuries: Diagnosis and treatment. J Trauma 51:279-285, 2001. https://doi.org/10.1097/00005373-200108000-00009
27. Mohamadpour M, Whitney K, Bergold PJ: The importance of therapeutic time window in the treatment of traumatic brain injury. Front Neurosci 13:07, 2019. https://doi.org/10.3389/fnins.2019.00007
28. Mostert CQB, Singh RD, Gerritsen M, Kompanje EJO, Ribbers GM, Peul WC, van Dijck JTJM: Long-term outcome after severe traumatic brain injury: A systematic literature review. Acta Neurochir 164:599-613, 2022. https://doi.org/10.1007/s00701-021-05086-6
29. Nasi D, di Somma L, Gladi M, Moriconi E, Scerrati M, Iacoangeli M, Dobran M: New or blossoming hemorrhagic contusions after decompressive craniectomy in traumatic brain injury: Analysis of risk factors. Front Neurol 9:11862019, 2019. https://doi.org/10.3389/fneur.2018.01186
30. Nazari P, Kasliwal MK, Wewel JT, Dua SG, Chen M: Delayed intracerebral hemorrhage from a pseudoaneurysm following a depressed skull fracture. Neurointervention 11:42-45, 2016. https://doi.org/10.5469/neuroint.2016.11.1.42
31. Patel J, Huynh TJ, Rao D, Brzezicki G: Vascular trauma in the head and neck and endovascular neurointerventional management. J Clin Imaging Sci 10:44, 2020. https://doi.org/10.25259/JCIS_96_2020
32. Rutman AM, Vranic JE, Mossa-Basha M: Imaging and management of blunt cerebrovascular injury. Radiographics 38:542-563, 2018. https://doi.org/10.1148/rg.2018170140
33. Schellenberg M, Benjamin E, Owattanapanich N, Inaba K, Demetriades D: The impact of delayed time to first CT head in traumatic brain injury. Eur J Trauma Emerg Surg 47:1511-1516, 2021. https://doi.org/10.1007/s00068-020-01421-1
34. Stocchetti N, Picetti E, Berardino M, Buki A, Chesnut RM, Fountas KN, Horn P, Hutchinson PJ, Iaccarino C, Kolias AG, Koskinen LO, Latronico N, Maas AI, Payen JF, Rosenthal G, Sahuquillo J, Signoretti S, Soustiel JF, Servadei F: Clinical applications of intracranial pressure monitoring in traumatic brain injury: Report of the Milan consensus conference. Acta Neurochir 156:1615-1622, 2014. https://doi.org/10.1007/s00701-014-2127-4
35. Teasdale G, Jennett B: Assessment of coma and impaired consciousness: A practical scale. Lancet 2:81-84, 1974. https://doi.org/10.1016/s0140-6736(74)91639-0
36. Thornhill S, Teasdale GM, Murray GD, McEwen J, Roy CW, Penny KI: Disability in young people and adults one year after head injury: Prospective cohort study. BMJ 320:1631-1635, 2000. https://doi.org/10.1136/bmj.320.7250.1631
37. Wan X, Fan T, Wang S, Zhang S, Liu S, Yang H, Shu K, Lei T: Progressive hemorrhagic injury in patients with traumatic intracerebral hemorrhage: Characteristics, risk factors and impact on management. Acta Neurochir 159:227-235, 2017. https://doi.org/10.1007/s00701-016-3043-6
38. Yuan Z, Wang Q, Sun Q, Li C, Xiong F, Li Z: Hypertensive intracerebral hemorrhage: Which one should we choose between laser navigation and 3D navigation mold? Front Surg 10:1040469, 2023. https://doi.org/10.3389/fsurg.2023.1040469
39. Zhao H, Zhang T, Li M, Gao Y, Wang S, Jiang R, Li Z: Three-dimensional laser combined with C-arm computed tomography-assisted puncture of intracerebral hemorrhage. Front Endocrinol 14:1198564, 2023. https://doi.org/10.3389/fendo.2023.1198564
40. Zhao HX, Liao Y, Xu D, Wang QP, Gan Q, You C, Yang CH: The value of intraoperative intracranial pressure monitoring for predicting re-operation using salvage decompressive craniectomy after craniotomy in patients with traumatic mass lesions. BMC Surg 15:111, 2015. https://doi.org/10.1186/s12893-015-0100-7

Turk Neurosurg 36(1):16-24, 2026
DOI: 10.5137/1019-5149.JTN.48436-25.3

Original Investigation
Neurotrauma

Received: 09.01.2025
Accepted: 03.05.2025
Published Online: 16.01.2026

Preventive Effects of Melatonin Against Post-Traumatic Contusional Expansion in Rats

Mehmet Arif ALADAG[1], Cengiz GOLCEK[2], Ramazan PASAHAN[1], Harika GOZUKARA[3]

[1]Inonu University Faculty of Medicine, Turgut Ozal Medical Center, Department of Neurosurgery, Malatya, Türkiye
[2]Pursaklar State Hospital, Department of Neurosurgery, Ankara, Türkiye
[3]Inonu University Faculty of Medicine, Department of Biostatistics, Malatya, Türkiye

Corresponding author: Mehmet Arif ALADAG ✉ marifaladag@hotmail.com

ABSTRACT

AIM: To provide insight into the molecular mechanism of contusional expansion (CE) by creating experimentally induced contusion cerebri (CC) in rats and investigating whether melatonin administration prevents CE or not.

MATERIAL and METHODS: Rats were randomized into four groups: Group 1 (control, n=5), group 2 (trauma, n=25), group 3 (trauma plus placebo, n=25), and, group 4 (trauma plus melatonin, n=25). Rats in the control group were sacrificed without undergoing any invasive procedure. Groups 2, 3, and 4 were further divided into 5 subgroups (A–E), with animals in each sacrificed at 12, 24, 72, 120, and 168 h after CC induction. Samples from these subgroups were analyzed for levels of caspase 3, caspase 8, and matrix metalloproteinase-9, as well as for evidence of ischemia, blood-brain barrier (BBB) breakdown, vasogenic edema (VE), and hemorrhage. Temporal progression of CE and correlations between these variables were also investigated.

RESULTS: Our results indicated that the ischemia, BBB breakdown, and VE are early events that initiate CE, with VE and hemorrhagic transformation due to BBB breakdown identified as key factors. Melatonin treatment prevented CE injury.

CONCLUSION: Melatonin, a safe and well-tolerated substance with minimal toxicity, may serve as a potential therapeutic agent for preventing CE injury.

KEYWORDS: Melatonin, Blood-brain barrier, Contusional expansion, Matrix metalloproteinase-9, Caspases

INTRODUCTION

Contusional expansion (CE) is a significant cause of secondary injury and subsequent clinical deterioration (28). Studies have indicated that the progression of cerebral contusions occurs in approximately half of patients (25). Among the early pathological changes in CE, the breakdown of the blood-brain barrier (BBB) is considered a key event. Studies have suggested that increased BBB permeability leads to vasogenic edema (VE) and ultimately hemorrhagic transformation, both of which represent important stages in CE development (11,14).

Several studies have posited that impact injuries to the cortex result in mechanical injury tears and disrupt the brain parenchyma and blood vessels, resulting in a primary injury. This mechanical injury often leads to the structural failure of microvessels. The ensuing ischemia, driven by microvascular dysfunction and primary brain parenchymal damage, can trigger several pathways, including activating apoptotic effectors such as caspase 3 (C3), caspase 8 (C8), and the proteolytic enzyme matrix metalloproteinase-9 (PP9). These processes contribute to two pathological outcomes. First, they result in more BBB disruption. Second, they result in increased VE, accompanied by hemorrhagic progression in the contusion area. Together, these factors drive the growth of the primary lesion, otherwise known as CE (2,3,8,9,10).

Mehmet Arif ALADAG : 0000-0003-3872-3741
Cengiz GOLCEK : 0000-0002-1969-9080
Ramazan PASAHAN : 0000-0002-3221-1422
Harika GOZUKARA : 0000-0003-1208-4072

The pathophysiology of CE injury is a complex process, and research has been unable to elucidate the underlying molecular mechanisms (10). Contemporary therapeutic interventions for CE are predominantly focused on reducing the intracranial hypertension associated with CE and are not focused on its prevention. This limits their clinical utility (12,14,16,25).

Melatonin has demonstrated the ability to cross morphophysiological barriers such as the BBB. It is considered safe, even at higher concentrations, and is well-tolerated by humans with minimal toxicity. As a multifunctional molecule, melatonin may be a useful therapeutic agent for the treatment of central nervous system injuries (20,26,27). Melatonin has also been reported to attenuate cerebral edema in a controlled cortical impact mouse model by inhibiting MMP9 (26), and reducing apoptotic cell death via C3 suppression in a rat subarachnoid hemorrhage model (4). Other studies have shown that melatonin inhibits MMP9 activity, subsequently decreasing the risk of hemorrhagic transformation following cerebral ischemia-reperfusion and traumatic spinal cord injury (13).

Given these previous findings, the present study was designed with two primary objectives. First, to evaluate the molecular pathophysiology underlying the hemorrhagic transformation associated with CE, and second, to investigate the effect of melatonin on this process.

MATERIAL and METHODS

This study was carried out in the Experimental Research Laboratory of the Inonu University Faculty of Medicine, complying with the approval of the ethic committee and the guidelines for care and use of experimental animals (2015/A-51). All applicable international, national, and/or institutional guidelines for the care and use of animals were followed.

The experiments were performed on 15-week-old 80 Wistar albino female rats, weighing between 200–250 g. The animals were kept under standard conditions, including a 12 hours (h) light/dark cycle, a constant ambient temperature of 20 °C, and humidity maintained between 40–60%. The rats had free access to standard dry pellets and tap water throughout the study. Rats were randomly divided into four groups: Group 1 (control, n=5), group 2 (trauma, n=25), group 3 (trauma plus placebo, n=25), and, group 4 (trauma plus melatonin, n=25). All rats were fasted one day before surgery and pre-treated with enrofloxacin (2.27 mg/kg subcutaneously, Bayer, Germany). The rats were anesthetized with ketamine hydrochloride (50 mg/kg) and xylazine (10 mg/kg) before surgery. All rats were placed on a heated surgical table to maintain a body temperature of 37°C. Supplemental doses of ketamine were provided as needed to maintain anesthesia.

The control group were sacrificed without undergoing any surgical procedure. The rats in groups 2, 3, and 4 underwent a standardized surgical procedure. The surgical area was shaved and cleaned antiseptically. A midline longitudinal incision was made on the scalp, and the underlying periosteum and muscles were dissected to expose the skull. A craniotomy (10 mm x 15 mm) was performed over the right parietal bone using a dental drill. To create the brain injury, the weight drop technique modified by Feeney et al. was used (7). A 9 g weight was dropped from a height of 50 cm onto a 10 mm diameter piston resting on the exposed dura, delivering an impact force of 450 g/cm.

To explore the temporal profile of the data, rats in groups 2, 3, and 4 were further divided into 5 subgroups (A–E), each comprising 5 rats. The subgroups were sacrificed at specific time points after injury: Subgroup A was sacrificed at 12 h, subgroup B was sacrificed after 24 h, subgroup C was sacrificed after 72 h, subgroup D was sacrificed after 120 h, and subgroup E was sacrificed after 168 h. Six hours after the procedure, intraperitoneal administration of 1 ml 2.5% alcohol or melatonin (purchased from Sigma; 20 mg/kg/day in 1 ml of 2.5% alcohol solution, warmed to 37 °C) was initiated in groups 3 and 4, respectively. Group 2, the trauma group, received no medication. Intraperitoneal melatonin or alcohol injections were continued until the time of sacrifice.

At the end of the specified period for each subgroup, the animals were re-anesthetized, and the ascending aorta was cannulated retrogradely through a thoracotomy. The craniocervical circulation was perfused with 200 ml of heparinized isosmotic phosphate buffer saline (0.1M, pH 7.4) at a physiological mean arterial pressure (80–90mmHg) using a peristaltic pump (May=PRS9508=991129-1). This was followed by perfusion with 200 ml of 0.1M phosphate buffer saline containing 4% paraformaldehyde. Brains were removed and the right and left hemispheres were separated. The right hemispheres, which contained the contusion epicenter, were post-fixed in 4% formalin and processed for paraffin embedding. Representative sections were sliced into 5 µm thick sections. A series of adjacent sections were used so that multiple histological and immunological markers could be examined in individual animals. The sections were also stained with hematoxylin-eosin (H&E) to enable evaluation of the degree of BBB breakdown, VE, and hemorrhage. For immunohistochemistry evaluation, immediately adjacent sections were processed simultaneously and stained with antibodies against C3, C8, and MMP9 (Abcam, polyclonal antibody for rats). These slides were then assessed by a neuropathologist. The number of positively stained cells was counted in 10 different sites, and the mean value was recorded.

VE results from dysfunction in the BBB. Both conditions are characterized by the movement of intravascular contents from the vasculature into the extracellular space and by the enlargement of the extracellular spaces (6). Therefore, we assessed both BBB breakdown and VE by measuring the extent of extracellular space enlargement, recorded as VE. A neuropathologist, blinded to group assignments, evaluated the edema on H&E-stained slides using a light microscope (Olympus, BX50, Tokyo, Japan). If the enlargement was minimal, VE was classified as grade 1. If the enlargement was moderate, VE was classified as grade 2. If the enlargement was severe, VE was classified as grade 3

The H&E-stained slides were assessed by a neuropathologist to evaluate the extent of hemorrhage and ischemia using a light microscope (Olympus, BX50, Tokyo, Japan). If the hemorrhage involved less than one-third of the high-power

field (HPF; x40 objectives), it was classified as grade 1. If hemorrhage involved between one-third to two-thirds of the HPF, it was classified as grade 2. If the hemorrhage involved over two-thirds of the HPF, it was classified as grade 3. To determine the extent of ischemia, the number of red neurons, which are typically observed in early ischemic damage, were used. Quantification of neuronal damage was performed by counting the number of pink acidophilic dead neurons (red neurons), following the method described by Kaku et al. (18). Red neurons were counted in 10 different HPFs (x40 objective) and the average number was calculated. If the number of red neurons was between 1–3, the degree of ischemia was classified as grade 1. If the number of red neurons was between 3–5, the degree of ischemia was classified as grade 2. If the number of red neurons was above 5, the degree of ischemia was classified as 3.

Statistical Analysis

The data from the control group were considered as the baseline values for all parameters. Data normality was evaluated using the Shapiro-Wilk test. Data were summarized as median (minimum-maximum) values. Group comparisons were performed using the Kruskal-Wallis test. When significant differences were detected, pairwise comparisons were performed using the Conover test. Statistically different groups, based on these pairwise comparisons, were indicated by different superscripts. For intra-temporal comparisons, a, b, and c superscripts were used, while x and y superscripts were used for comparisons between groups at each time point. Relationships between the variables across time points were evaluated using Spearman's rank correlation coefficient. A two-sided significance level of 0.05 was used for all analyses.

RESULTS

The median number of C3-positive cells was 0 (range = 0–0) in the control group. In groups 2 (trauma) and 3 (trauma plus placebo), the median C3-positive cell counts were 8 (6–10) and 8 (6–10) at 12 h, 15 (11–18) and 13 (11–17) at 24 h, 15 (12–17) and 15 (11–17) at 72 h, 9 (6–9) and 8 (5–10) at 120 h and, 2 (1–5) and 2 (1–4) at 168 h, respectively. In both groups, C3 levels began to increase immediately after trauma, peaked between 24 and 72 h, and significantly decreased thereafter ($p<0.05$). Significant differences were observed across all time points within these groups. C3 levels were significantly elevated in these groups across all time points compared to the control group ($p<0.05$), with no significant difference between groups 2 and 3. In group 4 (trauma plus melatonin), the median C3-positive cell counts were 3 (1–5), 7 (6–8), 7 (6–8), 4 (1–5), and 2 (1–3) at 12, 24, 72, 120, and 168 hours, respectively. Although group 4 followed a similar temporal pattern to groups 2 and 3, C3 levels in group 4 were significantly lower than in groups 2 and 3 at all time points except 160 h ($p<0.05$; Figure 1).

The median number of C8-positive cells was 0 (0–0) in the control group. In groups 2 and 3, the median C8-positive cell counts were 9 (6–10) and 9 (8–10) at 12 h, 13 (11–16) and 15 (12–15) at 24 h, 9 (6–10) and 9 (7–9) at 72 h, 8 (7–10) and 8 (7–10) at 120 h, and 3 (2–5) and 3 (2–5) at 168 h, respectively. In these groups, C8 began to increase immediately after trauma and continued to significantly increase until peaking at 24 h ($p<0.05$). In contrast to C3 levels, the C8 levels began to decrease immediately after peaking and continued to decline significantly up to 72 h post-injection ($p<0.05$). From 72 to 120 h, the decline slowed and remained relatively stable, followed by a further significant decrease after 120 h ($p<0.05$). C8 levels were significantly increased in groups 2 and 3 at all time points compared to the control group ($p<0.05$). However, no significant difference was observed between groups 2 and 3. In group 4, the median C8-positive cell counts were 2 (1–5), 6 (6–8), 7 (6–7), 2 (1–5), and 1 (1–2) at 12, 24, 72, 120, and 168 hours, respectively. C8 levels in group 4 were significantly lower than those in groups 2 and 3 at all time points ($p<0.05$). However, in contrast to C3, C8 levels in group 4 did not show a similar temporal pattern to groups 2 and 3 (Figure 2).

The median number of MMP9-positive cells was 0 (0–0) in the control group. In groups 2 and 3, the median MMP9-positive cell counts were 8 (6–10) and 8 (7–10) at 12 h, 13 (12–16) and 14 (12–16) at 24 h, 15 (13–18) and 15 (13–17) at 72 h, 9 (8–10) and 9 (8–10) at 120 h, and 9 (8–10) and 8 (8–9) at 168 h, respectively. In both groups, MMP9 levels showed a similar pattern to C3 levels. They began to significantly

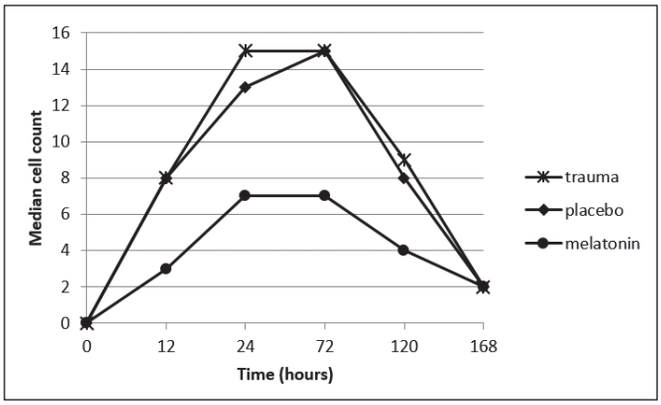

Figure 1: The temporal course of caspase 3 (C3) levels in the contusion areas.

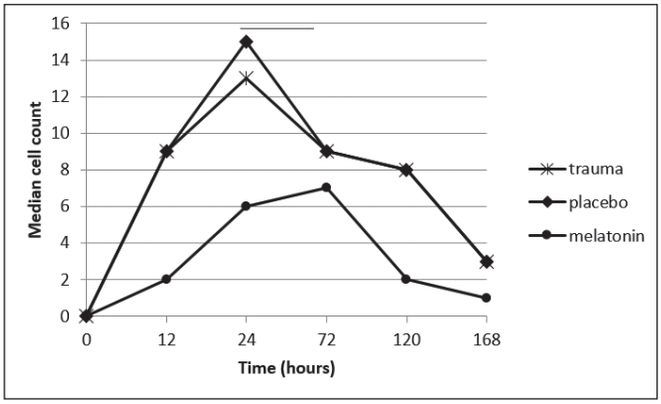

Figure 2: The temporal course of caspase 8 (C8) levels in the contusion areas.

increase immediately after trauma, peaking between 24 h and 72 h ($p<0.05$). A significant decline followed up to 120 h, after which levels remained stable. MMP9 levels were significantly increased in groups 2 and 3 at all time points compared to the control group ($p<0.05$), with no significant differences between groups 2 and 3. In group 4, the median MMP9-positive cell counts were 2 (1–3), 7 (6–8), 7 (6–8), 2 (1–3), and 2 (1–3) at 12, 24, 72, 120, and 168 hours, respectively. While there was no significant difference in MMP9 levels between 120 and 168 h, significant differences were observed between the other time points ($p<0.05$). MMP9 levels in group 4 were significantly lower compared to those in groups 2 and 3 at all time points ($p<0.05$; Figure 3).

The microscopic image of red neurons in the contusion area is shown in Figure 4. The median number of red neurons indicating ischemia was 0 (0–0) in the control group. In groups 2 and 3, the median red neuron counts were 10 (7–18) and 10 (8–17) at 12 h, 15 (5–18) and 14 (5–16) at 24 h, 15 (13–18) and 15 (14–17) at 72 h, 16 (14–18) and 15 (14–18) at 120 h, and 16 (14–17) and 16 (15–18) at 168 h, respectively. Ischemia levels were significantly higher in these groups compared to the control group at all time points ($p<0.05$); however, there was no significant difference between the groups at any time points. Ischemia levels started to increase immediately after trauma, showing an initial peak at 12 h and a second peak at 24 h ($p<0.05$). Following this, levels continued to increase more gradually. In group 4, the median red neuron counts were 6 (6–7), 5 (4–5), 7 (6–8), 7 (6–8), and 6 (5–8) at 12, 24, 72, 120, and 168 hours, respectively. Ischemia levels were significantly lower in group 4 compared to groups 2 and 3 at all time points ($p<0.05$; Figure 5).

Microscopic images of VE and red neurons in the contusion area are shown in Figure 4. The median grade of VE was 0 (0–0) in the control group. In groups 2 and 3, the median grades were 1 (0–2) and 1 (0–2) at 12 h, 1 (1–2) and 1 (1–2) at 24 h, 2 (1–2) and 2 (1–2) at 72 h, 1 (1–1) and 1 (1–1) at 120 h, and 1 (1–1) and 1 (1–1) at 168 h, respectively. In these groups, a significant increase in VE was observed at time points compared to the control group ($p<0.05$). However, there were no significant differences between groups 2 and 3. VE and BBB breakdown started to increase immediately after trauma, with an initial peak at 12 h. Their development then remained unchanged until 24 h, with a second peak then observed at 72 h. Following this, levels began to decrease until 120 h, at

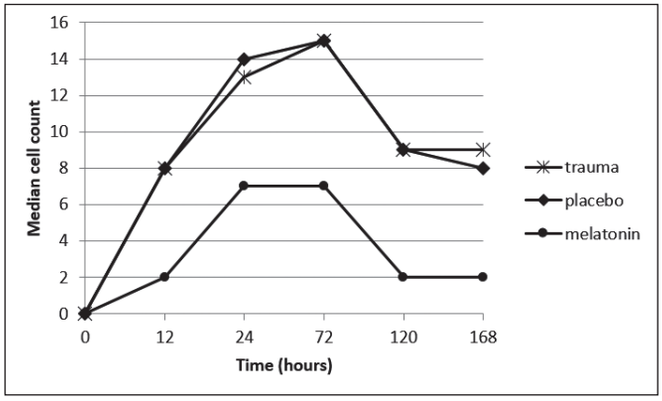

Figure 3: The temporal course of matrix metalloproteinase 9 (MMP9) levels in the contusion areas.

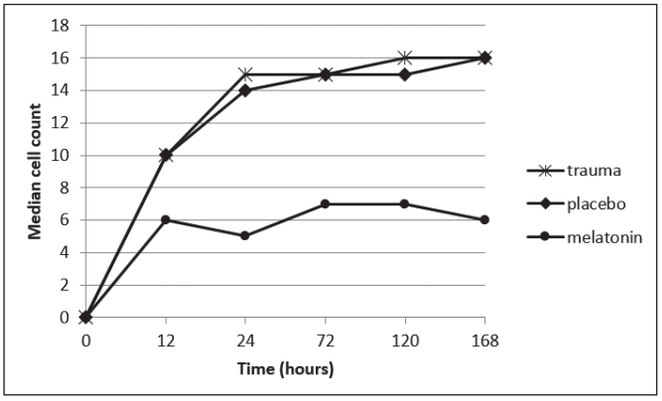

Figure 5: The temporal course of ischemia in the contusion areas.

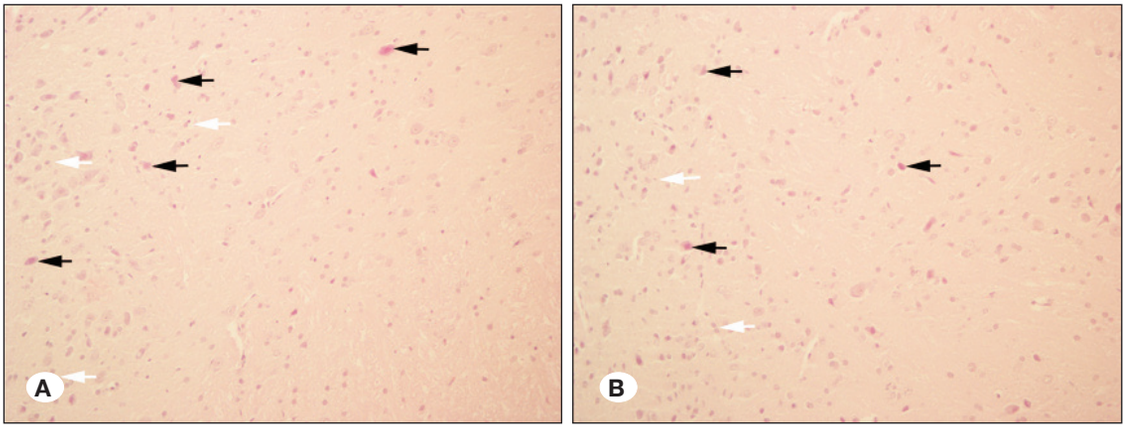

Figure 4: A microscopic image depicting ischemia, vasogenic edema (VE), and blood-brain barrier (BBB) breakdown, as well as red "ischemic" neurons in the contusion area. The enlargement of the extracellular spaces is a marker of VE. Red "ischemic" neurons are indicated by black arrows and glial proliferation by white arrows. **A)** Trauma group. **B)** Trauma plus melatonin group. Hematoxylin and Eosin, x90.

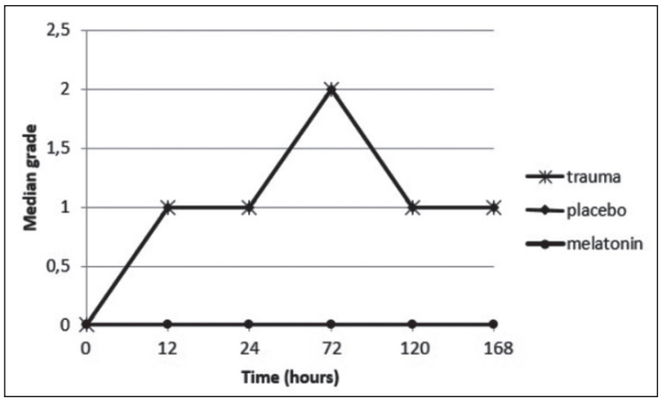

Figure 6: The temporal course of vasogenic edema (VE) in the contusion areas.

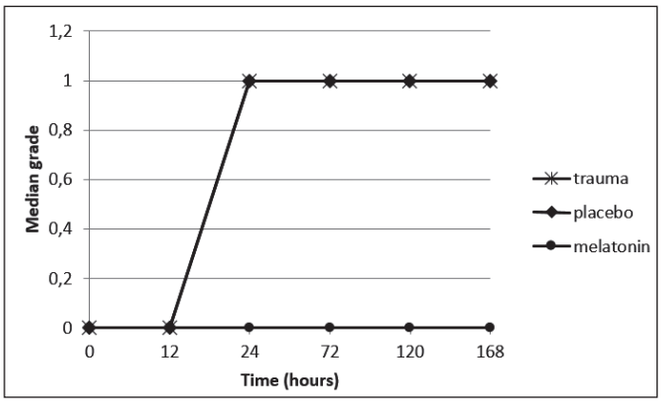

Figure 8: The temporal course of hemorrhagic transformation in the contusion areas.

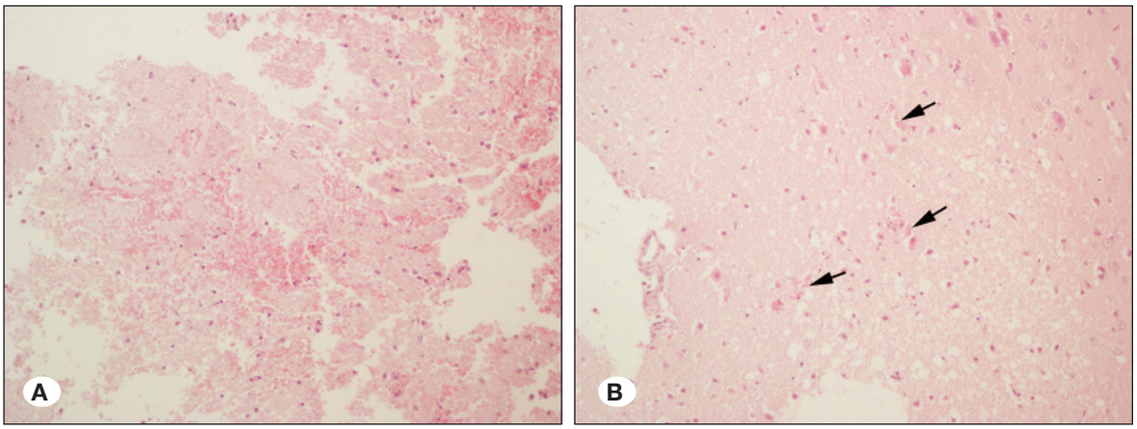

Figure 7: A microscopic image of hemorrhage in the contusion area. **A)** Trauma group; severe hemorrhage. Hematoxylin and Eosin, (HE), x10. **B)** Trauma plus melatonin group; minimal hemorrhage, "black arrows". HE, x90.

which point they remained stable. In group 4, the median VE grades were 0 (0–1), 0 (0–1), 0 (0–1), 0 (0–1), and 0 (0–1) at 12, 24, 72, 120, and 168 hours, respectively. Although there were no significant differences between time points within group 4, the levels of VE were markedly lower than in groups 2 and 3 across all time points (Figure 6).

Microscopic images of hemorrhage in the contusion area are shown in Figure 7. The median hemorrhage grade was 0 (0–0) in the control group. In groups 2 and 3, the median hemorrhage grades were 0 (0–1) and 0 (0–0) at 12 h, 1 (0–1) and 1 (0–1) at 24 h, 1 (1–2) and 1 (1–1) at 72 h, 1 (1–2) and 1 (1–2) at 120 h, and 1 (1–1) and 1 (1–1) at 168 h, respectively. No hemorrhagic progression was observed before 12 h in these groups. However, the level of hemorrhagic progression was significantly higher at 24, 72, 120, and 168 h in these groups compared to both the control group and 12 h subgroups ($p<0.05$). No significant difference was observed between groups 2 and 3. Hemorrhage levels started to increase 12 h after trauma, peaking at 24 h and then stabilizing. In group 4, the median hemorrhage grades were 0 (0–1), 0 (0–1), 0 (0–1), 0 (0–0), and 0 (0–0) at 12, 24, 72, 120, and 168 hours, respectively, indicating an absence of any substantial disparities among the subgroups in group 4. The level of hemorrhagic progression in group 4 was significantly lower than in groups 2 and 3 ($p<0.05$; Figure 8).

Table I illustrates the intercorrelations among parameters within specified time intervals. Between 0 h and 12 h, significant positive correlations were observed between levels of C3 and C8 (0.724, $p<0.001$), C3 and MMP9 (0.943, $p<0.001$), and C8 and MMP9 (0.702, $p<0.001$). Between 12 h and 24 h, positive correlations were observed between levels of C3 and ischemia (0.468, $p=0.009$), C8 and MMP9 (0.493, $p=0.006$), hemorrhage and VE (0.633, $p<0.001$), and hemorrhage and MMP9 (0.389, $p=0.034$). Between 24 h and 72 h, negative correlations were observed between levels of C3 and hemorrhage (–0.396, $p=0.030$) and C8 and MMP9 (–0.395, $p=0.031$), while positive correlations were observed between C3 and MMP9 (0.550, $p=0.002$), hemorrhage and VE (0.370, $p=0.044$), and VE and MMP9 (0.437, $p=0.016$). Between 72 h and 120 h, negative correlations were observed between C3 and C8 (–0.455, $p=0.012$), C3 and ischemia (–0.537, $p=0.002$), C8 and MMP9 (–0.544, $p=0.002$), C8 and VE (–0.469, $p=0.009$), and VE and ischemia (–0.509, $p=0.004$), while positive correlations were observed between C8 and ischemia (0.553, $p=0.002$) and hemorrhage and VE (0.399, $p=0.029$). Between 120 h and 168 h, positive correlations were observed between

Table I: The Correlations Among Parameters in Intervals at All Time

0 h – 12 h	**C 8**	**Hemorrhage**	**VE**	**Ischemia**	**MMP9**
C 3	**0.724 (p<0.001)**	0.058 (p=0.760)	0.001 (p=0.994)	-0.078 (p=0.683)	**0.943 (p<0.001)**
C 8	1.000	0.176 (p=0.352)	0.040 (p=0.837)	-0.196 (p=0.300)	**0.702 (p<0.001)**
Hemorrhage		1.000	0.056 (p=0.774)	-0.250 (p=0.183)	0.117 (p=0.537)
VE			1.000	0.056 (p=0.774)	0.161 (p=0.405)
Ischemia				1.000	-0.020 (p=0.918)
12 h – 24 h					
C 3	-0.290 (p=0.121)	0.020 (p=0.918)	-0.133 (p=0.484)	**0.468 (p=0.009)**	-0.099 (p=0.605)
C 8	1.000	0.161 (p=0.394)	0.010 (p=0.957)	-0.150 (p=0.429)	**0.493 (p=0.006)**
Hemorrhage		1.000	**0.633 (p<0.001)**	0.357 (p=0.053)	**0.389 (p=0.034)**
VE			1.000	0.105 (p=0.580)	-0.020 (p=0.918)
Ischemia				1.000	0.128 (p=0.499)
24 h – 72 h					
C 3	-0.042 (p=0.825)	**-0.396 (p=0.030)**	0.123 (p=0.518)	0.197 (p=0.296)	**0.550 (p=0.002)**
C 8	1.000	-0.315 (p=0.090)	-0.114 (p=0.547)	-0.016 (p=0.934)	**-0.395 (p=0.031)**
Hemorrhage		1.000	**0.370 (p=0.044)**	-0.289 (p=0.121)	0.002 (p=0.993)
V E			1.000	-0.068 (p=0.721)	**0.437 (p=0.016)**
Ischemia				1.000	-0.066 (p=0.730)
72 h – 120 h					
C 3	**-0.455 (p=0.012)**	-0.301 (p=0.106)	0.184 (p=0.330)	**-0.537 (p=0.002)**	-0.002 (p=0.992)
C 8	1.000	-0.174 (p=0.357)	**-0.469 (p=0.009)**	**0.553 (p=0.002)**	**-0.544 (p=0.002)**
Hemorrhage		1.000	**0.399 (p=0.029)**	-0.057 (p=0.763)	0.302 (p=0.105)
V E			1.000	**-0.509 (p=0.004)**	0.303 (p=0.104)
Ischemia				1.000	-0.148 (p=0.435)
120 h – 168 h					
C3	0.314 (p=0.092)	0.229 (p=0.223)	0.256 (p=0.172)	**0.438 (p=0.015)**	-0.062 (p=0.745)
C8	1.000	**0.390 (p=0.033)**	-0.278 (p=0.137)	**0.441 (p=0.015)**	-0.343 (p=0.063)
Hemorrhage		1.000	0.000 (p=1.000)	**0.447 (p=0.013)**	-0.174 (p=0.359)
VE			1.000	0.000 (p=1.000)	0.000 (p=1.000)
Ischemia				1.000	0.342 (p=0.065)

C3: *Caspase3,* ***C8:*** *Caspase8,* ***MMP9:*** *Matrix metalloproteinase-9,* ***VE:*** *Vasogenic edema and blood-brain barrier breakdown,* ***h:*** *Hour.*

C3 and ischemia (0.438, p=0.015), C8 and hemorrhage (0.390, p=0.033), C8 and ischemia (0.441, p=0.015), and hemorrhage and ischemia (0.447, p=0.013).

DISCUSSION

VE and hemorrhagic transformation are progressive processes and major causes of CE injury (12,14,18). Studies have indicated that VE formation begins immediately after trauma and typically peaks between 48 h and 72 h, while hemorrhagic progression most frequently occurs between the first 12 h and 24 h, peaking at 24 h (1,12,16,24,28). Our data indicated that no hemorrhagic progression occurred before 12 h post-injury, while VE, BBB breakdown, and ischemia levels began to increase immediately after trauma. Both VE and BBB breakdown levels initially peaked after 12 h, stabilized until 24 h, and had a second peak at 72 h. After this, they began to decrease until 120 h. The present findings lend further support

to previous studies, demonstrating that VE formation begins immediately following trauma and typically peaks between 48 h and 72 h, while hemorrhagic progression typically occurs between 12 h and 24 h, peaking at 24 h (1,12,16,24).

It is well established that the initial and most important contributors to BBB breakdown and ischemia after traumatic brain injury (TBI) are mechanical tears and shearing forces impacting the brain parenchyma and blood vessels (1,6,18,24). The initiation of BBB breakdown and subsequent ischemia triggers the activation of multiple pathways, including the activation of the apoptotic effectors C3 and C8 and the proteolytic enzyme MMP9. This results in further BBB disruption, subsequently increasing VE and promoting hematoma progression. This cascade leads to further expansion of the primary lesion (14,16,22,28).

Our study showed that C3, C8, and MMP9 levels increased alongside VE and BBB breakdown between 0 h and 12 h post-injury. Positive correlations were observed between levels of C3 and C8, C3 and MMP9, and C8 and MMP9 in this period. However, no significant correlations were observed between VE, ischemia, or hemorrhage, or between these factors and C3, C8, and MMP9 levels within the same interval. These findings indicate that C3, C8, and MMP9 are co-activated immediately after trauma and operate through interconnect pathways. These findings also support previous studies indicating that early edema, BBB breakdown, and ischemia following a TBI are direct consequences of mechanical tissue and vascular injury (14,16,22,28).

Our data indicated that between 12 h and 24 h post-injury, C3, C8, and MMP9, and ischemia levels continued to increase, while VE and BBB breakdown levels stabilized. This interval coincides with the onset and peak of hemorrhagic progression. Notably, correlations were observed between C3 and ischemia, C8 and MMP9, hemorrhagic progression and MMP9, hemorrhagic progression and VE, and hemorrhagic progression and BBB breakdown However, the correlation between hemorrhagic progression and MMP9 levels was lower than the correlation between hemorrhagic progression and VE and between C8 and MMP9.

These findings support those of previous studies, suggesting that apoptotic factors may contribute to microvascular disruption and exacerbate BBB damage as part of the secondary injury cascade (2,3,8,9,10,30). Furthermore, our findings highlight BBB breakdown and VE as central events driving hemorrhagic progression in CE. MMP9 likely plays a key role in initiating hemorrhagic transformation by increasing BBB breakdown and VE beyond a critical threshold level. This is presumably mediated by MMP9's capacity to degrade components of the basal lamina and disrupt tight junction proteins in both injured and intact vessels (23,29).

Our data demonstrated that between 24 h and 72 h, VE and MMP9 levels continued to rise, C8 levels started to decrease, and C3, ischemia, and hemorrhage levels remained unchanged. During this interval, negative correlations were observed between C3 and hemorrhagic progression and between C8 and MMP9, while positive correlations were observed between VE and hemorrhagic progression and VE and MMP9. These findings suggest that while MMP9 plays a critical role in exacerbating BBB breakdown and VE, other factors likely play additional roles in modulating these processes (10,14,22).

In the interval between 72 h and 120 h, C3, VE, and MMP9 levels started to decrease significantly, while the decline in C8 levels slowed until levels were near stable. Ischemia and hemorrhage levels also remained unchanged. Negative correlations were observed between C3 and C8, C3 and ischemia, C8 and edema, C8 and MMP9, and edema and ischemia. In contrast, positive correlations were observed between edema and hemorrhagic progression and C8 and ischemia. These findings suggest that endothelial apoptotic damage mediated by C8 persisted during this time. The positive correlation seen between C8 and ischemia may reflect the pro-inflammatory effects of C8 (19).

In the interval between 120 h and 168 h, C3 and C8 levels continued to decrease, ischemia levels continued to rise slowly, and MMP9, ischemia, VE, and hemorrhage levels remained unchanged. Positive correlations were observed between C3 and ischemia, C8 and hemorrhagic progression, C8 and ischemia, and between hemorrhagic progression and ischemia. These findings suggest that endothelial apoptotic damage continued to contribute to ischemia during this period. Additionally, hemorrhagic progression may have influenced ischemic progression, likely due to its mass effect (21).

In the current study, melatonin administration completely prevented VE and hemorrhagic transformation (i.e., CE) by reducing C3, C8, MMP9, and ischemia levels across all time points, except for 120 and 168 h post-injury in the case of MMP9. However, an incontinency was observed between the reduction rates of C3, C8, and MMP9 and those of VE and hemorrhagic progression, with C3, C8, and MMP9 levels decreasing partially but significantly, while VE and hemorrhagic progression levels decreased almost completely. This discrepancy may be explained by the involvement of additional pathways beyond C3, C8, and MMP9 in the development of CE, which melatonin may also inhibit (5,10,14,15,22).

In contrast to the near-complete reduction of VE and hemorrhage levels, melatonin administration only reduced ischemia levels partially, similar to its impact on C3, C8, and MMP9 levels. This may be attributed to continued primary vascular dysfunction (17). These findings support previous studies that suggested that the structural failure of microvessels caused by primary injuries triggers multiple pathways, ultimately leading to CE through increased VE and hemorrhagic progression in the primary lesion (2,3,8,9,10).

Taken together, the results of our study imply that:

1. CE is driven by a complex interplay of molecular, cellular, structural, and functional changes, including microcirculation dysfunction, ischemia, BBB breakdown, edema, and hemorrhage arising from both primary and secondary injuries.

2. BBB breakdown leads to VE and hemorrhagic transformation, which are key factors in CE development. VE formation begins immediately after trauma and follows a biphasic pattern (first peak at 12 h, second peak at 72 h), while hemorrhagic progression starts at 12 h and peaks at 24 h.
3. Ischemia, BBB breakdown, and VE are the initial changes that trigger CE. Hemorrhagic transformation occurs later once VE exceeds a certain threshold and is further promoted by MMP9, consequently exacerbating CE.
4. While C3, C8, and, in particular, MMP9 play key roles in CE pathogenesis, additional pathways are likely to contribute to its development.
5. Melatonin effectively prevented CE by inhibiting or modulating several key pathways involved in VE development and hemorrhagic transformation, supporting its potential use as a multifunctional therapeutic agent.

The current study has several limitations. First, we only investigated temporal changes in CE, not spatial changes. Second, we did not examine all potential factors or pathways that may influence CE. Further studies are needed to explore these potential factors and pathways, including their spatiotemporal distributions and interactions. Finally, BBB breakdown was assessed indirectly, with VE levels used as a surrogate marker.

CONCLUSION

The present study demonstrated that melatonin inhibits CE by preventing BBB breakdown and VE, which are key events that lead to hemorrhagic progression, and by ameliorating ischemia. These findings suggest that melatonin, a safe and well-tolerated molecule with minimum toxicity in humans, could be utilized as a potential therapeutic agent for CE prevention. However, further studies are required to validate this hypothesis.

Declarations

Funding: This study received financial support from The Scientific Research Projects Unit of Inonu University for financial support. (grant no:2015/81) The authors thank to Nusret Akpolat for his support in histopathological preparations and analysis, and to Hakan Parlakpinar for his support in the preparation of the article.

Availability of data and materials: The datasets generated and/or analyzed during the current study are available from the corresponding author by reasonable request.

Disclosure: The authors have no personal financial or institutional interests in any of the drugs, materials, or devices described in this article. The authors alone are responsible for the content and writing of the article. They declare no competing interests.

AUTHORSHIP CONTRIBUTION

Study conception and design: MAA, CG, RP
Data collection: MAA, CG, RP, HG
Analysis and interpretation of results: HG
Draft manuscript preparation: MAA
Critical revision of the article: MAA
Other (study supervision, fundings, materials, etc...): MAA, CG, RP, HG
All authors (MAA, CG, RP, HG) reviewed the results and approved the final version of the manuscript.

REFERENCES

1. Adatia K, Newcombe VFJ, Menon DK: Contusion progression following traumatic brain injury: A review of clinical and radiological predictors, and influence on outcome. Neurocrit Care 34:312-324, 2021. https://doi.org/10.1007/s12028-020-00994-4
2. Ahmadighadykolaei H, Lambert JA, Raeeszadeh-Sarmazdeh M: TIMP-1 protects tight junctions of brain endothelial cells from MMP-mediated degradation. Pharm Res 40:2121-2131, 2023. https://doi.org/10.1007/s11095-023-03593-y
3. Cash A, Theus MH: Mechanisms of blood–brain barrier dysfunction in traumatic brain injury. Int J Mol Sci 21:3344, 2020. https://doi.org/10.3390/ijms21093344
4. Chen J, Wang L, Wu C, Hu Q, Gu C, Yan F, Li J, Yan W, Chen G: Melatonin-enhanced autophagy protects against neural apoptosis via a mitochondrial pathway in early brain injury following a subarachnoid hemorrhage. J Pineal Res 56:12-19, 2014. https://doi.org/10.1111/jpi.12086
5. Dehghan F, Khaksari Hadad M, Asadikram G, Najafipour H, Shahrokhi N: Effect of melatonin on intracranial pressure and brain edema following traumatic brain injury: Role of oxidative stresses. Arch Med Res 44:251-258, 2013. https://doi.org/10.1016/j.arcmed.2013.04.002
6. Donkin JJ, Vink R: Mechanisms of cerebral edema in traumatic brain injury: Therapeutic developments. Curr Opin Neurol 23:293-299, 2010. https://doi.org/10.1097/WCO.0b013e328337f451.
7. Feeney DM, Boyeson MG, Linn RT, Murray HM, Dail WG: Responses to cortical injury: I. Methodology and local effects of contusions in the rat. Brain Res 211:67-77, 1981. https://doi.org/10.1016/0006-8993(81)90067-6
8. Gerzanich V, Kwon MS, Woo SK, Ivanov A, Simard JM: SUR1-TRPM4 channel activation and phasic secretion of MMP-9 induced by tPA in brain endothelial cells. PLoS One 13:e0195526. 2018. https://doi.org/10.1371/journal.pone.0195526
9. Glushakova OY, Glushakov AO, Borlongan CV, Valadka AB, Hayes RL, Glushakov AV: Role of caspase-3-mediated apoptosis in chronic caspase-3-cleaved tau accumulation and blood-brain barrier damage in the corpus callosum after traumatic brain injury in rats. J Neurotrauma 35:157-173, 2018. https://doi.org/10.1089/neu.2017.4999

10. Higashida T, Kreipke CW, Rafols JA, Peng C, Schafer S, Schafer P, Ding JY, Dornbos D 3rd, Li X, Guthikonda M, Rossi NF, Ding Y: The role of hypoxia-inducible factor-1α, aquaporin-4, and matrix metalloproteinase-9 in blood-brain barrier disruption and brain edema after traumatic brain injury. J Neurosurg 114: 92-101, 2011. https://doi.org/10.3171/2010.6.jns10207
11. Hu Y, Tao W: Microenvironmental variations after blood-brain barrier breakdown in traumatic brain injury. Front Mol Neurosci 14:750810, 2021. https://doi.org/10.3389/fnmol.2021.750810
12. Huang AP, Lee CW, Hsieh HJ, Yang CC, Tsai YH, Tsuang FY, Kuo LT, Chen YS, Tu YK, Huang SJ, Liu HM, Tsai JC: Early parenchymal contrast extravasation predicts subsequent hemorrhage progression, clinical deterioration, and need for surgery in patients with traumatic cerebral contusion. J Trauma 71:1593-1599, 2011. https://doi.org/10.1097/TA.0b013e31822c8865
13. Hung YC, Chen TY, Lee EJ, Chen WL, Huang SY, Lee WT, Lee MY, Chen HY, Wu TS: Melatonin decreases matrix metalloproteinase-9 activation and expression and attenuates reperfusion-induced hemorrhage following transient focal cerebral ischemia in rats. J Pineal Res 45:459-467, 2008. https://doi.org/10.1111/j.1600-079X.2008.00617.x
14. Jha RM, Kochanek PM, Simard JM: Pathophysiology and treatment of cerebral edema in traumatic brain injury. Neuropharmacology 145:230-246, 2019. https://doi.org/10.1016/j.neuropharm.2018.08.004
15. Jha RM, Simard JM: Glibenclamide for brain contusions: Contextualizing a promising clinical trial design that leverages an imaging-based TBI endotype. Neurotherapeutics 20:1472-1481, 2023. https://doi.org/10.1007/s13311-023-01389-x
16. Jirlow U, Hossain I, Korhonen O, Depreitere B, Rostami E: Cerebral contusions - Pathomechanism, predictive factors for progression and historical and current management. Brain Spine 4:103329, 2024. https://doi.org/10.1016/j.bas.2024.103329
17. Jullienne A, Obenaus A, Ichkova A, Savona-Baron C, Pearce WJ, Badaut J: Chronic cerebrovascular dysfunction after traumatic brain injury. J Neurosci Res 94:609-622, 2016. https://doi.org/10.1002/jnr.23732
18. Kaku Y, Yonekawa Y, Tsukahara T, Ogata N, Kimura T, Taniguchi T: Alterations of a 200 kDa neurofilament in the rat hippocampus after forebrain ischemia. J Cereb Blood Flow Metab 13:402-408, 1993 https://doi.org/10.1038/jcbfm.1993.54
19. Ke DQ, Chen ZY, Li ZL, Huang X, Liang H: Target inhibition of caspase-8 alleviates brain damage after subarachnoid hemorrhage. Neural Regen Res 15:1283-1289, 2020 https://doi.org/10.4103/1673-5374.272613
20. Kulsoom K, Ali W, Saba Z, Hussain S, Zahra S, Irshad M, Ramzan MS: Revealing melatonin's mysteries: Receptors, signaling pathways, and therapeutics applications. Horm Metab Res 56:405-418, 2024. https://doi.org/10.1055/a-2226-3971
21. Kurland D, Hong C, Aarabi B, Gerzanich V, Simard JM: Hemorrhagic progression of a contusion after traumatic brain injury: A review. J Neurotrauma 29:19-31, 2012. https://doi.org/10.1089/neu.2011.2122
22. Michinaga S, Inoue A, Yamamoto H, Ryu R, Inoue A, Mizuguchi H, Koyama Y: Endothelin receptor antagonists alleviate blood-brain barrier disruption and cerebral edema in a mouse model of traumatic brain injury: A comparison between bosentan and ambrisentan. Neuropharmacology 175:108182, 2020. https://doi.org/10.1016/j.neuropharm.2020.108182
23. Mrozek S, Delamarre L, Capilla F, Al-Saati T, Fourcade O, Constantin JM, Geeraerts T: Cerebral expression of glial fibrillary acidic protein, ubiquitin carboxy-terminal hydrolase-L1, and matrix metalloproteinase 9 after traumatic brain injury and secondary brain insults in rats. Biomark Insights 14:1177271919851515, 2019. https://doi.org/10.1177/1177271919851515
24. Oertel M, Kelly DF, McArthur D, Boscardin WJ, Glenn TC, Lee JH, Gravori T, Obukhov D, McBride DQ, Martin NA: Progressive hemorrhage after head trauma: Predictors and consequences of the evolving injury. J Neurosurg 96:109-116, 2002. https://doi.org/10.3171/jns.2002.96.1.0109
25. Pellot JE, De Jesus O: Cerebral Contusion. In: StatPearls [Internet]. Treasure Island (FL): StatPearls Publishing, 2025. PMID: 32965818. Available from: https://www.ncbi.nlm.nih.gov/books/NBK562147/
26. Robinson BD, Isbell CL, Anasooya Shaji C, Kurek S Jr, Regner JL, Tharakan B: Quetiapine protects the blood-brain barrier in traumatic brain injury. J Trauma Acute Care Surg 85:968-976, 2018. https://doi.org/10.1097/TA.0000000000002011
27. Seabra ML, Bignotto M, Pinto LR Jr, Tufik S: Randomized, double-blind clinical trial, controlled with placebo, of the toxicology of chronic melatonin treatment: J Pineal Res 29:193-200, 2000. https://doi.org/10.1034/j.1600-0633.2002.290401.x
28. Sheng J, Chen W, Zhuang D, Li T, Yang J, Cai S, Chen X, Liu X, Tian F, Huang M, Li L, Li K: A Clinical predictive nomogram for traumatic brain parenchyma hematoma progression. Neurol Ther 11:185-203, 2022. https://doi.org/10.1007/s40120-021-00306-8
29. Teng Z, Guo Z, Zhong J, Cheng C, Huang Z, Wu Y, Tang S, Luo C, Peng X, Wu H, Sun X, Jiang L: ApoE influences the blood-brain barrier through the NF-κB/MMP-9 pathway after traumatic brain injury. Sci Rep 7:6649, 2017. https://doi.org/10.1038/s41598-017-06932-3
30. Zhou C, Yamaguchi M, Kusaka G, Schonholz C, Nanda A, Zhang JH: Caspase inhibitors prevent endothelial apoptosis and cerebral vasospasm in dog model of experimental subarachnoid hemorrhage. J Cereb Blood Flow Metab 24:419-431, 2004. https://doi.org/10.1097/00004647-200404000-00007

Turk Neurosurg 36(1):25-33, 2026
DOI: 10.5137/1019-5149.JTN.49423-25.2

Original Investigation
Cerebrovascular-Endovascular

Received: 18.07.2025
Accepted: 08.10.2025
Published Online: 16.01.2026

Endovascular Treatment of Multiple Intracranial Aneurysms: A Multicenter Study from Türkiye on Morphology-Based Strategies and Clinical Outcomes

Levent AYDIN[1], Munibe Busra ERDEM[2], Caghan TONGE[2], Cagri ELBIR[2], Emrah KESKIN[3], Fatih YAKAR[4], Mehmet Erhan TURKOGLU[5]

[1]Medicana Beylikduzu International Hospital, Department of Neurosurgery, Istanbul, Türkiye
[2]Ankara Etlik City Hospital, Department of Neurosurgery, Ankara, Türkiye
[3]Zonguldak Bulent Ecevit University, School of Medicine, Department of Neurosurgery, Zonguldak, Türkiye
[4]Pamukkale University, School of Medicine, Department of Neurosurgery, Denizli, Türkiye
[5]Hacettepe University, School of Medicine, Department of Neurosurgery, Ankara, Türkiye

Corresponding author: Levent AYDIN ✉ mdleventaydin@gmail.com

ABSTRACT

AIM: To evaluate the role of recent endovascular techniques as less invasive alternatives in the management of multiple intracranial aneurysms, particularly in the context of heterogeneous aneurysm morphology and anatomical complexity.

MATERIAL and METHODS: This retrospective analysis included 65 patients with a total of 151 MIAs that were treated using endovascular approaches. Morphological parameters, anatomical location, and clinical features were evaluated. Treatment strategies included primary coiling, stent-assisted coiling, Y/X-stent coiling, flow diversion (with or without coiling), use of Woven EndoBridge devices, and parent artery occlusion. Patient outcomes were assessed radiologically (Raymond–Roy Occlusion Classification) and clinically (Modified Rankin Scale, Glasgow Outcome Scale).

RESULTS: Morphometric parameters significantly differed by aneurysm location. Flow diversion was preferred for wide-necked ınternal carotid artery aneurysms, while coiling was more commonly used for aneurysms at bifurcation sites. Complete occlusion (Class I) was achieved in 70.2% of the cases, while residual neck/sac (Classes II–IIIa) were observed in 29.8% of the cases. Incomplete occlusion was associated with higher aspect ratios and was more frequent in aneurysms in the anterior and posterior communicating arteries and at the middle cerebral artery bifurcation. The clinical outcomes were favorable, with median Modified Rankin Scale and Glasgow Outcome Scale scores of 0.5 and 5, respectively. The mortality rate was 12%, with a median follow-up of 8.5 months.

CONCLUSION: Endovascular therapy provides a safe and effective approach to treat MIAs. Aneurysm morphology, especially location and aspect ratio, significantly influences angiographic outcomes, supporting the need for individualized treatment plans.

KEYWORDS: Multiple intracranial aneurysm, Endovascular treatment, Aneurysm, Multicenter study

ABBREVIATIONS: Acom: Anterior communicating artery, **CT:** Computed tomography, **GCS:** Glasgow Coma Scale, **ICA:** Internal carotid artery, **MCA:** Middle cerebral artery, **MIA:** Multiple ıntracranial aneurysm, **Pcom:** Posterior communicating artery, **WFNS:** World Federation of Neurosurgical Societies

Levent AYDIN : 0000-0001-7015-4070
Munibe Busra ERDEM : 0000-0003-0373-8679
Caghan TONGE : 0000-0002-9921-1750
Cagri ELBIR : 0000-0002-8747-2187
Emrah KESKIN : 0000-0001-5326-741X
Fatih YAKAR : 0000-0001-7414-3766
Mehmet Erhan TURKOGLU : 0000-0001-7044-617X

INTRODUCTION

The management of multiple intracranial aneurysms (MIAs) is clinically complicated by heterogeneity in aneurysm size and location and the complexity of three-dimensional vasculature (12,19,26). Achieving precise anatomical orientation becomes particularly difficult in cases involving ruptured aneurysms. The disruption of natural arachnoid dissection planes further increases the complexity of microsurgical exposure and manipulation. When aneurysms are located in different vascular territories, simultaneous access through a single craniotomy may be unfeasible, often necessitating multiple surgical approaches and patient repositioning (10,19,21). While microsurgical clipping has traditionally been the standard treatment, it is often limited by anatomical constraints and increased perioperative morbidity in complex MIA cases.

Advances in endovascular techniques, such as stent-assisted coiling, flow-diverter stents, and intrasaccular devices, have significantly expanded the treatment horizons for MIAs. These minimally invasive approaches allow for single-session treatment of multiple lesions, reducing overall procedural burden and improving safety (7,22).

In this multicenter retrospective study, we analyzed patients with MIAs who underwent endovascular treatment over a 1-year period. We aimed to evaluate the contemporary role of endovascular management in MIAs, focusing on morphological predictors, treatment strategies, and clinical outcomes within an integrated neurovascular care framework.

MATERIAL and METHODS

Patients and Data Collection

This retrospective observational study included 65 patients diagnosed with a cumulative total of 151 MIAs. As an inclusion criterion, all patients underwent endovascular treatment, and the clinical, morphological, procedural, and outcome-related data were systematically analyzed to evaluate associations among aneurysm characteristics, treatment modalities, and clinical outcomes. Comorbidities included hypertension, diabetes mellitus, smoking, and other vascular risk factors.

Symptoms included headache, visual problems, seizure, vertigo, and paresthesia. Neurological grading was performed using the World Federation of Neurosurgical Societies (WFNS) scale and Glasgow Coma Scale (GCS). Pre-treatment cranial computed tomography (CT) findings were evaluated using the Fisher scale. Additionally, hemorrhage distribution in cranial cisterns was categorized into four groups: lamina terminalis, sylvian cistern, quadrigeminal cistern, and prepontine cistern. The presence of hydrocephalus was also assessed on initial CT scans.

For each treated cerebral aneurysm, the following information was documented: morphology (categorized as saccular, fusiform, dissecting, thrombosed); location (categorized as internal carotid artery [ICA] cervical, cavernous, clinoid, ophthalmic, communicating segment, posterior communicating artery [Pcom], ICA bifurcation, A1 segment, anterior communicating artery [Acom], A2 segment, M1 segment, middle cerebral artery [MCA] bifurcation, M2 segment, P1 segment, basilar tip, basilar trunk, superior cerebellar artery, anterior inferior cerebellar artery, posterior inferior cerebellar artery, and vertebral artery); neck width; dome-to-neck ratio; aspect ratio; and maximum diameter.

Endovascular treatment strategies included primary coiling, stent-assisted coiling, Y/X-stent coiling, flow-diverter stent (alone or combined with coiling), Woven EndoBridge devices, and parent artery occlusion. Procedural efficacy was radiologically stratified using Raymond–Roy Occlusion Classification and O'Kelly–Marotta grading. Clinical outcomes were evaluated using the Modified Rankin Scale and Glasgow Outcome Scale. Digital subtraction angiography was the primary modality for follow-up imaging at 3–6 months after treatment.

The study received approval from the ethics committee of Ankara Etlik City Hospital (Ethical ID: AEŞH BADEK1-2025-048).

Statistical Analysis

Statistical analyses were performed using parametric and non-parametric methods depending on the data distribution. Morphometric parameters across anatomical locations were compared using one-way analysis of variance. Categorical and ordinal data were compared using chi-square and Kruskal–Wallis tests, respectively. Relationships between parameters were quantified using Spearman's rho correlation. Longitudinal differences between parameters were analyzed using the Wilcoxon signed-rank test. All statistical analyses were performed using SPSS software for Windows, version 25.0, with the threshold of significance set at 0.05.

RESULTS

The mean patient age was 55.5 ± 15.3 years. Of the 65 enrolled patients, 37 were women and 28 men. Comorbidities included hypertension (45.3%), diabetes mellitus (15.6%), smoking (20.3%), and other vascular risk factors. At admission, 39.1% of the patients presented with subarachnoid hemorrhage, most frequently involving the distal Sylvian fissure (50.0%) and lamina terminalis (45.3%). Neurological grading was performed using the WFNS scale and GCS score. A majority of the patients (51.6%) were assessed to be in good clinical condition, with a WFNS grade of 1 and a GCS score of 15. Radiologic evaluation was conducted using the Fisher grading system. Grade 4 hemorrhage was identified in 42.2% of the cases (Table I).

The average neck width was 3.6 ± 1.1 mm, aspect ratio was 1.5 ± 0.9, dome-to-neck ratio was 1.3 ± 0.4, and maximum diameter was 6.4 ± 2.5 mm. Three morphometric parameters, namely neck width (analysis of variance, p=0.0012), aspect ratio (p=0.0471), and maximum diameter (p=0.0113), differed significantly across anatomical regions. Aneurysms in the proximal ICA tended to be larger in dimension, while those at bifurcation sites (e.g., Acom, middle cerebral artery bifurcation) demonstrated higher aspect ratios (Figures 1, 2).

Flow-diverter stents were preferentially used to manage wide-necked aneurysms of the ICA, whereas coiling approaches were applied to bifurcation or distal branch aneurysms.

Table I: Demographics and Clinical Characteristics of the Patients

Category	Subcategory / Label	n	% of Patients
Demographics	Mean Age ± SD (years)		55.5 ± 15.3
	Gender (Female : Male)	(n)	37 : 28
Comorbidities	Hypertension (HT)	29	45.3
	Diabetes Mellitus (DM)	10	15.6
	Smoking	13	20.3
	Chronic Lung Disease	5	7.8
	Hyperlipidemia	8	12.5
Symptoms	Headache	14	21.9
	Visual Problems	5	7.8
	Seizures	2	3.1
	Incidental Finding	8	12.5
	Dizziness	3	4.7
	Hemiparesis / Stroke Signs	5	7.8
Subarachnoid Hemorrhage		25	39.1
Clinical Admission	Antiaggregant Therapy	27	42.2
	Hydrocephalus	8	12.5
Glasgow Coma Scale (GCS) at Admission	4-8	12	18.7
	9	1	1.6
	10	4	6.2
	11	1	1.6
	12	3	4.7
	13	4	6.2
	14	6	9.4
	15	33	51.6
Patient Classification	Fisher Grade (4) (1/2/3/4)		25/5/7/27
	WFNS Grade (18) (1/2/3/4/5)		33/9/3/10/9
Cisternal Blood	Lamina terminalis (AComA region)	29	45.3
	Distal Sylvian fissure (MCA bifurcation)	32	50.0
	Quadrigeminal cistern	22	34.4
	Prepontine cistern	10	15.6
	Unknown / No detectable blood	25	39.1

WFNS: *World Federation of Neurological Surgeons,* ***AcomA:*** *Anterior communicating artery,* ***MCA:*** *Middle cerebral artery.*

Primary angiographic outcome was assessed using the Raymond–Roy classification: Class I (complete occlusion) was achieved in 70.2% of the cases, while Classes II and IIIa (residual neck or sac) were achieved in 27.2% and 2.6% of the cases, respectively (Figure 3). Aneurysm location significantly influenced occlusion rates (chi-square test, p=0.0002), with higher incomplete occlusion in Acom, Pcom, and MCA bifurcation aneurysms (Figures 4, 5). Aspect ratio was also a significant predictor of incomplete occlusion (Kruskal–Wallis test, p=0.0202), whereas dome-to-neck ratio and neck width did not exhibit significant associations (p=0.06). The mean Modified Rankin Scale and Glasgow Outcome Scale scores were 1.44 (median: 0.5) and 4.19 (median: 5.0), respectively, indicating that most of the patients recovered favorably. The overall mortality rate was 12% and the mean hospital stay was 12.2 days (range: 2–147 days). The median follow-up period was 8.5 months.

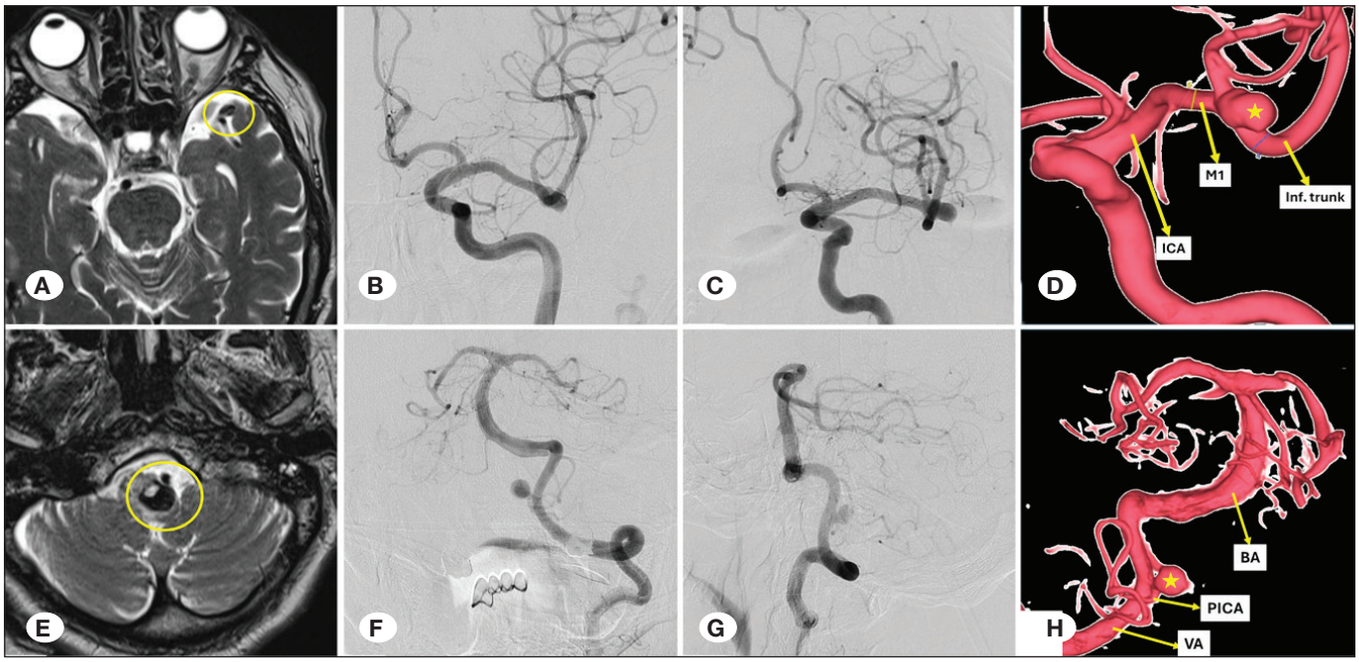

Figure 1: Pre-treatment imaging of a patient with non-ruptured left MCA bifurcation aneurysm and left PICA aneurysm. **A)** Axial T2-weighted MRI showing the left MCA bifurcation aneurysm. **B)** Anteroposterior (AP) view and **C)** oblique view DSA images demonstrating aneurysm location. **D)** 3D reconstructive DSA image showing a 7.3 × 4.2 mm saccular, wide-necked aneurysm. **E)** Axial T2-weighted MRI showing the left PICA aneurysm with a thrombosed component. **F)** AP view and **G)** lateral view DSA images demonstrating aneurysm location. **H)** 3D reconstructive DSA image showing a 12.4 × 8.3 mm saccular, wide-necked aneurysm.

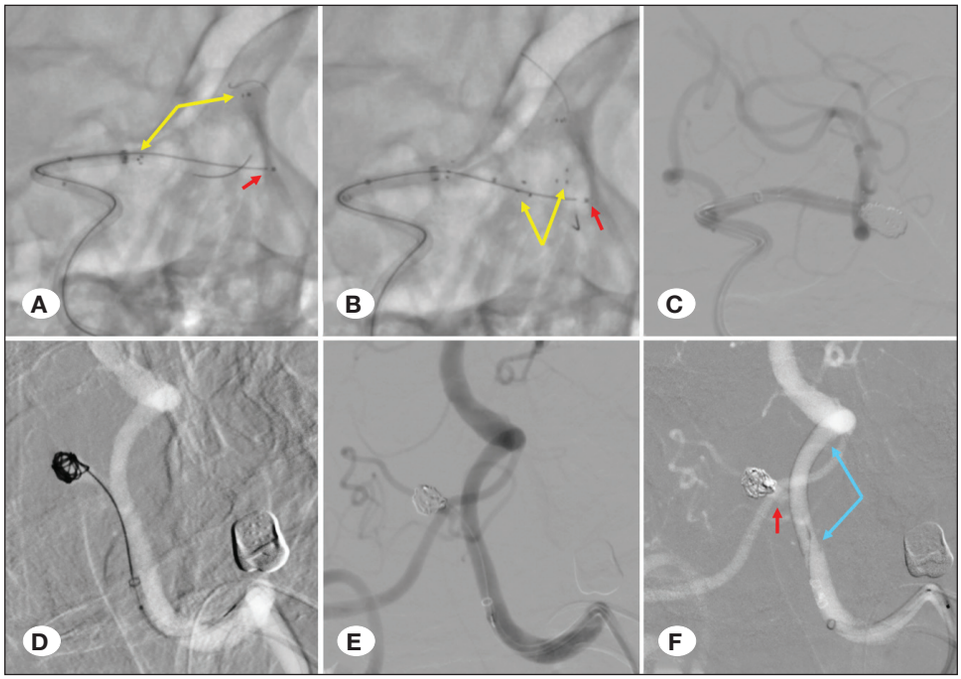

Figure 2: Treatment imaging of a patient with a left MCA bifurcation aneurysm and a left PICA aneurysm. **A)** In the Y-stent-assisted coil embolization procedure for the left MCA aneurysm, distal and proximal markers of the first stent (Acclino 3.5x25 mm) placed into the superior trunk (yellow arrows) and the coil microcatheter within the aneurysm dome (red arrow) are shown. **B)** Distal and proximal markers of the stent (Acclino 3.5x25 mm) placed into the inferior trunk (yellow arrows) and the coil microcatheter within the aneurysm dome (red arrow) are visible. **C)** Final control angiogram after completion of the coiling procedure. **D)** Initial coiling procedure performed for the left PICA aneurysm. **E)** Loose coiling at the aneurysm neck to preserve the proximal segment of the PICA. **F)** Distal and proximal markers of the DERIVO-2 4×15 mm flow diverter stent (blue arrows) placed to promote remodeling of the residual neck filling (red arrow) over time.

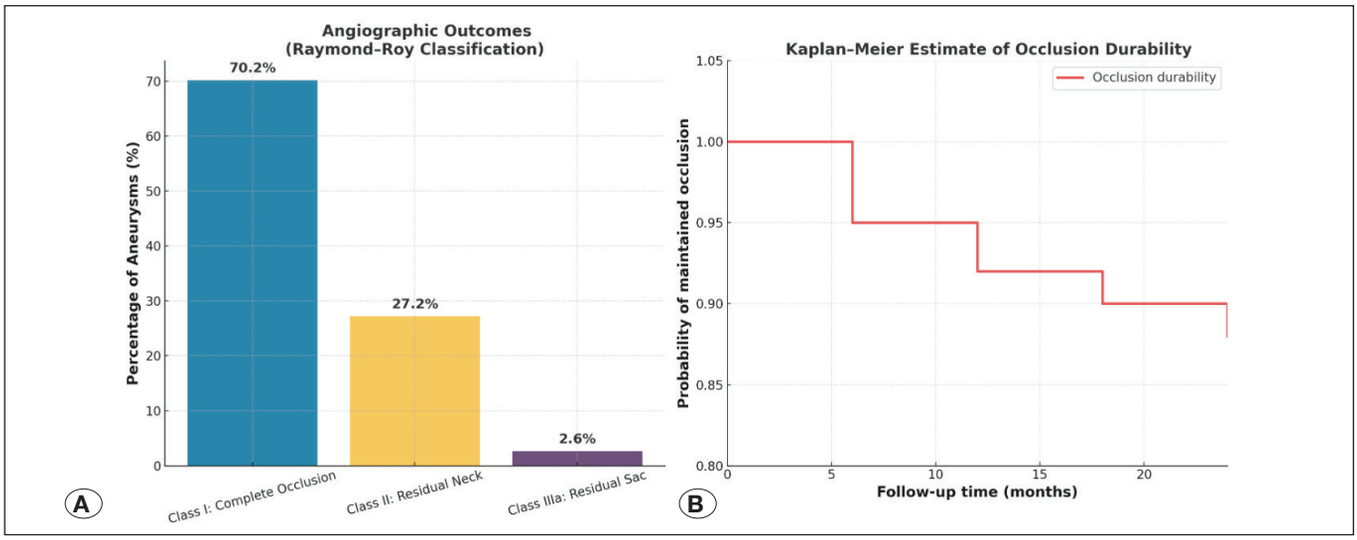

Figure 3: Summary of angiographic and follow-up outcomes in patients with multiple intracranial aneurysms treated endovascularly. **A)** Distribution of angiographic results according to the Raymond–Roy Occlusion Classification. Complete occlusion (Class I) was achieved in 70.2% of aneurysms, whereas residual neck (Class II) and residual sac (Class IIIa) were seen in 27.2% and 2.6%, respectively. **B)** Kaplan–Meier estimate of occlusion durability. The majority of aneurysms maintained stable occlusion during the first year of follow-up, with only a modest decline observed at 18–24 months. Median follow-up was 8.5 months and extended imaging data in a subset of patients confirmed continued stability without significant late recanalization.

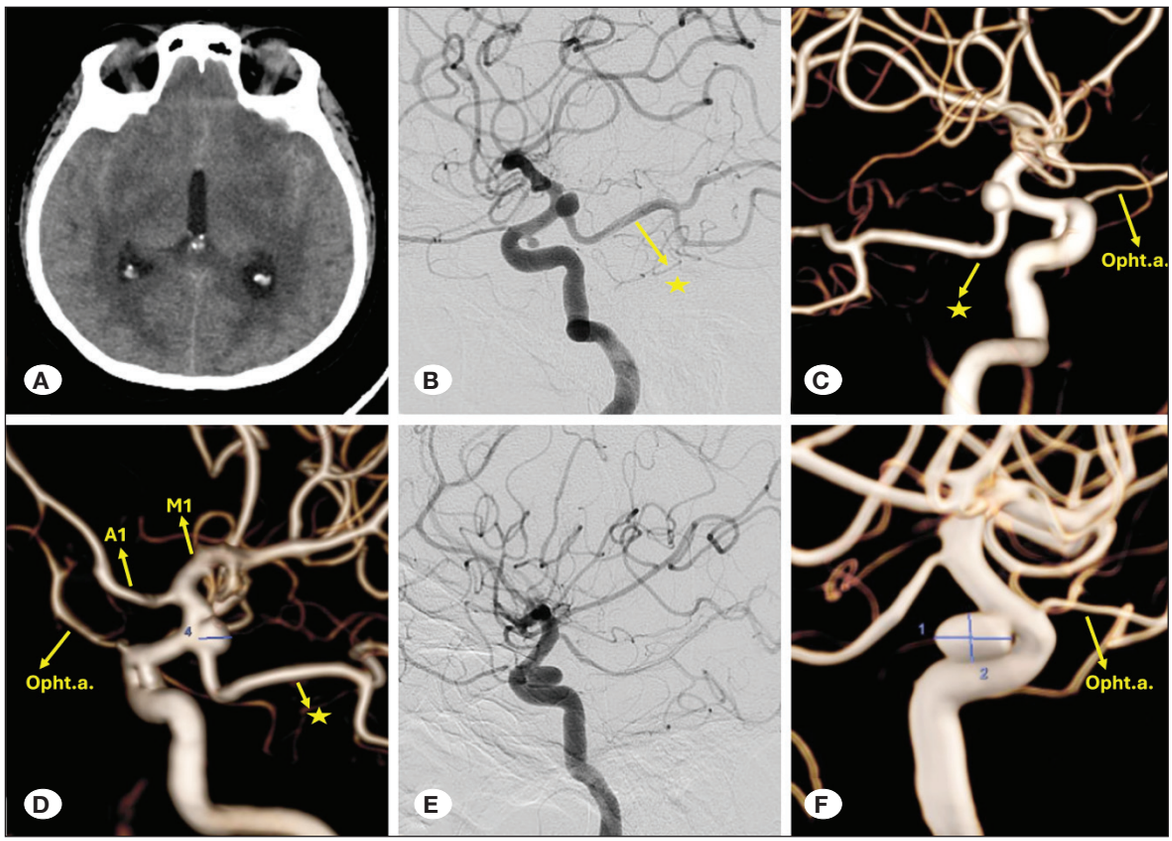

Figure 4: Pre-treatment imaging in a patient with bilateral ICA aneurysms. **A)** Axial cranial CT scan showing subarachnoid hemorrhage in the bilateral Sylvian cisterns. **B)** Lateral view DSA image following right ICA injection, demonstrating two saccular, wide-necked aneurysms: an inferiorly projecting aneurysm at the right ICA paraophthalmic segment measuring 2.8 × 2.4 mm, and an aneurysm originating from the right ICA Pcom segment measuring 6.6 × 4.4 mm. (yellow star: fetal Pcom). **C)** 3D reconstructed DSA image (oblique view) and **D)** posterior-anterior view of the same right ICA aneurysms. **E, F)** Lateral view and 3D reconstructed DSA image following left ICA injection, showing a saccular, wide-necked aneurysm at the left ICA paraophthalmic segment measuring 7.6 × 4.8 mm.

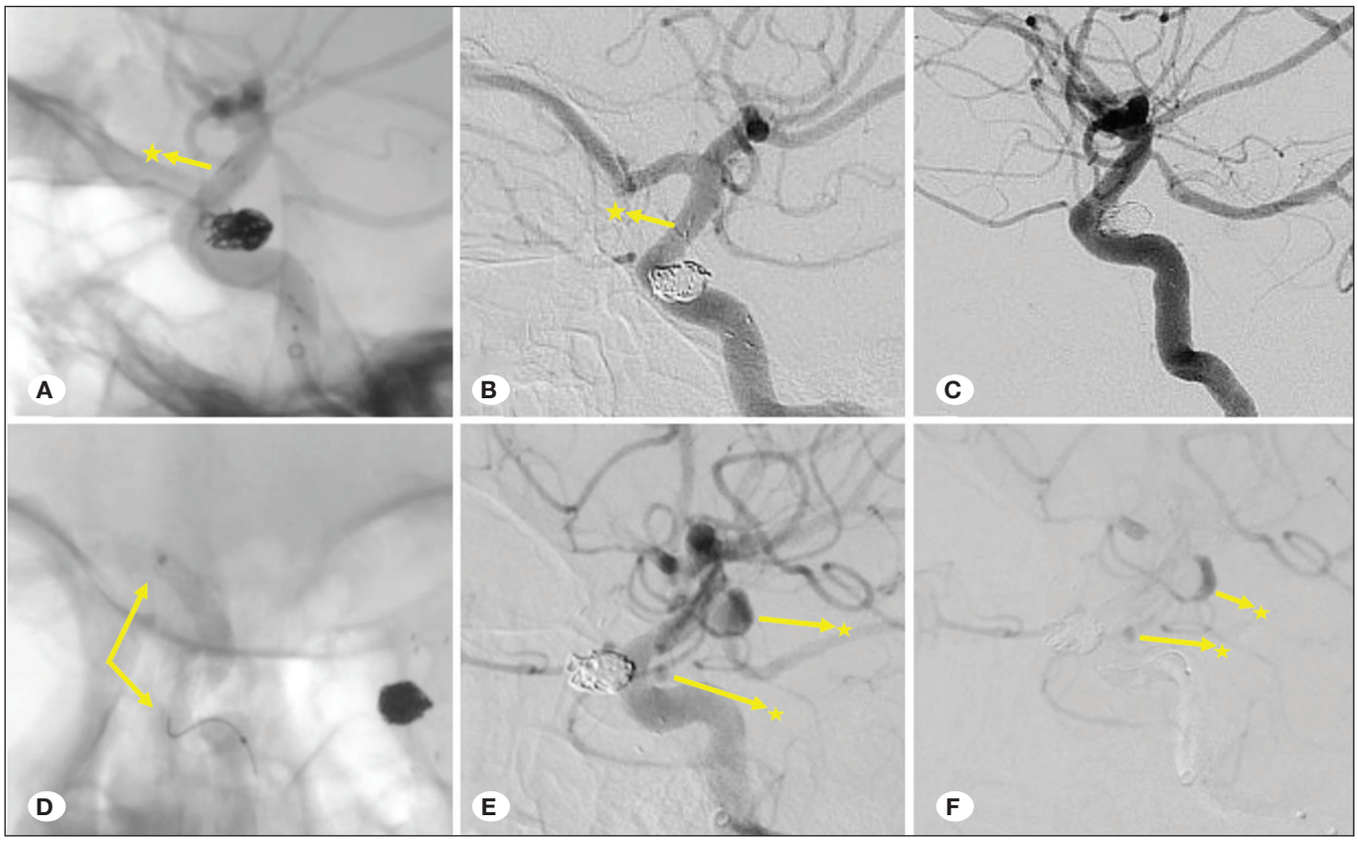

Figure 5: Treatment images of left and right ICA aneurysms. **A)** Unsubtracted view and **B)** subtracted view during stent-assisted coil embolization of the left ICA aneurysm, showing the proximal marker (yellow star) of the Neuroform Atlas stent (4.5 × 21 mm). **C)** Post-procedural control image in lateral projection in the same patient. **D)** Unsubtracted view during flow diverter stent placement for right ICA aneurysms, showing proximal and distal markers of the Surpass Evolve stent (4 × 17 mm). **E)** Delayed arterial phase and **F)** capillary phase images demonstrating contrast stagnation within the aneurysms located at the right ICA Pcom origin and paraophthalmic segment (yellow stars).

DISCUSSION

This multicenter retrospective study aimed to evaluate endovascular strategies in the treatment of MIAs, focusing on morphological predictors and clinical outcomes. Our findings demonstrated that endovascular strategies resulted in high overall occlusion rates with favorable clinical recovery. Moreover, our results highlighted the significant impact of aneurysm location and aspect ratio on treatment success. One of the most critical challenges in managing MIAs is accurately identifying the source of hemorrhage. Nehls et al. correctly localized bleeding aneurysms in up to 98% of the cases in their study through detailed CT and angiographic analysis, considering parameters such as aneurysm size, shape, wall irregularities, and adjacent vasospasm (16). In our cohort, prioritizing the treatment of the ruptured lesion was critical, often dictating the sequence and strategy for managing coexisting unruptured aneurysms.

Following the occlusion rate of the ruptured aneurysm, management of coexisting unruptured lesions can be considered either in the same session or in a staged approach. In particular, treating ipsilateral aneurysms sharing the same vascular access in a single session is advantageous because it minimizes vascular manipulation, reduces endothelial trauma, and facilitates neointimal healing when stents are deployed (15).

The choice between microsurgical clipping and endovascular intervention in the treatment of multiple aneurysms remains nuanced. With advancements in neurointerventional technology—particularly the development of flow-diverter stents and improved angiographic visualization—endovascular treatment has become increasingly preferred in recent years (7). Broad-necked aneurysms, often encountered in cases featuring multiple aneurysms, represent a challenge for microsurgical access but are amenable to endovascular techniques. At 10-year follow-up in the Barrow Ruptured Aneurysm Trial, clipping of anterior circulation aneurysms was associated with lower rates of rebleeding, retreatment, and incomplete occlusion compared with coiling, although both groups showed comparable clinical outcomes (25). At 1-year follow up in the International Subarachnoid Aneurysm Trial, endovascular coiling resulted in improved independent survival compared with surgery in favorable cases, but the trial results highlighted the necessity of follow-up to monitor the rare occurence of late rerupture (13). Morsy et al. reported an occlusion rate of 92.5% in wide-necked aneurysms treated with endovascular

methods, underscoring the efficacy of such methods (15). In our study, Raymond–Roy Class I and II occlusion rates were achieved by 97.4% of the patients (Class I: 70.2%, Class II: 27.2%), and aneurysm aspect ratio and location significantly influenced occlusion rates, with higher incomplete occlusion noted in Acom, Pcom, and MCA bifurcation aneurysms.

In cases involving giant aneurysms, which are frequently associated with multiple aneurysms, endovascular treatment is generally preferred due to the elevated perioperative risk associated with microsurgical clipping. Santoro et al. found that while both approaches yielded comparable mortality rates, microsurgery was associated with higher morbidity and intraoperative complication rates, whereas endovascular techniques were associated with lower morbidity but higher recurrence rates (20). In our study, we treated eight giant aneurysms using endovascular techniques.

Interestingly, aneurysm location may influence long-term outcomes depending on the treatment modality. Yamada et al. reported a reduced incidence of secondary normal-pressure hydrocephalus in patients treated with endovascular coiling compared with microsurgical clipping (28). Similarly, Dong et al. observed no persistent neurological deficits in the endovascular group, suggesting a potential safety advantage over microsurgery despite similar complication rates (3). In patients without massive subarachnoid hemorrhage or severe vasospasm, endovascular approaches are generally preferred due to their minimally invasive nature.

Liu et al. proposed a novel zonal classification of the cranial cavity from the falx cerebri to the tentorium cerebelli to guide the selection of treatment modality on the basis of aneurysm location (10). Furthermore, Song et al. demonstrated the safety and efficacy of single-session endovascular treatment in midline or symmetrically distributed aneurysms, such as mirror aneurysms (24). The ongoing debate between single-session and staged treatment strategies is especially relevant in MIA management. Several studies have advocated for single-session treatment to mitigate the risk of rebleeding during the interventional interval (9,22,23,29). However, Andic et al. emphasized that while single-session endovascular treatment is effective in complex cases, it may carry an elevated risk of thromboembolic complications, particularly in patients with bilateral ICA aneurysms. In such cases, a staged approach should be considered (1).

Deniwar reported that aneurysm size and location, radiological signs of impending rupture, and clinical presentation are critical factors in determining the optimal treatment modality and timing (2). Similarly, Kim and Song identified endovascular treatment as the standard of care for multiple aneurysms, cautioning that limiting treatment only to the ruptured lesion could underestimate the true risk of hemorrhage from untreated aneurysms (6). Supporting this recommendation, Massaud et al. reported superior outcomes and shorter procedural times for endovascular approaches in posterior circulation aneurysms, attributing this to the complexity of microsurgical access in such locations (11).

Several studies advocate for primary coil embolization in single-session treatments, citing its efficacy in reducing hemorrhage risk and limiting vessel trauma and dissection (4,17). In addition to primary coiling, other endovascular techniques such as stent-assisted coiling and primary stenting have demonstrated high success rates, especially in wide-necked or proximally situated multiple aneurysms (14,21,24,27).

In cases involving multiple ipsilateral aneurysms near the ophthalmic segment of the ICA, Tang et al. emphasized the importance of aneurysm geometry in selecting the optimal endovascular strategy, achieving complete occlusion through tailored techniques in a single session (26). Similarly, Lee et al. demonstrated that flow-diverter stents are effective in treating proximally spaced ipsilateral aneurysms, achieving successful occlusion across multiple lesions (8). In our study, flow-diverter stents were preferentially used in wide-necked aneurysms of the ICA, while coiling approaches were applied to bifurcation or distal branch aneurysms.

Limitations

This study has some limitations. First, the study is retrospective in design with a moderately sized patient cohort. Second, heterogeneity in endovascular devices, procedural protocols, operator experience, and institutional case volumes could have influenced treatment selection and outcomes. Finally, the relatively short median follow-up of 8.5 months may underestimate the incidence of late recanalization, particularly in bifurcation aneurysms treated with coiling. Nevertheless, the value of this study lies in its pioneering contribution to the understanding of treatment selection and efficacy in the management of multiple aneurysms. To strengthen the generalizability of these findings and support global standardization, future studies should aim for larger, prospectively collected datasets with standardized protocols.

CONCLUSION

Endovascular techniques represent a valuable treatment option for MIAs, achieving favorable occlusion rates and clinical outcomes. However, the choice of strategy should be individualized, considering aneurysm location, morphology, and patient-specific factors. Our findings underscore the importance of a morphology-driven, patient-tailored approach in optimizing treatment success. Further prospective multicenter studies with longer follow-up are warranted to validate these results and refine therapeutic strategies.

Declarations

Funding: This research did not receive any specific grant from funding agencies in the public, commercial, or not-for-profit sectors.

Availability of data and materials: The datasets generated and/or analyzed during the current study are available from the corresponding author by reasonable request.

Disclosure: The authors declare no competing interests.

AUTHORSHIP CONTRIBUTION

Study conception and design: LA, MBE, MET

Data collection: LA, MBE, CT

Analysis and interpretation of results: LA, EK, FY, CT

Draft manuscript preparation: LA, MBE, FY

Critical revision of the article: EK, FY, MET, CE

Other (study supervision, fundings, materials, etc...): LA, MBE, MET, CE

All authors (LA, MBE, CT, CE, EK, FY, MET) reviewed the results and approved the final version of the manuscript.

REFERENCES

1. Andic C, Aydemir F, Kardes O, Gedikoglu M, Akin S: Single-stage endovascular treatment of multiple intracranial aneurysms with combined endovascular techniques: Is it safe to treat all at once? J Neurointerv Surg 9:1069-1074, 2017. https://doi.org/10.1136/neurintsurg-2016-012745
2. Deniwar MA: Management of multiple and unruptured cerebral aneurysms. Egyptian J Neurosurg 37:1-10, 2022. https://doi.org/10.1186/s41984-023-00206-z
3. Dong QL, Gao BL, Cheng ZR, He YY, Zhang XJ, Fan QY, Li, CH, Yang ST, Xiang, C: Comparison of surgical and endovascular approaches in the management of multiple intracranial aneurysms. Int J Surg 32:129-135, 2016. https://doi.org/10.1016/j.ijsu.2016.07.004
4. Fisher CM, Kistler JP, Davis JM. Relation of cerebral vasospasm to subarachnoid hemorrhage visualized by computerized tomographic scanning. Neurosurgery 1980;6:1-9.
5. Jeon P, Kim BM, Kim DJ, Kim DI, Suh SH: Treatment of multiple intracranial aneurysms with 1-stage coiling. Am J Neuroradiol 35:1170-1173, 2014. https://doi.org/10.3174/ajnr.A3821
6. Kim YJ, Song KY: Endovascular coiling of multiple (more than four) intracranial aneurysms. Case report. Interv Neuroradiol 10:75-81, 2004. https://doi.org/10.1177/159101990401000110
7. Laurent D, Lucke-Wold B, Leary O, Randall MH, Porche K, Koch M, Chalouhi N, Polifka A, Hoh BL: The evolution of endovascular therapy for intracranial aneurysms: Historical perspective and next frontiers. Neurosci Insights 17:26331055221117560, 2022. https://doi.org/10.1177/26331055221117560
8. Lee CH, Luo CB, Lai YC, Chang FC, Lin CJ: Single flow diverter to manage multiple intracranial aneurysms in a parent artery. J Chin Med Assoc 86:289-294, 2023. https://doi.org/10.1097/JCMA.0000000000000868
9. Li TF, Shui SF, Han XW, Yan L, Ma J, Guo D: One-stage endovascular embolization for multiple intracranial aneurysms. Turk Neurosurg 28:43-47, 2018. https://doi.org/10.5137/1019-5149.JTN.18186-16.1
10. Liu H, Xu Q, Yang H: Application of zone classification in multiple intracranial aneurysmal subarachnoid hemorrhage treatment strategies. Heliyon 10:e26857, 2024. https://doi.org/10.1016/j.heliyon.2024.e26857
11. Massoud TF, Guglielmi G, Viñuela F, Duckwiler GR: Endovascular treatment of multiple aneurysms involving the posterior intracranial circulation. Am J Neuroradiol 17:549-554, 1996. https://doi.org/ 0195-6108/96/1703–054
12. Molyneux A, Kerr R, Birks J: Barrow ruptured aneurysm trial. J Neurosurg 119:139-141, 2013. https://doi.org/10.3171/2012.11.JNS121406
13. Molyneux AJ, Kerr RSC, Yu LM, Clarke M, Sneade M, Yarnold JA, Sandercock P; International Subarachnoid Aneurysm Trial (ISAT) Collaborative Group: International subarachnoid aneurysm trial (ISAT) of neurosurgical clipping versus endovascular coiling in 2143 patients with ruptured intracranial aneurysms: A randomised comparison of effects on survival, dependency, seizures, rebleeding, subgroups, and aneurysm occlusion. Lancet 366:809-817, 2005. https://doi.org/10.1016/S0140-6736(05)67214-5
14. Mont'alverne F, Tournade A, Riquelme C, Musacchio, M: Multiple intracranial aneurysms. Angiographic study and endovascular treatment. Interv Neuroradiol 8:95-106, 2002. https://doi.org/10.1177/159101990200800201
15. Morsy A, Mahmoud M, Abokresha AE, Moussa AA, Abdel-Tawab M, Othman M, Mahmoud, AM: Intracranial wide neck aneurysms: Clinical and angiographic outcomes of endovascular management. Egypt J Neurol Psychiatry Neurosurg 58:1-7, 2022. https://doi.org/10.1186/s41983-022-00546-x
16. Nehls DG, Flom RA, Carter LP, Spetzler RF: Multiple intracranial aneurysms: Determining the site of rupture. J Neurosurg 63:342-348, 1985. https://doi.org/10.3171/jns.1985.63.3.0342
17. Oh K, Lim YC: Single-session coil embolization of multiple intracranial aneurysms. J Cerebrovasc Endovasc Neurosurg 15:184-190, 2013. https://doi.org/10.7461/jcen.2013.15.3.184
18. Report of World Federation of Neurological Surgeons Committee on a Universal Subarachnoid Hemorrhage Grading Scale. J Neurosurg 68(6):985-986, 1988. doi:10.3171/jns.1988.68.6.0985
19. Rhoton AL, Saeki N, Perlmutter D, Zeal A: Microsurgical anatomy of common aneurysm sites. Clin Neurosurg 26:248-306, 1979. https://doi.org/10.1093/neurosurgery/26.cn_suppl_1.248
20. Santoro A, Armocida D, Paglia F, Iacobucci M, Berra LV, D'Angelo L, Cirelli C, Guidetti G, Biraschi F, Cantore G: Treatment of giant intracranial aneurysms: long-term outcomes in surgical versus endovascular management. Neurosurg Rev 45:3759-3770, 2022. https://doi.org/10.1007/s10143-022-01884-3
21. Serrone JC, Maekawa H, Tjahjadi M, Hernesniemi J: Aneurysmal subarachnoid hemorrhage: Pathobiology, current treatment and future directions. Expert Rev Neurother 15:367-380, 2015. https://doi.org/10.1586/14737175.2015.1018892
22. Shen X, Xu T, Ding X, Wang W, Liu Z, Qin H: Multiple intracranial aneurysms: Endovascular treatment and complications. Interv Neuroradiol 20:442-447, 2014. https://doi.org/10.15274/INR-2014-10037
23. Solander S, Ulhoa A, Viñuela F, Duckwiler GR, Gobin YP, Martin NA, Frazee JG, Guglielmi G: Endovascular treatment of multiple intracranial aneurysms by using Guglielmi detachable coils. J Neurosurg 90:857-864, 1999. https://doi.org/10.3171/jns.1999.90.5.0857
24. Song Y, Song G, Liu G, Mao L, An X, Peng C, Li J, Chen Y, Li H, Hou C, Wang B, Zhao Y, Wang X, Yin G, Yang X: Endovascular treatment of mirror aneurysms in subarachnoid hemorrhage patients: Single stage or multiple stage? Brain Behav 15: e70234, 2025. https://doi.org/10.1002/brb3.70234

25. Spetzler RF, McDougall CG, Zabramski JM, Albuquerque FC, Hills NK, Nakaji P, Karis JP, Wallace RC: Ten-year analysis of saccular aneurysms in the Barrow Ruptured Aneurysm Trial. J Neurosurg 132:771-776, 2019. https://doi.org/10.3171/2018.8.JNS181846
26. Tang K, Zhang C, Liu X, Zhao L, Wang X, Liu X, Ma S, Gao C, Gao S, Zhang G, Hu Y, Wu J: Endovascular treatment strategies and a new classification for multiple aneurysms of the ipsilateral ophthalmic segment of the internal carotid artery. Asian J Surg 46:3663-3672, 2023. https://doi.org/10.1016/j.asjsur.2023.03.134
27. Wang JW, Li CH, Liu JF, Li H, Guo H, Gao BL: Endovascular treatment of multiple intracranial aneurysms. Medicine 102:E36340, 2023. https://doi.org/10.1097/MD.0000000000036340
28. Yamada S, Ishikawa M, Yamamoto K, Ino T, Kimura T, Kobayashi S: Aneurysm location and clipping versus coiling for development of secondary normal-pressure hydrocephalus after aneurysmal subarachnoid hemorrhage: Japanese Stroke DataBank. J Neurosurg 123:1555-1561, 2015. https://doi.org/10.3171/2015.1.JNS142761
29. Zhang G, Zhang W, Chang H, Shen Y, Ma C, Mao L, Li Z, Lu H: Endovascular treatment of multiple intracranial aneurysms in patients with subarachnoid hemorrhage: One or multiple sessions? Front Neurol 14:1196725, 2023. https://doi.org/10.3389/fneur.2023.1196725

Turk Neurosurg 36(1):34-48, 2026
DOI: 10.5137/1019-5149.JTN.48396-25.2

Original Investigation
Cerebrovascular-Endovascular

Received: 02.01.2025
Accepted: 03.06.2025
Published Online: 16.01.2026

Evaluation of the Role of miRNAs Expression Profiles in Aneurysm

Sara Khadem ANSARI[1], Ebru ERZURUMLUOGLU GOKALP[1], Emre OZKARA[2], Ozlem AYKAC[3], Ertugrul COLAK[4], Ezgi SUSAM[1], Beyhan DURAK ARAS[1], Atilla Ozcan OZDEMIR[3], Sevilhan ARTAN[1]

[1]Eskisehir Osmangazi University, Faculty of Medicine, Department of Medical Genetics, Eskisehir, Türkiye
[2]Eskisehir Osmangazi University, Faculty of Medicine, Department of Neurosurgery, Eskisehir, Türkiye
[3]Eskisehir Osmangazi University, Faculty of Medicine, Department of Neurology, Eskisehir, Türkiye
[4]Eskisehir Osmangazi University, Faculty of Medicine, Department of Biostatistics, Eskisehir, Türkiye

Corresponding author: Sevilhan ARTAN ✉ sartan26@gmail.com

ABSTRACT

AIM: To evaluate the diagnostic and prognostic significance of miRNA signatures by identifying differences in miRNA expression between ruptured and unruptured intracranial aneurysm (IA) cases, as well as to pinpoint miRNAs that correlate with clinical severity in patients with aneurysmal subarachnoid hemorrhage (aSAH).

MATERIAL and METHODS: Peripheral blood samples were collected from 50 IA patients (25 without rupture and 25 with rupture) and 25 healthy controls. In the ruptured group, analyses were performed on samples collected on Days 3 and 5 after SAH. The clinical severity and outcomes of the disease were assessed using Fisher grades, WFNS grades, Hunt–Hess grades, and the Modified Rankin Scale.

RESULTS: We found that the expression levels of miR-21-5p and miR-15a were significantly altered in unruptured aneurysms (UA) patients compared to controls. The expression levels of 10 miRNAs were significantly decreased in ruptured aneurysms (RA) patients compared to controls. The ruptured group also exhibited an upregulation of 16 miRNAs relative to the unruptured group. Furthermore, we noted a significant increase in miR-24 expression in RA patients between Days 3 and 5, suggesting its potential role in the progression of aSAH. miR-9p-3p and miR-497 were found to be associated with aSAH severity. Moreover, the levels of miR-451a, miR-146a-5p, miR-502-5p, and miR-497 were significantly lower in patients with poor outcomes compared to those with favorable outcomes.

CONCLUSION: These findings suggest that specific miRNAs may serve as potential diagnostic and prognostic biomarkers for IA and subsequent SAH, particularly on Day 3 following aSAH.

KEYWORDS: Intracranial aneurysm, Aneurysmal subarachnoid hemorrhage, miRNA, Biomarker, Preipheral blood

ABBREVIATIONS: aSAH: Aneurysmal subarachnoid hemorrhage, **AUC:** Area under the ROC curve, **CSF:** Cerebrospinal fluid, **CVS:** Cerebral vasospasm, **DCI:** Delayed cerebral ischemia, **DCV:** Delayed cerebral vasospasm, **FC:** Fold change, **IA:** Intracranial aneurysm, **miRNAs:** MicroRNAs, **mRS:** Modified rankin scale, **RA:** Ruptured aneurysms, **ROC:** Receiver operating characteristic, **SAH:** Subarachnoid hemorrhage, **UA:** Unruptured aneurysms, **VSMC:** Vascular smooth muscle cells, **WFNS:** World Federation of Neurosurgical Societies

Sara Khadem ANSARI : 0000-0001-7951-2137
Ebru ERZURUMLUOGLU GOKALP : 0000-0002-1275-5174
Emre OZKARA : 0000-0001-5448-6446
Ozlem AYKAC : 0000-0003-4987-0050
Ertugrul COLAK : 0000-0003-3251-1043
Ezgi SUSAM : 0000-0003-3343-7797
Beyhan DURAK ARAS : 0000-0003-1881-1912
Atilla Ozcan OZDEMIR : 0000-0002-9864-6904
Sevilhan ARTAN : 0000-0001-7658-6309

INTRODUCTION

Subarachnoid hemorrhage (SAH) is the extravasation of blood within a vessel into the subarachnoid space, which is normally filled with cerebrospinal fluid (CSF) in the central nervous system (28). The most common cause of non-traumatic SAH is intracranial aneurysm (IA) rupture (40). Aneurysmal subarachnoid hemorrhage (aSAH) is a severe health problem due to both the direct effects of bleeding and complications such as vasospasm (37). aSAH has an incidence of approximately 6-16 per 100,000 individuals annually worldwide, with a mortality rate of 45% (19). Various modifiable and non-modifiable factors that affect the risk of aneurysm formation, growth, and rupture, such as smoking, alcohol use, female gender, and a family history of IA, have been identified (43). Although there have been remarkable advances in the diagnosis, treatment, and follow-up of the disease, it remains a significant cause of morbidity and mortality due to a lack of biomarkers that would allow for the screening and timely intervention of high-risk aneurysms. Therefore, there is an urgent need to identify robust markers with high sensitivity and specificity for the accurate identification of aSAH or prediction of aneurysmal rupture (41).

MicroRNAs (miRNAs) are single-stranded small conserved noncoding RNAs composed of 18-22 nucleotides that play critical roles in regulating gene expression at the post-transcriptional level (10). More than 2,500 miRNAs in humans have been identified as being able to regulate over 60% of protein-coding genes. These molecules play a role in various physiological processes, such as cell proliferation, cell differentiation, apoptosis, oxidative stress, and angiogenesis (49). Differential expression of miRNAs can often impair cellular and biological functions and contribute to the development and progression of disease. miRNAs are known to be involved in numerous diseases, including cancer, cardiovascular disease, and neurological conditions. Although limited, data showing that specific miRNAs may play a vital role in the development of IA and the progression of aSAH are available (10,20,27,40).

This case-control study aimed to determine miRNA expression differences in ruptured and unruptured IA cases, evaluate the diagnostic and prognostic significance of these miRNA signatures, and identify markers associated with clinical severity in aSAH patients.

MATERIAL and METHODS

Ethics Statement

This study was conducted in accordance with the guidelines presented in the Declaration of Helsinki for research experiments involving human subjects and approved by the Institutional Ethics Review Board of the Eskisehir Osmangazi University, Medical Faculty (2023-48). All participants provided written informed consent.

Literature Search

A preliminary search was conducted to identify miRNAs reported to have the potential to reveal the risk of aSAH among IA cases by examining relevant articles and databases such as PubMed, Embase, Ovid, Google Scholar, and miRbase. Based on previous studies, the expression profiles of 20 miRNAs, including miR-29a, miR-126, miR-200a-3p, miR-451a, miR-146a-5p, miR-1297, miR-27b-3p, miR-502-5p, miR-143-3p, miR-145-5p, miR-17-5p, miR-221-3p, miR-21-5p, miR-15a, miR-9-3p, miR-630, miR-24, miR-148b-3p, miR-497, and miR-183-5p (2,5,7,11,20,21,23,31-35,40,41,44,47,50-52,55), in the peripheral blood samples of IA cases were determined and compared with control blood samples.

Participants

Patients with ruptured aneurysms (RA) and unruptured aneurysms (UA) were recruited from the Neurosurgery and Neurology departments of the Medical Faculty, Eskisehir Osmangazi University, Turkey. The diagnosis of both IA and aSAH was based on clinical examination and neuro-imaging techniques, including computed tomography (CT), computed tomography angiography, digital subtraction angiography, and magnetic resonance angiography, as defined in the World Health Organization criteria. Cases with a medical history of cardiovascular or immunological diseases, cancer, and organ failure were excluded, as these conditions have the potential to change miRNA expression levels. Clinically healthy individuals of both sexes, without neurological and chronic/systemic diseases, IA, or a family history of IA/aSAH, constituted the control group of the study. Baseline demographic data, as well as details regarding vascular risk factors, such as hypertension, diabetes, smoking, and alcohol consumption, were gathered from all participants.

The present study included a total of 100 blood samples from IA/aSAH patients and controls: (A) 25 patients with unruptured IA (Group 1); (B) 25 patients with ruptured IA; samples from aSAH patients were collected post-SAH on Days 3 and 5 (Group 2); and (C) 25 healthy controls. All participants were from the Turkish population.

Whole Blood Collection and Total RNA Extraction

Venous whole blood was collected using PAXgene Blood RNA tubes (PreAnalytiX GmbH, Switzerland). To ensure the complete lysis of blood cells, each PAXgene Blood RNA tube was incubated at room temperature (15-25°) for a minimum of 2 hours before processing, per the manufacturer's protocol. Total RNA extraction was performed using the PAXgene Blood miRNA kit (PreAnalytiX, Qiagen, Switzerland) according to the manufacturer's recommendations. The RNA concentration was assessed using a NanoDrop ND-1000 spectrophotometer (PeQLab Biotechnologie GmbH), and the samples were subsequently stored at –80°C for further analysis.

Quantitative Real-Time PCR (qRT-PCR)

A total of 20 miRNAs were screened for. Reverse transcription of miRNA was carried out using the miRNA All-In-One cDNA Synthesis Kit (Cat#G898 ABM, CA, USA) following the manufacturer's instructions. Each reaction mixture consisted of 10 µl of 2X miRNA cDNA Synthesis SuperMix, 2 µl of Enzyme Mix, 2 µl of Total RNA, and 6 µL of nuclease-free water, bringing the total volume to 20 µL. Then, the reaction followed this cycling profile: 37 °C for 30 min, 50 °C for 15 min,

Table I: Clinical Parameters of IA Groups and Control Participants

Parameters	Controls (n=25)	Group 1: Unruptured IA (n=25)	Group 2: Ruptured IA (n=25)	p-value
Age (year)	61.42 ±11.28	56.32±14.06	59.12±12.20	0.585
Gender (females)	14 (56)	15 (60)	14 (56)	0.959
Hypertension	None	9 (36)	7 (28)	0.544

Data are presented as mean ± standard deviation or n (%); p value <0.05 is considered statistically significant.

85 °C for 5 min, and hold at 4 °C. Amplification was performed on a CFX-96 Real-Time PCR Detection System (C1000 Touch Thermal Cycler, BIO-RAD) with a reaction mixture containing 5 µl BrightGreen miRNA qPCR Master Mix, 0.35 µl forward primer, 0.35 µl reverse primer, 2 µl cDNA, and 2.3 µl nuclease-free water, reaching a final volume of 10 µl. U6 was used as a housekeeping gene (all from ABM, CA, USA). The RT-PCR protocol was as follows: incubation at 95 °C for 10 minutes, followed by 40 cycles at 95 °C for 10 seconds, 60 °C for 20 seconds, and 72 °C for 30 seconds. Cycle threshold (Ct) values were determined for each sample, and the relative miRNA level was calculated using the formula $2^{-\Delta\Delta Ct}$.

Statistical Analysis

Statistical analyses were performed using SPSS version 25.0 (IBM, NY, USA). The distribution of the variables was evaluated with the Shapiro–Wilk test. Comparisons were performed using Student's t-test for normally distributed variables. The Mann–Whitney U test was used to evaluate the differences between two groups, and the Kruskal–Wallis test assessed differences among more than two groups. Correlations between variables were evaluated using Spearman's rank correlation coefficient analysis. Receiver operating characteristic (ROC) curves were generated for each miRNA, and the area under the ROC curve (AUC), specificity, and sensitivity were calculated with a 95% confidence interval (95% CI) to evaluate the potential of these candidate miRNAs as diagnostic biomarkers.

RESULTS

Demographic and Clinical Features of the Study Groups

Among the 50 IA patients included in this study, 29 were female and 21 were male (mean age 57.72±13.10 years; range 29-79), and 16 had a history of hypertension. The healthy controls comprised 14 women and 11 men (mean age 61.43±11.28 years). No significant differences in age or gender were observed between the IA cases and the control cohort. The distribution of hypertension was similar in both RA and UA patients. The clinical features of the controls and IA patients are summarized in Table I. Clinical severity assessments at admission indicated that five cases (20%) were categorized as WFNS (World Federation of Neurosurgical Societies) Grades 3-5, while nine cases (36%) were classified as Hunt–Hess Grades 3-5. Brain CT results showed Fisher Grade 4 in 60% of patients. Regarding clinical outcomes, 40% of the patients showed a modified Rankin Scale (mRS) score of 3-6.

The clinical characteristics of aSAH patients are presented in Table II.

Table II: Clinical Characteristics of the Patients (n=25) with aSAH

Clinical profiles	n (%)
Symptoms	
Headache	16 (64.0)
Vomiting	6 (24.0)
Altered sensorium	6 (24.0)
Focal deficits	2 (8.0)
Seizures	7 (28.0)
Aneurysm location	
Anterior communicating artery	13 (52.0)
Middle cerebral artery	4 (16.0)
Internal carotid artery	2 (8.0)
Anterior cerebral artery	1 (4.0)
Posterior communicating artery	1 (4.0)
Multiple	4 (16.0)
Fisher grade (9)	
1-3	10 (40.0)
4	15 (60.0)
Hunt-Hess grade (12)	
1-2	16 (64.0)
3-5	9 (36.0)
WFNS grade (32)	
1-2	20 (80.0)
3-5	5 (20.0)
Modified Rankin Scale (mRS) (31)	
1-2	15 (60.0)
3-6	10 (40.0)

WFNS: *World Federation of Neurologic Surgeons.*

Comparison of the miRNA Expression Profiles in the Blood Samples of UA Cases and the Control Group

Among the 20 examined miRNAs, two miRNAs, namely miR-21-5p and miR-15a, were differentially represented in controls and UA patients: the expression level of miR-21-5p was significantly increased (Fold Change (FC)=2.07, p=0.006), whereas miR-15a was considerably decreased (FC=0.72, p=0.049) in UA cases compared with controls (Figure 1A). The sensitivity and specificity of these circulating miRNAs as diagnostic indicators were determined by analyzing the AUC for each miRNA. miR-21-5p and miR-15a had AUC values of 0.829 (p<0.0001) and 0.780 (p=0.001), respectively (Figure 1B). The findings suggest that these two miRNAs together can discriminate UA patients from healthy individuals.

Differently Expressed miRNAs Between the Ruptured and Control Groups

Expression analyses were conducted on blood samples taken on the third and fifth days post-hemorrhage to identify miRNAs that may contribute to prognostic assessment and clinical recovery in cases of rupture. The expression levels of circulating miRNAs in blood samples taken on the third and fifth days after bleeding from ruptured cases differed from those in the control group. Specifically, nine miRNAs on the

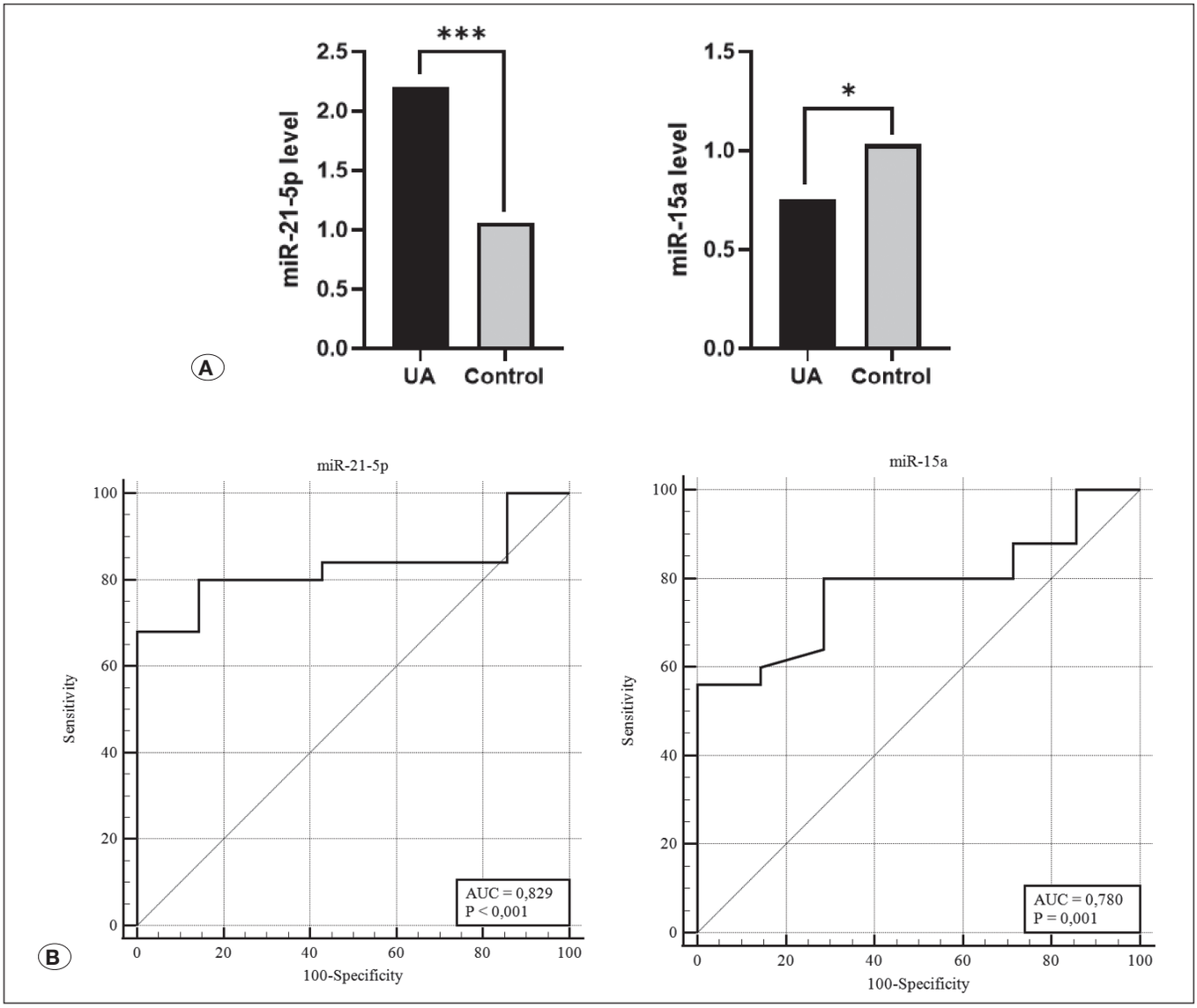

Figure 1: Expression levels of differentially expressed miRNAs in patients with unruptured aneurysms and healthy controls. **A)** Relative expression of miR-21-5p and miR-15a in unruptured aneurysm patients and controls. All miRNA levels are presented as fold changes. Data are shown as means. **B)** ROC curves to distinguish unruptured IA patients from healthy controls. The AUCs of miR-21-5p and miR-15a were 0.829 and 0.780, respectively. Statistically significant differences are marked with asterisks: ***p=0.0001-0.001, **p=0.001-0.01, *p=0.01-0.05. **AUC:** Area under the curve, **ROC:** Receiver operating characteristic.

third day after bleeding and six miRNAs on the fifth day post-bleeding were found to have statistically significant decreases in expression levels compared to the control group (Figure 2A, B). Subsequently, ROC and AUC analyses of these candidate circulating miRNAs revealed strong discriminatory potential between the patient and control groups, indicating their viability as potential biomarkers (Figure 2C and Table III).

Comparison of Circulating miRNA Expression Profiles in the Ruptured and Unruptured Cases

In comparing the RA and UA groups, the expression levels of 14 miRNAs in samples collected on the third day of bleeding, as well as 11 miRNAs from the fifth day, exhibited significant differences. Notably, miRNA expression was downregulated in the RA group relative to the UA group (Figure 3A, B). Several miRNAs demonstrated AUC values exceeding 0.8 on the third day, highlighting their effectiveness in distinguishing between patients with unruptured and ruptured aneurysms. These findings indicate that such miRNAs hold considerable promise for accurately differentiating between these two conditions and that alterations in their expression could potentially serve as predictors of aneurysmal rupture (Table IV).

Regarding whether specific miRNAs exhibit significant changes from the third to the fifth day, which may play a role in the progression of aSAH due to complications like vasospasm (that can arise after the fourth day in cases of aneurysm rupture), we compared miRNA expression levels between the two time points in patients with aneurysm rupture. A significant increase was noted in the level of miR-24 on the fifth day compared to the third day after aSAH (FC=1.70, p=0.013), with an AUC value of 0.814 (95% CI: 0.678-0.910; sensitivity=68.00, specificity=88.00, p<0.0001). These results suggest that miR-24 may contribute to the progression of aSAH.

Relationship Between miRNA Expression Patterns and the Clinical Characteristics of Patients with Ruptured Aneurysms

To identify miRNAs that could provide information about the development of ruptured aneurysms and be used as markers, miRNA expression patterns were compared based on the patients' Fisher grades (Grades 1-3 versus 4), Hunt–Hess grades (Grades 1-2 versus 3-5), WFNS grades (Grades 1-2 versus 3-4), and clinical outcomes (mRS scores of 1-2 versus 3-6). No significant difference was observed between miRNA levels and Fisher grades (p>0.05). However, when comparing miRNA levels based on neurological severity, on the third day, the expression of miR-9-3p was significantly reduced in patients with worse neurological conditions (WFNS Grades 3-5) compared to those in better condition (WFNS Grades 1-2; FC=0.53, p=0.047; AUC=0.747, p=0.020; Figure 4A). Similarly, miR-497 expression levels were significantly reduced on the third day in patients with Hunt–Hess Grades 3-5 (FC=0.45, p=0.023; AUC=0.840, p<0.0001; Figure 4B).

Table III: Receiver Operating Characteristic Curve Analysis for Detecting the Effectiveness of microRNAs with Biomarker Potential

Ruptured IA (Day 3 post-SAH) vs Control					**Ruptured IA (Day 5 post-SAH) vs Control**				
miRNA	**Sensitivity (%)**	**Specificity (%)**	**AUC (95% CI)**	**p-value**	**miRNA**	**Sensitivity (%)**	**Specificity (%)**	**AUC (95% CI)**	**p-value**
miR-15a	68.00	100.00	**0.783** (0.602-0.908)	**0.0004***	miR-15a	68.00	100.00	**0.846** (0.674-0.948)	**<0.0001***
miR-183-5p	84.00	100.00	**0.891** (0.731-0.973)	**<0.0001***	miR-183-5p	80.00	100.00	**0.874** (0.709-0.964)	**<0.0001***
miR-126	96.00	85.71	**0.903** (0.745-0.979)	**<0.0001***	miR-126	72.00	85.71	**0.803** (0.625-0.922)	**0.0002***
miR-146-5p	88.00	100.00	**0.914** (0.760-0.984)	**<0.0001***	miR-146-5p	80.00	100.00	**0.903** (0.745-0.979)	**<0.0001***
miR-502-5p	92.00	71.43	**0.866** (0.699-0.960)	**<0.0001***	miR-502-5p	88.00	71.43	**0.820** (0.644-0.933)	**0.0006***
miR-221-3p	92.00	85.71	**0.897** (0.738-0.976)	**<0.0001***	miR-497	64.00	100.00	**0.840** (0.668-0.945)	**<0.0001***
miR-24	88.00	100.00	**0.914** (0.760-0.984)	**<0.0001***					
miR-143-3p	84.00	71.43	**0.837** (0.664-0.943)	**<0.0001***					
miR-27b-3p	76.00	100.00	**0.834** (0.661-0.942)	**<0.0001***					

p value <0.05 is statistically significant,* ***AUC:* *Area under the ROC curve,* ***CI:*** *Confidence interval.*

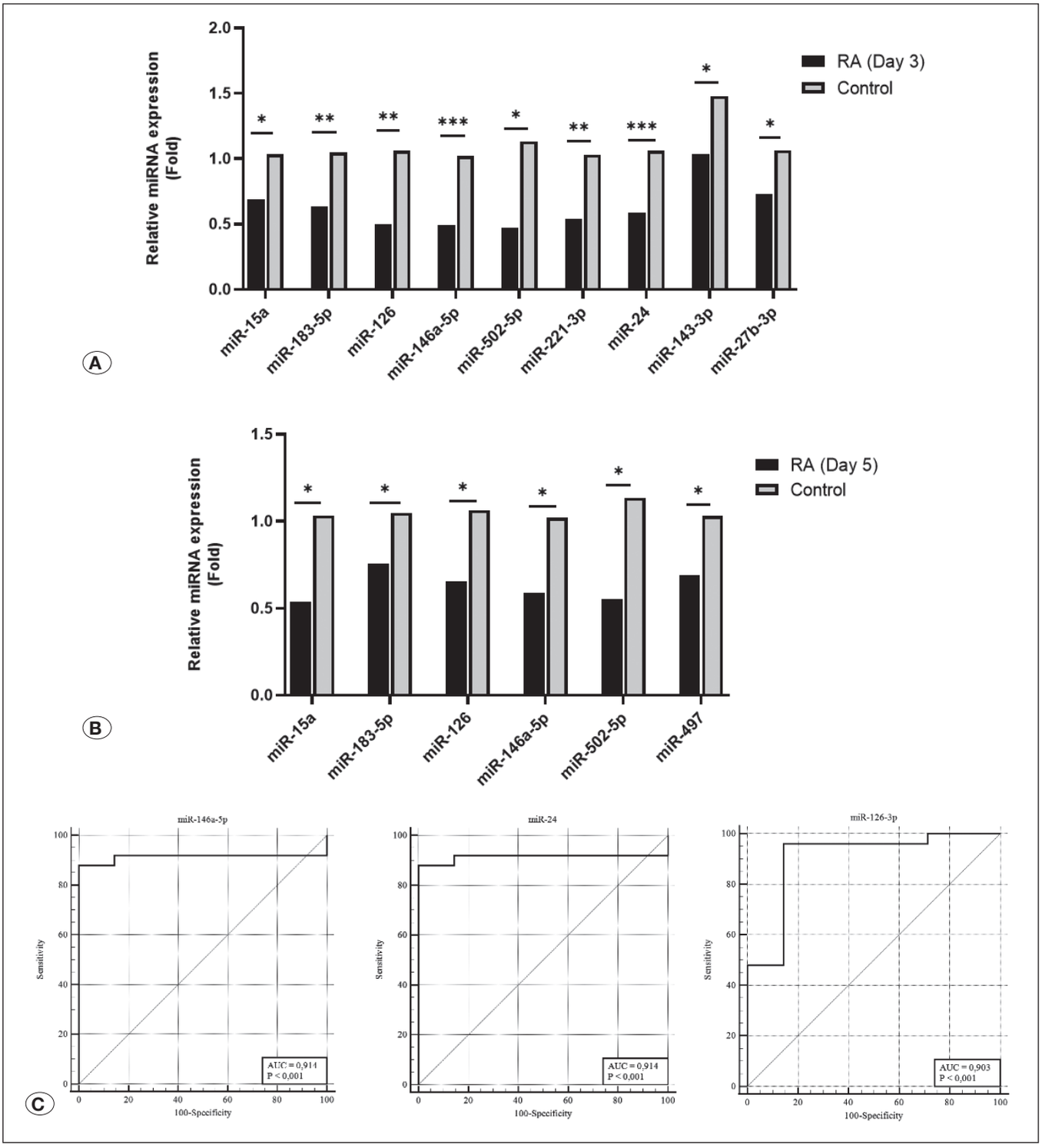

Figure 2: Differential miRNA expression levels in ruptured aneurysm patients versus healthy controls. **A)** Relative expression of miRNAs in ruptured aneurysm patients and controls, presented in bar graphs on a linear scale. miRNA expression levels were significantly downregulated in the RA group compared with controls on Day 3 post-aSAH. **B)** Bar graphs showing six downregulated miRNAs in the RA group compared with controls on Day 5 post-aSAH. Expression levels of all miRNAs are presented as fold changes. Data are shown as means. **C)** ROC curves of patients with ruptured IA and controls. miR-146a-5p, miR-24, and miR-126 achieved AUCs greater than 0.9 on Day 3. Statistically significant differences are marked with asterisks as follows: ***p=0.0001-0.001, **p=0.001-0.01, *p=0.01-0.05. **AUC:** area under the curve, **IA:** Intracranial aneurysm, **RA:** Ruptured aneurysms, **ROC:** Receiver operating characteristic.

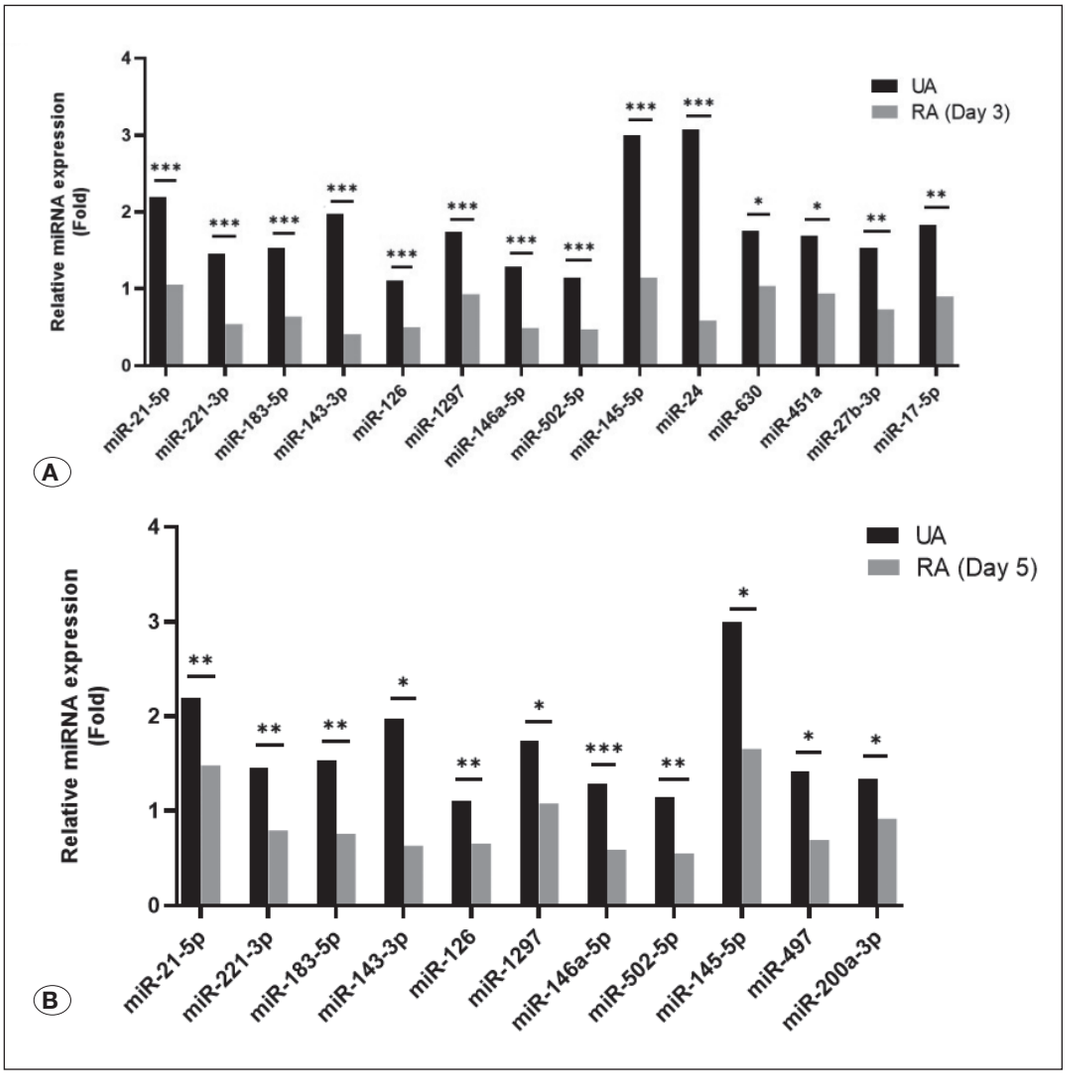

Figure 3: Comparison of the expression levels of differentially expressed miRNAs between groups. **A)** Relative miRNA levels, with a difference between ruptured and unruptured aneurysm cases on Day 3 post-aSAH. **B)** Relative miRNA levels, with a difference between ruptured and unruptured aneurysm cases on Day 5 post-aSAH. miRNA expression levels were significantly downregulated in the RA group compared with the UA group on Days 3 and 5. Statistically significant differences are marked with asterisks as follows: ***p=0.0001-0.001, **p=0.001-0.01, *p=0.01-0.05. **aSAH:** Aneurysmal subarachnoid hemorrhage, **RA:** Ruptured aneurysms, **UA:** Unruptured aneurysms.

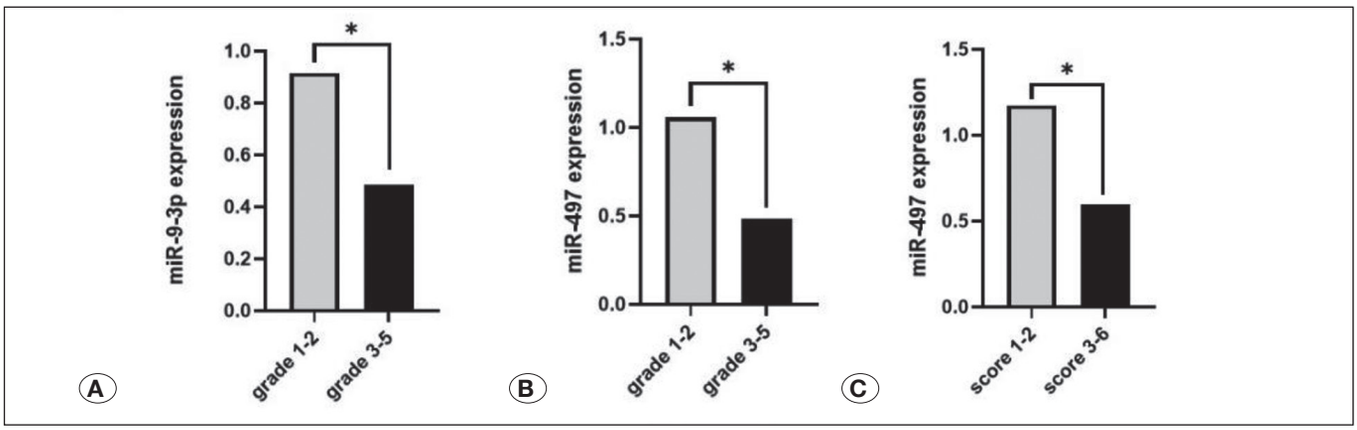

Figure 4: Comparison of miRNA expression in blood with clinical features in aSAH patients. **A)** Relative levels of miR-9-3p in aSAH patients with Hunt–Hess Grades 1-2 and 3-5. **B)** Relative levels of miR-497 in aSAH patients with WFNS Grades 1-2 and 3-5. **C)** Relative levels of miR-497 in aSAH patients with mRS Grades 1-2 (good recovery) and Grades 3-6 (disabled or dead). *A p-value <0.05 is statistically significant. **aSAH:** Aneurysmal subarachnoid hemorrhage, **mRS:** Modified Rankin Scale, **WFNS:** World Federation of Neurosurgical Societies.

Table IV: Receiver Operating Characteristic Curve Analysis for Detecting the Effectiveness of microRNAs with Biomarker Potential in Aneurysmal Rupture

Unruptured vs. Ruptured IA (Day 3 post-SAH)					Unruptured vs. Ruptured IA (Day 5 post-SAH)				
miRNA	**Sensitivity (%)**	**Specificity (%)**	**AUC (95% CI)**	**p-value**	**miRNA**	**Sensitivity (%)**	**Specificity (%)**	**AUC (95% CI)**	**p-value**
miR-21-5p	72.00	76.00	**0.806** (0.670-0.904)	**<0.0001***	miR-21-5p	80.00	76.00	**0.771** (0.631-0.878)	**0.0001***
miR-221-3p	88.00	96.00	**0.894** (0.775-0.963)	**<0.0001***	miR-221-3p	84.00	84.00	**0.849** (0.719-0.934)	**<0.0001***
miR-183-5p	84.00	76.00	**0.818** (0.683-0.913)	**<0.0001***	miR-183-5p	80.00	76.00	**0.784** (0.645-0.888)	**<0.0001***
miR-143-3p	88.00	80.00	**0.878** (0.755-0.954)	**<0.0001***	miR-143-3p	72.00	76.00	**0.730** (0.585-0.845)	**0.0022***
miR-126	88.00	80.00	**0.875** (0.751-0.952)	**<0.0001***	miR-126	60.00	92.00	**0.739** (0.596-0.853)	**0.0010***
miR-1297	88.00	72.00	**0.844** (0.714-0.931)	**<0.0001***	miR-1297	84.00	68.00	**0.758** (0.616-0.868)	**0.0005***
miR-146a-5p	88.00	88.00	**0.882** (0.759-0.956)	**<0.0001***	miR-146a-5p	80.00	88.00	**0.851** (0.722-0.936)	**<0.0001***
miR-502-5p	88.00	72.00	**0.825** (0.691-0.918)	**<0.0001***	miR-502-5p	84.00	72.00	**0.791** (0.653-0.893)	**<0.0001***
miR-145-5p	88.00	68.00	**0.789** (0.650-0.891)	**<0.0001***	miR-145-5p	60.00	80.00	**0.678** (0.531-0.803)	**0.0224***
miR-24	88.00	84.00	**0.867** (0.741-0.947)	**<0.0001***	miR-497	72.00	76.00	**0.761** (0.619-0.870)	**0.0002***
miR-630	72.00	84.00	**0.744** (0.601-0.857)	**0.0010***	miR-200a-3p	84.00	64.00	**0.742** (0.599-0.856)	**0.0008***
miR-451a	64.00	80.00	**0.739** (0.596-0.853)	**0.0008***					
miR-27b-3p	76.00	76.00	**0.775** (0.635-0.881)	**0.0001***					
miR-17-5p	72.00	76.00	**0.757** (0.615-0.867)	**0.0003***					

p value <0.05 is statistically significant,* ***AUC:* *Area under the ROC curve,* ***CI:*** *Confidence interval.*

Additionally, patients classified by clinical outcomes were grouped as well-recovered (mRS scores of 1-2) and those who died or were disabled (mRS scores of 3-6). The expression level of miR-497 was found to be significantly lower on the third day in patients with an mRS score of 3-6 compared to those with mRS scores of 1-2 (FC=0.51, p=0.037; AUC=0.753, p=0.015; Figure 4C).

In the group with mRS scores of 3-6, the expression levels of miR-451a, miR-146a-5p, and miR-502-5p (FC=0.65, FC=0.59, and FC=0.47, respectively) were significantly reduced on the fifth day after SAH. The AUC values for miR-451a, miR-146a-5p, and miR-502-5p were 0.753, 0.773, and 0.813, respectively. These data suggest that they can be used as potential biomarkers to predict clinical outcomes in aSAH patients (Figure 5A, B).

DISCUSSION

Despite considerable efforts to identify non-genetic factors that could serve as predictors for the risk of IA, clinical studies to date have only identified a few traditional risk factors for unruptured IAs, such as age, gender, smoking, and hypertension (47). Comprehensive data regarding the pathogenesis of IAs remain elusive. Additionally, as the early diagnosis of ruptured IAs, which continue to be a significant cause of morbid-

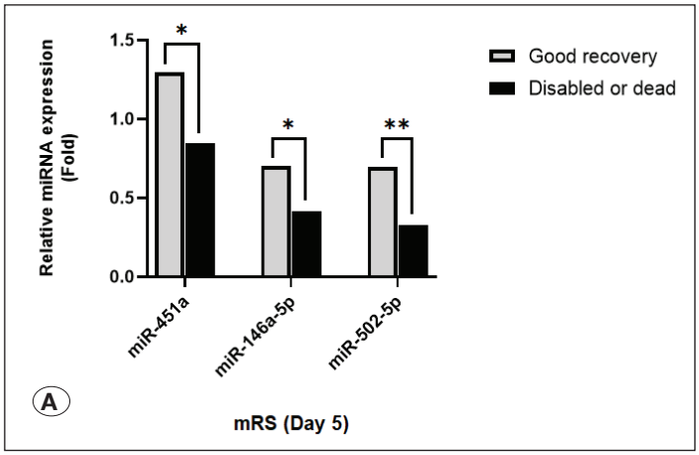

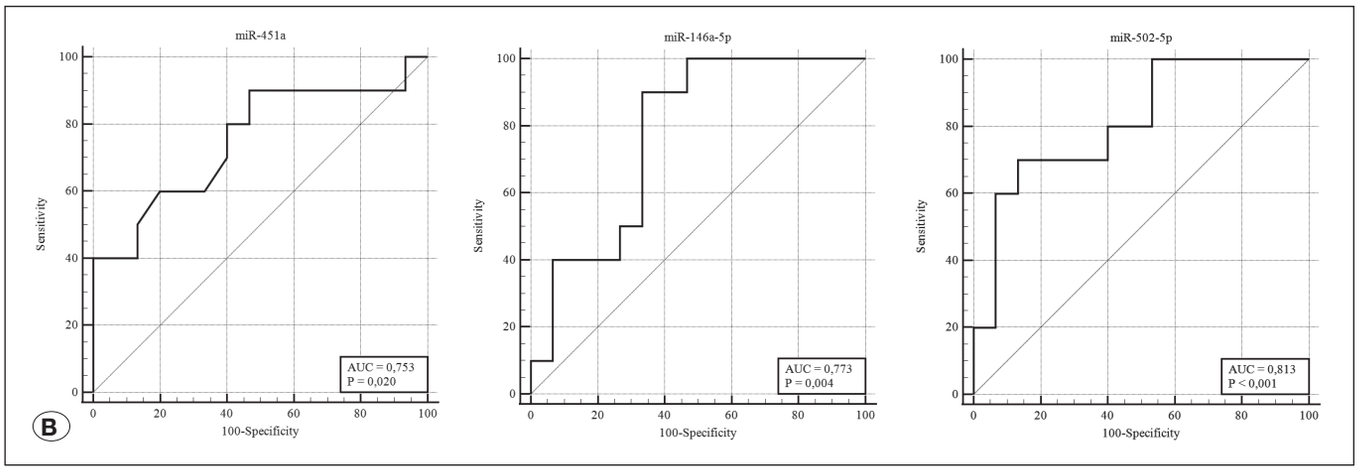

Figure 5: miRNA expression pattern in patients with good and poor clinical outcomes. **A)** Relative levels of miR-451, miR-146a-5p, and miR-502-5p in aSAH patients with good recovery and those who died or became disabled. Expression levels of miR-451, miR-146a-5p, and miR-502-5p were significantly lower in patients with a poor outcome (mRS Grades 3-6) than in those with a good clinical outcome (mRS Grades 1-2) on Day 5 post-SAH. All miRNA levels are presented as fold change. Data are shown as means. **p=0.001-0.01, *p=0.01-0.05. **B)** ROC curve analysis for potential miRNAs and predicted risk of poor outcomes after SAH. miR-502-5p had the strongest predictive value in discriminating patients with good outcomes and those with poor outcomes on Day 5 post-SAH, with an AUC of 0.813, sensitivity of 70%, and specificity of 86.67%. **aSAH:** Aneurysmal subarachnoid hemorrhage, **AUC:** Area under the curve, **mRS:** Modified Rankin Scale, **ROC:** Receiver operating characteristic.

ity and mortality and contribute to the global disease burden, increases the chance of achieving good outcomes, there is a pressing need for easily testable markers that can provide highly accurate information for IA risk, particularly in relation to predicting and prognosticating aSAH (40,53). miRNAs, which are non-coding RNAs, are found in various biological fluids, including plasma, serum, and CSF and are involved in many physiological processes through their roles in gene expression regulation. Therefore, their abnormal expression can often disrupt cellular and biological functions and contribute to the development and progression of disease. Due to their resistance to nucleases and high stability in body fluids (16), miRNAs have been demonstrated to be potential biomarkers for the development of numerous diseases, including cancer, cardiovascular disease, and neurological conditions (10,42). Recently, leveraging these characteristics of miRNAs to identify asymptomatic IAs, predict the risk of ruptured IAs, and provide information about clinical progression has gained importance. A feature of our study is that samples from ruptured cases were collected separately on the third and fifth days of bleeding and analyzed. The aim was to identify miRNAs that may influence the risk of clinical deterioration, such as vasospasm, around the fourth to fifth days post-bleeding.

Research on complications and prognosis following aSAH remains limited. Few studies have examined the relationship between miRNA expression and factors such as vasospasm, delayed cerebral ischemia (DCI), or overall prognosis. Unfortunately, many of these findings lack consistency across different cohorts because of methodological heterogeneities (8).

miRNAs have the potential to serve as prognostic biomarkers for patients with aSAH. Increase in the expression levels of let-7b-5p, miR-19b-3p, miR-125-5p, miR-221-3p, miR-21-5p, and miR-27a-3p in CSF have been associated with a higher risk of delayed cerebral vasospasm (DCV) in SAH patients. Similarly, elevated levels of let-7a-5p, miR-146a-5p, miR-204-5p, miR-221-3p, miR-23a-3p, and miR-497-5p expression in plasma samples taken 3 days post-aSAH have been linked to DCV (34).

miRNAs and their target genes play distinct roles in vascular endothelial inflammation and phenotypic changes of vessel cells. The formation and rupture of IAs have been reported to be associated with endothelial cell dysfunction. Therefore, miRNAs act as epigenetic elements involved in the inflammatory process of aneurysms (47,50).

In a study by Wang et al., the expression profiles of miRNAs in CSF and plasma samples collected from patients with and without DCV were compared 3 and 7 days after aneurysm rupture. Notably, in CSF, miRNAs including let-7b-5p, miR-15b-5p, miR-17-5p, miR-19b-3p, miR-20a-5p, miR-24-3p,

and miR-29a-3p demonstrated an AUC of 1, indicating perfect discrimination. Likewise, let-7a-5p, miR-146a-5p, miR-204-5p, miR-221-3p, miR-23a-3p, and miR-497-5p in plasma achieved AUCs greater than 0.8, demonstrating their strong potential to differentiate between DCV+ and DCV– 3 days after aSAH, even before the onset of DCV events. The authors highlighted their newly designed miRNA panel as a reliable predictor of DCV risk, offering substantial potential for the clinical management of aSAH patients. Previous studies also reported that elevated miR-21-5p and miR-221-3p levels in CSF correlated with DCI, while miR-221-3p, miR-132-3p, and miR-19b-3p in CSF were associated with DCV. Additionally, temporal changes of let-7b-5p and miR-92a-3p in CSF, as well as miR-15a in both the CSF and plasma of DCI patients, have been reported (50).

Jin et al. found that the relative expression of miR-21 was downregulated in the serum specimens of IA patients compared with controls. Of note, the reduction in miR-21 expression was most pronounced in the group with daughter aneurysms. They suggested that the decreased expression of miR-21 in IA cases might offer diagnostic insights regarding aneurysm rupture and could inform clinical intervention (15).

miRNA-21 regulates vascular smooth muscle activity by targeting proteins such as phosphatase and tensin homologous protein (PTEN), Bcl-2, and PDCD-4. When miRNA-21 is expressed at low levels, PTEN expression increases, which reduces the phosphorylation and activation of AKT. This reduction is significant because AKT is a key player in an anti-apoptotic and pro-proliferative pathway that limits IA expansion and the progression of vascular disorders. Recent scientific reports have highlighted the specific role of miR-21 in regulating the biological function of endothelial progenitor cells (EPCs). Studies have shown that exosomes derived from EPCs carry miR-21-5p, which specifically suppresses the expression of thrombospondin 1 (THBS1), an angiogenesis inhibitor, in endothelial cells, thereby facilitating the repair of vascular endothelial cells (11,32). A study conducted by Chen et al. in mouse models revealed that the miR-21 expression level influences the formation and rupture of IA through the JNK signaling pathway-mediated inflammatory response. This finding aligns with our research (4). When the expression of miRNA-21, which acts comprehensively and regulates multiple pathways, decreases, its protective efficacy diminishes, contributing to aneurysm formation due to wall remodeling. Therefore, circulating miRNA-21 expression levels may serve as a useful diagnostic/prognostic biomarker for IAs.

miR-15a plays a significant role in ischemia-induced cerebral vascular endothelial damage, vascular angiogenesis, and endothelial cell proliferation. Previously, increased and decreased expression of miR-15a have been reported to significantly reduce and increase cerebral vascular endothelial cell death due to oxygen-glucose deprivation, respectively. In addition, elevated miR-15a expression may contribute to vascular proliferation or angiogenesis, potentially leading to the development of vasospasm (56,57).

In a study by Supriya et al., miR-15a-5p expression was significantly increased in aSAH cases compared to controls (40). Conversely, Kikkawa et al. (18), in evaluating the chronological changes in miR-15a expression levels in plasma and CSF samples of patients with SAH, found that miR-15a expression decreased from Day 1 to Day 3 in plasma and increased in CSF. In contrast, its expression increased in plasma from Day 5 and remained constant on Day 7. In general, since delayed cerebral ischemia, which is the main cause of clinical deterioration in patients with SAH, mostly occurs between Days 4 and 10 after the onset of SAH, miR-15a expression may also be related to the clinical course of the cases. However, when the clinical scores and miRNA expression of the cases included in this study were compared, no relationship due to miR-15a expression was noted.

Ding et al. studied changes in CSF proteins in aSAH patients using multitargeted Olink proteomics (including a 96-neurology panel and a 96-inflammation panel) to elucidate the pathophysiology of DCI and provide valuable insights into its molecular basis for clinical applications. Based on the neurology panel, they identified several CSF proteins in aSAH patients, mainly MSR1, siglec-1, siglec-9, CTSC, and CTSS. These proteins are involved in defense response regulation, vesicle-mediated transport, and regulation of immune response. Additionally, differentially expressed proteins were notably enriched in various pathways, including the MAPK signaling pathway, RAS signaling pathway, cytokine-cytokine receptor interaction, and lysosome and phagosome pathways. In the inflammation panel, the predominantly identified proteins were IL-6, MCP-1, CXCL10, CXCL-9, and TRAIL, which are involved in the cellular responses to chemokines and chemokine-mediated signaling pathways. Additionally, these differentially expressed proteins were mainly enriched in cytokine-cytokine receptor interactions, viral protein interactions with cytokines and their receptors, chemokine signaling pathways, the NF-κB signaling pathway, and the Toll-like receptor signaling pathway (6). Lu et al. identified a panel of four miRNAs (miR-4532, miR-4463, miR-1290, and miR-4793) that can effectively distinguish SAH patients with DCI from those without DCI, achieving an AUC of 100%. The targets of these miRNAs were found to be enriched in various developmental pathways, including the Wnt, hedgehog, and oxytocin signaling pathways (24).

In our study, we observed a significant decrease in the expression of miR-143 in samples taken on the third day from ruptured cases compared to controls. This finding aligns with previous studies (14,16,39). Recently, the downregulation of miR-143-3p and miR-125b-5p was reported to be associated with worse neurological conditions and the occurrence of vasospasm (8). The downregulation of miR-143 has been identified as a critical step contributing to vascular smooth muscle cells (VSMC) phenotypic modulation, which is essential for cerebral aneurysm formation. In most IA walls, VSMCs migrate to the intima and undergo modulation from a contractile to a synthetic phenotype. This results in their dissociation and leads to myointimal hyperplasia. Several researchers have shown that this process leads to the loss of the structural integrity of the media, the layer that provides support to the vessel wall (1,3,52). Xu et al. reported that both miR-143 and miR-145 interact with the 3'-UTR of KLF5, inhibiting its

post-transcriptional expression (54). Consequently, the downregulation of miR-143/145, combined with the upregulation of KLF5, suggests that VSMC phenotypic modulation significantly influences the formation and growth of IAs. Moreover, NLRP1, a predicted target of miR-143-3p, is a member of the Ced-4 family of apoptosis proteins that can induce caspase-1 activation through the assembly of inflammasomes, which are critical for the production of mature proinflammatory cytokines, including IL-1β and IL-18. IL-18, a predicted target of miR-143-3p, enhances early-stage apoptosis of cultured human umbilical vein endothelial cells and increases vascular endothelial cell death. These interactions suggest that miR-143-3p may play a crucial role in the pathogenesis of IA by regulating apoptosis and inflammation-related pathways (14).

Ryu and colleagues reported that several miRNAs, specifically miR-4732-3p, miR-16-2-3p, miR-6885-3p, miR-29a-3p, miR-148b-3p, miR-374b-5p, and miR-26b-5p, displayed differing levels between patients with and without cerebral vasospasm (CVS). Interestingly, miR-148b-3p was the only differentially expressed miRNA that interacted with rho-associated protein kinase 1 (ROCK1). This interaction is significant, as ROCK1 plays a role in regulating endothelial and vascular tone during vasospasm, and miR-148b-3p was found to be upregulated in patients. The study showed that miR-148b-3p directly interacts with ROCK1, reducing its expression and influencing cell growth, migration, and invasion in human brain endothelial cells through the ROCK-LIMK-cofilin pathway. Moreover, disruption of the ROCK-LIMK-cofilin pathway leads to abnormal organization of the actin cytoskeleton, ultimately causing endothelial cell dysfunction, and may contribute to the development of vasospasm. Notably, cofilin has also been implicated in other forms of brain injury, such as intracerebral hemorrhage and traumatic brain injury, as it influences inflammation and synaptic plasticity. This highlights miR-148b-3p's potential as a promising biomarker and therapeutic target for CVS following aSAH (33).

An in vitro study that simulated the post-SAH extracellular environment highlighted the critical role of exosomal miR-630 in disease pathology. When brain microvascular endothelial cells (BMECs) were exposed to a culture medium containing blood-cerebrospinal fluid, a significant reduction in exosomal miR-630 level was observed, aligning closely with the alterations in CSF exosomal miR-630 in aSAH patients. Additionally, BMECs co-cultured with exosomes transfected with miR-630 mimics exhibited a marked upregulation of ICAM-1, VCAM-1, and the tight junction protein ZO-1 compared to the control group. These findings suggest that exosomal miR-630 may play a pivotal role in modulating cell adhesion and maintaining tight junction integrity in BMECs, potentially contributing to the enhancement of the brain microcirculation (21).

Lopes et al. utilized an NGS platform to analyze global miRNA profiling in whole blood samples from 26 patients, both with and without vasospasm. Their study identified five downregulated miRNAs (miR-7f-5p, miR-126-5p, miR-17-5p, miR-451a, and miR-486-5p) and three upregulated miRNAs (miR-146a-5p, miR-589-5p, and miR-941) that were differentially expressed in aSAH patients compared to controls. Notably, in silico analysis revealed that the THBS1 and VEGFA target genes are associated with aSAH (23). In another study involving serum samples from patients with intracerebral hemorrhage, miR-126 showed a significant decrease in patients compared to controls and was correlated with perihematomal edema. The authors proposed that miR-126 can be used as a potential biomarker for managing perihematomal edema (60). Additionally, Yang et al. (55) found significant alterations in miR-126 levels in patients with IA. Their results showed that both lesion size and miR-126 expression were independent risk factors for aneurysmal rupture, leading them to hypothesize that circulating miR-126 might be a potential diagnostic biomarker for IA occurrence and rupture. Our study also demonstrated that miR-126 expression was significantly decreased in ruptured cases compared to controls, suggesting its potential as an effective marker for distinguishing between ruptured and non-ruptured cases.

Supriya et al. (40) identified five downregulated miRNAs (miR-146a-5p, miR-376c-3p, miR-18b-5p, miR-24-3p, and miR-27b-3p) and three upregulated miRNAs (miR-15a-5p, miR-34a-5p, and miR-374a-5p) that can discriminate between aSAH patients and controls. In addition, circulating levels of miR-146a-5p and miR-27b-3p were associated with the severity of aSAH and patient outcomes. Functional analysis of these differentially expressed miRNAs showed that their target genes were involved in signaling pathways related to inflammation, suggesting they may play critical roles in IA pathology. In a preclinical study, a decreased level of miR-146a was observed in the perihematomal area 48 hours after intracerebral hemorrhage, confirming its anti-inflammatory potential (17).

A PCR array study indicated that circulating miRNA-183-5p, miRNA-let7b-5p, and miRNA-200a-3p were differentially expressed in aSAH patients. Most importantly, elevated levels of miRNA-200a-3p were found exclusively in aSAH patients and not in those with UA, indicating that circulating miR-200a-3p may influence the risk of aneurysmal rupture. Functional analyses of miRNA-183-5p and miRNA-200a-3p showed that their target genes were associated with signaling pathways involved in inflammation and cell proliferation. This evidence suggests that these miRNAs may serve as biomarkers for diagnosing IA and assessing the risk of its subsequent rupture (15,27).

Zheng et al. conducted a comparative analysis of the miRNA expression profiles of peripheral blood samples from patients with aSAH, reporting downregulated expression of miR-23b-3p, miR-590-5p, miR-20b-5p, miR-142-3p, and miR-29b-3p in aSAH patients compared to controls. These miRNAs target genes closely linked to the formation, progression, and rupture of IA, such as TGM2, EREG, EDN1, and COL4A1. Several pathways implicated in SAH were enriched in their analysis, including the Hippo signaling pathway, p53 signaling pathway, cellular senescence, AMPK signaling pathway, focal adhesion, osteoclast differentiation, and the cell cycle. Notably, altered expression of miRNA-23b-3p and miRNA-29b has been demonstrated in IA tissues compared to normal tissues. Additionally, miR-23b is linked to the inflammatory response,

while miR-20b-5p appears to influence the progression of IA by modulating actin cytoskeleton biogenesis. Further research indicates that the decreased expression of miR-590-5p in aSAH enhances angiotensin II-induced endothelial cell apoptosis (58).

Our study also explored the relationships between miRNAs, the severity of aSAH, and the clinical outcomes of the cases. Lai et al. identified significant changes in the expression of miR-502-5p and miR-1297 in aSAH patients (20). Furthermore, they reported a strong correlation between elevated expression levels of circulating miR-502-5p and poor neurological outcomes. These findings suggest that miR-502-5p may serve as a potential biomarker for the diagnosis and prognosis of aSAH. In another study, Bache et al. analyzed miRNA expression in CSF samples from 63 SAH patients and assessed its relationships with severity and post-SAH clinical outcomes (2). They found that high levels of miR-9-3p were associated with poor functional outcomes (mRS 3-6) 3 months later. Additionally, they found that high levels of miR-451a were associated with poor neurological status at admission, as measured by the WFNS grade. Two target genes of miR-451a, MMP-2 and MMP-9, are considered significant in the pathogenesis of SAH and its complications due to their roles in the extracellular matrix and immune responses (26,37). Studies on ischemic stroke have also shown that higher levels of miR-9 in CSF or plasma are associated with increased severity and larger infarct volume, suggesting its potential as a future research target (8). The differences in sample sizes make it challenging to directly compare these studies and our findings when assessing the severity of SAH and clinical outcomes.

Our data generally align with those of previous studies. However, small sample sizes, the heterogeneity of the specimens examined, varying sample collection time points, and different miRNA analysis methodologies may have caused discrepancies therein.

We acknowledge some limitations of our current study. First, the small size of our study cohort is an important limitation. Second, the samples could only be collected from RA patients at two time points (3 and 5 days post-SAH). The levels of differentially expressed miRNA in biofluids following SAH can be dynamic (18,32,35,36). Regularly monitoring changes in these miRNA levels could provide more accurate timing for predicting neurological outcomes and preventing complications, thus allowing physicians to adjust therapies for aSAH more effectively. Finally, utilizing additional approaches, such as high-throughput sequencing methods and miRNA-targeted gene expression studies, could help identify novel diagnostic and prognostic biomarkers of IAs and their subsequent rupture.

CONCLUSION

We demonstrated that miRNA expression differences are valuable for distinguishing aSAH cases. In particular, levels of circulating miR-146a-5p, miR-24, and miR-126 measured 72 h after aSAH showed an AUC value greater than 0.9. When comparing the RA and UA groups, several miRNAs were found to be significantly altered in patients with RA. Our results indicate that the levels of these miRNAs on the third day after aSAH can discriminate RA from UA with a higher predicted probability (AUC>0.8) compared to other time points. Additionally, we showed that circulating miR-9-3p and miR-497 have prognostic value for assessing the severity of aSAH, while miR-451a, miR-146a-5p, miR-502-5p, and miR-497 can predict poor clinical outcomes after admission. Future studies are needed to validate these findings in larger cohorts and better understand the specific roles of these miRNAs in the progression and rupture of IAs before they are implemented in clinical practice.

Declarations

Funding: This study was supported by the Scientific Research Projects Fund of Eskisehir Osmangazi University [TCD-2021-1737].

Availability of data and materials: The datasets generated and/or analyzed during the current study are available from the corresponding author by reasonable request.

Disclosure: The authors declare no competing interests.

AUTHORSHIP CONTRIBUTION

Study conception and design: SKA, EEG, EO, SA
Data collection: EO, AOO, OA
Analysis and interpretation of results: SKA, EEG, ES, BDA, SA, EC
Draft manuscript preparation: SKA, EEG, EO
Critical revision of the article: AOO, SA
Other (study supervision, fundings, materials, etc...): SA
All authors (SKA, EEG, EO, OA, EC, ES, BDA, AOO, SA) reviewed the results and approved the final version of the manuscript.

REFERENCES

1. Ali MS, Starke RM, Jabbour PM, Tjoumakaris SI, Gonzalez LF, Rosenwasser RH, Owens GK, Koch WJ, Greig NH, Dumont AS: TNF induces phenotypic modulation in cerebral vascular smooth muscle cells: Implications for cerebral aneurysm pathology. J Cereb Blood Flow Metab 33:1564-1573, 2013. https://doi.org/10.1038/jcbfm.2013.109
2. Bache S, Rasmussen R, Wolcott Z, Rossing M, Møgelvang R, Tolnai D, Hassager C, Forman JL, Køber L, Nielsen FC, Kimberly WT, Møller K: Elevated miR-9 in cerebrospinal fluid is associated with poor functional outcome after subarachnoid hemorrhage. Transl Stroke Res 11:1243-1252, 2020. https://doi.org/10.1007/s12975-020-00793-1
3. Boon RA, Dimmeler S: MicroRNAs and aneurysm formation. Trends Cardiovasc Med 21:172-177, 2011. https://doi.org/10.1016/j.tcm.2012.05.005
4. Chen Z, Song S, Zhu J, Lai X: Regulatory mechanism of MiR-21 in formation and rupture of intracranial aneurysm through JNK signaling pathway-mediated inflammatory response. Int J Clin Exp Pathol 13:1834-1841, 2020.
5. Cheng X, Ander BP, Jickling GC, Zhan X, Hull H, Sharp FR, Stamova B: MicroRNA and their target mRNAs change expression in whole blood of patients after intracerebral hemorrhage. J Cereb Blood Flow Metab 40:775-786, 2020. https://doi.org/10.1177/0271678X19839501

6. Ding R, Wu L, Wei S, Lu H, Qin X, Liu X, Wang Y, Liu W, Li H, Luo B, Xie T, Chen Z: Multi-targeted olink proteomics analyses of cerebrospinal fluid from patients with aneurysmal subarachnoid hemorrhage. Proteome Sci 22:11, 2024. https://doi.org/10.1186/s12953-024-00236-x
7. Feng X, Peng F, Zhang B, Wang L, Guo E, Li Y, Jiang C, Wu Z, Liu A: Lower miR-143/145 and higher matrix metalloproteinase-9 levels in circulation may be associated with intracranial aneurysm formation and rupture: A pilot study. Clin Neurol Neurosurg 173:124-129, 2018. https://doi.org/10.1016/j.clineuro.2018.08.010
8. Fernández-Pérez I, Macias-Gómez A, Suárez-Pérez A, Vallverdú-Prats M, Giralt-Steinhauer E, Bojtos L, Susin-Calle S, Rodriguez-Campello A, Guisado-Alonso D, Jimenez-Balado J, Jiménez-Conde J, Cuadrado-Godia E: The role of epigenetics in brain aneurysm and subarachnoid hemorrhage: A comprehensive review. Int J Mol Sci 25:3433, 2024. https://doi.org/10.3390/ijms25063433
9. Fisher CM, Kistler JP, Davis JM. Relation of cerebral vasospasm to subarachnoid hemorrhage visualized by computerized tomographic scanning. Neurosurgery 6:1-9, 1980.
10. Gareev I, Beylerli O, Yang G, Izmailov A, Shi H, Sun J, Zhao B, Liu B, Zhao S: Diagnostic and prognostic potential of circulating miRNAs for intracranial aneurysms. Neurosurg Rev 44:2025-2039, 2021. https://doi.org/10.1007/s10143-020-01427-8
11. Hu H, Wang B, Jiang C, Li R, Zhao J: Endothelial progenitor cell-derived exosomes facilitate vascular endothelial cell repair through shuttling miR-21-5p to modulate Thrombospondin-1 expression. Clinical Science 133:1629-1644, 2019. https://doi.org/10.1042/CS20190188
12. Hunt WE, Hess RM. Surgical risk as related to time of intervention in the repair of intracranial aneurysms. J Neurosurg 28(1):14-20, 1968. doi:10.3171/jns.1968.28.1.0014. PMID 5635959
13. Iwuchukwu I, Nguyen D, Sulaiman W: MicroRNA profile in cerebrospinal fluid and plasma of patients with spontaneous intracerebral hemorrhage. CNS Neurosci Ther 22:1015-1018, 2016. https://doi.org/10.1111/cns.12656
14. Jiang Y, Zhang M, He H, Chen J, Zeng H, Li J, Duan R: MicroRNA/mRNA profiling and regulatory network of intracranial aneurysm. BMC Med Genomics 6:1, 2013. https://doi.org/10.1186/1755-8794-6-36
15. Jin H, Jiang Y, Liu X, Meng X, Li Y: Cell-free microRNA-21: Biomarker for intracranial aneurysm rupture. Chinese Neurosurg J 6:1–11, 2020. https://doi.org/10.1186/s41016-020-00195-0
16. Kamal NNSBNM, Shahidan WNS: Non-exosomal and exosomal circulatory MicroRNAs: Which are more valid as biomarkers? Front Pharmacol 10:1500, 2020. https://doi.org/10.3389/fphar.2019.01500
17. Kashif H, Shah D, Sukumari-Ramesh S: Dysregulation of microRNA and intracerebral hemorrhage: Roles in neuroinflammation. Int J Mol Sci 22:8115, 2021. https://doi.org/10.3390/ijms22158115
18. Kikkawa Y, Ogura T, Nakajima H, Ikeda T, Takeda R, Neki H, Kohyama S, Yamane F, Kurogi R, Amano T, Nakamizo A, Mizoguchi M, Kurita H: Altered expression of MicroRNA-15a and kruppel-like factor 4 in cerebrospinal fluid and plasma after aneurysmal subarachnoid hemorrhage. World Neurosurg 108:909-916.e3, 2017. https://doi.org/10.1016/j.wneu.2017.09.008
19. Lai N, Wu D, Liang T, Pan P, Yuan G, Li X, Li H, Shen H, Wang Z, Chen G: Systemic exosomal miR-193b-3p delivery attenuates neuroinflammation in early brain injury after subarachnoid hemorrhage in mice. J Neuroinflammation 17:1-14, 2020. https://doi.org/10.1186/s12974-020-01745-0
20. Lai NS, Zhang JQ, Qin FY, Sheng B, Fang XG, Li ZB: Serum microRNAs are non-invasive biomarkers for the presence and progression of subarachnoid haemorrhage. Biosci Rep 37:1–10, 2017. https://doi.org/10.1042/BSR20160480
21. Liao L, Wang H, Wei D, Yi M, Gu Y, Zhang M, Wang L: Exosomal microRNAs: Implications in the pathogenesis and clinical applications of subarachnoid hemorrhage. Front Mol Neurosci 16:1-13, 2023. https://doi.org/10.3389/fnmol.2023.1300864
22. Liu D, Han L, Wu X, Yang X, Zhang Q, Jiang F: Genome-wide microRNA changes in human intracranial aneurysms. BMC Neurol 14:1-11, 2014. https://doi.org/10.1186/s12883-014-0188-x
23. Lopes KDP, Vinasco-Sandoval T, Vialle RA, Paschoal FM, Bastos VAPA, Bor-Seng-Shu E, Teixeira MJ, Yamada ES, Pinto P, Vidal AF, Ribeiro-Dos-Santos A, Moreira F, Santos S, Paschoal EHA, Ribeiro-Dos-Santos Â: Global miRNA expression profile reveals novel molecular players in aneurysmal subarachnoid haemorrhage. Sci Rep 8:1-11, 2018. https://doi.org/10.1038/s41598-018-27078-w
24. Lu G, Wong MS, Xiong MZQ, Leung CK, Su XW, Zhou JY, Poon WS, Zheng VZY, Chan WY, Wong GKC: Circulating MicroRNAs in delayed cerebral infarction after aneurysmal subarachnoid hemorrhage. J Am Heart Assoc 6:25-28, 2017. https://doi.org/10.1161/JAHA.116.005363
25. Maegdefessel L, Spin JM, Raaz U, Eken SM, Toh R, Azuma J, Adam M, Nagakami F, Heymann HM, Chernugobova E, Jin H, Roy J, Hultgren R, Caidahl K, Schrepfer S, Hamsten A, Eriksson P, McConnell M V., Dalman RL, Tsao PS: MiR-24 limits aortic vascular inflammation and murine abdominal aneurysm development. Nat Commun 5:1-13, 2014. https://doi.org/10.1038/ncomms6214
26. McGirt MJ, Lynch JR, Blessing R, Warner DS, Friedman AH, Laskowitz DT, Lawton MT, Awad IA, Max Findlay J, Friedlander RM: Serum von Willebrand factor, matrix metalloproteinase-9, and vascular endothelial growth factor levels predict the onset of cerebral vasospasm after aneurysmal subarachnoid hemorrhage. Neurosurgery 51:1128-1135, 2002. https://doi.org/10.1097/00006123-200211000-00005
27. Meeuwsen JAL, Van't Hof FNG, Van Rheenen W, Rinkel GJE, Veldink JH, Ruigrok YM: Circulating microRNAs in patients with intracranial aneurysms. PLoS One 12:1–11, 2017. https://doi.org/10.1371/journal.pone.0176558
28. Mijiti M, Mijiti P, Axier A, Amuti M, Guohua Z, Xiaojiang C, Kadeer K, Xixian W, Geng D, Maimaitili A: Incidence and predictors of angiographic vasospasm, symptomatic vasospasm and cerebral infarction in chinese patients with aneurysmal subarachnoid hemorrhage. PLoS One 11:1-12, 2016. https://doi.org/10.1371/journal.pone.0168657

29. Olivieri F, Prattichizzo F, Giuliani A, Matacchione G, Rippo MR, Sabbatinelli J, Bonafè M: miR-21 and miR-146a: The microRNAs of inflammaging and age-related diseases. Ageing Res Rev 70:101374, 2021. https://doi.org/10.1016/j.arr.2021.101374
30. Powers CJ, Dickerson R, Zhang SW, Rink C, Roy S, Sen CK: Human cerebrospinal fluid microRNA: Temporal changes following subarachnoid hemorrhage. Physiol Genomics 1240:361-366, 2021. https://doi.org/10.1152/physiolgenomics.00052.2015
31. Rankin J. Cerebral vascular accidents in patients over the age of 60. II. Prognosis. Scott Med J 2(5):200-215, 1957. doi:10.1177/003693305700200504. PMID 13432835. S2CID 29669359
32. Report of World Federation of Neurological Surgeons Committee on a Universal Subarachnoid Hemorrhage Grading Scale. J Neurosurg 68(6):985-986, 1988. doi:10.3171/jns.1988.68.6.0985
33. Ryu JY, Zhang J, Tirado SR, Dagen S, Frerichs KU, Patel NJ, Aziz-Sultan MA, Brown A, Rogers-Grazado M, Amr SS, Weiss ST, Du R: MiRNA expression profiling reveals a potential role of microRNA-148b-3p in cerebral vasospasm in subarachnoid hemorrhage. Sci Rep 14:1-12, 2024. https://doi.org/10.1038/s41598-024-73579-2
34. Segherlou ZH, Saldarriaga L, Azizi E, Vo KA, Reddy R, Siyanaki MRH, Lucke-Wold B: MicroRNAs' role in diagnosis and treatment of subarachnoid hemorrhage. Diseases 11:1-12, 2023. https://doi.org/10.3390/diseases11020077
35. Sheng B, Fang X, Liu C, Wu D, Xia D, Xu S, Lai N: Persistent high levels of miR-502-5p are associated with poor neurologic outcome in patients with aneurysmal subarachnoid hemorrhage. World Neurosurg 116:e92–e99, 2018. https://doi.org/10.1016/j.wneu.2018.04.088
36. Sheng B, Lai NS, Yao Y, Dong J, Li ZB, Zhao XT, Liu JG, Li XQ, Fang XG: Early serum miR-1297 is an indicator of poor neurological outcome in patients with aSAH. Biosci Rep 38:1–8, 2018. https://doi.org/10.1042/BSR20180646
37. Stylli SS, Adamides AA, Koldej RM, Luwor RB, Ritchie DS, Ziogas J, Kaye AH: miRNA expression profiling of cerebrospinal fluid in patients with aneurysmal subarachnoid hemorrhage. J Neurosurg 126:1131-1139, 2017. https://doi.org/10.3171/2016.1.JNS151454
38. Sun L, Zhang W, Li Z, Li M, Guo J, Wang H, Wang X: The expression of cerebrospinal fluid exosomal miR-630 plays an important role in the dysfunction of endothelial cells after subarachnoid hemorrhage. Sci Rep 9:1–8, 2019. https://doi.org/10.1038/s41598-019-48049-9
39. Supriya M, Christopher R, Devi BI, Bhat DI, Shukla D, Kalpana SR: Altered MicroRNA expression in intracranial aneurysmal tissues: Possible role in TGF-β signaling pathway. Cell Mol Neurobiol 42:2393-2405, 2022. https://doi.org/10.1007/s10571-021-01121-3
40. Supriya M, Christopher R, Indira Devi B, Bhat DI, Shukla D: Circulating MicroRNAs as potential molecular biomarkers for intracranial aneurysmal rupture. Mol Diagnosis Ther 24:351-364, 2020. https://doi.org/10.1007/s40291-020-00465-8
41. Taufique Z, May T, Meyers E, Falo C, Mayer SA, Agarwal S, Park S, Connolly ES, Claassen J, Schmidt JM: Predictors of poor quality of life 1 year after subarachnoid hemorrhage. Neurosurgery 78:256-263, 2016. https://doi.org/10.1227/NEU.0000000000001042
42. Terrinoni A, Calabrese C, Basso D, Aita A, Caporali S, Plebani M, Bernardini S: The circulating miRNAs as diagnostic and prognostic markers. Clin Chem Lab Med 57:932–953, 2019. https://doi.org/10.1515/cclm-2018-0838
43. Texakalidis P, Sweid A, Mouchtouris N, Peterson EC, Sioka C, Rangel-Castilla L, Reavey-Cantwell J, Jabbour P: Aneurysm formation, growth, and rupture: The biology and physics of cerebral aneurysms. World Neurosurg 130:277-284, 2019. https://doi.org/10.1016/j.wneu.2019.07.093
44. Tsai PC, Liao YC, Wang YS, Lin HF, Lin RT, Juo SHH: Serum microrna-21 and microrna-221 as potential biomarkers for cerebrovascular disease. J Vasc Res 50:346–354, 2013. https://doi.org/10.1159/000351767
45. Unda SR: microRNAs potential biomarkers and therapeutic targets for intracranial aneurysm. J Clin Epigenetics 4:3-5, 2018. https://doi.org/10.21767/2472-1158.100087
46. Vlak MHM, Rinkel GJE, Greebe P, Greving JP, Algra A: Lifetime risks for aneurysmal subarachnoid haemorrhage: Multivariable risk stratification. J Neurol Neurosurg Psychiatry 84:619-623, 2013. https://doi.org/10.1136/jnnp-2012-303783
47. Wang RK, Sun YY, Li GY, Yang HT, Liu XJ, Li KF, Zhu X, Yu GY: MicroRNA-124-5p delays the progression of cerebral aneurysm by regulating FoxO1. Exp Ther Med 22:1-8, 2021. https://doi.org/10.3892/etm.2021.10606
48. Wang WH, Wang YH, Zheng LL, Li XW, Hao F, Guo D: MicroRNA-29a: A potential biomarker in the development of intracranial aneurysm. J Neurol Sci 364:84-89, 2016. https://doi.org/10.1016/j.jns.2016.03.010
49. Wang WX, Springer JE, Hatton KW: Micrornas as biomarkers for predicting complications following aneurysmal subarachnoid hemorrhage. Int J Mol Sci 22:9492, 2021. https://doi.org/10.3390/ijms22179492
50. Wang WX, Springer JE, Xie K, Fardo DW, Hatton KW: A Highly predictive MicroRNA panel for determining delayed cerebral vasospasm risk following aneurysmal subarachnoid hemorrhage. Front Mol Biosci 8:1-12, 2021. https://doi.org/10.3389/fmolb.2021.657258
51. Wang Y, Song Y, Pang Y, Yu Z, Hua W, Gu Y, Qi J, Wu H: miR-183-5p alleviates early injury after intracerebral hemorrhage by inhibiting heme oxygenase-1 expression. Aging (Albany NY) 12:12869-12895, 2020. https://doi.org/10.18632/aging.103343
52. Wei Y, Schober A, Weber C: Pathogenic arterial remodeling: The good and bad of microRNAs. Am J Physiol - Hear Circ Physiol 304:1050-1059, 2013. https://doi.org/10.1152/ajpheart.00267.2012
53. Wright MC, Medel R, Dumont AS, Amenta PS: Understanding the role of microRNAs in the pathogenesis of intracranial aneurysms. J Dis Markers 22:1033, 2015
54. Xu J, Yan S, Tan H, Ma L, Feng H, Han H, Pan M, Yu L, Fang C: The miR-143/145 cluster reverses the regulation effect of KLF5 in smooth muscle cells with proliferation and contractility in intracranial aneurysm. Gene 679:266-273, 2018. https://doi.org/10.1016/j.gene.2018.09.010

55. Yang F, Xing WW, Shen DW, Tong MF, Xie FM: Effect of miR-126 on intracranial aneurysms and its predictive value for rupture of aneurysms. Eur Rev Med Pharmacol Sci 24:3245–3253, 2020. https://doi.org/10.26355/eurrev_202003_20691

56. Yin KJ, Deng Z, Hamblin M, Xiang Y, Huang H, Zhang J, Jiang X, Wang Y, Chen YE: Peroxisome proliferator-activated receptor δ regulation of miR-15a in ischemia-induced cerebral vascular endothelial injury. J Neurosci 30:6398-6408, 2010. https://doi.org/10.1523/JNEUROSCI.0780-10.2010

57. Yin KJ, Olsen K, Hamblin M, Zhang J, Schwendeman SP, Chen YE: Vascular endothelial cell-specific MicroRNA-15a inhibits angiogenesis in hindlimb ischemia. J Biol Chem 287:27055–27064, 2012. https://doi.org/10.1074/jbc.M112.364414

58. Zheng L, Zhang X, Liu L, Pu Y: Altered expression of specific MicroRNAs in plasma of aneurysmal subarachnoid hemorrhage patients. Front Neurol 13:1-9, 2022. https://doi.org/10.3389/fneur.2022.842888

59. Zhou Y, Yang L, Bo C, Zhang X, Zhang J, Li Y: Microrna-9-3p aggravates cerebral ischemia/ reperfusion injury by targeting fibroblast growth factor 19 (Fgf19) to inactivate gsk-3β/nrf2/are signaling. Neuropsychiatr Dis Treat 17:1989-2002, 2021. https://doi.org/10.2147/NDT.S290237

60. Zhu Y, Wang JL, He ZY, Jin F, Tang L: Association of altered serum micro RNAs with perihematomal edema after acute intracerebral hemorrhage. PLoS One 10:1-11, 2015. https://doi.org/10.1371/journal.pone.0133783

Turk Neurosurg 36(1):49-63, 2026
DOI: 10.5137/1019-5149.JTN.48929-25.1

Original Investigation
Cerebrovascular-Endovascular

Received: 16.04.2025
Accepted: 03.06.2025
Published Online: 16.01.2026

Genetic Association Between Systemic Lupus Erythematosus and Cerebrovascular Disorders

Yu GUO[1,2]*, Yonggang XU[3]*, Chao LIU[3], Meilin CHEN[4], Hengzhu ZHANG[1,2], Wenmiao LUO[3]

[1]Northern Jiangsu People's Hospital Affiliated to Yangzhou University, Department of Neurosurgery, Yangzhou, Jiangsu, China
[2]Northern Jiangsu People's Hospital, Department of Neurosurgery, Yangzhou, Jiangsu, China
[3]Xiamen Susong Hospital, Department of Neurosurgery, Xiamen, China
[4]Xiamen Susong Hospital, Department of Pathology, Xiamen, China

*Yu Guo and Yonggang Xu are joint first authors.

Corresponding author: Wenmiao LUO ✉ wenmiaoluo@outlook.com

ABSTRACT

AIM: To evaluate the potential genetic differences between systemic lupus erythematosus (SLE) and cerebrovascular disorders (CVDs) patients.

MATERIAL and METHODS: This genetic association study conducted Mendelian randomization (MR) analyses on the derived exposures and outcomes from summary statistics of genome-wide association studies (GWAS). This study employed univariate MR (UVMR) analysis, multivariable MR (MVMR) analysis, and meta-analysis, using data from large genomic databases such as the UK Biobank, FinnGen, and OpenGWAS. These methods aim to overcome confounding factors by using genetic variants as instrumental variables to infer causal relationships.

RESULTS: UVMR analysis revealed a genetic causal relationship between SLE and ischemic stroke, with a positive correlation (odds ratio [OR] 1.000367; 95% confidence interval [CI] 1.000074--1.00066; p=0.014). No evidence of a genetic causal relationship was found between SLE and other types of CVDs, including cerebral aneurysm, intracerebral hemorrhage, subarachnoid hemorrhage, stroke, and transient ischemic attack. MVMR analysis, after adjusting for confounders such as smoking and type 2 diabetes, confirmed the robustness of the association between SLE and ischemic stroke. Furthermore, a meta-analysis of multiple MR outcomes was conducted to verify the stability of the results (OR, 1.00037; 95% CI, 1.00008-1.00067).

CONCLUSION: Our study enhances the understanding of the genetic basis between SLE and various CVDs, particularly suggesting a positive causal association between SLE and ischemic stroke, and we emphasize the need for further research.

KEYWORDS: Systemic lupus erythematosus, Cerebrovascular disorders, Mendelian randomization, Genetic susceptibility

ABBREVIATIONS: SLE: Systemic lupus erythematosus, **CVDs:** Cerebrovascular disorders, **MR:** Mendelian randomization, **UVMR:** Univariate Mendelian randomization, **MVMR:** Multivariable Mendelian randomization, **LD:** Linkage disequilibrium, **IS:** Ischemic stroke, **AN:** Cerebral aneurysm, **ICH:** Intracerebral hemorrhage, **SAH:** Subarachnoid hemorrhage, **TIA:** Transient ischemic attack

Yu GUO : 0000-0003-0969-5913
Yonggang XU : 0000-0003-2978-2715
Chao LIU : 0000-0001-6994-8703
Meilin CHEN : 0009-0003-1787-5823
Hengzhu ZHANG : 0000-0003-3240-5689
Wenmiao LUO : 0000-0003-0340-9867

INTRODUCTION

Systemic lupus erythematosus (SLE) is a multifaceted, chronic autoimmune condition, and its development is influenced by genetic, environmental, and immune factors, leading to impacts on various organ systems. Recently, a growing body of epidemiological research has indicated that SLE patients face a substantially increased risk of cerebrovascular disorders (CVDs), including both ischemic and hemorrhagic strokes (40). The likelihood of CVDs in individuals with SLE is reported to be 2 to 10 times greater than that in the general population (12). However, despite these findings highlighting a link between SLE and CVDs, the causal relationship remains unclear, largely owing to the challenges posed by potential confounding factors and reverse causality in observational studies, which complicate the ability to draw definitive conclusions (15).

CVDs rank among the primary causes of illness and death globally. In patients with SLE, the intricate progression of the disease, combined with conventional risk factors such as hypertension, diabetes, and smoking, highlights the critical need for investigating the genetic predisposition of individuals with SLE to various forms of CVDs (14).

The advent of Mendelian randomization (MR) techniques offers a robust means to address these limitations by employing genetic variants as instrumental variables (IVs) to infer causality. Owing to the random distribution of genetic variants, this method is less susceptible to biases from unmeasured confounding or reverse causation (30). However, previous MR analyses have produced inconsistent findings when examining the connection between SLE and the risk of CVDs (16, 21). Furthermore, while prior research has focused primarily on specific cardiovascular events, such as one study identifying a significant link between SLE and ischemic stroke and another failing to replicate this finding, our study broadens the scope by thoroughly examining the relationship between SLE and a wide range of cerebrovascular outcomes. In this study, the core scientific challenge lies in the selection and validation of appropriate genetic instruments for MR analysis. It is crucial to ensure that these IVs are strongly associated with SLE and that their effect on stroke risk is mediated solely through SLE, without confounding due to horizontal pleiotropy. This study enhances the robustness of the findings by applying stringent criteria for selecting IVs, using sensitivity analyses to assess pleiotropy, and incorporating data from diverse populations. Finally, a meta-analysis of MR outcomes across various datasets was conducted to validate the robustness of the conclusions.

This study conducts two-sample MR analysis, along with multivariable MR analysis (MVMR) and meta-analysis, by leveraging data from several extensive genomic databases, including the UK Biobank (UKB), FinnGen, and OpenGWAS, to investigate the genetic links between SLE and a range of CVDs. By addressing the shortcomings of prior research, this study aims to offer stronger evidence for the causal connections between SLE and specific CVDs, such as ischemic stroke (IS), cerebral aneurysm (AN), intracerebral hemorrhage (ICH), subarachnoid hemorrhage (SAH), stroke, and transient ischemic attack (TIA).

MATERIAL and METHODS

This study adheres to the STROBE-MR guidelines, which are essential for reporting observational epidemiological research employing MR framework (31). Statistical analyses were conducted via R version 4.2.3, which employs the TwoSampleMR and MR packages for robust computational processing (18).

No human subjects were directly involved in this study. All data used in this study were derived from existing de-identified biospecimens from previous studies. Therefore, this study did not require ethical approval or patient consent.

Study Design

In our MR analysis, we articulate three principal hypotheses: (i) There exists a robust association between IVs and exposures. (ii) These IVs are statistically independent of confounding variables. (iii) The influence of IVs on the risk of outcomes is mediated directly via exposure rather than through alternative pathways. Figure 1 presents the flowchart of the study design.

Instrumental Variables Selection

The data on SLE and CVDs were obtained from a study of the European population (Table I). The SLE data were derived from the study conducted by Bentham et al. (3). For cerebrovascular diseases, data on AN, ICH, IS, SAH, stroke, and TIA were extracted from the UKB (33). From the FinnGen database, data on AN, ICH, SAH, stroke, and TIA were obtained (23). Additionally, from the Genome-Wide Association Studies (GWAS), we extracted stroke data on AN, ICH, ischemic stroke, and SAH published by Sakaue et al. (27); stroke data published by Donertas et al. (11); TIA data published by Traylor et al. (36); data on ICH, SAH, and TIA published by Jiang et al. (22); and IS and stroke data published by Malik et al. (25). Using the TwoSampleMR package, genome-wide significant SNPs ($p<5\times10^{-8}$) were identified and combined to maintain independence, with a linkage disequilibrium (LD) threshold of $r^2<0.001$ and a distance of 10,000 kb. LD refers to the nonrandom association between adjacent genes or genetic markers in the genome. By using stringent criteria to select IVs, studies can better explain causal relationships while reducing confounding effects caused by LD (32). To assess the strength of the association between the selected IVs and exposures, F statistics are computed for each instrumental variable. To evaluate the robustness of the genetic instruments, an F statistic threshold of 10 is applied to determine instrument validity, reducing the risk of bias introduced by weak instruments (17). Additionally, sensitivity analyses are performed via the MR-PRESSO approach to further assess the robustness of the results.

Study Outcomes

UKB is a biomedical database and research resource that contains genetic, lifestyle, and health information of approximately 500,000 participants aged between 40 and 69 years from the UK (8). Data from individuals of pan-European ancestry were obtained from the UKB. Stroke-related data of interest were selected, and summary statistics were downloaded from the Neale-UKB project portal website.

FinnGen is a research resource that includes analyses of genomic and health registry data of approximately 500,000 Finn-

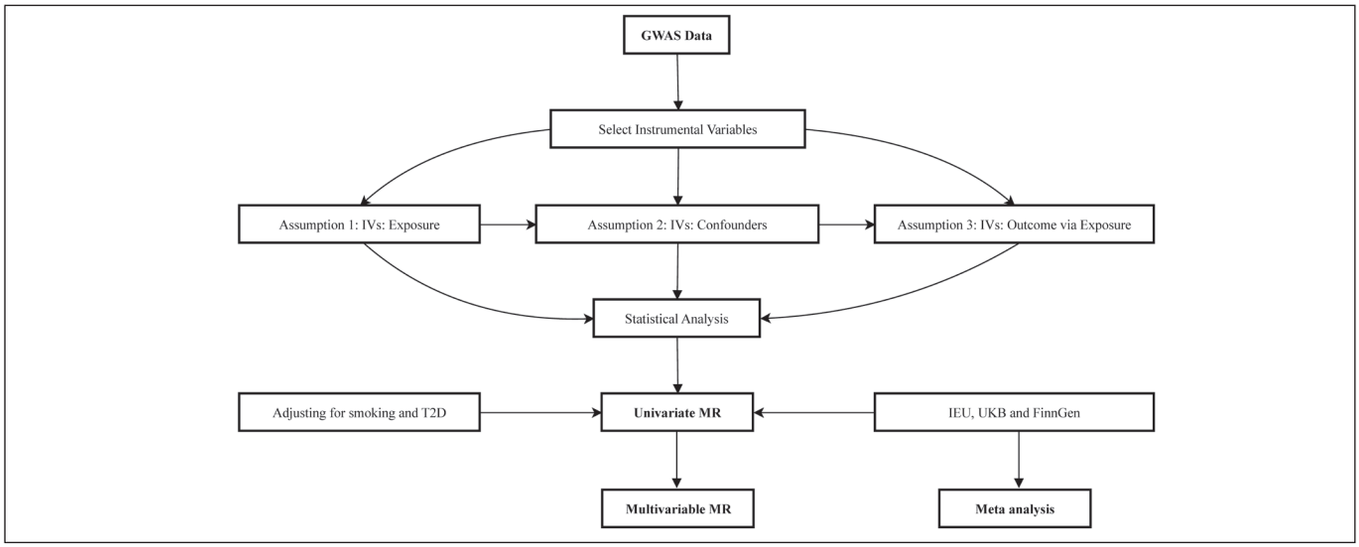

Figure 1: A diagram of the study workflow.

Table I: Characteristics of the Genome Wide Association Studies Used in This Study

Data sources	Traits	GWAS ID	Sample.size	Cases	Controls	Ancestry	R^2 for SLE	F statistic for SLE
Bentham J.	SLE	ebi-a-GCST003156	14267	5201	9066	European		
UK Biobank	AN	I9_ANEURYSM	361194	225	360969	European	0.223	97.5
UK Biobank	ICH	ICD10_I61	361197	496	360701	European	0.238	90.2
UK Biobank	IS	I9_STR_EXH	361194	3314	357880	European	0.253	96.2
UK Biobank	SAH	ICD10_I60	361178	626	360552	European	0.256	94.7
UK Biobank	Stroke	ICD10_I64	361194	742	360452	European	0.258	93.1
UK Biobank	TIA	20002_1082	361141	1369	359772	European	0.271	95.2
FinnGen	AN	I9_ANEURYSM	345255	2582	342673	European	0.271	95.2
FinnGen	ICH	I9_ICH	343663	3749	339914	European	0.271	95.2
FinnGen	IS	I9_STR_EMBOLIC	344046	1373	342673	European	0.254	96.4
FinnGen	SAH	I9_SAH	343211	3289	339922	European	0.265	98.0
FinnGen	Stroke	I9_STR	311635	39818	271817	European	0.221	91.0
FinnGen	TIA	I9_TIA	360692	18398	342294	European	0.237	87.6
Sakaue	AN	ebi-a-GCST90018816	473683	945	472738	European	0.271	95.2
Sakaue	ICH	ebi-a-GCST90018870	473513	1935	471578	European	0.271	95.2
Sakaue	IS	ebi-a-GCST90018864	484121	11929	472192	European	0.237	87.6
Sakaue	SAH	ebi-a-GCST90018923	473255	1693	471562	European	0.271	95.2
Handan	Stroke	ebi-a-GCST90038613	484598	6925	477673	European	0.271	95.2
Traylor	TIA	ebi-a-GCST90014123	232596	7338	225258	European	0.234	91.1
Jiang L	ICH	GCST90043996	456348	158	456190	European	0.226	88.0
Malik R	IS	ebi-a-GCST005843	440328	34217	406111	European	0.266	98.5
Jiang L	SAH	GCST90043993	456348	832	455516	European	0.271	95.2
Malik R	Stroke	ebi-a-GCST005838	446696	40585	406111	European	0.266	98.5
Jiang L	TIA	GCST90044001	456348	2045	454303	European	0.269	96.8

*F statistic= ((N-K-1) / K) * (R/(1-R)) R^2 = 2 * eaf * (1 - eaf) * **beta² N:** Sample size of the exposure GWAS study. **K:** Number of SNPs. **beta:** Column containing the effect size for each SNP. **R^2:** Proportion of variance in the exposure explained by the IVs. **eaf:** Column containing the effect allele frequency for each SNP.*

ish individuals, encompassing low-frequency and high-impact variants (23). Stroke-related data of interest were selected, and summary statistics were downloaded from the FinnGen portal website.

To replicate the causal relationship between SLE and CVDs, data on SLE and CVD-related aspects of European populations were downloaded from the OpenGWAS API (13,18). The definitions of SLE, AN, ICH, ischemic stroke, SAH, stroke, and TIA, as well as the number of individuals in the experimental and control groups, are presented in Table I.

Statistical and Sensitivity Analyses

The statistical analysis for MR was performed via the two-sample MR, Mendelian randomization, and MR-PRESSO packages in R (version 4.2.3) (18,41). The primary approach applied is the inverse variance weighted (IVW) method, with additional analyses conducted using the MR Egger technique as secondary methods (4,5,7,17). The sensitivity tests include heterogeneity, multiplicative heterogeneity, and leave-one-out analysis (9,39). Heterogeneity was evaluated through IVW analysis and MR-Egger regression, with Cochran's Q test p values indicating the level of heterogeneity. To detect and correct for horizontal pleiotropy, the MR-PRESSO method is employed, identifying and adjusting outliers ($p<0.05$) to compare estimates before and after correction. A leave-one-out test is conducted to verify the robustness of the MR analysis. The outcomes are reported as odds ratios (ORs) with 95% confidence intervals (CIs), along with beta coefficients and standard errors (se). P values less than 0.05 were considered statistically significant.

The positive results of UVMR analysis are expanded through MVMR. After adjusting for potential confounding factors such as smoking and type 2 diabetes (T2D), a direct causal relationship between SLE and stroke outcomes associated with UVMR was confirmed. For false discovery rate (FDR) correction in MVMR analysis, adjusted P values are calculated via the Benjamini-Hochberg procedure, which ranks the P values from smallest to largest and applies a correction factor on the basis of the number of tests performed. A significance threshold of $p<0.05$ after FDR correction was used to identify statistically significant associations (26).

Meta-Analysis Approach

To validate the consistency and generalizability of our findings, a meta-analysis is conducted by synthesizing results from multiple independent datasets, including the UKB, FinnGen, and OpenGWAS datasets. To assess the robustness of the analysis, Cochran's Q test and the I^2 statistic were used to quantify between-study heterogeneity. A random-effects model is applied to account for potential variability across studies, minimizing bias and providing more conservative effect estimates.

IVW effect estimates for SLE on different types of CVDs are separately calculated using data from UKB, FinnGen, and OpenGWAS. These estimates are then combined in a random-effects meta-analysis (38). Dichotomous data with ORs and corresponding 95% CIs were used as effect measures. Prediction intervals are employed to estimate the range of outcomes in future studies while considering interstudy variability and uncertainty. Heterogeneity was assessed via Cochran's Q test, with significance set at $p<0.1$, and further quantified via the I^2 statistic. An I^2 value less than 50% indicates low heterogeneity, whereas values between 50% and 75% suggest high heterogeneity (10). The findings revealed a significant association between SLE and various types of stroke, with a bilateral $p<0.05$ considered potentially significant. The meta-analysis was conducted via the meta package in R (1).

RESULTS

The study included individual data of European descent extracted from UKB, FinnGen, and other extensive cohort studies. Definitions and sources of disease diagnoses for SLE, AN, ICH, ischemic stroke, SAH, stroke, and TIA are provided in Table I. On the basis of the correlation between SLE and different CVDs, genetic markers were identified (Table II-III). The UVMR effects of genetic proxies for SLE on different types of CVDs were estimated separately in UKB, FinnGen and other large databases (Table III). After adjusting for confounders such as smoking and T2D, MVMR outcomes were analysed to validate the robustness of the outcomes (Table IV). The IVs and outcomes extracted from the reverse UVMR analysis are presented in Tables V-VI. The UVMR outcomes were then combined in a random-effects meta-analysis. All IVs demonstrated strong validity (F statistic greater than 10) (Table I). No significant abnormalities were observed in horizontal pleiotropy or heterogeneity tests for any of the MR analyses (Table III).

Associations Between SLE and the Risk of Different Types of CVDs

Univariate Mendelian Randomization

When the UKB was used as the primary exposure outcome, the results of univariate MR-IVW analysis suggested a genetic causal relationship between SLE and ischemic stroke. We observed a positive correlation between genetically predicted SLE and ischemic stroke (OR, 1.000367; 95% CI, 1.000074--1.00066; p=0.014; Figure 2 and Table III). We further validated other types of CVDs in the UKB and found no evidence of a correlation between SLE and the risk of AN, ICH, SAH, stroke, or TIA (Table III). We conducted sensitivity analyses via MR-Egger mode. In the sensitivity analysis of SLE and stroke, only the MR-Egger results were contrary to those of the other methods. The results of the remaining sensitivity analyses were consistent with the direction of IVW. The scatter plots indicate that in all association analyses, the MR-Egger intercept did not significantly deviate from 0, and there was no evidence of pleiotropy (pleiotropy test >0.05) (Figure 3 and Table III). Leave-one-out analysis was used to validate the reliability of the results (Figure 3).

We further validated in other cohort studies that there was no evidence of a correlation between SLE and the risk of ischemic stroke. In all cohorts, we found no evidence of a genetic causal relationship between SLE and AN, ICH, SAH, stroke, or TIA (Table III).

Table II: Identifying Robust Instrumental Variables for SLE

SNP	Sample size	p-value	Se	Beta	Effect allele	Other allele
rs6679677	14267	4.55E-13	0.046485	0.336472	A	C
rs4661543	14267	9.40E-11	0.042376	0.274437	G	T
rs10912578	14267	1.65E-15	0.030992	0.24686	A	G
rs17849501	14267	1.81E-59	0.049864	0.81093	T	C
rs6671847	14267	6.64E-12	0.028965	0.198851	A	G
rs4916215	14267	5.07E-11	0.033969	0.223144	T	C
rs12094036	14267	1.37E-08	0.05786	0.328504	T	C
rs13019891	14267	1.65E-83	0.029034	0.562119	G	T
rs2573219	14267	1.13E-42	0.042929	0.587787	C	A
rs10200680	14267	4.96E-09	0.042484	0.248461	C	T
rs268124	14267	8.60E-09	0.03237	0.18633	T	C
rs2459611	14267	7.62E-09	0.045245	0.261365	T	C
rs4274624	14267	9.73E-66	0.032679	0.559616	C	T
rs10048743	14267	2.04E-08	0.041206	0.231112	G	T
rs34703115	14267	4.08E-09	0.104778	0.616186	T	C
rs1464446	14267	2.79E-16	0.04015	0.328504	G	T
rs9852014	14267	2.26E-36	0.049273	0.620577	G	A
rs13136219	14267	3.50E-10	0.027787	0.174353	C	T
rs1078324	14267	7.11E-20	0.078167	0.71335	C	A
rs4388254	14267	3.71E-10	0.060398	0.378436	T	C
rs2431697	14267	2.60E-14	0.029296	0.223144	T	C
rs6889239	14267	2.19E-18	0.03174	0.277632	C	T
rs389884	14267	2.92E-102	0.043232	0.928219	G	A
rs9274357	14267	1.28E-38	0.035196	0.457425	T	C
rs7768653	14267	3.11E-12	0.029689	0.207014	C	T
rs12524498	14267	2.48E-08	0.120793	0.673345	G	T
rs58721818	14267	3.38E-18	0.075594	0.65752	T	C
rs150180633	14267	2.66E-41	0.068957	0.928219	T	C
rs35000415	14267	1.86E-45	0.041539	0.587787	T	C
rs2736332	14267	4.83E-18	0.032069	0.277632	C	G
rs7823055	14267	1.64E-34	0.028621	0.350657	G	T
rs7899626	14267	4.19E-08	0.033253	0.182322	T	C
rs7097397	14267	8.60E-11	0.028712	0.18633	G	A
rs58688157	14267	2.97E-11	0.033565	0.223144	A	G
rs353608	14267	2.93E-11	0.02802	0.18633	G	A
rs73050535	14267	9.11E-09	0.124134	0.71335	C	T
rs597808	14267	3.51E-08	0.029474	0.162519	A	G
rs1143679	14267	5.03E-48	0.039987	0.582216	A	G
rs13332649	14267	5.43E-17	0.037568	0.314711	A	G
rs143123127	14267	2.23E-08	0.084034	0.470004	A	G
rs35251378	14267	3.61E-13	0.032427	0.235722	G	A
rs73068668	14267	4.40E-08	0.05749	0.314711	G	A
rs3747093	14267	2.88E-14	0.034506	0.262364	A	G

Select genome-wide significant SNPs for SLE ($p<5\times10-8$), ensuring independence with an $r^2 < 0.001$ for linkage disequilibrium and a distance of 10,000 kb. ***Se:*** *Standart error.*

Table III: The Univariate Mendelian Randomization of Genetic Proxies for SLE on IS, AN, ICH, SAH, Stroke and TIA in the UK Biobank, FinnGen, IEU and GWAS Catalog Databases.

Outcomes	Method	SNPs	Beta	Se	p-value	Heterogeneity tests	Pleiotropy test
						Q p-value	p-value
UK Biobank							
Ischemic stroke	MR Egger	38	0.0004545	0.0003141	0.1565208	0.1330163	0.7524929
	IVW	38	0.000367	0.0001493	**0.0139635***	0.1558752	
Cerebral aneurysm	MR Egger	33	-0.0001177	8.43E-05	0.1728961	0.2166895	0.2964794
	IVW	33	-0.0000389	4.02E-05	0.3332591	0.2089223	
Intracerebral hemorrhage	MR Egger	38	-0.0001262	0.0001247	0.3181248	0.2130197	0.7063034
	IVW	38	-0.0000846	0.0000587	0.1495237	0.2422703	
Subarachnoid hemorrhage	MR Egger	39	-0.0002222	0.0001236	0.0803506	0.6111911	0.1372706
	IVW	39	-0.0000579	0.0000598	0.3327382	0.5485976	
Stroke	MR Egger	40	-0.0000023	0.0001429	0.9870552	0.3077826	0.6064423
	IVW	40	0.0000626	0.0000685	0.3607582	0.3369019	
Transient ischemic attack	MR Egger	41	-0.0000751	0.0001927	0.6990531	0.1420934	0.6878885
	IVW	41	-0.0000069	0.0000929	0.9404493	0.1631692	
FinnGen							
Ischemic stroke	MR Egger	38	0.0268424	0.0500244	0.5948539	0.7928841	0.5810486
	IVW	38	0.0021593	0.0231927	0.9258213	0.8150444	
Cerebral aneurysm	MR Egger	41	0.0186737	0.0395707	0.6396221	0.1692403	0.9777643
	IVW	41	0.019656	0.0181996	0.2801319	0.1983929	
Intracerebral hemorrhage	MR Egger	41	-0.0503262	0.0323408	0.1277578	0.2055257	0.357942
	IVW	41	-0.02372	0.0150735	0.1155749	0.2076139	
Subarachnoid hemorrhage	MR Egger	39	0.0122422	0.0371933	0.743897	0.1014085	0.6470525
	IVW	39	0.0274719	0.0169944	0.105982	0.1171651	
Stroke	MR Egger	35	-0.0261687	0.0135192	0.0615134	0.2402225	0.1082091
	IVW	35	-0.006117	0.0060882	0.3150282	0.1761803	
Transient ischemic attack	MR Egger	39	-0.0133896	0.017999	0.4616303	0.1295774	0.3983252
	IVW	39	0.0004787	0.0077546	0.9507814	0.1339409	
IEU							
Ischemic stroke	MR Egger	38	-0.0033896	0.011596	0.7717279	0.5575338	0.781113
	IVW	38	-0.0004924	0.0052316	0.9250126	0.6003995	
Cerebral aneurysm	MR Egger	41	-0.0270455	0.0561382	0.6326646	0.7195153	0.680128
	IVW	41	-0.0064915	0.026518	0.8066129	0.7505296	
Intracerebral hemorrhage	MR Egger	41	0.0012602	0.0325245	0.9692916	0.3979051	0.8730485
	IVW	41	-0.0033626	0.0150381	0.8230633	0.4407831	
Subarachnoid hemorrhage	MR Egger	41	-0.0331494	0.0391241	0.4020033	0.0898489	0.4778944
	IVW	41	-0.0083868	0.018234	0.6455498	0.0973094	

Table III: Cont.

Outcomes	Method	SNPs	Beta	Se	p-value	Heterogeneity tests	Pleiotropy test
						Q p-value	p-value
Stroke	MR Egger	41	-0.0002526	0.0002999	0.4048778	0.3395831	0.2205481
	IVW	41	0.0000739	0.0001466	0.6142352	0.3157272	
Transient ischemic attack	MR Egger	37	0.0351295	0.0259391	0.1843189	0.4464989	0.4785699
	IVW	37	0.018841	0.0123974	0.1285717	0.4695658	
GWAS Catalog							
Ischemic stroke	MR Egger	39	-0.0022559	0.0121873	0.8541578	0.1933407	0.6194726
	IVW	39	0.0031688	0.0055303	0.5666545	0.2166684	
Intracerebral hemorrhage	MR Egger	37	-0.0879597	0.1449075	0.5477648	0.5056632	0.7689564
	IVW	37	-0.05069	0.0717484	0.479879	0.5492968	
Subarachnoid hemorrhage	MR Egger	41	-0.1075429	0.0588226	0.0751672	0.8832752	0.101926
	IVW	41	-0.0215335	0.0286975	0.4530363	0.824411	
Stroke	MR Egger	39	0.0022268	0.0113727	0.8458378	0.1922506	0.9264027
	IVW	39	0.0012885	0.0051804	0.8035746	0.2243507	
Transient ischemic attack	MR Egger	40	-0.0241888	0.0379735	0.5279504	0.4621167	0.8404686
	IVW	40	-0.0174683	0.0184679	0.3442112	0.5060334	

, p value <0.05.
***SNPs:** Single nucleotide polymorphisms; **Se:** Standard error; **IVW:** Inverse variance weighted.*

Table IV: The Multivariable Mendelian Randomization Effect of SLE on Ischemic Stroke After Adjusting for Smoking and Type 2 Diabetes

Exposure	Outcome	beta	Se	p-value	Adjusted p-values	F statistic	Q stat	Q p-value
Systemic lupus erythematosus	Ischemic stroke	0.000387	0.000141	**0.00677**	0.020311	23.55347	187.8418	0.065384
Diabetes Mellitus, Type 2	Ischemic stroke	0.000648	0.000384	0.09335	0.140025	56.39439	187.8418	0.065384
Tobacco Smoking, Current	Ischemic stroke	0.00959	0.006624	0.149605	0.149605	6.307108	187.8418	0.065384

***Se:** Standard error.*

Table V. Identifying Robust Instrumental Variables for Ischemic Stroke in UK Biobank

SNP	Sample size	p-value	Se	Beta	Effect allele	Other allele
rs116676869	361194	2.13539e-06	0.000447294	0.00212028	A	G
rs117184775	361194	2.67794e-06	0.00110861	0.00520402	A	G
rs118001501	361194	1.6788e-06	0.000668369	-0.00320066	G	T
rs12665721	361194	4.00247e-06	0.000230751	0.00106407	C	T
rs142726048	361194	4.56208e-06	0.000649805	0.00297874	A	G
rs149541600	361194	4.52765e-06	0.000936969	0.00429659	T	C
rs151319393	361194	1.84923e-06	0.000681006	0.00324793	T	A
rs16955419	361194	1.0722e-06	0.000487215	0.00237663	G	T
rs17336988	361194	5.91489e-07	0.000875933	0.00437447	A	G
rs35847387	361194	7.22471e-07	0.000410946	0.00203637	T	C

Table V. Cont.

SNP	Sample size	p-value	Se	Beta	Effect allele	Other allele
rs4307235	361194	1.13945e-06	0.000237493	0.00115564	T	C
rs6054662	361194	3.16397e-08	0.000317744	-0.00175783	T	C
rs62174635	361194	4.35309e-06	0.000789791	0.00362817	T	C
rs6564437	361194	3.95323e-06	0.000264794	-0.00122173	C	T
rs66961966	361194	4.42965e-06	0.000598503	0.00274725	G	C
rs7085903	361194	7.79616e-07	0.000273432	-0.00135089	T	C
rs72781382	361194	1.15692e-06	0.000980832	0.00476975	C	T
rs7501414	361194	3.23506e-06	0.000328134	-0.00152759	C	A
rs75238399	361194	4.01368e-06	0.000833806	0.00384447	A	G
rs75259736	361194	9.38906e-08	0.000285389	-0.00152349	A	T
rs75415430	361194	3.15976e-06	0.000576427	0.00268628	T	C
rs76307406	361194	2.58378e-06	0.000475683	0.00223641	A	C

Select genome-wide significant SNPs for SLE (p<5×10−6), ensuring independence with an r^2<0.001 for linkage disequilibrium and a distance of 10,000 kb.

Table VI. The Univariate Mendelian Randomization of Genetic Proxies for IS on SLE in the UK Biobank

Outcomes	Method	SNPs	Beta	Se	p-value	Heterogeneity tests	Pleiotropy test
						Q p-value	p-value
UK Biobank							
Ischemic stroke	MR Egger	16	-6.4407259	16.11462417	0.695	0.7418789	0.80194265
	IVW	16	-7.2543813	7.1918339	0.313	0.8019426	

SNPs: *Single nucleotide polymorphisms;* ***Se:*** *Standard error;* ***IVW:*** *Inverse variance weighted.*

Reverse UVMR analyses revealed that the genome-wide significant SNPs ($p<5\times10^{-6}$) for ischemic stroke provided by the UKB may not exhibit a causal association with systemic lupus erythematosus (SLE) (p=0.802) (Tables V-VI).

Multivariable Mendelian Randomization

Within the MVMR framework, the positive results of UVMR analysis were extended via MVMR. After adjusting for potential confounders such as smoking and T2D, we validated a more direct causal relationship between SLE and ischemic stroke outcomes that was associated with UVMR (Table IV). We found that after adjusting for the effects of smoking and T2D, the causal relationship between SLE and ischemic stroke in the UKB remained stable (beta, 0.000387; se, 0.000141; p=0.007). When the FDR method was used to correct for potential Type I errors, a positive association between SLE and ischemic stroke was observed (P-adjust =0.02).

Meta-analysis

A meta-analysis of all outcomes between SLE and different types of CVDs revealed a positive causal association between SLE and ischemic stroke (OR, 1.00037; 95% CI, 1.00008-1.00067; Figure 4). There was no evidence of heterogeneity or pleiotropy. In the meta-analysis of SLE patients with AN, ICH, SAH, stroke, and TIA outcomes, we found no evidence of a genetic causal relationship. Similarly, there was no evidence of heterogeneity or pleiotropy (Figure 5).

DISCUSSION

Previous observational studies and several recent MR analyses have provided inconsistent explanations regarding the associations between SLE and CEVs (12,16,21). Our study further provided genetic evidence supporting the association between SLE and ischemic stroke, as demonstrated through UVMR (OR, 1.000367; 95% CI, 1.000074--1.00066) and MVMR (beta, 0.000387; se, 0.000141; p=0.007). Furthermore, a meta-analysis integrating data from various genetic levels indicated that SLE patients may have an elevated risk of ischemic stroke (OR, 1.00037; 95% CI, 1.00008-1.00067). Nevertheless, there is currently no evidence of a causal relationship between SLE and AS, ICH, SAH, stroke, or TIA. Reverse UVMR analysis indicated that ischemic stroke, as indicated by the UKB, may not be causally associated with SLE (p=0.802). These findings suggest that there may be a unidirectional causal relationship between SLE and ischemic stroke.

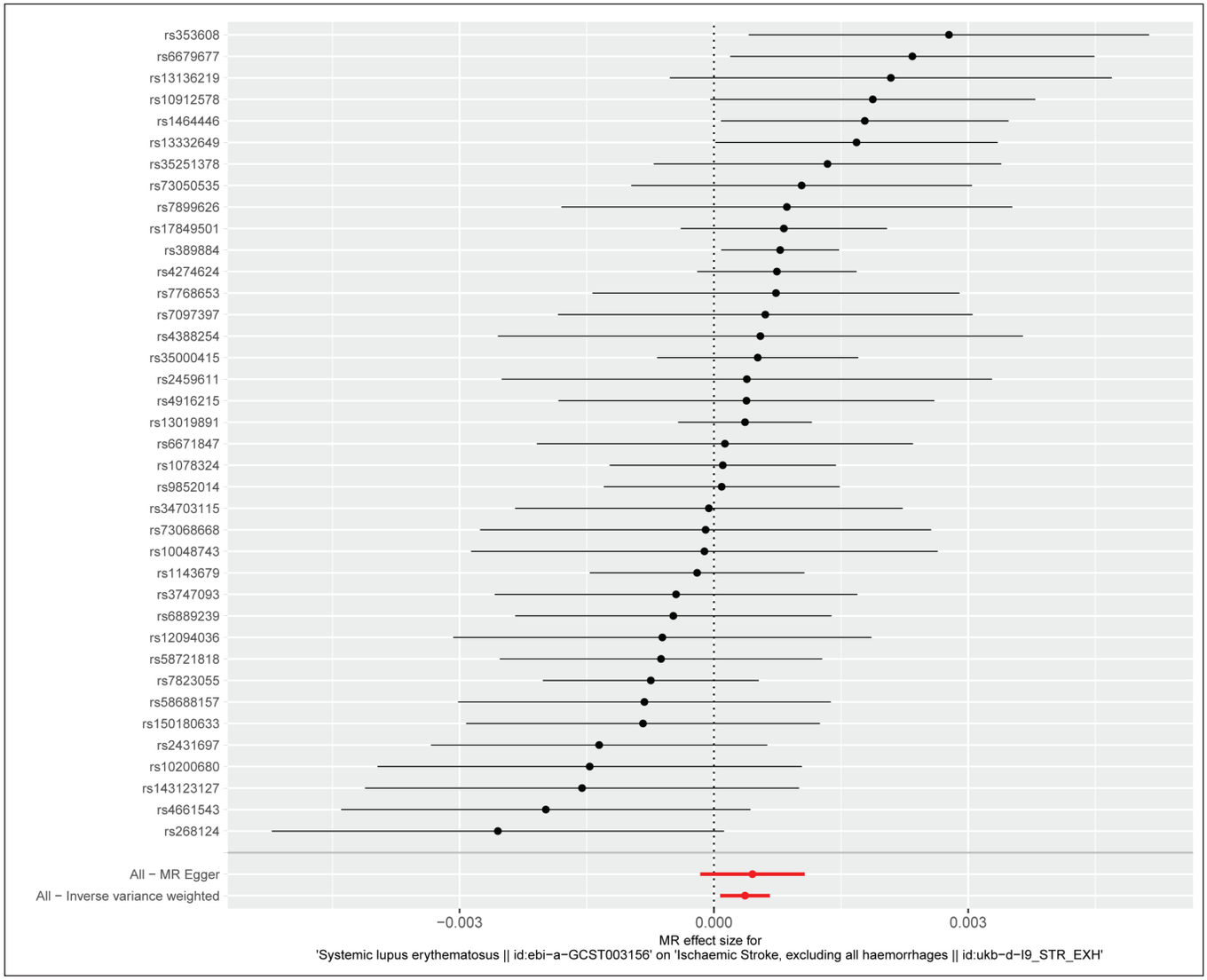

Figure 2: MR effect size for systemic lupus erythematosus on ischemic stroke.

Global Incidence and Risks in SLE

Recent studies have reported that approximately 3.4 million people worldwide are affected by SLE. Each year, 400,000 new cases of systemic lupus erythematosus are diagnosed globally (19,29). Observational studies have emphasized that SLE patients face an increased risk of cardiovascular and cerebrovascular diseases. However, researchers have objectively noted that most of the literature focuses on data from national registries, where significant discrepancies in the incidence and prevalence of SLE are observed. Additionally, the associations between SLE and various CVDs have not been well explained. Observational studies may have potential confounding or reverse causality biases (2,24). For example, hypertension or oral anticoagulants in SLE patients may influence CVDs, but such factors are difficult to control in clinical studies. MR, which is based on genetic variations assigned at birth, is not affected by drugs, the environment, or other factors and can be used to assess the correlation between genetic markers of SLE and CVDs effectively. Unfortunately, recent MR analyses have not provided consistent evidence for a causal relationship between SLE and CVDs (16,21,34). The primary considerations are pleiotropy and heterogeneity between studies, as well as limitations in study populations. It is necessary to conduct larger MR analyses, combining outcomes from different databases and study populations.

Potential Problems

Our study effectively analysed the correlation between SLE genetic susceptibility and different cerebrovascular diseases via MR analysis. CVDs include ischemic CVDs and hemorrhagic CVDs, with the former being more common in SLE patients. Compared with that in non-SLE patients, the incidence of ischemic stroke in SLE patients is as high as 90%, whereas the incidence of nonischemic stroke is 63%. Additionally, the incidence of widespread cerebral infarction in SLE patients is significantly greater than that in non-SLE patients (69.4% vs. 18.7%) (37). Previous studies have shown that the risk of

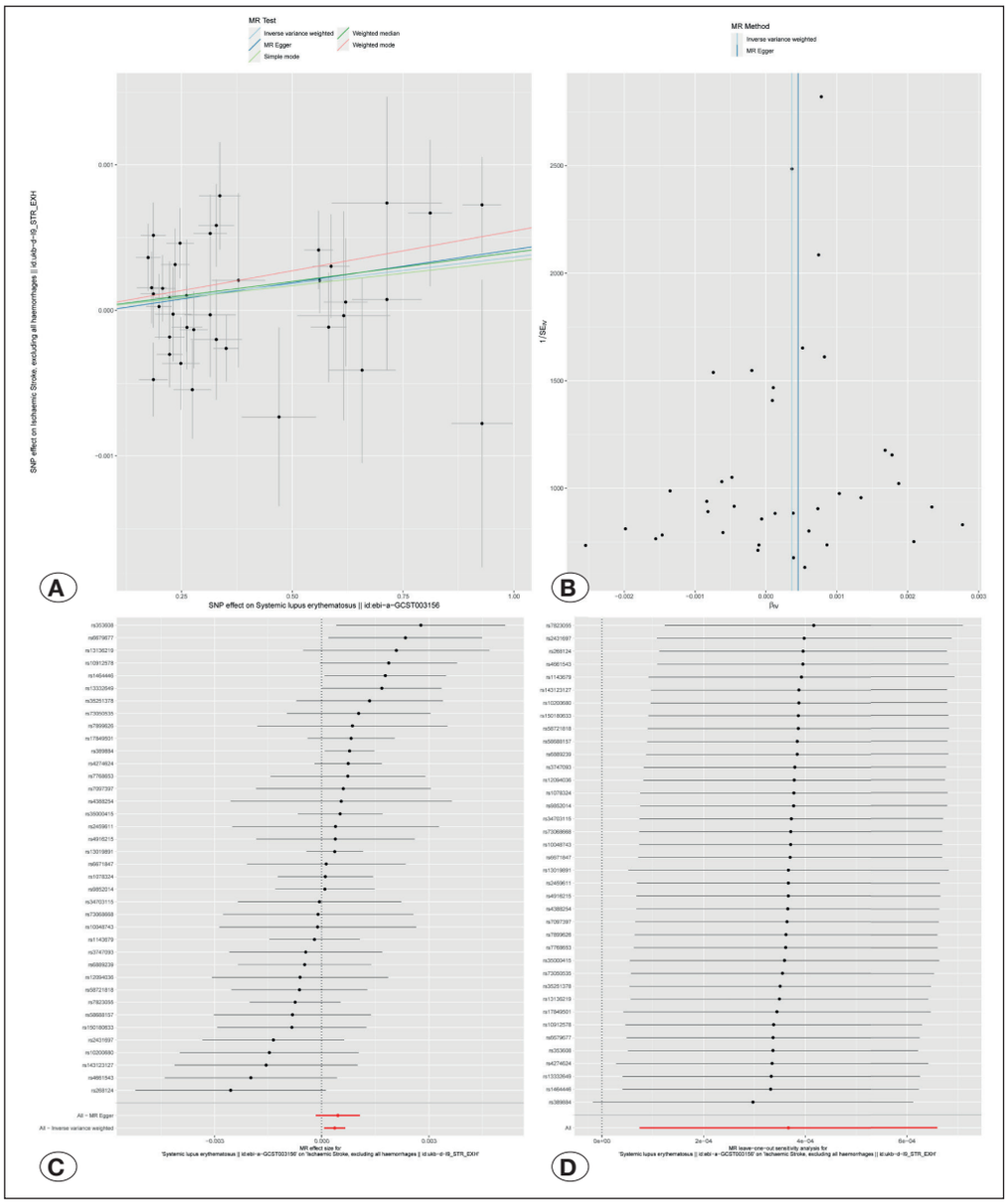

Figure 3: The UVMR effect of SLE-associated SNPs on ischemic stroke in the UKB.

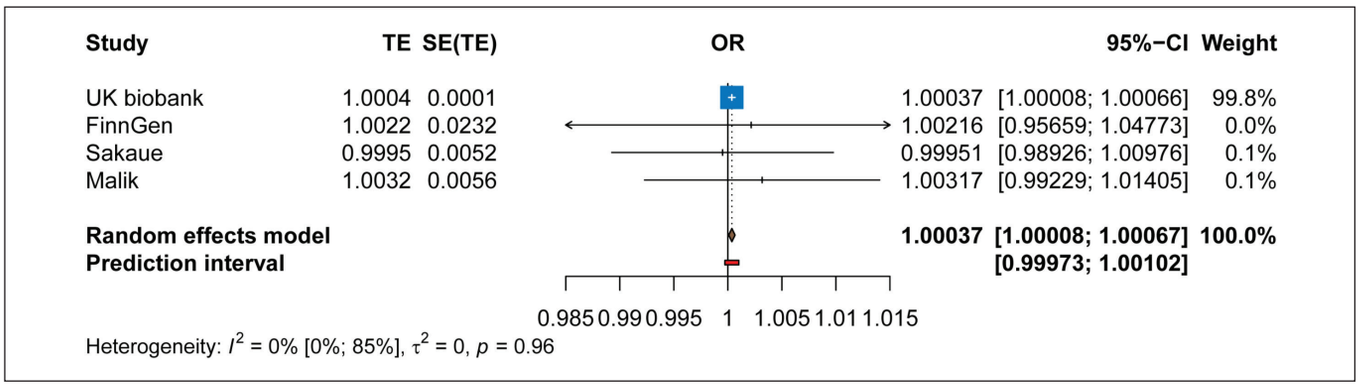

Figure 4: Combined random-effects model meta-analysis of the effect of SLE on ischemic stroke in the UK Biobank, FinnGen, IEU and GWAS Catalog.

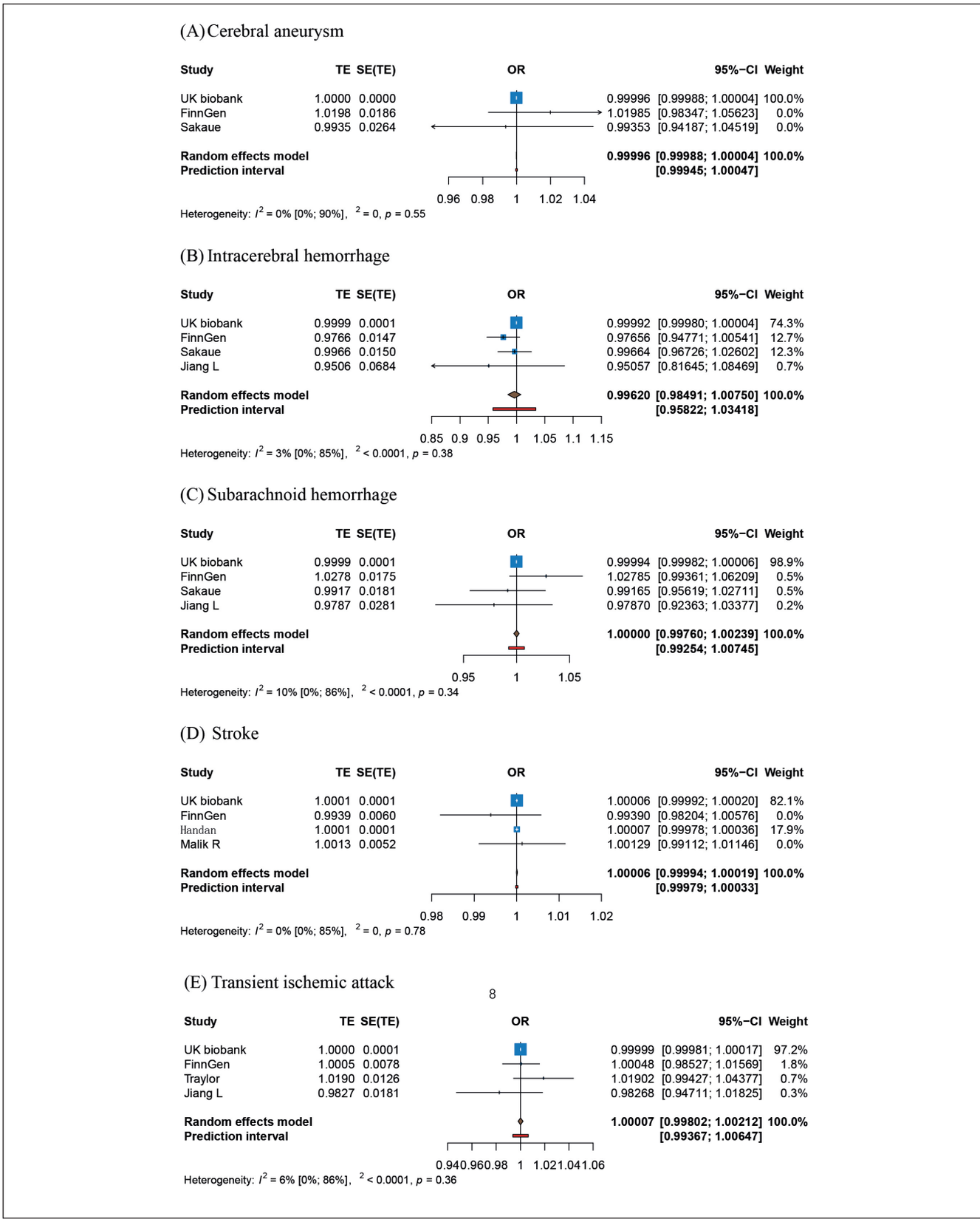

Figure 5: Combined random-effects model meta-analysis of the effect of SLE on AN, ICH, SAH, Stroke, and TIA in the UK Biobank, FinnGen, IEU and GWAS Catalog.

thrombosis persists throughout the course of SLE, accelerating atherosclerosis and vascular calcification and thereby increasing the risk of ischemic stroke. SLE patients often have other cardiovascular risk factors, such as smoking and diabetes, which further increase the risk of CVDs (28). Therefore, it is crucial to comprehensively assess and manage the impact of these comorbidities and validate the correlation between SLE and CVDs. We used MVMR to adjust for potential confounding factors such as smoking and type 2 diabetes, further validating the correlation between SLE genetic susceptibility and a high risk of ischemic stroke. Moreover, our MR analysis did not reveal a correlation between SLE genetic susceptibility and AN, ICH, SAH, overall stroke, or TIA. This finding does not align with the outcomes of observational studies, and the underlying mechanisms are currently unclear. The mechanisms of AN, ICH, SAH, overall stroke, and TIA are closely related to the structural integrity of the vascular wall, blood pressure control, and endothelial function, and these pathological processes may not be directly influenced by SLE-related genes. SLE genetic susceptibility may be related to immune system abnormalities (such as the production of autoantibodies and complement system activation), and these factors may have limited direct effects on vascular lesions. For example, chronic immune activation in SLE, characterized by elevated levels of autoantibodies and inflammatory cytokines such as TNF-α and IL-6, has been associated with endothelial dysfunction and plaque formation in cerebral arteries (40). These immune-mediated processes can disrupt vascular homeostasis, promote atherosclerosis and increase the risk of ischemic stroke. Additionally, complement activation, a hallmark of SLE, has been linked to vascular injury and an increased risk of thromboembolic events, potentially contributing to the pathogenesis of ischemic stroke (6). The deposition of immune complexes and the generation of complement-derived anaphylatoxins can further exacerbate endothelial damage and microvascular thrombosis, creating a pro-thrombotic environment that predisposes SLE patients to cerebrovascular events (20). MR analysis relies on the validity of the selected instrumental variables, specifically whether these genetic variations affect the risk of AN, ICH, and TIA by influencing SLE risk. If the instrumental variables do not fully meet this assumption (e.g., they also affect vascular health through other pathways), the study results may be biased, making it difficult to detect significant associations. We included data from several large databases, all of which involved European populations (Table I), to minimize the interference caused by population stratification features such as race and geography (32). Of course, we acknowledge that we cannot fully control for confounding factors related to population stratification. Therefore, we conducted heterogeneity tests to assess the degree of heterogeneity and further evaluate the reliability of the outcomes (42,43).

Influence on Clinicians

In our study, we further optimized the MR analysis by ensuring the selection of robust instrumental variables. Additionally, we applied various sensitivity analysis methods and combined meta-analyses to verify the stability of the outcomes. However, further studies with larger sample sizes and multicenter studies are still needed. A longitudinal study design combined with MR analysis was used to track the occurrence of cardiovascular events in SLE patients over time (35). The associations between SLE populations with different characteristics, such as sex or age, and various CVD subgroups should be investigated, confounding factors should be reduced, and genetic associations should be further elucidated (34). While our MR analysis suggested a genetic causal relationship between SLE and ischemic stroke, it was important to recognize the inherent limitations of MR in establishing causality. While robust, MR findings are ultimately observational in nature and require experimental validation to confirm causality. Future studies should aim to validate these genetic associations through experimental approaches, such as animal models or in vitro studies, to directly assess the impact of SLE-related genetic variants on vascular pathology and stroke risk. Additionally, clinical trials targeting specific pathways identified in this study (e.g., immune system activation or complement regulation) could provide further insights into the causal mechanisms linking SLE to ischemic stroke (19).

Limitations

Our study revealed a causal association between SLE genetic susceptibility and CVDs, but it is important to acknowledge the limitations of the methodology and data sources.

1) Sample population limitations: The genetic data analysed in this study were predominantly derived from European populations, limiting the generalizability of our findings to non-European cohorts. Furthermore, a systematic review of the literature revealed no large-scale genetic studies investigating SLE-CVDs relationships in non-European populations, underscoring the reliance on Eurocentric datasets and the uncertain applicability of our conclusions to ethnically diverse cohorts.

2) Selection of instrumental variables: Although we used stringent criteria to screen instrumental variables ($p<5\times10^{-8}$, LD r^2 <0.001), there remains the possibility that instrumental variables may not have completely eliminated potential bias. Specifically, instrumental variables might influence stroke risk through pathways other than SLE, which could lead to biased results.

3) Limitations of genetic data sources: Although we used multiple large databases (e.g., UKB, FinnGen, and OpenGWAS) for data analysis, the coverage and accuracy of certain genetic variants in these databases may be limited, potentially affecting the robustness of the study results.

4) Unmeasured confounding factors: We acknowledge that unmeasured confounding factors, such as diet, physical activity, or other environmental exposures, could still bias our results. Furthermore, while our sensitivity analyses provided some reassurance against horizontal pleiotropy, they cannot entirely rule out its presence, particularly if pleiotropic effects are correlated with IV-exposure associations.

5) Limitations of the study design: Although MR analysis partially avoids reverse causation and confounding bias, it relies on the assumption of a gene-phenotype association, which may make it difficult to fully capture the impact of SLE on stroke risk under certain complex biological

mechanisms. While we employed robust sensitivity analyses (e.g., MR-Egger, MR-PRESSO) to address these issues, residual biases may still exist. Furthermore, MR findings are inherently observational and cannot replace experimental evidence. Therefore, our results should be interpreted as suggestive of a causal relationship, with further validation through experimental and clinical studies. Future research should incorporate longitudinal study designs to assess the incidence of CVDs in SLE patients more comprehensively more comprehensively. These limitations highlight the caution needed when interpreting the association between SLE and CVDs in this study and provide directions for further improvements in future research.

CONCLUSION

This study utilized MR analysis to explore the potential causal associations between SLE and multiple CVDs. Our findings present novel genetic evidence supporting a causal link between SLE and ischemic stroke. However, no significant genetic causal associations were identified between SLE and other types of CVDs. These results highlight the necessity of further investigations to validate and expand our findings.

ACKNOWLEDGEMENTS

We acknowledge the participants of the UK Biobank and FinnGen studies for their contributions to science. We also appreciate the IEU OpenGWAS and GWAS Catalog databases for providing the genome-wide association statistics.

Declarations

Funding: This research was conducted in the absence of any commercial or financial relationships that could be construed as potential conflicts of interest.

Availability of data and materials: The datasets generated and/or analyzed during the current study are available from the corresponding author by reasonable request.

Disclosure: The authors declare no competing interests.

AUTHORSHIP CONTRIBUTION

Study conception and design: WL , YG

Data collection: YG, YX, MC, CL, HZ, WL

Analysis and interpretation of results: YG, YX, MC, WL

Draft manuscript preparation: YG, YX, MC, WL

Critical revision of the article: YG, YX, MC, WL

Other (study supervision, fundings, materials, etc...): YG, YX, MC, WL

All authors (YG, YX, CL, MC, HZ, WL) reviewed the results and approved the final version of the manuscript.

REFERENCES

1. Balduzzi S, Rücker G, Schwarzer G: How to perform a meta-analysis with R: A practical tutorial. Evid Based Ment Health 22:153-160, 2019. https://doi.org/: 10.1136/ebmental-2019-300117
2. Bello N, Meyers KJ, Workman J, Hartley L, McMahon M: Cardiovascular events and risk in patients with systemic lupus erythematosus: Systematic literature review and meta-analysis. Lupus 32:325-341, 2023. https://doi.org/: 10.1177/09612033221147471
3. Bentham J, Morris DL, Graham DSC, Pinder CL, Tombleson P, Behrens TW, Martín J, Fairfax BP, Knight JC, Chen L, Replogle J, Syvänen AC, Rönnblom L, Graham RR, Wither JE, Rioux JD, Alarcón-Riquelme ME, Vyse TJ: Genetic association analyses implicate aberrant regulation of innate and adaptive immunity genes in the pathogenesis of systemic lupus erythematosus. Nat Genet 47:1457-1464, 2015. https://doi.org/: 10.1038/ng.3434
4. Bowden J, Davey Smith G, Burgess S: Mendelian randomization with invalid instruments: effect estimation and bias detection through Egger regression. Int J Epidemiol 44:512-525, 2015. https://doi.org/: 10.1093/ije/dyv080
5. Bowden J, Davey Smith G, Haycock PC, Burgess S: Consistent estimation in mendelian randomization with some invalid instruments using a weighted median estimator. Genet Epidemiol 40:304-314, 2016. https://doi.org/: 10.1002/gepi.21965
6. Buch MH, Mallat Z, Dweck MR, Tarkin JM, O'Regan DP, Ferreira V, Youngstein T, Plein S: Current understanding and management of cardiovascular involvement in rheumatic immune-mediated inflammatory diseases. Nat Rev Rheumatol 20:614-634, 2024. https://doi.org/: 10.1038/s41584-024-01149-x
7. Burgess S, Thompson SG: Interpreting findings from Mendelian randomization using the MR-Egger method. Eur J Epidemiol 32:377-389, 2017. https://doi.org/: 10.1007/s10654-017-0255-x
8. Bycroft C, Freeman C, Petkova D, Band G, Elliott LT, Sharp K, Motyer A, Vukcevic D, Delaneau O, O'Connell J, Cortes A, Welsh S, Young A, Effingham M, McVean G, Leslie S, Allen N, Donnelly P, Marchini J: The UK Biobank resource with deep phenotyping and genomic data. Nature 562:203-209, 2018. https://doi.org/: 10.1038/s41586-018-0579-z
9. Cho Y, Haycock PC, Sanderson E, Gaunt TR, Zheng J, Morris AP, Davey Smith G, Hemani G: Exploiting horizontal pleiotropy to search for causal pathways within a Mendelian randomization framework. Nat Commun 11:1010, 2020. https://doi.org/: 10.1038/s41467-020-14452-4
10. Cumpston M, Li T, Page MJ, Chandler J, Welch VA, Higgins JP, Thomas J: Updated guidance for trusted systematic reviews: A new edition of the cochrane handbook for systematic reviews of interventions. Cochrane Database Syst Rev 10:Ed000142, 2019. https://doi.org/: 10.1002/14651858.Ed000142
11. Donertas HM, Fabian DK, Valenzuela MF, Partridge L, Thornton JM: Common genetic associations between age-related diseases. Nat Aging 1:400-412, 2021. https://doi.org/: 10.1038/s43587-021-00051-5
12. Durcan L, O'Dwyer T, Petri M: Management strategies and future directions for systemic lupus erythematosus in adults. Lancet 393:2332-2343, 2019. https://doi.org/: 10.1016/s0140-6736(19)30237-5
13. Elsworth B, Lyon M, Alexander T, Liu Y, Matthews P, Hallett J, Bates P, Palmer T, Haberland V, Smith GD: The MRC IEU OpenGWAS data infrastructure. BioRxiv 2020. https://doi.org/10.1101/2020.08.10.244293

14. Fanouriakis A, Kostopoulou M, Andersen J, Aringer M, Arnaud L, Bae SC, Boletis J, Bruce IN, Cervera R, Doria A, Dörner T, Furie RA, Gladman DD, Houssiau FA, Inês LS, Jayne D, Kouloumas M, Kovács L, Mok CC, Morand EF, Moroni G, Mosca M, Mucke J, Mukhtyar CB, Nagy G, Navarra S, Parodis I, Pego-Reigosa JM, Petri M, Pons-Estel BA, Schneider M, Smolen JS, Svenungsson E, Tanaka Y, Tektonidou MG, Teng YO, Tincani A, Vital EM, van Vollenhoven RF, Wincup C, Bertsias G, Boumpas DT: EULAR recommendations for the management of systemic lupus erythematosus: 2023 update. Ann Rheum Dis 83:15-29, 2024. https://doi.org/: 10.1136/ard-2023-224762
15. Fanouriakis A, Tziolos N, Bertsias G, Boumpas DT: Update on the diagnosis and management of systemic lupus erythematosus. Ann Rheum Dis 80:14-25, 2021. https://doi.org/: 10.1136/annrheumdis-2020-218272
16. Gao N, Kong M, Li X, Wei D, Zhu X, Hong Z, Ni M, Wang Y, Dong A: Systemic lupus erythematosus and cardiovascular disease: A mendelian randomization study. Front Immunol 13:908831, 2022. https://doi.org/: 10.3389/fimmu.2022.908831
17. Hartwig FP, Davey Smith G, Bowden J: Robust inference in summary data Mendelian randomization via the zero modal pleiotropy assumption. Int J Epidemiol 46:1985-1998, 2017. https://doi.org/: 10.1093/ije/dyx102
18. Hemani G, Zheng J, Elsworth B, Wade KH, Haberland V, Baird D, Laurin C, Burgess S, Bowden J, Langdon R, Tan VY, Yarmolinsky J, Shihab HA, Timpson NJ, Evans DM, Relton C, Martin RM, Davey Smith G, Gaunt TR, Haycock PC: The MR-Base platform supports systematic causal inference across the human phenome. Elife 30:7:e34408, 2018. https://doi.org/: 10.7554/eLife.34408
19. Hoi A, Igel T, Mok CC, Arnaud L: Systemic lupus erythematosus. Lancet 403:2326-2338, 2024. https://doi.org/: 10.1016/S0140-6736(24)00398-2
20. Huang JA, Lin CH, Wu MJ, Chen YH, Chang KC, Hou CW: Ten-year follow-up investigation of stroke risk in systemic lupus erythematosus. Stroke Vasc Neurol 9:1-7, 2024. https://doi.org/: 10.1136/svn-2022-001499
21. Huang S, Huang F, Mei C, Tian F, Fan Y, Bao J: Systemic lupus erythematosus and the risk of cardiovascular diseases: A two-sample Mendelian randomization study. Front Cardiovasc Med 9:896499, 2022. https://doi.org/: 10.3389/fcvm.2022.896499
22. Jiang L, Zheng Z, Fang H, Yang J: A generalized linear mixed model association tool for biobank-scale data. Nat Genet 53:1616-1621, 2021 https://doi.org/: 10.1038/s41588-021-00954-4
23. Kurki MI, Karjalainen J, Palta P, Sipilä TP, Kristiansson K, Donner KM, Reeve MP, Laivuori H, Aavikko M, Kaunisto MA, Loukola A, Lahtela E, Mattsson H, Laiho P, Della Briotta Parolo P, Lehisto AA, Kanai M, Mars N, Rämö J, Kiiskinen T, Heyne HO, Veerapen K, Rüeger S, Lemmelä S, Zhou W, Ruotsalainen S, Pärn K, Hiekkalinna T, Koskelainen S, Paajanen T, Llorens V, Gracia-Tabuenca J, Siirtola H, Reis K, Elnahas AG, Sun B, Foley CN, Aalto-Setälä K, Alasoo K, Arvas M, Auro K, Biswas S, Bizaki-Vallaskangas A, Carpen O, Chen CY, Dada OA, Ding Z, Ehm MG, Eklund K, Färkkilä M, Finucane H, Ganna A, Ghazal A, Graham RR, Green EM, Hakanen A, Hautalahti M, Hedman Å K, Hiltunen M, Hinttala R, Hovatta I, Hu X, Huertas-Vazquez A, Huilaja L, Hunkapiller J, Jacob H, Jensen JN, Joensuu H, John S, Julkunen V, Jung M, Junttila J, Kaarniranta K, Kähönen M, Kajanne R, Kallio L, Kälviäinen R, Kaprio J, Kerimov N, Kettunen J, Kilpeläinen E, Kilpi T, Klinger K, Kosma VM, Kuopio T, Kurra V, Laisk T, Laukkanen J, Lawless N, Liu A, Longerich S, Mägi R, Mäkelä J, Mäkitie A, Malarstig A, Mannermaa A, Maranville J, Matakidou A, Meretoja T, Mozaffari SV, Niemi MEK, Niemi M, Niiranen T, CJ OD, Obeidat ME, Okafo G, Ollila HM, Palomäki A, Palotie T, Partanen J, Paul DS, Pelkonen M, Pendergrass RK, Petrovski S, Pitkäranta A, Platt A, Pulford D, Punkka E, Pussinen P, Raghavan N, Rahimov F, Rajpal D, Renaud NA, Riley-Gillis B, Rodosthenous R, Saarentaus E, Salminen A, Salminen E, Salomaa V, Schleutker J, Serpi R, Shen HY, Siegel R, Silander K, Siltanen S, Soini S, Soininen H, Sul JH, Tachmazidou I, Tasanen K, Tienari P, Toppila-Salmi S, Tukiainen T, Tuomi T, Turunen JA, Ulirsch JC, Vaura F, Virolainen P, Waring J, Waterworth D, Yang R, Nelis M, Reigo A, Metspalu A, Milani L, Esko T, Fox C, Havulinna AS, Perola M, Ripatti S, Jalanko A, Laitinen T, Mäkelä TP, Plenge R, McCarthy M, Runz H, Daly MJ, Palotie A: FinnGen provides genetic insights from a well-phenotyped isolated population. Nature 613:508-518, 2023. https://doi.org/: 10.1038/s41586-022-05473-8
24. Lu X, Wang Y, Zhang J, Pu D, Hu N, Luo J, An Q, He L: Patients with systemic lupus erythematosus face a high risk of cardiovascular disease: A systematic review and Meta-analysis. Int Immunopharmacol 94:107466, 2021. https://doi.org/: 10.1016/j.intimp.2021.107466
25. Malik R, Traylor M, Pulit SL, Bevan S, Hopewell JC, Holliday EG, Zhao W, Abrantes P, Amouyel P, Attia JR, Battey TW, Berger K, Boncoraglio GB, Chauhan G, Cheng YC, Chen WM, Clarke R, Cotlarciuc I, Debette S, Falcone GJ, Ferro JM, Gamble DM, Ilinca A, Kittner SJ, Kourkoulis CE, Lemmens R, Levi CR, Lichtner P, Lindgren A, Liu J, Meschia JF, Mitchell BD, Oliveira SA, Pera J, Reiner AP, Rothwell PM, Sharma P, Slowik A, Sudlow CL, Tatlisumak T, Thijs V, Vicente AM, Woo D, Seshadri S, Saleheen D, Rosand J, Markus HS, Worrall BB, Dichgans M: Low-frequency and common genetic variation in ischemic stroke: The METASTROKE collaboration. Neurology 86:1217-1226, 2016. https://doi.org/: 10.1212/wnl.0000000000002528
26. Reiner A, Yekutieli D, Benjamini Y: Identifying differentially expressed genes using false discovery rate controlling procedures. Bioinformatics 19:368-375, 2003. https://doi.org/: 10.1093/bioinformatics/btf877
27. Sakaue S, Kanai M, Tanigawa Y, Karjalainen J, Kurki M, Koshiba S, Narita A, Konuma T, Yamamoto K, Akiyama M, Ishigaki K, Suzuki A, Suzuki K, Obara W, Yamaji K, Takahashi K, Asai S, Takahashi Y, Suzuki T, Shinozaki N, Yamaguchi H, Minami S, Murayama S, Yoshimori K, Nagayama S, Obata D, Higashiyama M, Masumoto A, Koretsune Y, Ito K, Terao C, Yamauchi T, Komuro I, Kadowaki T, Tamiya G, Yamamoto M, Nakamura Y, Kubo M, Murakami Y, Yamamoto K, Kamatani Y, Palotie A, Rivas MA, Daly MJ, Matsuda K, Okada Y: A cross-population atlas of genetic associations for 220 human phenotypes. Nat Genet 53:1415-1424, 2021. https://doi.org/: 10.1038/s41588-021-00931-x
28. Schoenfeld SR, Kasturi S, Costenbader KH: The epidemiology of atherosclerotic cardiovascular disease among patients with SLE: A systematic review. Semin Arthritis Rheum 43:77-95, 2013. https://doi.org/: 10.1016/j.semarthrit.2012.12.002

29. Siegel CH, Sammaritano LR: Systemic lupus erythematosus: A review. JAMA 331:1480-1491, 2024 https://doi.org/: 10.1001/jama.2024.2315
30. Skrivankova VW, Richmond RC, Woolf BAR, Davies NM, Swanson SA, VanderWeele TJ, Timpson NJ, Higgins JPT, Dimou N, Langenberg C, Loder EW, Golub RM, Egger M, Davey Smith G, Richards JB: Strengthening the reporting of observational studies in epidemiology using mendelian randomisation (STROBE-MR): Explanation and elaboration. BMJ 375:n2233, 2021. https://doi.org/: 10.1136/bmj.n2233
31. Skrivankova VW, Richmond RC, Woolf BAR, Yarmolinsky J, Davies NM, Swanson SA, VanderWeele TJ, Higgins JPT, Timpson NJ, Dimou N, Langenberg C, Golub RM, Loder EW, Gallo V, Tybjaerg-Hansen A, Davey Smith G, Egger M, Richards JB: Strengthening the reporting of observational studies in epidemiology using mendelian randomization: The STROBE-MR statement. JAMA 326:1614-1621, 2021. https://doi.org/: 10.1001/jama.2021.18236
32. Smith GD, Ebrahim S: Mendelian randomization: Prospects, potentials, and limitations. Int J Epidemiol 33:30-42, 2004. https://doi.org/: 10.1093/ije/dyh132
33. Sudlow C, Gallacher J, Allen N, Beral V, Burton P, Danesh J, Downey P, Elliott P, Green J, Landray M, Liu B, Matthews P, Ong G, Pell J, Silman A, Young A, Sprosen T, Peakman T, Collins R: UK biobank: An open access resource for identifying the causes of a wide range of complex diseases of middle and old age. PLoS Med 12:e1001779, 2015. https://doi.org/: 10.1371/journal.pmed.1001779
34. Tang C, Ruan R, Pan B, Xu M, Huang J, Xiong Z, Zhang Z: The relationship between autoimmune disorders and intracranial aneurysms in East Asian and European populations: A bidirectional and multivariable two-sample Mendelian randomization study. Front Neurol 15:1412114, 2024. https://doi.org/: 10.3389/fneur.2024.1412114
35. Tian J, Zhang D, Yao X, Huang Y, Lu Q: Global epidemiology of systemic lupus erythematosus: A comprehensive systematic analysis and modelling study. Ann Rheum Dis 82:351-356, 2023. https://doi.org/: 10.1136/ard-2022-223035
36. Traylor M, Persyn E, Tomppo L, Klasson S, Abedi V, Bakker MK, Torres N, Li L, Bell S, Rutten-Jacobs L, Tozer DJ, Griessenauer CJ, Zhang Y, Pedersen A, Sharma P, Jimenez-Conde J, Rundek T, Grewal RP, Lindgren A, Meschia JF, Salomaa V, Havulinna A, Kourkoulis C, Crawford K, Marini S, Mitchell BD, Kittner SJ, Rosand J, Dichgans M, Jern C, Strbian D, Fernandez-Cadenas I, Zand R, Ruigrok Y, Rost N, Lemmens R, Rothwell PM, Anderson CD, Wardlaw J, Lewis CM, Markus HS: Genetic basis of lacunar stroke: A pooled analysis of individual patient data and genome-wide association studies. Lancet Neurol 20:351-361, 2021. https://doi.org/: 10.1016/s1474-4422(21)00031-4
37. Tsoi LK, Mok CC, Man BL, Fu YP: Imaging pattern and outcome of stroke in patients with systemic lupus erythematosus: A case-control study. J Rheumatol 48:533-540, 2021 https://doi.org/: 10.3899/jrheum.200664
38. Tufanaru C, Munn Z, Stephenson M, Aromataris E: Fixed or random effects meta-analysis? Common methodological issues in systematic reviews of effectiveness. Int J Evid Based Healthc 13:196-207, 2015. https://doi.org/: 10.1097/xeb.0000000000000065
39. Verbanck M, Chen CY, Neale B, Do R: Detection of widespread horizontal pleiotropy in causal relationships inferred from Mendelian randomization between complex traits and diseases. Nat Genet 50:693-698, 2018. https://doi.org/: 10.1038/s41588-018-0099-7
40. Wiseman SJ, Ralston SH, Wardlaw JM: Cerebrovascular disease in rheumatic diseases: A systematic review and meta-analysis. Stroke 47:943-950, 2016 https://doi.org/: 10.1161/strokeaha.115.012052
41. Yavorska OO, Burgess S: Mendelian randomization: An R package for performing Mendelian randomization analyses using summarized data. Int J Epidemiol 46:1734-1739, 2017. https://doi.org/: 10.1093/ije/dyx034
42. Zeng W, Hu M, Zhou L, Cun D, Ma L, Zhang J, Huang F, Jiang Z: Exploring genetic links between blood metabolites and gout susceptibility. Clin Rheumatol 43:3901-3912, 2024. https://doi.org/: 10.1007/s10067-024-07215-9
43. Zeng W, Wu Y, Liang X, Cun D, Ma L, Zhang J, Huang F, Jiang Z: Causal associations between human gut microbiota and osteomyelitis: A Mendelian randomization study. Front Cell Infect Microbiol 14:1338989, 2024. https://doi.org/: 10.3389/fcimb.2024.1338989

Turk Neurosurg 36(1):64-73, 2026
DOI: 10.5137/1019-5149.JTN.47854-24.2

Original Investigation
Cerebrovascular-Endovascular

Received: 18.11.2024
Accepted: 12.01.2025
Published Online: 16.01.2026

Revascularization in Pediatric Patients with Moyamoya Disease

Emre DURDAG[1], Baran BABAYIGIT[2], Mustafa MAZICAN[3], Sibel CATALCA[4], Ben Ali OMARI[1], Soner CIVI[1], Cagatay ANDIC[3], Halil Ibrahim SUNER[1], Ozgur KARDES[1], Ilknur EROL[5], Kadir TUFAN[1], Cem YILMAZ[2]

[1]Baskent University Adana Dr. Turgut Noyan Training and Research Hospital, Department of Neurosurgery, Adana, Türkiye
[2]Baskent University Ankara Hospital, Department of Neurosurgery, Ankara, Türkiye
[3]Baskent University Adana Dr. Turgut Noyan Training and Research Hospital, Department of Interventional Radiology, Adana, Türkiye
[4]Baskent University Adana Dr. Turgut Noyan Training and Research Hospital, Department of Anesthesiology, Adana, Türkiye
[5]Baskent University Adana Dr. Turgut Noyan Training and Research Hospital, Department of Pediatric Neurology, Adana, Türkiye

This study has been presented at the Turkish Neurosurgical Society 36th Scientific Congress between 27 and 30 April 2023, Antalya, Türkiye

Corresponding author: Emre DURDAG ✉ emredurdag@yahoo.com

To watch the surgical videoclip, please visit https://youtu.be/cToaxjztGrA?si=R4zkd3SOrS5DVbbI.

ABSTRACT

AIM: To evaluate the patients who underwent surgery with a diagnosis of Moyamoya disease (MMD), and to contribute to the literature from a single-center in Türkiye.

MATERIAL and METHODS: Patients were evaluated retrospectively based on age, symptoms, history of cerebrovascular events (CVE), genetic disorders, pre-operative (pre-op) radiological stage, surgical technique, post-operative (post-op) improvement, and post-op radiological staging. The absence of new CVEs and reduced seizure frequency were considered indicators of clinical improvement.

RESULTS: A total of 7 patients, 4 of whom had bilateral MMD, underwent surgery. The average age was 11.8 ± 5 years. 4 patients (57%) presented with cerebrovascular events as symptoms, and the remaining 3 patients (43%) presented with headaches. Cranial digital subtraction angiography (DSA) revealed that the patients were in advanced stages (Suzuki Stage 4.9 ± 1.1). Encephalo Duro Arterio Myo Synangiosis (EDAMS) surgical technique was performed on 10 hemispheres, and a combined bypass (EDAMS + direct) was performed on 1 hemisphere. Clinical improvement was observed approximately 6 months postoperatively. During follow-up, disease progression in the contralateral hemisphere with associated symptoms was noted in 4 patients, and these patients subsequently underwent surgery on the contralateral hemisphere. The average time between the first and second surgeries was 15 ± 7.7 months. Post-operative follow-up was conducted with DSA, and radiological success was defined as Lucia Stage 2 ± 0.85. No clinical difference was observed between craniotomy and craniectomy as surgical techniques. No differences were found between vessel selection and clinical outcomes.

CONCLUSION: The EDAMS protocol has proven to be an effective treatment method for pediatric patients with MMD. Post-operative clinical improvements are rapidly observed, followed by radiological improvements. Patients may experience progression from unilateral to bilateral disease, which can progress quickly.

KEYWORDS: Moyamoya, EDAMS, Incision technique, Craniotomy, Türkiye

Emre DURDAG : 0000-0001-6939-5491
Baran BABAYIGIT : 0009-0002-1283-841X
Mustafa MAZICAN : 0000-0003-1142-213X
Sibel CATALCA : 0000-0002-8899-1106
Ben Ali OMARI : 0009-0006-4242-5922
Soner CIVI : 0000-0002-1055-5152
Cagatay ANDIC : 0000-0001-8581-8685
Halil Ibrahim SUNER : 0000-0002-5957-8611
Ozgur KARDES : 0000-0003-2854-941X
İlknur EROL : 0000-0002-3530-0463
Kadir TUFAN : 0000-0003-1509-4575
Cem YILMAZ : 0000-0002-2353-8044

INTRODUCTION

Moyamoya disease (MMD), which was first reported in 1957, is an idiopathic condition characterized by nonatherosclerotic progressive stenosis of intracranial arteries, and it typically involves the distal internal carotid artery (ICA), the proximal branches of the anterior cerebral artery (ACA), and the middle cerebral artery (MCA). This stenosis results in irregular neovascularization and elevates the risk of infarction and hemorrhage (3,43). Cerebrovascular events (CVE), including transient ischemic attacks (TIA), stroke, and hemorrhage, are the most frequent symptoms reported by these patients (23). Ischemic CVEs are more prevalent in pediatric patients, whereas hemorrhagic CVEs are more common in adults (10). It is not uncommon for MMD to progress from unilateral to bilateral involvement, and the brain parenchyma can be affected unilaterally or bilaterally (27).

The diseased prevalence is 0.086 per 100,000 individuals, with the highest prevalence among Japanese children (6.03 per 100,000) (36). MMD exhibits a bimodal age distribution, with peaks at ages 5–9 and 35–50 years, and it predominantly affects females (8).

Although medical and endovascular techniques have been employed in treatment, their long-term efficacy is restricted (16,17,33). Currently, surgical revascularization techniques including direct and indirect bypass are considered as the most effective treatment modality for MMD (33).

This study aimed to contribute to Turkish literature by sharing our surgical experiences and clinical outcomes related to this disease.

MATERIAL and METHODS

The Institutional Review Board approved the study (Baskent University Clinical Research Ethics Board, KA24/348, 09/10/2024).

The data of seven patients who underwent surgical treatment for MMD in our clinic between January 2019 and January 2024 were retrospectively evaluated. During the postoperative follow-up, progression in the contralateral hemisphere was noted in 4 of these patients who underwent surgery on the contralateral hemisphere, resulting in a total of 11 hemispheres that were operated on. The symptoms, radiological findings, and surgical techniques employed during the second surgery in the bilaterally operated patients were also documented. Antiepileptic drug (AED) treatments and acetylsalicylic acid (ASA) were either maintained at an appropriate dosage or introduced in the drug regimen of all patients.

Cerebral digital subtraction angiography (DSA) and brain magnetic resonance imaging (MRI) were employed for preoperative and postoperative follow-up imaging. DSA follow ups were performed every six months for the first year and annually thereafter. Interventional radiologists, blinded to the patient data, conducted the radiological staging. The Suzuki staging system was utilized for preoperative staging, while the radiological staging system described by Lucia et al. was employed for postoperative follow-up (30,42).

Suzuki staging is based on conventional angiographic findings and classifies the MMD progression into six stages (Table I) (42). The staging system described by Lucia et al. is also angiography-based, and assesses distal perfusion following a superficial temporal artery (STA)-MCA anastomosis (Table II) (30).

Surgical Technique

Direct by-pass in one patient and indirect by-pass (encephaloduroarteriomyosynangiosis (EDAMS protocol) in the other surgical procedures were performed**.** The primary aim of the EDAMS protocol is to establish anastomosis between the STA and MCA to enhance perfusion. All patients were placed in a supine position with the head completely turned to the contralateral side. Mild hypertension and hypercapnia were

Table I: Suzuki Grading System (42)

Stage I	Narrowing of Terminal ICA
Stage II	Initiation of moyamoya vessels in basal carotid circulation, dilation of intracerebral arteries
Stage III	Intensification of moyamoya vessels, severe carotid stenosis, defection of ACA and MCA
Stage IV	Minimization of moyamoya vessels, defection of PCA
Stage V	Further reduction of moyamoya, disappearance of major cerebral arteries
Stage VI	Disappearance of moyamoya collaterals and ICA, cerebral blood supply comes from external carotid arteries via leptomeningeal anastomoses

Table II: Angiographic Staging System Proposed by Lucia et al. (30)

Stage	Definition	Findings
I	Poor	No filling of the MCA territory
II	Moderate	Antegrade filling of one or two MCA branches
III	High	Complete filling of the MCA territory

preferred for preventing perfusion disruption and facilitating technical ease via vasodilation. A skin Doppler was employed to trace the STA and its branches, and these were evaluated along with DSA imaging. A question mark-shaped incision was utilized to increase arterial mobilization in patients with an increased distance between the artery and the Sylvian fissure. For patients with a reduced distance, a linear incision was implemented. The STA was employed as the donor artery in all surgeries. After performing an appropriate skin incision, the STA was dissected in accordance with microvascular surgical principles, ensuring 360-degree isolation, and it was suspended. The temporal muscle was then incised in a cruciate shape and suspended. After two burr holes were made, a circular craniotomy was performed. Subsequently, a cruciate opening was created in the dura mater, preserving the middle meningeal artery as much as possible, and the edges were folded inward. Following the opening of the Sylvian fissure, the STA was sutured to the pia near the MCA using microvascular surgical techniques (Figure 1). The tissue adhesive was applied without suturing the dura mater, and standard closure procedures were performed.

Craniectomy was preferred to craniotomy in cases where the selected STA branch's thickness was deemed insufficient to ensure adequate perfusion to maximize the contact between the temporal muscle and the brain parenchyma without replacing the bone. In other cases, the craniotomy flap was affixed to the intact bone.

The presenting symptom, age at initial symptom onset, sex, preoperative ischemic events, presence of syndromes, consanguinity, and a history of genetic diseases in the patient or their family were analyzed. Furthermore, data regarding the surgical technique, skin incision type, donor artery, preference for craniotomy or craniectomy, perioperative complications, symptoms during follow-up, and the interval between the first and second surgeries were obtained. The absence of new ischemic events or hemorrhage, reduced seizure frequency, improved ischemic findings, and the absence of new ischemic events or hemorrhage were regarded as indicators of clinical improvement during the postoperative period.

RESULTS

The average age of the patients at initial presentation was 11.8±5 years. Only one patient was male, while the remaining six were female (M/F ratio: 1/6). At initial presentation, two patients (28%) exhibited hemiplegia/paresis, two (28%) presented with monoplegia/paresis, and three (43%) experienced headaches. One of the patients with hemiplegia also reported a history of focal seizures (14%). Vomiting was noted as an additional symptom in two patients. Upon reviewing the patients' medical histories, it was observed that one patient had been previously diagnosed with migraines, while another had been experiencing headaches and nausea/vomiting attacks for four years.

Regarding genetic predisposition, one patient had Down syndrome, another had Poland syndrome, while a third was being monitored for NF-1. Genetic screening for MTHFR, factor V, prothrombin, and prothrombin activator inhibitor (PAI) mutations was performed in four out of seven patients. A heterozygous MTHFR mutation was present in one patient, while a homozygous mutation was present in the other. The patient with the homozygous mutation had a history of consanguinity. Genetic screening data for the remaining three patients could not be retrieved due to follow-up at other centers. DSA performed preoperatively revealed that the patients were predominantly in the advanced stages of the disease (Suzuki stage 4.9 ± 1.1).

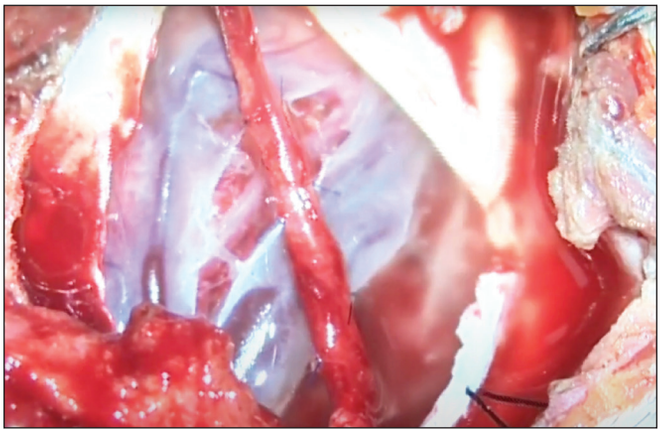

Figure 1: Intraoperative imaging during the EDAMS procedure. Please check "Surgical Technique" and/or "Surgical Videoclip" for attention in details.

Antiepileptic drugs (AEDs) were administered by a pediatric neurologist following the initial diagnosis in four patients (one on carbamazepine, three on levetiracetam). Levetiracetam was administered perioperatively as AED prophylaxis to the remaining three patients. The treatment doses for patients who were already receiving AEDs preoperatively were not modified. AEDs prescribed prophylactically were altered or tapered based on clinical and EEG-based monitoring under the guidance of the pediatric neurologist. The prophylactically prescribed AEDs were discontinued within three months postoperatively. All patients were administered aspirin (ASA) at an appropriate dose (100 mg) based on their body weight, which was Continued postoperatively.

Seven patients underwent surgery, with 11 hemispheres being operated on, including bilateral operations in four patients. The EDAMS protocol was implemented in ten hemispheres (91%), while the combined bypass technique [direct + indirect (EDAMS)] was performed in one hemisphere (9%). A longitudinal linear incision anterior to the tragus was used in seven hemispheres (63%), while a question mark-shaped incision was utilized in four hemispheres (36%). The frontal branch of the STA was used in three hemispheres (27%), the parietal branch in four hemispheres (36%), and both the major branches of the STA in four hemispheres (36%). Craniotomy was performed to access three hemispheres (27%), while craniectomy was performed for acessing the remaining eight hemispheres (63%).

In the early postoperative phase, one patient developed an epidural hematoma, requiring reoperation. The remaining

patients did not experience any additional early postoperative complications. One patient experienced a focal seizure on the fifth postoperative day. In terms of surgical success, no clinical difference was observed between craniotomy and craniectomy. The question mark incision technique was implemented in four surgeries, while linear incisions were used in seven surgeries. Two patients with question mark-shaped incisions experienced wound dehiscence following suture removal; these wounds were allowed to heal through secondary intention. No wound complications were observed in patients with linear incisions. No clinically significant difference in outcomes was observed based on the choice of donor artery.

The follow-up period was 30.57 ± 14.48 months. No lateralizing symptoms were idenified on the side of the body innervated by the operated hemisphere during the follow-up period. Two patients reported persistent headaches, the intensity of which decreased following the initial surgery and did not continue to affect their quality of life (18%). Unrelated to the surgery, one patient developed stage 2 essential hypertension and was initiated on antihypertensive therapy.

Based on the radiological findings, bilateral involvement was observed in three patients at the time of diagnosis. One of these patients experienced stroke-like symptoms on both sides of the body, including left upper limb plegia and right upper limb paresis (power: 4/5). The right hemisphere, which was the more symptomatic side, was operated on first. The left hemisphere was operated one year later, as planned. The other two patients were symptomatic on only one side of the body; therefore, the symptomatic hemisphere was operated on first. These patients were monitored for contralateral symptoms, and a second surgery was scheduled when the symptoms manifested. However, in one patient, the second surgery was postponed for more than 24 months due to insurance coverage issues. In another patient, the unilateral disease was diagnosed initially; however, subsequent DSA revealed the involvement of the contralateral hemisphere. Therefore, contralateral surgery was performed after the patient became symptomatic. Hypesthesia was the most prevalent symptom in all patients who underwent bilateral surgery. None of the patients developed early postoperative complications. The average duration between the first and second surgeries was 15 ± 6 months (Table III).

According to the first post-operative DSA performed at 6 months Lucia stage was 1.81 ± 0.87. Last radiological stage based on last DSA was identified as 2 ± 0.85 (Figure 2, 3) (Table IV). Although there were insufficient data to make a statistical assessment, there was no significant difference between early and late results.

DISCUSSION

Moyamoya disease is a cerebrovascular condition characterized due to ischemic and hemorrhagic stroke caused by stenosis or occlusion at the terminal ICA and ACA-MCA proximal regions, although its pathophysiology remains incompletely understood. Moyamoya syndrome refers to similar clinical and vascular manifestations observed in patients with underlying conditions such as autoimmune diseases, meningitis, cranial tumors, Down syndrome, NF-1, or cranial radiation exposure (27). Although it does not meet the diagnostic criteria for Moyamoya disease, it has been linked to sickle cell anemia, renal artery stenosis, antiphospholipid syndrome, and intracranial atherosclerotic disease (39). The diagnostic criteria most recently revised by the Moyamoya Disease Research Committee in 2021 (27). The definitive diagnosis is determined based on angiography. Historically, DSA was essential for a definitive

Table III: Involved Side, Symptomatology, Surgery, and Follow-Up Chart of Study Participants

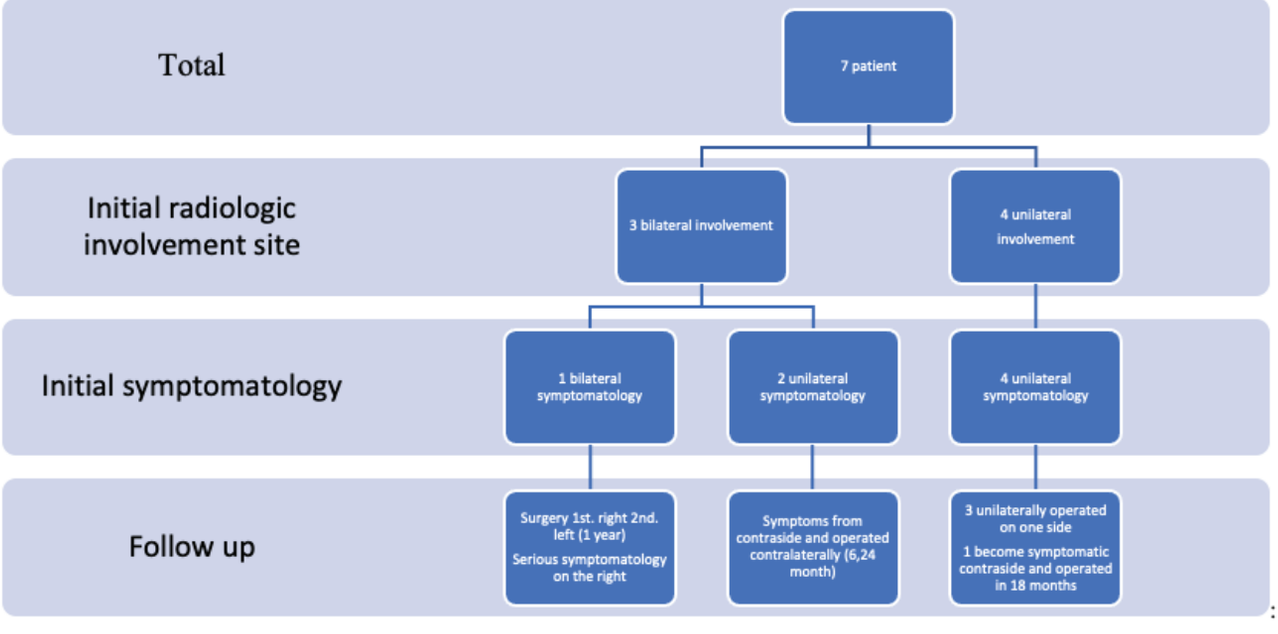

diagnosis; however, current diagnostic protocols may utilize MR angiography. DSA may still be implemented in the event of diagnostic uncertainty or for temporal imaging (27,33). Surgical revascularization is recognized as the most effective treatment for the disease (34).

In our case series, we noted that most patients were female (F:M = 6:1). Epidemiological studies in the literature have also suggested a higher disease prevalence among females, with a general female predominance ratio of 1–2:1 (37,48). The female-to-male ratio was 4.25:1 in a case series conducted by Kraemer and colleagues in Germany (25).

The absence of adult patients in our study cohort is inconsistent with Moyamoya's bimodal age distribution (mean age 11.8 ± 5 years) (37,48). This could be attributed to the fact that our center has only recently begun administering Moyamoya treatments within the past four years as well as a result of our collaboration with the pediatric neurology department, leading to a predominance of pediatric patients in our study population.

Table IV: DSA Results of Procedures

Number of Procedures	Patient Number	Side	Pre-operative Suzuki stage	Post-operative Lucia stage on 6th month DSA	Lucia stage on last DSA (Follow-Up)
1	1	Right	6	2	3 (3th year)
2	1	Left	4	1	1 (2nd year)
3	2	Right	5	2	2 (6th month)
4	2	Left	5	1	1 (2nd year)
5	3	Right	2	1	1 (6th month)
6	3	Left	5	2	2 (2nd year)
7	4	Right	5	1	2 (2nd year)
8	5	Right	5	3	3 (2nd year)
9	6	Right	6	3	3 (2nd year)
10	6	Left	5	3	3 (12th month)
11	7	Left	6	1	1 (6th month)

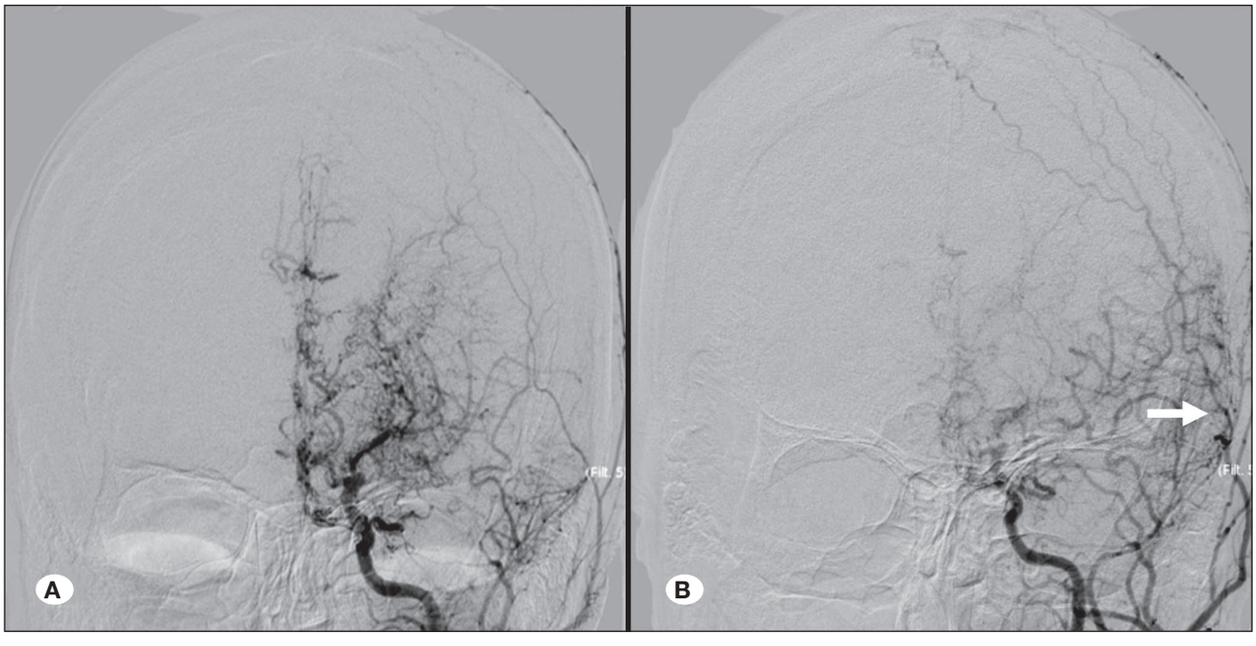

Figure 2: A) Classic "puff of smoke" sign observed on pre-operative DSA imaging of the patient, **B)** In the fourth year of postoperative follow-up, white arrow mentioned anastomosis site. The Moyamoya disease-involved arteries have disappeared and the MCA filling now occurs through the ECA.

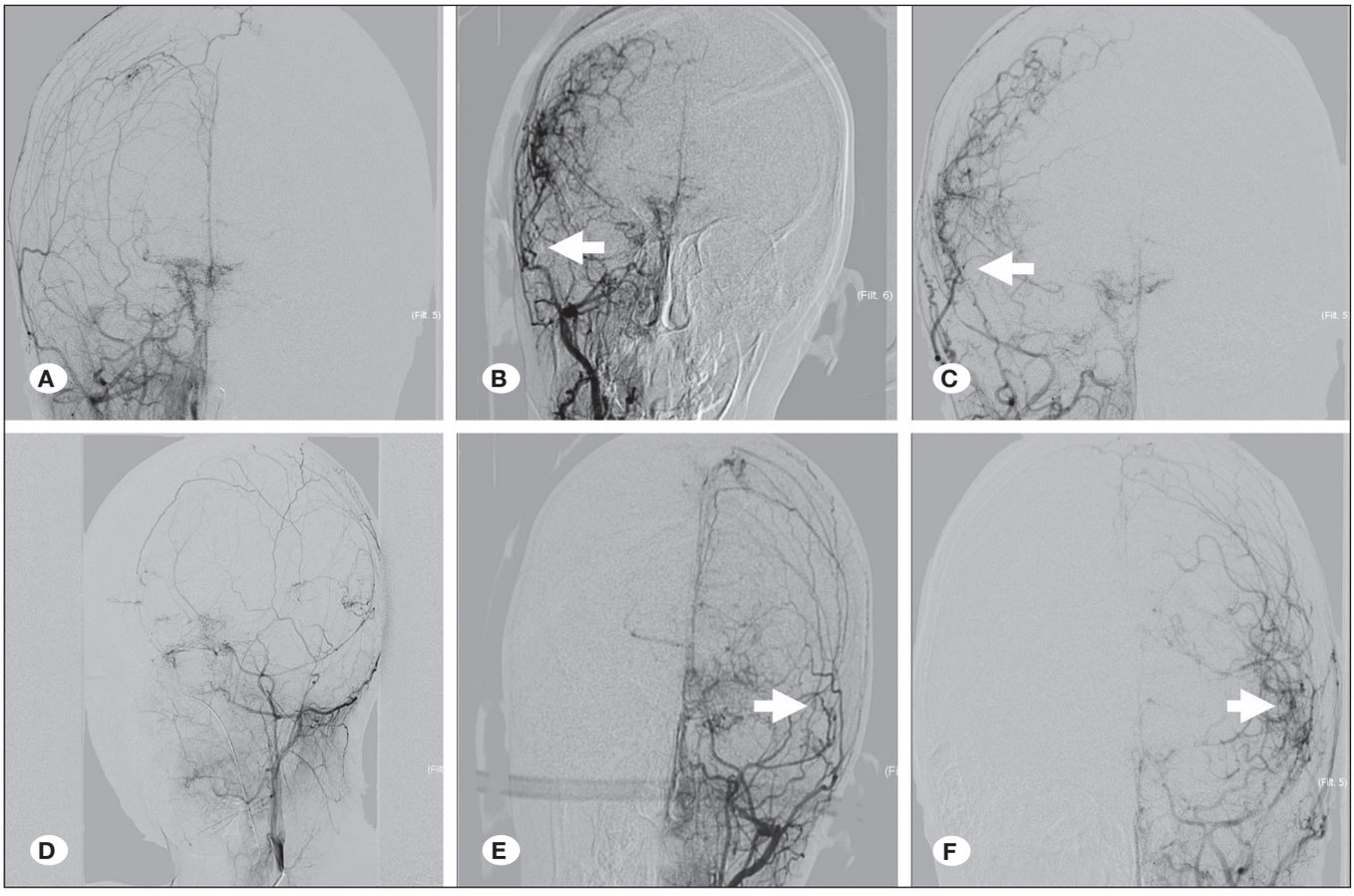

Figure 3: DSA images of another patient who underwent bilateral EDAMS protocol: **A)** preoperative, **B, C)** patient's 6th month and 18th follow-up (right), **D)** preoperative, **E, F)** patient's 6th month and 18th follow-up (left). White arrow mentioned anastomosis sites.

There are two principal methods for managing patients with bilateral disease: simultaneous bilateral surgery or a two-stage approach, in which the more symptomatic hemisphere is operated initially. Xu et al. demonstrated that patients who underwent simultaneous bilateral surgery had longer hospital stays, a greater incidence of postoperative ischemic stroke, and a shorter stroke-free survival compared to those who underwent staged surgeries (47). Deckers et al. have shown that unilateral surgery in patients with bilateral involvement also enhances perfusion in the contralateral hemisphere (7). Given that our patient population was pediatric and considering the higher risks associated with bilateral surgery, we selected a two-stage surgical approach. Our objective in monitoring patients during asymptomatic periods was to gain a more comprehensive understanding of the natural progression of the disease. The interval between operations was 15 ± 6 months in the four patients who underwent bilateral surgery.

During the second year of DSA-based monitoring, one patient initially exhibited unilateral involvement; however, progression to the contralateral hemisphere was observed. Existing literature indicates that patients with unilateral involvement can progress to develop bilateral disease; thus, the 2021 revision of the Moyamoya Diagnostic Criteria now includes patients with unilateral MMD (27). Lee and colleagues found that 29% of patients progressed from unilateral to bilateral disease in their investigation of young adults (29). Conversely, Church et al. reported a lower rate of 8.3% (5). Kelly et al. found a 38% progression rate, with an average time of 12.7 months (20). A mean progression time of 43.7 months was reported in another study (28). We recommend close monitoring of the diagnosed patients for potential disease progression. Bilateral progression in one of our four patients with initial unilateral involvement by the second postoperative year is consistent with the literature.

In pediatric patients with CVE, genetic and metabolic disorders should be considered. We conducted a differential diagnosis by assessing the homocysteine levels, factor V, prothrombin, prothrombin activator inhibitor (PAI), and MTHFR mutations in our patients. Unlike MMD patients, those with homocystinuria exhibit significant clinical improvement by normalizing homocysteine levels through vitamin B12 and folate supplementation (9). In two patients, the homocysteine levels were marginally elevated. Due to the absence of the characteristic phenotypes associated with homocystinuria (mental retardation, atypical facies, lens subluxation), MMD was considered the primary diagnosis, with the MTHFR polymorphism identified as a risk factor. Although all of our patients underwent MTHFR gene screening, the current

literature suggests that MTHFR analysis without homocysteine level assessment is unnecessary (35). Nevertheless, due to the increased risk of thrombosis associated with elevated homocysteine levels, vitamin B12 and folate supplementation were administered, and homocysteine levels were regularly monitored.

In 3 of our 7 patients, syndromic diseases were noted. One patient had Down syndrome, and another was diagnosed with NF-1. The association of these conditions with MMD has been documented in literature. Therefore, in patients with these syndromes, the presence of neurological symptoms should prompt the consideration of MMD as a differential diagnosis (44). One of our patients had Poland syndrome, and to our knowledge, this is the first reported case of the coexistence of MMD and Poland syndrome. Although there is insufficient data to ascertain whether this is incidental, this association may offer a novel insight into the pathogenesis of MMD. The high number of patients with syndromes in our study could be attributed to the fact that our patient population was predominantly from the Eastern and Southeastern Anatolia regions of Turkey, which are known for their high ethnic diversity (45).

It was observed that most patients experienced prodromal symptoms prior to their initial presentation. These nonparetic symptoms may result in a delayed diagnosis, as MMD is a rare disease and does not always manifest with the typical symptoms of CVE (14). Non-paretic symptoms in these patients can be misinterpreted as epileptic seizures, and similarly, epileptic seizures may be confounded with stroke or transient ischemic attack (TIA) (14,46). These scenarios underscore the significance of EEG and perfusion imaging in such cases (46). At the initial presentation, four patients (57%) presented with ischemic stroke, while three patients (43%) reported headaches. One of the patients with ischemic stroke also experienced focal seizures (14%). These findings are consistent with previous studies, indicating that MMD presents differently from other ischemic strokes (4,18,19,35).

In terms of revascularization, both direct bypass (STA-MCA) and indirect bypass techniques are accessible. In direct bypass, a patent artery is connected to the affected artery's distal segment. Conversely, indirect revascularization involves the placement of a patent artery or tissue supplied by an artery in contact with the brain parenchyma to facilitate spontaneous vascularization (12). Indirect techniques, including encephaloduroarteriosynangiosis (EDAS), encephalomyosynangiosis (EMS), encephalomyoarteriosynangiosis (EMAS), encephaloduroaortic synangiosis (EDAMS), and omental transplantation, have been developed (12). These techniques are frequently preferred in patients possessing a cortical artery that is suitable for anastomosis. However, there are concerns that indirect methods alone may be inadequate to prevent ischemia (4). Fujimura et al. reported that direct STA-MCA anastomosis is safe and effective for all age groups (11). Certain studies indicate that the direct bypass technique is more effective for achieving radiological improvement, as it rapidly resolves hypoperfusion (22,32). However, direct bypass surgery also carries risks, primarily due to the fragility of the vascular walls in these patients, necessitating the use of precise surgical techniques. Another potential complication of the direct bypass technique is postoperative hyperperfusion injury (26). The current literature is divided on the advantages of direct versus indirect bypass techniques.

The EDAMS technique was employed at 91% of the cerebral bypass surgeries in our clinic. The donor arteries were chosen based on the distance of the STA branches from the Sylvian fissure and their diameter. A combined direct-indirect bypass technique was performed in one patient, as the STA and MCA branches were considered appropriate for anastomosis due to their larger diameter. In other cases, the risk of anastomosis was deemed excessive due to the small size of the STA branches. Rapid clinical improvement was observed postoperatively, and no new neurological findings were noted on the affected side. Our clinical experience suggests that indirect bypass can yield favorable results in pediatric MMD patients. However, given our limited experience with direct bypass, assessing the superiority of different surgical techniques is beyond the scope of this study.

Although data are insufficient for establishing statistical significance, we observed that epithelialization was completed by postoperative day 14 in patients with linear skin incisions, and scabs were fully resolved. Conversely, wound healing did not progress as quickly in patients with question mark-shaped incisions, and two patients experienced wound dehiscence. Linear incisions seem superior as they preserve skin perfusion and facilitate easier suturing. This observation is consistent with the results of previous studies (1).

In terms of complications, one patient (14%) experienced early postoperative epidural hemorrhage, while another experienced focal seizure during the first postoperative week (14%). No new ischemic stroke occurred in the operated hemispheres of any patient. In a 2024 review conducted by Batista et al., hemorrhagic, ischemic, and epileptic complications were reported at rates of 4%, 6%, and 3%, respectively, with no significant difference in the complication rates between the pediatric and adult populations (2).

In 3 of the 11 surgeries that were performed, a craniectomy was conducted, while the other 8 entailed a craniotomy. In all cases, the bone flap was removed employing a single-burr keyhole technique with an average diameter of 4 cm. The objective was to reduce the surgical field and mitigate the risk of potential hemorrhage or parenchymal injury. Shimizu et al. have reported that larger craniotomies elevate the risk of surgical complications (38). Nevertheless, there is no consensus on the optimal craniotomy size, as larger craniotomies may expand the area of indirect revascularization, a critical factor in postoperative progression (26). Considering that potential complications in pediatric patients could be more severe, we opted for a craniotomy size of approximately 4 cm^2 in all patients.

While the Suzuki staging system is the standard for the radiological classification of MMD, multiple classifications have been proposed for evaluating vascular structures postoperatively, and no consensus has been reached in the

literature (6,31). For the radiological follow-up of our patients, we employed the classification described by Lucia et al., which is simple to understand and practical to implement. This classification also demonstrated positive surgical outcomes (30).

Our clinical experience indicates that clinical symptoms are likely to develop after a significant occlusion is detected radiologically. Clinical improvement typically manifests within the first six months of the postoperative period, followed by radiological improvement. However, clinical improvement was also noted in three patients without the evidence of angiographic improvement. This could be attributed to an increase in perfusion, even if there was no morphological evidence of new vessel formation. So et al. observed that MR perfusion SPECT results significantly correlated with clinical outcomes, although SPECT and angiographic findings were not always correlated (40,41). We believe that digital subtraction angiography (DSA) is essential for bypass patency assessment. Clinical follow-up and angiography alone may not always be sufficient. The growing availability of 3 Tesla MR and perfusion imaging provides more comprehensive information and can serve as a supplementary follow-up method in managing MMD in addition to direct angiography (21).

Study Limitations

The study's results were consistent with the literature, and certain relationships could be established. However, the small sample size undermines the ability to conduct statistical analyses. A more extensive, multi-center study is required. Another study limitation is the absence of genetic studies on the patients. Han et al. demonstrated that the prevalence of asymptomatic familial Moyamoya disease (MMH) is higher than anticipated through family screening using transcranial Doppler ultrasonography (18). In our study, the absence of family screening resulted in the scarcity of information regarding the familial background of our patients. Investigating genes associated with MMD and performing family screenings may provide valuable insights for future research, particularly given our patient population's high rate of consanguineous marriages. Transcranial Doppler ultrasonography could be a cost-effective and noninvasive screening procedure for family members in our country.

Although the surgery demonstrated symptomatic benefits, no follow-up was conducted to assess the status of patients' social reintegration or participation in daily life. Tools such as the Modified Rankin Scale or Pediatric Stroke Outcome Measure could be employed in this regard (15,24). Because the patients in our study were from the pediatric population, it is crucial to determine the extent to which they benefit from surgery and how they cope with such a condition and adapt to social life (13). The absence of psychological, mental, and social participation assessments during preoperative and postoperative follow-up restricts our understanding in this area.

From a radiological standpoint, the lack of perfusion imaging in the patients implies that, while increased vascular filling could be demonstrated via DSA, it is insufficient in providing quantitative data when compared to MRI or CT perfusion imaging (40). Additionally, the fact that all surgeries were conducted by a single surgeon in a single clinic setup introduces potential bias, further limiting the data reliability.

CONCLUSION

The EDAMS protocol is an effective surgical technique for treating Moyamoya disease. Although the global literature on the disease has advanced significantly, the absence of sufficient studies in our country renders this research important in contributing to the literature. Future studies and long-term follow-ups should assess the epidemiology and genetic background of Moyamoya disease in Turkey, as well as the comparison of various surgical techniques.

Declarations

Funding: This research did not receive any specific grant from funding agencies in the public, commercial, or not-for-profit sectors.

Availability of data and materials: The datasets generated and/or analyzed during the current study are available from the corresponding author by reasonable request.

Disclosure: The authors declare no competing interests.

AUTHORSHIP CONTRIBUTION

Study conception and design: ED
Data collection: BB, MM
Analysis and interpretation of results: CA, SC
Draft manuscript preparation: BAO, IE
Critical revision of the article: SC, IS
Other (study supervision, fundings, materials, etc...): CY, OK, KT
All authors (ED, BB, MM, SC, BAO, SC, CA, HIS, OK, IE, KT, CY) reviewed the results and approved the final version of the manuscript.

REFERENCES

1. Acker G, Schlinkmann N, Fekonja L, Grünwald L, Hardt J, Czabanka M, Vajkoczy P: Wound healing complications after revascularization for Moyamoya vasculopathy with reference to different skin incisions. Neurosurg Focus 46:E12, 2019. https://doi.org/10.3171/2018.11.FOCUS18512
2. Batista S, Koester S, Bishay AE, Bertani R, Oberman DZ, de Abreu LV, Bocanegra-Becerra JE, Amaral D, Isaacs AM, Dewan M, Figueiredo EG: Complications associated with combined direct and indirect bypass in moyamoya disease: a meta-analysis. Neurosurg Rev 47:58, 2024. https://doi.org/10.1007/s10143-024-02285-4
3. Berry JA, Cortez V, Toor H, Saini H, Siddiqi J: Moyamoya: An update and review. Cureus 12:e10994, 2020. https://doi.org/10.7759/cureus.10994
4. Burke GM, Burke AM, Sherma AK, Hurley MC, Batjer HH, Bendok BR: Moyamoya disease: A summary. Neurosurg Focus 26:E11, 2009. https://doi.org/10.3171/2009.1.FOCUS08310
5. Church EW, Bell-Stephens TE, Bigder MG, Gummidipundi S, Han SS, Steinberg GK: Clinical course of unilateral Moyamoya disease. Neurosurgery 87:1262-1268, 2020. https://doi.org/10.1093/neuros/nyaa284

6. Czabanka M, Peña-Tapia P, Scharf J, Schubert GA, Münch E, Horn P, Schmiedek P, Vajkoczy P: Characterization of direct and indirect cerebral revascularization for the treatment of European patients with Moyamoya disease. Cerebrovasc Dis 32:361-369, 2011. https://doi.org/10.1159/000330351
7. Deckers PT, van Hoek W, Kronenburg A, Yaqub M, Siero JCW, Bhogal AA, van Berckel BNM, van der Zwan A, Braun KPJ: Contralateral improvement in cerebrovascular reactivity and TIA frequency after unilateral revascularization surgery in Moyamoya vasculopathy. Neuroimage Clin 30:102684, 2021. https://doi.org/10.1016/j.nicl.2021.102684
8. Duan L, Bao XY, Yang WZ, Shi WC, Li DS, Zhang ZS, Zong R, Han C, Zhao F, Feng J: Moyamoya disease in China: Its clinical features and outcomes. Stroke 43:56-60, 2012. https://doi.org/10.1161/STROKEAHA.111.621300
9. Erol M, Gayret OB, Yigit O, Serefoglu Cabuk K, Toksoz M, Tiras M: A case of homocystinuria misdiagnosed as Moyamoya disease: A case report. Iran Red Crescent Med J 18:e30332, 2016. https://doi.org/10.5812/ircmj.30332
10. Fox BM, Dorschel KB, Lawton MT, Wanebo JE: Pathophysiology of vascular stenosis and remodeling in Moyamoya disease. Front Neurol 12:661578, 2021. https://doi.org/10.3389/fneur.2021.661578
11. Fujimura M, Kaneta T, Tominaga T: Efficacy of superficial temporal artery-middle cerebral artery anastomosis with routine postoperative cerebral blood flow measurement during the acute stage of childhood Moyamoya disease. Childs Nerv Syst 24:827-832, 2008. https://doi.org/10.1007/s00381-007-0551-y
12. Fukui M: Current state of the study on Moyamoya disease in Japan. Surg Neurol 47:138-143, 1997. https://doi.org/10.1016/S0090-3019(96)00358-8
13. Funaki T, Takahashi JC, Miyamoto S: Late cerebrovascular events and social outcome after adolescence: Long-term outcome of pediatric Moyamoya disease. Neurol Med Chir 58:240-246, 2018. https://doi.org/10.2176/nmc.ra.2018-0026
14. Ghosh R, Das S, Roy D, Ray A, Benito-León J: Moyamoya angiopathy in a case of Klinefelter syndrome. Childs Nerv Syst 38:1195-1199, 2022. https://doi.org/10.1007/s00381-021-05371-w
15. Goren O, Hendrix P, Peled A, Kimchi G, Zauberman J, Griessenauer C, Feldman Z: Encephaloduroarteriosynangiosis with dural inversion for Moyamoya disease in a pediatrics and adult population: A single-center 20-year experience. World Neurosurg 149:e16-21, 2021. https://doi.org/10.1016/j.wneu.2021.02.102
16. Gross BA, Thomas AJ, Frerichs KU: Endovascular treatment of symptomatic Moyamoya. Neurosurg Rev 37:579-583, 2014. https://doi.org/10.1007/s10143-014-0542-x
17. Hallemeier CL, Rich KM, Grubb RL Jr, Chicoine MR, Moran CJ, Cross DT 3rd, Zipfel GJ, Dacey RG Jr, Derdeyn CP: Clinical features and outcomes in north American adults with Moyamoya phenomenon. Stroke 37:1490-1496, 2006. https://doi.org/10.1161/01.STR.0000221787.70503.ca
18. Han C, Feng H, Han YQ, Liu WW, Zhang ZS, Yang WZ, Duan L: Prospective screening of family members of Moyamoya disease patients. PLoS One 9:e88765, 2014. https://doi.org/10.1371/journal.pone.0088765
19. Houkin K, Yoshimoto T, Kuroda S, Ishikawa T, Takahashi A, Abe H: Angiographic analysis of moyamoya disease-how does moyamoya disease progress? Neurol Med Chir 36:783-787, 1996. https://doi.org/10.2176/nmc.36.783
20. Kelly ME, Bell-Stephens TE, Marks MP, Do HM, Steinberg GK: Progression of unilateral Moyamoya disease: A clinical series. Cerebrovasc Dis 22:109-115, 2006. https://doi.org/10.1159/000093238
21. Kikuta K: Experiences using 3-tesla magnetic resonance imaging in the treatment of Moyamoya disease. Acta Neurochir Suppl 103:123-126, 2008. https://doi.org/10.1007/978-3-211-76589-0_22
22. Kim H, Jang DK, Han YM, Sung JH, Park IS, Lee KS, Yang JH, Huh PW, Park YS, Kim DS, Han KD: Direct bypass versus indirect bypass in adult Moyamoya angiopathy with symptoms or hemodynamic instability: A meta-analysis of comparative studies. World Neurosurg 94:273-284, 2016. https://doi.org/10.1016/j.wneu.2016.07.009
23. Kim JS: Moyamoya disease: Epidemiology, clinical features, and diagnosis. J Stroke 18:2-11, 2016. https://doi.org/10.5853/jos.2015.01627
24. Kitchen L, Westmacott R, Friefeld S, MacGregor D, Curtis R, Allen A, Yau I, Askalan R, Moharir M, Domi T, deVeber G: The pediatric stroke outcome measure: A validation and reliability study. Stroke 43:1602-1608, 2012. https://doi.org/10.1161/STROKEAHA.111.639583
25. Kraemer M, Heienbrok W, Berlit P: Moyamoya disease in Europeans. Stroke 39:3193-3200, 2008. https://doi.org/10.1161/STROKEAHA.107.513408
26. Kuroda S: Bypass surgery for Moyamoya disease, part 1: Special considerations and techniques. No Shinkei Geka 50:806-818, 2022. https://doi.org/10.11477/mf.1436204624.
27. Kuroda S, Fujimura M, Takahashi J, Kataoka H, Ogasawara K, Iwama T, Tominaga T, Miyamoto S; Research Committee on Moyamoya Disease (Spontaneous Occlusion of Circle of Willis) of the Ministry of Health, Labor, and Welfare, Japan: Diagnostic criteria for Moyamoya disease-2021 revised version. Neurol Med Chir 62:307-312, 2022. https://doi.org/10.2176/jns-nmc.2022-0072
28. Kuroda S, Hashimoto N, Yoshimoto T, Iwasaki Y; Research Committee on Moyamoya Disease in Japan: Radiological findings, clinical course, and outcome in asymptomatic Moyamoya disease: Results of multicenter survey in Japan. Stroke 38:1430-1435, 2007. https://doi.org/10.1161/STROKEAHA.106.478297
29. Lee WJ, Jeong SK, Han KS, Lee SH, Ryu YJ, Sohn CH, Jung KH: Impact of endothelial shear stress on the bilateral progression of unilateral Moyamoya disease. Stroke 51:775-783, 2020. https://doi.org/10.1161/STROKEAHA.119.028117
30. Lucia K, Acker G, Mrosk F, Beyaztas D, Vajkoczy P: Longitudinal angiographic characterization of the efficacy of combined cerebral revascularization using minimally invasive encephalodurosynangiosis in patients with Moyamoya angiopathy. Neurosurg Rev 45:3689-3698, 2022. https://doi.org/10.1007/s10143-022-01862-9

31. Matsushima T, Inoue T, Suzuki SO, Fujii K, Fukui M, Hasuo K: Surgical treatment of Moyamoya disease in pediatric patients-comparison between the results of indirect and direct revascularization procedures. Neurosurgery 31:401-405, 1992. https://doi.org/10.1227/00006123-199209000-00003
32. Nielsen TH, Abhinav K, Sussman ES, Han SS, Weng Y, Bell-Stephens T; CNRN; Heit JJ, Steinberg GK: Direct versus indirect bypass procedure for the treatment of ischemic Moyamoya disease: Results of an individualized selection strategy. J Neurosurg 134:1578-1589, 2020. https://doi.org/10.3171/2020.3.JNS192847
33. Ott WP, Bellamy S, Onyali CB: A rare case of Moyamoya disease in a Hispanic woman: Unveiling non-Asian ethnicity and atypical risk factors. Am J Case Rep 24:e940353, 2023. https://doi.org/10.12659/AJCR.940353
34. Pang CH, Cho WS, Kang HS, Kim JE: Benefits and risks of antiplatelet medication in hemodynamically stable adult Moyamoya disease. Sci Rep 11:19367, 2021. https://doi.org/10.1038/s41598-021-99009-1
35. Per H, Unal E, Poyrazoglu HG, Ozdemir MA, Donmez H, Gumus H, Uzum K, Canpolat M, Akyildiz BN, Coskun A, Kurtsoy A, Kumandas S: Childhood stroke: Results of 130 children from a reference center in Central Anatolia, Turkey. Pediatr Neurol 50:595-600, 2014. https://doi.org/10.1016/j.pediatrneurol.2013.12.023
36. Said S, Cooper CJ, Alkhateeb H, Galvis JM, Hernandez GT, Salameh HJ: Moyamoya in hispanics: not Only in Japanese. Neurol Int 6:5369, 2014. https://doi.org/10.4081/ni.2014.5369
37. Shang S, Zhou D, Ya J, Li S, Yang Q, Ding Y, Ji X, Meng R: Progress in moyamoya disease. Neurosurg Rev 43:371-382, 2020. https://doi.org/10.1007/s10143-018-0994-5
38. Shimizu T, Aihara M, Yamaguchi R, Sato K, Aishima K, Yoshimoto Y: Large craniotomy increases the risk of minor perioperative complications in revascularization surgery for Moyamoya disease. World Neurosurg 141:e498-507, 2020. https://doi.org/10.1016/j.wneu.2020.05.227
39. Shoukat S, Itrat A, Taqui AM, Zaidi M, Kamal AK: Moyamoya disease: A clinical spectrum, literature review and case series from a tertiary care hospital in Pakistan. BMC Neurol 9:15, 2009. https://doi.org/10.1186/1471-2377-9-15
40. So Y, Lee HY, Kim SK, Lee JS, Wang KC, Cho BK, Kang E, Lee DS: Prediction of the clinical outcome of pediatric Moyamoya disease using postoperative basal/acetazolamide stress brain perfusion SPECT after revascularization surgery. Stroke 36:1485-1489, 2005. https://doi.org/10.1161/01.STR.0000170709.95185.b1
41. Suzuki J, Kodama N: Moyamoya disease-A review. Stroke 14:104-109, 1983. https://doi.org/10.1161/01.STR.14.1.104
42. Suzuki J, Takaku A: Cerebrovascular "Moyamoya" disease. Disease showing abnormal net-like vessels in the base of the brain. Arch Neurol 20:288-299, 1969. https://doi.org/10.1001/archneur.1969.00480090076012
43. Takeuchi K: Hypoplasia of bilateral internal carotid arteries. No To Shinkei 9:37-43, 1957.
44. Tatli B, Ekici B, Sencer A, Sencer S, Aydin K, Aydinli N, Caliskan M, Ozmen M, Kiris T: Clinical features, prothrombotic risk factors, and long-term follow-up of eight pediatric Moyamoya patients. J Clin Neurol 8:100-103, 2012. https://doi.org/10.3988/jcn.2012.8.2.100
45. Türkiye İstatistik Kurumu, Evlenme ve Boşanma İstatistikleri, 2023, Yayım Tarihi :22 Şubat 2024, Saat: 10:00, Sayı: 53707, https://data.tuik.gov.tr/Bulten/Index?p=Evlenme-ve-Bosanma-Istatistikleri-2023-53707
46. Volkan-Salanci B, Lay Ergun E, Genc Sel C, Yalnizoglu D, Turanli G: The role of brain perfusion SPECT in Moyamoya disease. Rev Esp Med Nucl Imagen Mol 31:216-218, 2012. https://doi.org/10.1016/j.remn.2012.02.006
47. Xu R, Xie ME, Kim J, Kothari R, Sun LR, Jackson EM, Tamargo RJ, Huang J, Ahn ES, Cohen AR: Same-day versus staged revascularization of bilateral Moyamoya arteriopathy in pediatric patients. Childs Nerv Syst 39:1207-1213, 2023. https://doi.org/10.1007/s00381-023-05916-1
48. Zhang X, Xiao W, Zhang Q, Xia D, Gao P, Su J, Yang H, Gao X, Ni W, Lei Y, Gu Y: Progression in Moyamoya disease: Clinical features, neuroimaging evaluation, and treatment. Curr Neuropharmacol 20:292-308, 2022. https://doi.org/10.2174/1570159X19666210716114016

Turk Neurosurg 36(1):74-81, 2026
DOI: 10.5137/1019-5149.JTN.49659-25.3

Original Investigation
Spine and Peripheral Nerves

Received: 12.08.2025
Accepted: 24.10.2025
Published Online: 16.01.2026

Patient-Specific Lattice Cage Design for Cervical Spinal Fusion

Bulent BOZYIGIT[1], Mehmet Akif OYMAK[2], Erkan BAHCE[2], Gurminder SINGH[3]

[1]Izmir Private Health Hospital, Department of Neurosurgery, Izmir, Türkiye
[2]Inonu University, Department of Mechanical Engineering, Malatya, Türkiye
[3]Indian Institute of Technology Bombay, Department of Mechanical Engineering, Mumbai, India

Corresponding author: Bulent BOZYIGIT ✉ bulentbzt@yahoo.com

ABSTRACT

AIM: To propose a patient-specific interbody cage with graded stiffness distributions analogous to the Young's modulus of the cervical spinal bone interface in order to improve mechanical compatibility, promote physiological load sharing, and enhance osseointegration.

MATERIAL and METHODS: A synthetic database of spinal bone Young modulus values was used, incorporating anatomical regions (cervical, thoracic, lumbar) and patient-specific factors (age, bone density, health status). A parametric generative design approach allowed dynamic modification of lattice unit cell geometry to achieve target stiffness values (200–3000 MPa) while preserving structural integrity.

RESULTS: Finite element endplate analysis demonstrated a 30%–50% reduction in stress shielding compared with conventional solid or homogeneous mesh lattices. Additively manufactured prototypes showed tunable stiffness–porosity trade-offs, achieving yield strength ≥150 MPa while supporting osseointegration.

CONCLUSION: This study demonstrates improved load distribution and reduced risk of cage collapse compared with cadaveric spine data. Integrating computational design, biomechanical compatibility, and additive manufacturing may facilitate the development of patient-specific spinal implants with superior mechanical and biological performance.

KEYWORDS: Interbody cage implant, Young's modulus, Lattice generative design, Additive manufacturing, Finite element analysis

ABBREVIATIONS: AM: Additive manufacturing, **CT:** Computed tomography, **GA:** Genetic algorithm, **PEEK:** Polyetheretherketone

INTRODUCTION

The cervical spine provides substantial flexibility and essential protection for the spinal cord. However, its continuous movement makes it highly susceptible to degenerative disorders, traumatic injuries, and diseases, which may lead to chronic pain, spinal instability, and serious neurological impairment (13).

When conservative treatments fail, surgical intervention becomes necessary. Cervical spinal fusion is an established procedure used to restore spinal stability by immobilizing the affected vertebral segment and promoting bone union (8). The success of cervical fusion is closely linked to the type of interbody implant, which preserves disc height and facilitates osseous integration for solid fusion (14). Autologous iliac crest bone grafting, the original "gold standard," has several limitations, including donor-site morbidity and limited graft availability (8). These drawbacks have led to the widespread adoption of interbody cages made of materials such as polyetheretherketone (PEEK). Because of PEEK's favorable

Bulent BOZYIGIT : 0000-0001-5038-2260
Mehmet Akif OYMAK : 0000-0001-8251-3106
Erkan BAHCE : 0000-0001-5389-5571
Gurminder SINGH : 0000-0001-5921-9638

mechanical rigidity compared with metallic implants, it has become a popular material for interbody cages. However, its bioinert characteristics limit cellular response, often leading to fibrous encapsulation rather than bone formation. This limitation underscores the need for surface modifications or bioactive coatings to enhance long-term osseointegration (18). The emergence of additive manufacturing (AM), or 3D printing, has transformed orthopedic implant design. Unlike conventional manufacturing, AM enables the fabrication of complex, patient-specific geometries (4). This shift allows the development of advanced internal cage architectures, moving beyond simple hollow designs toward highly porous, interconnected structures that better mimic the natural bone environment (4,11). Current implant innovations incorporate lattice structure design and topology optimization based on the principle of biomimicry, which emulates nature's optimized structural systems. The aim is to create scaffolds that closely replicate the mechanical properties and lattice architecture of bone, enabling more physiological load transfer and improving the potential for osseointegration (6). These lattice implants are engineered as dynamic scaffolds that enhance osseointegration by replicating the porous structure of bone. This design facilitates osteoblast infiltration, promotes vascularization, and establishes a strong interface between the implant and the host vertebra. Ti-6Al-4V alloy has emerged as the preferred material for load-bearing orthopedic implants due to its high strength, low density, corrosion resistance, and excellent biocompatibility. Its mechanical properties closely approximate those of bone, thereby reducing stress shielding and improving long-term stability. Recent advances in surface modification and nanoparticle reinforcements have further expanded its clinical applications (1). AM allows the effective stiffness of Ti-6Al-4V lattice structures to be precisely tuned to match the mechanical properties of adjacent bone tissue, thereby enhancing osseointegration and minimizing stress shielding (7). Achieving this mechanical balance is critical, as an overly stiff implant can transfer excessive stress away from surrounding bone, leading to bone resorption and potential collapse. Personalized implant design, tailored to individual anatomical variations, represents an important future direction for spinal implant technology. Prefabricated implants often provide a suboptimal fit, which can lead to instability, localized stress concentrations, and an increased risk of subsidence into the softer spinal bone. In contrast, patient-specific designs uses computed tomography (CT) data to fabricate implants that conform precisely to individual anatomy, maximizing endplate contact, enhancing initial stability, and promoting even distribution of mechanical loads. This creates a stronger foundation for successful fusion. This study employs a genetic algorithm (GA), a machine learning-based optimization technique inspired by natural selection, to address the critical design challenge of developing patient-specific cervical cage implants. The GA explores a wide range of design variables, including strength, stiffness, and porosity. By selecting optimal candidates, combining favorable features through "crossover," and introducing incremental variations through "mutation," the algorithm iteratively refines implant geometry to identify an optimal configuration with balanced mechanical and structural properties. The "fitness" of each implant design generated by the GA was evaluated using finite element analysis (FEA) in a virtual simulation environment. This advanced modeling technique allows non-destructive evaluation of implant performance under physiologically relevant loading conditions. Each patient-specific design was subjected to multiple simulated force applications replicating natural cervical spine movements: axial compression (representing head weight), flexion–extension (nodding), lateral bending (side-to-side tilting), and torsion (rotational movement indicating "no"). This study integrates GA and FEA into a unified, simulation-driven design workflow. Three patient-specific cervical fusion implants made of Ti-6Al-4V were computationally designed using this GA–FEA approach to optimize structural and mechanical performance before fabrication. Although alternative materials such as magnesium alloys have attracted interest because of their bone-like elastic modulus and biodegradability, fabricating magnesium with a controlled, uniform porous architecture using AM remains technically challenging. Therefore, Ti-6Al-4V alloy, which has been clinically validated and can be reliably produced using additive printing, was selected for this study. Beyond providing precise mechanical compatibility and physiological load sharing, this simulation-driven approach offers a scalable and efficient pathway for the rapid production of complex spinal implants, potentially improving long-term outcomes in cervical fusion surgery. Each implant's internal structure was custom designed to withstand the complex loading environment of the cervical spine while accommodating patient-specific anatomical variation, resulting in a bone-like, functionally graded cage. The key innovation of this study lies in the computational validation of a generative design methodology. Generative design enables the construction of interbody cages with graded mechanical stiffness tailored to individual patients, supporting the heterogeneous distribution of Young's modulus in cervical spinal bone and adjacent tissues.

MATERIAL and METHODS

Ethical approval was not required for this study, as no patient data or human participants were involved.

Patient-Specific Design and Geometric Optimization

A patient-specific parametric model was developed to design a cervical spine implant that ensures both anatomical conformity and biomechanical compatibility. CT scans were obtained using a Siemens SOMATOM Definition Edge system with a slice thickness of 0.5 mm to accurately reconstruct cervical anatomy. The raw DICOM data were processed with Mimics 21.0 software (Materialise, Belgium) to segment the vertebral structures and generate a three-dimensional surface model. The reconstructed geometry was exported in STL format for subsequent design and optimization. This digital model formed the foundation of a patient-specific implant design workflow integrating geometry reconstruction with computational optimization techniques to produce an implant that precisely fits the targeted cervical segment. A parametric approach rapid adjustment of the design to accommodate anatomical variability, aligning with modern personalized medicine strategies. Geometric optimization was performed using

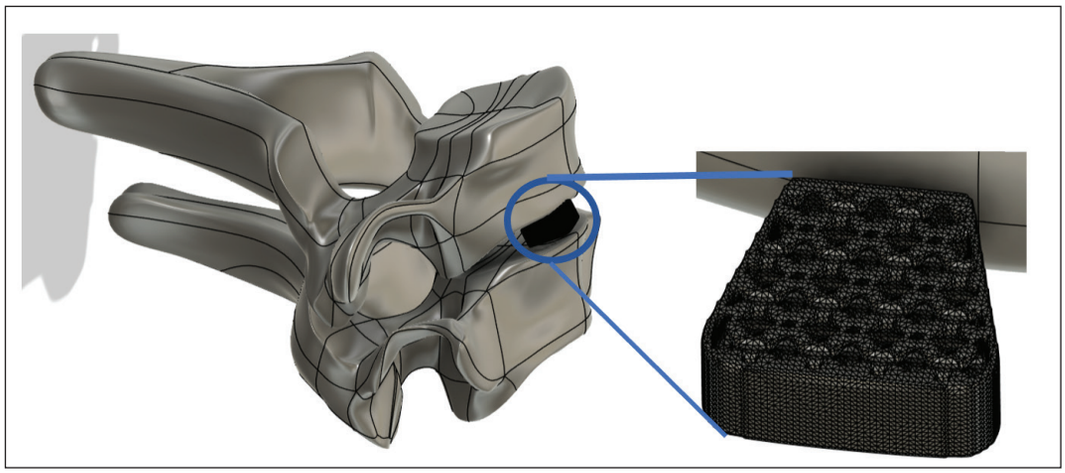

Figure 1: Patient-specific lattice implant at the C4–C5 level.

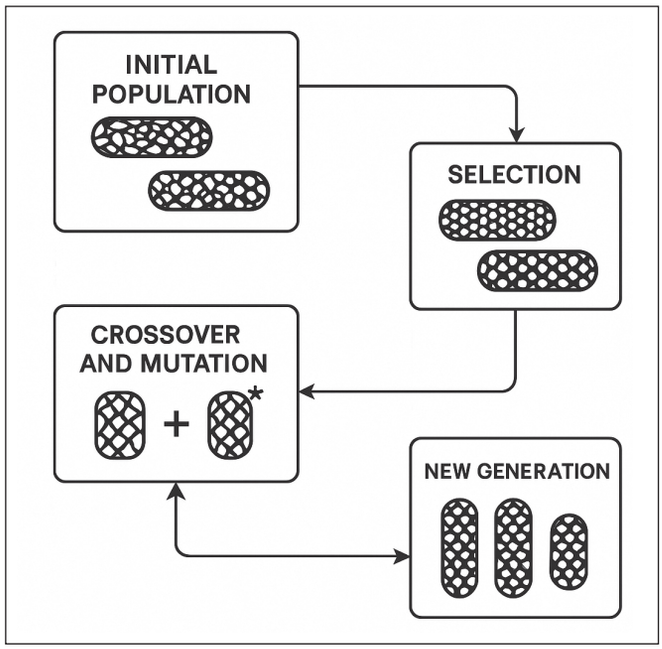

Figure 2: Genetic algorithm implant design scheme.

the Topology Optimization module of Autodesk Fusion 360 to create a lightweight, mechanically robust structure. Optimization of selective laser-melted Ti-6Al-4V lattice scaffolds aimed to reduce implant mass while preserving load-bearing capacity. Implant mass was reduced by up to 40% without compromising mechanical strength, in accordance with established design criteria. This stage of the workflow integrated structural performance goals with manufacturability constraints to ensure that the optimized geometry could be reliably produced using AM. The design process also minimized stress concentrations and preserved fatigue performance. Additionally, optimization accounted for adequate bone–implant contact surfaces to support osseointegration and maintain a stable mechanical interface with the vertebrae. The final geometry achieved a balance between structural efficiency and clinical applicability by integrating functional and biological requirements.

GA-based optimization was integrated into the final design phase to enhance the biomechanical performance of the implant and refine its geometry. The cervical spine implant was embedded in a cage structure tailored to the patient's anatomy to ensure controlled load transfer and optimal integration with the surrounding bone. The assembly process involved aligning the implant within the cervical region, optimizing contact surfaces, and accurately positioning the cage within the targeted spinal segment. This procedure was carried out using Autodesk Fusion 360. Figure 1 illustrates the complete workflow, from anatomical reconstruction to final implant assembly. This integrated digital design and assembly approach demonstrates how advanced computational tools enable the development of patient-specific implants. By combining anatomical data, topology optimization, and evolutionary computation in a single workflow, this study highlights the potential to produce implants that meet manufacturability, structural integrity, and clinical performance requirements.

Lattice Structure Optimization Using GA

The cage structure parameters of the cervical spine implant were optimized using a multi-objective genetic algorithm (MOGA) (3). This evolutionary algorithm was selected for its ability to simultaneously balance mechanical and biological design criteria. The optimization targeted three key objectives: maintaining a von Mises stress distribution below 350 MPa to ensure structural integrity, achieving a fatigue life of at least 10^6 cycles to support long-term durability under physiological loading, and establishing a porosity level between 50% and 80% to balance mechanical stability with biocompatibility. To refine the cage design configurations and achieve an optimal balance between the defined constraints, the evolutionary algorithm was run iteratively, as illustrated in Figure 2. Candidate solutions were generated, screened against mechanical and biological criteria, and evaluated using FEA for stress distribution. The algorithm optimized key geometric parameters, including support thickness, unit cell size, and cage orientation,s to produce a design that maximizes structural strength, enhances fatigue performance, and promotes bone ingrowth. This approach enabled the development a patient-specific implant that is both physiologically beneficial and mechanically durable over the long term.

GAs are among the most effective machine learning methods, inspired by the principles of crossover, mutation, and selection in biological evolution. They are particularly well suited for spinal implant design because of their ability to efficiently explore large and complex design spaces. By iteratively refining candidate solutions toward optimal configurations, GAs can identify designs that balance multiple and often competing biomechanical requirements. This capability is especially valuable in the development of patient-specific implants, where geometry and material distribution must be precisely tailored to individual anatomy to ensure both mechanical performance and clinical safety. In this study, GAs were employed to generate and refine lattice-based spinal implant designs that achieve a balance between structural strength, fatigue resistance, and bone ingrowth potential. The optimization process was implemented using the Rhino Grasshopper visual programming environment, enabling rapid parametric modeling and the evaluation of multiple design iterations. As shown in Figure 3, the algorithm-driven workflow produced multiple candidate geometries, which were subsequently evaluated for stress distribution, implant–bone interface behavior, and manufacturability. This integrated computational approach ensures that the final implant design is biomechanically optimized while remaining precisely tailored to the patient's unique cervical anatomy.

The selection of the optimal porosity was achieved through a multi-objective optimization approach that considered bone ingrowth, biocompatibility, and mechanical strength. The cage architecture was customized for each case by integrating patient-specific anatomical data derived from preoperative CT scans and bone quality assessments. To ensure an optimal balance between load-bearing capacity and osseointegration potential, the mechanical performance of each design was evaluated using FEA. This comprehensive design strategy enables the fabrication of implants that are both mechanically robust and anatomically conforming, thereby supporting improved clinical outcomes. Furthermore, variability in surgical placement (e.g., drilling or curettage of cartilage endplates) was addressed by tailoring the implant shape to the intended implantation site based on preoperative imaging and planned surgical preparation. This integrated approach facilitates the production of anatomically compatible and mechanically strong implants, enhancing the likelihood of favorable therapeutic results.

Biomechanical Analysis and Validation

Figure 4 illustrates the definition of the force and support regions used in the FEA conducted with ANSYS for the spinal implant optimized using a GA. In this model, a fixed support (boundary condition) was applied to the bone-contacting surfaces to replicate realistic physiological constraints, while loading conditions were applied at defined anatomical locations to simulate forces transmitted through the cervical spine. This approach enables a detailed assessment of the implant's biomechanical behavior, allowing the prediction of load-carrying capacity and the identification of potential stress concentrations or weak points. This analysis represents a critical

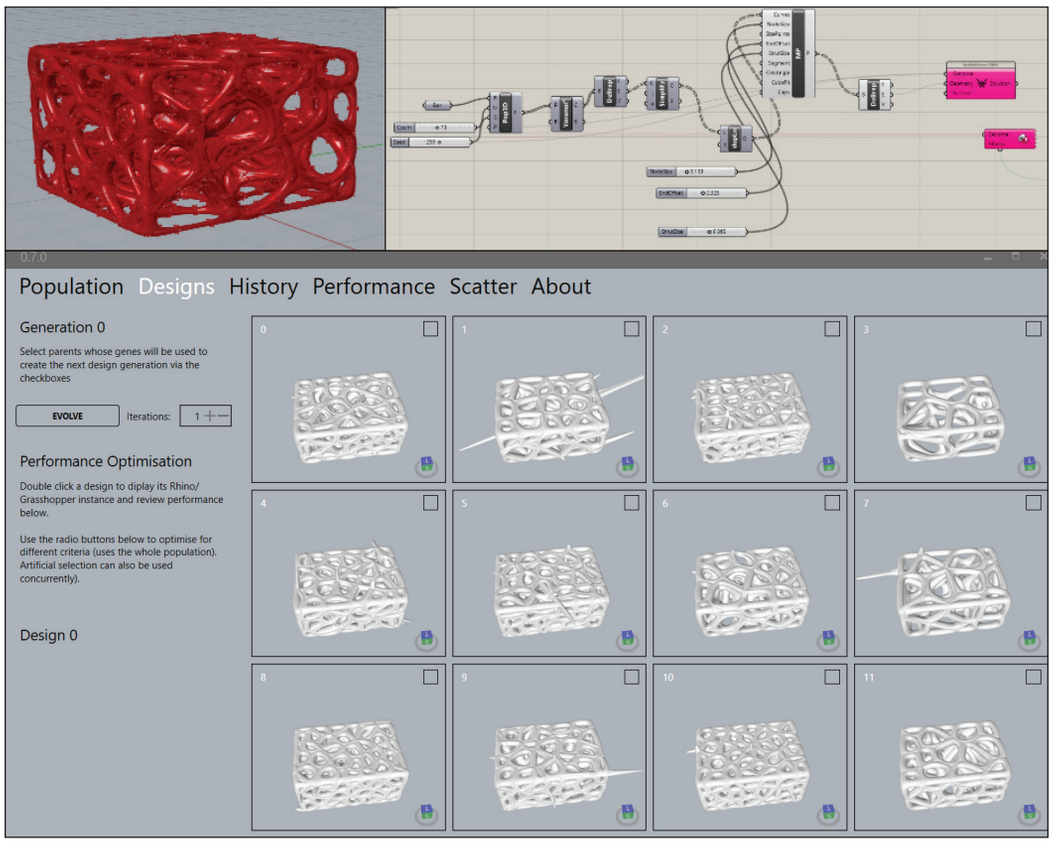

Figure 3: Genetic algorithm design using Rhino Grasshopper program.

step in verifying the structural integrity and performance of the GA-derived implant design. Following this, the C4–C5 vertebrae and the designed interbody cage were assembled and imported into the FEA environment for simulation and validation.

The spine and cage assemblies were incorporated into the 3D finite element model, and meshing was performed as shown in Figure 4. The mesh consisted of 351,749 nodes and 295,642 elements. A finite element-based approach was developed to evaluate both vertebral bone and lattice implant performance under physiological loading. To minimize element distortions commonly observed in purely Lagrangian formulations, the Arbitrary Lagrangian–Eulerian (ALE) method with mesh integration was employed. Boundary fixation points and loading application regions were defined according to established cervical spine anatomical and biomechanical constraints. The loading protocol used in this study was based on well-characterized cervical spine biomechanics and benchmarked against predictive models reported in the literature.

For the C4–C5 motion segment, physiological cervical loading conditions were simulated to replicate postoperative spinal mechanics. During flexion, a load of approximately 230 N (0.34 body weight) was applied, whereas in the upright position, a maximum compressive load of 1000 N (1.82 body weight) was considered, based on reported in vivo measurements (2). Additional loading scenarios adapted from the literature were implemented, consisting of a 7.5 N·m moment for lateral bending, flexion, and torsion, combined with an axial compressive force of 1200 N. The inferior surface of the C5 vertebra was defined as the fixation site (boundary condition), while the superior surface of the C4 vertebra was subjected to the applied forces and moments (Figure 5). This configuration accurately replicates physiological loading paths and boundary conditions for evaluating postoperative cervical implant performance.

RESULTS

The implant's resistance to a maximum von Mises stress of 90 MPa is of critical clinical importance.

The equivalent elastic strain pattern under an axial force of 1200 N and a 7.5 N.m moment during lateral bending, torsion, and flexion is shown in Figure 6A–C.

The maximum deformation was measured as follows: 0.722 mm under lateral bending (Figure 6A), 0.603 mm under torsion (Figure 6B), and 0.795 mm under flexion (Figure 6C).

DISCUSSION

The GA-based optimization approach presented in this study provided substantial mechanical advantages for patient-spe-

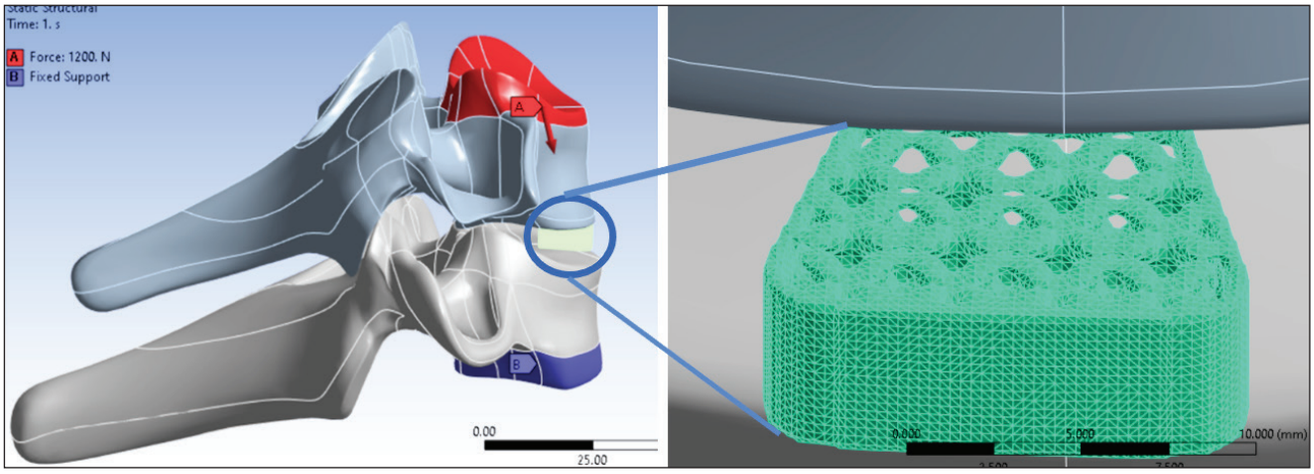

Figure 4: Definition of loading and boundary conditions for the C4–C5 vertebra and interbody implant in ANSYS.

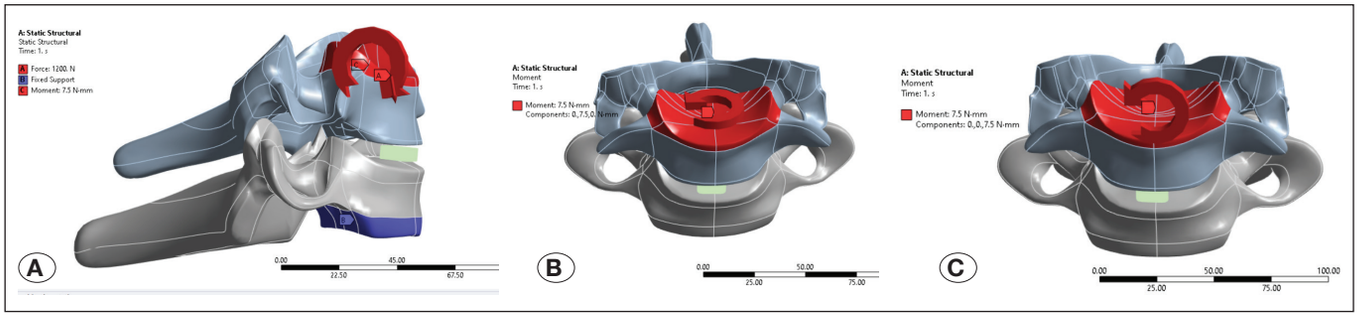

Figure 5: Finite element, force, moment, and fixation model of the genetic algorithm-designed interbody cage: **A)** 7.5 N.m lateral bending moment, **B)** 7.5 N.m torsion, and **C)** 7.5 N.m flexion, each combined with a 1200 N axial force.

cific spinal implant design. The results demonstrate a 60% improvement in mechanical performance compared with conventional porous structures with the same volume occupancy. This finding supports the potential of GAs in biomedical applications, as reported by Ghaheri et al. (5).

Figure 8 illustrates the maximum von Mises stress and its distribution obtained from the analyses. Similar studies by Wang et al. have shown that stress levels below this threshold significantly increase implant life (12). A uniform stress distribution can also enhance osseointegration by minimizing micromotion at the bone–implant interface (15,16).

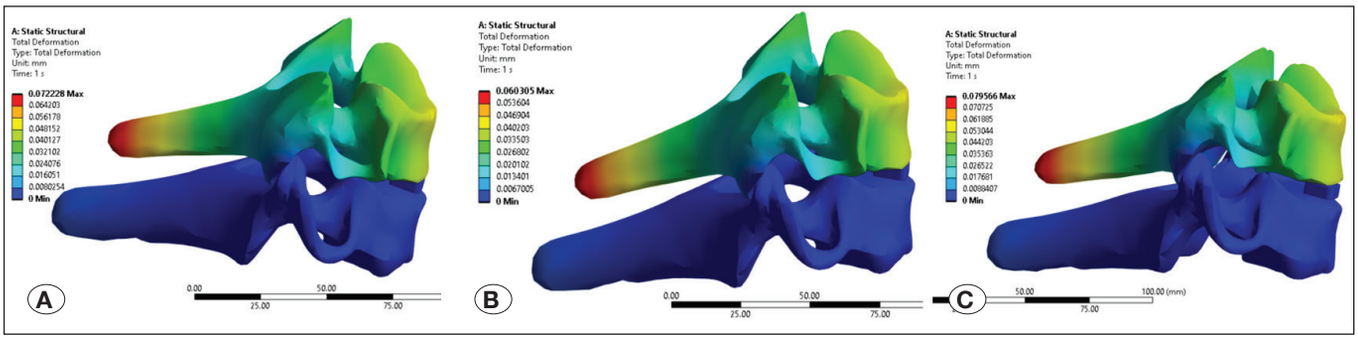

Figure 6: C4–C5 spinal bone and lattice-designed interbody cage under 1200 N axial force: **A)** 7.5 N.m lateral bending, **B)** 7.5 N.m torsion, and **C)** 7.5 N.m flexion, showing total deformation and strain distribution.

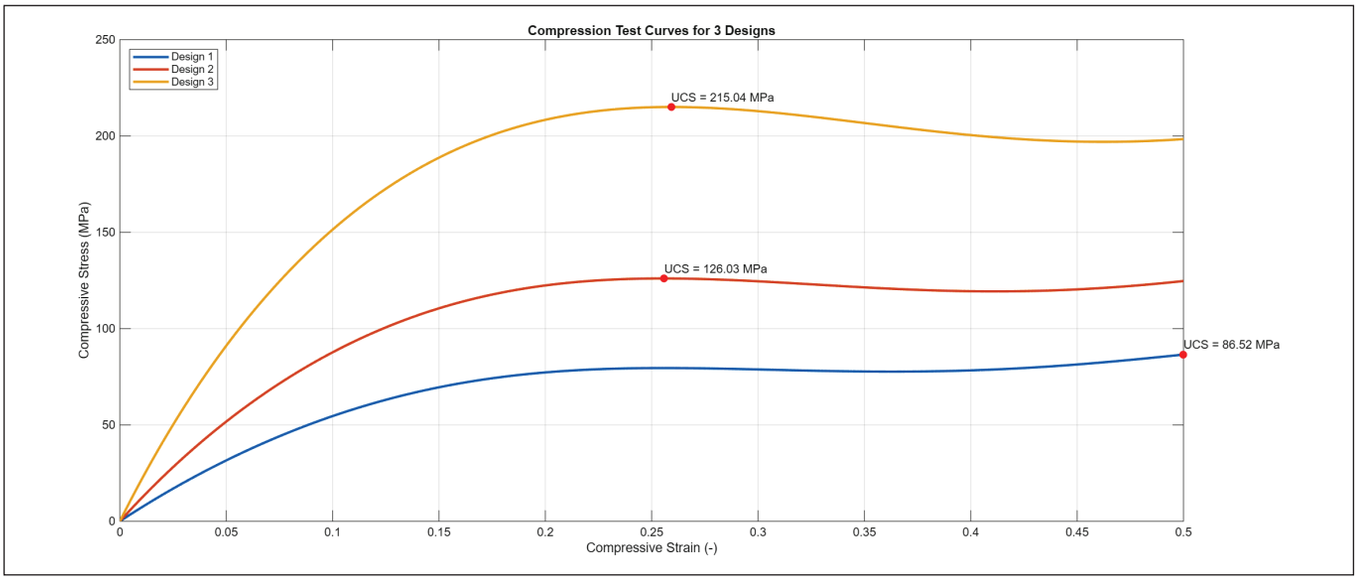

Figure 7: Numerical maximum von Mises stress–strain graph.

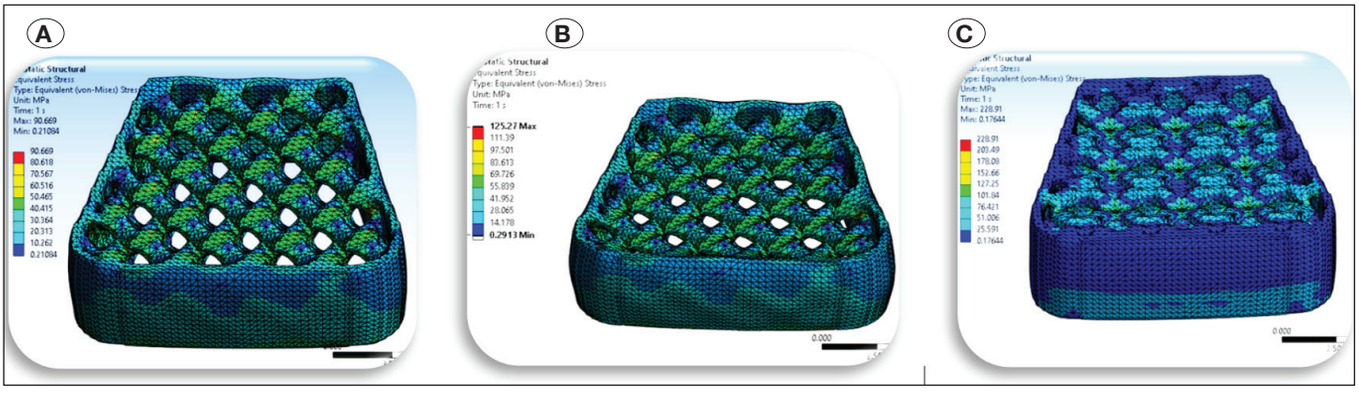

Figure 8: Maximum von Mises stress and its distribution obtained from the analysis.

The locations of maximum stress, strain, and potential failure points correspond to previously reported experimental findings (2,9).

Clinical Implications

The optimization process demonstrated in this study provides two major clinical advantages. First, it minimizes the risk of implant collapse by maintaining structural integrity under physiological loading conditions. This is clinically significant, as implant failure can lead to postoperative complications, compromised surgical outcomes, and delayed patient recovery (10). Second, a biomechanically driven design strategy enhance compatibility between the implant and the surrounding bone tissue, ensuring a more stable and durable interface.

A homogeneous stress distribution at the bone–implant interface plays a critical role in reducing localized stress concentrations. By lowering the degree of stress shielding, this approach may help prevent bone resorption and preserve the structural stability of the adjacent vertebrae over time (17,18). Collectively, these findings highlight the clinical potential of patient-specific, optimization-based implant design to improve both immediate surgical safety and long-term functional outcomes.

CONCLUSION

In this study, optimized cage structures for patient-specific spinal implants were designed using a GA, and their biomechanical performance was comprehensively analyzed. The findings demonstrate that the proposed methodology offers significant structural and biological advantages compared with conventional implant designs.

The GA-optimized implant achieved up to 60% better stress distribution than traditional porous structures with equivalent porosity and maintained its integrity under a maximum von Mises stress of 90 MPa. Furthermore, the optimized modulus distribution minimized stress shielding by approximately 60%, thereby improving mechanical compatibility with the surrounding spinal bone.

Customizable designs tailored to variations in age, bone density, and health status were achieved through an adaptive parametric algorithm informed by patient-specific data.

Comparative analyses using clinically relevant cadaveric spinal data demonstrated improved load distribution and a reduced risk of implant collapse, underscoring the potential for long-term clinical success.

In conclusion, this study shows that a computational design approach supported by GAs provides an effective and innovative solution for developing spinal implants that are both biomechanically compatible and manufacturable. Future research should incorporate biological modeling and in vivo testing to further validate the clinical applicability of this method and support its transition to larger patient populations.

Declarations

Funding: This research did not receive any specific grant from funding agencies in the public, commercial, or not-for-profit sectors.

Availability of data and materials: The datasets generated and/or analyzed during the current study are available from the corresponding author by reasonable request.

Disclosure: The authors declare no competing interests.

AUTHORSHIP CONTRIBUTION

Study conception and design: BB
Data collection: MAO
Analysis and interpretation of results: GS
Draft manuscript preparation: BB
Critical revision of the article: GS, EB
Other (study supervision, fundings, materials, etc...): EB
All authors (BB, MAO, EB, GS) reviewed the results and approved the final version of the manuscript.

REFERENCES

1. Abd-Elaziem W, Darwish MA, Hamada A, Daoush WM: Titanium-Based alloys and composites for orthopedic implants applications: A comprehensive review. Mater Des 241:112850, 2024. https://doi.org/10.1016/j.matdes.2024.112850
2. Bozyigit B, Oymak MA, Bahce E, Uzunyol OF: Finite element analysis of lattice designed lumbar interbody cage based on the additive manufacturing. Proc Inst Mech Eng H 237:991-1000, 2023. https://doi.org/10.1177/09544119231184379
3. Deb K, Pratap A, Agarwal S, Meyarivan T: A fast and elitist multiobjective genetic algorithm: NSGA-II. IEEE Trans Evol Comput 6:182-197, 2002. https://doi.org/10.1109/4235.996017
4. Emir E, Bahce E: Investigation of the mechanical properties triple periodic minimal surfaces lattice structures with functional graded of porosity. J Cell Plast 59:251-268, 2023. https://doi.org/10.1177/0021955X231175179
5. Ghaheri A, Shoar S, Naderan M, Hoseini SS: The applications of genetic algorithms in medicine. Oman Med J 30:406-416, 2015. https://doi.org/10.5001/omj.2015.82
6. Huang D, Li Z, Li G, Zhou F, Wang G, Ren X, Su J: Biomimetic structural design in 3D-printed scaffolds for bone tissue engineering. Mater Today Bio 32:101664, 2025. https://doi.org/10.1016/j.mtbio.2025.101664
7. McGregor M, Patel S, McLachlin S, Vlasea M: Architectural bone parameters and the relationship to titanium lattice design for powder bed fusion additive manufacturing. Addit Manuf 47: 102273, 2021. https://doi.org/10.1016/j.addma.2021.102273
8. Rho JY, Kuhn-Spearing L, Zioupos P: Mechanical properties and the hierarchical structure of bone. Med Eng Phys 20:92-102, 1998. https://doi.org/10.1016/S1350-4533(98)00007-1
9. Sanjay D, Kumar N, Chanda S: Stress-strain distribution in intact L4-L5 vertebrae under the influence of physiological movements: A finite element (FE) investigation. IOP Conf Ser: Mater Sci Eng 1206:012024, 2021. https://doi.org/10.1088/1757-899X/1206/1/012024

10. Smith JS, Kelly MP, Buell TJ, Ben-Israel D, Diebo B, Scheer JK, Line B, Lafage V, Lafage R, Klineberg E, Kim HJ, Passias P, Gum JL, Kebaish K, Mullin JP, Eastlack R, Daniels A, Soroceanu A, Mundis G, Hostin R, Protopsaltis TS, Hamilton DK, Gupta M, Lewis SJ, Schwab FJ, Lenke LG, Shaffrey CI, Burton D, Ames CP, Bess S; International Spine Study Group: Adult cervical deformity patients have higher baseline frailty, disability, and comorbidities compared with complex adult thoracolumbar deformity patients: A comparative cohort study of 616 patients. Glob Spine J 15:846-857, 2023. https://doi.org/10.1177/21925682231214059
11. Tamayo JA, Riascos M, Vargas CA, Baena LM: Additive manufacturing of Ti6Al4V alloy via electron beam melting for the development of implants for the biomedical industry. Heliyon 7:e06892, 2021. https://doi.org/10.1016/j.heliyon.2021.e06892
12. Wang Q, Zhang ZZ, Bai SZ, Zhang SF: Biomechanical analysis of stress around the tilted implants with different cantilever lengths in all-on-4 concept. BMC Oral Health 22:469, 2022. https://doi.org/10.1186/s12903-022-02520-8
13. Weiner S, Wagner HD: The material bone: Structure-mechanical function relations. Annu Rev Mater Sci 28:271-298, 1998. https://doi.org/10.1146/annurev.matsci.28.1.271
14. Wilke HJ, Kettler A, Claes L: Primary stabilizing effect of interbody fusion devices for the cervical spine: An in vitro comparison between three different cage types and bone cement. Eur Spine J 9:410-416, 2000. https://doi.org/10.1007/s005860000168
15. Zhang C, Zeng C, Wang Z, Zeng T, Wang Y: Optimization of stress distribution of bone-implant interface (BII). Biomater Adv 147:213342, 2023. https://doi.org/10.1016/j.bioadv.2023.213342.
16. Zhang L, Song B, Yang L, Shi Y: Tailored mechanical response and mass transport characteristic of selective laser melted porous metallic biomaterials for bone scaffolds. Acta Biomater 112:298-315, 2020. https://doi.org/10.1016/j.actbio.2020.05.038
17. Zhao G, Luo J, Ma J, Wang J: Decreased stress shielding with poly-ether-ether-ketone tibial implant for total knee arthroplasty: A preliminary study using finite element analysis. Heliyon 10:e27204, 2024. https://doi.org/10.1016/j.heliyon.2024.e27204
18. Zhu C, He M, Mao L, Li T, Zhang L, Liu L, Feng G, Song Y: Titanium-interlayer mediated hydroxyapatite coating on poly-etheretherketone: A prospective study in patients with single-level cervical degenerative disc disease. J Transl Med 19:14, 2021. https://doi.org/10.1186/s12967-020-02688-z

Turk Neurosurg 36(1):82-88, 2026
DOI: 10.5137/1019-5149.JTN.49271-25.2

Original Investigation
Spine and Peripheral Nerves

Received: 10.06.2025
Accepted: 27.10.2025
Published Online: 16.01.2026

Intra-Articular vs Medial Branch Pulsed Radiofrequency in the Management of Lumbar Facet Joint-Related Low Back Pain: A Prospective Randomized Trial

Burak ERKEN[1], Suat DEMIR[2], Ipek Saadet EDIPOGLU[3]

[1]University of Health Sciences, Basaksehir Cam and Sakura City Hospital, Department of Anesthesiology, Division of Pain Medicine, Istanbul, Türkiye
[2]University of Health Sciences, Basaksehir Cam and Sakura City Hospital, Department of Neurosurgery, Istanbul, Türkiye
[3]University Hospital Lewisham, Department of Anaesthetics and Pain Management, London, United Kingdom

Corresponding author: Suat DEMIR ✉ suatdemir57@gmail.com

ABSTRACT

AIM: To compare the efficacy of intra-articular PRF (IA-PRF) and medial branch PRF (MB-PRF) in the treatment of facet joint-related low back pain.

MATERIAL and METHODS: In this prospective observational study, 116 patients with ≥50% pain relief after diagnostic intra-articular anesthetic injection were included. Patients underwent IA-PRF (n=60) or MB-PRF (n=56). Pain and disability were assessed using the Numerical Rating Scale (NRS) and Oswestry Disability Index (ODI) at baseline and 1 and 6 months post-treatment.

RESULTS: Both groups showed significant improvements in NRS and ODI scores at 1 and 6 months ($p<0.001$). In the IA-PRF group, NRS scores improved from 6.55 ± 0.65 to 3.23 ± 0.43 (1 month) and 3.70 ± 0.46 (6 months); ODI scores improved from 49.70 ± 3.75 to 25.13 ± 1.66 and 26.90 ± 2.13, respectively. In the MB-PRF group, NRS scores decreased from 6.43 ± 0.66 to 3.13 ± 0.33 (1 month) and 3.57 ± 0.49 (6 months); ODI scores decreased from 49.18 ± 3.49 to 24.71 ± 1.34 (1 month) and 26.68 ± 2.20 (6 months). No significant intergroup differences were observed at follow-ups ($p>0.05$). No complications occurred.

CONCLUSION: IA-PRF and MB-PRF are effective and safe in treating LFJ-induced pain after 6 months of follow-up. Significant pain control and functional improvement were achieved with both methods, with no significant difference between them regarding clinical efficacy. Our findings suggest that treatment selection should be individualized according to patient characteristics. Randomized studies with large samples and long-term follow-up are needed to improve the level of evidence in this field.

KEYWORDS: Chronic low back pain, Intra-articular pulsed radiofrequency, Lumbar facet joint (LFJ) pain, Medial branch pulsed radiofrequency, Pulsed radiofrequency

ABBREVIATIONS: LFJ: Lumbar facet joint, **IA:** Intra-articular, **IA-PRF:** Intra-articular pulsed radiofrequency, **MB-PRF:** Medial branch pulsed radiofrequency, **NRS:** Numerical rating scale, **ODI:** Oswestry disability index, **PRF:** Pulsed radiofrequency

INTRODUCTION

Lumbar facet joint (LFJ)-induced pain is one of the important causes of chronic low back pain and is a common condition in clinical practice (12). The prevalence of facet joint-related low back pain reportedly varies between 15% and 45% (16,17,24). Degenerative changes of the facet joints increase especially with age and contribute to the pathogenesis of mechanical low back pain (22). Since facet joint pathology is difficult to differentiate from other causes of lumbar pain, the diagnosis is mostly based on a combination

Burak ERKEN : 0000-0002-7369-0618 Suat DEMIR : 0000-0001-8344-4210 Ipek Saadet EDIPOGLU : 0000-0002-3510-5991

of the patient's clinical symptoms, physical examination findings, and interventional methods, especially diagnostic injections (6). Although the presence of pathologic changes can be demonstrated with imaging methods, the correlation between radiologic findings and clinical pain is reportedly poor (13).

Intra-articular local anesthetic injections for diagnostic purposes are frequently used in the confirmation of LFJ-induced pain (7). A ≥50% pain reduction after diagnostic injection is reportedly be indicative of facet-induced pain (8,25,30). Therefore, only patients who showed significant pain relief after diagnostic intra-articular injection were included in the present study.

Interventional approaches come to the forefront in the treatment of LFJ pain in patients who do not get results with conservative methods (6). Conventional radiofrequency ablation (CRF) provides analgesia by thermal damage to the medial branch nerves; however, side-effects such as neuritic pain, dysesthesia and nerve damage may develop with this method (1,5,6). Pulsed radiofrequency (PRF), wherein the temperature does not exceed 42 ºC and causes minimal tissue destruction, aims to alleviate pain with neuromodulatory effect (26,27). Although the exact mechanism of action of PRF has not yet been fully elucidated, it is thought to modulate neural transmission and suppress local inflammation through the applied electrical field (27).

Intra-articular PRF (IA-PRF) has recently been proposed as an alternative method for the management of LFJ pain (20,22). IA-PRF reportedly provides significant reduction in pain by directly targeting the joint pathology compared to medial branch PRF (MB-PRF) (20). However, the number of studies directly comparing both methods is limited and there is no consensus regarding which technique is superior; the need for prospective studies on this subject continues.

In this study, we aimed to compare the efficacy of IA-PRF and MB-PRF. In our study, the short-term results of 116 patients whose LFJ-induced pain was confirmed by diagnostic intra-articular injection and subsequently treated with IA-PRF or MB-PRF were evaluated at the 1- and 6-month follow-ups by using Numerical Rating Scale (NRS) and Oswestry Disability Index (ODI) scores. With the findings obtained, it is aimed to contribute to the determination of the optimal interventional approach in the treatment of LFJ pain.

MATERIAL and METHODS

Patient Population

This prospective study was conducted between December 2021 and November 2023 on patients admitted to the algology clinic of our institution with complaints of low back pain and diagnosed with LFJ-induced chronic low back pain and registered in the clinicaltrials.gov database (registration number, NCT06157294). Ethical approval for the study was obtained from our institution (ethics committee decision number, 2002.05.102), and the study was conducted in accordance with the ethical principles of the Declaration of Helsinki. Written informed consent was obtained from all patients before participation in the study.

Inclusion criteria were defined as the presence of low back pain that persisted for at least 3 months and was considered to have an LFJ origin, no response to previous conservative treatments (analgesic therapy, physical therapy, manual therapy, etc.), pain severity ≥ 6 as assessed by NRS at the time of admission, and subjective pain reduction of ≥50% after intra-articular local anesthetic injection for diagnostic purposes.

Exclusion criteria were as follows: history of previous surgery in the lumbar region, presence of coagulopathy or bleeding diathesis, pregnancy, presence of active infection findings or systemic diseases that may interfere with the interventional procedure, and cognitive impairment such that patients were unable to complete the assessment scales such as NRS and ODI completely and accurately during the follow-up period. A total of 130 patients were initially enrolled in the study. However, 14 patients were excluded from the final analysis owing to loss to follow-up (n=10), incomplete questionnaire data (n=3), or withdrawal of consent (n=1). Consequently, 116 patients were included in the final evaluation (IA-PRF group, n=60; MB-PRF group, n=56). Patients were selected by a researcher not involved in the procedure and were randomized using a computer-generated program. All patients were systematically followed up with NRS and ODI scores at 1 and 6 months.

Procedure

All interventional procedures were performed by a single experienced pain physician, thereby ensuring procedural standardization. All procedures were performed under sterile conditions, in the operating room environment and under fluoroscopic guidance at the levels between L3 and S1, either unilaterally or bilaterally, as determined by clinical and radiologic findings.

In the IA-PRF application, the patient was intravenously accessed and monitored, sterile conditions were provided in the prone position, and the targeted facet joints were determined with appropriate fluoroscopy (Shimadzu Opescope Acteno; Shimadzu Corporation, Kyoto, Japan) angles. A 10-cm-long, 10-mm-active tip, 20-gauge, radiofrequency needle (Cosman RF Injection Electrode; Cosman Medical Inc., Burlington, MA, USA) was advanced into the target joint space. After intra-articular localization was confirmed by fluoroscopic imaging, PRF was applied with radiofrequency generator (G4 radiofrequency generator; Cosman Medical Inc.) using the following parameters: voltage, 45 V; frequency, 2 Hz; pulse width, 20 ms; duration, 6 minutes; and maximum temperature, 42°C. No sensory or motor stimulation was applied during the procedure (Figure 1A).

In MB-PRF, the patient was placed in the prone position and the anatomical localization of the targeted medial branch was determined under fluoroscopic guidance. A 10-cm-long, 10-mm-active tip, 20-gauge, radiofrequency needle was inserted at the intersection of the superior articular process and the transverse process. After the needle position was confirmed with lateral and oblique fluoroscopic projections, paresthesia and contraction in the lumbar region with sensory

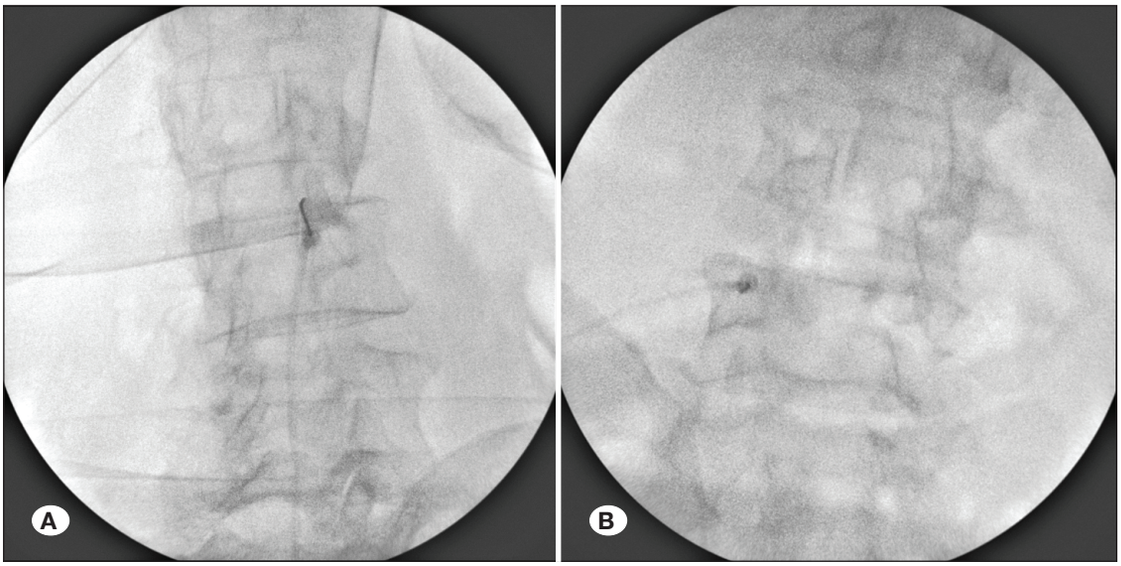

Figure 1: Fluoroscopic images demonstrating PRF techniques for lumbar facet joint pain. **A)** Anteroposterior fluoroscopic image demonstrating IA-PRF, with the cannula advanced into the facet joint space at the L3–L4 level. **B)** Anteroposterior fluoroscopic image showing appropriate placement of the radiofrequency cannula targeting the L5 medial branch for MB-PRF. (**IA-PRF:** intra-articular pulsed radiofrequency, **MB-PRF:** medial branch pulsed radiofrequency, **PRF:** pulsed radiofrequency)

stimulation under 0.5 V and muscle contraction with motor stimulation were observed to confirm the accuracy of nerve localization. PRF was then applied with the same parameters (maximum temperature, 42 °C; voltage, 45 V; frequency, 2 Hz; pulse width, 20 ms; and duration, 6 minutes) (Figure 1B).

After both procedures, patients were discharged on the same day after post-procedural controls and no additional medical treatment was given except for standard post-procedural recommendations.

Clinical Evaluation Criteria

Clinical evaluations of the patients were performed using NRS and ODI scores. These scales were administered to all patients before treatment, and at the 1- and 6-month follow-ups and the data were recorded prospectively.

Statistical Analysis

The distribution of the data obtained in the study was evaluated with histograms and Q-Q graphs; nonparametric analysis methods were preferred for the data that were found not to show normal distribution. Friedman's test was applied for repeated measurements within groups, and in cases where a significant difference was found, pairwise comparisons were made with Wilcoxon signed-rank test. The Mann–Whitney U test was used for intergroup comparisons. Chi-square test was preferred for the analysis of categorical variables. The significance level was accepted as $p<0.05$ in all statistical analyzes. Statistical analyses were performed using JASP software (Version 0.19.3; The JASP Team, Amsterdam, The Netherlands).

RESULTS

Overall, 116 patients were included in the study. Of these, 60 patients were in the IA-PRF group and 56 patients were in the MB-PRF group. The mean age was 59.2 ± 8.17 years in the IA-PRF group and 58.5 ± 8.28 years in the MB-PRF group, and there was no statistically significant difference in age between the groups ($p=0.632$). Gender distribution (IA-PRF: 56.7% female; MB-PRF: 53.6% female, $p=0.738$) and side of administration (right-left-bilateral) ($p=0.831$) were similar between the groups (Table I).

Clinical Variation within Groups

In the IA-PRF group, the mean NRS score reflecting the pain level was 6.55 ± 0.65 before treatment, 3.23 ± 0.43 at 1 month and 3.70 ± 0.46 at 6 months. In the same group, the mean ODI score was 49.70 ± 3.75 at baseline and decreased to 25.13 ± 1.66 at 1 month and 26.90 ± 2.13 at 6 months. When the change over time was analyzed with Friedman test, a statistically significant difference was found in both NRS and ODI scores ($p<0.001$ for both). Pairwise comparisons using the Wilcoxon test showed a significant decrease between pretreatment and both 1-month and 6-month values ($p<0.001$).

Similarly, in the MB-PRF group, the mean pretreatment NRS score was 6.43 ± 0.66, which decreased to 3.13 ± 0.33 at 1 month and 3.57 ± 0.49 at 6 months. ODI scores were 49.18 ± 3.49 at baseline, 24.71 ± 1.34 at 1 month and 26.68 ± 2.20 at 6 months. In the within-group analysis, the change over time was found to be significant for both NRS and ODI using Friedman's test ($p<0.001$) and in pairwise comparisons using Wilcoxon test, statistically significant improvements were obtained at both follow-up times compared to baseline ($p<0.001$). The mean values of the changes in NRS and ODI scores over time in both groups are presented in Figure 2.

Table I: Demographic Characteristics of the Patients

Variable	IA-PRF (n=60)	MB-PRF (n=56)	p-value
Age, years (mean ± SD)	59.2 ± 8.17	58.5 ± 8.28	0.632
Sex, n (%)			0.738
Female	34 (56.7)	30 (53.6)	
Male	26 (43.3)	26 (46.4)	
Side, n (%)			0.831
Right	31 (51.7)	28 (50.0)	
Left	22 (36.7)	23 (41.1)	
Bilateral	7 (11.6)	5 (8.9)	

IA-PRF: *Intra-articular pulsed radiofrequency,* ***MB-PRF:*** *Medial branch pulsed radiofrequency.*

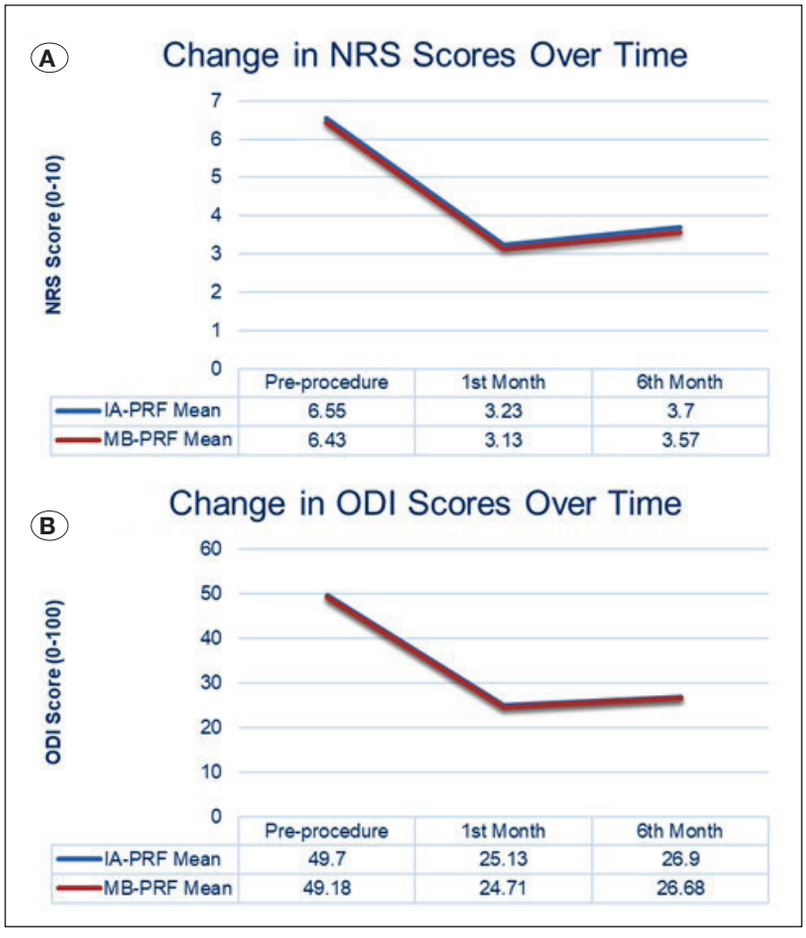

Figure 2: A) Change in NRS scores over time in IA-PRF and MB-PRF groups. **B**) Time course of ODI scores in the same groups. <A statistically significant decrease was found in both groups at the 1st and 6th month follow-ups compared to pretreatment (p 0.001). (**IA-PRF:** intra-articular pulsed radiofrequency, **MB-PRF:** medial branch pulsed radiofrequency, **NRS:** Numerical Rating Scale, **ODI:** Oswestry Disability Index)

Comparison Between Groups

There was no statistically significant difference between IA-PRF and MB-PRF groups in terms of NRS and ODI scores obtained at 1 and 6 months after treatment. At 1 month, NRS scores were 3.23 ± 0.43 in the IA-PRF group and 3.13 ± 0.33 in the MB-PRF group (p = 0.133); at 6 months, these values were 3.70 ± 0.46 and 3.57 ± 0.49, respectively (p=0.153). No significant difference was observed between the groups regarding ODI scores; at 1 month, the mean ODI score was 25.13 ± 1.66 in the IA-PRF group and 24.71 ± 1.34 in the MB-PRF group (p=0.186); at 6 months, it was 26.90 ± 2.13 and 26.68 ± 2.20, respectively (p=0.591).

Table II: Comparison of NRS and ODI Scores Between IA-PRF and MB-PRF Groups at Pre-procedure, 1st Month, and 6th Month

Time Point	Assessment	IA-PRF Mean ± SD (Min – Max)	MB-PRF Mean ± SD (Min – Max)	Intergroup p-value†	Intragroup p-value‡
Pre-procedure	NRS	6.55 ± 0.65 (6-8)	6.43 ± 0.66 (6-8)	0.225	–
Post-procedure 1st Month	NRS	3.23 ± 0.43 (3-4)	3.13 ± 0.33 (3-4)	0.133	**<0.001***
Post-procedure 6th Month	NRS	3.70 ± 0.46 (3-4)	3.57 ± 0.49 (3-4)	0.153	**<0.001***
Pre-procedure	ODI	49.70 ± 3.75 (44-58)	49.18 ± 3.49 (44-58)	0.498	–
Post-procedure 1st Month	ODI	25.13 ± 1.66 (24-30)	24.71 ± 1.34 (22-28)	0.186	**<0.001***
Post-procedure 6th Month	ODI	26.90 ± 2.13 (24-30)	26.68 ± 2.20 (24-30)	0.591	**<0.001***

IA-PRF: *Intra-articular pulsed radiofrequency,* ***MB-PRF:*** *Medial branch pulsed radiofrequency,* ***NRS:*** *Numerical Rating Scale,* ***ODI:*** *Oswestry Disability Index,* ***SD:*** *Standard deviation,* ***†*** *Intergroup comparison by Mann–Whitney U test,* ***‡*** *Intragroup change over time by Friedman test, *<0.05 was considered significant.*

Although clinically significant pain and functional improvement was achieved in both treatment groups, the differences between the groups did not reach statistical significance. In addition, no complications developed during the intervention or during the short-term follow-up period in both procedure groups. Detailed findings regarding the comparative analysis of NRS and ODI scores between the groups are presented in Table II.

DISCUSSION

This prospective randomized study compared the short-term results of the efficacy of IA-PRF and MB-PRF in patients with confirmed LFJ pain by diagnostic intra-articular injection. Treatment response was evaluated on the NRS and ODI. Results showed that both methods provided statistically significant clinical improvement in LFJ-induced low back pain; however, there was no significant difference in clinical efficacy between the methods. These results indicate that both IA-PRF and MB-PRF may be effective in the short-term treatment of LFJ-related pain.

LFJ-induced pain is one of the important causes of chronic low back pain and is usually diagnosed with diagnostic injections (7). As recommended in the literature, patients with at least 50% reduction in pain after diagnostic block were included in the present study (8,25,30). Interventional methods are preferred in patients who do not respond to conservative approaches in the treatment of LFJ-induced low back pain (6). Although CRF applied to the medial branch is frequently used, it may cause undesirable effects such as permanent damage to nerve structures, burning sensation and neuritic pain by creating thermal lesions (1,5,6). In this context, PRF applications, which operate at low temperature and provide a neuromodulatory effect with minimal tissue destruction, are considered as a safer alternative (11,18,27). However, there is still no universally accepted gold standard for radiofrequency applications in the treatment of LFJ pain (14).

PRF is an interventional treatment method that works with intermittent electrical energy pulses at low temperature (≤42 °C) and aims to provide analgesic effect without thermal damage to the target tissue, unlike CRF applications (4). Although the mechanism of action of PRF has not been fully explained, available evidence suggests that this method shows neuromodulatory effects at multiple biological levels. Electron microscopic studies have shown that PRF application causes structural changes especially in small diameter C and Aδ fibers involved in nociceptive transmission (11). Moreover, PRF reportedly activates the endogenous opioid system and increases opioid precursor mRNAs and corresponding peptides such as proenkephalin, proopiomelanocortin and prodynorphin (19). In addition, it has been shown in animal models that PRF administration suppresses the expression of proinflammatory cytokines such as tumor necrosis factor-α and interleukin-6, while modulating the expression of genes involved in pain transmission such as GABAB-R1 receptor, Na/K ATPase, 5-HT3 receptor and c-Fos (28). These multilevel biological effects suggest that PRF may be effective not only as a method to suppress nerve conduction, but also through regulation of inflammation and modulation of neuroimmune response.

The target in MB-PRF application is the medial branches of the dorsal spinal nerves that provide sensation of the facet joints (6). These nerves play a role in the transmission of nociceptive inputs, especially in the facet joint capsule and paraspinal soft tissues; pathological examinations have shown that both sensory and autonomic nerve fibers are densely present in these structures (31). With PRF application, pain transmission is inhibited by decreasing neuroexcitability in these nerves (11). However, the anatomical variation of the medial branch nerves makes accurate localization difficult, especially in fluoroscopic interventions, and may cause variable efficacy due to the regenerative capacity of the nerves (10,21,23,29). In addition, the application requires technical skill due to its proximity to the nerve structure and the level of invasiveness is relatively high (20).

IA-PRF is based on direct intra-articular application of the PRF technique and specifically targets the suppression of synovial inflammation and capsular tension (9). It has been shown that the facet joint capsule has intense nociceptive innervation and this area becomes hypersensitized in degenerative processes

due to proinflammatory cytokines, synovial hyperplasia and increased pain mediators in the joint fluid (2). IA-PRF application modulates axoplasmic conduction and cell membrane permeability in local nerve endings by generating an electrical field in this region; thus, the transmission of peripheral nociceptive signals is suppressed and central sensitization of pain can be prevented (9,15). As reported by Schianchi, IA-PRF provides long-term reduction in pain with high success rates when applied in small and large joints (22). Chang et al. showed that IA-PRF application in patients with refractory LFJ pain provided a significant reduction in pain for up to 6 months and no serious complications were reported (4). Do et al. reported that IA-PRF offered similar short-term effects compared to intra-articular steroid injection, but the efficacy lasted longer (9). In addition, IA-PRF may be technically easier to administer than MB-PRF due to the larger target area and may provide a wider analgesic effect with less needle placement (3).

The prospective nature of our study provides an important methodological advantage in terms of data integrity and quality of follow-up. Furthermore, the fact that the patients were selected by diagnostic injection and the evaluation parameters were systematically monitored increases the clinical validity of the findings. The limited number of studies directly comparing these two techniques in the literature makes the findings of our study significant.

Limitations

Although our study was prospectively designed and supported by systematic follow-up data, it has some limitations. First of all, the study was conducted in a single center and the findings reflect only a specific patient population. Although the sample size is considered adequate for interventional pain treatments, multicenter studies are needed to confirm the results in larger clinical settings. Furthermore, only short-term follow-up data (1 and 6 months) were evaluated and long-term treatment efficacy was not analyzed. Another limitation is that contrast agent injection to verify intraarticular spread after RF needle placement was not performed. Instead, correct needle positioning at each level was ensured using anteroposterior, lateral, and oblique fluoroscopic views. These limitations partially limit the external validity of the study and the generalizability of the results.

Future Directions

In order to compare the efficacy of IA-PRF and MB-PRF more clearly and to guide clinical decision-making, multicenter, large-scale and long-term follow-up studies are needed. In addition, separate evaluation of both applications in subgroups with different age groups, degeneration levels and comorbidities may enable the development of patient-based treatment approaches. Further studies investigating the relationship between radiologic imaging findings and treatment response and evaluation of the biological effects of PRF with objective biomarkers or neurophysiologic tests will contribute to a better understanding of treatment mechanisms. Furthermore, the synergistic effects of IA-PRF and combination therapies (e.g. steroid injection or physical therapy) should also be investigated.

CONCLUSION

In this prospective study, the short-term efficacy of IA-PRF and MB-PRF for diagnostically confirmed LFJ pain was compared, and both methods were shown to provide pain control and functional improvement at the 1- and 6-month follow-ups. Although no statistically significant difference was found between the methods, both techniques stand out as effective and safe interventional options. Considering the lack of prospective data directly comparing these two methods in the literature, our study provides original information that will contribute to clinical practice with its findings. The findings support the necessity of individualizing the treatment approach according to patient characteristics. Future studies with larger samples and longer-term follow-up are still needed regarding this topic.

Declarations

Funding: This research did not receive any specific grant from funding agencies in the public, commercial, or not-for-profit sectors.

Availability of data and materials: The datasets generated and/or analyzed during the current study are available from the corresponding author by reasonable request.

Disclosure: The authors declare no competing interests.

AUTHORSHIP CONTRIBUTION

Study conception and design: BE, SD, ISE

Data collection: BE, ISE

Analysis and interpretation of results: BE, SD, ISE

Draft manuscript preparation: BE, SD

Critical revision of the article: BE, SD, ISE

All authors (BE, SD, ISE) reviewed the results and approved the final version of the manuscript.

REFERENCES

1. Arias Garau J: Radiofrequency denervation of the cervical and lumbar spine. Phys Med Rehabil Clin N Am 29:139-154, 2018. https://doi.org/10.1016/j.pmr.2017.08.011
2. Ashton IK, Ashton BA, Gibson SJ, Polak JM, Jaffray DC, Eisenstein SM: Morphological basis for back pain: The demonstration of nerve fibers and neuropeptides in the lumbar facet joint capsule but not in ligamentum flavum. J Orthop Res 10:72-78, 1992. https://doi.org/10.1002/jor.1100100109
3. Bogduk N, Long DM: The anatomy of the so-called "articular nerves" and their relationship to facet denervation in the treatment of low-back pain. J Neurosurg 51:172-177, 1979. https://doi.org/10.3171/jns.1979.51.2.0172
4. Chang MC, Cho YW, Ahn DH, Do KH: Intraarticular pulsed radiofrequency to treat refractory lumbar facet joint pain in patients with low back pain. World Neurosurg 112:e140-e144, 2018. https://doi.org/10.1016/j.wneu.2017.12.181
5. Civelek E, Cansever T, Kabatas S, Kırcelli A, Yılmaz C, Musluman M, Ofluoglu D, Caner H: Comparison of effectiveness of facet joint injection and radiofrequency denervation in chronic low back pain. Turk Neurosurg 22:200-206, 2012. https://doi.org/10.5137/1019-5149.JTN.5207-11.1

6. Cohen SP, Bhaskar A, Bhatia A, Buvanendran A, Deer T, Garg S, Hooten WM, Hurley RW, Kennedy DJ, McLean BC, Moon JY, Narouze S, Pangarkar S, Provenzano DA, Rauck R, Sitzman BT, Smuck M, van Zundert J, Vorenkamp K, Wallace MS, Zhao Z: Consensus practice guidelines on interventions for lumbar facet joint pain from a multispecialty, international working group. Reg Anesth Pain Med 45:424-467, 2020. https://doi.org/10.1136/rapm-2019-101243
7. Cohen SP, Raja SN: Pathogenesis, diagnosis, and treatment of lumbar zygapophysial (facet) joint pain. Anesthesiology 106:591-614, 2007. https://doi.org/10.1097/00000542-200703000-00024
8. Cohen SP, Williams KA, Kurihara C, Strassels SA, Foster L, Burney R, Griffith SR, Larkin TM, Crooks M, Nguyen C, Su S, Jones SS: Multicenter, randomized, comparative cost-effectiveness study comparing 0, 1, and 2 diagnostic medial branch (facet joint nerve) block treatment paradigms before lumbar facet radiofrequency denervation. Anesthesiology 113:395-405, 2010. https://doi.org/10.1097/ALN.0b013e3181e33ae5
9. Do KH, Ahn SH, Cho YW, Chang MC: Comparison of intra-articular lumbar facet joint pulsed radiofrequency and intra-articular lumbar facet joint corticosteroid injection for management of lumbar facet joint pain: A randomized controlled trial. Medicine (Baltimore) 96:e6524, 2017. https://doi.org/10.1097/MD.0000000000006524
10. Dreyfuss P, Baker R, Leclaire R, Fortin L, Lambert R, Bergeron Y, Rossignol M: Radiofrequency facet joint denervation in the treatment of low back pain: A placebo-controlled clinical trial to assess efficacy. Spine (Phila Pa 1976) 27: 556-557, 2002. https://doi.org/10.1097/00007632-200203010-00026
11. Erdine S, Bilir A, Cosman ER, Cosman ER Jr: Ultrastructural changes in axons following exposure to pulsed radiofrequency fields. Pain Pract 9:407-417, 2009. https://doi.org/10.1111/j.1533-2500.2009.00317.x
12. Jacobson RE, Palea O, Granville M: Bipolar radiofrequency facet ablation of the lumbar facet capsule: An adjunct to conventional radiofrequency ablation for pain management. Cureus 9:e1635, 2017. https://doi.org/10.7759/cureus.1635
13. Kalichman L, Kim DH, Li L, Guermazi A, Hunter DJ: Computed tomography-evaluated features of spinal degeneration: Prevalence, intercorrelation, and association with self-reported low back pain. Spine J 10:200-208, 2010. https://doi.org/10.1016/j.spinee.2009.10.018
14. Li SJ, Zhang SL, Feng D: A comparison of pulsed radiofrequency and radiofrequency denervation for lumbar facet joint pain. J Orthop Surg Res 18:331, 2023. https://doi.org/10.1186/s13018-023-03814-5
15. Lim JW, Cho YW, Lee DG, Chang MC: Comparison of intraarticular pulsed radiofrequency and intraarticular corticosteroid injection for management of cervical facet joint pain. Pain Phys 20:E961-E967, 2017. https://doi.org/10.36076/ppj.20.5.E961
16. Manchikanti L, Pampati V, Fellows B, Baha AG: The inability of the clinical picture to characterize pain from facet joints. Pain Phys 3:158-166, 2000. https://doi.org/10.36076/ppj.2000/3/158
17. Manchikanti L, Pampati V, Fellows B, Bakhit CE: Prevalence of lumbar facet joint pain in chronic low back pain. Pain Phys 2:59-64, 1999. https://doi.org/10.36076/ppj.1999/2/59
18. Maretto F, Vennik M, Albers KI, van Duijn B: TNFα secretion of monocytes exposed to pulsed radiofrequency treatment: A possible working mechanism of PRF chronic pain management. Pain Pract 14:399-404, 2014. https://doi.org/10.1111/papr.12101
19. Moffett J, Fray LM, Kubat NJ: Activation of endogenous opioid gene expression in human keratinocytes and fibroblasts by pulsed radiofrequency energy fields. J Pain Res 5:347-357, 2012. https://doi.org/10.2147/JPR.S35076
20. Moussa WM, Khedr W: Percutaneous radiofrequency facet capsule denervation as an alternative target in lumbar facet syndrome. Clin Neurol Neurosurg 150:96-104, 2016. https://doi.org/10.1016/j.clineuro.2016.09.004
21. Qi LN, Sun Y, Shi YT, Yang JH, Yang YR, Qin XZ: Comparison of the efficacy of different radiofrequency techniques for the treatment of lumbar facet joint pain: Combined with anatomy. Curr Pain Headache Rep 28:699-708, 2024. https://doi.org/10.1007/s11916-024-01241-7
22. Schianchi PM: A new technique to treat facet joint pain with pulsed radiofrequency. Anesth Pain Med 5:e21061, 2015. https://doi.org/10.5812/aapm.21061
23. Schofferman J, Kine G: Effectiveness of repeated radiofrequency neurotomy for lumbar facet pain. Spine (Phila Pa 1976) 29:2471-2473, 2004. https://doi.org/10.1097/01.brs.0000143170.47345.44
24. Schwarzer AC, Aprill CN, Derby R, Fortin J, Kine G, Bogduk N: Clinical features of patients with pain stemming from the lumbar zygapophysial joints. Is the lumbar facet syndrome a clinical entity? Spine (Phila Pa 1976) 19:1132-1137, 1994. https://doi.org/10.1097/00007632-199405001-00006
25. Sehgal N, Dunbar EE, Shah RV, Colson J: Systematic review of diagnostic utility of facet (zygapophysial) joint injections in chronic spinal pain: An update. Pain Physician 10:213-228, 2007. https://doi.org/10.36076/ppj.2007/10/213
26. Shealy CN: Percutaneous radiofrequency denervation of spinal facets: Treatment for chronic back pain and sciatica. J Neurosurg 43:448-451, 1975. https://doi.org/10.3171/jns.1975.43.4.0448
27. Sluijter ME, Imani F: Evolution and mode of action of pulsed radiofrequency. Anesth Pain Med 2:139-141, 2013. https://doi.org/10.5812/aapm.10213
28. Vallejo R, Tilley DM, Williams J, Labak S, Aliaga L, Benyamin RM: Pulsed radiofrequency modulates pain regulatory gene expression along the nociceptive pathway. Pain Phys 16:E601-E613, 2013. https://doi.org/10.36076/ppj.2013/16/E601
29. van Kleef M, Barendse GA, Kessels A, Voets HM, Weber WE, de Lange S: Randomized trial of radiofrequency lumbar facet denervation for chronic low back pain. Spine (Phila Pa 1976) 24:1937-1942, 1999. https://doi.org/10.1097/00007632-199909150-00013
30. van Wijk RM, Geurts JW, Wynne HJ, Hammink E, Buskens E, Lousberg R, Knape JT, van Kleef M: Radiofrequency denervation of lumbar facet joints in the treatment of chronic low back pain: A randomized, double-blind, sham lesion-controlled trial. Clin J Pain 21:335-344, 2005. https://doi.org/10.1097/01.ajp.0000120792.69705.c9
31. Zhou L, Schneck CD, Shao Z: The anatomy of dorsal ramus nerves and its implication in lower back pain. Neurosci Med 3:192-201, 2012. https://doi.org/10.4236/nm.2012.32025

Turk Neurosurg 36(1):89-98, 2026
DOI: 10.5137/1019-5149.JTN.47941-24.4

Original Investigation
Spine and Peripheral Nerves

Received: 23.10.2024
Accepted: 17.05.2025
Published Online: 16.01.2026

Distal Junctional Failure in Posterior Thoracolumbar Surgery: An Analysis of Spinopelvic Alignment and Surgical Outcomes

Numan KARAARSLAN[1], Hidayet Safak CINE[1], Ece UYSAL[2], Mehmet Ali KAHRAMAN[1], Emre HERDAN[1], Mohammed ALADDAM[1], Abdullah Talha SIMSEK[1], Mahmut DEMIRKOL[1], Burak BAYRAKTAR[1], Yunus Emre OZBILGI[1]

[1]Istanbul Medeniyet University, Prof. Dr. Suleyman Yalcin City Hospital, Department of Neurosurgery, Istanbul, Türkiye
[2]University of Health Sciences, Prof. Dr. Cemil Tascioglu City Hospital, Department of Neurosurgery, Istanbul, Türkiye

Corresponding author: Numan KARAARSLAN ✉ numankaraarslan@yahoo.com

ABSTRACT

AIM: To evaluate the incidence, risk factors, and spinopelvic alignment parameters associated with distal junctional failure (DJF) following posterior thoracolumbar stabilization surgery.

MATERIAL and METHODS: This retrospective cohort study included 40 patients who underwent thoracolumbar stabilization between 2018 and 2024. Patients were divided into two groups: those who developed DJF (n=20) and those who did not (n=20, control group). Radiographic evaluations, including pre- and postoperative lateral radiographs, were used to assess spinopelvic parameters such as lumbar lordosis (LL), pelvic incidence (PI), and PI–LL mismatch. Statistical analyses were conducted to examine the correlation between these parameters and DJF occurrence.

RESULTS: The DJF group exhibited a significant postoperative reduction in LL and an increase in PI–LL mismatch compared to the control group, which maintained better sagittal alignment postoperatively ($p < 0.05$). Patients with higher preoperative PI–LL mismatch were more likely to develop DJF, highlighting the importance of preoperative planning and correction to prevent this complication.

CONCLUSION: Optimizing spinopelvic alignment, particularly LL and PI–LL mismatch, is crucial for reducing the risk of DJF after thoracolumbar stabilization surgery. Future studies should aim to refine surgical techniques and strategies to enhance postoperative outcomes and minimize complications.

KEYWORDS: Distal junctional failure, Thoracolumbar stabilization surgery, Spinopelvic parameters, Lumbar lordosis, PI-LL mismatch

ABBREVIATIONS: CT: Computed tomography, **DEXA:** Dual-energy x-ray absorptiometry, **DJF:** Distal junctional failure, **DJK:** Distal junctional kyphosis, **ESV:** End segment vertebra, **IQR:** Interquartile range, **LIV:** Lower instrumented vertebra, **LL:** Lumbar lordosis, **MRI:** Magnetic resonance imaging, **NPV:** Negative predictive value, **PI:** Pelvic incidence, **PI–LL Mismatch:** Pelvic incidence and lumbar lordosis mismatch, **PPV:** Positive predictive value, **PT:** Pelvic tilt, **SD:** Standard deviation, **SS:** Sacral slope, **SVA:** Sagittal vertical axis

Numan KARAARSLAN : 0000-0001-5590-0637
Hidayet Safak CINE : 0000-0002-0808-5921
Ece UYSAL : 0000-0002-2355-8395
Mehmet Ali KAHRAMAN : 0009-0005-3719-654X
Emre HERDAN : 0000-0003-2046-2133
Mohammed ALADDAM : 0009-0004-2289-2975
Abdullah Talha SIMSEK : 0000-0002-8668-3935
Mahmut DEMIRKOL : 0009-0009-4286-6690
Burak BAYRAKTAR : 0009-0006-4317-5961
Yunus Emre OZBILGI : 0009-0004-8394-402X

INTRODUCTION

Posterior transpedicular fixation is the most commonly used and widely accepted method for treating adult spinal deformities, thoracolumbar fractures, and scoliosis (5). The primary goal of this stabilization technique is to achieve a balanced spine in both the coronal and sagittal planes while preserving as much functional movement as possible and preventing future complications (21). However, despite successful stabilization, motion persists in the unfused segments, leading to increased stress and movement in the adjacent upper and lower segments. This biomechanical shift may result in adjacent segment disease.

While much of the existing literature has focused on the proximal junction-where insufficiencies are most commonly observed-distal junctional failure (DJF) is also a significant complication that warrants attention (19). Distal junctional kyphosis (DJK) refers to the development of kyphosis at the caudal end of the instrumentation, typically defined by a sagittal Cobb angle greater than 10 degrees between the vertebrae in the caudal region (13). DJF, in contrast, refers to failure at the most caudal end of the instrumented segments, which may occur even in the absence of kyphosis. It is characterized by clinical and radiological changes at the distal segment (20).

Clinically, DJF may present with lower back and hip pain, loss of function, neurological symptoms, and postural deformity. Radiologic findings include progressive loss of lumbar lordosis, degeneration of the adjacent disc at the lower end of the instrumentation, loss of vertebral height, wedging, fractures of the distal instrumented or adjacent vertebrae, and implant-related issues such as screw breakage, loosening, stenosis, and instability at the segment adjacent to the distal instrumented vertebra (2).

The incidence of DJF following adult spinal deformity surgery ranges from 1.8% to 15.6%, significantly impacting patients' quality of life, leading to increased deformities, repeated surgeries, and reduced productivity (6). Prevention of DJF requires a comprehensive assessment of various spinal parameters. The sagittal vertical axis (SVA) is a widely used measure of sagittal alignment, but it can be influenced by compensatory mechanisms such as pelvic retroversion, knee flexion, and patient posture (12). Among the most critical parameters to evaluate during stabilization surgery are the pelvic parameters, including lumbar lordosis (LL), pelvic tilt (PT), pelvic incidence (PI), sacral slope (SS), and PI–LL mismatch. These should be carefully evaluated preoperatively, as they play a vital role in maintaining sagittal balance (16).

Despite the recognized importance of these parameters, few studies have specifically investigated their role in patients who develop DJF following thoracolumbar stabilization. This study aims to investigate the causes of DJF in patients who have undergone thoracolumbar posterior stabilization, focusing on the surgical levels involved, identification of the last instrumented vertebra, and relevant sagittal pelvic parameters. Furthermore, the study seeks to explore the relationship between the timing of DJF onset and these parameters, with the ultimate goal of informing strategies to prevent this complication.

MATERIAL and METHODS

Study Design

This study protocol received approval from the Usak University Ethics Board (approval no. 448-448-13/2024). Due to the retrospective design and institutional regulations for research, specific informed consent from patients was not required.

This retrospective study includes patients treated for spinal stenosis, deformity, or trauma who underwent posterior transpedicular stabilization at our institution between 2018 and 2024. All procedures were performed by different surgeons within the same clinic. The surgical approach involved a posterior midline incision followed by posterolateral transpedicular screw fixation, including both cases with and without decompression and fusion.

Out of 237 patients who underwent lumbar rigid stabilization and were initially reviewed, 116 were excluded based on the inclusion criteria. Of the remaining 121 patients, 20 were identified as having developed DJF. These patients were categorized into two groups. The first group consisted of patients who had undergone revision surgery due to DJF following their initial posterior stabilization surgery. For the control group, patients without DJF were randomized at a ratio of 5:1 (100 patients) to ensure the reliability of the study. Hence, the failure group included only cases that required revision within six years post-surgery. Medical histories, surgical reports, follow-up reports, and diagnostic imaging (radiographs, CT, and MRI) of all patients stored in the hospital's digital archive were reviewed.

A patient was assigned to the DJF group if a failure occurred at the last instrumented fused level or the immediately adjacent caudal vertebra and met one or more of the following criteria:

- Pullout or loosening of the pedicle screws,
- mechanical breakage of rods or screws,
- adjacent segment pathology (e.g., stenosis/disc/listhesis).

Inclusion Criteria

The inclusion criteria included patients who underwent posterior transpedicular fixation with rigid rods in the thoracolumbar region. There were no age restrictions. Patients who presented with pain, neurological deficits, or other clinical symptoms confirmed through imaging (e.g., CT, X-ray, or MRI) during follow-up were included as part of the DJF group. Patients who did not exhibit any clinical pain or neurological symptoms and showed no evidence of DJF on radiological imaging were included in the control group. Patients with a coronal balance <5 degrees were included in the study.

Exclusion Criteria

Patients who underwent anterior or anterolateral fixation as well as those who had fixation methods other than transpedicular screw fixation were not included in the study. Patients stabilized with dynamic or semi-dynamic systems were also excluded. Patients were monitored for osteoporosis using DEXA scans either preoperatively or postoperatively.

Those with advanced osteoporosis were excluded from the study to avoid conflicts, as were patients who underwent interbody fusion. Patients with a coronal balance >5 degrees were excluded from the study.

Radiological Evaluation

Spinopelvic parameters were assessed in both groups using available lateral standing radiographs that included the entire spine or at least the C2 to femoral heads. For radiological evaluation, pelvic parameters were assessed at three key time points: preoperatively, within three months postoperatively, and immediately prior to revision surgery (for the DJF group). Spinopelvic parameters were analyzed using Surgimap software (Nemaris Inc, New York, NY, www.surgimap.com), a validated, freely available tool designed for surgical planning and spinal measurement. Following prior studies, the following spinopelvic parameters were measured for each patient.

Spinopelvic Parameters: Sagittal and pelvic parameters included LL, PT, PI, SS, and PI–LL mismatch.

Timing of Failure: For the failure group, the time between the first and second surgeries was calculated to determine the timing of DJF onset.

Surgical Details: The number of levels stabilized, whether the lumbar and/or thoracic regions were involved, and the lowest instrumented vertebra (LIV) were recorded for all patients.

Statistical Analyses

Statistical analyses were conducted using the Shapiro–Wilk test to assess normality of the data distribution. For comparisons between groups, either the Student's t-test or Mann–Whitney U test was applied to continuous variables, depending on whether the data were normally distributed. Categorical variables were analyzed using the Chi-square test or Fisher's exact test as appropriate. Parametric variables are presented as mean ± standard deviation (SD) along with minimum–maximum (min–max) values, while categorical variables are reported as percentages (%).

Correlations were assessed using either Pearson or Spearman correlation coefficients, based on data distribution. Statistical significance was set at $p<0.05$. All analyses were performed using SPSS (Statistical Package for the Social Sciences), version 26.0.

RESULTS

A total of 40 patients were included in the study, equally divided between the control group (n=20) and the DJF group (n=20). The overall mean age was 59.62 ± 12.85 years, with an interquartile range (IQR) of 55.0–68.0 years. The control group had a mean age of 58.90 ± 13.02 years (range: 23–80 years; IQR 54.5–66.5 years), while the DJF group had a mean age of 60.35 ± 12.97 years (range: 25–80 years; IQR 57.25–68.25 years).

In terms of gender distribution, 67.5% of all patients were female and 32.5% were male. The control group consisted of 65.0% females and 35.0% males, while the DJF group consisted of 70.0% females and 30.0% males. Regarding surgical location, 92.5% of patients underwent procedures in the lumbar region, 5.0% in the thoracolumbar region, and 2.5% in the thoracic region. Specifically, in the control group, 95.0% of patients underwent lumbar surgery and 5.0% thoracolumbar surgery. In the DJF group, 90.0% had lumbar procedures, 5.0% thoracolumbar, and 5.0% thoracic.

The distribution of LIV varied. Across all patients, LIV was at L5 in 65.0% of cases, S1 in 25.0%, L3 in 5.0%, L1 in 2.5%, and T7 in 2.5%. In the control group, LIV was at L5 in 55.0% of cases, S1 in 40.0%, and L2 in 5.0%. In the DJF Group, LIV was at L5 in 75.0% of cases, L3 in 10.0%, S1 in 10.0%, and T7 in 5.0%.

The mean number of instrumented fused levels was 3.27 ± 1.20 (range: 2.00–7.00 levels; IQR: 2.75–4.00) for all patients. The control group had a mean of 3.10 ± 0.91 fused levels (range: 2.00–6.00), while the DJF group had a mean of 3.45 ± 1.43 fused levels (range 2.00–7.00). In the DJF Group, the mean interval between the first and second surgeries was 39.40 ± 29.21 months (range: 5.0–108.0 months; IQR: 18.75–57.5 months) (Table I, Figure 1).

The preoperative LL for all patients was 47.33 ± 14.37 degrees (range: 18.3–73.9 degrees). The control group had a mean preoperative LL of 43.97 ± 15.08 degrees, while the DJF group had a mean of 50.68 ± 13.14 degrees. The difference between the groups was not statistically significant (p=0.14). Postoperatively, overall LL was 45.63 ± 13.65 degrees. The control group had a significantly higher mean LL (50.14 ± 8.91 degrees) than the DJF group (41.11 ± 16.13 degrees; p=0.03).

Preoperative PT averaged 21.30 ± 11.97 degrees. The control group had a mean of 19.06 ± 12.93 degrees, while the DJF Group had a mean of 23.53 ± 10.78 degrees (p=0.24). Postoperatively, PT decreased to 19.10 ± 11.08 degrees overall, with the control group at 15.83 ± 10.92 degrees and the DJF group at 22.37 ± 10.49 degrees. This difference did not reach statistical significance (p=0.06).

PI averaged 54.45 ± 11.27 degrees preoperatively, with no significant difference between the control group (51.65 ± 9.40 degrees) and the DJF group (57.24 ± 12.49 degrees; p=0.12). PI remained stable postoperatively (p=0.24).

Preoperative SS was 33.43 ± 11.74 degrees overall, with no statistically significant difference between groups (control: 32.65 ± 11.18 degrees; DJF: 34.21 ± 12.51 degrees; p=0.68). Postoperative SS increased slightly to 35.90 ± 9.87 degrees for all patients, without significant between-group differences (p=0.43).

The preoperative PI–LL mismatch was 12.60 ± 10.07 degrees overall, with no statistically significant difference between the control group (15.11 ± 10.15 degrees) and the DJF group (10.09 ± 9.58 degrees; p=0.12). Postoperatively, the PI–LL mismatch increased slightly to 13.56 ± 11.89 degrees for all patients. The DJF group had a significantly higher mismatch (17.98 ± 14.13 degrees) than the control group (9.13 ± 7.02 degrees; p=0.02) (Table II). Among patients with L5 as the LIV, no statistically significant difference was observed in either

Table I: Demographic and Clinical Characteristics of Patients in the Control and DJF Groups

Data	All Patients (n=40)	Control Group (n=20)	DJF Group (n=20)
	n (%) / M ± SD (min - max) [Q1 Q3]		
Age	59.62 ± 12.85 [55.0-68.0]	58.90 ± 13.02 (23-80) [54.5-66.5]	60.35 ± 12.97 (25-80) [57.25-68.25]
Gender	Female (67.5%) Male (32.5%)	Female (65.0%) Male (35.0%)	Female (70.0%) Male (30.0%)
Region	Lumbar (92.5%) Thoracolumbar (5.0%) Thoracic (2.5%)	Lumbar (95.0%) Thoracolumbar (5.0%)	Lumbar (90.0%) Thoracolumbar (5.0%) Thoracic (5.0%)
Lower Instrumented vertebra (LIV)	L5 (65.0%) S1 (25.0%) L3 (5.0%) L1 (2.5%) T7 (2.5%)	L1 (55.0%) S1 (40.0%) L2 (5.0%)	L5 (75.0%) L3 (10.0%) S1 (10.0%) T7 (5.0%)
Instrumental fused levels	3.27 ± 1.20 [2.00 - 7.00] [2.75-4.0]	3.10 ± 0.91 [2.00 - 6.00]	3.45 ± 1.43 [2.00 - 7.00]
Duration between first and second surgery (month)	39.40 ± 29.21 (5.0-108.0) [18.75-57.5]		39.40 ± 29.21 (5.0-108.0) [18.75-57.5]

DJF: *Distal junctional failure,* ***LIV:*** *Lower Instrumented Vertebra,* ***M:*** *Mean,* ***SD:*** *Standard Deviation,* ***min:*** *Minimum,* ***max:*** *Maximum,* ***Q1:*** *First Quartile,* ***Q3:*** *Third Quartile.*

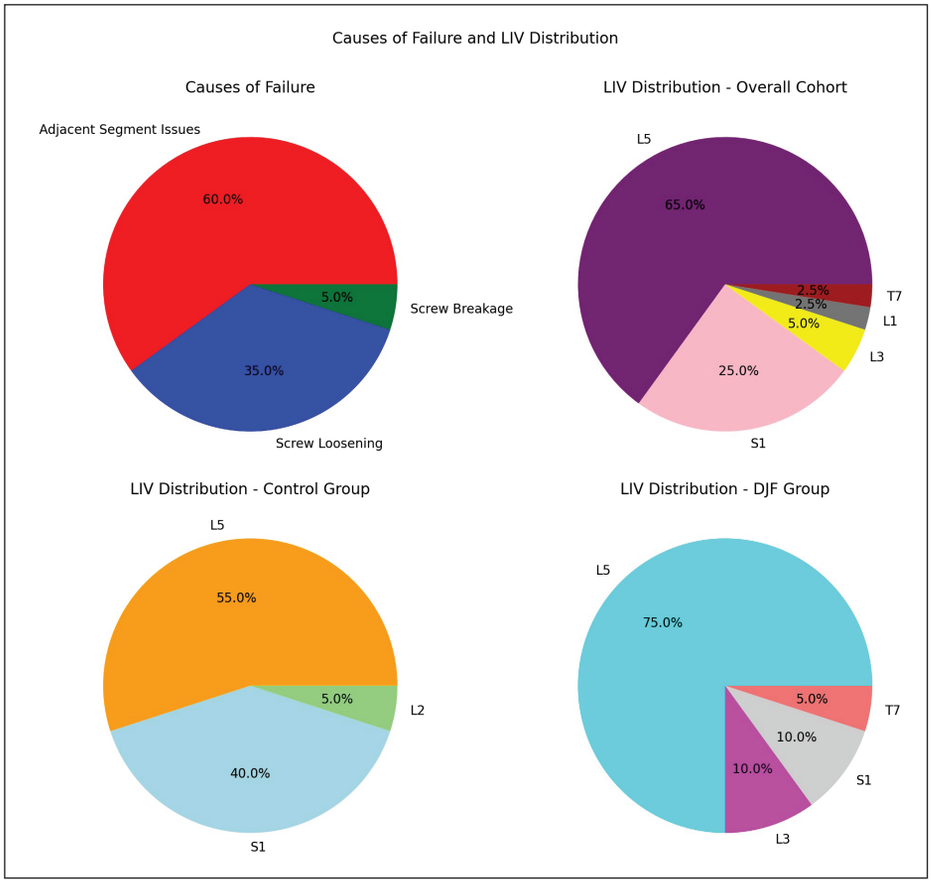

Figure 1: Causes of Failure and Distribution of Lower Instrumented Vertebra (LIV) in the Overall Cohort, Control Group, and DJF Group. This figure illustrates the distribution of failure causes, including screw breakage, screw loosening, and adjacent segment issues, alongside the distribution of the LIV in the overall cohort, control group, and DJF group. The pie charts provide a visual breakdown of the distribution of L5, S1, L3, L1, and T7 as the lower instrumented vertebrae in each group.

Table II: Preoperative and Postoperative Spinopelvic Parameters of Patients in the Control and DJF Groups

Parameter	All Patients (n=40)	Control Group (n=20)	DJF Group (n=20)	p-value
	n (%) / M ± SD (min - max) [Q1 Q3]			
Preoperative LL	47.33 ± 14.37 (18.3-73.9) [35.63-57.38]	43.97 ± 15.08 (18.3-67.9) [30.88-56.73]	50.68 ± 13.14 (27.8-73.9) [43.05-62.57]	0.14
Postoperative LL	45.63 ± 13.65 (6.9-87.7) [38.9-50.3]	50.14 ± 8.91 (37.6-75.0) [45.25-53.65]	41.11 ± 16.13 (6.9-87.7) [34.7-46.6]	**0.03***
Preoperative PT	21.30 ± 11.97 (0.2-50.9) [13.15-29.58]	19.06 ± 12.93 (0.2-43.6) [9.1-25.35]	23.53 ± 10.78 (6.5-50.9) [14.9-30.53]	0.24
Postoperative PT	19.10 ± 11.08 (3.0-50.9) [12.45-25.83]	15.83 ± 10.92 (3.0-40.1) [6.88-19.92]	22.37 ± 10.49 (4.4-50.9) [14.73-27.28]	0.06
Preoperative PI	54.45 ± 11.27 (34.9-80.2) [47.48-62.22]	51.65 ± 9.40 (34.9-68.2) [45.75-57.55]	57.24 ± 12.49 (36.8-80.2) [47.65-66.38]	0.12
Postoperative PI	54.68 ± 12.18 (35.3-83.3) [45.73-61.13]	52.38 ± 11.74 (35.3-83.3) [44.28-57.2]	56.99 ± 12.46 (36.5-80.3) [48.0-65.98]	0.24
Preoperative SS	33.43 ± 11.74 (4.4-56.3) [27.08-41.0]	32.65 ± 11.18 (8.3-48.4) [25.23-40.8]	34.21 ± 12.51 (4.4-56.3) [27.83-41.0]	0.68
Postoperative SS	35.90 ± 9.87 (5.2-60.8) [30.65-40.88]	37.16 ± 6.42 (26.6-50.2) [32.2-40.63]	34.63 ± 12.47 (5.2-60.8) [26.8-42.3]	0.43
Preoperative PI-LL mismatch	12.60 ± 10.07 (1.2-45.3) [5.48-18.10]	15.11 ± 10.15 (1.2-45.3) [8.05-19.0]	10.09 ± 9.58 (1.4-34.0) [2.65-12.65]	0.12
Postoperative PI-LL mismatch	13.56 ± 11.89 (1.6-68.4) [7.8-16.55]	9.13 ± 7.02 (1.6-29.5) [3.475-12.08]	17.98 ± 14.13 (1.72-68.4) [9.48-20.03]	**0.02***
Preoperative LL (LIV L5)		43.89 ± 12.51 (22.7 - 59.5) [35.05-53.85]	52.84 ± 14.16 (27.8 - 73.9) [43.75-64.70]	0.11
Postoperative LL (LIV L5)		47.95 ± 4.73 (38.9 - 55.0) [45.95-50.40]	42.38 ± 18.48 (6.9 - 87.7) [34.20-50.25]	0.34

LL: *Lumbar lordosis,* ***PT:*** *Pelvic tilt,* ***PI:*** *Pelvic incidence,* ***SS:*** *Sacral slope,* ***PI-LL mismatch:*** *Pelvic incidence - Lumbar Lordosis mismatch,* ***M:*** *Mean,* ***SD:*** *Standard Deviation,* ***min:*** *Minimum,* ***max:*** *Maximum,* ***Q1:*** *First Quartile,* ***Q3:*** *Third Quartile,* ****:*** *p<0.05.*

preoperative or postoperative LL values (p=0.011, p=0.34, respectively).

A comparison between preoperative and postoperative spinopelvic parameters revealed significant changes in both groups. Both groups showed significant improvement in LL after surgery (control: p=0.03; DJF: p=0.01). PT, PI, and SS did not show statistically significant preoperative to postoperative changes in either group (PT: control p=0.22, DJF p=0.25; PI: control p=0.51, DJF p=0.07; SS: control p=0.06, DJF p=0.68). Postoperatively, the PI–LL mismatch significantly improved in both the control group (p=0.01) and the DJF group (p=0.01) (Table III).

The change in LL differed significantly between groups (p=0.01). The DJF group showed a mean decrease in LL of –9.58 degrees, while the control group had a mean increase of 6.18 degrees. Postoperatively, the PI–LL mismatch increased in the DJF group by 7.9 degrees and decreased by 5.98 degrees in the control group, a statistically significant difference (p=0.01). Changes in PT, PI, and SS did not significantly differ between groups (p=0.45, p=0.37, p=0.11, respectively) (Table IV, Figure 2).

The PI–LL mismatch and the change in PI–LL mismatch were evaluated in terms of sensitivity, specificity, positive predictive value (PPV), and negative predictive value (NPV). For postoperative PI–LL mismatch, sensitivity was 0.65, specificity was 0.75, PPV was 0.722, and NPV was 0.682. When analyzing the change in PI–LL mismatch, sensitivity was 0.8, specificity was 0.9, PPV was 0.889, and NPV was 0.818 (Table V, Figures 3 and 4).

DISCUSSION

The incidence of DJF has been reported to range between 1.8% and 15.6% (15). DJF refers to mechanical failure occurring at the distal end of the instrumented spine. Some patients may remain asymptomatic, with DJF identified only through radiographic findings, while others may experience

Table III: Comparison of Preoperative and Postoperative Spinopelvic Parameters in Control and DJF Groups

Parameter	Control Group p-value	DJF Group p-value
Preoperative LL vs Postoperative LL	**0.03***	**0.01***
Preoperative PT vs Postoperative PT	0.22	0.25
Preoperative PI vs Postoperative PI	0.51	0.07
Preoperative SS vs Postoperative SS	0.06	0.68
Preoperative PI-LL mismatch vs Postoperative PI-LL mismatch	**0.01***	**0.01***

***LL:** Lumbar lordosis, **PT:** Pelvic tilt, **PI:** Pelvic incidence, **SS:** Sacral slope, **PI-LL mismatch:** Pelvic incidence - Lumbar Lordosis mismatch, *: p<0.05.*

Table IV: Postoperative Changes in Spinopelvic Parameters for DJF and Control Groups

Parameter	DJF Group Change	DJF Group Description	Control Group Change	Control Group Description	p-value
LL change after surgery	-9.58	Decreased	6.18	Increased	**0.01**
PT change after surgery	-1.17	Decreased	-3.23	Decreased	0.45
PI change after surgery	-0.26	Decreased	0.73	Increased	0.37
SS change after surgery	0.42	Increased	4.51	Increased	0.11
PI-LL mismatch change after surgery	7.9	Increased	-5.98	Decreased	**0.01**

***LL:** Lumbar lordosis, **PT:** Pelvic tilt, **PI:** Pelvic incidence, **SS:** Sacral slope, **PI-LL mismatch:** Pelvic incidence - Lumbar Lordosis mismatch, *: p<0.05.*

Table V: Sensitivity, Specificity, and Predictive Values for Postoperative and Change in PI-LL Mismatch

Metric	Postoperative PI-LL Mismatch	Change in PI-LL Mismatch
Sensitivity	0.65	0.8
Specificity	0.75	0.9
PPV	0.722	0.889
NPV	0.682	0.818

***PI-LL mismatch:** Pelvic incidence - lumbar lordosis mismatch, **PPV:** Positive predictive value, **NPV:** Negative predictive value.*

more acute symptoms, often describing an audible sound or a sensation linked to hardware failure, such as a rod or screw fracture (15). In other cases, DJF presents more gradually, with persistent postoperative pain, leading to the discovery of pseudarthrosis or adjacent segment disease on advanced imaging (14).

In our study, the primary causes of failure in patients undergoing thoracolumbar posterior stabilization were adjacent segment disease (60%), screw loosening (35%), and screw breakage (5%). This distribution aligns with findings in the literature, although variations exist depending on patient demographics, surgical techniques, and follow-up durations. Adjacent segment disease was the most frequent cause of failure in our cohort, accounting for 60% of all failures (7). Screw loosening was responsible for 35% of failures, while screw breakage accounted for 5%. Screw loosening is often attributed to poor bone quality, incorrect screw positioning, or excessive stress at the instrumented junctional segment. Screw-related issues, including loosening and breakage, are particularly common in patients with osteoporosis or those undergoing long instrumented fusions (3,20). Hardware complications such as screw breakage are frequently preceded by loosening, as increased micromotion weakens the screw–bone interface over time. Additionally, variability in surgical technique (e.g., using stronger, larger diameter screws or dual–rod systems) may also influence these outcomes.

In our study, most patients had LIV at L5, which is consistent with literature emphasizing the importance of selecting the distal-most instrumented vertebra, often referred to as the end segment vertebra (ESV). The use of L5 as the LIV has been a subject of ongoing debate due to its anatomical position and the biomechanical stresses placed on the L5–S1. Studies suggest that fusions ending at L5 may predispose patients to degeneration, sagittal imbalance, and ultimately DJF (8). Thus, while L5 may be appropriate for certain patients—particularly those with a healthy L5–S1 disc and short fusions—surgeons must carefully consider individual anatomical and alignment factors.

LL is a crucial parameter in maintaining spinal sagittal balance. Normal LL values typically range from 40 to 60 degrees,

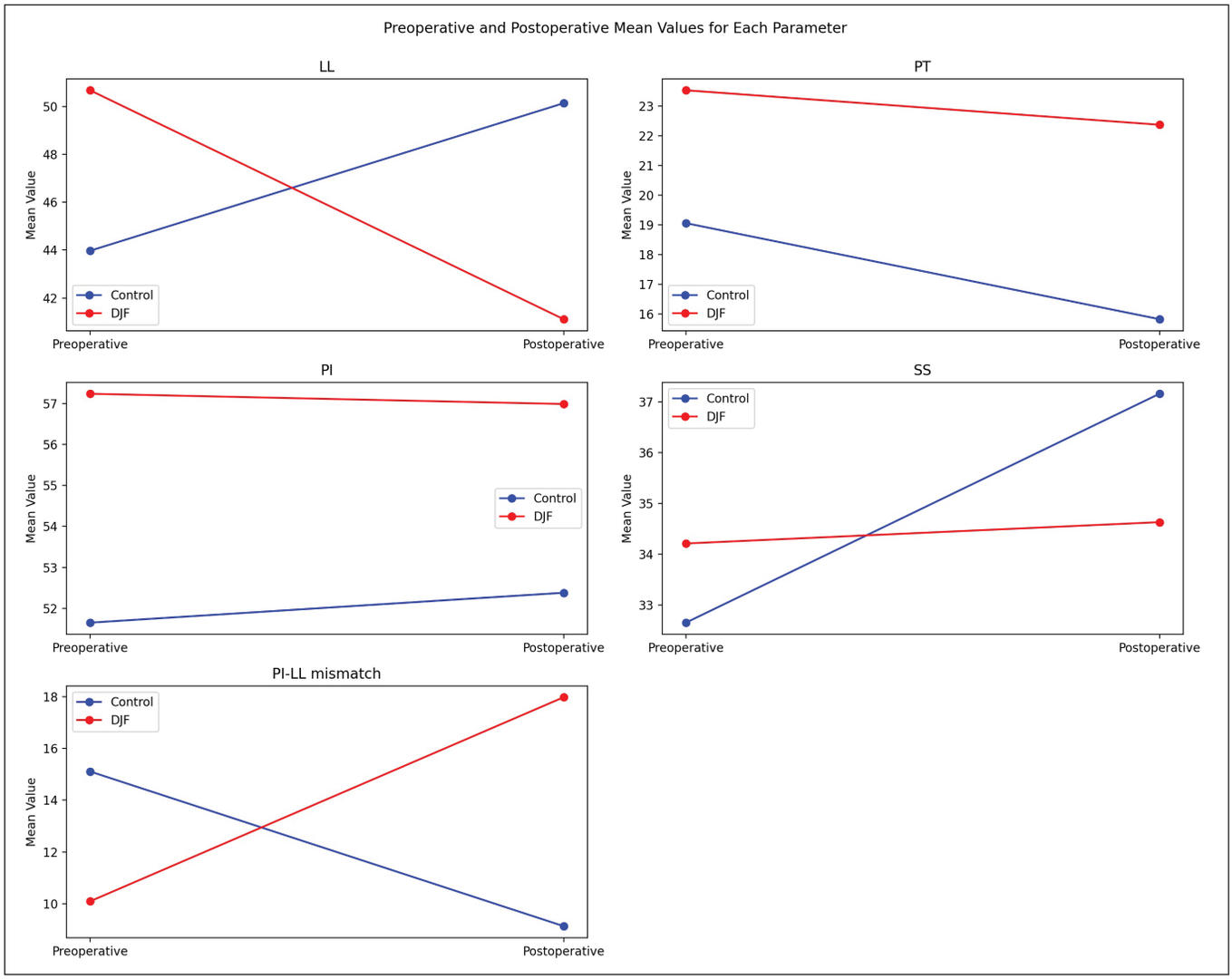

Figure 2: Preoperative and Postoperative Mean Values for Lumbar Lordosis (LL), Pelvic Tilt (PT), Pelvic Incidence (PI), Sacral Slope (SS), and PI–LL Mismatch in the Control and DJF Groups. This figure illustrates the comparison of mean preoperative and postoperative values for LL, PT, PI, SS, and PI–LL mismatch between the control and DJF groups. The graphs depict the trends and differences in each parameter after surgical intervention.

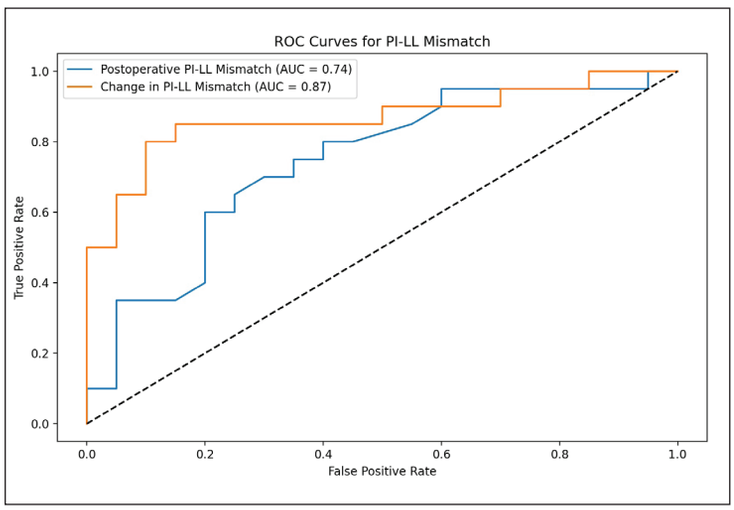

Figure 3: ROC Curves for Postoperative PI–LL Mismatch and Change in PI–LL Mismatch. This figure displays the receiver operating characteristic (ROC) curves comparing the postoperative PI–LL mismatch (AUC = 0.74) and the change in PI–LL mismatch (AUC = 0.87), illustrating the diagnostic performance of these metrics in predicting outcomes.

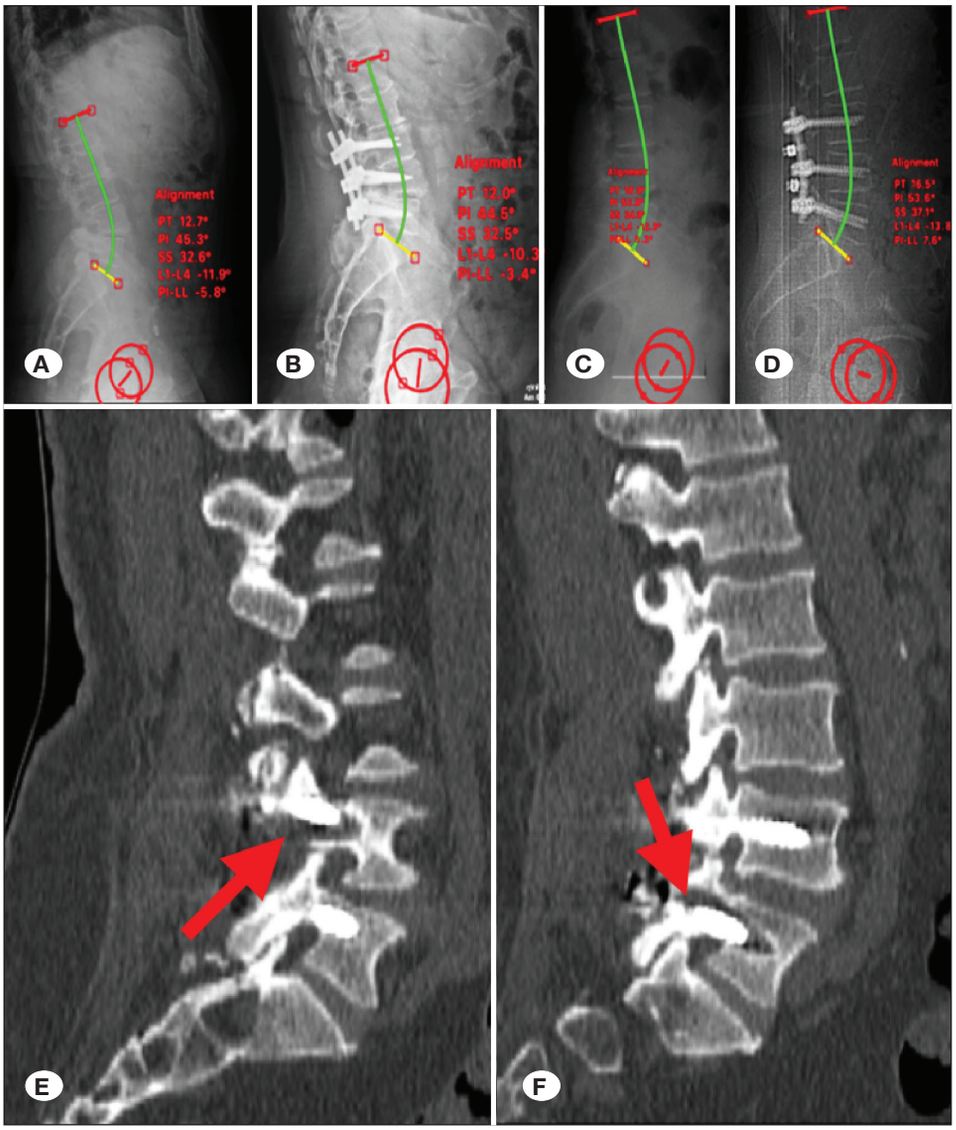

Figure 4: A, C) depict preoperative images showing the measurement of pelvic parameters in patient case examples,
B, D) show the postoperative measurements of the same pelvic parameters in these cases,
E, F) are sagittal CT images from the cases, highlighting screw loosening, indicated by the red arrows.

depending on pelvic morphology (9). This curvature facilitates appropriate force distribution along the spine and plays a critical role in overall posture and mobility (4). Achieving or restoring optimal LL is essential, as inadequate correction is associated with postoperative complications, including DJF. In our study, the DJF group exhibited a postoperative reduction in LL of –9.58 degrees, whereas the control group showed a mean increase of 6.18 degrees. Several studies have suggested that overcorrecting LL, particularly when L5 is selected as the LIV, may elevate the risk of DJF (10). However, we found no statistically significant difference in DJF rates between patients whose fusions ended at L5 and those whose fusions did not, despite similar LIV selection across groups.

The PI–LL mismatch is widely considered a critical indicator of sagittal balance. PI is a constant anatomical parameter that determines the optimal degree of lordosis for an individual (18). A PI–LL mismatch greater than 10 degrees is considered pathologic and has been strongly linked to poor surgical outcomes, including DJF (17). In our analysis, patients who developed DJF exhibited an increased postoperative PI–LL mismatch, whereas those without DJF maintained a more balanced alignment. These findings support previous reports suggesting that both insufficient correction and overcorrection of the PI–LL mismatch may contribute to the development of DJF. Maintaining this mismatch within a physiologic range is critical for minimizing the mechanical burden at both the proximal and distal junctions. Ailon et al. similarly observed a significantly increased DJF risk in patients with a postoperative mismatch exceeding 15 degrees (1), reinforcing our conclusions.

Limitations

This study has several limitations. First, its retrospective design may introduce selection bias, as data were collected from existing medical records, and not all relevant variables could be consistently controlled. Second, the relatively small

sample size—40 patients divided into two groups—may limit the generalizability of our findings. Nevertheless, given the rarity of DJF, this number remains acceptable for initial analysis. Another limitation is the variable follow-up period. Although some patients were followed for up to six years, longer-term data would offer deeper insight into the durability of surgical corrections and the development of DJF over time.

Additionally, while the study focused on spinopelvic parameters such as LL and PI–LL mismatch, other potentially influential factors—such as bone quality, comorbidities, and specific surgical techniques—were not comprehensively analyzed. Our reliance on radiographic evidence to identify DJF may have also overlooked subtler or purely clinical manifestations, as some patients remain asymptomatic despite radiologic evidence of failure. Future research should incorporate advanced imaging modalities and detailed functional assessments to better capture the full spectrum of DJF.

We excluded patients with advanced osteoporosis to better isolate other contributing factors to DJF. However, we recommend future subgroup analyses focusing on osteoporotic patients, as preoperative osteoporosis is a known risk factor for postoperative DJF. The American National Osteoporosis Foundation advises preoperative vitamin D and calcium supplementation for surgical cases, and a study by Liu et al. found a lower incidence of adjacent segment pathology in patients receiving osteoporosis treatment (11). Furthermore, the use of expandable or cement-augmented cannulated screws has been suggested to reduce DJF risk in osteoporotic individuals (14).

CONCLUSION

To minimize the risk of DJF in posterior thoracolumbar fusion surgery, it is essential to achieve an optimal LL. Both overcorrection and undercorrection can disrupt sagittal balance and increase mechanical stress on distal segments, leading to DJF. Maintaining an appropriate PI–LL mismatch is equally critical in reducing the biomechanical burden on junctional regions and improving long-term surgical outcomes.

Declarations

Funding: The authors did not receive support from any organization for the submitted work. The authors have no relevant financial or non-financial interests to disclose.

Availability of data and materials: The datasets generated and/or analyzed during the current study are available from the corresponding author by reasonable request.

Disclosure: The authors declare no competing interests.

AUTHORSHIP CONTRIBUTION

Study conception and design: HSC, NK, EU

Data collection: HSC, EU, YEO

Analysis and interpretation of results: MD, ATS, BB

Draft manuscript preparation: HSC, EU, YEO

Critical revision of the article: NK

Other (study supervision, fundings, materials, etc...): MAK, EH, MA

All authors (NK, HSC, EU, MAK, EH, MA, ATS, MD, BB, YEO) reviewed the results and approved the final version of the manuscript.

REFERENCES

1. Ailon T, Smith JS, Shaffrey CI, Lenke LG, Brodke D, Harrop JS, Fehlings M, Ames CP: Degenerative spinal deformity. Neurosurgery 77 Suppl 4:S75-91, 2015. https://doi.org/10.1227/NEU.0000000000000938.
2. Arlet V, Aebi M: Junctional spinal disorders in operated adult spinal deformities: Present understanding and future perspectives. Eur Spine J 22 Suppl 2:95, 2013. https://doi.org/10.1007/s00586-013-2676-x.
3. Berjano P, Damilano M, Pejrona M, Langella F, Lamartina C: Revision surgery in distal junctional kyphosis. Eur Spine J 29 Suppl 1:86-102, 2020. https://doi.org/10.1007/s00586-020-06304-y.
4. Cho KJ, Suk SI, Park SR, Kim JH, Kang SB, Kim HS, Oh SJ: Risk factors of sagittal decompensation after long posterior instrumentation and fusion for degenerative lumbar scoliosis. Spine 35:1595-1601, 2010. https://doi.org/10.1097/BRS.0b013e3181bdad89.
5. Deville R, Khalifé M, Rollet ME, Chatelain L, Guigui P, de Loubresse CG, Ferrero E: Readmission rate after adult scoliosis surgery on primary cases over 45 years-old with long-term follow-up. Eur Spine J 33:3880-3886, 2024 https://doi.org/10.1007/s00586-024-08429-w.
6. Faulks CR, Biddau DT, Munday NR, McKenzie DP, Malham GM: Patient-specific spinal rods in adult spinal deformity surgery reduce proximal junctional failure: A review of patient outcomes and surgical technique in a prospective observational cohort. J Spine Surg 9:409-421, 2023. https://doi.org/10.21037/jss-23-85.
7. Hosthota A, Govindasamy R, Rudrappa S: Distal junctional failure secondary to nontraumatic fracture of lower instrumented vertebra: Our experience and review of literature. Int J Spine Surg 15:1031-1038, 2021. https://doi.org/10.14444/8131.
8. Kuhns CA, Bridwell KH, Lenke LG, Amor C, Lehman RA, Buchowski JM, Edwards C 2nd, Christine B: Thoracolumbar deformity arthrodesis stopping at L5: Fate of the L5-S1 disc, minimum 5-year follow-up. Spine 32:2771-2776, 2007. https://doi.org/10.1097/BRS.0b013e31815a7ece.
9. Legaye J: The femoro-sacral posterior angle: An anatomical sagittal pelvic parameter usable with dome-shaped sacrum. Eur Spine J 16:219-225, 2007. https://doi.org/10.1007/s00586-006-0090-3.

10. Lee NJ, Marciano G, Puvanesarajah V, Park PJ, Clifton WE, Kwan K, Morrissette CR, Williams JL, Fields M, Hassan FM, Angevine PD, Mandigo CE, Lombardi JM, Sardar ZM, Lehman RA, Lenke LG: Incidence, mechanism, and protective strategies for 2-year pelvic fixation failure after adult spinal deformity surgery with a minimum six-level fusion. J Neurosurg Spine 38:208-216, 2022. https://doi.org/10.3171/2022.8.SPINE22755.
11. Liu D, Hu Z, Tang Z, Li P, Yuan W, Li F, Chen Q, Min W, Zhao C: Early risk assessment and prediction model for osteoporosis based on traditional Chinese medicine syndromes. Heliyon. 9:e21501, 2023. https://doi.org/10.1016/j.heliyon.2023.e21501.
12. Liu Y, Yuan L, Zeng Y, Li W: Risk factors for distal junctional problems following long instrumented fusion for degenerative lumbar scoliosis: Are they related to the paraspinal muscles. Orthop Surg 15:3055-3064, 2023. https://doi.org/10.1111/os.13878.
13. Lowe TG, Lenke L, Betz R, Newton P, Clements D, Haher T, Crawford A, Letko L, Wilson LA: Distal junctional kyphosis of adolescent idiopathic thoracic curves following anterior or posterior instrumented fusion: Incidence, risk factors, and prevention. Spine 31:299-302, 2006. https://doi.org/10.1097/01.brs.0000197221.23109.fc.
14. Marciano GF, Simhon ME, Lehman RA, Lenke LG: Strategies to avoid distal junctional pathology. Neurosurg Clin N Am 34:585-597, 2023. https://doi.org/10.1016/j.nec.2023.06.006.
15. McDonnell JM, Ahern DP, Wagner SC, Morrissey PB, Kaye ID, Sebastian AS, Butler JS: A systematic review of risk factors associated with distal junctional failure in adult spinal deformity surgery. Clin Spine Surg 34:347-354, 2021. https://doi.org/10.1097/BSD.0000000000001224.
16. Montanari S, Griffoni C, Cristofolini L, Girolami M, Gasbarrini A, Barbanti Bròdano G: Correlation between sagittal balance and mechanical distal junctional failure in degenerative pathology of the spine: A retrospective analysis. Global Spine J 10:21925682231195954, 2023. https://doi.org/10.1177/21925682231195954.
17. Schwab FJ, Blondel B, Bess S, Hostin R, Shaffrey CI, Smith JS, Boachie-Adjei O, Burton DC, Akbarnia BA, Mundis GM, Ames CP, Kebaish K, Hart RA, Farcy JP, Lafage V; International Spine Study Group (ISSG): Radiographical spinopelvic parameters and disability in the setting of adult spinal deformity: A prospective multicenter analysis. Spine 38: E803-12, 2013. https://doi.org/10.1097/BRS.0b013e318292b7b9.
18. Tartara F, Garbossa D, Armocida D, Di Perna G, Ajello M, Marengo N, Bozzaro M, Petrone S, Giorgi PD, Schirò GR, Legrenzi S, Boeris D, Piazzolla A, Passarelli AC, Longo A, Ducati A, Penner F, Tancioni F, Bona A, Paternò G, Tassorelli C, De Icco R, Lamaida GA, Gallazzi E, Pilloni G, Colombo EV, Gaetani P, Aimar E, Zoia C, Stefini R, Rusconi A, Querenghi AM, Brembilla C, Bernucci C, Fanti A, Frati A, Manelli A, Muzii V, Sedia M, Romano A, Baram A, Figini S, Ballante E, Gioia G, Locatelli M, Pluderi M, Morselli C, Bassani R, Costa F, Cofano F: Relationship between lumbar lordosis, pelvic parameters, PI–LL mismatch and outcome after short fusion surgery for lumbar degenerative disease. Literature review, rational and presentation of public study protocol: RELApSE study (registry for evaluation of lumbar artrodesis sagittal alignEment). World Neurosurg X 18:100162, 2023. https://doi.org/10.1016/j.wnsx.2023.100162.
19. Wang Y, Li J, Xi Y, Zeng Y, Yu M, Sun Z, Ma Y, Liu Z, Chen Z, Li W: Distal junctional failures in degenerative thoracolumbar hyperkyphosis. Orthop Surg 16:830-841, 2024. https://doi.org/10.1111/os.13973.
20. Wang Y, Zhu W, Sun K, Kong C, Wang W, Lu S: Selecting proper distal fusion level in severe thoracolumbar kyphosis secondary to late osteoporotic vertebral compression fracture to limit distal complications. J Orthop Sci 27:1177-1184, 2022. https://doi.org/10.1016/j.jos.2021.07.025.
21. Wilk B, Karol LA, Johnston CE 2nd, Colby S, Haideri N: The effect of scoliosis fusion on spinal motion: A comparison of fused and nonfused patients with idiopathic scoliosis. Spine (Phila Pa 1976) 31:309-314, 2006. https://doi.org/10.1097/01.brs.0000197168.11815.ec.

Turk Neurosurg 36(1):99-107, 2026
DOI: 10.5137/1019-5149.JTN.48739-25.2

Original Investigation
Spine and Peripheral Nerves

Received: 11.03.2025
Accepted: 01.06.2025
Published Online: 16.01.2026

The Role of DTI and DTT in the Evaluation of Cervical Extramedullary Tumors

Zeynep FIRAT[1], Cumhur Kaan YALTIRIK[2], Aysegul GORMEZ[1], Osman Melih TOPCUOGLU[1], Gazanfer EKINCI[1], Ugur TURE[3]

[1]Yeditepe University Hospitals, Department of Radiology, Istanbul, Türkiye
[2]Maltepe University, School of Medicine, Department of Neurosurgery, Istanbul, Türkiye
[3]Yeditepe University Hospitals, Department of Neurosurgery, Istanbul, Türkiye

Corresponding author: Zeynep FIRAT ✉ zfirat@yeditepe.edu.tr

ABSTRACT

AIM: To evaluate the efficacy of diffusion tensor imaging (DTI) and diffusion tensor tractography (DTT) in establishing the relationship between cervical extramedullary tumors and the spinal cord with reference to, especially treatment planning, clinical outcome prediction and diagnostic accuracy.

MATERIAL and METHODS: This was a retrospective study conducted on 15 patients diagnosed with cervical extramedullary tumors, wherein each patient underwent standard 3.0-T magnetic resonance imaging, DTI, and DTT to evaluate microstructural changes and neural tract displacement. Fractional anisotropy (FA) values were examined, and the relationship of tractography results with clinical presentation and outcomes was evaluated.

RESULTS: FA values revealed disturbances in the microstructure, which exhibited marked changes in lesion areas compared with that of normal tissue and displaced spinal cord (DSC). The DTT of each patient revealed neural tract anomalies or deformities related to the degree of their clinical symptoms. Receiver operating characteristic curve analysis demonstrated the excellent diagnostic accuracy of FA in separating lesions from normal tissue (AUC = 0.880) and DSC (AUC = 0.840).

CONCLUSION: FA values could help particularly in detecting early myelopathic changes due to cervical cord displacement, which might be a critical indication for surgical decisions. This study supports the usage of DTI and DTT in evaluating cervical extramedullary lesions, surgical planning, and outcome prediction by exposing microstructural changes and lesion–tract relationships.

KEYWORDS: Cervical extramedullary tumors, Diffusion tensor imaging, Diffusion tensor tractography, Cervical spinal cord, Surgical planning

INTRODUCTION

The cervical spinal cord is a fundamental anatomical structure for neural signals where lesions can significantly affect function and quality of life. Magnetic resonance imaging (MRI) is a basic technique for the diagnosis and differentiation of lesions in the cervical spinal cord, helping in surgical planning and patient management (4). Diffusion tensor imaging (DTI) and diffusion tensor tractography (DTT) provide spinal imaging with a novel viewpoint and essential knowledge of the microstructural integrity of neural pathways (2,5-7). These two techniques are quite helpful in evaluating patients with different spinal diseases, including intramedullary and extramedullary tumors, vascular malformations, and traumatic spinal cord injury. They provide comprehensive information on the directionality and integrity of fiber tracts (11,13,16,22).

Zeynep FIRAT : 0000-0001-6810-6360
Cumhur Kaan YALTIRIK : 0000-0002-4312-5685
Aysegul GORMEZ : 0000-0001-5620-2881
Osman Melih TOPCUOGLU : 0000-0002-4008-3395
Gazanfer EKINCI : 0000-0002-1589-1833
Ugur TURE : 0000-0002-7449-6171

DTI and DTT can effectively detect changes in neural tracts and their surroundings. They can provide details on deviation, deformation, and disturbance, which would be vital for determining the degree of damage and organizing surgical treatments (3,8,19,21,22). Furthermore, there is ongoing research on the predictive power of these imaging techniques in deciding outcomes and guiding therapy development. Some studies have also demonstrated a correlation between DTT results and neurological examination findings (19,22). Despite these advances, it is necessary to investigate the application of DTI and DTT in the framework of cervical extramedullary lesions and their efficacy in this particular context. Accordingly, this study was conducted to explore the usefulness of DTI and DTT to address the knowledge gap in the relationship between cervical extramedullary tumors and the spinal cord. Moreover, by analyzing the impact, we attempted to examine in detail how cervical extramedullary tumors interact with the spinal cord, thus guiding treatment strategies, clinical outcomes, and surgical approach.

MATERIAL and METHODS

Ethical Considerations

This study was conducted according to the Declaration of Helsinki and approved by the Yeditepe University Ethical Committee (IRB Approval Number: 1344). Informed consent was obtained from each study participant.

Study Design and Patient Population

This retrospective study was conducted between January 2018 and May 2024 in a tertiary care center on 15 patients, including 8 men and 7 women, who were diagnosed with extramedullary cervical spine lesions. Patients were included, irrespective of whether they were advised for either conservative management or surgical intervention after confirming extramedullary cervical spine lesions. All patients underwent the cervical MRI protocol, which also included a focused DTI sequence for microstructural analysis and lesion evaluation. Exclusion criteria were incomplete or low-quality imaging data, intramedullary or other cervical lesion type, and previous cervical spine surgery.

Imaging Protocol

All participants underwent MRI on a 3.0-T system (GE Discovery MR750w, GE Healthcare, Waukesha, USA) with a 24-channel neck coil covering the C1–C7 levels. A T2-weighted fast spin-echo (FSE) sequence was performed with a TR of 3450 ms, a TE of 96.1 ms, and a matrix size of 416 × 288. The focused DTI sequence was acquired using a spin-echo echo-planar imaging (SE/EPI) technique with a TR of 6000 ms, a TE of 71.9 ms, and a matrix size of 128 × 34, applying diffusion weighting along 16 directions (b-values: 0 and 800 s/mm^2). Both sequences were acquired in the sagittal plane with a field of view (FOV) of 18 cm, a slice thickness of 3.0 mm, and 16 slices with no interslice gap.

Diffusion Tensor Tractography

A specialized workstation (GE, AWS Portal 3.2 Ext. 4.0) was used to generate fractional anisotropy (FA) maps and perform tractography analyses. Although the FA maps were generated automatically, regions of interest (ROIs) were manually placed on the normal-appearing spinal cord, above and below the lesion to initiate fiber tracking.

Data Analysis

Demographic and clinical data, including age, gender, and clinical presentation, were recorded. Imaging findings from conventional MRI, DTI metrics (FA values), and DTT results were analyzed. FA measurements were obtained using ROIs (10–30 mm in size) from the normal-appearing cervical spinal cord, the cervical spinal cord near the lesion, and directly over the lesion. Tractography results were analyzed to determine the relationship between lesions and the surrounding structures, which were categorized as normal, deviated, deformed, or interrupted fibers. The relationship between DTT results and clinical symptoms was evaluated to explore the potential impact of extramedullary lesions on the microstructure and function of the cervical spinal cord.

Statistical Analysis

Statistical analyses were conducted using the SPSS software (version 27, IBM Corp., Armonk, NY, USA). Skewness and kurtosis coefficients were calculated to determine whether the values for each continuous variable followed a normal distribution. Categorical variables were expressed as frequencies (n, %), and continuous variables were summarized using mean and standard deviation.

The Mann–Whitney U test was applied to compare continuous variables between two groups, whereas comparisons between more than two groups were performed using the Kruskal–Wallis test. Post hoc analysis to determine the groups that contributed to significant differences was performed using Dunnett's multiple comparison test. Within-group repeated measures were analyzed using the Friedman test, and subgroup repeated measures were analyzed using the Wilcoxon signed-rank test.

The diagnostic performance of FA scores in differentiating the presence of lesions was evaluated using receiver operating characteristic (ROC) curve analysis. The optimal FA cutoff was determined using the Youden index. The diagnostic performance of FA was expressed in terms of sensitivity, specificity, positive predictive value, negative predictive value, and accuracy. Categorical data were compared using Fisher's exact test. Results were considered statistically significant at $p<0.05$ (two-tailed) within a 95% confidence interval.

RESULTS

The mean age of the 15 participants was 48.73 ± 12.55 (range: 33–68) years, and there were 7 (47%) women and 8 (53%) men. The following tumor types were identified: meningioma in 6 patients (40%), schwannoma in 6 patients (40%), chordoma in 2 patients (13%), and osteoblastoma in 1 patient (6.7%). The mean tumor size was 34.80 ± 18.16 (range: 12–88) mm. Table I shows the detailed characteristics of the patients.

DTI Measurements and FA

The mean FA values for normal tissue, displaced spinal cord (DSC), and lesion areas were 0.54 ± 0.13, 0.51 ± 0.12, and 0.31 ± 0.16, respectively. The FA values showed a statistically significant difference based on the measurement region (χ^2 = 25.200; p<0.001). Subgroup analysis showed that FA values were significantly lower in the lesion area than in the normal tissue and DSC (p<0.001). However, the FA values were not statistically significantly different between normal tissue and DSC (p>0.05).

Patients classified as "normal" on DTI/DTT analysis exhibited no significant differences in FA values between normal tissue, DSC, and lesion areas (p>0.05). In contrast, patients classified as "deviation" showed a significant decrease in FA values from normal tissue to the lesion area (χ^2 = 20.667; p<0.001).

Table I: Patient/Lesion / MR Characteristics

Variables			**n (%)**
Patient			
	Age (years)	Mean ± SD (range)	48.73 ± 12.55 (33–68)
	Gender		
		Female	7 (46.7)
		Male	8 (53.3)
Lesion			
	Size (mm)	Mean ± SD (range)	34.80 ± 18.16 (12–88)
	Histological Type		
		Meningioma	6 (40)
		Schwannoma	6 (40)
		Others	3 (20)
	Localization		
		C1	1 (6.7)
		C1–2	4 (26.7)
		C1–4	1 (6.7)
		C2	3 (20)
		C2–3	2 (13.3)
		C2–5	1 (6.7)
		C6–7	2 (13.3)
		C7–T1	1 (6.7)
Magnetic Resonance Imaging Characteristics			
	T1 Signal Intensity		
		Hypointense	5 (33.3)
		Heterogeneous/Isointense	10 (66.7)
	T2 Signal Intensity		
		Hyperintense	8 (53.3)
		Heterogeneous/Isointense	7 (46.7)

For meningiomas and schwannomas, the FA values of lesions were significantly lower than those of normal tissue and DSC (χ^2 = 10.333–9.333; p<0.01). However, the FA values of DSC were higher for meningiomas and schwannomas than for other tumor types (Z = –2.028; p=0.043) (Table II).

FA Diagnostic Performance (ROC Analysis)

Although the ability of FA to differentiate normal tissue from DSC was poor and not statistically significant (AUC = 0.607; p=0.320), FA demonstrated excellent performance in distinguishing lesions from normal tissue (AUC = 0.880; 95% confidence interval (CI): 0.756–1; p<0.001) and lesions from DSC (AUC = 0.840; 95% CI: 0.693–0.987; p=0.002). The optimal cutoff points for distinguishing lesions from normal tissue and DSC were 0.39 and 0.36, respectively. The sensitivity, specificity, and accuracy of FA for distinguishing lesions from normal tissue were 93.3%, 80%, and 86.7%, respectively, and the respective values for distinguishing lesions from DSC were 100%, 60%, and 80% (Table III).

Patient Complaints and Symptoms

The most common symptom was neck pain in 9 patients (60%), followed by radiculopathy in 5 patients (33.3%), numbness in 4 patients (26.7%), and loss of balance in 1 patient (6.7%). Multiple symptoms were found in 6 patients (40%), and neurological findings were detected in 7 patients (46.7%). Symptoms were more common in patients classified as "deviation" on DTI/DTT analysis; however, these differences did not reach statistical significance (p>0.05). There was also no significant association between lesion type and symptom frequency (p>0.05) (Table IV).

Table II: Fractional Anisotropy (FA) Measurement Results

Variables	Normal (a)	DSC (b)	Lesion (c)	χ^2	p-value	a vs b	a vs c	b vs c
All Patients	0.54 ± 0.13	0.51 ± 0.12	0.31 ± 0.16	25.200	**<0.001***	**0.053**	**<0.001***	**<0.001***
DTI/DTT Classification								
Normal	0.46 ± 0.17	0.48 ± 0.13	0.32 ± 0.13	4.667	0.097	-	-	-
Deviation	0.56 ± 0.12	0.52 ± 0.12	0.31 ± 0.17	20.667	**<0.001***	**0.023*****	**0.002****	**0.002****
Z/P-value	1.231/0.218	–0.362/0.717	–0.217/0.828					
Lesion Type								
Meningioma (1)	0.54 ± 0.15	0.49 ± 0.11	0.38 ± 0.17	10.333	**0.006****	0.249	**0.028*****	**0.027*****
Schwannoma (2)	0.61 ± 0.10	0.60 ± 0.06	0.29 ± 0.16	9.333	**0.009****	0.345	**0.028*****	**0.027*****
Others (3)	0.41 ± 0.03	0.37 ± 0.02	0.19 ± 0.03	6.000	0.050	-	-	-
K-Wχ^2/P-value	5.057/0.080	7.592/**0.022*****	3.651/0.161					
Difference†		3 < 2						
Lesion Type								
Meningioma/ Schwannoma	0.57 ± 0.13	0.54 ± 0.10	0.34 ± 0.17	19.500	**<0.001***	0.136	**0.002****	**0.002****
Others	0.41 ± 0.03	0.37 ± 0.02	0.19 ± 0.03	6.000	0.050	-	-	-
Z/P-value	–2.028/**0.043*****	–2.318/**0.020*****	–1.664/0.096					

DTI: *Diffusion tensor imaging,* ***DTT:*** *Diffusion tensor tractography*

Table III: Diagnostic Performance of FA (ROC Analysis Results)

Diagnostic Performance	Normal Tissue vs. DSC	Normal Tissue vs. Lesion	DSC vs. Lesion
AUC (95% CI)	0.607 (0.401–0.813)	0.880 (0.756–1)*	0.840 (0.693–0.987)**
Cut-off Point	0.65	0.39	0.36
Sensitivity	40%	93.3%	100%
Specificity	86.7%	80%	60%
Positive Predictive Value	75%	82.4%	71.4%
Negative Predictive Value	59.1%	92.3%	100%
Accuracy	63.3%	86.7%	80%

DSC: *Displaced spinal cord.*

Table IV: Patient Complaints/Symptoms

Complaints/Symptoms	n	DTI/DTT Normal	Deviation	p-value (a)
Neck pain, n (%)	9	1 (33.3)	8 (66.7)	0.525
Radiculopathy, n (%)	5	0 (0)	5 (41.7)	0.505
Numbness, n (%)	4	2 (66.7)	2 (16.7)	0.154
Loss of equilibrium, n (%)	1	0 (0)	1 (8.3)	>0.999
Multiple symptoms, n (%)	6	0 (0)	6 (50)	0.229
Neurological findings, n (%)	7	2 (66.7)	5 (41.7)	0.569
Complaints/Symptoms	**n**	**Lesion Type Meningioma/ Schwannoma**	**Other**	**p-value (a)**
Neck pain, n (%)	9	7 (58.3)	2 (66.7)	>0.999
Radiculopathy, n (%)	5	4 (33.3)	1 (33.3)	>0.999
Numbness, n (%)	4	4 (33.3)	0 (0)	0.516
Loss of equilibrium, n (%)	1	0 (0)	1 (33.3)	0.200
Multiple symptoms, n (%)	6	5 (41.7)	1 (33.3)	>0.999
Neurological findings, n (%)	7	6 (50)	1 (33.3)	>0.999
DTI/DTT				**p-value**
Normal, n (%)	3	3 (25)	0 (0)	>0.999
Deviation, n (%)	12	9 (75)	3 (100)	

*p>0.05, Fisher's exact test.

DISCUSSION

The findings of this study emphasize the significance of DTI and DTT in the evaluation of cervical extramedullary lesions and indicate their possible impact on surgical planning and neurological outcomes. Consistent with previous research demonstrating the sensitivity of DTI in identifying minor pathological changes within the spinal cord, the variations in FA values observed in our study patients indicate the microstructural changes occurring near extramedullary lesions (4,7,13). The ability of DTI to visualize the displacement or deformation of neural tracts provides invaluable guidance for surgical planning, enabling the preservation of neural integrity and possibly improving postoperative outcomes (19,22).

DTI and DTT have been confirmed to be valuable tools in distinguishing between intramedullary and extramedullary spinal lesions (1). Furthermore, they provide functional insights that complement conventional MRI (12,15). The general pattern of extramedullary lesions typically displaces and compresses the spinal cord (14). Intramedullary lesions often infiltrate and disrupt spinal cord tracts (10). DTI metrics such as FA may predict damage to the axon, which remains relatively preserved in extramedullary tumors but is significantly reduced in intramedullary lesions (9). In extramedullary lesions, DTT revealed that intact white matter tracts were displaced, whereas in intramedullary lesions, these tracts were disrupted or interrupted. These findings are consistent with those of previous studies, which indicate that DTI and DTT provide valuable microstructural information that helps in clinical decision-making and accurately characterizing the lesions, particularly in the context of surgical planning and predicting neurological outcomes (12,20).

This study emphasizes that DTI and DTT can contribute to surgical planning by supporting the diagnosis and clinical findings. The significant reduction in FA values effectively identified compression and microstructural changes in neural pathways, playing a pivotal role in preserving neural integrity during surgery and improving postoperative neurological outcomes. The high diagnostic performance of FA in distinguishing cervical extramedullary tumors from normal tissue and DSC underscores its clinical applicability. Moreover, the differences in FA values between tumor types suggest that DTI could serve as a complementary tool for tumor characterization.

Our findings correlated with the clinical presentation of the patients. Patients with pronounced deviation and deformation of neural tracts often presented with more severe neurological symptoms, including motor weakness and sensory deficits.

Conversely, patients with less pronounced imaging changes tended to have milder or asymptomatic changes, suggesting that DTI and DTT findings have prognostic implications for neurological outcomes. Previous studies have demonstrated a correlation between DTI metrics and clinical symptoms, suggesting that these imaging modalities are biomarkers of the integrity and function of the spinal cord (19,22). In addition, the use of DTT in surgical planning, as demonstrated in our study subjects, reflects the potential of this technology to minimize surgical morbidity by guiding the surgeon to avoid critical neural structures (7,19).

Our findings demonstrate that cervical extramedullary tumors impact spinal cord tracts differently based on tumor type and location. Meningiomas caused variable displacement, ranging from minimal to significant (Figures 1–2), whereas cystic schwannoma resulted in complete tract displacement and

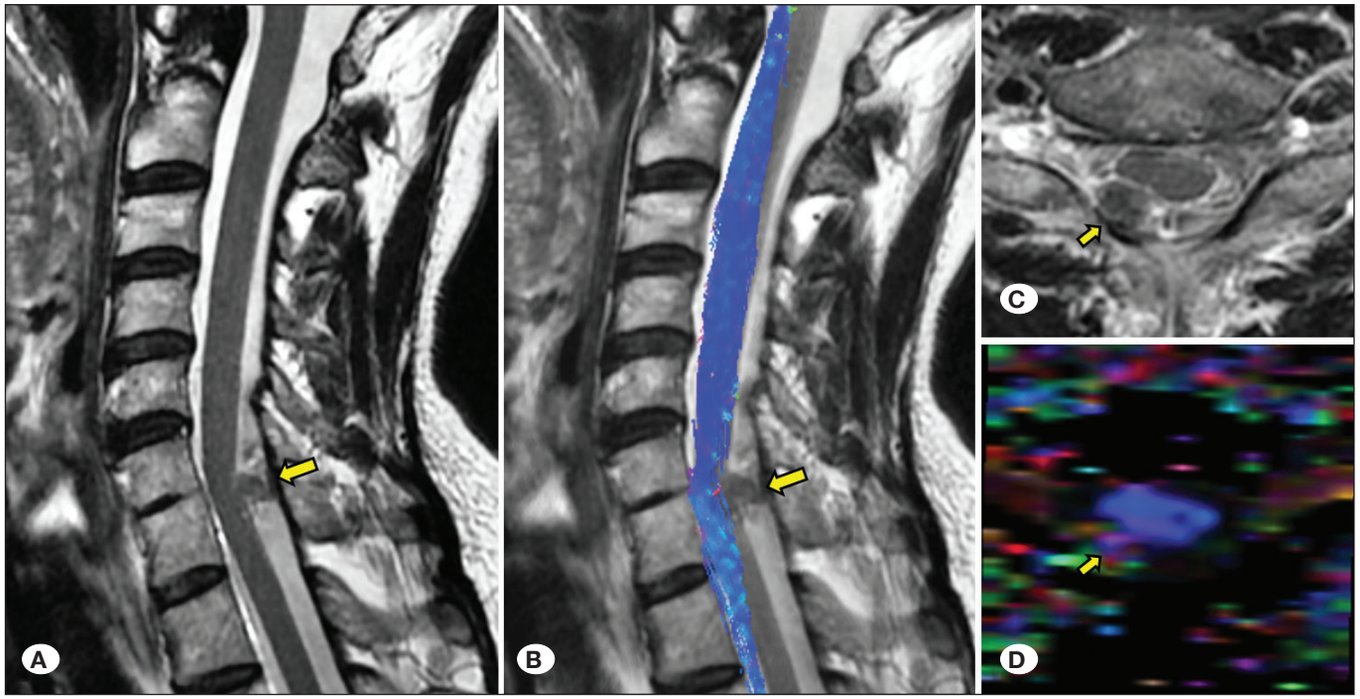

Figure 1: A 60-year-old woman with head and neck pain had a meningioma at C6–C7 (yellow arrows) with minimal displacement of the spinal cord tract. T2-weighted sagittal image **(A)**, tracts superimposed on a T2-weighted sagittal image **(B)**, a T2-weighted fat-saturated axial image **(C)**, and a color-coded FA map **(D)**.

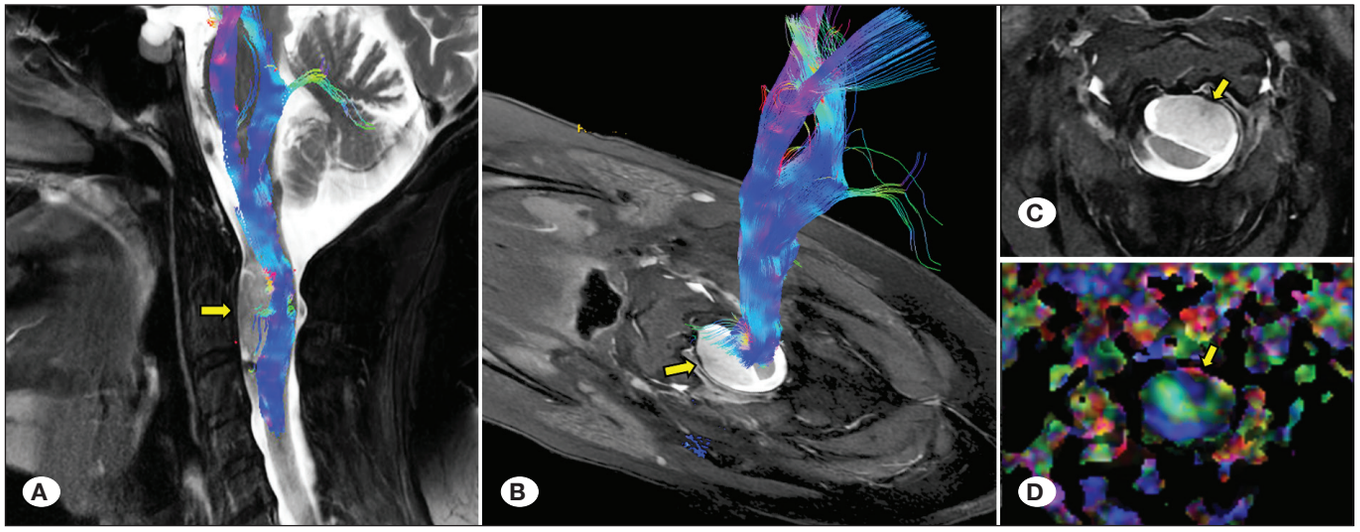

Figure 2: A 61-year-old woman with numbness in her extremities had a meningioma at C1–C2 (yellow arrows) causing displacement of spinal cord tracts. T2-weighted sagittal fat-saturated image **(A)**, T2-weighted axial fat-saturated image with cervical cord tracts **(B)**, T2-weighted axial fat-saturated image **(C)**, and color-coded FA map **(D)**.

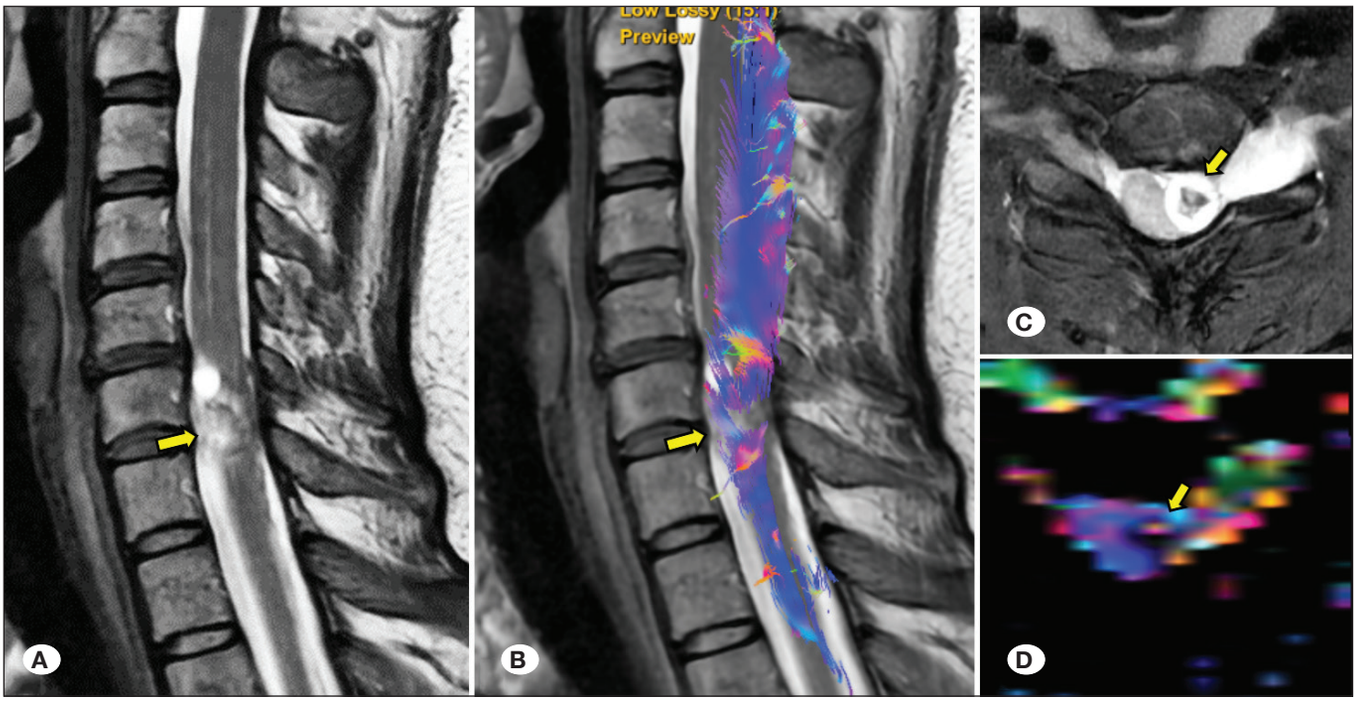

Figure 3: A 35-year-old woman with arm pain and numbness of the fingers showed a schwannoma with a cystic component at C6–C7 (yellow arrows) causing complete displacement of the spinal cord tract. T2-weighted sagittal image **(A)**, tracts superimposed on a T2-weighted sagittal image **(B)**, a T2-weighted fat-saturated axial image **(C)**, and a color-coded FA map **(D)**.

severe symptoms (Figure 3). These results emphasize the significance of DTI and DTT in correlating neural compression patterns with clinical presentation.

Although our study demonstrates the innovative and valuable role of DTI and DTT in preserving neural structures, technical challenges, such as motion artifacts, inhomogeneity, and the need for specialized expertise in analysis, limit generalizability (17). Moreover, the lack of a statistically significant relationship between clinical symptoms and DTI/DTT findings emphasizes the need for prospective studies with larger cohorts.

The limitations of our study include its retrospective design and the small sample size. Technical issues, including motion artifacts and the requirement for specialist analysis tools, may also limit the clinical adoption of these techniques (4,22). Nonetheless, their ability to advance knowledge and outcomes in spinal cord pathology warrants further prospective studies with larger cohorts (18).

Finally, the contribution of FA to the determination of microstructural changes may be important for decision-making regarding treatment or surgical approach. By revealing the microstructural changes and lesion–tract relationships, our study supports the use of DTI and DTT in evaluating cervical extramedullary lesions for surgical planning and outcome prediction.

CONCLUSION

Although DTI and DTT are generally applied in the evaluation of intra-axial brain tumors or intramedullary cervical tumors, they can provide valuable input in some cases of extramedullary cervical tumors, especially if the lesion causes displacement or compression of vital white matter tracts, and can assist in treatment and surgical planning. This study emphasizes the important role and clinical utility of DTI and DTT in the evaluation of extramedullary cervical tumors. The contribution of FA to the determination of microstructural changes may contribute to the early diagnosis of myelopathy findings, which may be a critical indicator for surgical decision-making.

Differences in the type, location, and size of cervical extramedullary tumors can provide information regarding the orientation of the tracts, the degree of spinal cord compression, and the associated clinical picture. Although larger scale studies are required to increase the reliability and clinical applicability of DTI and DTT in the evaluation of extramedullary cervical tumors, our findings may provide important contributions for understanding the effects of DTI and DTT on neural pathways in distinguishing extramedullary from intramedullary tumors and predicting neurological outcomes.

ACKNOWLEDGEMENTS

The authors would like to thank the patients and clinical staff for their participation and support throughout the study.

Declarations

Funding: This research did not receive any specific grant from funding agencies in the public, commercial, or not-for-profit sectors.

Availability of data and materials: The datasets generated and/or analyzed during the current study are available from the corresponding author by reasonable request.

Disclosure: The authors declare no competing interests.

AUTHORSHIP CONTRIBUTION

Study conception and design: ZF

Data collection: ZF, CKY, AG

Analysis and interpretation of results: ZF, CKY

Draft manuscript preparation: ZF, CKY, OMT

Critical revision of the article: GE, UT

Other (study supervision, fundings, materials, etc...): GE, UT

All authors (ZF, CKY, AG, OMT, GE, UT) reviewed the results and approved the final version of the manuscript.

REFERENCES

1. Beall DP, Googe DJ, Emery RL, Thompson DB, Campbell SE, Ly JQ, DeLone D, Smirniotopoulos J, Lisanti C, Currie TJ: Extramedullary intradural spinal tumors: A pictorial review. Curr Probl Diagn Radiol 36:185-198, 2007. https://doi.org/10.1067/j.cpradiol.2006.12.002
2. Calabrese E, Adil SM, Cofer G, Perone CS, Cohen-Adad J, Lad SP, Johnson GA: Postmortem diffusion MRI of the entire human spinal cord at microscopic resolution. Neuroimage Clin 18:963-971, 2018. https://doi.org/10.1016/j.nicl.2018.03.029
3. Choudhri AF, Whitehead MT, Klimo P, Jr., Montgomery BK, Boop FA: Diffusion tensor imaging to guide surgical planning in intramedullary spinal cord tumors in children. Neuroradiology 56:169-174, 2014. https://doi.org/10.1007/s00234-013-1316-9
4. Costanzo R, Brunasso L, Paolini F, Benigno UE, Porzio M, Giammalva GR, Gerardi RM, Umana GE, di Bonaventura R, Sturiale CL, Visocchi M, Iacopino DG, Maugeri R: Spinal tractography as a potential prognostic tool in spinal cord injury: A systematic review. World Neurosurg 164:25-32, 2022. https://doi.org/10.1016/j.wneu.2022.04.103
5. Dauleac C, Frindel C, Pelissou-Guyotat I, Nicolas C, Yeh FC, Fernandez-Miranda J, Cotton F, Jacquesson T: Full cervical cord tractography: A new method for clinical use. Front Neuroanat 16:993464, 2022. https://doi.org/10.3389/fnana.2022.993464
6. D'Souza MM, Choudhary A, Poonia M, Kumar P, Khushu S: Diffusion tensor MR imaging in spinal cord injury. Injury 48:880-884, 2017. https://doi.org/10.1016/j.injury.2017.02.016
7. Ducreux D, Fillard P, Facon D, Ozanne A, Lepeintre JF, Renoux J, Tadie M, Lasjaunias P: Diffusion tensor magnetic resonance imaging and fiber tracking in spinal cord lesions: Current and future indications. Neuroimaging Clin N Am 17:137-147, 2007. https://doi.org/10.1016/j.nic.2006.11.005
8. Egger K, Hohenhaus M, Van Velthoven V, Heil S, Urbach H: Spinal diffusion tensor tractography for differentiation of intramedullary tumor-suspected lesions. Eur J Radiol 85:2275-2280, 2016. https://doi.org/10.1016/j.ejrad.2016.10.018
9. Firat Z, Topcuoglu OM, Yaltirik CK, Gormez A, Ekinci G, Ture U: Can qualitative cervical tractography predict clinical findings as effectively as it aids surgical planning today? Turk Neurosurg 34:1066-1072, 2024. https://doi.org/10.5137/1019-5149.JTN.46234-24.1
10. Hohenhaus M, Merz Y, Klingler JH, Scholz C, Hubbe U, Beck J, Wolf K, Egger K, Reisert M, Kremers N: Diffusion tensor imaging in unclear intramedullary tumor-suspected lesions allows separating tumors from inflammation. Spinal Cord 60:655-663, 2022. https://doi.org/10.1038/s41393-021-00741-2
11. Krisa L, Middleton DM, Saksena S, Faro SH, Leiby BE, Mohamed FB, Mulcahey MJ: Clinical utility of diffusion tensor imaging as a biomarker to identify microstructural changes in pediatric spinal cord injury. Top Spinal Cord Inj Rehabil 28:1-12, 2022. https://doi.org/10.46292/sci21-00048
12. Li DC, Malcolm JG, Rindler RS, Baum GR, Rao A, Khurpad SN, Ahmad FU: The role of diffusion tensor imaging in spinal pathology: A review. Neurol India 65:982-992, 2017. https://doi.org/10.4103/neuroindia.NI_198_17
13. Liang KN, Feng PY, Feng XR, Cheng H: Diffusion tensor imaging and fiber tractography reveal significant microstructural changes of cervical nerve roots in patients with cervical spondylotic radiculopathy. World Neurosurg 126:e57-e64, 2019. https://doi.org/10.1016/j.wneu.2019.01.154
14. Liu X, Tian W, Chen H, LoStracco TA, Zhang J, Li MY, Germin B, Wang HZ: Advanced neuroimaging in the evaluation of spinal cord tumors and tumor mimics: Diffusion tensor and perfusion-weighted imaging. Semin Ultrasound CT MR 38:163-175, 2017. https://doi.org/10.1053/j.sult.2016.07.006
15. Ottenhausen M, Ntoulias G, Bodhinayake I, Ruppert FH, Schreiber S, Forschler A, Boockvar JA, Jodicke A: Intradural spinal tumors in adults-update on management and outcome. Neurosurg Rev 42:371-388, 2019. https://doi.org/10.1007/s10143-018-0957-x
16. Rindler RS, Chokshi FH, Malcolm JG, Eshraghi SR, Mossa-Basha M, Chu JK, Kurpad SN, Ahmad FU: Spinal diffusion tensor imaging in evaluation of preoperative and postoperative severity of cervical spondylotic myelopathy: Systematic review of literature. World Neurosurg 99:150-158, 2017. https://doi.org/10.1016/j.wneu.2016.11.141
17. Rutman AM, Peterson DJ, Cohen WA, Mossa-Basha M: Diffusion tensor imaging of the spinal cord: Clinical value, investigational applications, and technical limitations. Curr Probl Diagn Radiol 47:257-269, 2018. https://doi.org/10.1067/j.cpradiol.2017.07.005
18. Scullen T, Milburn J, Aria K, Mathkour M, Tubbs RS, Kalyvas J: The use of diffusion tensor imaging in spinal pathology: A comprehensive literature review. Eur Spine J 33:3303-3314, 2024. https://doi.org/10.1007/s00586-024-08231-8
19. Shabani S, Kaushal M, Budde M, Kurpad SN: Correlation of magnetic resonance diffusion tensor imaging parameters with American Spinal Injury Association score for prognostication and long-term outcomes. Neurosurg Focus 46:E2, 2019. https://doi.org/10.3171/2018.12.FOCUS18595
20. Wang J, Huang J, Cui B, Yang H, Tian D, Ma J, Duan W, Dong H, Chen Z, Lu J: Diffusion tensor imaging identifies cervical spondylosis, myelitis, and spinal cord tumors. Diagnostics 14:1225, 2024. https://doi.org/10.3390/diagnostics14121225

21. Zaninovich OA, Avila MJ, Kay M, Becker JL, Hurlbert RJ, Martirosyan NL: The role of diffusion tensor imaging in the diagnosis, prognosis, and assessment of recovery and treatment of spinal cord injury: A systematic review. Neurosurg Focus 46:E7, 2019. https://doi.org/10.3171/2019.1.FOCUS18591
22. Zhu F, Liu Y, Zeng L, Wang Y, Kong X, Yao S, Chen K, Jing X, Yang L, Guo X: Evaluating the severity and prognosis of acute traumatic cervical spinal cord injury: A novel classification using diffusion tensor imaging and diffusion tensor tractography. Spine 46:687-694, 2021. https://doi.org/10.1097/BRS.0000000000003923

Turk Neurosurg 36(1):108-118, 2026
DOI: 10.5137/1019-5149.JTN.48508-25.3

Systematic Review

Received: 23.01.2025
Accepted: 01.05.2025
Published Online: 16.01.2026

SPECT/CT in the Assessment of Postoperative Spine: A Comprehensive Literature Review

Aydın Sinan APAYDIN[1], Mehmet Denizhan YURTLUK[2], Mounica PATURU[3], Brittany Grace FUTCH[3], Khoi D THAN[3], Muhammad ABD-EL-BARR[3]

[1]Karabuk University, Faculty of Medicine, Department of Neurosurgery, Karabuk, Turkiye
[2]Bezmialem Vakıf University, Faculty of Medicine, Istanbul, Turkiye
[3]Duke University, Department of Neurosurgery, Durham, USA

Corresponding author: Aydın Sinan APAYDIN ✉ dr.sinanapaydin@yahoo.com

ABSTRACT

Back pain is a widespread and debilitating condition that significantly impairs quality of life, often eroding patients' sense of autonomy and independence, and contributes to global disability rates. The initial management of back pain generally follows a conservative approach, encompassing physical therapy, pharmacological interventions, and lifestyle modifications aimed at alleviating symptoms and restoring functionality. Spine surgery, while frequently beneficial in addressing underlying structural issues, carries certain inherent risks. Among the most challenging outcomes of spine surgery is the persistence or recurrence of pain, a condition commonly referred to as failed back surgery syndrome (FBSS). The effective management of FBSS requires a comprehensive and meticulous approach. When conservative measures for FBSS fail to yield satisfactory results, revision surgery can be considered. The role of advanced imaging techniques is critical in these cases. Standard imaging modalities each involve unique advantages and limitations, and a multimodal approach is therefore important to achieve a comprehensive and accurate evaluation of the patient's condition. In recent years, single-photon emission computed tomography combined with computed tomography (SPECT/CT) has gained recognition as a valuable tool in the postoperative assessment of spine surgery patients. SPECT/CT has demonstrated superior efficacy in detecting specific complications, such as pseudoarthrosis, hardware failure, and screw loosening. By integrating metabolic activity data from the spine and surrounding bony structures with the three-dimensional reconstruction capabilities of CT, SPECT/CT enhances diagnostic accuracy and informs more precise treatment decisions. This review aims to synthesize the current body of literature on the application of SPECT/CT in the postoperative evaluation of spine surgery patients, while also providing a comparative overview of other imaging modalities within this context. Our objective is to underscore the pivotal role that advanced imaging techniques play in improving patient outcomes after spine surgery, reducing the incidence of FBSS, and shortening its duration.

KEYWORDS: Postoperative back pain, SPECT/CT, Pseudoarthrosis, Hypermetabolism, Hardware failure

ABBREVIATIONS: CT: Computerized tomography, **MRI:** Magnetic resonance imaging, **SPECT:** Single photon emission computed tomography, **CSF:** Cerebrospinal fluid, **PET:** Positron emission tomography, **ACR:** American college of radiology, **US:** Ultrasound, **18F-NaF:** 18F Sodium fluoride, **18F-FDG:** 18F-Fluorodeoxyglucose, **FBSS:** Failed back surgery syndrome

Aydın Sinan APAYDIN : 0000-0002-2916-9550
Mehmet Denizhan YURTLUK : 0009-0004-9101-6311
Mounica PATURU : 0000-0003-0543-8469
Brittany Grace FUTCH : 0000-0002-1059-9470
Khoi D THAN : 0000-0003-2026-7004
Muhammad ABD-EL-BARR : 0000-0003-4558-7119

INTRODUCTION

Back pain is a leading cause of disability and diminished quality of life in the global population, with up to 85% of individuals experiencing it at least once in their lifetime (2,7,41). The related economic burden includes both direct healthcare costs and societal impacts such as lost productivity and early retirement. Treatment strategies are individualized, and initial emphasis is placed on conservative approaches such as physical therapy and analgesic medications. When these fail or neurological symptoms arise, surgical intervention may be necessary. While spine surgery is effective, it carries risks, including major neurological deficits (<1%) and complications like instrumentation failure, infection, and persistent pain (5,9,13,16,17).

A particularly challenging condition related to poor postoperative outcomes is failed back surgery syndrome (FBSS). FBSS is characterized by persistent or recurrent back pain, with or without accompanying sciatica, following one or more spinal surgeries (4,30). Its etiology is multifactorial, complicating management. Radiological evaluation is critical in diagnosing FBSS, typically utilizing plain radiography, CT, and MRI. While effective, these methods are limited for evaluating metabolic processes. Nuclear medicine imaging modalities, such as SPECT/CT and PET/CT, integrate structural and metabolic assessment and enhance diagnostic accuracy.

This review examines the role of SPECT/CT in postoperative spinal evaluation, providing a comparison of various imaging modalities to improve diagnostic accuracy and patient outcomes.

MATERIAL and METHODS

Literature Search

This systematic review was conducted according to the Preferred Reporting Items for Systematic Reviews and Meta-Analyses (PRISMA) guidelines (1). Pubmed, ScienceDirect, and Scopus databases were searched from 27.03.2024, using Medical Subject Headings (MeSH) terms and keywords. The Boolean operators “OR and “AND” were used as follows: (“SPECT/CT” OR “single photon emission computed tomography”) AND (“postoperative spine” OR “spinal surgery” OR FBSS OR pseudoarthrosis OR “screw loosening”) AND (diagnosis OR “diagnostic accuracy” OR sensitivity OR specificity) AND (comparison OR MRI OR CT OR “PET/CT”). Search result references were uploaded into Rayyan (https://www.rayyan.ai) for duplicate removal and screening.

Study Selection

Articles were screened under the following inclusion/exclusion criteria. The inclusion criteria were 1) case reports or case series reporting non-pooled data on clinical radiographic evaluation by SPECT/CT imaging, treatment procedures, and follow-up results; and 2) studies written in English. Exclusion criteria were as follows: 1) literature reviews, meta-analyses, autopsy reports, editorials, and conference abstracts; 2) studies only reporting histopathologic or radiologic results without any clinical, demographic, and follow-up data; 3) non-English language articles and non-peer-reviewed sources.

Data Extraction

The following data was extracted from the included studies: first author, publication year, study design, sample size, the primary indication for SPECT/CT (persistent postoperative pain, infection, screw loosening, arthropathy), the type of radiotracer (99mTc-MDP, 99mTc-UBI 29-41), reported spinal level and location (lumbar vertebrae, facet joints, sacroiliac joint, thoracolumbar fusion levels), type of instrumentation (pedicle screws, interbody cages), postoperative infection status, sensitivity, specificity, and AUC values when compared with other modalities. One reviewer (M.D.Y.) extracted data from each study, and two more reviewers (A.S.A.) and (K.D.T.) independently verified the data.

Data Synthesis and Quality Assessment

Two independent authors (M.D.Y. and A.S.A.) evaluated the risk of bias using the Joanna Briggs Institute checklists for case reports and case series, and assessed the quality of evidence according to the 2011 Oxford Centre for Evidence-Based Medicine standards (2-4).

Statistical Analysis

The Jamovi (version 2.4.7) MAJOR module was used for all statistical analyses. Continuous variables were summarized as medians (ranges), and categorical variables were summarized as frequencies (percentages). The themes of the studies were categorized as Infection Diagnosis, Pseudoarthrosis/Nonunion, Screw Loosening/Hardware Complications, and Facetogenic/Mechanical Pain.

RESULTS

Our search strategy yielded 391 results (PubMed: 26, Science Direct: 351, Scopus: 14). Following duplicate removal and screening, 15 studies, including several case reports, were included in our review (Figure 1).

The studies included a total of 1022 patients. There were four prospective case reports, and eight retrospective case series with a weighted mean patient age of 55.1 years (43.4% Male). The most common tracer utilized was 99mTc-MDP, appearing in 14 studies. All studies included SPECT/CT in their assessments. However, the limited number of studies reporting demographic and clinical data, along with the heterogeneity of these data and low evidence levels (IV–V), prevented the calculation of hazard ratios and precluded a meta-analysis.

SPECT/CT vs Conventional Imaging Modalities for Spinal Pathologies

Several studies compared conventional imaging and SPECT/CT for postoperative patient assessment. These reports revealed the superiority of SPECT/CT for diagnosing pathology in cases where MRI results were ambiguous (1,3,8,19,23,26). Lehman et al. reported that the management strategy was altered in 79% of cases due to SPECT/CT results, for which MRI had been inconclusive (23). Furthermore, Hudayana et al. showed 100% sensitivity and 89.7% specificity in diagnosing screw loosening through SPECT/CT imaging (19). However, Paez et al. reported contradictory results for infection detection,

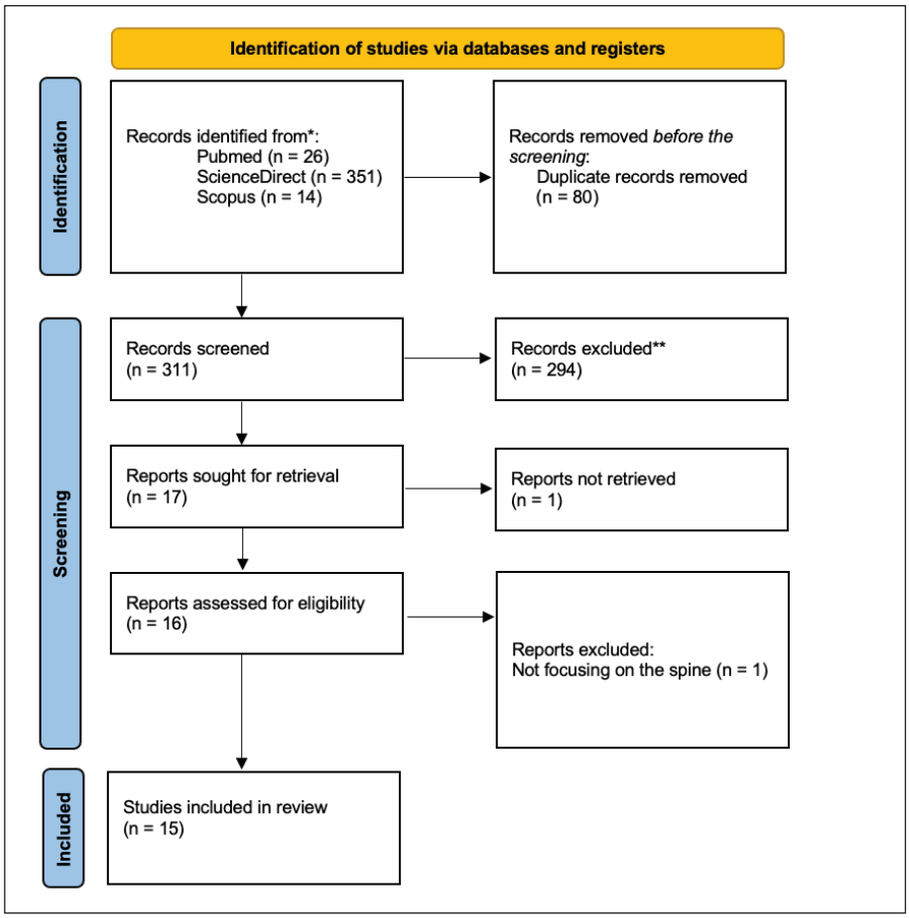

Figure 1: PRISMA 2020 flow diagram for new systematic reviews which included searches of databases and registers only. *Consider, if feasible to do so, reporting the number of records identified from each database or register searched (rather than the total number across all databases/registers). **If automation tools were used, indicate how many records were excluded by a human and how many were excluded by automation tools (27).

with SPECT/CT producing suboptimal results compared to MRI (26). Finally, Carsten et al. presented a case in which CT results were normal, with pathology uncovered using SPECT/CT; this case highlights the discordance between structural integrity and metabolic activity (8).

Impact on Clinical Decision-Making

Several studies explored different clinical strategy options based on SPECT/CT findings (3,19–21,23,34). Kaiser et al. utilized SPECT/CT in degenerative disc disease patients and showed significant improvements in VAS and ODI scores in postoperative compared to preoperative assessments (20). In an attempt to prevent extensive fusion, Kato et al. utilized SPECT/CT to localize specific pain generators in elderly patients, using this information to manage these patients conservatively (21). Furthermore, in their cohort, Shapovalov et al. demonstrated that patients benefited more and had greater pain relief following SPECT/CT-guided revision surgeries (34). SPECT/CT was also used to diagnose and alter the management planning for patients with facet arthropathy and hardware loosening (19,23).

Biomechanical Correlation and Metabolic Activity

Correlations between tracer uptake and several factors—including mechanical stress, anatomical abnormalities, and degenerative disease progression—were investigated in several studies (8,12,32). Russo et al. found that Modic type I changes and Pfirrmann grade IV discs were associated with high tracer uptake, indicating a more metabolically active region, presumably connected to greater pain generation (32). Dharia et al. found increased tracer uptake in patients with elevated pelvic incidence and sacral slope, and sacroiliac joint pathologies (12). Finally, Carsten et al. demonstrated increased uptake associated with minimal degenerative changes; meanwhile, severely degenerated regions exhibited minimal uptake, indicating that metabolic activity represents early degenerative changes (8).

Detection of Hardware Failure, Pseudoarthrosis, and Other Complications

Detecting recent complications in the postoperative setting can be challenging. Several studies aimed to clarify these changes utilizing SPECT/CT. Rager et al. used SPECT/CT to differentiate true and pseudoarthrosis from other causes of pain, demonstrating greater sensitivity when compared to CT (29). In further studies, Rager et al. demonstrated that the absence of tracer uptake does not correlate with an absence of complications in patients with broken screws (28). Tamm and Abele reported that SPECT/CT is equivalent to spinal MRI in the capacity to detect spinal infection. This is especially useful when MRI is contraindicated (36).

DISCUSSION

Causes of Postsurgical Back Pain

Complication rates for spinal procedures range between 4% and 19%; these issues can be broadly categorized into acute and chronic causes of pain (10,35,38) (Table I). Chronic complications, such as hardware failure, may manifest months after surgery and include problems like the loosening or fracture of pedicle screws, cage migration, and rod breakage, all of which can lead to fusion failure. Fusion failure can result in spondylolisthesis and spinal instability, especially in the case of rod fractures. Early radiologic assessment is vital for detecting these complications, identifying sources of pain, and enabling timely surgical revision to prevent further deterioration.

Table I: Acute and Chroic Causes of Postoperative Back Pain

Acute	Chronic
Hemorrhage	Hardware Failure
Edema	Chronic infection
Postoperative Inflammation	Spondylolisthesis
Screw malpositioning	Infection
Infection	Dural tears
Nerve root injury	Pseudoarthrosis
	Facet joint degeneration
	Adjacent segment degeneration
	Sacroiliac Joint secondary to previous spinal surgery
	Cage subsidence

In addition to hardware-related issues, other complications such as infection, spinal or epidural hematoma, pseudomeningocele, and nerve root injury can contribute to persistent postoperative pain. Early identification and management of these complications are crucial, as they can quickly progress to permanent neurological deficits or even death. Postsurgical pseudomeningocele, though rare, often arises from inadvertent meningeal tears or inadequate closure during surgery, and can lead to symptoms such as wound swelling, headaches, and radicular pain. Another potential issue, known as "battered root syndrome," can cause persistent radicular pain following lumbar surgery. This is often due to prolonged and aggressive root retraction, excessive bleeding, or the presence of a conjoined nerve root. Surgery may also lead to arachnoiditis, a condition where persistent inflammation of the arachnoid mater causes irritation of the nerve roots, resulting in pain that can affect both the spine and lower limbs.

Postoperative Radiologic Assessment of the Spinal Column

Plain radiographs, CT, and MRI scans are the primary radiological tools used for postoperative evaluation. These modalities are crucial for monitoring spinal column alignment, hardware integrity, and the progression of bony fusion. Regular follow-up with thorough clinical and radiological assessments is essential to ensure optimal outcomes. However, each of these imaging techniques has limitations and should not be relied upon in isolation; they must be interpreted in the context of a patient's symptoms and medical history to provide accurate diagnoses (Table II). Plain radiography is cost-effective for evaluating bone structure and hardware integrity. Static radiographs can detect hardware failure, while dynamic mo-

Table II: Comparing the Imaging Modalities Utilized in The Studies

Modality	Strengths	Limitations	Clinical Application
SPECT/CT	High sensitivity for detecting metabolically active pain generators (e.g., pseudoarthrosis, facet degeneration, screw loosening); increased efficacy for postoperative assessment with metal hardware	Increased Radiation exposure; limited in early postoperative phase due to bone healing activity shows as increased tracer uptake; cannot effectively differentiate inflammation from infection	Postoperative back pain with ambigious CT/MRI scans; suspected hardware loosening, pseudoarthrosis, and facet degeneration
PET/CT (FDG)	Superior for infection detection (spondylodiscitis, osteomyelitis); less affected by metal artifact	High cost; limited availability; not routinely used in mechanical pain diagnosis; also increased radiation exposure	Suspected postoperative infection or systemic inflammation; early discitis/osteomyelitis with negative MRI
MRI	Gold Standard for soft tissue, nerve root, and scar tissue as well as spinal cord and disc assessment	Metal artifacts limits postoperative imaging; decreaced efficacy in visualizing fusion long scan time	Initial evaluation for soft tissue/ spinal pathology; radiculopathy or cord compression; disc herniation
CT	Superior bone detail and hardware visualization; 3D reconstruction; Effective in detecting nonunion and foraminal stenosis	No functional/metabolic information; increased radiation exposure	Excellent structural evaluation of bone, hardware, and nonunion in the early postoperative period

dalities assess spinal instability (6,25). Spondylolisthesis can be identified, but soft tissue and neural impingement cannot be assessed. Meanwhile, CT provides detailed 3D visualization of bone and hardware, excelling in detecting nonunion and foraminal stenosis in FBSS (11,39). MRI is the best tool for soft tissue evaluation, and can identify conditions like stenosis, disc disease, and infections (37). Research has shown that the extent of scar tissue is directly linked to the recurrence of radicular pain, with a 25% increase in scar tissue doubling the risk (22,31). Despite its strengths, MRI has certain limitations, particularly in evaluating the bony cortex or assessing fusion across operated levels. Metallic implants can also introduce artifacts that complicate imaging, although modern titanium hardware typically causes fewer problems. Moreover, advances in metallic artifact reduction sequences, when appropriately selected, can effectively address both in-plane and through-plane artifacts by using multi-acquisition variable resonance image combinations and slice-encoding techniques to enhance image quality (24). However, patients with chronic pain may struggle to remain still for the lengths of time required to obtain high-quality multiplanar images, and reactions to contrast agents can limit the widespread use of MRI in the postoperative population. These considerations highlight the importance of selecting appropriate imaging modalities and techniques to maximize diagnostic accuracy while minimizing patient discomfort.

SPECT/CT

SPECT utilizes the pharmacokinetic properties of specific radionuclide substances to detect areas of altered or hypermetabolic activity within the bone structure of the spinal column. This can identify anatomical or functional sources of postoperative pain. Common radiotracers include technetium-99m, which binds to hydroxyapatite—a key mineral in the bone cortex—^{18}F Sodium Fluoride (^{18}F-NaF), and ^{18}F-fluorodeoxyglucose (^{18}F-FDG). These tracers are incorporated into the bone matrix with hydroxyapatite and are also taken up by inflammatory cells, enabling the detection of metabolically active cells within the spine through SPECT and positron emission tomography (PET) imaging.

Recent advancements in imaging technology have given rise to hybrid techniques like SPECT/CT and PET/CT, which seamlessly integrate the metabolic insights of SPECT and PET with the detailed 3D anatomical reconstructions provided by CT scans (2). This powerful combination enables the precise evaluation of metabolically active sites, even in challenging areas such as around implanted hardware or regions affected by infection, where metabolic activity is often heightened. The studies included in our systematic review have consistently demonstrated the prognostic utility of SPECT/CT in revealing pathologies missed by CT or MRI scans. This is especially useful in the postoperative period, in which artifacts caused by instrumentation can impede image quality (Table III). Lehman

Table III: Summarization of Studies with Key Findings

Study	Study Aim	Key Results	Added Benefit of SPECT/CT	Evidence & Quality
Lehman et al., (23)	Postoperative back pain	Patient management strategy changed in 79% of cases	MRI scans cannot increased tracer uptake at facet joints	JBI: High OCEBM: IV
Hudyana et al., (19)	Screw loosening, Hardware Failure	SPECT/CT had 100% sensitivity, and 89.7% specifity	SPECT/CT outperformed CT	JBI: High OCEBM: IV
Rager et al., (29)	Pseudarthrosis vs facet pain	SPECT/CT has increased efficacy inpain generator localization	Detected facet joint tracer uptake not visible on CT	JBI: High OCEBM:IV
Kaiser et al., (20)	DDD in patients with positive SPECT/CT findings	Improved ODI and VAS scores after SPECT/CT imaging targeted fusions	Increased uptake by ı-increased metabolic activity has improved outcomes	JBI: High OCEBM: III
Kato et al., (21)	Exploring, Management and assessment of elderly patients presenting with back pain with SPECT/CT	SPECT/CT has guided and help avoid surgery in multilevel disease in elderly patients	Conservative management guided by SPECT	JBI: High OCEBM: IV
Awosika et al., (3)	Systematic review and case series on the utilization of SPECT/CT and PET scan on postoperative spine assessment	Confirmed superior detection of facet degeneration through SPECT/CT scan	They have concluded through systematic review that SPECT/CT is a valuable adjunsct were traditional imaging fails	JBI: High OCEBM: I

Table III: Cont.

Study	Study Aim	Key Results	Added Benefit of SPECT/CT	Evidence & Quality
Paez et al., (26)	Multicenter, prospective study in evaluating postoperative infection assessment through PET/CT and SPECT/CT	FDG PET/CT superior to SPECT with UBI in detecting postoperative infections	MRI + FDG has the AUC of 0.938	JBI: Moderate OCEBM: II
Dharia et al., (12)	Sacroiliac joint pain	Increased uptake correlated with increased pelvic tilt and other spinopelvic parameters	While SPECT/CT is superior in assessing postoperative osteoblastic activity, PET/CT showed incresed efficacy in assessing postoperative infectious assessment	JBI: Moderate OCEBM: IV
Shapovalov et al., (34)	Postoperative cervical spine fusion syndrome	SPECT-guided revision improved patient outcomes	Higher revision success in patients assessed with SPECT/CT vs non-SPECT	JBI: Moderate OCEBM: IV
Russo et al., (32)	Evaluation of chronic back pain with SPECT/CT	Increased Uptake associated with Modic I and Pfirrmann grade 5 disc degenerations	Metabolic confirmation of degenerative pain	JBI: Moderate OCEBM: IV
Rager et al., (28)	Differentiating pseudoarthrosis from other causes of postoperative back pain	Controversially SPECT/CT -failed to detect broken screw	underscoring the importance of metabolic activity in SPECT/CT	JBI: Moderate OCEBM: IV
Carstensen et al., (8)	Chronic facet joint pain assess by SPECT/CT	SPECT showed increased uptake in facet joints in patients with no appearent facet disease on CT scan	SPECT/CT showed metabolic activity in patients without any symptoms and structural degeneration	JBI: Moderate OCEBM: IV
Acosta et al., (1)	Postoperative lumbar spine fusion syndrome	Localized pain generator not seen on MRI revealed by SPECT/CT	Management strategy altered based on metabolic activity seen on SPECT/CT	JBI: Moderate OCEBM: IV
Tamm and Abele, (36)	Assessment of suspected spondylodiscitis	SPECT/CT is equivalent to MRI in infection detection	Viable alternative in stiuations where MRI is contraindicated	JBI: Moderate OCEBM: IV

SPECT/CT: *Single photon emission computed tomography/computed tomography,* ***PET/CT:*** *Positron emission tomography/computed tomography,* ***FBSS:*** *Failed back surgery syndrome,* ***DDD:*** *Degenerative disc disease,* ***ODI:*** *Oswestry disability index,* ***VAS:*** *Visual analog scale,* ***MRI:*** *Magnetic resonance imaging,* ***CT:*** *Computed tomography,* ***FDG:*** *Fluorodeoxyglucose,* ***UBI:*** *Ubiquicidin,* ***JBI:*** *Joanna Briggs Institute,* ***OCEBM:*** *Oxford center for evidence-based medicine levels.*

et al. emphasized the clinical utility of SPECT/CT in treatment planning; SPECT/CT findings led to changes in the treatment plans of 79% of patients through the identification of facet joint abnormalities previously missed by MRI (23). Meanwhile, Rager et al. and Hudyana et al. reported that SPECT/CT effectively revealed metabolically active areas with increased tracer uptake in patients with postoperative back pain, which had been missed on CT scans (19,29). Finally, Carstensen et al. illustrated that ambiguous CT findings could be visualized as metabolically active sites by SPECT/CT (8). This shows the capacity of SPECT/CT to capture lesions before any radiographically significant changes occur. Notably, focal intensities detected by these hybrid methods can remain positive for up to a year following surgery, potentially signaling issues such as nonunion or pseudoarthrosis. In contrast, diffuse activity may indicate increased bone turnover in a normally fused spine, reflecting the body's ongoing healing process. Furthermore, the use of technetium-labeled white blood cells enhances the ability to detect infections in the operated area, providing a comprehensive toolset for assessing complex postoperative conditions (37). The updated American College of Radiology (ACR) Appropriateness Criteria endorse SPECT/CT as the standard for identifying radiographically hidden spondylosis as a pain generator in younger patients (Figure

2) (14). SPECT/CT is also recommended as an adjunctive imaging technique for detecting pseudoarthrosis and screw loosening in patients who have undergone prior lumbar surgery, with or without radiculopathy (14). Hudyana et al. reported that SPECT/CT significantly outperformed CT for the diagnosis of screw loosening, with sensitivity of 100% and specificity around 90 (19). However, in consecutive studies, Rager et al. underscored that metabolic activity may not always be present in the event of mechanical failure of a construct. While it can be deduced from these studies that the presence of a metabolically active site can confidently indicate pseudoarthrosis, a negative scan does not necessarily exclude the possibility (28,29). In a systematic review, Awosika et al. highlighted the superiority of SPECT/CT in diagnosing pseudoarthrosis and adjacent segment disease, and guiding further revision surgeries (3). One study explored the relationship between SPECT/CT findings and the outcomes of revision surgery in patients with FBSS, and determined the modality's use in identifying sources of pain in patients with suspected inflammatory back pathology, thereby guiding more effective treatment strategies (Figure 3). The utility of SPECT/CT for guiding patient management has been indicated by several studies. Kaiser et al. found that patients benefited more when treated at SPECT/CT positive levels compared to SPECT/CT negative or other non-targeted levels, reporting overall reduced postoperative pain and increased functional improvement (20). Kato et al. investigated the conservative treatment of active pain generators using SPECT/CT in older patients. Use of the technique allowed these patients to receive conservative management and avoid surgery (21). Furthermore, Shapovalov et al. demonstrated that SPECT/CT-guided revision surgeries had better outcomes than traditional image-guided revision surgeries (34). These findings underscore the wide utility of SPECT/CT, not only in diagnosis but also in improving patient outcomes. Together, these results suggest a paradigm shift for the assessment of radiologically ambiguous cases.

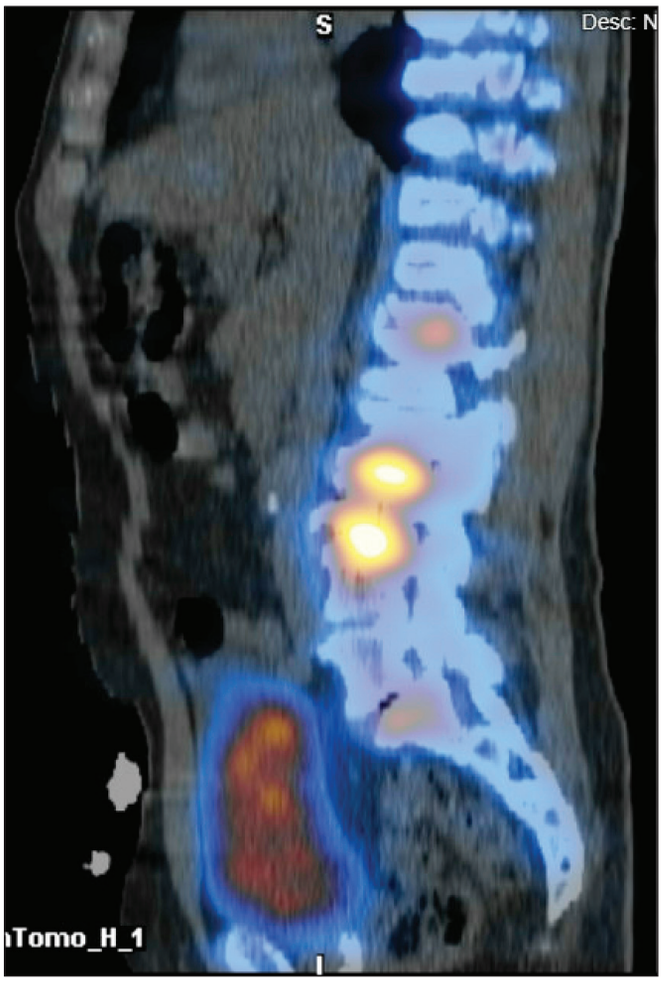

Figure 2: 71-year-old male who had a Lumbar MRI performed, which demonstrated multilevel degenerative disc disease as well as multilevel neural foraminal stenosis at L2-L3, L3-L4, and L5-S1 bilaterally. SPECT/CT demonstrated metabolic activity at multiple levels, including T12-L1, L2-L3, and L3-L4, though the greatest degree of tracer uptake was noted at L3-L4 end plates. He had an L2-4 prone trans psoas lateral fusion and was followed up with 1 year later. He reported his pain level to be at a zero at his 1-year follow-up.

Figure 3: 70-year-old Male with a history of L3-L4, L4-L5, and L5-S1 transforaminal lumbar interbody fusion (TLIF) intervention. MRI demonstrated multiple-level degenerative disease. His SPECT/CT demonstrated activity at the L2-L3 disc space. He subsequently had L2-L3 extension TLIF. Subsequently, pain improved from a 6 at his baseline consult visit to a 2 at 6 months follow.

Patients with positive SPECT/CT results—indicating conditions such as facet arthritis, disc inflammation, or pedicle screw loosening—responded better to re-operation than those with negative SPECT/CT findings (18). While research on the use of SPECT/CT as an adjunct to other imaging modalities is still emerging, there is already substantial evidence demonstrating its added value. Significantly, SPECT/CT can detect active metabolic sites not only at operated levels but also those adjacent and in other load-bearing structures, such as the sacroiliac joints. This capability is particularly useful in guiding targeted injections, which can provide significant relief for patients. However, it is crucial to distinguish asymmetrical increased uptake in the sacroiliac joints, often seen at bone grafting sites, from inflammatory processes.

SPECT/CT has increasingly been established as a valuable imaging modality for evaluating conditions such as pseudoarthrosis, hardware failure, metallic work fractures, screw loosening, and misalignment, especially in cases where other imaging techniques yield inconclusive results. A recent systematic review by Awosika et al. highlighted SPECT/CT's superiority in detecting facet degeneration compared to CT alone (3). Their findings suggest that SPECT/CT has higher diagnostic accuracy than conventional imaging methods and can provide additional information for identifying pain-generating sites, including pseudoarthrosis, hardware loosening, and facet joint degeneration. Furthermore, ^{18}F-FDG PET/CT was noted for its efficacy in detecting postoperative infections; increased FDG uptake was associated with increased inflammatory activity, aiding in the diagnosis of suspected infection. Additionally, Hudyana et al. demonstrated that SPECT/CT could detect screw loosening with remarkable accuracy, boasting a sensitivity of 100% and a specificity of 89.7% (19). Besides hardware assessments, SPECT/CT also showed efficacy in identifying other sources of recurrent back pain, including active fact degeneration and degenerative changes in the discs and sacroiliac joint.

SPECT/CT is particularly effective in identifying pain generators related to adjacent segment degeneration following spinal surgery, offering a clear differentiation between tracer uptake by facet joints and pedicle screws. This is crucial in cases of device subsidence, where CT scans might overestimate lucencies, potentially leading to false diagnoses. SPECT/CT helps to distinguish between physiological height loss and pathological processes, with the latter showing increased tracer uptake and CT evidence of subsidence (15). Huang et al. investigated the utility of SPECT/CT in FBSS, and found it to be effective in pinpointing sources of persistent pain and identifying facet joint inflammation and pedicle screw loosening (37). Moreover, patients exhibiting more positive findings in SPECT were reported to have more favorable outcomes following revision surgery compared to patients with high uptake and increased signal intensity on imaging.

Pedicle screw loosening, seen in 18% to 31% of patients, typically appears as a rim of lucency around the screw on CT scans. SPECT/CT provides valuable information by identifying increased metabolic activity associated with this process (33,39). However, caution is advised when using SPECT/CT in the early postoperative period, as the heightened metabolic activity of osteoblasts during tissue repair may lead to misdiagnosis or overdiagnosis. Russo et al. demonstrated increased tracer uptake with degenerative disc changes, further showing the correlation between increased uptake and inflammation (32). Further studies reported similar observations in the sacroiliac and facet joints (8,12).

Experts, including Al-Riyami and Gnanasegaran, have recommended the use of SPECT/CT in patients with persistent postoperative pain lasting 12 months or more, especially when other modalities produce inconclusive results (2,15). They also underscored the robustness of SPECT/CT for detecting pseudoarthrosis and hardware failure even in very close proximity to the instrumented level, yielding highly detailed information. Gnanasegaran et al. further validated the efficacy of SPECT/CT in detecting pseudoarthrosis, hardware failure, and adjacent segment disease (15).

Interestingly, SPECT/CT can also uncover significant findings in asymptomatic patients with clean radiographic images. For example, Rager et al. reported on six patients with normal CT scans, who were later found to have facet joint disease upon SPECT/CT evaluation (Figure 4) (29). Despite the normal CT images, SPECT/CT was able to capture the active sites of facet disease on the anatomical landmarks provided by the original scan.

If we compare PET/CT and SPECT/CT for postoperative spinal evaluation, both provide valuable information. While PET/CT shows increased utility in identifying postoperative infection, particularly with FDG tracers, SPECT/CT has demonstrated superiority for detecting mechanical complications, including pseudoarthrosis and hardware failure, due to its ability to assess osteoblastic activity. The choice of imaging modality should be based on the clinical scenario and initial evaluation.

SPECT/CT has certain limitations, particularly in the evaluation of disc herniations, cord and root compressions, and listhesis, where it may not provide sufficient detail. Furthermore, in the immediate preoperative period, SPECT/CT may not be as well adapted as it is in the later treatment periods. Inflammation caused by the trauma of surgery and early osteoblastic activity can be easily misinterpreted as infection or pseudoarthrosis. Unfortunately, there is no established evidence-based cutoff in follow-up duration for when best to utilize this modality. As a further limitation, SPECT/CT may not be able to differentiate infection from inflammation due to other causes, including pseudoarthrosis, facet joint degeneration, adjacent disease, and hardware failure; the patient's clinical and other biomarkers should be taken into account when making a diagnosis of postoperative infectious disease. Finally, in cases of concurrent multiple complications, SPECT/CT may fall short in differentiation, and may lead to the underdiagnosis of certain conditions. Moreover, this procedure requires ingestion of certain chemicals, which may not be feasible in patients with chronic kidney disease or allergies.

Future directions for SPECT/CT should focus on its implementation in preoperative planning, alongside improvements in accounting for anatomical variations and individual meta-

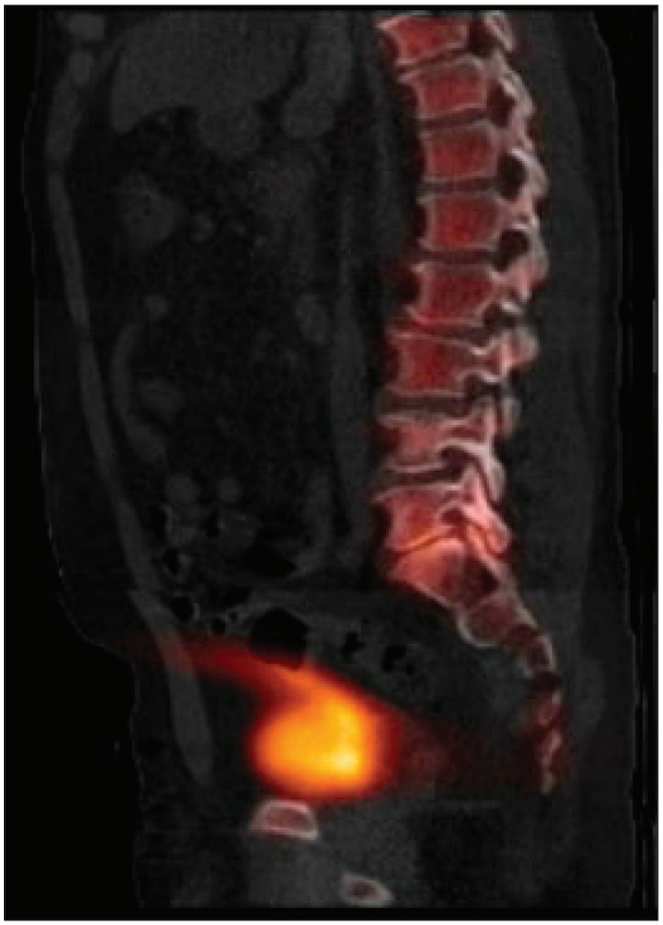

Figure 4: 51-years-old, Male with a history of T12-L1 Laminectomy. SPECT CT was performed and demonstrated L5-S1 disc & facet joint uptake. He ended up receiving an L5-S1 TLIF. Pain at baseline before most recent surgery was a 7, at 3 months it was a 0, and at 6 months it was a 4.

bolic profiles. Progress in these factors would allow for a more individualized approach for patients and enhance the clinical utility of SPECT/CT. Furthermore, research focused on radiotracers specific to spinal pathologies could enhance the diagnostic sensitivity of SPECT/CT. Integration with other imaging modalities, such as functional MRI, could also improve preoperative planning and patient outcomes. Naturally, these modalities are costly, so optimization and standardization of imaging protocols are necessary, especially in the postoperative term, for the differentiation of inflammation and bone healing from other common complications.

CONCLUSION

Postoperative pain that recurs or persists despite initial treatment necessitates a comprehensive approach, combining both clinical evaluation and advanced radiological investigations. SPECT/CT and PET/CT have become widely used for evaluating postoperative spinal conditions, and can effectively pinpoint sources of persistent pain. These hybrid imaging techniques merge metabolic and anatomical data to accurately detect issues like nonunion, pseudoarthrosis, and infection. Identifying active metabolic sites, both proximal and distal from surgical areas, enables targeted treatments such as guided injections, enhancing patient outcomes. As evidence of its efficacy grows, SPECT/CT is poised to become a mainstay in diagnosing complex spinal pathologies. Nevertheless, clinicians must interpret results carefully to differentiate between pathological findings and normal postoperative changes. Further large-scale patient studies are needed to better define the role of SPECT/CT in managing complex postoperative pain complications.

Declarations

Funding: This research did not receive any specific grant from funding agencies in the public, commercial, or not-for-profit sectors.

Availability of data and materials: The datasets generated and/or analyzed during the current study are available from the corresponding author by reasonable request.

Disclosure: The authors declare no competing interests.

AUTHORSHIP CONTRIBUTION

Study conception and design: ASA, MDY, BGF, KDT, MAEB
Data collection: ASA, MDY, MP, KDT
Analysis and interpretation of results: ASA, MDY, MP, BGF, KDT
Draft manuscript preparation: ASA, MDY, MAEB
Critical revision of the article: ASA, MDY, KDT, MAEB
Other (study supervision, fundings, materials, etc...): ASA, MDY, MP, BGF, KDT, MAEB
All authors (ASA, MDY, MP, BGF, KDT, MAEB) reviewed the results and approved the final version of the manuscript.

REFERENCES

1. Acosta FL, Shapovalov VS, Lobo BM, Liker MA: Radiographic evaluation of low back pain after lumbar fusion using Technetium-99 single-photon emission computed tomography: Impact on clinical decision-making and outcome. Interdiscip Neurosurg 24:101089, 2021. https://doi.org/10.1016/j.inat.2021.101089
2. Al-Riyami K, Gnanasegaran G, Van den Wyngaert T, Bomanji J: Bone SPECT/CT in the postoperative spine: A focus on spinal fusion. Eur J Nucl Med Mol Imaging 44:2094-2104, 2017. https://doi.org/10.1007/s00259-017-3765-6
3. Awosika T, Davidar AD, Hersh AM, Menta A, Weber-Levine C, Alomari S, Khan MA, Theodore N: SPECT/CT and PET/CT for the evaluation of persistent or recurrent pain after spine surgery: A systematic review and case series. World Neurosurg 182:e344-e359, 2024. https://doi.org/10.1016/j.wneu.2023.11.108
4. Baber Z, Erdek MA: Failed back surgery syndrome: Current perspectives. J Pain Res 9:979-987, 2016. https://doi.org/10.2147/JPR.S92776
5. Barber SM, Fridley JS, Konakondla S, Nakhla J, Oyelese AA, Telfeian AE, Gokaslan ZL: Cerebrospinal fluid leaks after spine tumor resection: Avoidance, recognition and management. Ann Transl Med 7:217, 2019. https://doi.org/10.21037/atm.2019.01.04

6. Borkar SA, Sharma R, Mansoori N, Sinha S, Kale SS: Spinopelvic parameters in patients with lumbar degenerative disc disease, spondylolisthesis, and failed back syndrome: Comparison vis-à-vis normal asymptomatic population and treatment implications. J Craniovertebr Junction Spine 10:167-171, 2019. https://doi.org/10.4103/jcvjs.JCVJS_70_19
7. Buchbinder R, Blyth FM, March LM, Brooks P, Woolf AD, Hoy DG: Placing the global burden of low back pain in context. Best Pract Res Clin Rheumatol 27:575-589, 2013. https://doi.org/10.1016/j.berh.2013.10.007
8. Carstensen MH, Al-Harbi M, Urbain JL, Belhocine TZ: SPECT/CT imaging of the lumbar spine in chronic low back pain: A case report. Chiropr Man Therap 19:2, 2011. https://doi.org/10.1186/2045-709X-19-2
9. Cramer DE, Maher PC, Pettigrew DB, Kuntz C: Major neurologic deficit immediately after adult spinal surgery: Incidence and etiology over 10 years at a single training institution. J Spinal Disord Tech 22:565-570, 2009. https://doi.org/10.1097/BSD.0b013e318193452a
10. Dekutoski MB, Norvell DC, Dettori JR, Fehlings MG, Chapman JR: Surgeon perceptions and reported complications in spine surgery. Spine (Phila Pa 1976) 35:S9-S21, 2010. https://doi.org/10.1097/BRS.0b013e3181d830de
11. Dhagat PK, Jain M, Singh SN, Arora S, Leelakanth K: Failed back surgery syndrome: Evaluation with magnetic resonance imaging. J Clin Diagn Res 11:TC06-TC09, 2017. https://doi.org/10.7860/JCDR/2017/24930.9817
12. Dharia AA, Guillotte AR, De Stefano FA, Rouse AG, Ohiorhenuan IE: Biomechanical predictors of sacroiliac joint uptake on single-photon emission computed tomography/computed tomography. World Neurosurg 188:e606-e612, 2024. https://doi.org/10.1016/j.wneu.2024.05.176
13. Esses SI, Sachs BL, Dreyzin V: Complications associated with the technique of pedicle screw fixation. A selected survey of ABS members. Spine (Phila Pa 1976) 18:2231-2238; discussion 2238-2239, 1993. https://doi.org/10.1097/00007632-199311000-00015
14. Expert Panel on Neurological Imaging, Hutchins TA, Peckham M, Shah LM, Parsons MS, Agarwal V, Boulter DJ, Burns J, Cassidy RC, Davis MA, Holly LT, Hunt CH, Khan MA, Moritani T, Ortiz AO, O'Toole JE, Powers WJ, Promes SB, Reitman C, Shah VN, Singh S, Timpone VM, Corey AS: ACR appropriateness criteria® low back pain: 2021 update. J Am Coll Radiol 18:S361-S379, 2021. https://doi.org/10.1016/j.jacr.2021.08.002
15. Gnanasegaran G, Paycha F, Strobel K, van der Bruggen W, Kampen WU, Kuwert T, Van den Wyngaert T: Bone SPECT/CT in postoperative spine. Semin Nucl Med 48:410-424, 2018. https://doi.org/10.1053/j.semnuclmed.2018.06.003
16. Guerin P, El Fegoun AB, Obeid I, Gille O, Lelong L, Luc S, Bourghli A, Cursolle JC, Pointillart V, Vital JM: Incidental durotomy during spine surgery: Incidence, management and complications. A retrospective review. Injury 43:397-401, 2012. https://doi.org/10.1016/j.injury.2010.12.014
17. Hamilton DK, Smith JS, Sansur CA, Glassman SD, Ames CP, Berven SH, Polly DW, Perra JH, Knapp DR, Boachie-Adjei O, McCarthy RE, Shaffrey CI, Scoliosis Research Society Morbidity and Mortality Committee: Rates of new neurological deficit associated with spine surgery based on 108,419 procedures: a report of the scoliosis research society morbidity and mortality committee. Spine (Phila Pa 1976) 36:1218-1228, 2011. https://doi.org/10.1097/BRS.0b013e3181ec5fd9
18. Huang BR, Peng BR, Pan LK, Chen CY: Potential usefulness of single photon emission computed tomography/computed tomography in management of patients with failed back surgery syndrome. J Med Imaging Health Inform 9:1386-1392, 2019. https://doi.org/10.1166/jmihi.2019.2782
19. Hudyana H, Maes A, Vandenberghe T, Fidlers L, Sathekge M, Nicolai D, Van de Wiele C: Accuracy of bone SPECT/CT for identifying hardware loosening in patients who underwent lumbar fusion with pedicle screws. Eur J Nucl Med Mol Imaging 43:349-354, 2016. https://doi.org/10.1007/s00259-015-3158-7
20. Kaiser R, Varga M, Lang O, Waldauf P, Vaněk P, Saur K, Beneš V, Netuka D: Spinal fusion for single-level SPECT/CT positive lumbar degenerative disc disease: The SPINUS I study. Acta Neurochir 165:2633-2640, 2023. https://doi.org/10.1007/s00701-023-05666-8
21. Kato S, Demura S, Matsubara H, Inaki A, Shinmura K, Yokogawa N, Murakami H, Kinuya S, Tsuchiya H: Utility of bone SPECT/CT to identify the primary cause of pain in elderly patients with degenerative lumbar spine disease. J Orthop Surg Res 14:185, 2019. https://doi.org/10.1186/s13018-019-1236-4
22. Lee YS, Choi ES, Song CJ: Symptomatic nerve root changes on contrast-enhanced MR imaging after surgery for lumbar disk herniation. AJNR Am J Neuroradiol 30:1062-1067, 2009. https://doi.org/10.3174/ajnr.A1497
23. Lehman VT, Murphy RC, Maus TP: 99mTc-MDP SPECT/CT of the spine and sacrum at a multispecialty institution: Clinical use, findings, and impact on patient management. Nucl Med Commun 34:1097-1106, 2013. https://doi.org/10.1097/MNM.0b013e328364bfa6
24. Lu W, Pauly KB, Gold GE, Pauly JM, Hargreaves BA: SEMAC: Slice encoding for metal artifact correction in MRI. Magn Reson Med 62:66-76, 2009. https://doi.org/10.1002/mrm.21967
25. Mehta VA, Amin A, Omeis I, Gokaslan ZL, Gottfried ON: Implications of spinopelvic alignment for the spine surgeon. Neurosurgery 76 Suppl 1:S42-56; discussion S56, 2015. https://doi.org/10.1227/01.neu.0000462077.50830.1a
26. Paez D, Sathekge MM, Douis H, Giammarile F, Fatima S, Dhal A, Puri SK, Erba PA, Lazzeri E, Ferrando R, Almeida Filho P, Peter Magboo V, Morozova O, Núñez R, Pellet O, Mariani G, Giammarile FGiammarile F: Comparison of MRI, [18 F]FDG PET/CT, and 99m Tc-UBI 29-41 scintigraphy for postoperative spondylodiscitis-a prospective multicenter study. Eur J Nucl Med Mol Imaging 48:1864-1875, 2021. https://doi.org/10.1007/s00259-020-05109-x/Published

27. Page MJ, McKenzie JE, Bossuyt PM, Boutron I, Hoffmann TC, Mulrow CD, Shamseer L, Tetzlaff JM, Akl EA, Brennan SE, Chou R, Glanville J, Grimshaw JM, Hróbjartsson A, Lalu MM, Li T, Loder EW, Mayo-Wilson E, McDonald S, McGuinness LA, Stewart LA, Thomas J, Tricco AC, Welch VA, Whiting P, Moher D: The PRISMA 2020 statement: An updated guideline for reporting systematic reviews BMJ 372:n71, 2021. https://doi.org/10.1136/bmj.n71.
28. Rager O, Amzalag G, Varoquaux A, Schaller K, Ratib O, Tessitore E: SPECT-CT assessment of pseudarthrosis after spinal fusion: diagnostic pitfall due to a broken screw. Case Rep Orthop 2013:1-3, 2013. https://doi.org/10.1155/2013/502517
29. Rager O, Schaller K, Payer M, Tchernin D, Ratib O, Tessitore E: SPECT/CT in differentiation of pseudarthrosis from other causes of back pain in lumbar spinal fusion: Report on 10 consecutive cases. Clin Nucl Med 37:339-343, 2012. https://doi.org/10.1097/RLU.0b013e318239248b
30. Reisener MJ, Pumberger M, Shue J, Girardi FP, Hughes AP: Trends in lumbar spinal fusion-a literature review. J Spine Surg 6:752-761, 2020. https://doi.org/10.21037/jss-20-492
31. Ross JS, Robertson JT, Frederickson RC, Petrie JL, Obuchowski N, Modic MT, deTribolet N: Association between peridural scar and recurrent radicular pain after lumbar discectomy: Magnetic resonance evaluation. ADCON-L European Study Group. Neurosurgery 38:855-861; discussion 861-3, 1996.
32. Russo VM, Dhawan RT, Dharmarajah N, Baudracco I, Lazzarino AI, Casey AT: Hybrid bone single photon emission computed tomography imaging in evaluation of chronic low back pain: Correlation with modic changes and degenerative disc disease. World Neurosurg 104:816-823, 2017. https://doi.org/10.1016/j.wneu.2017.03.107
33. Sandén B, Olerud C, Petrén-Mallmin M, Johansson C, Larsson S: The significance of radiolucent zones surrounding pedicle screws. Definition of screw loosening in spinal instrumentation. J Bone Joint Surg Br 86:457-461, 2004. https://doi.org/10.1302/0301-620x.86b3.14323
34. Shapovalov V, Lobo B, Liker M: SPECT/CT imaging for diagnosis and management of failed cervical spine surgery syndrome. Interdiscip Neurosurg 32: 101699, 2023. https://doi.org/10.1016/j.inat.2022.101699
35. Smith JS, Fu KMG, Polly DW, Sansur CA, Berven SH, Broadstone PA, Choma TJ, Goytan MJ, Noordeen HH, Knapp DR, Hart RA, Donaldson WF, Perra JH, Boachie-Adjei O, Shaffrey CI: Complication rates of three common spine procedures and rates of thromboembolism following spine surgery based on 108,419 procedures: A report from the Scoliosis Research Society Morbidity and Mortality Committee. Spine (Phila Pa 1976) 35:2140-2149, 2010. https://doi.org/10.1097/BRS.0b013e3181cbc8e7
36. Tamm AS, Abele JT: Bone and gallium single-photon emission computed tomography-computed tomography is equivalent to magnetic resonance imaging in the diagnosis of infectious spondylodiscitis: A retrospective study. Can Assoc Radiol J 68:41-46, 2017. https://doi.org/10.1016/j.carj.2016.02.003
37. Van Goethem JWM, Van den Hauwe L, Parizel PM: Spinal imaging: Diagnostic imaging of the spine and spinal cord. Am J Neuroradiol 29:e60-e61, 2008. https://doi.org/10.3174/ajnr.A0984
38. Veeravagu A, Cole TS, Azad TD, Ratliff JK: Improved capture of adverse events after spinal surgery procedures with a longitudinal administrative database. J Neurosurg Spine 23:374-382, 2015. https://doi.org/10.3171/2014.12.SPINE14659
39. Waguespack A, Schofferman J, Slosar P, Reynolds J: Etiology of long-term failures of lumbar spine surgery. Pain Med 3:18-22, 2002. https://doi.org/10.1046/j.1526-4637.2002.02007.x
40. Winter RB: Complications after transpedicular stabilization of the spine. Spine (Phila Pa 1976) 20:1847-1848, 1995.
41. Wu A, March L, Zheng X, Huang J, Wang X, Zhao J, Blyth FM, Smith E, Buchbinder R, Hoy D: Global low back pain prevalence and years lived with disability from 1990 to 2017: Estimates from the Global Burden of Disease Study 2017. Ann Transl Med 8:299, 2020. https://doi.org/10.21037/atm.2020.02.175

Turk Neurosurg 36(1):119-135, 2026
DOI: 10.5137/1019-5149.JTN.46779-24.2

Original Investigation
Neuro-Oncology

Received: 18.07.2024
Accepted: 17.06.2025
Published Online: 16.01.2026

Effective Management of Brainstem Tumors: A Study of 22 Patient Experiences

Ersin HACIYAKUPOGLU[1], Evren YUVRUK[2], Ayca Ersen DANYELI[3], Sebahattin HACIYAKUPOGLU[4]

[1]Heinrich-Braun-Klinikum, Zwickau, Department of Neurosurgery, Zwickau, Germany
[2]Umraniye Education and Research Hospital, Department of Neurosurgery, Istanbul, Türkiye
[3]Acibadem University, School of Medicine, Department of Medical Pathology, Istanbul, Türkiye
[4]Acibadem University, School of Medicine, Department of Neurosurgery, Adana, Türkiye

This study has been presented at the 37th Scientific Congress of the Turkish Neurosurgical Society between 18 and 21 April, 2024 at Antalya, Türkiye

Corresponding author: Ersin HACIYAKUPOGLU ✉ haciyakupoglu@yahoo.com

ABSTRACT

AIM: To evaluate the surgical outcomes, extent of resection, and postoperative clinical improvement in 22 patients with brainstem tumors.

MATERIAL and METHODS: We performed surgery on 22 patients with brainstem tumors using various approaches to access the pathology. Our goal was to achieve gross total resection wherever feasible, although this was not possible in all cases. Spontaneous breathing was preferred during surgery, and resection was halted if any disturbance occurred. Bipolar or monopolar coagulation was avoided, and smooth compression and irrigation were used for bleeding control. Neuromonitoring was employed during surgery for all patients.

RESULTS: Among the 22 patients included in this study, 4 presented with long tract symptoms, 3 had hydrocephalus, 5 had papillary stasis, 4 had cerebellar findings, 3 had gait disturbances, 1 had respiratory disturbance, and 1 had dysphagia. Gross total resection was achieved in 10 patients, near-total resection in 4, and partial resection in 8.

CONCLUSION: Surgery enables histologic diagnosis, relieves mass effect, and improves symptoms in brainstem tumors. While gross total resection is ideal, it should not be insisted on in infiltrative tumors; partial or subtotal resection may provide long-term benefit in focal and exophytic lesions. Careful neuromonitoring and anatomical planning are essential to minimize morbidity.

KEYWORDS: Brainstem tumors, Exophytic, Focal, Diffuse, Infiltrative

ABBREVIATIONS: CNS: Central nervous system, **NF1:** Neurofibromatosis type 1, **NF2:** Neurofibromatosis type 2, **VA:** Vertebral artery, **BA:** Basilar artery, **PICA:** Posterior inferior cerebellar artery, **BST:** Brainstem tumor, **GBM:** Glioblastoma multiforme, **GTR:** Gross total resection, **DIPG:** Diffuse intrinsic pontine glioma, **MRI:** Magnetic resonance imaging, **PNET:** Primitive neuroectodermal tumor, **RT:** Radiotherapy, **HE:** Hematoxylin and eosin, **GCS:** Glasgow coma scale

INTRODUCTION

Approximately 5% of all intracranial tumors and 25% of posterior fossa tumors arise in the brainstem, with 80% located in the pons and 86% of those histologically classified as diffuse infiltrative fibrillary astrocytoma grade II (6,11,23). Although these tumors are typically classified as low-grade histologically, they frequently behave like supratentorial high-grade gliomas in children, demonstrating infiltrative, aggressive, and progressive characteristics, with no clear demarcation lines and symmetrical metastasis in vertical and transverse directions (11,18,23).

Ersin HACIYAKUPOGLU : 0000-0002-9712-9913
Evren YUVRUK : 0000-0002-2945-743X
Ayca ERSEN DANYELI : 0000-0001-8015-9916
Sebahattin HACIYAKUPOGLU : 0000-0002-0700-7593

Brainstem tumors (BSTs) are most commonly detected in children, particularly males; moreover, these tumors often remain asymptomatic until they reach a significant size due to their midline location (7,28). The most common symptoms of BSTs include headache, vomiting, and gait disturbances, whereas the most prominent clinical findings include papilledema, ataxia, strabismus, nystagmus, vertigo, cranial nerve deficits, long tract signs, and head bobbing (27,28). In cases with hydrocephalus, shunt procedures may be required (2).

Approximately 90% of BSTs originate from astrocytic lineage and include diffuse fibrillary, pilocytic, pilomyxoid, pleomorphic xanthoastrocytoma, and other histological variants (11,19) The less frequent pathologies include oligodendroglioma, ependymoma, primitive neuroectodermal tumor (PNET), atypical teratoid/rhabdoid tumor (AT/RT), hamartoma, tuberculoma, and fungal granulomas (9,10,14).

Based on anatomical and radiological characteristics, BSTs may be classified as focal, anterior, posterior, lateral, exophytic, diffuse, infiltrative, or intrinsic (18). Magnetic resonance imaging (MRI) is the most preferred imaging modality for BSTs as it provides valuable data on their localization, extent, neighborhood, and differential diagnosis (8,18,32).

Focal exophytic midbrain, medullary, and cervicomedullary tumors can be treated via gross total resection (GTR), whereas diffuse infiltrative pontine gliomas (DIPGs) without an exophytic component cannot be treated surgically (23). Instead, these lesions can be treated using radiotherapy, chemotherapy, immunologic therapies, stereotactic radiosurgery, genetic therapies, and targeted molecular agents including IL-13 receptor-targeted approaches (13,15,16,22).

In this study, we evaluated 22 patients with brainstem tumors who had undergone surgical treatment between 2010 and 2023. We analyzed their outcomes based on the extent of resection—gross total, near-total, or partial—and assessed the role of follow-up in stable lesions. A comprehensive literature review was also performed.

MATERIAL and METHODS

Of the 22 BSTs analyzed in this study, 3 were located in the midbrain and 2 in the peduncle. These five tumors were resected through pterional craniotomy. We reached the tumor after opening the Sylvian fissure, opticocarotid complex, and carotico-oculomotor triangle (Figure 1).

A tectal tumor was removed using the occipital transcallosal approach by splitting the splenium.

We resected three DIPGs; of these, two were ventral exophytic tumors that were resected through pterional craniotomy and by opening the prechiasmatic and interpeduncular cisterns (21). We used a thin-tipped ultrasonic suction tube to partially resect the tumor. In a patient with a posterior exophytic tumor, subependymal protrusion and portions obstructing the aqueduct were surgically removed using a classic posterior fossa approach through the cisterna magna, involving partial vermis splitting (22). The same procedure was used for four posterior exophytic medullary tumors. We resected 1/3 of the bottom part of the vermis (18). The same approach was used for two focal medullary tumors subjected to GTR. Three lateral exophytic medullary tumors were accessed through posterolateral incision and retromastoid craniotomy, similar to the approach used for pontocerebellar angle (PCA) tumors (25).

We did not perform a midline incision into the floor of the fourth ventricle. Furthermore, we did not descend beyond the base of the fourth ventricle, unless necessary (21). The tumor was resected from the center to the periphery (Figure 2).

If there was uncertainty regarding tissue identification, a frozen section was performed; meanwhile, the patient was monitored, and a stimulator was used (28). We preferred spontaneous respiration in all cases. If any alteration in respiratory or cardiac rhythm was observed, the surgery was stopped and resumed after recovery.

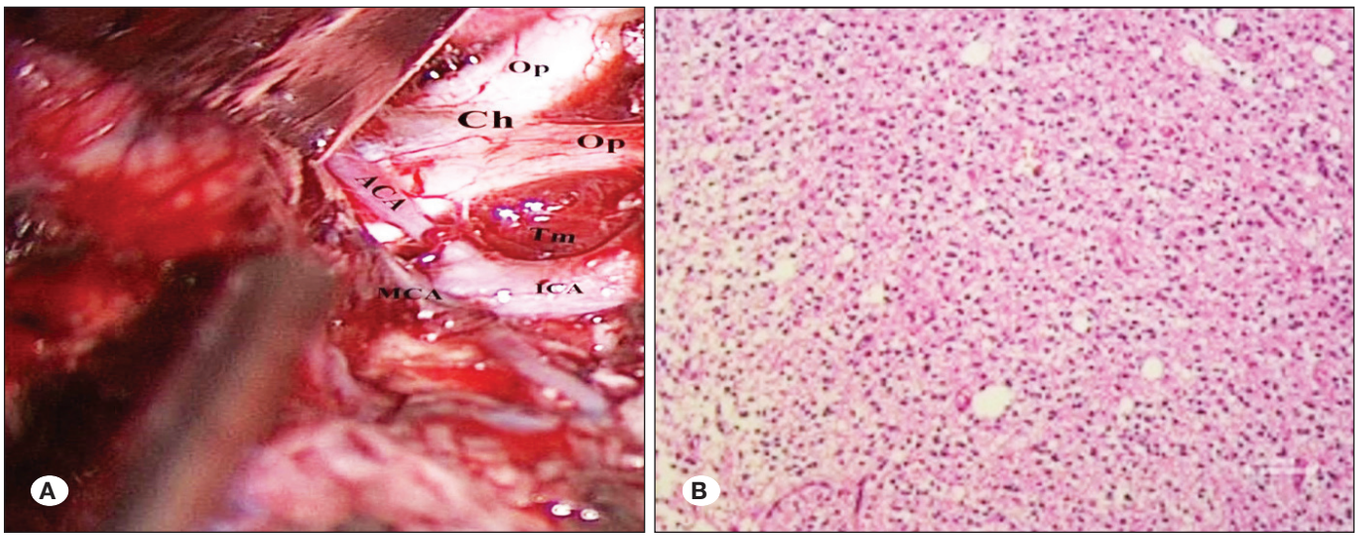

Figure 1: A) Surgical exposure via prechiasmatic, opticocarotid, and cortico-oculomotor triangle. **B)** Astrocytoma composed of fibrillary astrocytic cells with cytoplasm and fusiform nuclei. Hematoxylin and eosin (H&E) staining, ×100.

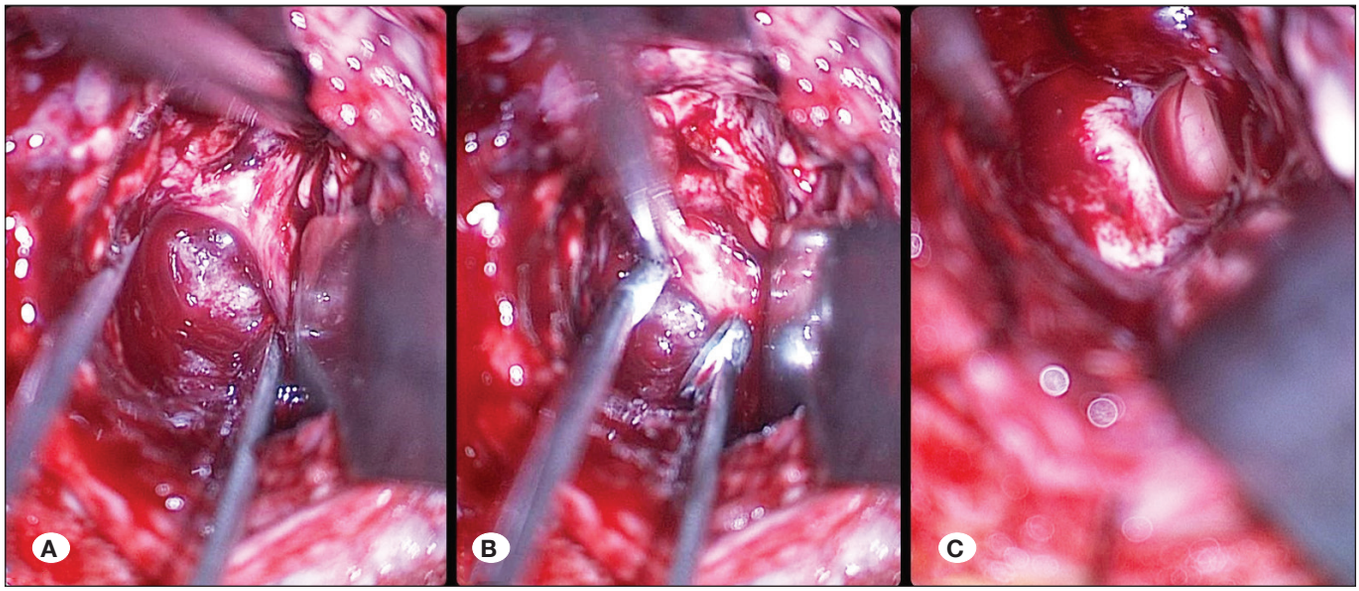

Figure 2: Patient #11. Piecemeal removal of the tumor from center to periphery; no glial barrier observed, consistent with infiltrative growth.

We gained access to the tumor through a cystic, discolored, protruding area with abnormal vascularization, choosing the shortest route to reach the exophytic region (22). We avoided the use of laser and bipolar cautery whenever possible. Bleeding ceased after applying gentle pressure with a wet cotton compress. Seven cervicomedullary tumors were surgically excised via a midline incision, adhering to standard microsurgical guidelines for accessing the fourth ventricle. However, a midline approach was not used for all cases; instead, a mediolateral approach was used when a protruding cystic area was present (28).

This retrospective study was conducted in accordance with the principles of the Declaration of Helsinki (32). All surgical and diagnostic procedures had been performed under the standard institutional regulations in place at the time of treatment, and written informed consent had been obtained from all patients and/or their legal guardians.

RESULTS

In 3 of the 22 patients with BSTs, the tumors were located in the midbrain. One patient with a tectal tumor was 35 years old and had papillary stasis and Parinaud's syndrome. In this patient, GTR was performed, and he was pathologically diagnosed with mature teratoma. The conditions resolved postoperatively. The other two patients were 3- and 7-year-old girls with a peduncular tumor who were pathologically diagnosed with pilocytic astrocytoma. Their symptoms, i.e., headache, nausea, and vomiting, improved after partial resection.

Two male patients aged 3 and 4 years had ventral exophytic DIPGs. One patient had primary optic atrophy, hydrocephalus, and a Glasgow Coma Scale (GCS) score of 5. In this patient, partial resection was performed and a V–P shunt was inserted for hydrocephalus. This patient was pathologically diagnosed with pilocytic astrocytoma and was found to gain consciousness postoperatively. However, the other patient showed no neurological symptoms, underwent partial resection, and was pathologically diagnosed with astrocytoma grade II.

A 6-year-old male patient with a dorsal exophytic DIPG had hydrocephalus and gait disturbance. After partial resection, the hydrocephalus improved. He was pathologically diagnosed with astrocytoma grade II.

Four patients had dorsal exophytic medullary focal tumors. The first patient was a 38-year-old man with cerebellar findings. He underwent GTR and was pathologically diagnosed with glioblastoma multiforme (GBM). The second patient was an 18-year-old woman with hydrocephalus and papillary stasis. She underwent GTR and was pathologically diagnosed with GBM. The third patient was a 21-year-old woman with cerebellar findings. She underwent near-total resection and was pathologically diagnosed with GBM. The fourth patient was an 11-year-old boy with multiple cranial nerve paralysis, gait imbalance, and diplopia. He underwent GTR and was pathologically diagnosed with ganglioglioma.

Three patients had lateral exophytic focal medullary tumors. The first patient was a 3-year-old girl with hydrocephalus and papillary stasis. She underwent GTR and was pathologically diagnosed with ependymoma. The second patient was a 4-year-old boy with hemiparesis and strabismus. He underwent partial resection and was pathologically diagnosed with ependymoma. The third patient was a 9-year-old boy with gait disturbance. He underwent partial resection and was pathologically diagnosed with pilocytic astrocytoma.

Two patients with focal medullary tumors underwent GTR. One patient was an 8-year-old boy with imbalance and diplopia who was pathologically diagnosed with astrocytoma grade II (Figure 3).

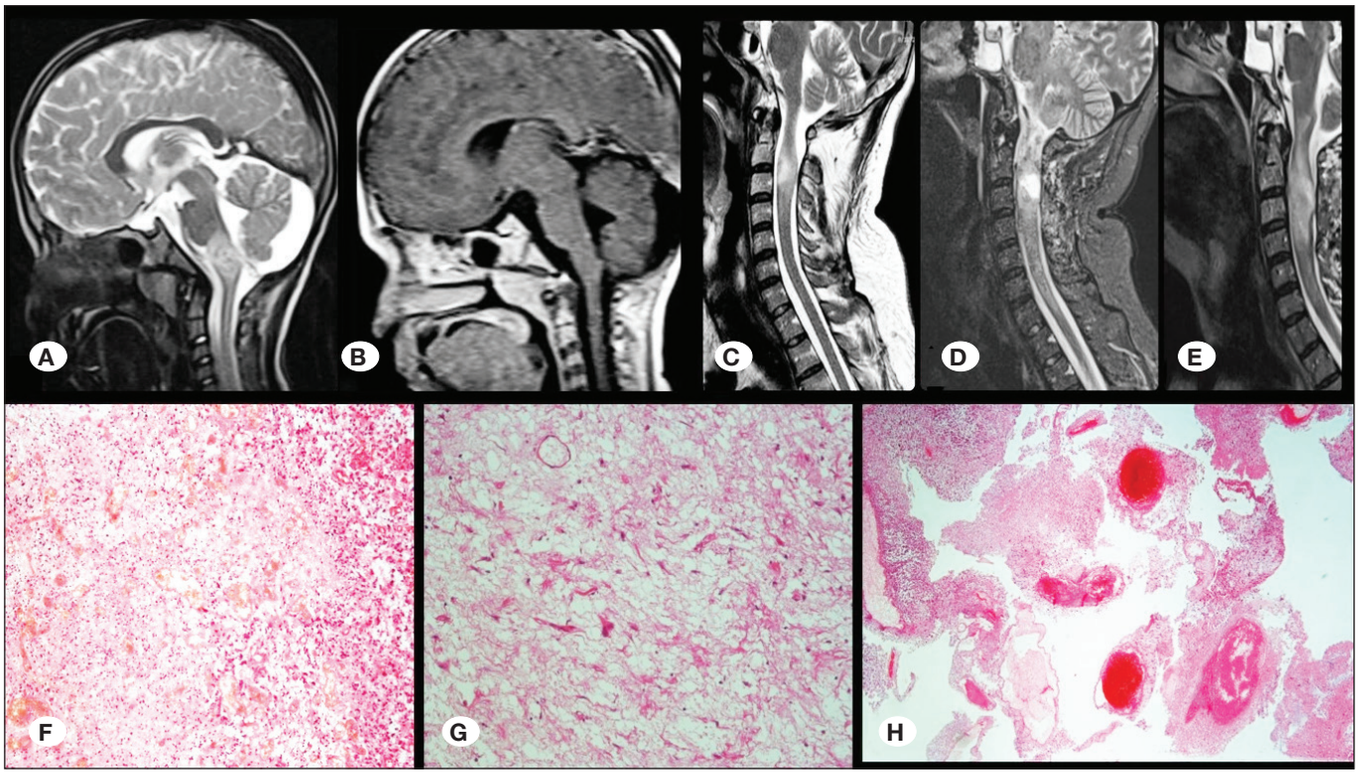

Figure 3: Patient #16. Focal medullary tumor, preoperative **(A)** and postoperative **(B)** MRI scans. Cervicomedullary Glioblastoma multiforme (GBM), preoperative **(C, D)** and postoperative **(E)** views. **F)** GBM, Hematoxylin and Eosin (H&E) staining, ×200. **G)** GBM, immunohistochemical staining, ×200. **H)** Thrombus mass in a dilated vessel of GBM, H&E, ×200, consistent with vascular invasion.

The other patient was a 13-year-old girl with gait disturbance who was pathologically diagnosed with oligodendroglioma.

Seven patients had cervicomedullary tumors. The first patient was a 27-year-old man with quadriparesis and respiratory disturbance. He underwent near-total resection and was pathologically diagnosed with GBM. His findings improved, except for the mild left hemiparesis. On postoperative day 2, he experienced irregular nocturnal breathing, which occurred at 7–8-h intervals. Breathing was supported, but the residual tumor quickly expanded to the distal and proximal areas. The patient died on postoperative day 75 due to respiratory arrest.

The second patient was a 20-year-old man with arm weakness. He underwent GTR and was pathologically diagnosed with GBM. The third patient was a 7-year-old girl with dysphagia. She underwent GTR and was pathologically diagnosed with pilocytic astrocytoma. Her condition improved in 1 week (Figure 4).

The fourth patient was a 4-year-old girl with papillary stasis and hydrocephalus. She underwent GTR and was pathologically diagnosed with ependymoma. Her pathological findings improved after GTR. The fifth patient was a 5-year-old girl with hemiparesis. She underwent partial resection and was pathologically diagnosed with astrocytoma grade II. Her hemiparesis improved after partial resection. The sixth patient was a 41-year-old man with papillary stasis and quadriparesis who was pathologically diagnosed with ependymoma (Figure 5).

The seventh patient was a 38-year-old man with quadriparesis, left spasmodic torticollis, and glossopharyngeal neuralgia. He underwent GTR and was pathologically diagnosed with hemangioblastoma. We accessed the saccular aneurysm at the origin of the posterior inferior cerebellar artery by following the left vertebral artery. His conditions improved postoperatively (Figure 6).

Except for the children, all patients suffered from headache and vomiting. The study population consisted of 22 patients, including 12 female and 10 male patients. Of them, eight were adults (mean age: 29.8 years) and four were children (mean age: 6.2 years). The mean age of all patients was 14.7 years.

Of the 22 patients in this study, 4 had long tractus symptoms, 3 had hydrocephalus, 5 had papillary stasis, 4 had cerebellar findings, 3 had gait disturbance, 1 had respiratory disturbance, and 1 had aglutition. Ten, four, and eight patients underwent GTR, near-total resection, and partial resection, respectively.

The detailed demographic and clinical characteristics of all 22 patients are summarized in Table I.

DISCUSSION

Advances in anesthesia and asepsis led to significant improvements in abdominal and thoracic surgeries during the 19th century. However, brain tumor surgery could not be significantly improved because it is difficult to accurately localize these tumors (9). In 1884, Richman Godlee localized an IC

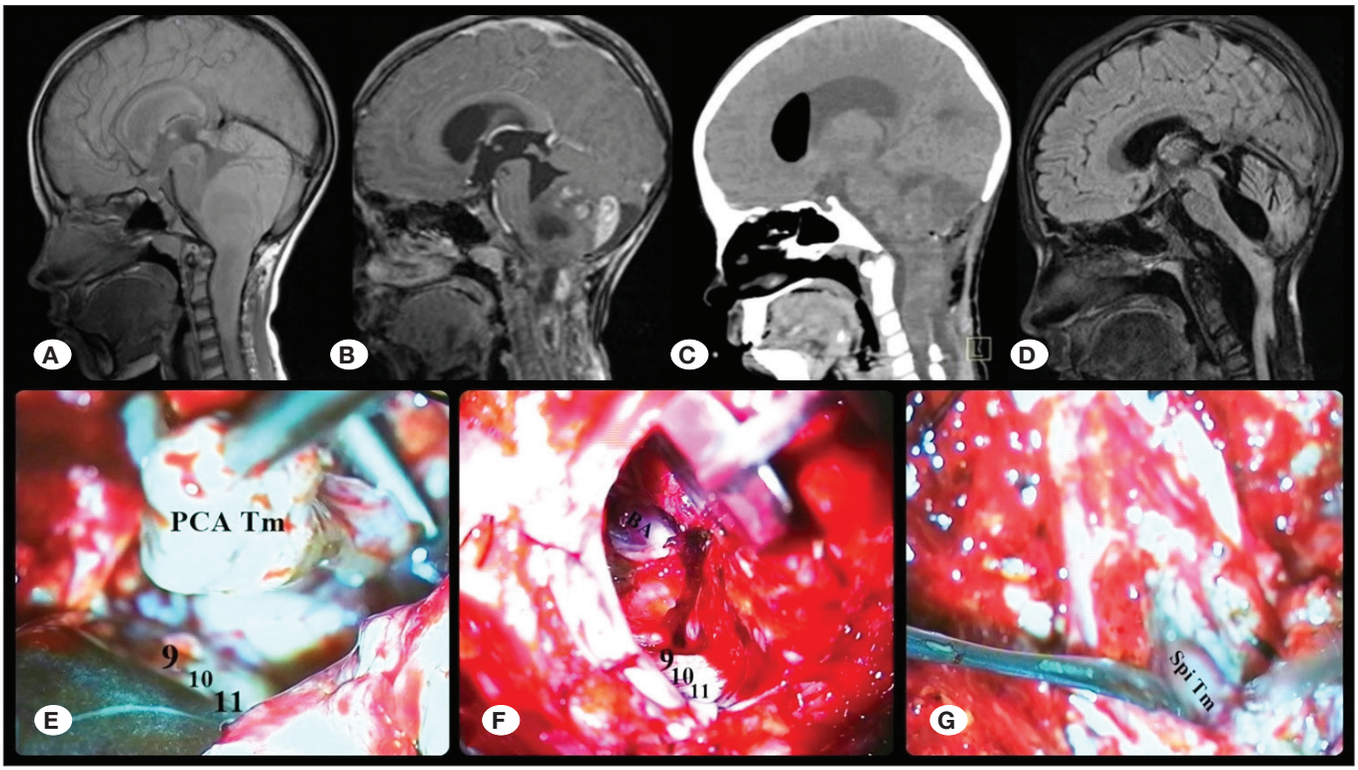

Figure 4: Patient #18. Pilocytic astrocytoma extending to the fourth ventricle, posterior cranial area (PCA), and cervicomedullary region. **A)** Preoperative T1W sagittal MR imaging. **B)** Multiple cystic structures and heterogeneous contrast enhancement in T1W sagittal MR image. **C)** Early postoperative CT scan. **D)** Late postoperative period (1 year after surgery). **E–G)** Cervicomedullary tumor with exophytic lateral extension into the PCA; postoperative follow-up shows resolution of hydrocephalus and gait disturbance.

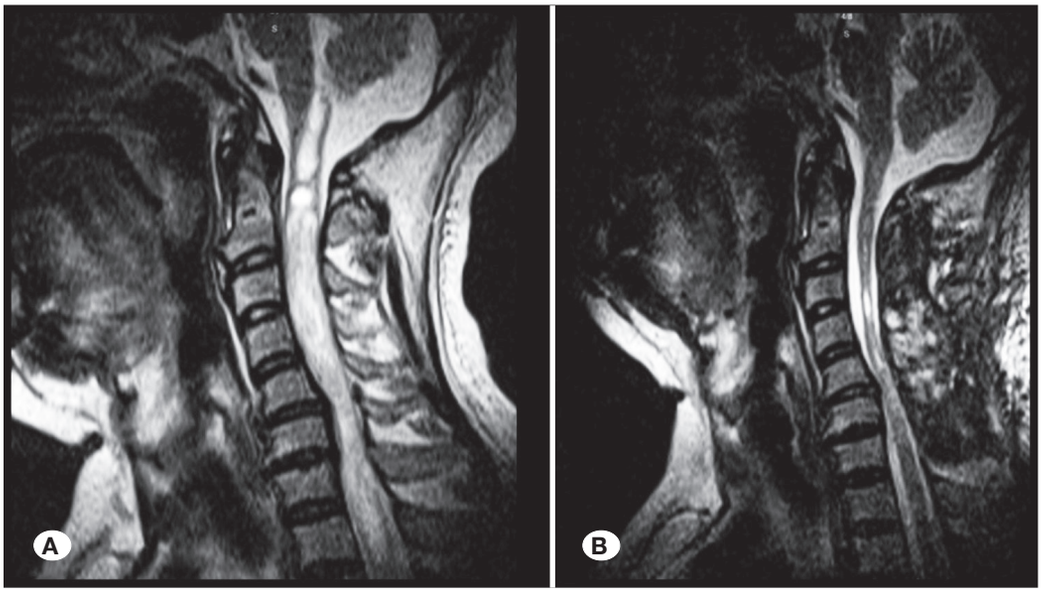

Figure 5: (Patient #19) T2W sagittal MRI scans. Preoperative **(A)** and postoperative **(B)**.

tumor in a patient with focal epilepsy through neurological examination and performed a successful operation (17). During this period, some brave surgeons attempted to treat desperate patients through craniotomy; however, most of them were unsuccessful as they could not localize the lesion (15). In the 1950s, advancements in neurology deepened our understanding of brain anatomy and physiology. Consequently, a significant increase in the rates of intracranial tumor surgery and GTR was observed, except for BSTs (3). At the end of the 20th century, advancements in imaging techniques allowed for precise tumor localization and a preliminary understanding of its histological characteristics (9). Furthermore, advances in

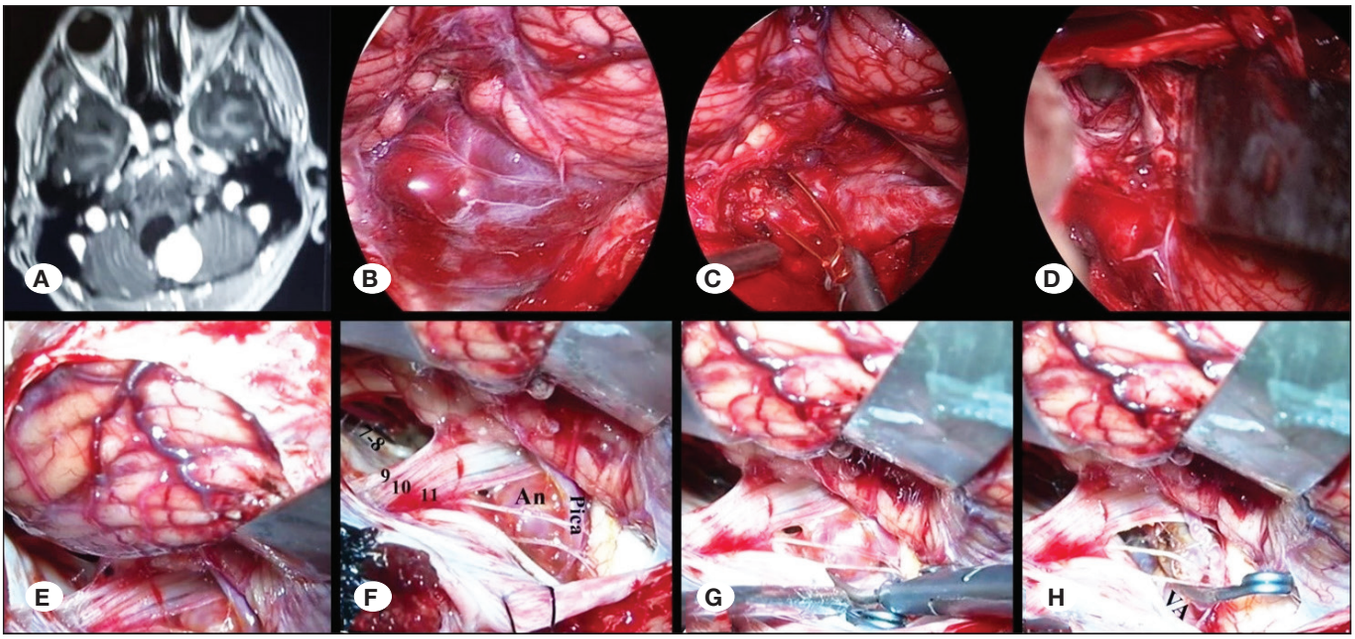

Figure 6: Patient #22. **A)** Preoperative axial contrast enhanced T1W MRI, **B–D)** Cervicomedullary hemangioblastoma in operative micrographs. **E–H)** PICA aneurysm coexisting with cervicomedullary hemangioblastoma. Complete removal of the hemangioblastoma and associated PICA aneurysm confirmed.

Table I: Detailed Demographic and Clinical Characteristics of All 22 Patients

Case	Age (years)	Sex	Tumor Location	Surgical Approach	Extent of Resection	Histopathology
1	35	F	Midbrain	Posterior transcallosal	GTR	Teratoma
2	3	F	Peduncle	Pterional	Partial	Pilocytic astrocytoma
3	7	F	Peduncle	Pterional	Partial	Pilocytic astrocytoma
4	3	M	Pons	Pterional	Partial	Pilocytic astrocytoma
5	4	M	Pons	Pterional	Partial	Astrocytoma, WHO Grade II
6	6	M	Pons	Posterior fossa	Partial	Astrocytoma, WHO Grade II
7	38	M	Medulla	Posterior fossa	GTR	GBM
8	18	F	Medulla	Posterior fossa	GTR	GBM
9	21	F	Medulla	Posterior fossa	Near-total	GBM
10	11	M	Medulla	Posterior fossa	GTR	Ganglioglioma
11	3	F	Medulla	Retromastoid	GTR	Ependymoma
12	4	M	Medulla	Retromastoid	Partial	Ependymoma
13	9	M	Medulla	Retromastoid	Partial	Pilocytic astrocytoma
14	8	M	Medulla	Posterior fossa	GTR	Astrocytoma, WHO Grade II
15	13	F	Medulla	Posterior fossa	GTR	Oligodendroglioma
16	27	M	Cervico-medullary	Posterior fossa	Near-total	GBM
17	20	M	Cervico-medullary	Posterior fossa	GTR	GBM
18	7	F	Cervico-medullary	Posterior fossa	GTR	Pilocytic astrocytoma
19	4	F	Cervico-medullary	Posterior fossa	GTR	Ependymoma
20	5	F	Cervico-medullary	Posterior fossa	Partial	Astrocytoma, WHO Grade II
21	41	M	Cervico-medullary	Posterior fossa	GTR	Ependymoma
22	38	M	Cervico-medullary	Posterior fossa	GTR	Hemangioblastoma

GBM: *Glioblastoma multiforme,* ***GTR:*** *Gross total resection*

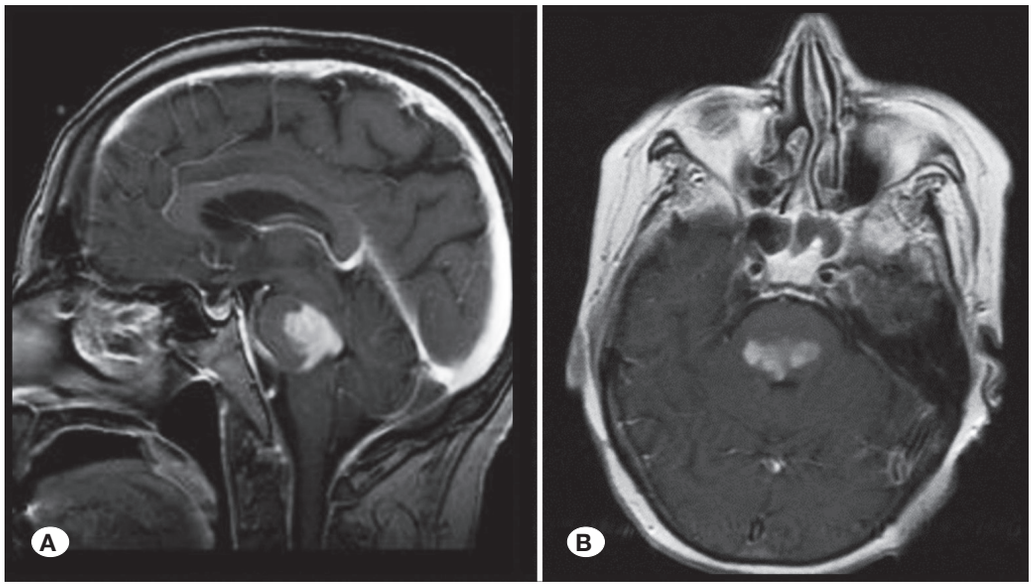

Figure 7: Sagittal **(A)** and axial **(B)** T1W contrast enhanced MR images show symmetric expansion of DIPGs in both transverse and vertical planes [image(s) courtesy of the authors' archive].

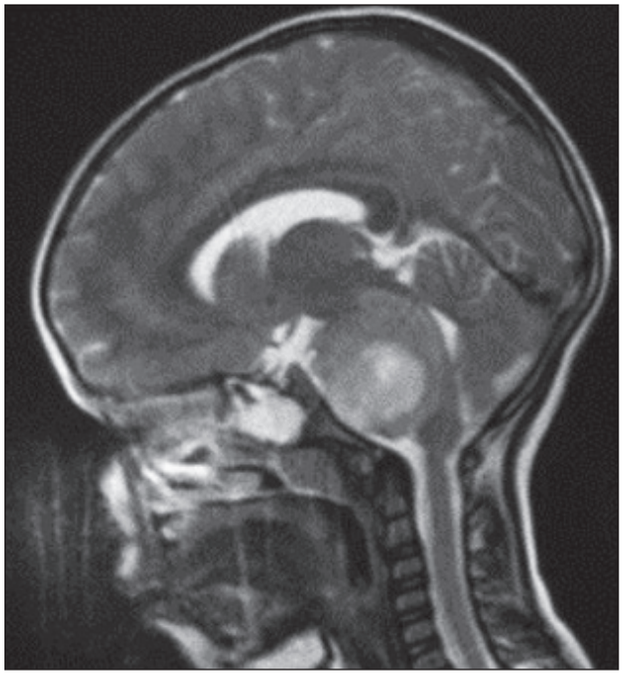

Figure 8: Enlarged (fat) pons [image(s) courtesy of the authors' archive].

microsurgical instruments increased the likelihood of a successful surgery. However, no success has been observed in the treatment of BSTs because most of them are diffuse, aggressive, highly invasive, infiltrative, and malignant. Moreover, they lack clear demarcation and are surrounded by normal tissues, leading to a high recurrence rate (17). BSTs exhibit life-threatening, extensive, and critical anatomical structures and progress rapidly. Furthermore, determining a functional entrance route to reach the tumor is challenging (15,17).

The brainstem contains corticopedal and corticofugal pathways, projection tracts, nuclei of the reticular formation, and centers responsible for respiratory and cardiovascular functions (24). It plays a pivotal role in muscle tonus, consciousness, awareness, and regulation of motor responses to stimuli (15). The nuclei of all cranial nerves and neurons, except for the first two cranial nerves, are settled in the brainstem (24).

Catecholamine, indolamine, encephalin, and many other neurotransmitters are secreted from the brainstem. Therefore, currently, these tumor types are not treated via surgery (24).

In the 2000s, developments in MRI technologies, including diffusion tensor imaging, functional MRI, spectroscopic MRI, and diffusion MRI, allowed for precise identification of brainstem tumors, their cellular characteristics, surrounding tissues, and functional access points (10). During operation, the use of MRI, ultrasound (USG), somatosensory evoked potential, motor evoked potential (12), multimodality evoked potential, and nerve and nucleus stimulation along with neuronavigation assistance enables successful BST resection and minimizes morbidity and mortality (28).

Sulci, gyri, and a functional area at the base of the fourth ventricle do not develop before the age of 4 years (6,15). Furthermore, cortical stimulation is inexcitable before the age of 8 years. Therefore, navigation (mapping) cannot be performed. Since 75% of BSTs develop in children, problems remain unsolved (1,8).

In DIPGs, which constitute 80% of BSTs, surgery is not indicated if the exophytic component is absent. Although approximately 86% of DIPGs in children are histologically classified as diffuse infiltrative fibrillary astrocytoma grade II (15), these tumors often behave like supratentorial high-grade gliomas in the pediatric population. They are infiltrative, aggressive, and progressive in nature, lacking encapsulation or clear demarcation lines, and tend to spread symmetrically in both vertical and transverse directions (15,28) (Figure 7).

If RT is not applied, malignant transformation does not occur. Pons enlarges (fat pons) (Figure 8). The midbrain, medulla, and

peduncles sometimes have an anterior exophytic component and rarely a posterior exophytic component (31).

It pushes the fourth ventricle back and causes a subependymal bulging at the rhomboid fossa (Figure 9).

Subarachnoid spread occurs and envelops at the vertebral artery (VA) and basilar artery (BA) in 50% of the patients (19,31). Tumor may spread to the prepontine, interpeduncular, prechiasmatic, and suprachiasmatic cisterns and diencephalon. It spreads through fibers and attaches to critical areas. It can be cystic, and focal growth may develop in 10% of cases. Furthermore, leptomeningeal infiltration may be detected in 5%–25% of cases, which can often lead to death in a short time. Spontaneous regression can also occur occasionally (31) (Figure 10).

Pilocytic astrocytoma in the pons is the second most frequently observed tumor. Dysembryoplastic neuroepithelial tumor, PNET, AT/RT, ependymoma, and primary and secondary GBM can also be detected (25). Hemisphere tumors can infiltrate the pons (20) (Figure 11).

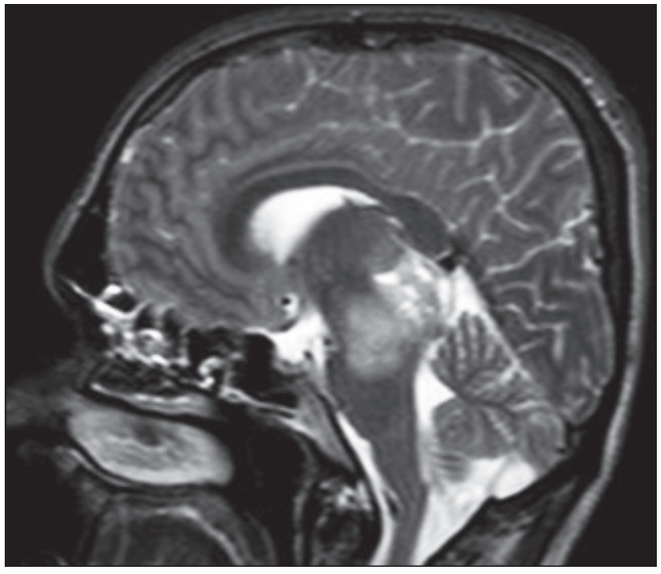

Figure 9: Infiltration of a tectal tumor into the pons [image(s) courtesy of the authors' archive].

In 2018, we encountered a case of a patient with DIPG who had hydrocephalus. The tumor had spread to the prepontine prechiasmatic cistern. His GCS score was 5, and due to his unconscious state, a ventricular drain was inserted. He was later discharged from the hospital as he could not be operated. Subsequently, he was admitted to our hospital and subjected to ventriculoperitoneal shunt, pterional craniotomy, and Sylvian dissection. We explored the tumor through the triangular opening of opticocarotid and carotico-oculomotor. Tumor tissues in the cisterns were removed using a thin pointed ultrasonic suction until the BA was seen (9) (Figure 12).

The patient regained his consciousness and was discharged from the hospital on the 10th day. He underwent chemotherapy and was pathologically diagnosed with pilocytic astrocytoma. He has been living without assistance for the last 5 years.

However, it was noted that attempting resection would provide minimal benefit. We partially resected one ventral exophytic pontine tumor and two midbrain peduncular tumors using the same approach, without any complication. The pathological diagnosis of the DIPG was astrocytoma grade II, whereas the peduncular tumors were diagnosed as pilocytic astrocytoma. Although 5% of pilocytic astrocytomas are reportedly associated with neurofibromatosis types I and II (NF1 and NF2), none of our cases presented with NF. Peduncular tumors can be removed using the infratemporal approach, which involves opening the tentorium through the corridor inside the transchoroideal fissure; however, we do not have any experience in this approach (20).

A DIPG with a posterior exophytic component at the left superior fossa occluded the aqueduct entrance of the fourth ventricle and resulted in hydrocephalus. To reach the lesion, we nearly had to totally separate the cerebellar vermis. In patients who undergo total vermis separation, mutism can develop due to the dentato rubro thalamic tract lesion; however, we

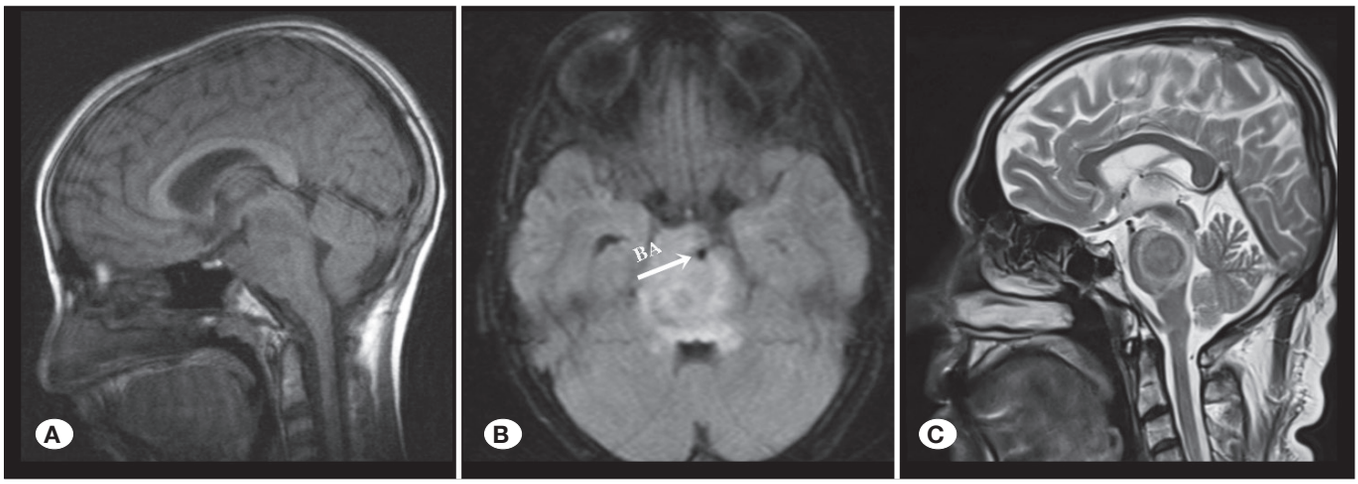

Figure 10: Infiltration of a ventral exophytic pontine tumor into the midbrain and medulla; basilar artery (BA) surrounded [image(s) courtesy of the authors' archive].

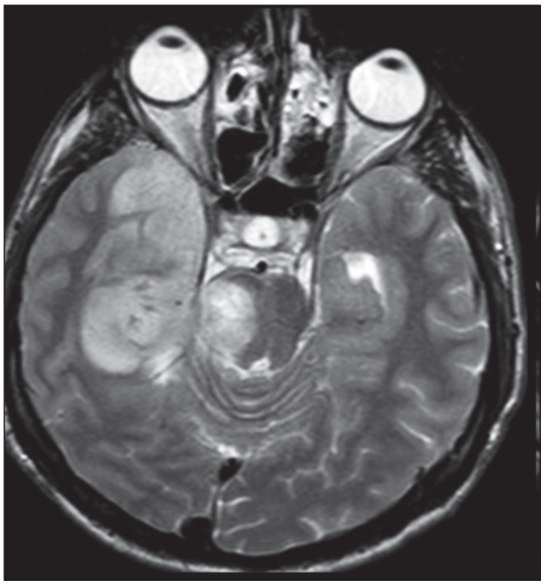

Figure 11: Infiltration of a hemispheric tumor into the pons [image(s) courtesy of the authors' archive].

did not detect mutism in any of our cases (1,23). We opened the subependymal and obliterated parts of the aqueduct. No additional neurological deficit developed. The pathological diagnosis was diffuse fibrillary astrocytoma grade II.

Midbrain tectal tumor is rare and exhibits an indolent course if hydrocephalus is absent (18). Surgical management of these tumors requires careful planning and proper technical approaches (30). A 35-year-old woman had headache, hydrocephalus, and Parinaud's syndrome. She underwent GTR, in which the splenium was opened using the posterior transcallosal approach, and was pathologically diagnosed with teratoma. Her conditions improved postoperatively (12) (Figure 13).

Small tectal tumors have a high likelihood of being hamartomas; moreover, they can be indolent for a long time. We followed up three patients for 10 years and no changes were observed during the follow-up (6,10) (Figure 14).

Most tectal tumors are astrocytomas and have an indolent course (5). They can be cystic, low-grade, and anaplastic

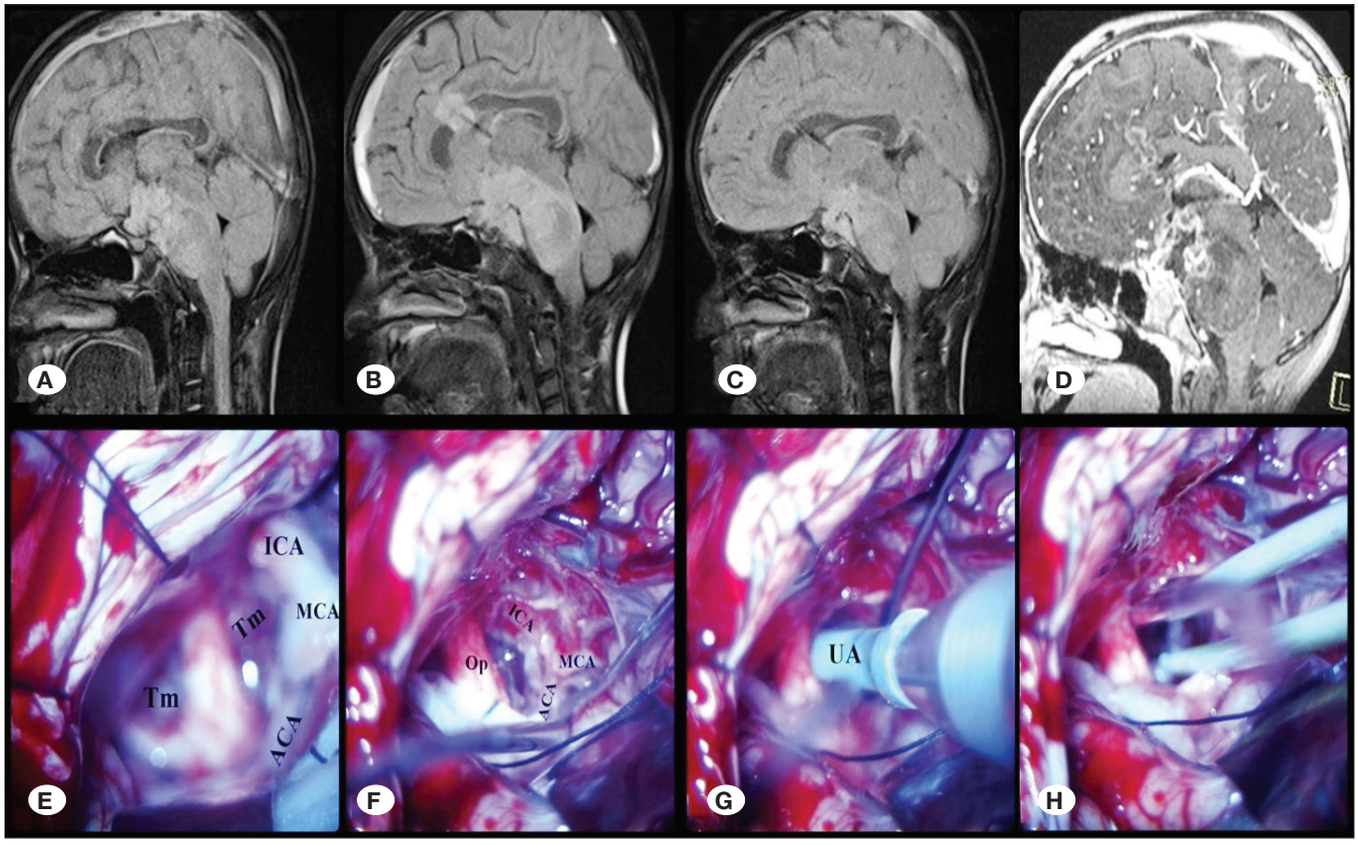

Figure 12: Patient #3. **A)** Preoperative sagittal T1-weighted MRI demonstrating the brainstem tumor. **B)** Preoperative sagittal MRI showing the lesion and its relationship to the surrounding structures. **C)** Early postoperative sagittal MRI confirming decompression of the brainstem and adequate tumor debulking. **D)** Late postoperative sagittal MRI at follow-up demonstrating stable postoperative changes without radiological progression. **E)** Intraoperative microscopic view after pterional craniotomy and Sylvian fissure dissection, showing the tumor (T) and surrounding vascular structures (ICA, MCA). **F)** Intraoperative view demonstrating further tumor exposure and debulking within the operative field. **G)** Intraoperative view showing the ultrasonic aspirator (UA) in the prechiasmatic cistern, used for piecemeal tumor removal. **H)** Final intraoperative view after debulking, illustrating decompression of the critical neurovascular structures.

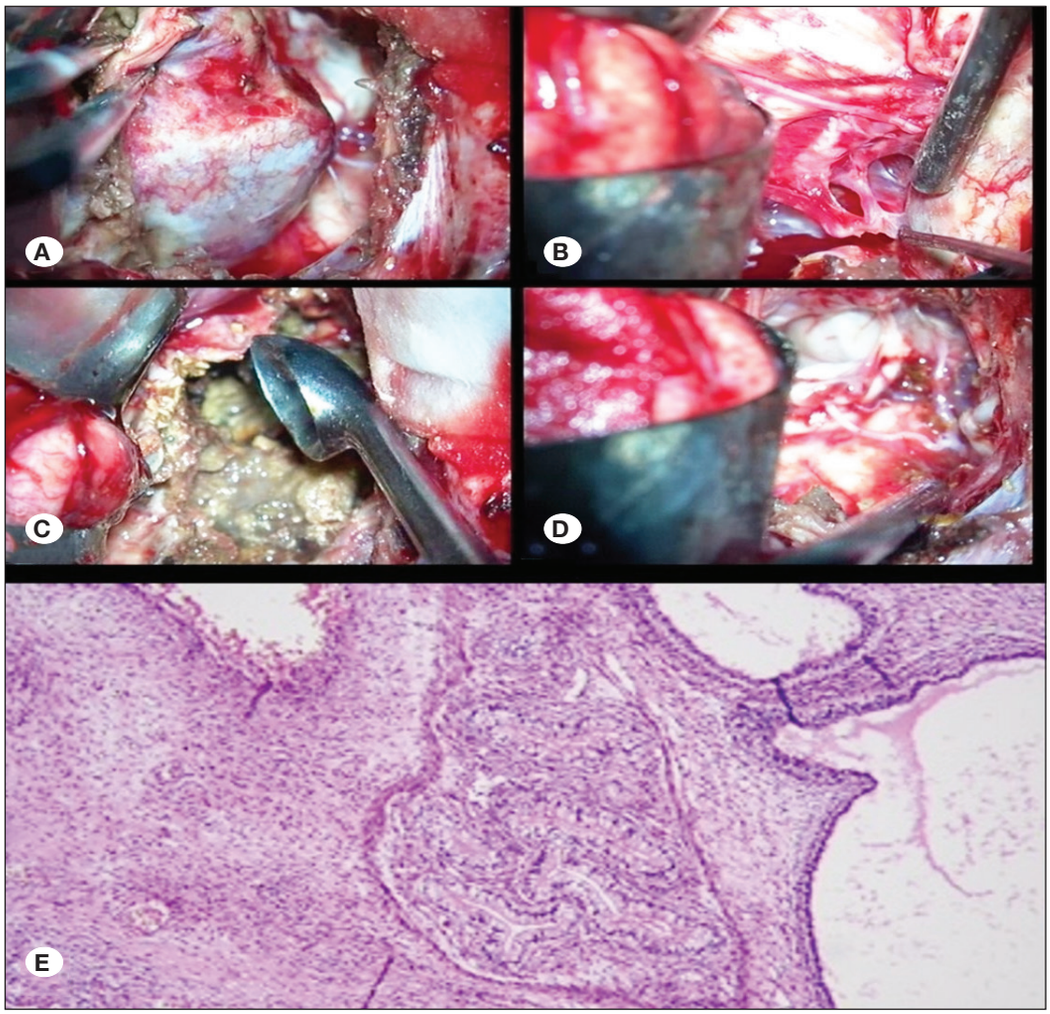

Figure 13: Patient #1. Posterior transcallosal teratoma located at the superior colliculus. **A)** Removal of the collicular component. **B)** Separation of vascular adherence. **C)** Tumor decompression. **D)** Total resection of the superior colliculus and pineal and cavum vergae components. **E)** Teratoma composed of multiple germ layers, including gastrointestinal-type glands lined with columnar epithelium. (H&E staining, ×200).

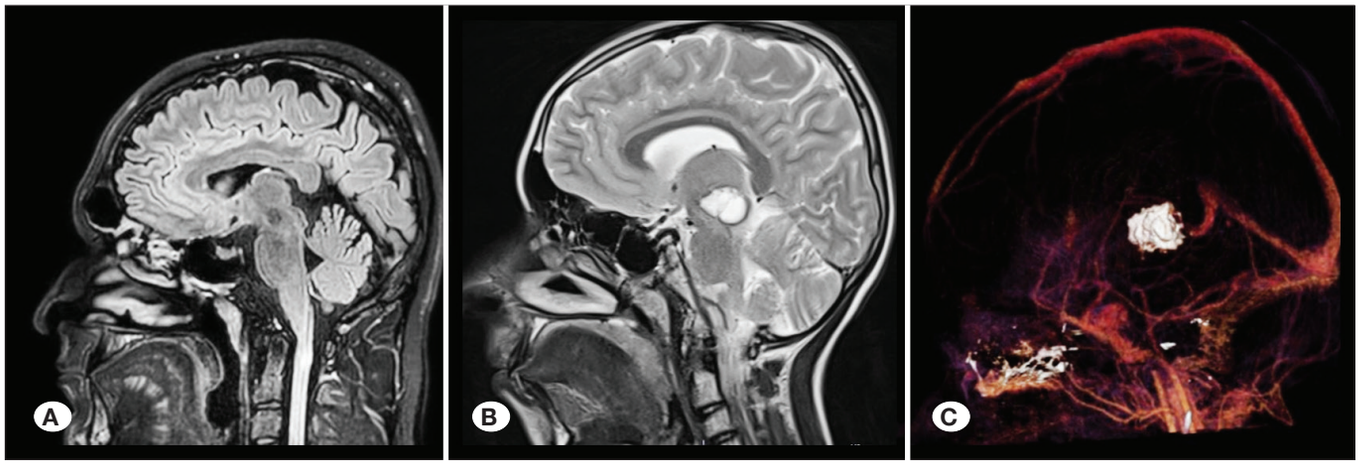

Figure 14: A tumor in the mesencephalon remaining indolent over several years [image(s) courtesy of the authors' archive].

gangliogliomas, gangliocytomas, or oligodendrogliomas or even PNETs (12). As observed in our cases, other conditions such as Parinaud's syndrome, head bobbing, Weber's syndrome, Benedict's syndrome, and strabismus can also be observed in patients with tectal tumors (1,23).

The midbrain has a perfect vascular structure (26). If tracts and nuclei are not damaged, then neurological deficits are not likely to occur. Sometimes, despite the development of hydrocephalus, computed tomography does not reveal a lesion (11) and can be misdiagnosed as idiopathic aquaeductus stenosis (25).

MRI enables the localization of tumors and identification of their histological characteristics, rendering biopsy nonessential to treatment (33). Sampling is inadequate in 35% of cases, and in 30%, it is inaccurate and lacks correlation with nondiagnostic results, resulting in 3% mortality and 4% morbidity. Stimulation of the trigeminal tractus results in an intense pain sensation (4). In instances where MRI displays atypical presentation and suggests the possibility of a noncancerous tumor, a diagnosis is typically made via an image-guided stereotactic biopsy in 96% of cases (14). DIPG is resistant to chemotherapy as macromolecules are unable to pass through an intact blood–brain barrier. Microantibodies (15) and cytokine overexpression occur in 70% of cases (23). Inhibiting agents are used, but their effects remain controversial. Radiotherapy serves as the primary treatment modality (31).

Most medullary and cervicomedullary tumors are of focal and posterior exophytic types (28). They are demarcated and convenient for GTR; however, GTR is not recommended as most of these tumors are of low grade and pilocytic astrocytomas (20) (Figure 15).

Even after partial resection, patients can live for a long time independently (19). Anaplastic astrocytoma, GBM, ganglioglioma, ependymoma, hemangioma, oligoastrocytoma, and endothelioma are rare (18) (Figure 16).

In general, cervicomedullary tumors are unable to pass through the decussation pyramidalis and tractus; therefore, they push the medulla and fourth ventricle upward (28). At this site, the tumor becomes distorted and forms an exophytic portion by protruding posteriorly. The long tracts are also pushed and become flattened (28). This area can be used for the careful delivery of the tumor to the tracti (28).

Occasionally, the tumor extends to the decussation, fills the cisterna magna, and displaces the obex (28). It can also invade the CPA and attach to the 9th, 10th, and 11th cranial nerves (low group). Aspiration pneumonia may develop due to hydrocephalus and dysphagia (22). The children admit to

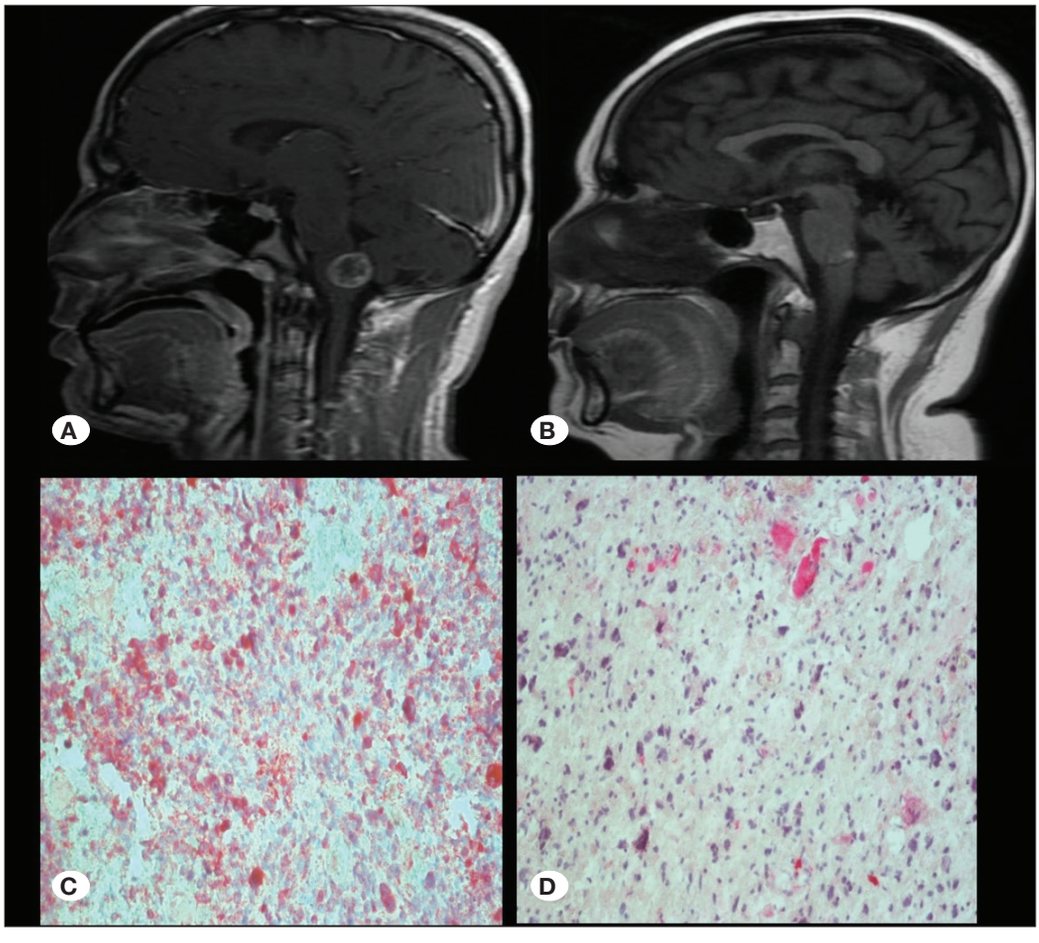

Figure 15: Patient #14. Medullary focal tumor. **A)** Preoperative sagittal T1W contrast enhanced MRI. **B)** Postoperative sagittal T1W MRI. **C)** Low-grade astrocytoma (H&E staining, ×100), **D)** immunohistochemical staining, ×200.

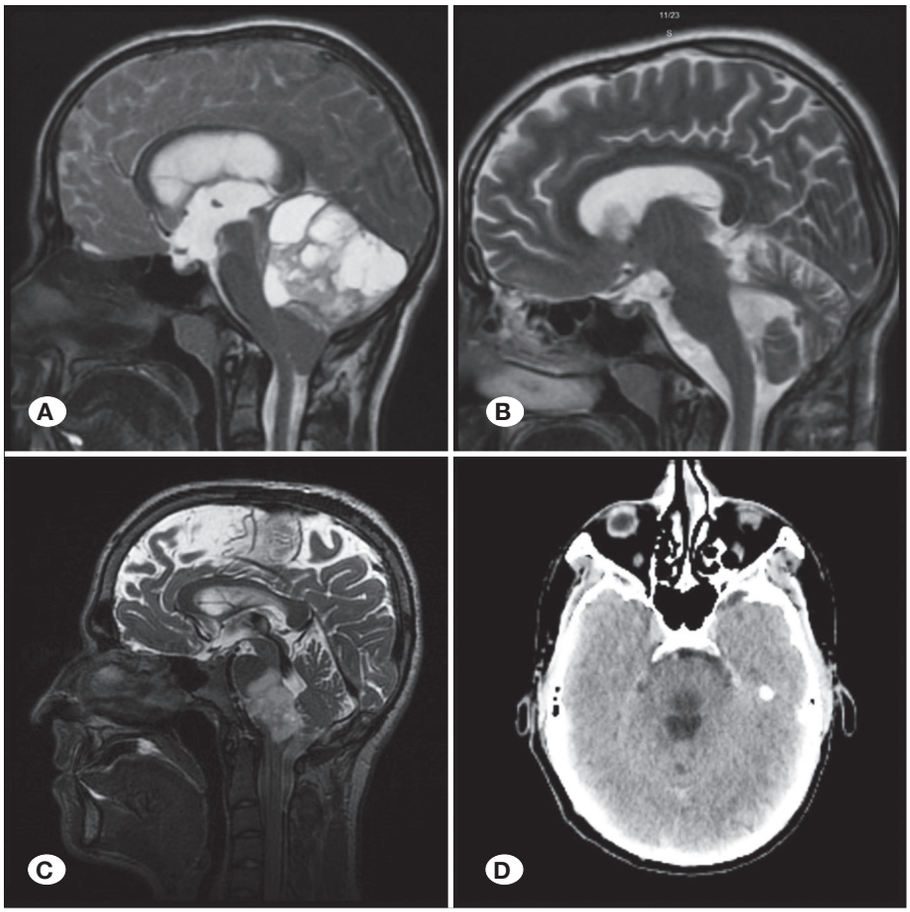

Figure 16: Patient #15. Dorsal exophytic medullary tumor. **A and C)** Preoperative T2W sagittal MRIs. Postoperative **B)** sagittal T2W MRI and **D)** axial CT images. No recurrence observed on postoperative imaging.

Figure 17: Cervicomedullary tumor exceeding the decussation pyramidalis and occupying the fourth ventricle, causing hydrocephalus in sagittal MR image [image(s) courtesy of the authors' archive].

gastroenterology and lung disease centers. The children have a long natural history, with 80% of them having headache with vomiting (27) (Figure 17).

In our patients with cervicomedullary tumors, the tumor passed decussation pyramidalis, filled cisterna magna, and displaced obex (28). Both patients had papillary stasis, and one had hydrocephalus. In one of our patients with cervicomedullary tumor, the tumor reached the PCA, involved the lower group, and caused dysphagia. This patient developed aspiration pneumonia and dysphagia and recovered in the first month. Almost all patients experienced headache. Notably, headache can be present with benign causes during childhood (27) (Figure 4).

Lateral exophytic medulla tumors have symptoms similar to those of PCA tumors and are resected through retromastoid craniectomy (22). Cysts and mural nodules are present in most of these tumors; furthermore, they expand to the subependymal area and displace the fourth ventricle (29). Tumors that fill the ventricles are resected in a similar manner to posterior fossa tumors (28). C1–2 laminectomy can be used based on the situation of the occiput and tonsil. For patients up to 4 years of age, the operation is performed in the concorde position (28,29). For older children and adults, the operation is performed in the sitting position, taking precautions for air embolism. Because we are used to the

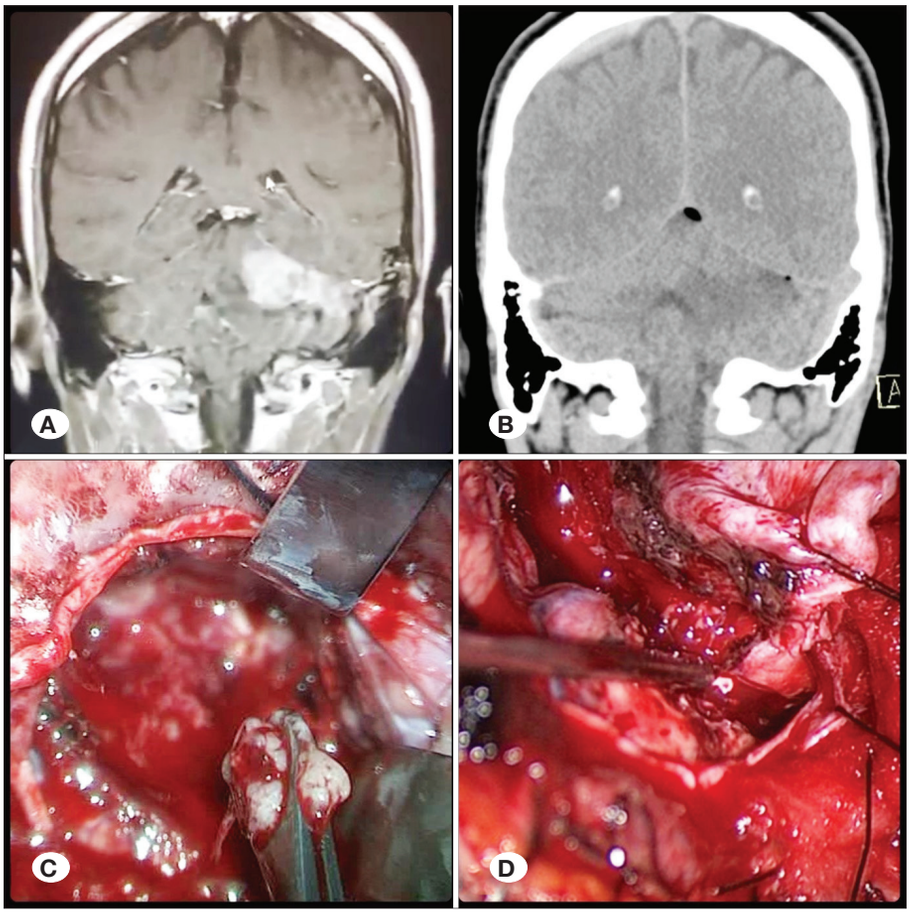

Figure 18: Patient #10. **A)** Preoperative T1W contrast enhanced coronal MRI. **B)** Postoperative coronal reconstructed CT scan. **C)** Piecemeal tumor removal. **D)** Gross total resection (GTR) confirmed.

sitting position, we preferred this for patients over 8 years old, with no complications other than pneumocephalus reported (22,28) (Figure 18).

The symptoms of cervicomedullary tumors are similar to those of spinal intramedullary tumors, and torticollis, irregular nocturnal breathing, and abscess can develop (28). They generally benefit from surgery. In one series 5 of 16 cases who underwent medulla and cervicomedullary junction surgery had favorable outcomes (28). A 38-year-old man was diagnosed with a focal medulla tumor, and GTR was performed in 2011. He was pathologically diagnosed with GBM. We recommended RT and chemotherapy and sent him to the oncology department (8). Subsequently, in 2017, he was admitted to our clinic due to the complaints of headache and vomiting (17); his MRI revealed tumor recurrence. Thus, we performed GTR again. Multiple metastases developed 1 year later; thus, we recommended chemotherapy (7) (Figure 19).

Of the seven patients who underwent surgery for cervicomedullary tumors, five had long tractus defect, two had hemiparesis, one had bilateral arm weakness, two had quadriparesis, and one had glossopharyngeal neuralgia and spasmodic torticollis. Based on these findings, we considered that the tumor involved the left lower cranial nerves (22).

Craniectomy was performed through a midline incision in the posterior fossa, and laminectomy was performed up to the C3 level. The bleeding tumor with intermedullary components was completely removed via resection, and temporary clips were applied during the procedure to areas with severe bleeding, where a possible vertebral aneurysm was suspected (28). After the GTR procedure, we removed the clips and exposed the fourth ventricle but found no evidence of a tumor. We then followed the VA to locate the glossopharyngeal neuralgia and identified and clipped a saccular aneurysm at the posterior inferior cerebral artery's exit (Figure 6).

We detected insignificant C7 hypoesthesia in two patients. Postoperatively, these patients developed left hemiparesis, and these symptoms resolved quickly after surgery.

We detected a cervicomedullary tumor in a 27-year-old man who had hypoesthesia on the left arm. He refused to undergo any operation. However, 3 months later, he was admitted to our clinic due to quadriparesis and dyspnea. Consequently, operation was performed urgently. We applied near-total resection with C2–3 laminectomy and midline cord incision. Postoperatively, deficits other than insignificant left hemiparesis resolved, but breathing distress at intervals of 5–6 h continued. On the 3rd day, irregular nocturnal breathing started (28). Tracheostomy was performed 1 week later, and he was pathologically diagnosed with GBM. Diaphragmatic

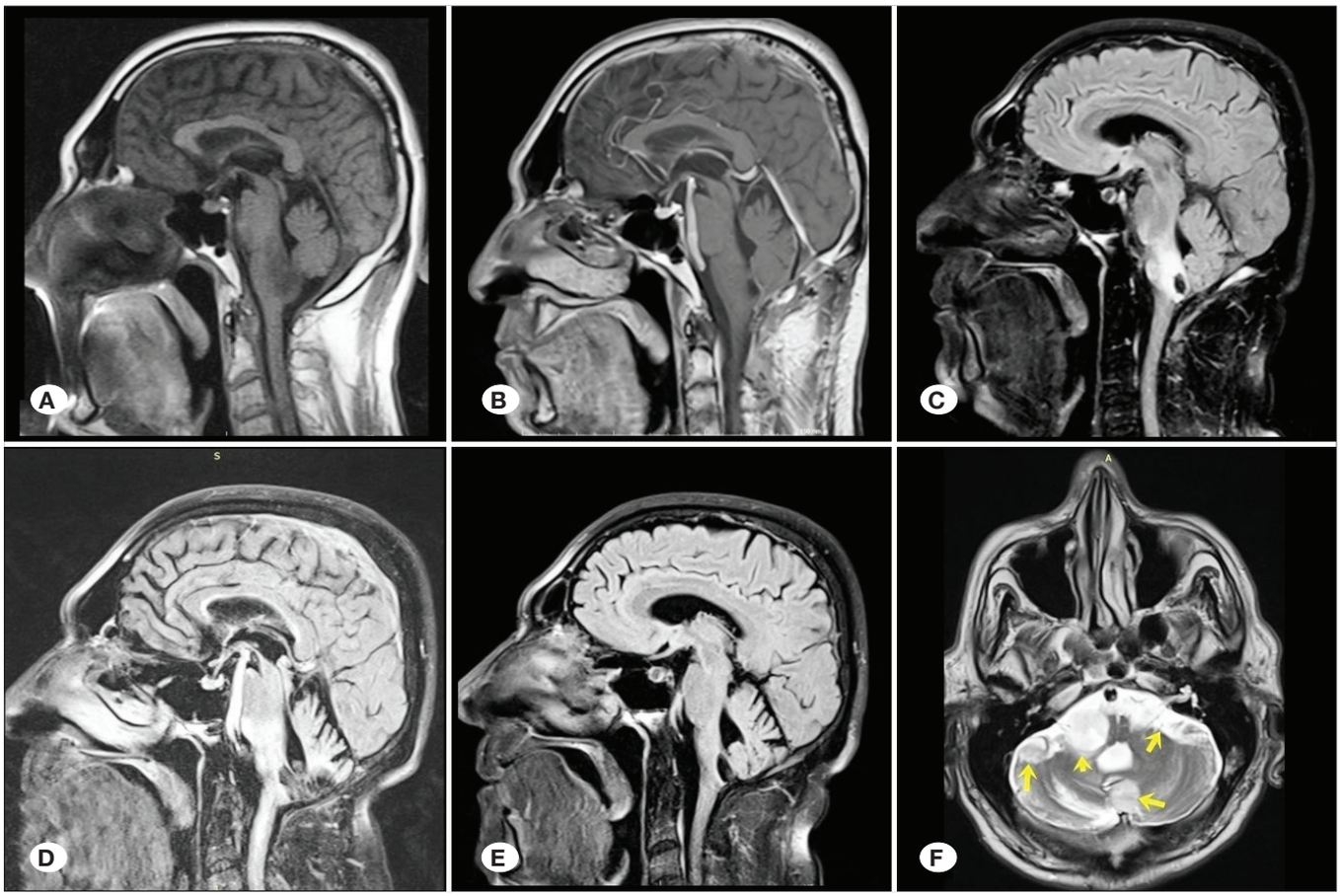

Figure 19: Patient #17. Medullary GBM. **A)** Preoperative sagittal T1W MRI at the time of diagnosis. **B)** T1W contrast enhanced sagittal MRI after first operation. **C)** FLAIR sagittal MRI after radiotherapy (2015). **D)** Sagittal T1W contrast enhanced MRI shows residual tumor (2018). **E)** FLAIR sagittal MRI after second operation. **F)** T2W axial MRI shows multiple metastatic lesions (2020).

respiration was insufficient, and the intercostal muscles were normal (Figure 3C-E).

Although Tsai and Rutka stated that recovery will be extremely slow, all symptoms resolved, except for breathing (28). Because of breathing distress, we could not apply RT and chemotherapy. At 2 months postoperatively, breathing support was provided at night. At the end of 2 months, proximal and distal tumor progression was detected. The patient died 2.5 months later due to respiratory arrest. Among the other two patients with medullary tumors, one with a cervicomedullary tumor developed recurrence within 3 years following RT and chemotherapy. Tsai and Rutka reported that 10%–20% of cervical tumors are of high grade (28). Two of our seven patients were diagnosed with GBM.

At times, it is impossible to differentiate tumor tissues from normal tissues surrounding the tumor (22). In this case, intraoperative MRI and USG can be used. However, due to the lack of opportunity, we performed frozen biopsy (29). In one case, we initially believed that the tumor had been completely removed; however, frozen biopsy of the surrounding tissue revealed astrocytoma grade II.

We avoided putting the patient at risk when the ultrasound imaging was unable to distinguish between the normal and tumor tissues. Postoperative MRI revealed a near-total resection. In another case, cavernous malformation was observed at the medulla; moreover, bleeding tissues were detected at the base of the fourth ventricle, but no cavernomas were observed. We performed frozen biopsy and pathologically diagnosed astrocytoma grade II (29) (Figure 20).

We performed GTR. The primary treatment option for BST is surgical intervention. Surgical intervention enables histologic diagnosis, alleviates symptoms, removes the influence of the tumor mass, and decreases the numbers of malignant and stem cells. To obtain these effects, the tumor should be resected at least 10 ml (18,29).

BSTs must be subjected to GTR; however, caution must be exercised and this approach should not be insisted upon as most midbrain, medullary, and cervicomedullary tumors are focal, exophytic, and benign.

Partial, subtotal, and near-total resections enable free survival with longer prognosis (19,29). RT and chemotherapy are also effective. To demonstrate the benefits of chemotherapy, a reduction of at least 50% of the tumor volume should be observed. Operation should be performed with maximum exposure and minimum retraction. The aim should be maximum reduction (29).

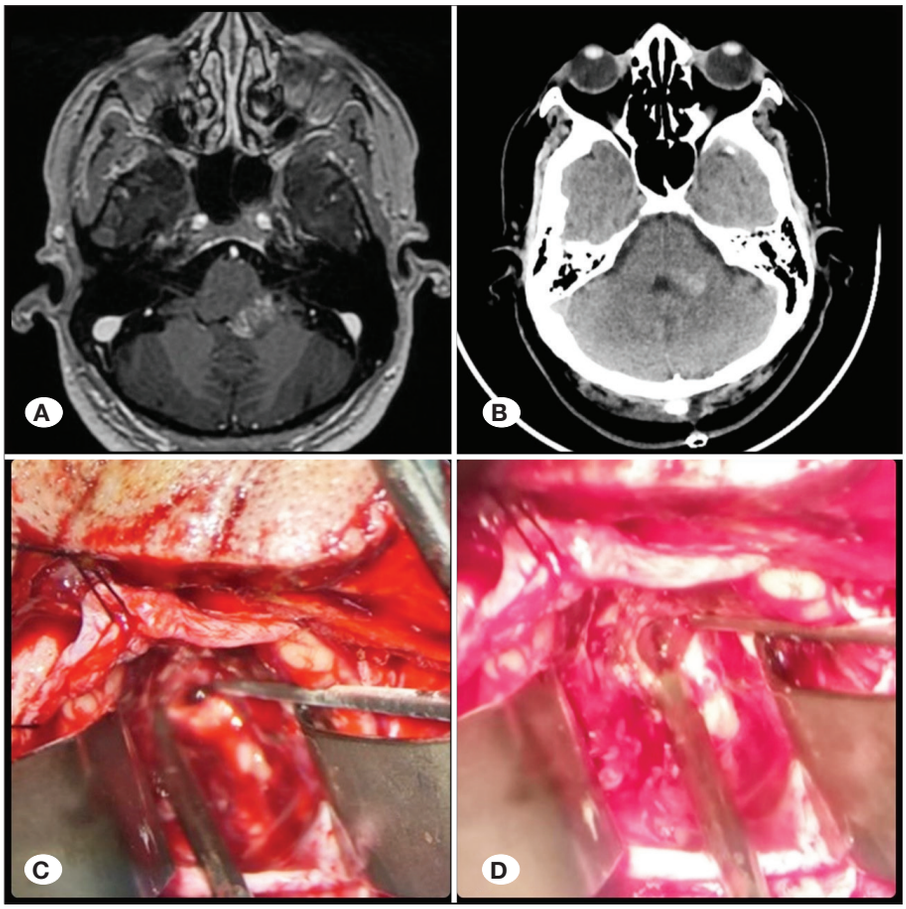

Figure 20: Patient #13. A cerebellar peduncular lesion initially suggestive of cavernoma; however, it was finally diagnosed as pilocytic astrocytoma. **A)** Preoperative T1W contrast enhanced axial MRI. **B)** Postoperative axial CT scan. Intraoperative views **C)** before and **D)** after resection. Final histopathology confirmed pilocytic astrocytoma.

Before opening the entrance to the tumor, the operation area should be examined using a microscope; the fourth ventricle and its base, subependymal cyst, discoloration, abnormal vascularization, bulging, protrusion, asymmetry, and displacement areas should be determined; and the shortest trajectory for entrance should be identified (20). Entrance through the medullary midline should be avoided due to the possibility of bilateral nuclear lesion development. Entrance from the cervicomedullary area should be preferred (28). Postoperatively, filling of the blood in the spinal canal can be mistaken for metastasis. Therefore, preoperative spinal MRI should be performed and compared with MRI performed on postoperative days 4–5 to confirm that the spinal canal is clear (28).

During the operation, to prevent the disruption of the tumor and avoid confusion with normal tissue under the microscope, thermal and biochemical coagulation using bipolar and laser techniques should not be applied to stop bleeding (28). The brainstem is highly sensitive to compression; therefore, mechanical hemostasis is provided mildly with a wet cotton compress. Normally, in the brainstem, perforating vessels exit with opposite angle to reduce the blood flow. Bleeding from vessels without laminin, fibronectin, and neuron can be stopped with mild compression; in cases where it does not work, Tisseel LYO (Baxter Turkey Renal Hizmetler A.S., Istanbul, Türkiye), fibrin sealant, can be used (28).

Using the posterior exophytic part of the medulla tumor as an entrance, the tumor can be removed up to the base of the fourth ventricle (22). A piecemeal technique can also be applied for the removal of tumors, which involves removing a tumor from the center to the periphery while staying within the tumor boundaries (22). If a cyst is present, it can be used as an entrance; a mural nodule should be totally resected (11).

In BSTs, a glial barrier is not present and the surrounding cuff is normal tissue; therefore, maximal care should be taken for this area (28).

Because flattened and distorted tracts are pushed even if they are not touched, their movement to the original area following tumor removal can lead to their damage (5).

We used nuclear and neuronal stimulators for BSTs (28). Although we did not receive a pathological stimulus from the monitor, we detected postoperative paresis of long tractus. Therefore, we aimed for spontaneous respiration from anesthesia in all patients with posterior fossa tumors. We halted the operation until the respiration and heart rhythm changes recovered. We terminated the operation in cases with frequent changes (28). The most important stimulus in operation was the deterioration in heart and respiratory rhythms. In cases where we were unsure about the differentiation of the tumor tissues from the surrounding tissues, we performed frozen section from a very small tissue.

As a result, if a tumor forms a place for itself by pushing the surrounding tissues, GTR can be applied if the entrance is found. However, infiltrative, invasive tumors that spread through the tractus are not amenable to safe resection; only their exophytic components can be removed (11,28)

CONCLUSION

Surgical treatment remains the cornerstone in the management of BSTs, offering histological diagnosis, mass effect elimination, symptom improvement, and cyst reduction. While GTR is the ideal treatment goal, it should not be insisted upon, particularly for midbrain, medullary, and cervicomedullary tumors that are often focal, exophytic, and benign in nature. In such cases, partial or subtotal resection can provide long-term survival with favorable outcomes.

Critical intraoperative considerations include vigilant monitoring of cardiac and respiratory parameters, maximal exposure with minimal retraction, and avoidance of aggressive maneuvers in infiltrative tumors. GTR is feasible when the tumor displaces surrounding tissue and allows a safe entry corridor; however, diffusely infiltrative tumors remain largely inoperable, aside from their exophytic components.

Our 13-year single-center experience suggests that individualized, anatomy-based surgical strategies, which are guided by neuromonitoring and advanced imaging, can lead to meaningful clinical improvement, even in complex cases.

ACKNOWLEDGEMENTS

The authors thank the neurosurgical and pathology teams involved in patient follow-up and data collection.

Declarations

Funding: This research did not receive any specific grant from funding agencies in the public, commercial, or not-for-profit sectors.

Availability of data and materials: The datasets generated and/or analyzed during the current study are available from the corresponding author by reasonable request.

Disclosure: The authors declare no competing interests.

AUTHORSHIP CONTRIBUTION

Study conception and design: EH

Data collection: EH, EY

Analysis and interpretation of results: EH, AED

Draft manuscript preparation: EH, EY, SH

Critical revision of the article: SH, EH

All authors (EH, EY, AED, SH) reviewed the results and approved the final version of the manuscript.

REFERENCES

1. Albers AC, Gutmann DH: Gliomas in patients with neurofibromatosis type 1. Expert Rev Neurother 9:535-539, 2009. https://doi.org/10.1586/ern.09.4
2. Amano T, Inamura T, Nakamizo A, Inoha S, Wu CM, Ikezaki K: Case management of hydrocephalus associated with the progression of childhood brain stem gliomas. Childs Nerv Syst 18:599-604, 2002. https://doi.org/10.1007/s00381-002-0637-5
3. Asthagiri RA, Warren EK, Lonser RR: Brain tumors associated with neurofibromatosis. In: Kaye HA, Laws ER, (eds). Brain Tumors. Edinburgh: Elsevier; 2012:558-599. https://doi.org/10.1016/B978-0-443-06967-3.00030-2
4. Başarır M, Özek MM: Beyin sapı tümörlerinde güncel tedavi seçenekleri. Türk Nöroşir Derg 26:43-51, 2016
5. Bowers DC, Georgiades C, Aronson LJ, Carson BS, Weingart JD, Wharam MD, Melhem ER, Burger PC, Cohen KJ: Tectal gliomas: Natural history of an indolent lesion in pediatric patients. Pediatr Neurosurg 32:24-29, 2000. https://doi.org/10.1159/000028893
6. Chico-Ponce de León F, Perezpena-Diazconti M, Castro-Sierra E, Guerrero-Jazo FJ, Gordillo-Domínguez LF, Gutiérrez-Guerra R, Salamanca T, Sosa-Sainz G, Santana-Montero BL, DeMontesinos-Sampedro A: Stereotactically-guided biopsies of brainstem tumors. Childs Nerv Syst 19:305-310, 2003. https://doi.org/10.1007/s00381-003-0737-x
7. Di Maio S, Gul SM, Cochrane DD, Hendson G, Sargent MA, Steinbok P: Clinical, radiologic and pathologic features and outcome following surgery for cervicomedullary gliomas in children. Childs Nerv Syst 25:1401-1410, 2009. https://doi.org/10.1007/s00381-009-0956-x
8. Donaldson SS, Laningham F, Fisher PG: Advances toward an understanding of brainstem gliomas. J Clin Oncol 24:1266-1272, 2006. https://doi.org/10.1200/JCO.2005.04.6599
9. Dubey A, Patwardhan RV, Sampath S, Santosh V, Kolluri S, Nanda A: Intracranial fungal granuloma: Analysis of 40 patients and review of the literature. Surg Neurol 63:254-260, 2005. https://doi.org/10.1016/j.surneu.2004.04.020
10. Farrell CJ, Plotkin SR: Genetic causes of brain tumors. Neurol Clin 25:925-946, 2007. https://doi.org/10.1016/j.ncl.2007.07.008
11. Fisher PG, Breiter SN, Carson BS, Wharam MD, Williams JA, Weingart JD, Foer DR, Goldthwaite PT, Tihan T, Burger PC: A clinicopathologic reappraisal of brain stem tumor classification. Identification of pilocystic astrocytoma and fibrillary astrocytoma as distinct entities. Cancer 89:1569-1576, 2000. https://doi.org/10.1002/1097-0142(20001001)89:7<1569::AID-CNCR22>3.0.CO;2-0
12. Gupta M, Chan TM, Santiago-Dieppa DR, Yekula A, Sanchez CE, Elster JD, Crawford JR, Levy ML, Gonda DD: Robot-assisted stereotactic biopsy of pediatric brainstem and thalamic lesions. J Neurosurg Pediatr 27:317-324, 2021. https://doi.org/10.3171/2020.7.PEDS20373
13. Greenberg ML, Fisher PG, Freeman C, Korones DN, Bernstein M, Friedman H, Blaney S, Hershon L, Zhou T, Chen Z, Kretschmar C: Etoposide, vincristine, and cyclosporin A with standard-dose radiation therapy in newly diagnosed diffuse intrinsic brainstem gliomas: A pediatric oncology group phase I study. Pediatr Blood Cancer 45:644-648, 2005. https://doi.org/10.1002/pbc.20382

14. Hamisch C, Kickingereder P, Fischer M, Simon T, Ruge MI: Update on the diagnostic value and safety of stereotactic biopsy for pediatric brainstem tumors: A systematic review and meta-analysis of 735 cases. J Neurosurg Pediatr 20:261-268, 2017. https://doi.org/10.3171/2017.2.PEDS1665
15. Joshi BH, Puri RA, Leland P, Varricchio F, Gupta G, Kocak M, Gilbertson RJ, Puri RK: Identification of interleukin-13 receptor α2 chain overexpression in situ in high-grade diffusely infiltrative pediatric brainstem glioma. Neuro Oncol 10:265-274, 2008. https://doi.org/10.1215/15228517-2007-066
16. Kawakami M, Kawakami K, Takahashi S, Abe M, Puri RK: Analysis of interleukin-13 receptor alpha2 expression in human pediatric brain tumors. Cancer 101:1036-1042, 2004. https://doi.org/10.1002/cncr.20470
17. Kaye HA, Laws ER: Historical perspective of brain tumor surgery. In: Kaye HA, Laws ER, (eds). Brain Tumors. New York: Elsevier, 2012:1-6. https://doi.org/10.1016/B978-0-443-06967-3.00001-6
18. Laigle-Donadey F, Doz F, Delattre JY: Brainstem gliomas in children and adults. Curr Opin Oncol 20:662-667, 2008. https://doi.org/10.1097/CCO.0b013e32831186e0
19. Lorincz KN, Gorodezki D, Schittenhelm J, Zipfel J, Tellermann J, Tatagiba M, Ebinger M, Schuhmann MU: Surgery in pediatric low-grade gliomas with brainstem involvement. Childs Nerv Syst 40:3037-3050, 2024. https://doi.org/10.1007/s00381-024-06561-y
20. Narayan P, Mapstone T: Dorsally exophytic brainstem gliomas. In: Berger MS, Prados MD, (eds). Textbook of Neuro-Oncology. Philadelphia: Saunders, 2005:634-637. https://doi.org/10.1016/B978-0-7216-8148-1.50086-3
21. Pollack IF: Intrinsic tumors of the brainstem. In: Batjer HH, Loftus CM, (eds). Textbook of Neurological Surgery. Philadelphia: Lippincott Williams & Wilkins, 2005:974-985.
22. Pollack IF, Hoffman HJ, Humphreys RP, Becker L: The long-term outcome after surgical treatment of dorsally exophytic brain-stem gliomas. J Neurosurg 78:859-863, 1993. https://doi.org/10.3171/jns.1993.78.6.0859
23. Robison NJ, Kieran MW: Diffuse intrinsic pontine glioma: A reassessment. J Neurooncol 119:7-15, 2014. https://doi.org/10.1007/s11060-014-1448-8
24. Salunke P, Sura S, Tewari MK, Gupta K, Khandelwal NK: An exophytic brain stem glioblastoma in an elderly presenting as a cerebellopontine angle syndrome. Br J Neurosurg 26:96-98, 2012. https://doi.org/10.3109/02688697.2011.585670
25. Samadani U, Judy KD: Stereotactic brainstem biopsy is indicated for the diagnosis of a vast array of brainstem pathology. Stereotact Funct Neurosurg 81:5-9, 2004. https://doi.org/10.1159/000075097
26. Serra C, Türe H, Fırat Z, Staartjes VE, Yaltırık CK, Ekinci G, Sav A, Türe U: Microsurgical management of midbrain gliomas: Surgical results and long-term outcome in a large, single-surgeon, consecutive series. J Neurosurg 140:104-115, 2023. https://doi.org/10.3171/2023.5.JNS222219
27. Smith MA, Freidlin B, Ries LAG, Simon R: Trends in reported incidence of primary malignant brain tumors in children in the United States. J Natl Cancer Inst 90:1269-1277, 1998. https://doi.org/10.1093/jnci/90.17.1269
28. Tsai CE, Rutka JT: Cervicomedullary gliomas. In: Berger MS, Prados MD, (eds). Textbook of Neuro-Oncology. Philadelphia: Saunders, 2005:638-645. https://doi.org/10.1016/B978-0-7216-8148-1.50087-5
29. Upadhyaya SA, Koschmann C, Muraszko K, MD, Venneti S, Garton HJ, Hamstra DA, Maher CO, Betz BL, Brown NA, Wahl D, Weigelin HC, DuRoss KE, Leonard AS, Robertson PL: Brainstem low-grade gliomas in children—excellent outcomes with multimodality therapy. J Child Neurol 32:194-203, 2017. https://doi.org/10.1177/0883073816675547
30. Wang C, Zhang J, Liu A, Sun B, Zhao Y: Surgical treatment of primary midbrain gliomas. Surg Neurol 53:41-51, 2000. https://doi.org/10.1016/S0090-3019(99)00165-2
31. Warren KE, Killian K, Suuriniemi M, Wang Y, Quezado M, Meltzer PS: Genomic aberrations in pediatric diffuse intrinsic pontine gliomas. Neuro Oncol 14:326-332, 2012. https://doi.org/10.1093/neuonc/nor190
32. World Medical Association Declaration of Helsinki: ethical principles for medical research involving human subjects. JAMA 27;310(20):2191-2194, 2013. doi: 10.1001/jama.2013.281053
33. Yin L, Zhang L: Correlation between MRI findings and histological diagnosis of brainstem glioma. Can J Neurol Sci 40:348-354, 2013. https://doi.org/10.1017/S0317167100014293

Turk Neurosurg 36(1):136-144, 2026
DOI: 10.5137/1019-5149.JTN.49153-25.2

Original Investigation
Neuro-Oncology

Received: 17.05.2025
Accepted: 23.07.2025
Published Online: 16.01.2026

Stereotactic Radiosurgery-Induced Peritumoral Edema in Asymptomatic Convexity, Parasagittal, and Parafalcine Meningiomas

Osman Burak CAN[1], Mete RUKSEN[2], Burcu DURMAK ISMAN[1], Mehmet Orbay ASKEROGLU[1], Seray ZORLU[3], Alper YUKSEL[3], Dilsat CAMLI[3], Ali AKAY[4]

[1]Acibadem Kent Hospital, Department of Radiation Oncology, Izmir, Türkiye
[2]Acibadem Kent Hospital, Department of Neurosurgery, Izmir, Türkiye
[3]Acibadem Kent Hospital, Department of Radiology, Izmir, Türkiye
[4]Izmir University of Economics, Medical Point Hospital, Department of Neurosurgery, Izmir, Türkiye

Corresponding author: Osman Burak CAN ✉ osmanburakcan@gmail.com

ABSTRACT

AIM: To evaluate the incidence and identify the risk factors of stereotactic radiosurgery (SRS)-induced peritumoral edema (PTE) in the asymptomatic convexity, parasagittal, and parafalcine meningiomas without pre-existing PTE.

MATERIAL and METHODS: We retrospectively analyzed 52 patients with asymptomatic convexity, parasagittal, or parafalcine meningiomas without pre-existing PTE who underwent single-fraction Gamma Knife radiosurgery between 2019 and 2024. The median tumor volume and the maximum tumor diameter were 3.3 cc (range: 0.31–10.2 cc) and 2.0 cm (range: 0.98–3.1 cm), respectively. The median margin dose was 12 Gy (range: 11 Gy–13 Gy). The median radiological and clinical follow-up durations were 21 months (range: 6–65 months) and 26 months (range: 12–66 months), respectively.

RESULTS: SRS-induced PTE occurred in 5.8% of patients (n=3), exclusively in elderly individuals (≥65 years) with parasagittal or parafalcine meningiomas. No cases were observed in convexity meningiomas (0/24). Multivariable analysis revealed a trend toward statistical significance for the association between age and SRS-induced PTE (p=0.074). In the overall cohort, the incidence of SRS-induced PTE was significantly higher in elderly patients compared to younger patients (<65 years) (3/14 vs. 0/38, p=0.016), and this difference remained significant within the parasagittal/parafalcine subgroup (3/7 vs. 0/21, p=0.011).

CONCLUSION: SRS appears to be a safe treatment modality in terms of PTE risk in patients aged below 65 years with asymptomatic convexity, parasagittal, or parafalcine meningiomas without pre-existing PTE. In contrast, elderly patients with parasagittal or parafalcine meningiomas may be more susceptible to SRS-induced PTE, thereby warranting a more cautious approach to SRS in this subgroup. Additional studies involving larger cohorts are warranted to validate these findings.

KEYWORDS: Stereotactic radiosurgery, Meningioma, Brain edema

ABBREVIATIONS: SRS: Stereotactic radiosurgery, **PTE:** Peritumoral edema, **RANO:** Response Assessment in Neuro-Oncology

Osman Burak CAN : 0000-0001-5184-8990
Mete RUKSEN : 0000-0002-0521-8143
Burcu DURMAK ISMAN : 0009-0000-4515-2444
Mehmet Orbay ASKEROGLU : 0000-0001-7126-6373
Seray ZORLU : 0000-0002-0912-3264
Alper YUKSEL : 0009-0006-7436-4749
Dilsat CAMLI : 0009-0001-0225-3306
Ali AKAY : 0000-0002-7187-398X

INTRODUCTION

Meningiomas are the most common benign brain tumors (21). The detection of incidental meningiomas has increased in recent years due to the rising use and widespread availability of brain magnetic resonance imaging (MRI) (30). Consensus guidelines recommend active surveillance to avoid treatment-related complications in patients with asymptomatic meningiomas (5,11). However, delaying treatment until symptoms emerge could result in inevitable surgical intervention or neurological deficits. In a retrospective analysis, Kim et al. reported that approximately two-thirds of patients with asymptomatic meningiomas exhibited tumor growth, and one-third eventually requiring surgical intervention during follow-up (14). In addition, a prospective study that assessed the growth rate of incidental meningiomas revealed that 75% of tumors demonstrated a volume increase of over 15% over a mean duration of 2.2 years (1). Additionally, tumors that grow during surveillance may fall outside the window of opportunity for stereotactic radiosurgery (SRS). Moreover, prolonging follow-up times can lead to patient anxiety, referred to as "scanxiety" (2). Consequently, the optimal management strategy for incidental meningiomas remains a subject of ongoing debate.

The question of whether performing SRS constitutes overtreatment in the management of incidental meningiomas remains controversial; however, SRS has been shown to be both safe and effective for treating these tumors. A recent international multicenter study, the Incidental Meningioma Progression During Active Surveillance or After Stereotactic Radiosurgery (IMPASSE), demonstrated that SRS provides superior radiological tumor control compared to the observation of incidental meningiomas (26). This enhanced tumor control was achieved without an increased risk of neurological deficits. The IMPASSE study provides a new perspective on the management of asymptomatic meningiomas.

Although SRS is an effective treatment option, it carries the potential risk of inducing or exacerbating peritumoral edema (PTE). This represents the most common complication of SRS for non-skull-base meningiomas. The reported incidence of SRS-induced PTE in patients with meningioma ranged from 15.3% to 38.2% (3,4,7,8,15,19,20,27). While most cases were asymptomatic, 5% to 15.1% of patients experienced new or worsening neurological symptoms, including headache, seizures, or focal deficits due to edema. Although a majority of these symptoms resolve with corticosteroid treatment, 1%–5.2% of patients may suffer progressive symptoms, with a few patients requiring surgical intervention (15,23,27).

Further, several studies have revealed that convexity, parafalcine, and, in particular, parasagittal meningiomas are associated with an increased risk of SRS-induced PTE or radiation-related complications compared to skull-base meningiomas (23,24,27). Additionally, pre-existing PTE has been identified as a strong predictor of SRS-induced PTE (3,8,17). Therefore, in our clinical practice, treatment with SRS for asymptomatic meningiomas located in high-risk regions such as the convexity, parasagittal, and parafalcine areas is usually avoided if PTE is present. However, the safety of SRS in terms of the development of PTE for incidental meningiomas that lack pre-existing PTE and are located in high-risk regions remains unclear. Therefore, in this retrospective study, our objective is to assess the incidence and factors associated with SRS-induced PTE in asymptomatic convexity, parasagittal, and parafalcine meningiomas without PTE at the time of diagnosis.

MATERIAL and METHODS

Patients

This study included patients diagnosed with incidental and asymptomatic meningiomas located in the cerebral convexity, parasagittal, or parafalcine locations, with no evidence of PTE prior to SRS and a clinical follow-up period of at least 12 months. Patients with biopsy-confirmed World Health Organization (WHO) grades 2 or 3 meningiomas as well as those with a history of prior radiotherapy or surgery were excluded. "Asymptomatic" was defined as the absence of any symptoms or signs attributable to the tumor's specific location (8). Between 2019 and 2024, 224 patients with meningioma underwent Gamma Knife radiosurgery at our institution, of whom 52 met the inclusion criteria and were enrolled in this study.

Ethical approval for this retrospective study was obtained from the local ethics committee (ATADEK; Decision No: 2024-10/379, Date: 18.07.2024). Informed consent was obtained from all patients.

Treatment Decision Process

Treatment decisions were made after informing patients of the available options, including surgery, SRS, or active surveillance. A thorough discussion of the potential risks, benefits, and side effects of each option was conducted with each patient, and informed consent from the patients was obtained prior to SRS.

Radiosurgery Technique

All patients underwent single-fraction SRS using the Gamma Knife Perfexion system (Elekta AB, Stockholm, Sweden). A Leksell stereotactic frame was applied under local anesthesia. Following frame placement, stereotactic MRI was performed, obtaining post-contrast T1-weighted MPR sequence images with a slice thickness of 1 mm. Treatment planning was collaboratively conducted by a neurosurgeon and a radiation oncologist. The median margin dose was 12 Gy (range: 11 Gy–13 Gy), with a mean margin dose of 12.1 Gy. The median isodose line was 50% (range: 45%–55%). Radiosurgery parameters are detailed in Table I.

Follow-Up

Post-SRS follow-up included a contrast-enhanced brain MRI at six months, followed by annual imaging thereafter. Following treatment, clinical evaluations were recommended twice annually to assess the neurological status and identify any potential complications.

The Primary Objective: SRS-Induced PTE

The primary objective of this study was to determine the incidence and to identify the risk factors for SRS-induced PTE, defined as the newly developed peritumoral T2 hyperintensity

Table I: Radiosurgery Parameters

Radiosurgery Parameters	Median (range)
Margin Dose (Gy)	12 (11–13)*
Maximum Tumor Dose (Gy)	24 (22–26.7)
Mean Tumor Dose (Gy)	16.9 (14.9–19.6)
Prescribed Isodose Line (%)	50 (45–55)
Tumor Coverage (%)	99 (98–100)
Gradient Index	2.83 (2.53–3.20)
Selectivity	0.86 (0.77–0.96)
Number of Shots	22 (4–75)

**Among the total cohort of 52 patients, a margin dose of 11 Gy was administered to 4 patients, 12 Gy to 39 patients, and 13 Gy to 9 patients.*

observed on MRI in the absence of tumor progression. Symptomatic edema was defined as the presence of edema-related symptoms that required corticosteroid therapy.

Tumor Response

Tumor responses were evaluated according to the Response Assessment in Neuro-Oncology (RANO) criteria for meningiomas, based on the sum of the products of perpendicular diameters of all target lesions. Partial response was defined as a decrease of ≥50%, minor response as a decrease of ≥25% but <50%, progressive disease as an increase of ≥25%, and stable disease as changes not meeting the criteria for other categories, with all changes sustained for at least eight weeks or until the next scheduled scan, whichever was longer (9).

Statistical Analysis

Chi-Square (χ^2) test or Fisher's exact test was performed for categorical variables, while the Mann–Whitney U test was applied for continuous variables. The Kruskal–Wallis test was employed to assess differences between groups based on tumor location. Variables included in the multivariable model were selected based on their statistical significance in the univariable analysis and/or their established relevance to PTE in previous studies, such as tumor location and volume. Due to the relatively small sample size and the low event rate of SRS-induced PTE, a post hoc power analysis was performed to assess the robustness of statistically significant findings.

RESULTS

The median patient age was 55 years (range: 34–76 years). Among the 52 patients, 8 (15.4%) were male, and 44 (84.6%) were female. SRS was performed in 14 patients (26.9%) due to tumor progression detected during active surveillance, while the remaining 38 patients (73.1%) underwent SRS immediately after diagnosis. The median tumor volume was 3.3 cc (range: 0.31–10.2 cc), and the median maximum tumor diameter was 2.0 cm (range: 0.98–3.1 cm). The median clinical follow-up duration was 26 months (range: 12–66 months), while the median radiological follow-up duration was 21 months (range: 6–65 months). A median of two MRI scans (range: 1–5) were performed after SRS.

Local tumor control was achieved in 100% of cases. According to the RANO criteria, 7 patients (13.5%) exhibited a partial response, 6 patients (11.5%) exhibited a minor response, and the remaining 39 patients (75%) had stable disease. There were no significant differences in age, gender, tumor volume, maximum tumor diameter, margin dose, or follow-up durations among patients with convexity, parafalcine, and parasagittal meningiomas (Table II).

Among the 52 patients, one patient (1.9%) with a parasagittal meningioma developed symptomatic PTE and two patients (3.8%) with a parafalcine meningioma developed asymptomatic PTE. Notably, no cases of PTE were observed in convexity meningiomas (0/24). Overall, SRS-induced PTE (both asymptomatic and symptomatic) occurred in 5.8% of patients. No additional late-onset complications related to SRS were observed. A moderately positive and statistically significant association was observed between age and tumor volume (ρ=0.495, p<0.001). The univariable analysis revealed a significant association between age and SRS-induced PTE (p=0.026). The multivariable model demonstrated a good overall fit (McFadden's R^2 = 0.632), and age revealed a trend toward statistical significance (p=0.074). Moreover, SRS-induced PTE was detected in 3 out of 14 elderly patients (≥ 65 years), whereas no cases were observed in younger patients (<65 years; 0/38), with this difference being statistically significant (p=0.016). In addition, no significant association was found between SRS-induced PTE and gender, maximum tumor diameter, tumor volume, margin dose, or tumor location. Comorbidities such as diabetes mellitus and hypertension were also not found to be associated with the development of SRS-induced PTE (Table III).

In the overall cohort, since SRS-induced PTE was exclusively observed in patients with parasagittal/parafalcine meningiomas, these 28 patients were analyzed separately, excluding those with convexity meningiomas. SRS-induced PTE was found to be significantly more frequent in elderly patients compared to younger patients with parasagittal/parafalcine meningiomas (3/7 vs. 0/21, p=0.011).

Although the observed differences were statistically significant for age in the univariable analysis and in comparisons between elderly and younger patients—both in the overall cohort and among those with parasagittal/parafalcine meningiomas—the post hoc statistical power of these analyses was <80%.

DISCUSSION

SRS-induced symptomatic PTE typically manifests among patients between three- and nine-months post-treatment, with its cumulative incidence increasing until 12 months and subsequently resolving within 2 years following SRS (8,29). Based on this timeframe, we included only patients with a clinical follow-up period of at least 12 months in this study. The median radiological and clinical follow-up durations were

Table II: Patient, Tumor, and Treatment Characteristics and the Incidence of PTE

	Entire Cohort n=52	Convexity n=24	Parafalcine n=17	Parasagittal n=11	p-value*
Age, Median (range) (years)	55 (34–76)	59 (34–71)	51 (36–76)	47 (34–70)	0.275
Gender					0.795
Male, n (%)	8 (15.4)	4 (16.7)	3 (17.6)	1 (9)	
Female, n (%)	44 (84.6)	20 (83.3)	14 (82.4)	10 (91)	
Tumor diameter (max), median, range (cm)	2.0 (0.98–3.1)	1.75 (1–3)	2.1 (0.98–3.1)	2.3 (1.4–2.9)	0.164
Tumor volume, median, range (ml)	3.3 (0.31–10.2)	2.25 (0.31–10.1)	4.1 (0.5–10.2)	4.3 (1.23–8.4)	0.444
Timing of SRS					0.924
Following tumor progression, n (%)	14 (26.9)	7 (29.2)	4 (23.5)	3 (27.3)	
Immediately after diagnosis, n (%)	38 (73.1)	17 (70.8)	13 (76.5)	8 (72.7)	
Margin dose	12 Gy (11 Gy–13 Gy)	12 Gy (11 Gy–13 Gy)	12 Gy (11 Gy–13 Gy)	12 Gy (11 Gy–13 Gy)	0.683
Follow-up (months)					
Clinical, median, (range)	26 (12–66)	24.5 (13–59)	32 (12–66)	26.5 (13–54)	0.714
Radiological, median, (range)	21 (6–65)	24 (7-48)	29 (6-65)	14.5 (6-35)	0.139
SRS-induced symptomatic PTE, n (%)	1 (1.9)	0 (0.0)	0 (0.0)	1 (9.0)	0.155
SRS-induced asymptomatic PTE, n (%)	2 (3.8)	0 (0.0)	2 (11.8)	0 (0.0)	0.122
SRS-induced symptomatic or asymptomatic PTE, n (%)	3 (5.8)	0 (0.0)	2 (11.8)	1 (9.0)	0.251

Statistical differences among the convexity, parasagittal, and parafalcine groups.* ***SRS:* *Stereotactic radiosurgery.* ***PTE:*** *Peritumoral edema.*

Table III: Risk factors for SRS-induced PTE (n=52)

Factors	Univariable Analysis	Multivariable Analysis
	p-value	
Age	**0.026**	0.074
≥65 vs. <65	**0.016**	-
Gender		
Male vs. Female	0.447	-
Tumor Diameter (maximum)	0.145	-
Tumor Volume	0.272	0.153
Margin Dose	0.407	-
Tumor Location	0.208	0.997
Convexity vs. Parafalcine	0.166	-
Convexity vs. Parasagittal	0.314	-
Convexity vs. Parafalcine/Parasagittal	0.240	-
Parasagittal vs. Parafalcine	0.823	-
Hypertension	0.546	-
Diabetes Mellitus	0.553	-

SRS: *Stereotactic radiosurgery.* ***PTE:*** *Peritumoral edema.*

21 and 26 months, respectively, which were deemed sufficient to assess SRS-induced PTE (3,17,29). Although the follow-up durations were not sufficient to reliably evaluate tumor control or response rates, these data were descriptively presented to provide a comprehensive overview of post-SRS outcomes. However, it should be emphasized that the primary focus of this study was the evaluation of SRS-induced PTE.

While asymptomatic PTE is primarily a radiological finding, symptomatic PTE is of greater clinical significance because it necessitates medical or surgical intervention. In our cohort, only one patient (1.9%) developed symptomatic PTE following SRS. At four months post-SRS, this patient presented with headaches and seizures, which were successfully managed with antiepileptic and corticosteroid therapy, thereby resulting in complete symptom resolution (Figures 1 and 2). In two patients (3.8%) with SRS-induced asymptomatic PTE, the edema did not require intervention and spontaneously resolved during follow-up.

Although a moderate positive correlation between age and tumor volume was observed in this study, this finding may be influenced by our clinical approach to managing meningiomas in elderly patients. In our clinical practice, small-volume meningiomas in elderly patients are more likely to be managed with surveillance rather than immediate intervention.

It is noteworthy that SRS-induced PTE was not observed in any of the 38 patients (0%) aged below 65 years, whereas it occurred in 3 out of 14 elderly patients (21.4%). Sheehan et al. identified meningiomas located in the parasagittal/parafalcine regions as being at higher risk for developing SRS-induced PTE, likely due to tumor abutment or the invasion of venous sinuses or other vascular structures (27). Although our study did not demonstrate a statistically significant difference in the

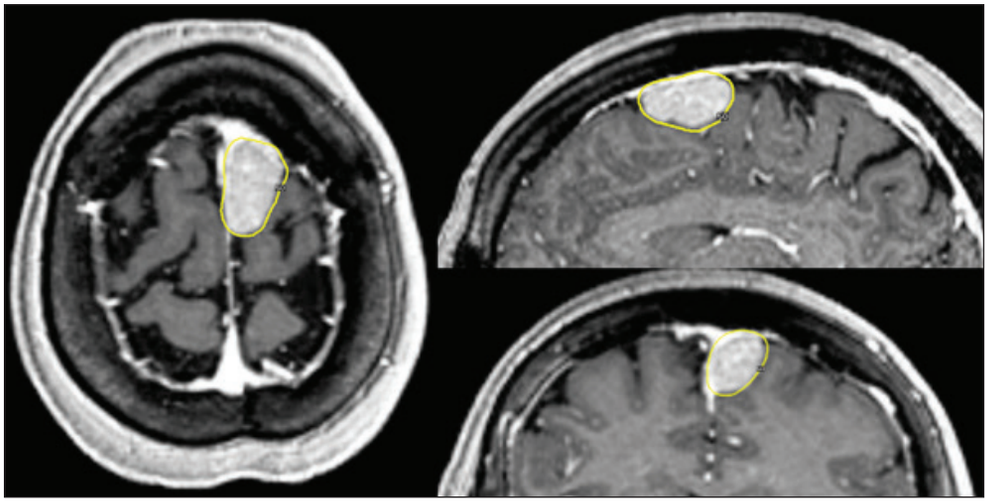

Figure 1: Axial, sagittal, and coronal post-contrast T1W MRI images show an asymptomatic parasagittal meningioma (tumor volume: 4.2 ml) in a 68-year-old female patient. The prescribed Gamma Knife treatment plan was a dose of 12 Gy to the 50% isodose line (yellow contours).

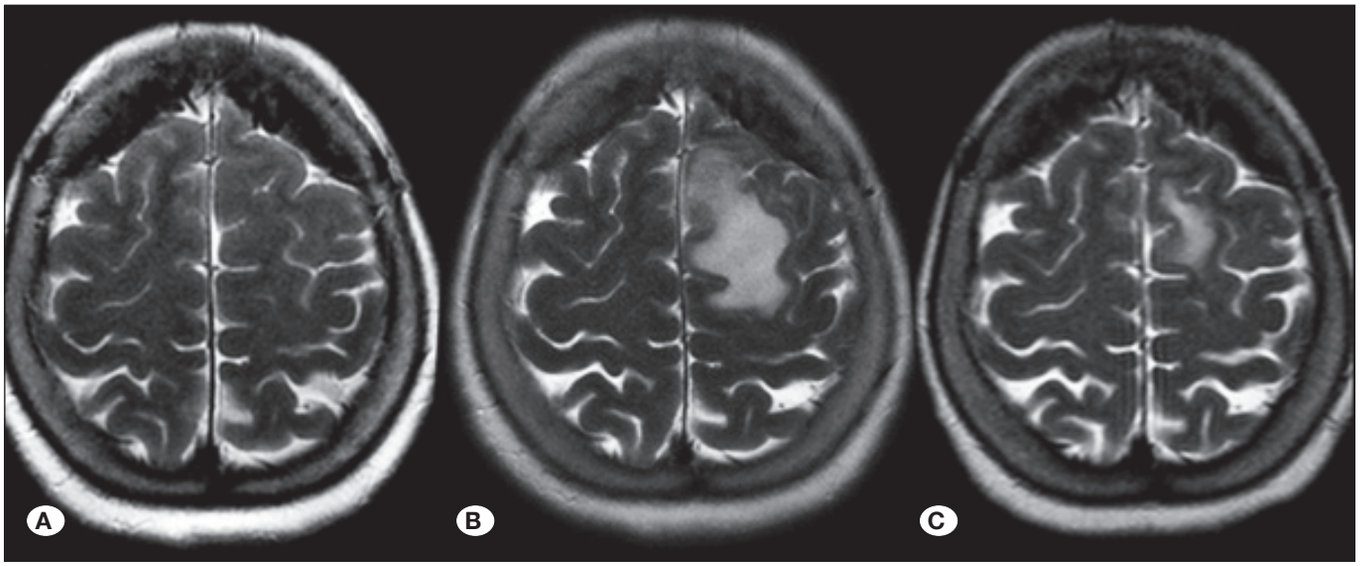

Figure 2: T2W axial MRI images obtained before Gamma Knife treatment **(A)**, post-treatment at 4 months **(B)**, and at 11 months **(C)**.

incidence of SRS-induced PTE between parasagittal/parafalcine and convexity meningiomas—possibly due to the small sample size or limited number of events—all three cases of SRS-induced PTE in our cohort occurred in elderly patients with parasagittal or parafalcine meningiomas. In line with our findings and those of previous studies, when the analysis was restricted to parasagittal/parafalcine meningiomas, we found that 42.9% (3/7) of elderly patients developed PTE, while none (0/21) of the younger patients did.

While the limited number of SRS-induced PTE cases and small sample size may constrain the statistical power to establish a definitive association between age (or elderly status) and the development of SRS-induced PTE, the complete absence of edema among younger patients remains a key observation in our study.

Thus, these findings suggest that SRS may represent a safe treatment modality with respect to SRS-induced PTE development in patients below 65 years of age and presenting with asymptomatic convexity, parasagittal, or parafalcine meningiomas without pre-existing edema, as no cases were observed in this group. In contrast, elderly patients with parasagittal or parafalcine tumors may be at increased risk of developing SRS-induced PTE. Therefore, the indication for SRS in this subgroup should be approached with caution and further evaluated in larger cohorts.

Several studies have investigated factors associated with the risk of SRS-induced PTE. Well-established risk factors include larger initial tumor volume, higher margin dose, pre-existing PTE, and non-skull-base tumor location. Additionally, venous sinus invasion and a large tumor–brain contact interface area have been identified as significant predictors of SRS-induced PTE (15,17). In a few studies, increased age has also been associated with SRS-induced PTE (3,15). In a study evaluating 331 patients with meningioma treated with SRS, PTE was observed in 15.4% of cases, and Kollová et al. reported that age over 60 years was a significant risk factor for the development of edema (15). Although the age threshold in our study was slightly higher (≥65 years), our findings support the previously reported association between increasing age and a higher risk of SRS-induced PTE.

Mechanism of SRS-Induced PTE

PTE in meningiomas is predominantly vasogenic, a phenomenon attributed to SRS-induced increases in capillary permeability, which subsequently leads to enhanced edema formation (21). Elevated levels of vascular endothelial growth factor (VEGF) have also been implicated in this process (13,22). Moreover, Cai et al. proposed that SRS-induced damage to the arachnoid membrane and pia mater at the tumor–brain interface significantly contribute to the development of PTE (3).

Tumor Location

Several studies have examined the correlation between tumor location and SRS-induced PTE in meningiomas (4,17,23). Although skull-base meningiomas may present long-term complications, such as cranial nerve deficits, SRS-induced PTE is relatively uncommon in these tumors. In contrast, meningiomas located in the convexity, parasagittal, and parafalcine locations—often referred to as cerebral hemispheric meningiomas—demonstrate a higher incidence of SRS-induced PTE compared to skull-base meningiomas. Chang et al. reported a 21.2% rate of symptomatic imaging changes in MRIs for cerebral hemispheric meningiomas and a 40% rate for parasagittal meningiomas, whereas skull-base meningiomas had a significantly lower incidence of 1.3% (4).

In a multicenter retrospective study, Sheehan et al. examined the risk factors for post-SRS PTE, specifically in parasagittal and parafalcine meningiomas. At a median dose of 14 Gy, new or worsening edema was observed in 38.2% of cases, and 5.2% of patients experienced progressive edema. Furthermore, 15.1% and 2.4% of patients required steroids or bevacizumab, respectively, while 7.1% underwent surgery due to edema. The patient population in their study may have been more susceptible to edema development because it included grades 2 and 3 meningiomas, which necessitate higher margin doses. Additionally, neurological deficits or symptoms were common prior to SRS, with 45.3% of patients exhibiting pre-existing PTE. In our study, SRS-induced PTE developed in 3 out of 28 (10.7%) parasagittal/parafalcine meningiomas; notably, all patients were asymptomatic at diagnosis and had no pre-existing PTE prior to treatment (27).

In another study, Cai et al. reported that among 105 meningiomas without pre-existing PTE, 16.19% of the patients developed edema following SRS. They also identified the tumor–brain contact interface area as one of the most significant risk factors for post-SRS PTE; specifically, for each increase of 1 cm^2 in the interface area, the likelihood of developing edema increased by 26% (3). Furthermore, some studies have indicated that parasagittal locations are particularly susceptible to PTE following SRS (17,23). Patil et al. demonstrated that the risk of post-SRS symptomatic edema was four times higher in parasagittal meningiomas compared to non-midline supratentorial meningiomas, with symptomatic edema occurring in 35.2% of parasagittal meningiomas versus 7.8% of non-parasagittal supratentorial meningiomas (23).

In our study, although we were unable to establish a correlation between tumor location and SRS-induced PTE, the absence of SRS-induced PTE in all 21 patients with parasagittal/parafalcine meningiomas aged below 65 years and in all 24 patients with convexity meningiomas is a noteworthy finding that may provide supportive evidence for the safety of SRS in these subgroups.

Pre-Existing PTE

Pre-existing PTE is a critical predictor of the risk of SRS-induced PTE (3,8,17). Cai et al. demonstrated that the risk of SRS-induced PTE is six times higher in meningiomas with pretreatment edema than in those without (3). Similarly, Hoe et al. found that the presence of PTE prior to SRS is significantly associated with an increased risk of developing SRS-induced PTE, even in asymptomatic meningiomas (8). Consequently, we generally refrain from treating edematous convexity, parasagittal, and parafalcine meningiomas in asymptomatic patients due to the relatively high risk of SRS-induced PTE.

Tumor Volume

Kollová et al. reported that the risk of post-SRS PTE reaches up to 30% in meningiomas that exceed 10 ml in volume, compared to only 10% in tumors smaller than 5 ml (15). Similarly, Han et al. found that large-volume meningiomas (>10 ml, median 15.2 ml) exhibited a 33.3% rate of symptomatic complications, even when treated with relatively low SRS doses (median dose of 12 Gy) (6). In a recent review, Islim et al. stated that SRS is not recommended for meningiomas with a volume that exceeds 10 ml (11). Based on these findings, our clinical practice does not employ single-fraction SRS for meningiomas larger than 10 ml. In our study, the median tumor volume was 3.3 ml, with the largest tumor measuring 10.2 ml.

Margin Dose

In studies reporting SRS-induced symptomatic PTE in over 10% of cases, the median margin doses ranged from 13.6 Gy to 18 Gy (7,8,15,19,27). Higher margin doses have been shown to significantly correlate with an increased risk of SRS-induced PTE (17). Based on this evidence, we opted for relatively lower doses, as inducing symptoms in asymptomatic patients with incidental meningiomas is undesirable. This low-dose strategy may have contributed to the low incidence of SRS-induced symptomatic PTE observed in our study, with the majority of our patients receiving a dose of 12 Gy. Although a dose of ≥13 Gy is generally considered effective for treating meningiomas, multiple studies have demonstrated that a dose of approximately 12 Gy is also sufficient for achieving long-term tumor control (10,15,28). Further, based on recent findings, Lee et al. recommended a margin dose of between 11 Gy and 14 Gy to achieve long-term local control in non-skull-base meningiomas. They also demonstrated that D98%—the dose received by 98% of the tumor volume—was a significant factor for local control, with a cutoff value of 11 Gy (16). In our study, the median tumor coverage was 99% (range, 98%–100%). Consequently, even for the meningiomas that received a margin dose of 11 Gy (n=4) in our study, tumor coverage was at least 98%, which is consistent with the recommendations of Lee et al. (16).

SRS-Induced Toxicity in Asymptomatic Meningiomas

Hoe et al. analyzed 320 asymptomatic meningioma patients treated with SRS. Approximately two-thirds of the meningiomas were located in the hemispheric regions, while the remainder were skull-base meningiomas. In their study, 5.9% of patients exhibited pretreatment PTE. Following SRS (with a median dose of 13 Gy), 15.3% of patients developed new or increased PTE, 8.8% became symptomatic, and 1.3% experienced persistent neurological symptoms. Large tumor volumes (>4.2 cc), hemispheric tumor locations, and the presence of pretreatment PTE were associated with an increased risk of post-SRS PTE (8).

In the recent multicenter IMPASSE study, which included both skull-base and non-skull-base asymptomatic meningiomas, new neurologic deficits were reported in 2.3% of patients treated with SRS, while excellent local tumor control was achieved (99% over a mean follow-up of 57.2 months). The mean margin dose was 12.9 Gy (26). Our toxicity outcomes were comparable to those of the IMPASSE study, with 1.9% of our patients developing neurologic deficits due to SRS-induced PTE.

SRS vs. Surgery

If therapeutic intervention is considered for a non-skull-base asymptomatic meningioma, surgical resection is preferable over SRS when the tumor volume exceeds 10 ml (4); this may also be a more appropriate option in the presence of PTE (3,8,17,29). Additionally, surgery may be considered even for SRS-eligible tumors, such as those included in this study—particularly when located in the convexity, parasagittal, or parafalcine locations—as surgery can achieve high rates of complete resection with low permanent morbidity (25). Moreover, a key advantage of surgery is the ability to establish a pathological diagnosis, which is critical for detecting higher-grade tumors. However, it is well established that the vast majority of incidental meningiomas (94%) are WHO grade 1, while grade 3 tumors account for less than 1% (12). Notably, the IMPASSE trial revealed that only 1% of patients with asymptomatic meningiomas progressed after SRS, despite the absence of histological confirmation (9). Furthermore, one of the most significant advantages of SRS compared to surgery is its minimally invasive nature—frame-based Gamma Knife radiosurgery requires only local anesthesia, while mask-based SRS is a completely non-invasive procedure. Importantly, SRS does not appear to increase the risk of malignant transformation in meningiomas compared to surgery alone (19).

Limitations

The main limitations of this study include its retrospective design, its single-institution setting, and the small number of SRS-induced PTE cases (n=3), all of which may limit the generalizability of the results. Additionally, it is possible that the relatively small sample size (n=52) limited the statistical power to detect more subtle associations. Consequently, we were unable to demonstrate an association between SRS-induced PTE and factors such as tumor volume and margin dose, which have been well established as predictors of SRS-induced PTE in previous studies. Moreover, in our cohort, 75% of patients received a margin dose of 12 Gy, 17.3% received 13 Gy, and only 7.7% (n=4) received 11 Gy. The limited variability in margin doses (11 Gy–13 Gy) possibly constrained our ability to identify dose-related effects. In addition, we were unable to evaluate the effects of pre-existing PTE on the development of SRS-induced PTE, as asymptomatic patients with pre-existing PTE were not included in this study due to our clinical policy of avoiding SRS in such cases.

CONCLUSION

Considering that no SRS-induced PTE was observed among patients below 65 years of age, our findings suggest that SRS, when administered with a median margin dose of 12 Gy (range: 11 Gy–13 Gy), may be a safe treatment modality in terms of PTE risk for this population, with asymptomatic convexity, parasagittal, or parafalcine meningiomas without pre-existing PTE. However, elderly patients with asymptomatic parasagittal or parafalcine meningiomas may be at an in-

creased risk of developing SRS-induced PTE. Therefore, the decision to treat such patients with SRS should be made cautiously, taking into account the potential risk of complications; moreover, the safety profile of SRS should be further validated in studies with larger patient populations.

ACKNOWLEDGEMENTS

The authors are grateful to Mustafa K. Baskaya, MD and Steven Goodman, PhD for their critical reading and editing of our manuscript.

Declarations

Funding: This research did not receive any specific grant from funding agencies in the public, commercial, or not-for-profit sectors.

Availability of data and materials: The datasets generated and/or analyzed during the current study are available from the corresponding author by reasonable request.

Disclosure: The authors declare no competing interests.

AUTHORSHIP CONTRIBUTION

Study conception and design: OBC, MR, BDI, AA
Data collection: OBC, SZ, AY, DC, OA
Analysis and interpretation of results: OBC, MR
Draft manuscript preparation: OBC
Critical revision of the article: OBC, MR, BDI
Other (study supervision, fundings, materials, etc...): AY, AA, OBC
All authors (OBC, MR, BDI, OA, SZ, AY, DC, AA) reviewed the results and approved the final version of the manuscript.

REFERENCES

1. Behbahani M, Skeie GO, Eide GE, Hausken A, Lund-Johansen M, Skeie BS: A prospective study of the natural history of incidental meningioma – Hold your horses! Neurooncol Pract 6:438-450, 2019. https://doi.org/10.1093/nop/npz011
2. Bui KT, Liang R, Kiely BE, Brown C, Dhillon HM, Blinman P: Scanxiety: A scoping review about scan-associated anxiety. BMJ Open 11:e043215, 2021. https://doi.org/10.1136/bmjopen-2020-043215
3. Cai R, Barnett GH, Novak E, Chao ST, Suh JH: Principal risk of peritumoral edema after stereotactic radiosurgery for intracranial meningioma is tumor-brain contact interface area. Neurosurgery 66:513-522, 2010. https://doi.org/10.1227/01.NEU.0000365366.53337.88
4. Chang JH, Chang JW, Choi JY, Park YG, Chung SS: Complications after gamma knife radiosurgery for benign meningiomas. J Neurol Neurosurg Psychiatry 74:226-230, 2003. https://doi.org/10.1136/jnnp.74.2.226
5. Goldbrunner R, Stavrinou P, Jenkinson MD, Sahm F, Mawrin C, Weber DC, Preusser M, Minniti G, Lund-Johansen M, Lefranc F, Houdart E, Sallabanda K, Le Rhun E, Nieuwenhuizen D, Tabatabai G, Soffietti R, Weller M: EANO guideline on the diagnosis and management of meningiomas. Neuro Oncol 23:1821-1834, 2021. https://doi.org/10.1093/neuonc/noab150
6. Han JH, Kim DG, Chung HT, Park CK, Paek SH, Kim CY, Jung HW: Gamma knife radiosurgery for skull base meningiomas: Long-term radiologic and clinical outcome. Int J Radiat Oncol Biol Phys 72:1324-1332, 2008. https://doi.org/10.1016/j.ijrobp.2008.03.028
7. Hasegawa T, Kida Y, Yoshimoto M, Iizuka H, Ishii D, Yoshida K: Gamma Knife surgery for convexity, parasagittal, and falcine meningiomas. J Neurosurg 114:1392-1398, 2011. https://doi.org/10.3171/2010.11.JNS10112
8. Hoe Y, Choi YJ, Kim JH, Kwon DH, Kim CJ, Cho YH: Peritumoral brain edema after stereotactic radiosurgery for asymptomatic intracranial meningiomas: Risks and pattern of evolution. J Korean Neurosurg Soc 58:379-384, 2015. https://doi.org/10.3340/jkns.2015.58.4.379
9. Huang RY, Bi WL, Weller M, Kaley T, Blakeley J, Dunn I, Galanis E, Preusser M, McDermott M, Rogers L, Raizer J, Schiff D, Soffietti R, Tonn JC, Vogelbaum M, Weber D, Reardon DA, Wen PY: Proposed response assessment and endpoints for meningioma clinical trials: Report from the response assessment in neuro-oncology working group. Neuro Oncol 21:26-36, 2019. https://doi.org/10.1093/neuonc/noy137
10. Huo M, Laperriere N, van Prooijen M, Shultz D, Coolens C, Hodaie M, Cusimano M, Gentili F, Zadeh G, Payne D, Schwartz M, Tsang DS: Efficacy of stereotactic radiosurgery for radiation-induced meningiomas. J Neurooncol 148:299-305, 2020. https://doi.org/10.1007/s11060-020-03515-7
11. Islim AI, Millward CP, Mills SJ, Fountain DM, Zakaria R, Pathmanaban ON, Mathew RK, Santarius T, Jenkinson MD: The management of incidental meningioma: An unresolved clinical conundrum. Neurooncol Adv 5:i26-i34, 2023. https://doi.org/10.1093/noajnl/vdac109
12. Islim AI, Mohan M, Moon RDC, Srikandarajah N, Mills SJ, Brodbelt AR, Jenkinson MD: Incidental intracranial meningiomas: A systematic review and meta-analysis of prognostic factors and outcomes. J Neurooncol 142:211-221, 2019. https://doi.org/10.1007/s11060-019-03104-3
13. Iwado E, Ichikawa T, Kosaka H, Otsuka S, Kambara H, Tamiya T, Kondo S, Date I: Role of VEGF and matrix metalloproteinase-9 in peritumoral brain edema associated with supratentorial benign meningiomas. Neuropathology 32:638-646, 2012. https://doi.org/10.1111/j.1440-1789.2012.01312.x
14. Kim KH, Kang SJ, Choi JW, Kong DS, Seol HJ, Nam DH, Lee JI: Clinical and radiological outcomes of proactive Gamma Knife surgery for asymptomatic meningiomas compared with the natural course without intervention. J Neurosurg 130:1740-1749, 2018. https://doi.org/10.3171/2017.12.JNS171943
15. Kollová A, Liscák R, Novotný J Jr, Vladyka V, Simonová G, Janousková L: Gamma Knife surgery for benign meningioma. J Neurosurg 107:325-336, 2007. https://doi.org/10.3171/JNS-07/08/0325
16. Lee EJ, Chung HT, Park H, Kim JW, Kim DG, Paek SH: Factors associated with radiation toxicity and long-term tumor control more than 10 years after Gamma Knife surgery for non-skull base, nonperioptic benign supratentorial meningiomas. J Neurosurg 138:1580-1590, 2022. https://doi.org/10.3171/2022.8.JNS22422

17. Milano MT, Sharma M, Soltys SG, Sahgal A, Usuki KY, Saenz JM, Grimm J, El Naqa I: Radiation-induced edema after single-fraction or multifraction stereotactic radiosurgery for meningioma: A critical review. Int J Radiat Oncol Biol Phys 101:344-357, 2018. https://doi.org/10.1016/j.ijrobp.2018.03.026
18. Nakasu S, Notsu A, Na K, Nakasu Y: Malignant transformation of WHO grade I meningiomas after surgery or radiosurgery: Systematic review and meta-analysis of observational studies. Neurooncol Adv 2:vdaa129, 2020. https://doi.org/10.1093/noajnl/vdaa129
19. Nakasu S, Notsu A, Nakasu Y: Prevalence of incidental meningiomas and gliomas on MRI: A meta-analysis and meta-regression analysis. Acta Neurochir (Wien) 163:3401-3415, 2021. https://doi.org/10.1007/s00701-021-04919-8
20. Novotný J Jr, Kollová A, Liscák R: Prediction of intracranial edema after radiosurgery of meningiomas. J Neurosurg 105:120-126, 2006. https://doi.org/10.3171/sup.2006.105.7.120
21. Ostrom QT, Cioffi G, Gittleman H, Patil N, Waite K, Kruchko C, Barnholtz-Sloan JS: CBTRUS statistical report: Primary brain and other central nervous system tumors diagnosed in the United States in 2012-2016. Neuro Oncol 21: v1-v100, 2019. https://doi.org/10.1093/neuonc/noz150
22. Park SH, Hwang JH, Hwang SK: Change in plasma vascular endothelial growth factor after gamma knife radiosurgery for meningioma: A preliminary study. J Korean Neurosurg Soc 57:77-81, 2015. https://doi.org/10.3340/jkns.2015.57.2.77
23. Patil CG, Hoang S, Borchers DJ 3rd, Sakamoto G, Soltys SG, Gibbs IC, Harsh GR 4th, Chang SD, Adler JR Jr: Predictors of peritumoral edema after stereotactic radiosurgery of supratentorial meningiomas. Neurosurgery 63:435-440, 2008. https://doi.org/10.1227/01.NEU.0000325257.58684.92
24. Pollock BE, Stafford SL, Link MJ, Brown PD, Garces YI, Foote RL: Single-fraction radiosurgery of benign intracranial meningiomas. Neurosurgery 71:604-612, 2012. https://doi.org/10.1227/NEU.0b013e31825ea557
25. Reinert M, Babey M, Curschmann J, Vajtai I, Seiler RW, Mariani L: Morbidity in 201 patients with small sized meningioma treated by microsurgery. Acta Neurochir (Wien) 148:1257-1265, 2006. https://doi.org/10.1007/s00701-006-0909-z
26. Sheehan J, Pikis S, Islim AI, Chen CJ, Bunevicius A, Peker S, Samanci Y, Nabeel AM, Reda WA, Tawadros SR, El-Shehaby AMN, Abdelkarim K, Emad RM, Delabar V, Mathieu D, Lee CC, Yang HC, Liscak R, Hanuska J, Alvarez RM, Patel D, Kondziolka D, Moreno NM, Tripathi M, Speckter H, Albert C, Bowden GN, Benveniste RJ, Lunsford LD, Jenkinson MD: An international multicenter matched cohort analysis of incidental meningioma progression during active surveillance or after stereotactic radiosurgery: The IMPASSE study. Neuro Oncol 24:116-124, 2022. https://doi.org/10.1093/neuonc/noab132
27. Sheehan JP, Cohen-Inbar O, Ruangkanchanasetr R, Bulent Omay S, Hess J, Chiang V, Iorio-Morin C, Alonso-Basanta M, Mathieu D, Grills IS, Lee JY, Lee CC, Dade Lunsford L: Post-radiosurgical edema associated with parasagittal and parafalcine meningiomas: A multicenter study. J Neurooncol 125:317-324, 2015. https://doi.org/10.1007/s11060-015-1911-1
28. Skeie BS, Enger PO, Skeie GO, Thorsen F, Pedersen PH: Gamma knife surgery of meningiomas involving the cavernous sinus: Long-term follow-up of 100 patients. Neurosurgery 66:661-668, 2010. https://doi.org/10.1227/01.NEU.0000366112.04015.E2
29. Unger KR, Lominska CE, Chanyasulkit J, Randolph-Jackson P, White RL, Aulisi E, Jacobson J, Jean W, Gagnon GJ: Risk factors for posttreatment edema in patients treated with stereotactic radiosurgery for meningiomas. Neurosurgery 70:639-645, 2012. https://doi.org/10.1227/NEU.0b013e3182351ae7
30. Vernooij MW, Ikram MA, Tanghe HL, Vincent AJ, Hofman A, Krestin GP, Niessen WJ, Breteler MM, van der Lugt A: Incidental findings on brain MRI in the general population. N Engl J Med 357:1821-1828, 2007. https://doi.org/10.1056/NEJMoa070972

Turk Neurosurg 36(1):145-150, 2026
DOI: 10.5137/1019-5149.JTN.48438-25.2

Original Investigation

Neuroanatomy

Received: 08.02.2025
Accepted: 18.06.2025

Published Online: 16.01.2026

The Anterior Endoscopic Transcervical Approach: A Cadaveric Study on Anatomical Challenges and Surgical Limitations in Odontoidectomy

Odhan YUKSEL[1], Seckin AYDIN[2], Aysegul Esen AYDIN[2], Galip Zihni SANUS[3]

[1]Baskent University, Faculty of Medicine, Department of Neurosurgery, Antalya, Türkiye
[2]University of Health Sciences, Prof. Dr. Cemil Tascioglu City Hospital, Department of Neurosurgery, Istanbul, Türkiye
[3]Istanbul University - Cerrahpasa, Cerrahpasa Medical Faculty, Department of Neurosurgery, Istanbul, Türkiye

Corresponding author: Odhan YUKSEL ✉ drodhanyuksel@hotmail.com

ABSTRACT

AIM: To investigate the anatomical characteristics, procedural constraints, and technical details of anterior endoscopic transcervical approach (AETCA) through cadaveric dissection.

MATERIAL and METHODS: Nine human cadaver heads, transected at the C6–C7 level and preserved in 10% formalin for no less than 4 weeks, were utilized. A 0° endoscope and surgical drills were used for odontoid removal. The resection extent was determined through volumetric analysis using CT scans performed before and after the procedure. Fluoroscopy was employed for orientation, and volumetric measurements were used to assess the resection outcomes.

RESULTS: Across the specimens, the average resection rate of the dens was 54%. Complete removal was achieved in two cases, subtotal in another two, and partial in five. The use of angled drills yielded significantly greater resection compared to flat-ended variants. No significant vascular or neurological injuries were noted. In seven cases, the resection extended to the odontoid's posterior wall. Challenges included the narrow and elongated operative corridor and difficulty maintaining midline orientation; however, these were addressed with the assistance of a custom-designed tubular trocar.

CONCLUSION: AETCA offers notable benefits, such as reduced risk of postoperative infections, shorter hospitalization, and decreased morbidity and healthcare expenditure. The study underscores the importance of technical expertise and enhanced instrumentation in achieving successful outcomes, particularly for complete odontoid removal while preserving adjacent anatomy. AETCA emerges as a viable and safer alternative for odontoidectomy, enhancing procedural efficiency. These findings contribute to the understanding of anatomical and technical factors relevant to the approach, supporting its clinical adoption and potentially shortening the learning curve.

KEYWORDS: Odontoidectomy, Anterior endoscopic transcervical approach, Cadaveric study, Craniovertebral junction, Surgical techniques

ABBREVIATIONS: AETCA: Anterior endoscopic transcervical approach

Odhan YUKSEL : 0000-0001-7339-1784
Seckin AYDIN : 0000-0003-1195-9084
Aysegul Esen AYDIN : 0000-0001-7444-8156
Galip Zihni SANUS : 0000-0001-6539-7254

INTRODUCTION

Multiple challenges are associated with surgical approaches to the craniocervical junction when addressing odontoid process pathologies (5,15). The outcome of such procedures is influenced by the distinct anatomical and biomechanical properties of this region. In addition to the established transoral and transcervical approaches, endoscopic techniques have also been employed in recent years.

The anterior endoscopic transcervical approach (AETCA) offers certain benefits, including its extrapharyngeal trajectory, which lowers the risk of bacterial contamination at the surgical site, as well as postoperative morbidity and hospital stay duration (3). Despite the inherent technical challenges of this method, AETCA appears to provide an appropriate surgical corridor for managing odontoid process pathologies. In this study, our objective was to assess the anatomical features of AETCA and explore its potential surgical limitations.

MATERIAL and METHODS

This study was conducted in the Microsurgical Neuroanatomy Laboratory of Cerrahpasa Medical Faculty and received approval from the Institutional Ethics Committee (Approval No: 83045809-604.01.02). A total of nine human cadaver heads, sectioned at the C6–C7 level, were utilized. All specimens have been preserved in a 10% formalin solution for a minimum duration of 4 weeks. For the resection procedures, a 5-mm diameter, 0˚ angled, 306-mm-long endoscope (Storz) was employed. A modified lumbar spinal endoscopy trocar was also used during the procedures.

Bone resections were conducted using different drill configurations: for the first five specimens, a straight attachment and straight-tip burr motor (Faro F632, Faro USA, Burlingame, CA, USA) operating at 30,000 rpm was used. For the remaining four specimens, a 30˚ angled burr motor (Medtronic, Midas Legend) with AT10 and ATT12 attachments, running at 75,000 rpm and equipped with a 2-mm burr tip, was utilized.

Anatomy of the Craniovertebral Junction

The vascular supply of this region is provided by the vertebral artery (VA) and the meningeal branches of the internal carotid artery. The third segment of the VA (V3) begins after the C2 level, extending laterally toward the transverse foramen of C1. After traversing this foramen, the artery reaches the posterior atlanto-occipital membrane and subsequently the dura mater. At this juncture, the fourth segment (V4) of the VA commences. Notably, anterior fixation procedures in this region carry a risk of complications due to possible screw penetration into these arterial structures.

Surgical Technique

The dissection began at the C5–C6 level with the cadaver positioned neutrally, using fluoroscopic assistance and a standard Smith–Robinson incision made from the right anterior cervical region. A skin incision was made at this level, and under fluoroscopic control, alignment with the odontoid process was achieved to establish the optimal trajectory. A trocar was introduced through the incision, and the endoscope was advanced via the trocar, allowing visualization of the anterior C2–C3 disc space and the anteroinferior portion of the C2 vertebral body. Following the opening of the platysma, dissection proceeded medially to the sternocleidomastoid muscle. The carotid sheath was retracted laterally, while the trachea was retracted medially, continuing in a superomedial direction. In the upper cervical region, after reaching the anterior surfaces of the vertebral bodies, the prevertebral muscles were retracted. The endoscopic trocar was then repositioned at approximately a 30˚ angle at the level of the odontoid process. Resection of the odontoid process was carried out using an endoscope and a drill inserted through the trocar (Figure 1).

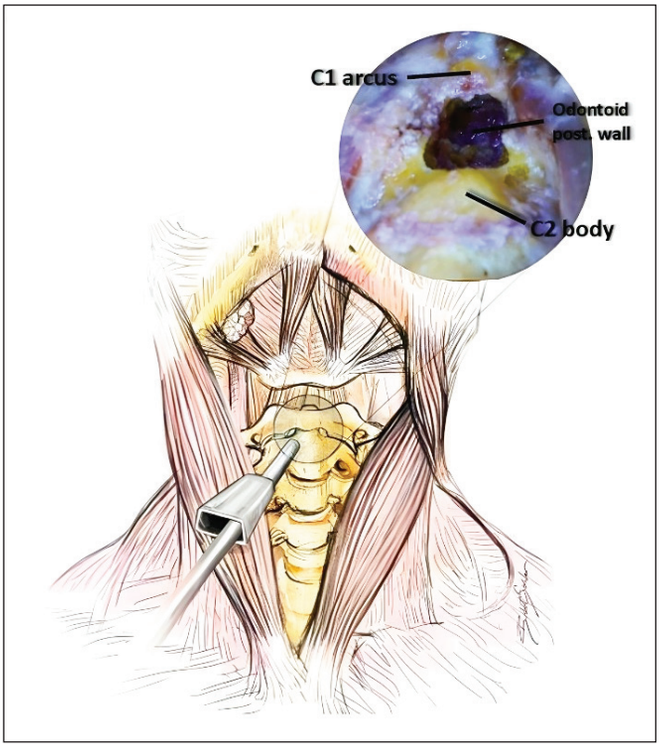

Figure 1: Diagram illustrating the surgical technique for resecting the odontoid process. The procedure starts with a right anterior cervical Smith–Robinson incision at the C5–C6 level, guided by fluoroscopy. The carotid sheath is retracted laterally and the trachea medially to allow access to the cervical spine. The prevertebral muscles are retracted to expose the anterior surface of the vertebral bodies. An endoscopic trocar is positioned at roughly a 30˚ angle at the odontoid process level, enabling resection with a drill passed through the trocar. The inset shows the endoscopic view, identifying key anatomical landmarks such as the C1 arch, the posterior wall of the odontoid process, and the C2 body. Figure 1 presents a basic anterior perspective of the surgical approach, created by a medical illustrator. The trocar is inserted through a skin incision at the C5–C6 level and advanced toward the odontoid process under alignment guidance. An example of the endoscopic view is shown in the upper right corner.

Radiological Evaluation

Once the prevertebral region was accessed during the procedure, the position of the odontoid process was identified using fluoroscopy in both sagittal and coronal planes, guided by the endoscopic trocar. Three-dimensional (3D) CT images centered on the craniovertebral junction were obtained for all specimens before and after the resection. Using the Radiology Workstation (Carestream Solutions®), the volume of resected odontoid tissue and its proportion relative to the total odontoid volume were calculated. The quantification of the resected volume was based on pre- and post-resection 3D CT imaging, and the percentage of resection was determined for each specimen.

RESULTS

The resection data from the nine cadaveric specimens are presented in Table I. On average, 54% of the dens volume was resected. In the first five specimens, where a flat-end drill tip was employed, the mean volume of resection was 28.5%. In contrast, the use of an angled drill in the remaining four specimens resulted in a markedly higher resection percentage, averaging 85.8%. These volumetric values were calculated by comparing pre- and post-resection 3D CT scans using the Radiology Workstation software, which allowed for accurate measurement of the removed odontoid volume in relation to the original anatomical structure (Table II). In seven specimens, it was possible to resect the anterior arch of C1 and reach the posterior cortical wall of the odontoid process. In cases where near-complete resection of the odontoid was achieved, no significant arterial, venous, or neural injuries were identified in any of the cadavers. Following resection, 3D CT imaging focused on the craniovertebral junction was obtained for all specimens (Figure 2).

DISCUSSION

The dens axis represents an anatomically critical area, where surgical intervention carries significant risk due to its proximity to vital anatomical structures (7,10,11). Furthermore, a thorough understanding of the complex anatomy of this region—difficult to access because of its deep location and limited surgical corridors—is essential for evaluating different surgical techniques and selecting the most appropriate method for individual patients (3,19,21). While transoral (transpharyngeal) approaches offer a broad surgical view and access for ventral decompression, particularly in cases of basilar invagination, they have been associated with notable postoperative morbidity in some instances (1,2,4,6,9). In addition, when supplementary procedures such as Le Fort osteotomy or mandibulotomy are required to enlarge the surgical field, the overall morbidity increases and hospital stays become longer (12,14). These concerns have prompted the exploration of alternative approaches to the traditional transoral technique. Advances in endoscopic technology have played a key role in this development. The AETCA was introduced as a means to avoid the complications linked to traditional transoral and endonasal pathways in surgeries addressing the dens, particularly in the context of platybasia.

Common complications associated with transpharyngeal approaches—both transoral and endonasal—include direct exposure to oral and nasal flora, extended intubation periods,

Table I: Drill and Resection Data of All Specimens

Specimen No	Drill type	Resected volume ratio (%)	Resected of C1 anterior arcus	Extending posterior odontoid wall
1	Flat-end	17.8	No	No
2	Flat-end	16.5	No	No
3	Flat-end	35.7	Yes	Yes
4	Flat-end	41.1	Yes	Yes
5	Flat-end	31.4	Yes	Yes
6	Angled	57.8	Yes	Yes
7	Angled	85.7	Yes	Yes
8	Angled	100.0	Yes	Yes
9	Angled	100.0	Yes	Yes

Table II: Resection Data According to Drill Type

Drill type	Resection ratio (%)	Resection of C1 anterior arcus (%)	Extending posterior odontoid wall (%)
Flat-end group	28.5	40	40
Angled group	85.8	100	100

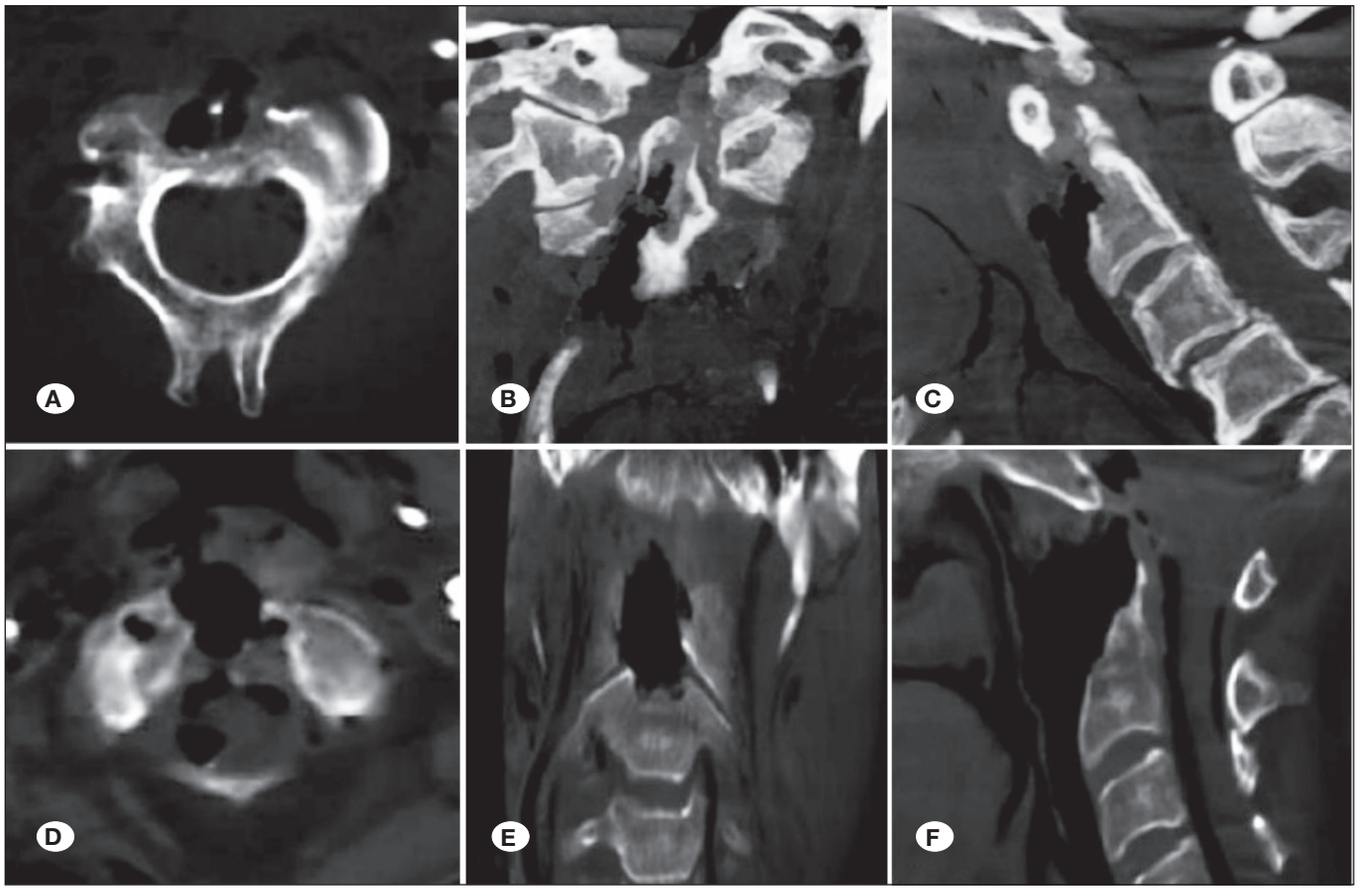

Figure 2: Three-dimensional CT images of the craniovertebral junction from cadaver specimens following odontoid process resection. **A–C)** Axial, coronal, and sagittal views displaying partial resection of the posterior wall of the odontoid cortex and the anterior arch of C1. **D–F)** Additional axial, coronal, and sagittal views demonstrating the odontoid process and adjacent anatomical structures after complete resection.

the need for tracheostomy in certain cases, reliance on nasogastric tube feeding postoperatively, cosmetic concerns particularly in transmandibular approaches, and prolonged hospitalizations. To address and potentially eliminate these issues, the AETCA was developed (5,13,15,19,20,22). The primary advantage of AETCA over endoscopic transoral and endonasal techniques lies in the fact that the pharyngeal mucosa remains intact, significantly reducing the risk of bacterial contamination and subsequent infection. Since this approach avoids mucosal incision, unlike the transoral route, it minimizes the likelihood of postoperative infection. As there is no clinical studies on AETCA currently available in the literature, these anticipated benefits can only be evaluated through cadaveric studies such as this one. Moreover, minimizing infection risk and removing the need for postoperative nasogastric tube placement can lead to reduced hospital stays, thereby decreasing morbidity and lowering overall healthcare costs. In a study by Dogan et al., the authors noted that posterior endoscopic procedures resulted in shorter hospital stays and were more cost-effective than anterior approaches (8). Consequently, patients undergoing AETCA experience no delay in postoperative feeding, eliminating the need for further interventions such as PEG placement. It has also been demonstrated that AETCA allows for earlier extubation and reduced hospitalization time, thereby lowering associated morbidities and care expenses (18).

There are several challenges when applying the AETCA technique compared to transoral and endonasal approaches. The primary anatomical difficulties include the length and narrowness of the surgical corridor and the challenges of accurately identifying the midline (18). To achieve precise midline localization and complete resection in clinical practice, technical aids such as neuronavigation, intraoperative CT, or fluoroscopy should be available (14,16,17). In our dissections, fluoroscopy in sagittal and coronal planes was used for surgical orientation once the prevertebral area was reached. The drawback of the long surgical corridor is lessened by using a trocar, which allows retraction without tissue damage within the corridor. Although the use of a specialized trocar is necessary, familiarity with anterior dissection at the C5–C6 level is important when comparing this technique to other endoscopic retropharyngeal approaches (16-18). A specially designed tubular trocar is employed for AETCA. Its tubular shape offers a 360° safe working space, and during our

dissections, no major arterial, venous, or esophageal–tracheal injuries were noted in any cadavers. However, since three or more surgical instruments (such as the endoscope, drill, and aspirator) are often used simultaneously within the trocar, surgical manipulation and the surgeon's movements can become relatively more difficult. This may prolong the surgical time and potentially influence the success of the resection. Additionally, trocar movement during surgery could cause microtrauma in the neck region of patients, though there is currently no data in the literature addressing this issue, and further clinical studies are required.

In odontoidectomy performed via AETCA, the adequacy of technical equipment is the primary factor influencing surgical success. The type of drill used affected the dens resection rates observed in cadavers. Clinical series in the literature generally employed angled endoscopes (25–30°), but except for one study, all have used non-angled drills (22). In our study, a 0° endoscope was used, while bone resection was carried out with drills of different angles. The use of drills with varying angles also affected the odontoid resection rates in our dissections. With a flat-end drill, reaching the posterior wall of the odontoid was not possible. When comparing resection amounts between the two drill types, cadavers treated with angled drills showed significantly higher resection rates.

The second factor contributing to the AETCA's success is the accumulation of surgical experience (21). Two major challenges to gaining proficiency in endoscopic surgery are the steep learning curve and the absence of depth perception due to two-dimensional imaging (22). Our study also showed the impact of increased surgical experience on resection outcomes. In cadavers where flat-end drills were used, resection rates improved from 17.8% to 31.4% over time, while in those with angled drills, the rate increased from 57.8% to 100%.

Other approaches, such as transoral and endoscopic endonasal techniques, have the advantage of better access to the posterior section of the odontoid (13,15). In AETCA, accessing the posterior section of the dens is more challenging because of the angle of the endoscope relative to the dens axis. In odontoidectomies—especially those performed on patients with basilar invagination—surgical success depends on the adequacy of brainstem decompression, with the goal of achieving sufficient decompression. Moreover, surgical outcomes reported in the literature have not been evaluated volumetrically, nor have specific criteria been established to define the extent of resection. Our study measured the extent of resection volumetrically and reported it as a percentage of the original odontoid volume. This method allowed for an objective comparison of different surgical instruments and techniques employed during AETCA.

The first limitation of our study is that the AETCA technique was mainly evaluated in terms of its anatomical features, limitations, and characteristics. However, because this was a cadaveric study, were unable to evaluate surgical success or the risks of complications. The second limitation is the absence of the cadavers' bodies, which allowed us to adjust the head position during dissection as needed—an advantage not possible in live patients. It is also important to note that accessing the odontoid region via AETCA may be difficult or impossible in patients with broad chests, severe obesity, or marked thoracic kyphosis. The third limitation is that our technical setup required resection of the C1 arch to achieve complete odontoidectomy. With increased surgical experience, advancements in endoscopic and drilling techniques, and improved equipment, it may become possible to preserve the C1 arch. Further anatomical and surgical studies are needed to refine and enhance the technique.

CONCLUSION

AETCA offers benefits including a reduced risk of postoperative infection, shorter hospital stays, prevention of potential morbidities, and lower healthcare costs. However, challenges such as a long surgical corridor and difficulties with midline orientation are associated with the technique. Nevertheless, success can be achieved by utilizing specially designed trocars, angled drills, and supplementary imaging methods. This cadaver study, which focused on the technical and anatomical aspects of AETCA, aims to shorten the learning curve and help surgeons gain experience prior to performing odontoidectomy on patients.

Future clinical studies are needed to evaluate patient outcomes following AETCA.

ACKNOWLEDGEMENTS

Preparation for publication of this article is partially supported by the Turkish Neurosurgical Society.

Declarations

Funding: This research did not receive any specific grant from funding agencies in the public, commercial, or not-for-profit sectors.

Availability of data and materials: The datasets generated and/or analyzed during the current study are available from the corresponding author by reasonable request.

Disclosure: The authors declare no competing interests.

AUTHORSHIP CONTRIBUTION

Study conception and design: OY, SA
Data collection: OY, SA, GZS
Analysis and interpretation of results: OY, SA, GZS
Draft manuscript preparation: OY, SA, AEA
Critical revision of the article: SA, AEA
Other (study supervision, fundings, materials, etc...): SA, AEA
All authors (OY, SA, AEA,GZS) reviewed the results and approved the final version of the manuscript.

REFERENCES

1. Apuzzo ML, Weiss MH, Heiden JS: Transoral exposure of the atlantoaxial region. Neurosurgery 3:201-207, 1978. https://doi.org/10.1227/00006123-197809000-00012

2. Arbit E, Patterson RH Jr: Combined transoral and median labiomandibular glossotomy approach to the upper cervical spine. Neurosurgery 8:672-674, 1981. https://doi.org/10.1227/00006123-198106000-00006
3. Baird CJ, Conway JE, Sciubba DM, Prevedello DM, Quiñones-Hinojosa A, Kassam AB: Radiographic and anatomic basis of endoscopic anterior craniocervical decompression: A comparison of endonasal, transoral, and transcervical approaches. Neurosurgery 65:158-163, 2009. https://doi.org/10.1227/01.NEU.0000345641.97181.ED
4. Balasingam V, Anderson GJ, Gross ND, Cheng CM, Noguchi A, Dogan A, McMenomey SO, Delashaw JB Jr, Andersen PE: Anatomical analysis of transoral surgical approaches to the clivus. J Neurosurg 105:301-308, 2006. https://doi.org/10.3171/jns.2006.105.2.301
5. Cavallo LM, Cappabianca P, Messina A, Esposito F, Stella L, de Divitiis E, Tschabitscher M: The extended endoscopic endonasal approach to the clivus and cranio-vertebral junction: Anatomical study. Childs Nerv Syst 23:665-671, 2007. https://doi.org/10.1007/s00381-007-0332-7
6. Chatain GP, Chee K, Finn M: Review of transoral odontoidectomy. Where do we stand? Technical note and a single-center experience. Interdiscip Neurosurg 29:101549, 2022. https://doi.org/10.1016/j.inat.2022.101549
7. Cirpan S, Sayhan S, Yonguc GN, Eyuboglu C, Guvencer M, Naderi S: Surgical anatomy of neurovascular structures related to ventral C1-2 complex: An anatomical study. Surg Radiol Anat 40:581-586, 2018. https://doi.org/10.1007/s00276-017-1961-5
8. Dogan I, Bayatli E, Eray HA, Erdogan K, Terzi M, Hasimoglu S, Tekneci O, Beton S, Eroglu U, Ozgural O, Kahilogullari G, Caglar YS: Single-institution comparative analysis for odontoid resection: Posterior transaxis versus anterior transnasal approach. Neurosurg Focus 54(3):E12, 2023. https://doi.org/10.3171/2022.12.FOCUS22624
9. Gladi M, Iacoangeli M, Specchia N, Re M, Dobran M, Alvaro L, Moriconi E, Scerrati M: Endoscopic transnasal odontoid resection to decompress the bulbo-medullary junction: A reliable anterior minimally invasive technique without posterior fusion. Eur Spine J 21:55-60, 2012. https://doi.org/10.1007/s00586-012-2220-4
10. Hoh DJ, Maya M, Jung A, Ponrartana S, Lauryssen CL: Anatomical relationship of the internal carotid artery to C-1: clinical implications for screw fixation of the atlas. J Neurosurg Spine 8:335-340, 2008. https://doi.org/10.3171/SPI/2008/8/4/335
11. Hong JT, Lee SW, Son BC, Sung JH, Kim IS, Park CK: Hypoglossal nerve palsy after posterior screw placement on the C-1 lateral mass. Case report. J Neurosurg Spine 5:83-85, 2006. https://doi.org/10.3171/spi.2006.5.1.83
12. James D, Crockard HA: Surgical access to the base of skull and upper cervical spine by extended maxillotomy. Neurosurgery 29:411-416, 1991. https://doi.org/10.1097/00006123-199109000-00012
13. Kassam AB, Snyderman C, Gardner P, Carrau R, Spiro R: The expanded endonasal approach: A fully endoscopic transnasal approach and resection of the odontoid process: Technical case report. Neurosurgery 57:E213, 2005. https://doi.org/10.1227/01.NEU.0000163687.64774.E4
14. Menezes AH: Surgical approaches: Postoperative care and complications "transoral-transpalatopharyngeal approach to the craniocervical junction". Childs Nerv Syst 24:1187-1193, 2008. https://doi.org/10.1007/s00381-008-0599-3
15. Messina A, Bruno MC, Decq P, Coste A, Cavallo LM, de Divittis E, Cappabianca P, Tschabitscher M: Pure endoscopic endonasal odontoidectomy: anatomical study. Neurosurg Rev 30:189-194, 2007. https://doi.org/10.1007/s10143-007-0084-6
16. Ohara Y, Nakajima Y, Kimura T, Kikuchi N, Sagiuchi T: full-endoscopic transcervical ventral decompression for pathologies of craniovertebral junction: Case series. Neurospine 17:138-144, 2020. https://doi.org/10.14245/ns.2040172.086
17. Ohara Y, Uchikado H, Hara T, Nojiri H, Abe E, Kikuchi N, Kimura T: Endoscopic approach for a difficult cervical area: fully endoscopic uniportal transcervical approach for ventral pathologies of the craniovertebral junction. J Minim Invasive Spine Surg Tech 8:21-27, 2023. https://doi.org/10.21182/jmisst.2023.00612
18. Ruetten S, Hahn P, Oezdemir S, Baraliakos X, Merk H, Godolias G, Komp M: Full-endoscopic uniportal odontoidectomy and decompression of the anterior cervicomedullary junction using the retropharyngeal approach. Spine (Phila Pa 1976) 43:911-918, 2018. https://doi.org/10.1097/BRS.0000000000002561
19. Seker A, Inoue K, Osawa S, Akakin A, Kilic T, Rhoton AL Jr: Comparison of endoscopic transnasal and transoral approaches to the craniovertebral junction. World Neurosurg 74:583-602, 2010. https://doi.org/10.1016/j.wneu.2010.06.033
20. Visocchi M, Di Martino A, Maugeri R, González Valcárcel I, Grasso V, Paludetti G: Videoassisted anterior surgical approaches to the craniocervical junction: Rationale and clinical results. Eur Spine J 24:2713-2723, 2015. https://doi.org/10.1007/s00586-015-3873-6
21. Wolinsky JP, Sciubba DM, Suk I, Gokaslan ZL: Endoscopic image-guided odontoidectomy for decompression of basilar invagination via a standard anterior cervical approach. Technical note. J Neurosurg Spine 6:184-191, 2007. https://doi.org/10.3171/spi.2007.6.2.184
22. Zenga F, Pacca P, Tardivo V, Pennacchietti V, Garbossa D, Pecorari G, Ducati A: Endoscopic endonasal approach to the odontoid pathologies. World Neurosurg 89:394-403, 2016. https://doi.org/10.1016/j.wneu.2016.02.011

Turk Neurosurg 36(1):151-157, 2026
DOI: 10.5137/1019-5149.JTN.49641-25.2

Perspective

Received: 11.08.2025
Accepted: 30.10.2025
Published Online: 16.01.2026

Honoring the Mentors from 2024: A Tribute to Their Legacy

Francisco TERZANO[1,2], Francisco ZARRA[2], Andrea L. CASTILLO[3], Adnan Hussain SHAHID[4], Ismail BOZKURT[5,6], Bipin CHAURASIA[7], Alejandro Mercado SANTORI[8]

[1]Clínica la Sagrada Familia, Department of Neurosurgery, Ciudad Autónoma de Buenos Aires, Argentina
[2]University of Buenos Aires School of Medicine, Department of Neurosurgery, Buenos Aires, Argentina
[3]LINT, Facultad de Medicina, Universidad Nacional de Tucumán, Tucumán, Argentina
[4]University of South Alabama, Department of Neurosurgery, Mobile, United States
[5]Yuksek Ihtisas University, Faculty of Medicine, Department of Neurosurgery, Ankara, Türkiye
[6]Medical Park Ankara Hospital, Department of Neurosurgery, Ankara, Türkiye
[7]Neurosurgeon at the Department of Neurosurgery, Neurosurgery Clinic, Birgunj 44300
[8]Hospital Marcial Quiroga, Department of Neurosurgery, San Juan, Argentina

Corresponding author: Francisco ZARRA ✉ franciscozarra@hotmail.com

ABSTRACT

The concept of a mentor represents one of the most important pillars of medical training. It constitutes one of the oldest and noblest arts that has contributed to the growth of this specialty for generations. Mentorship is the essential way to transmit knowledge and values to future generations, ensuring the continuation of legacy in the field. Therefore, the experience and knowledge of current neurosurgeons reflect the influence of previous neurosurgeons. This article aims to show respect to the educators and mentors who passed away in 2024 around the world, with deep gratitude, as learning from those who preceded us helps build a lasting legacy in neurosurgery.

A literature review was conducted to examine the deaths of neurosurgeons in 2024 worldwide, without limitation to the English language.

A total of 35 neurosurgeons were identified worldwide: one from Africa (Egypt), ten from Asia (Bangladesh, Japan, South Korea, India, and Pakistan); eleven from Europe (Greece, Poland, Spain and Türkiye), seven from North America (Canada and the United States), and six from South America (Argentina, Brazil, Chile, Colombia, and Mexico).

In 2024 there was a great loss to the global neurosurgical community. The deceased neurosurgeons left an indelible mark and a legacy that will endure through their disciples and students. The main lesson is to remain proud and grateful for sharing this discipline across generations, preserving the true values of human knowledge.

KEYWORDS: Ethics, Legacy, Medical education, Mentors

INTRODUCTION

The concept of a mentor is profound and transcendent. It is much more than a friendship with a professor and constitutes a cornerstone of medical training (1). This tribute to the legacy of mentors serves as a reflection on and acknowledgment of these individuals who unintentionally guide their disciples to pursue neurosurgical training, clinically and academically, and to transcend these boundaries (2,3).

In respect and honor of the neurosurgeons who passed away around the world in 2024, we have prepared a humble tribute highlighting their achievements in neurosurgery, categorized according to their country of residence (Table I).

Francisco ZARRA : 0009-0002-9565-6944
Andrea L. CASTILLO : 0000-0001-6596-1177
Adnan Hussain SHAHID : 0000-0003-2703-3497
Ismail BOZKURT : 0000-0002-6719-5522
Bipin CHAURASIA : 0000-0002-8392-2072
Alejandro Mercado SANTORI : 0009-0003-0932-5194

Table I: Neurosurgeons Known to have passed away in 2024, Categorized by Continent-Country (4)

Full name	Continent	Country	Field	Date
Mohammed Tawfik Hosny	Africa	Egypt	Skull Base	1980-2024
Tipu Aziz	Asia	Bangladesh	Functional Neurosurgery	1959-2024
Annaswamy Raja		India	Cerebrovascular diseases	1951-2024
Jagtar Singh Tiwana		India	Spine surgery	1936-2024
Raj Ghoniya		India	General neurosurgery	1990-2024
Sandip Chaterjee		India	Pediatric neurosurgery	1960-2024
Sunil Pandya		India	General neurosurgery	1940-2024
Vijay Kumar Kak		India	Pediatric neurosurgery	1938-2024
Takanori Fukushima		Japan	Skull Base	1942-2024
Saeed A. Bajwa		Pakistan	General neurosurgery	1951-2024
Tae Sung Park		South Korea	Pediatric neurosurgery	1947-2024
George Samandouras	Europe	Greece	Neuro-oncology	1967-2024
Jacek M. Malik		Poland	Spine neurosurgery	1957-2024
José Gerardo Martín Rodríguez		Spain	Functional neurosurgery	1941-2024
Ant Metin Atasoy		Türkiye	General neurosurgery	1951-2024
Aysima Altınok		Türkiye	General neurosurgery	1929-2024
Cahit Özşeker		Türkiye	General neurosurgery	1945-2024
Cem Akkurt		Türkiye	Neuro-oncology	1958-2024
Mehmet Akif Yürürdurmaz		Türkiye	General neurosurgery	1963-2024
Nuriye Güzin Özdemir		Türkiye	General neurosurgery	1969-2024
Osman Ekin Özcan		Türkiye	General neurosurgery	1947-2024
Zeki Buharalı		Türkiye	General neurosurgery	1938-2024
Douglas Cochrane	North America	Canada	Pediatric neurosurgery	1950-2024
David G. Kline		United States	Peripheral nerve	1934-2024
Frances Conley		United States	Spine neurosurgery	1940-2024
John P. Girvin		United States	Functional neurosurgery	1934-2024
L. Nelson “Nick” Hopkins III		United States	Endovascular neurosurgery	1943-2024
Mark E. Shaffrey		United States	Skull Base	1961-2024
Rupert Smith, Jr		United States	Skull Base	1932- 2024
Daniel D’Osvaldo	South America	Argentina	Skull Base	1953-2024
Marcos Flavio Ghizoni		Brazil	Neuro-oncology	1946-2024
Renato Chiorino Radaelli		Chile	Neuro-oncology	1930-2024
Victor Hugo Bastos Pardo		Colombia	Cerebrovascular diseases	1968-2024
Antonio M. Zárate Méndez		Mexico	Cerebrovascular diseases	1944-2024
Fernando Rueda Franco		Mexico	Pediatric neurosurgery	1936-2024

The table is organized alphabetically by continent and country, respectively.

AFRICA

Prof. Dr. Mohammed Tawfik Hosny, Egypt (1980–2024)

Dr. Tawfik Hosny was a distinguished military neurosurgeon from Egypt. He served as a professor of neurosurgery and dean of the School of Medicine, achieving the rank of Major General in the armed forces. He published several peer-reviewed scientific articles in neurosurgery and participated in numerous international conferences. Dr. Hosny left an indelible legacy in the Egyptian Armed Forces and the field of Egyptian neurosurgery.

ASIA

Prof. Dr. Tipu Aziz, Bangladesh (1959–2024)

Born in Bangladesh in 1956, Dr. Aziz pursued his early education there before moving to the United Kingdom, where he studied neurophysiology at the University of London and developed an interest in deep brain stimulation and functional neurosurgery. He earned his doctorate from the University of Manchester, focusing his research on Parkinson's disease in primates. His groundbreaking work greatly benefited the medical community. In 2013, he received the "Service to Medicine Award" at the British Muslim Awards, and in 2024, he was honored by the British Society for Stereotactic and Functional Neurosurgery for his outstanding contributions to global neurosurgery. A legend in his field, Dr. Aziz will always be remembered for his compassion, mentorship, and dedication to patients.

Prof. Dr. Annaswamy Raja, India (1951–2024)

Dr. Raja was a distinguished neurosurgeon and educator in India. He earned his MBBS from Madras University (1967–1972) and completed his MS in Neurosurgery (1974–1979). He served in Kasturba Medical College, Manipal, progressing through academic ranks to become Head of the Department in 2010. He published numerous papers in national and international journals. His expertise included aneurysm, vascular surgery, arteriovenous malformations, acoustic schwannomas, microsurgical excision of spinal cord AVMs, and intramedullary spinal cord tumors. He introduced several innovative microsurgical techniques and is regarded as one of India's legendary neurosurgeons.

Prof. Dr. Jagtar Singh Tiwana, India (1936–2024)

Dr. Tiwana was a dedicated educator, mentor, and pioneer in neurosurgery. He obtained his Master of Surgery from the Sanjay Gandhi Postgraduate Institute of Medical Sciences and later completed a fellowship in spine surgery. He worked as a Professor of Neurosurgery at Park Hospital in Panipat, Haryana, India. He authored several national and international peer-reviewed publications. He was deeply respected as a spine specialist and a compassionate human being.

Prof. Dr. Raj Ghoniya, India (1990–2024)

Dr. Ghoniya was a 34-year-old neurosurgeon who graduated with an MBBS from R. D. Gardi Medical College, Vikram University. He served at the Department of Neurosurgery at All India Institute of Medical Sciences and authored several papers in the field. He will be remembered for his energy, professionalism, and commitment to excellence.

Prof. Dr. Sandip Chaterjee, India (1960–2024)

Dr. Chatterjee was born and raised in Kolkata, India, where he graduated from medical school with outstanding academic performance. Later, he moved to the United Kingdom, earning the Fellowship of the Royal Colleges of Surgeons (FRCS) in Edinburgh. He specialized in pediatric neurosurgery, was regarded as a true master in his field, and made exceptional contributions in his field. He served as a former president of the Indian Society of Pediatric Neurosurgery and former Editor-in-Chief of several prestigious indexed journals. With over 150 published scientific papers and 30 book chapters to his credit, his scholarly achievements were remarkable. His students and colleagues will always remember his passion, compassion, and dedication toward his patients. He lived with courage and strength—his love, teachings, and contributions will remain with us forever.

Prof. Dr. Sunil Pandya, India (1940–2024)

Dr. Pandya began his medical training at Seth GS Medical College and KEM Hospital in Mumbai. He continued his career at Jaslok Hospital and Research Centre in the same city thereafter. His contributions to neurosurgery in Mumbai and across India were exceptional. His passion and love for his profession will always be remembered.

Prof. Dr. Vijay Kumar Kak, India (1938–2024)

Born in India in 1938, Dr. Kak was an educator, neurosurgeon, and researcher who made significant contributions to neurosurgery. He graduated with honors from Sarojini Naidu Medical College in 1960 and completed his residency at the Royal Victoria Hospital in Belfast, earning his FRCS from the United Kingdom. Later, he joined the Postgraduate Institute of Medical Education and Research, where he achieved remarkable scientific advancements. Moreover, he served as the Dean of the Post Graduate Institute of Medical Education and Research (PGIMER) School of Medicine in Chandigarh for several years. His interests included vascular and pediatric neurosurgery. He will be fondly remembered for his devotion to his patients and students.

Prof. Dr. Takanori Fukushima, Japan (1942–2024)

Dr. Fukushima graduated with honors from the School of Medicine at University of Tokyo in 1968. He served for nearly a decade as Professor of Neurosurgery and Chief of Neurosurgery at Mitsui Memorial Hospital. He is recognized as a pioneer in skull base surgery and the inventor of keyhole surgery, earning worldwide acclaim as a true legend in his field. His groundbreaking work and dedication to neurosurgical education and innovation will continue to shape the field for generations to come.

Prof. Dr. Saeed Bajwa, Pakistan (1951–2024)

Originally from Pakistan, Dr. Bajwa graduated from Nishtar Medical College, University of Punjab, Lahore, and completed his neurosurgery residency at the Military Hospital in Lahore.

Later, he migrated to the United States of America in 1980 to continue his medical career and worked for many years with Universal Health Services. A leader in advancing neurosurgical techniques, Dr. Bajwa was known for his dedication, compassion, and patient-centered care. His demise is a great loss not only to neurosurgery but also to his many patients and mentees.

Prof. Dr. Tae Sung Park, South Korea (1947–2024)

Dr. Park was born in South Korea and graduated from Yonsei University College of Medicine, where he completed his neurosurgery residency. He pursued advanced training in the United States at the University of Virginia and Ohio State University, with research fellowships in pediatric neurosurgery at Harvard Medical School and the University of Toronto. His research focused on vascular injuries in neonatal brains and syringomyelia. A pioneer of selective dorsal rhizotomy, Dr. Park was regarded as a legend in pediatric neurosurgery. He joined Washington University in 1989 and served for over 35 years as Professor and Surgeon in the Division of Pediatric Neurosurgery. He passed away at the age of 77, leaving a legacy of excellence, compassion, and innovation that continues to inspire neurosurgeons worldwide.

EUROPE

Prof. Dr. George Samandouras, Greece (1967–2024)

Dr. Samandouras was born in Greece in 1967 and completed his neurosurgery residency in Oxford in 2007, followed by a neuro-oncology fellowship in France in 2008. His main field of expertise was brain tumors. He was a consultant neurosurgeon at the Victor Horsley Department and the editor of The Neurosurgeon's Handbook. He will be remembered for his remarkable life philosophy, dedication to patient care, and his status as a true legend in the field of neurosurgery.

Prof. Dr. Jacek M. Malik, Poland (1957–2024)

Dr. Malik was born in Wroclaw, Poland, in 1957, and graduated with honors in Medicine from the Medical University of Wroclaw. Later, he completed his neurosurgery residency at the University of Virginia in Charlottesville. He served as Professor of Neurosurgery and Head of the Department at the Veterans Affairs Hospital in Little Rock, Arkansas, for several years. Throughout his career, he specialized in spinal surgery. We will always remember his great legacy and his deep love for his patients and students.

Prof. Dr. José Gerardo Martín Rodríguez, Spain (1941–2024)

Dr. Martín Rodríguez, affectionately known as "Pepe" among Spanish and international neurosurgeons, was a highly respected figure in the global neurosurgical community. Within the World Federation of Neurosurgical Societies (WFNS), he made significant contributions as Secretary under Dr. Ed Laws and co-founded the WFNS Foundation alongside Dr. Madjid Samii. For over three decades, this foundation has supported the training of neurosurgeons and improved care in underserved regions. In recognition of his lifelong commitment and enduring legacy, the Spanish Society of Neurosurgery has dedicated the WFNS World Congress in Madrid 2025 to his memory.

Prof. Dr. Ant Metin Atasoy, Türkiye (1951–2024)

Dr. Atasoy began his career in mining engineering but later pursued medicine. He completed his medical degree and neurosurgery residency at Ankara University. Eager to enhance his skills, he undertook additional training and observation excursions in Japan, the United States, Switzerland, Germany, Canada, and the United Kingdom. Upon returning to Turkey, he applied the knowledge gained abroad to revitalize the Department of Neurosurgery at Eskişehir Osmangazi University. Dr. Atasoy served as a mentor and cornerstone for his students, leaving a lasting legacy in Turkish neurosurgery.

Prof. Dr. Aysima Altınok, Türkiye (1929–2024)

Dr. Aysima Altınok was born in 1929 in Erzincan, Turkey. She graduated from Istanbul University School of Medicine with honors, ranking third in her class. She completed her residency under the mentorship of Dr. Hami Dilek at Haydarpaşa Numune Hospital. In 1959, she became Turkey's first female neurosurgeon and one of the earliest female neurosurgeons in the world, serving as an inspiration for generations of women in neurosurgery. In 1968, she became a clinic chief and a founding member of the Turkish Neurosurgical Society. She retired in 1992, continuing to engage in the activities she loved. Her legacy remains indelible for future generations of female neurosurgeons.

Prof. Dr. Cahit Özşeker, Türkiye (1945–2024)

Born in 1945 in Bursa, Turkey, Dr. Özşeker was an accomplished educator and neurosurgeon. A graduate of Bursa Erkek Lisesi, he was a lifelong and dedicated member of the Turkish Neurosurgical Society, serving the profession for 50 years. His steadfast commitment and contributions to neurosurgery will always be remembered with the highest respect.

Prof. Dr. Cem Akkurt, Türkiye (1958–2024)

Dr. Cem Akkurt was a remarkable Turkish neurosurgeon specializing in neuro-oncology. He graduated from Istanbul University Faculty of Medicine in 1981 and completed his neurosurgery residency at Hacettepe University Faculty of Medicine in 1990. Later, he served as a professor and attending neurosurgeon at Düzce Atatürk and Muş State Hospitals. He passed away at the age of 66, leaving behind a legacy of clinical excellence and dedication.

Prof. Dr. Mehmet Akif Yürürdurmaz, Türkiye (1963–2024)

Dr. Yürürdurmaz graduated in medicine in Bursa and trained in neurosurgery in Istanbul, achieving an outstanding professional career. Thereafter, he continued his practice in Izmir, leaving an enduring impact on his patients, students, and the history of neurosurgery in Turkey.

Prof. Dr. Nuriye Güzin Özdemir, Türkiye (1969–2024)

Dr. Güzin Özdemir was a dedicated Turkish neurosurgeon and educator known for her compassion and professionalism. She made significant contributions to primary cerebral lymphomas

and played an important role in the advancement of women in Turkish neurosurgery. Her legacy remains a permanent part of the country's neurosurgical history.

Prof. Dr. Osman Ekin Özcan, Türkiye (1947–2024)

Originally from Turkey, Dr. Özcan was one of the key founders of the Turkish Neurosurgical Society. He graduated with honors from Hacettepe University School of Medicine. He will be remembered as a great neurosurgeon for his dedication to his patients and for his important role in shaping the history of Turkish neurosurgery.

Prof. Dr. Zeki Buharalı, Türkiye (1938–2024)

Dr. Buharalı devoted his career to teaching and mentoring countless neurosurgeons at Ankara Training and Research Hospital. His lifelong commitment to education helped shape the future of neurosurgery in Turkey. His contributions and influence will forever be respected and honored.

NORTH AMERICA

Prof. Dr. Douglas Cochrane, Canada (1950–2024)

Dr. Cochrane was born in Cambridge, Ontario, Canada, in 1950. He studied medicine at the University of Toronto Medical School and completed his neurosurgery residency at the University of Calgary. Later, he pursued a fellowship in Pediatric Neurosurgery at the Hospital for Sick Children in Toronto. He enjoyed an outstanding 30-year partnership with Dr. Paul Steinbok in the Division of Pediatric Neurosurgery at the British Columbia Children's Hospital. Over his career, he performed more than 3000 neurosurgical operations and trained generations of medical students, residents, and fellows. Moreover, Dr. Cochrane served in several healthcare leadership roles across the province. He is fondly remembered for his dedication, intensity, and pursuit of excellence.

Prof. Dr. David G. Kline, United States (1934–2024)

Dr. Kline was born in Philadelphia in 1934 and became a trailblazer in neurosurgery, revolutionizing the treatment of nerve tumors and peripheral nerve injuries. He graduated from the University of Pennsylvania and completed his neurosurgical residency at the University of Michigan. Dr. Kline served in the U.S. Army at Walter Reed General Hospital and received the prestigious Cushing Medal in 2006. A member of numerous national and international neurosurgical societies, his humanity, compassion, and brilliance as a surgeon defined his legacy. His passing marks a great loss to the field.

Prof. Dr. Frances Conley, United States (1940–2024)

Originally from Palo Alto, California, Dr. Conley completed her medical studies at Stanford University in 1966 with outstanding distinction. She became the first woman to practice neurosurgery at Stanford University and, in 1975, the first female faculty member in the Department of Neurosurgery. In 1986, she became the first woman to chair a neurosurgery department at any North American university. She will be remembered as an inspirational role model for female neurosurgeons worldwide.

Prof. Dr. John P. Girvin, United States (1934–2024)

Dr. Girvin was born in Detroit, Michigan, in 1934. He obtained his MD from Western University in 1958 with honors, followed by a PhD in neurophysiology and neurological training at the Montreal Neurological Institute. He furthered his studies in Glasgow and Cleveland. In 1977, he established the Epilepsy Program at Western University and was deeply devoted to the training of neurology residents and fellows. Dr. Girvin led significant advances in surgical techniques, particularly in brain electrical stimulation and awake epilepsy surgery. He will be remembered forever as a passionate and dedicated neurosurgeon.

Prof. Dr. L. Nelson "Nick" Hopkins III, United States (1943–2024)

Dr. Hopkins was considered as one of the fathers of endovascular neurosurgery and a world-renowned neurosurgeon, neuroradiologist, and researcher. He completed medical school at Albany Medical College with distinction, followed by neurosurgical residency at Case Western Reserve University. He spent much of his career at Buffalo University, where he was the chairman of the Department of Neurosurgery. A former president of the AANS, Dr. Hopkins was a pioneer in neuroradiology, ushering in a new era in stroke management and leaving an indelible mark on the field.

Prof. Dr. Mark E. Shaffrey, United States (1961–2024)

Dr. Shaffrey was born in West Virginia, United States and earned his Bachelor of Science degree in Biochemistry and Biology in 1983. He completed medical school at the University of Virginia. Then, he enlisted in the United States Air Force. Dr. Shaffrey completed his neurosurgical residency between 1988 and 1994, serving as Chief Resident from 1993 to 1994. After fulfilling his Air Force obligation, he joined the University of Virginia Health Sciences Center as Associate Professor and Vice-Chairman (1997–2003). From 2008 until his passing, he held the David D. Weaver Professorship and chaired the Department of Neurological Surgery. His academic achievements included more than 150 publications, and he was recognized as one of *America's Top Surgeons*. An active member of American Association of Neurological Surgeons (AANS), Congress of Neurological Surgeons (CNS), and Society of Neurological Surgeons (SNS), he was a healer, mentor, and loyal friend who devoted his life to patient care—a true legend in neurosurgery.

Prof. Dr. Rupert Smith, Jr., United States (1932–2024)

Dr. Smith was born in Greenville, Illinois. He completed medical school at Washington University with distinction, followed by neurosurgical training at Johns Hopkins and Barnes Hospital, and fellowships in neuroanatomy at Washington University and Oxford. In 1966, he became the founding Chairman of Neurosurgery at Saint Louis University Hospital. A pioneer in the field, Dr. Smith advanced neuroanatomical research, trained generations of neurosurgeons, and contributed significantly to professional organizations. His enduring legacy lives on in the lives he touched.

SOUTH AMERICA

Prof. Dr. Daniel D'Osvaldo, Argentina (1953–2024)

He was an esteemed educator and neurosurgeon from Argentina. He graduated with honors from the Facultad de Medicina, Universidad de Buenos Aires (UBA), and completed his neurosurgery training at the Hospital de Clínicas José de San Martín in Buenos Aires. He pursued further studies at the Instituto de Neurocirugía Costa Buero and at the Institute of Rome, Italy. As a dedicated professor of neurosurgery at UBA and a member of the Argentine College of Neurosurgeons, his main fields of expertise included brain tumors, pituitary gland tumors, and vascular malformations. His passion, energy, and commitment to patient care were exceptional. We will always remember his warmth, humility, and devotion.

Prof. Dr. Marcos Flavio Ghizoni, Brazil (1946–2024)

Dr. Marcos Flavio Ghizoni was born in Urubici, Santa Catarina. After completing his formal education in Neurosurgery, he joined the medical staff of Hospital Nossa Senhora da Conceição in 1979. Then, he established the hospital's Neurosurgery Center and promoted the installation of its first CT scanner. He earned a Master's degree in Health Sciences from the University of Southern Santa Catarina, where he also served as a professor. In 2013, he was honored by the Legislative Assembly of Santa Catarina for developing a novel surgical technique for brachial plexus injuries—a procedure now cited in more than 50 journals and presented internationally. He was also recognized for performing awake brain surgeries for tumor removal. Remembered as an educator and pioneer in neurosurgery, his legacy continues to inspire the neurosurgical community.

Prof. Dr. Renato Chiorino-Radaelli, Chile (1930–2024)

Dr. Chiorino was a pioneer in neurosurgery and neuropathology, and a dedicated educator and mentor from Chile. He trained at the Instituto de Neurocirurgia Capixaba, specializing in neuropathology. At the age of 71, he received the "Dr. Héctor Valladares Medal" from the Chilean Society of Neurosurgery and was later honored by Society of Neurology, Psychiatry and Neurosurgery (SONEPSYN) as a "Master of Neurosurgery." He founded one of Chile's most advanced neuropathology laboratories. His legacy remains indelible.

Prof. Dr. Victor Hugo Bastos Pardo, Colombia (1968–2024)

Dr. Bastos Pardo served as Professor of Neurosurgery at the Universidad Nacional de Colombia and was affiliated with the Hospital Universitario Nacional for over 20 years. He was an active member of the Asociación Colombiana de Neurocirugía, making a significant impact on neurosurgery in Latin America. His main area of expertise was vascular surgery. He will be remembered for his passion for neurosurgery and for leaving an enduring mark on the legacy of Colombian neurosurgery.

Prof. Dr. Antonio M. Zárate Méndez, Mexico (1944–2024)

Dr. Zárate Méndez was a renowned Mexican neurosurgeon who dedicated his life to cerebrovascular and stereotactic surgery, areas in which he became a true master. He studied medicine at the Benemérita Universidad Autónoma de Puebla and completed his neurosurgery training at Centro Hospitalario 20 de Noviembre. In 1994 and 1995, he pursued advanced training in stereotactic surgery at the Detroit Medical Center, Michigan, Wayne State University, as well as at the Cologne University Hospital and Phillips University Hospital in Germany. He published numerous papers in indexed journals and authored several books. We will always remember his unwavering dedication, focus, and pursuit of excellence.

Prof. Dr. Fernando Rueda Franco, Mexico (1936–2024)

Dr. Franco was born in Mexico City in 1936 and completed his medical education at the Universidad Nacional Autónoma de México, earning his degree in 1960 with a thesis titled "Cerebral blood circulation and vascular malformations of the brain," and obtained his doctorate. In 1963, he began his neurosurgery specialization at the Children's Hospital of Mexico, continuing at the Neurological Institute of New York. He spent most of his career at the Neurology and Neurosurgery Service of the Mexican Institution for Assistance to Children (IMAN), now the National Institute of Pediatrics. A tireless researcher, prolific writer, and critical reader, his publications addressed important topics in pediatric neurosurgery. He will be remembered as a true legend among Mexican neurosurgeons.

Limitations

The authors were unable to identify every neurosurgeon worldwide who passed away in 2024. Another limitation was the inability to include personal photographs in this manuscript to protect intellectual property rights. We recognize these limitations but still honor and respect these unsung heroes whose legacies remain enduring and profound.

CONCLUSION

In 2024, there was a profound loss for the global neurosurgical community. Each of these neurosurgeons left a lasting legacy that endures in their students, apprentices, and colleagues. Their lives exemplified generosity, compassion, and professional mastery, leaving an indelible imprint on the scientific world. We remain thankful and proud to continue passing this science from generation to generation, preserving the authentic values of human wisdom. Despite our best efforts, some names may have been inadvertently omitted. We sincerely acknowledge this limitation and honor all the unnamed pioneers whose contributions continue to shape the history of neurosurgery.

ACKNOWLEDGEMENTS

Neurosurgery cocktail.

The authors of this tribute express their respect and tribute to the neurosurgeons who left us in 2024. The authors have intellectual property rights (IPR) over the opinions they express in writing and the figures provided in the paper; it can be cited by other authors after their publication in the journal.

Declarations

Funding: This research did not receive any specific grant from funding agencies in the public, commercial, or not-for-profit sectors.

Availability of data and materials: The datasets generated and/or analyzed during the current study are available from the corresponding author by reasonable request.

Disclosure: The authors declare no competing interests.

Use of artificial intelligence (AI)-assisted technology for manuscript preparation: The authors confirm that there was no use of artificial intelligence (AI)-assisted technology for assisting in the writing or editing of the manuscript, and no images were manipulated using AI.

AUTHORSHIP CONTRIBUTION

The authors (FT, FZ, ALC, AHS, IB, BC, AMS) confirm responsibility for the following: study conception and design, data collection, analysis and interpretation of results, and manuscript preparation.

REFERENCES

1. Ahmed A, Waheed A, Yaqoob E, Jabeen R, Chaurasia B, Javed S: Carving a path to the brain: A study on neurosurgery career choices. World Neurosurg 188:e405-e413, 2024. doi: 10.1016/j.wneu.2024.05.126
2. Deora H, Yagnick NS, Tripathi M: Mentor-mentee relationship in neurosurgery: Standing on the shoulder of giants. World Neurosurg 141:110-112, 2020. doi: 10.1016/j.wneu.2020.05.208
3. Graziano F, Gerardi RM, Scalia G, et al: Women in neurosurgery: From a matter of fortuitous occasions toward a conscious choice. World Neurosurg 148:129-135, 2021. doi:10.1016/j.wneu.2021.01.049
4. WFNS Member Societies. Available from: https://wfns.org/all-member-societies/?menu=18

Turk Neurosurg 36(1):158-162, 2026
DOI: 10.5137/1019-5149.JTN.47761-24.2

Case Report

Received: 29.10.2024
Accepted: 07.01.2025
Published Online: 16.01.2026

Percheron Artery Implicance in Bi-Thalamic Stroke Following Endoscopic Endonasal Approach for Infundibulo-Neurohypophysitis: A Combination of Two Rare Entities

Lucila DOMECQ LAPLACE[1], Mauro RUELLA[1], Pablo VILLANUEVA[2], Débora Adela KATZ[3], María Florencia BATTISTONE[3], Andrés CERVIO[1]

[1]Neurosurgery Department, Fleni, Buenos Aires, Argentina
[2]Hospital Regional San Martín de los Andes, Neurosurgery Department, Neuquén, Argentina
[3]Neuroendocrinology Department, Fleni, Buenos Aires, Argentina

Corresponding author: Lucila DOMECQ LAPLACE ✉ domecq.lucila@gmail.com / ldomecq@fleni.org.ar

ABSTRACT

Bi-thalamic stroke is rarely reported in the literature as a complication of an endonasal endoscopic procedure. It has been associated with presence of a Percheron artery variant, as well as with top of the basilar syndrome, both of which significantly increase patient surgical morbidity. Infundibulo-neurohypophysitis in turn, is an unusual inflammatory disorder affecting the infundibulum, the pituitary stalk, and the neurohypophysis. We present the case of a patient with visual impairment and an abnormal hormone profile compatible with infundibulo-neurohypophysitis, in whom tumor resection was conducted through an endoscopic endonasal approach (EEA). Patient developed postoperative bi-thalamic stroke due to Percheron artery infarct. A review of both conditions is included. This is the fourth case reported in the literature of a Percheron artery infarct, and to the best of our knowledge, the first linking it to endoscopic treatment of neurohypophysitis, itself an infrequent condition.

KEYWORDS: Bi-thalamic stroke, Endoscopic endonasal approach, Percheron artery, Infundibulo-neurohypophysitis, Diagnosis, Outcome

ABBREVIATIONS: AOP: Artery of percheron, **EEA:** Endoscopic endonasal approach, **INHP:** Infundibulo-neurohypophysitis, **MRA:** Magnetic resonance angiography, **MRI:** Magnetic resonance imaging, **PCA:** Posterior cerebral artery

INTRODUCTION

Infundibulo-neurohypophysitis (INHP) is an uncommon inflammatory condition affecting the infundibulum, the pituitary stalk, and the neurohypophysis (3,6,13,14). Patients typically present with central diabetes insipidus and normal anterior pituitary function. The most common pathogenesis involves lymphocytic infiltration, with destruction of normal structures and replacement by fibrotic tissue (6,14). Gadolinium-enhanced pituitary magnetic resonance imaging (MRI) is considered the diagnostic gold standard. Findings suggestive of INHP include pituitary stalk thickening and absence of posterior pituitary bright spot on T1 weighted images (3,4). Surgery is usually indicated in cases not responding to conservative treatment, or presenting significant mass effect and visual deficit (3,4). Endoscopic endonasal surgery may be indicated when diagnosis is unclear and a biopsy is needed for diagnostic confirmation, or for total lesion excision for symptom relief (10,11,14).

Lucila DOMECQ LAPLACE : 0000-0002-7882-9236
Mauro RUELLA : 0000-0003-2198-6801
Pablo VILLANUEVA : 0000-0001-7227-4164
Débora Adela KATZ : 0000-0003-3966-2223
María Florencia BATTISTONE : 0000-0001-5305-3999
Andrés CERVIO : 0000-0001-7617-1605

The artery of Percheron (AOP) is a normal anatomical variant of the posterior cerebral circulation. When present, it will impact classification of the small branches at the P1 segment of the posterior cerebral artery (PCA) as well as affect circulation and hemodynamic blood flow characteristics within this part of the brain (14).

Although extremely uncommon, injury to the AOP will usually result in bi-thalamic stroke. AOP is present in 4-12% of the population, and responsible for infarction in 0.5-2% of all strokes (1,7,9,11).

Correlation with use of an endonasal sellar approach for diagnosis or treatment is even more infrequent. To date, only three AOP infarctions have been reported following pituitary surgery. These occurred after endonasal resection of pituitary adenomas (2,10,11). This case we believe is the first to be linked to an inflammatory etiology.

CASE REPORT

We present the case of a 47-year-old female patient with a 7-year history of pituitary incidentaloma, initially diagnosed as a Rathke cleft cyst. Progressive growth observed on control MRI prompted referral to our neurosurgical center. Imaging at this time showed a 24.5 x 14.5 x 15.5mm retro-pituitary cyst (Figure 1). Hormonal profile and ophthalmological examination were abnormal. Patient presented symptoms of ADH deficiency and a bilateral inferior longitudinal visual defect. Differential diagnoses considered included craniopharyngioma, Rathke cleft cyst and hypophysitis.

Resection of the cyst and its dense content was performed through an endoscopic endonasal approach (EEA) (Figure 2) with no intraoperative complications.

Patient was extubated after surgery, but remained obtunded for 24 hours. Signs of somnolence persisted after 48 hours, and non-reactive right mydriasis, consistent with incomplete third cranial nerve (CN III) palsy, as well as mild right hemiparesis were observed. No signs of hematoma or acute hydrocephalus were detected on CT. MRI and magnetic resonance angiography (MRA) showed acute bi-thalamic infarction, and presence of a fetal variant of the right posterior cerebral artery (PCA), with Percheron artery origin from the P1 segment of the right PCA. Vessel caliber reduction and distal signal attenuation suggested artery of Percheron infarct (Figure 3).

Length of hospital stay was a total of 10 days, with 6 days in ICU. Patient was discharged to a rehabilitation center, in a stupor awareness state, with no significant changes on neurological examination.

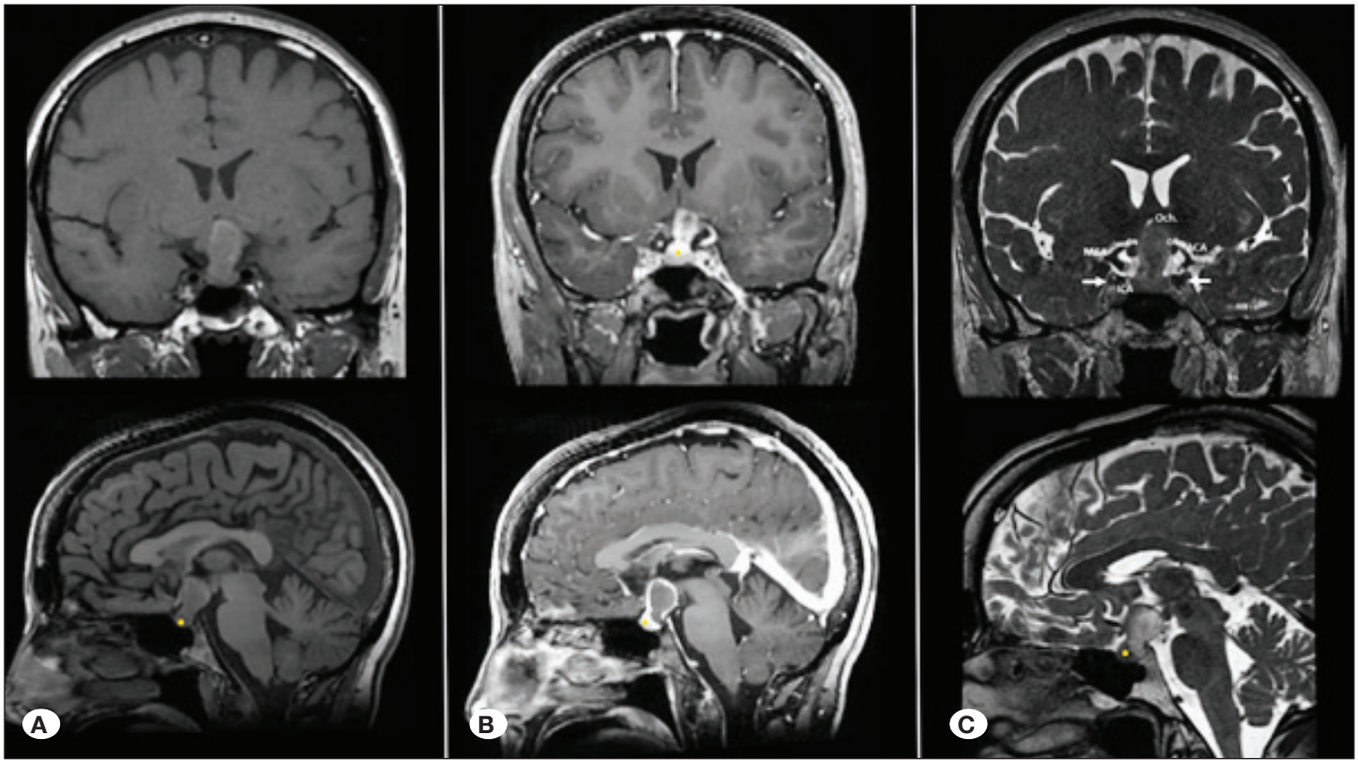

Figure 1: Preoperative T1W **(A)**, T1W post-gadolinium **(B)**, and T2W **(C)** Coranal ünd sagittal images showing a homogeneous, mild T1 spontaneously hyperintense, and T2 hypointense retro pituitary and infundibular lesion, with suprasellar extension and upward displacement (C) of the optic chiasm (Och.). Notice pituitary gland enhancement (yellow dot) and stalk thickening due to the lesion (B). Evidence of loss of posterior pituitary bright spot is observed on T1(A), sellar floor remains intact. In combination with clinical findings these images suggest presence of infundibulo-neurohypophysitis. **ON:** Optic nerve; **ACA:** Anterior cerebral artery; **MCA:** Middle cerebral artery; **ICA:** Internal carotid artery; **White arrows:** Oculomotor cistern and third cranial nerve (CN III).

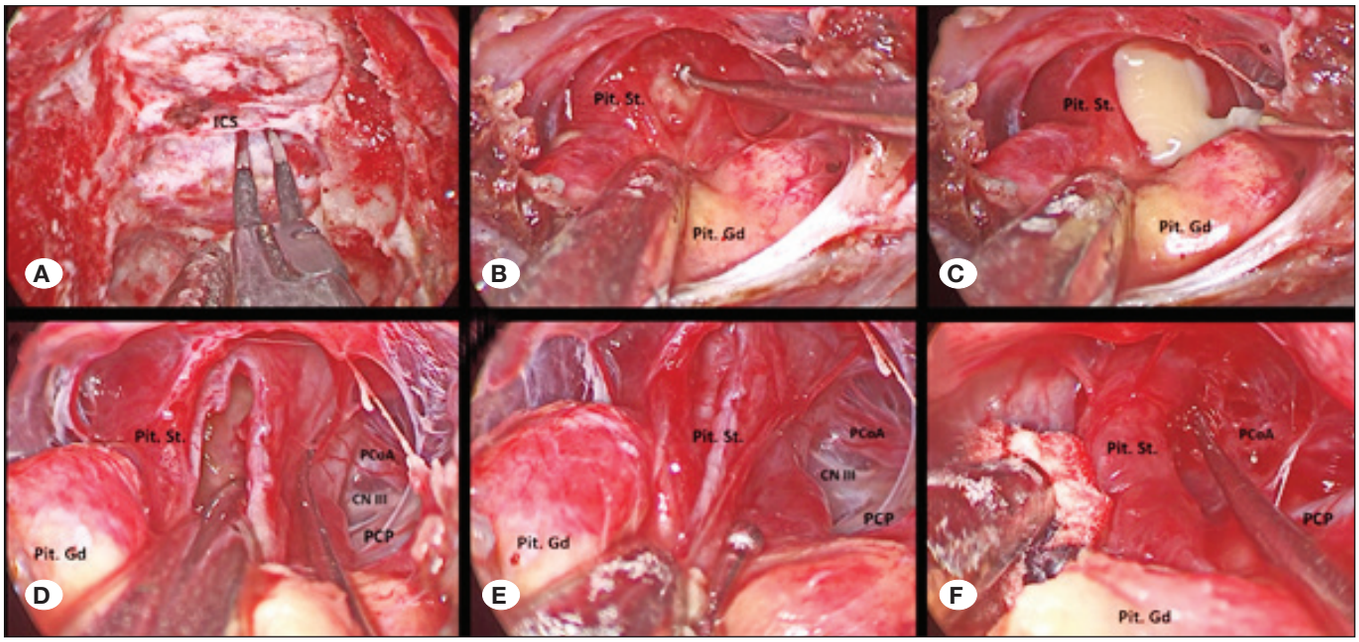

Figure 2: Intraoperative endoscopic images illustrating extended EEA to the sella **(A)**. Notice how the lesion is widening and displacing the pituitary gland (Pit. Gd.) and stalk (Pit. St.), with no clear limit between them **(B)**. Careful dissection is performed across the fibers of the stalk to access the cystic lesion from behind. Careful capsulotomy allows purulent inflammatory content evacuation **(B and D)**. Once lesion is emptied, a thinned pituitary stalk is repositioned. The posterior arachnoid is preserved **(E and F)**.

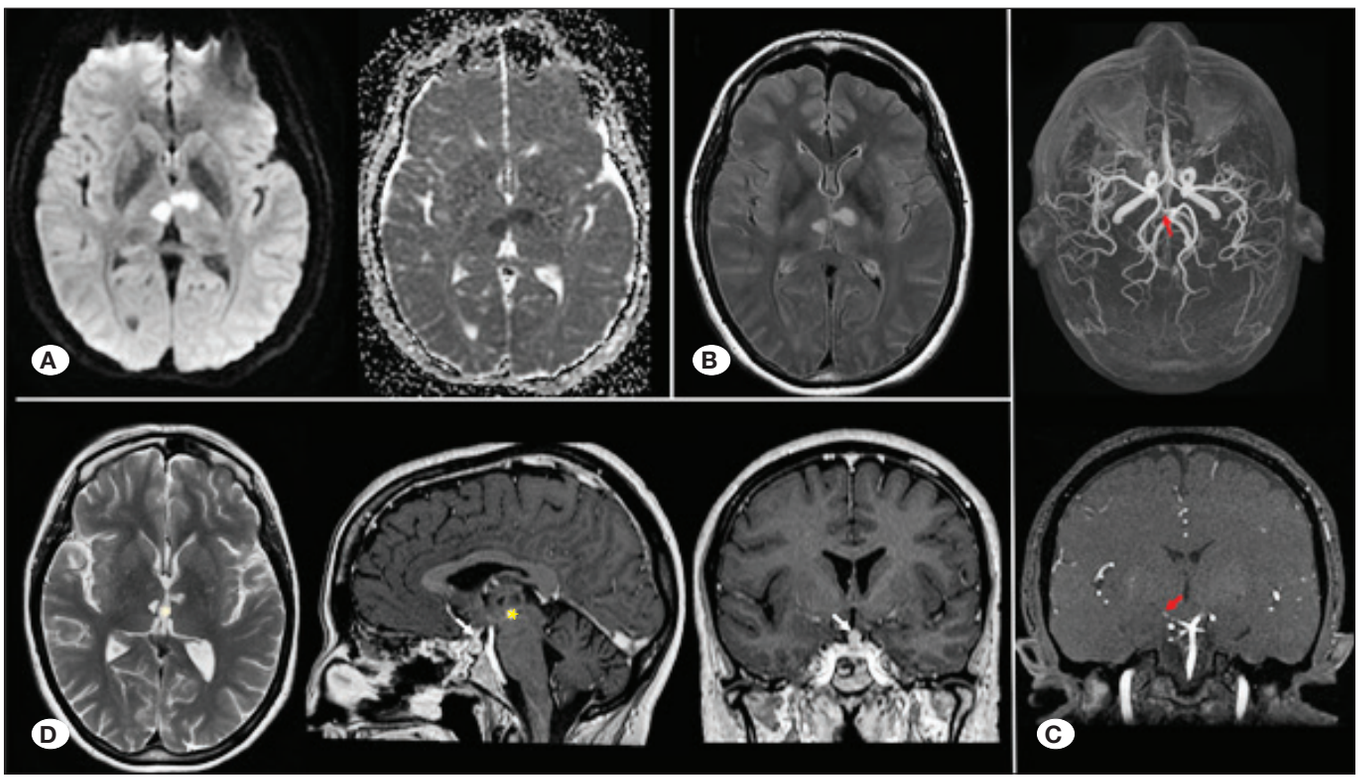

Figure 3: Early postoperative MRI shows bi-thalamic restrictive signal **(A)** on DWI sequence (diffusion-weighted), ADC (apparent diffusion coefficient), and hyperintensity on T2/FLAIR correlating with bi-thalamic ischemia **(B)**. MRA shows fetal variant of right PCA and Percheron artery origin at P1 segment of the right PCA, with evidence of caliber reduction and distal signal attenuation (red arrow) **(C)**. Postop MRI at three months **(D)** showing bi-thalamic increased T2 and decreased T1 signal (yellow asterisk), as well as persistence of pituitary stalk thickening (white arrow).

Pathology report confirmed inflammatory disease compatible with hypophysitis. Tissue cultures were negative.

Considerable neurological improvement was observed after rehabilitation. Patient was discharged after 4 months, and continued treatment as an outpatient. Both neurological and visual field symptoms improved after the surgery. However, panhypopituitarism and diabetes insipidus persisted, requiring hormone replacement therapy and desmopressin.

Despite the presence of minor visual deficit and mild cognitive impairment 1-year after surgery, patient was able to conduct daily life activities independently.

DISCUSSION

The artery of Percheron (AOP) is a normal anatomical variation of the posterior cerebral circulation, originally described by Gerard Percheron in 1973 (1). When present, not only does it impact classification of the small branches at the P1 segment of the posterior cerebral artery (PCA), it also affects circulation and hemodynamic blood flow characteristics within this region of the brain (14).

Prevalence ranges between 4 and 12% in the general population, and AOP infarction accounts for 0.5-2% of all isquemic strokes (1,7,9,11). Because it supplies blood flow to bilateral paramedian thalamic regions, AOP infarction will generate clinical symptoms reflecting midbrain involvement of areas such as the corticospinal tract, subthalamic nucleus, third cranial nerve nucleus, and the dentato-rubro-thalamic tract. Neurological syndromes such as those described by Weber, Benedikt and Claude have also been observed (1,8,9).

The most common underlying causes of an AOP occlusion are small artery disease and cardiac embolism (1,5), but it can also occur secondary to diabetes, smoking, tumors, inflammation, coagulation disorders and hypotension, among others (10).

Not only is the presence of an AOP anatomically significant, as it is a single trunk supplying both the right and left paramedian thalamic nucleus, it also has hemodynamic consequences. This territory is a “watershed zone” presenting increased risk of infarction due to occlusion, inflammation, or hypotension (1). In the case we describe, no direct involvement of the artery or other perforating branches was observed during the surgical procedure, and the arachnoid plane was preserved (see Figure 2). However, the hypoplastic right P1 origin of the AOP with a fetal variation of the CPA (Figure 3), as well as the inflammatory nature of the underlying disease (aseptic purulent hypophysitis) may have played a role in triggering vessel occlusion/stenosis.

Infundibulo-neurohypophysitis (INHP) is an unusual inflammatory disorder affecting the infundibulum, pituitary stalk, and neurohypophysis (3,6,13,14). Overall, hypophysitis is classified according to extension of inflammation and etiology (3,4). In cases of INHP, the usual MRI findings include loss of the posterior pituitary “bright spot’ (which reflects normal vasopressin and oxytocin storage) and thickening of the pituitary stalk. Bright spot absence in INHP indicates a vasopressin storage defect, though it is not considered a pathognomonic sign, as it can be absent in up to 20 % of normal individuals (6).

Other radiological signs that help differentiate INHP from pituitary adenomas or craniopharyngiomas are a homogeneous pre-contrast appearance, full contrast enhancement, an intact sellar floor and in some cases, a dural tail reaction (3,4). (Figure 1).

Hypophysitis is defined as primary, if the inflammation involves the pituitary gland. Autoimmune etiology is usually assumed. Whereas hypophysitis is considered secondary, when focal pituitary lesions are present. Possible causes include craniopharyngioma, adenoma, germinoma, and Rathke cleft cyst (6,3,13). Patients typically present with central diabetes insipidus and normal anterior pituitary function.

Clinical signs and symptoms, biochemical parameters, and MRI findings all contribute to a correct diagnosis (6,14). The endoscopic endonasal approach can be used to obtain a biopsy and confirm histology, or for complete surgical excision in patients not responding to conservative treatment, or presenting significant mass effect and loss of vision (4,6,10,12).

We report a case of Percheron artery infarction, as postoperative complication after endoscopic endonasal INHP resection.

CONCLUSION

Both, artery of Percheron infarction as well as infundibulo-neurohypophysitis are two extremely rare conditions. To the best of our knowledge, their combined occurrence has not been previously reported in the literature. We present the case of a patient who, after endonasal endoscopic resection of a pituitary lesion diagnosed as INHP, developed AOP infarction. No further postoperative complications were observed.

The etiology of the resulting bi-thalamic stroke remains unclear. Nevertheless, the fact that the AOP in this particular case originated from a hypoplastic right P1, with a fetal variation of the CPA, in addition to the inflammatory nature of the underlying disease (purulent aseptic hypophysitis), may have played an important role in causing vessel occlusion/stenosis.

Declarations

Funding: This research received no specific grant from any funding agency in the public, commercial, or not-for-profit sectors.

All authors have seen and agree with the contents of the manuscript and have no financial interest to report.

Availability of data and materials: The datasets generated and/or analyzed during the current study are available from the corresponding author by reasonable request.

Disclosure: The authors declare no competing interests.

AUTHORSHIP CONTRIBUTION

Study conception and design: LDL MR

Data collection: LDL MR PV

Analysis and interpretation of results: LDL MR PV DAK MFB AC

Draft manuscript preparation: LDL MR PV

Critical revision of the article: DAK MFB AC

All authors (LDL, MR, PV, DAK, MFB, AC) reviewed the results and approved the final version of the manuscript.

REFERENCES

1. Agarwal N, Chaudhari A, Hansberry DR, Prestigiacomo CJ: Redefining thalamic vascularization vicariously through Gerald Percheron: A historical vignette. World Neurosurg 81:198-201, 2014. https://doi.org/10.1016/j.wneu.2013.01.030
2. Aryan S, Thakar S, Hegde AS: Artery of percheron infarction after endoscopic pituitary surgery. Acta Neurochir 158):1973-1975, 2016. https://doi.org/10.1007/s00701-016-2925-y.
3. Caranci F, Leone G, Ponsiglione A, Muto M, Tortora F, Muto M, Cirillo S, Brunese L, Cerase A: Imaging findings in hypophysitis: A review. Radiol Med 125:319-328, 2020. https://doi.org/10.1007/s11547-019-01120-x.
4. Chiloiro S, Capoluongo ED, Tartaglione T, Giampietro A, Bianchi A, Giustina A, Pontecorvi A, De Marinis L: The changing clinical spectrum of hypophysitis. Trends Endocrinol Metab 30:590-602, 2019. https://doi.org/10.1016/j.tem.2019.06.004.
5. Hawkes MA, Arena JE, Rollán C, Pujol-Lereis VA, Romero C, Ameriso SF: Bilateral paramedian thalamic infarction. Neurologist 20:89-92, 2015. https://doi.org/10.1097/NRL.0000000000000047. PMID: 26566040.
6. Johnston PC, Chew LS, Hamrahian AH, Kennedy L: Lymphocytic infundibulo-neurohypophysitis: A clinical overview. Endocrine 50:531-536, 2015. https://doi.org/10.1007/s12020-015-0707-6.
7. Kheiralla O, Alghamdi S, Aljondi R, Tajaldeen A, Bakheet A: Artery of percheron infarction: A characteristic pattern of ischemia and variable clinical presentation: A literature review. Curr Med Imaging 17:669-674, 2021. https://doi.org/10.2174/1573405616666201130095801.
8. Kichloo A, Jamal SM, Zain EA, Wani F, Vipparala N: Artery of percheron infarction: A short review. J Investig Med High Impact Case Rep 7:2324709619867355, 2019. https://doi.org/10.1177/2324709619867355.
9. Kocaeli H, Yilmazlar S, Kuytu T, Korfali E: The artery of Percheron revisited: A cadaveric anatomical study. Acta Neurochir (Wien) 155:533-539, 2013. https://doi.org/10.1007/s00701-012-1548-1.
10. Li J, Ge J, Yang S, Yao G: Clinical review and analysis of artery of Percheron infarction. IBRO Neurosci Rep 15:17-23, 2023. https://doi.org/10.1016/j.ibneur.2023.04.006.
11. Pilonieta M, Pérez P, Prevedello DM: The clinical relevance of the thalamogeniculate arteries in endoscopic endonasal surgery for giant pituitary adenomas in the interpeduncular fossa. J Neurol Surg A Cent Eur Neurosurg 85:100-104, 2024. https://doi.org/10.1055/s-0042-1748773.
12. Sankar T, Souster J, Steinke DE: Bilateral thalamic infarction following transsphenoidal surgery. Can J Neurol Sci 35:522-525, 2008. https://doi.org/10.1017/s0317167100009264.
13. Tkatch J, Szuman G, Agüero M, Alfieri A, Ballarino MC, Bamberger E, Battistone MF, Boero L, Danilowicz K, Donoso M, Fainstein-Day P, Furioso A, Glerean M, Gonzalez Pernas M, Guitelman M, Katz D, Loto M, Pignatta A, Slavinsky P, Sosa S, Mallea-Gil MS, Rogozinski A: Primary hypophysitis: Diagnosis and treatment multicenter study. Medicina (B Aires) 83:744-752, 2023 (in Spanish)
14. Tubridy N, Saunders D, Thom M, Asa SL, Powell M, Plant GT, Howard R: Infundibulohypophysitis in a man presenting with diabetes insipidus and cavernous sinus involvement. J Neurol Neurosurg Psychiatry 71:798-801, 2001. https://doi.org/10.1136/jnnp.71.6.798.

Turk Neurosurg 36(1):163-167, 2026
DOI: 10.5137/1019-5149.JTN.47959-24.2

Case Report

Received: 29.10.2024
Accepted: 20.01.2025
Published Online: 16.01.2026

Dural Amyloidoma Located in the Falx Cerebri and Spinal Dura: Two Case Reports

Ilhan AYDIN[1], Abdullah Safa KURSUN[1], Muhsin GUNBOZ[1], Seda Yagmur KARATAS OKUMUS[1], Gokcen GUNDOGDU UNVERENGIL[2], Erhan EMEL[1]

[1]Bakirkoy Prof. Dr. Mahzar Osman Teaching Hospital for Neurology, Neurosurgery and Psychiatry, Department of Neurosurgery, Istanbul, Türkiye
[2]Istanbul University, Istanbul Faculty of Medicine, Department of Pathology, Istanbul, Türkiye

This study has been presented at the Annual Scientific Congress of European Association of Neurosurgical Societies (EANS), Sofia, Bulgaria, 2024 and Annual Scientific Congress of Turkish Neurosurgical Society (TNS), Antalya, Türkiye, 2024

Corresponding author: Ilhan AYDIN ✉ ilhanaydinmd@gmail.com

ABSTRACT

Amyloidosis is a progressive disorder marked by the aggregation of insoluble fibrillar proteins in various tissues, leading to tissue damage. Localised amyloidosis, known as amyloidoma, is particularly rare in the central nervous system and may be mistaken for a neoplastic lesion due to similar radiological features. Consequently, the general treatment approach often involves total excision. However, it is important to consider that a biopsy of the amyloidoma, rather than total excision, may suffice for complete recovery when paired with appropriate systemic treatment. This report presents two rare cases of amyloidoma: one located in the falx cerebri and the other in the lumbar spine. Both cases were successfully operated on, with the patients recovering without complications following treatment. (1)

KEYWORDS: Amyloidoma, Amyloidosis, Dural amyloidoma, Cerebral amyloidoma

ABBREVIATIONS: MRI: Magnetic resonance imaging, **CT:** Computed tomography, **CNS:** Central nervous system

INTRODUCTION

Amyloidosis is a progressive, heterogeneous group of disorders caused by the abnormal deposition of toxic, insoluble fibrillar protein aggregates in various tissues, leading to tissue damage. For this reason, it is called a protein-folding disorder. The aetiology of amyloidosis remains unclear. The disease can be localised, wherein amyloid accumulates in different tissues and causes a mass effect. This condition is known as amyloidoma, and its clinical presentation varies depending on the affected tissue (1,4-6).

The incidence of amyloidosis is 1-2 per 100,000 per year in Western countries. In the United States, 1,275 to 3,200 new cases are reported annually (3). However, specific data on amyloidoma are limited due to its rarity. Cerebral amyloidoma cases are reported predominantly in middle-aged individuals, with a female predilection. Amyloidoma is most frequently seen in the kidneys and gastrointestinal system, whereas brain involvement is uncommon. The involvement of the dura is also quite rare, and information about this condition is primarily based on case reports, challenging the acquisition of precise epidemiological data (2). Intracranial amyloid accumulation is extremely rare and can be seen in the cerebral parenchyma, skull base, pituitary gland and cerebellopontine angle. Parenchymal involvement is frequently observed in systemic amyloidosis, particularly in AL amyloidosis. Amyloid deposits

Ilhan AYDIN : 0000-0001-7681-8528
Abdullah Safa KURSUN : 0000-0001-8824-164X
Muhsin GUNBOZ : 0009-0009-3618-3500
Seda Yagmur KARATAS OKUMUS : 0000-0003-3104-8755
Gokcen GUNDOGDU UNVERENGIL : 0000-0003-3177-7851
Erhan EMEL : 0000-0002-0584-9164

in the calvarium often show a predilection for the skull base and are described as calcified lesions (5).

While the diagnosis of amyloidoma is confirmed through histochemical methods, it is often mistaken for other conditions before biopsy due to its radiological features. These lesions are contrast-enhancing and can mimic high-grade lymphomas and glial neoplasms, as demonstrated in a case report on a spinal extradural mass (1,2,4,6).

In this report, we present two cases: those of a young woman presenting with headache and dizziness, diagnosed with an amyloidoma involving the falx cerebri, and an older woman presenting with lower back and leg pain, diagnosed with a lumbar dural amyloidoma.

CASE REPORTS

Cerebral Dural Amyloidoma

A 32-year-old female patient presented with headaches, dizziness, and nasal bleeding lasting a few weeks. Her medical history, neurological examination, and blood tests were normal upon admission. Cranial imaging revealed a gadolinium-enhancing, hyperintense lesion on T2-weighted magnetic resonance images (MRI) and a hyperdense lesion on computed tomography (CT). The lesion measured 34 × 11 × 93 mm and was extra-axial, located in the frontal interhemispheric area and extending to both sides of the falx cerebri (Figure 1). Central nervous system (CNS) lymphoma, meningioma, or glial tumours were considered primary differential diagnoses, and the patient underwent surgery using an anterior interhemispheric approach. During the surgery, the tumour was observed to be associated with the dura. The lesion was successfully sub-totally removed. A pathological analysis confirmed the diagnosis of amyloidoma. Congo red and crystal violet histochemical stains were positive, and immunohistochemical analysis showed a polytypic reaction for kappa and lambda light chains (Figure 2).

Postoperative examinations were normal, and the patient was referred to the Haematology Department for further investigation of systemic amyloidosis. No systemic amyloidosis was detected, so systemic treatment was required. Three months after the surgery, follow-up imaging showed spontaneous regression of the tumour (Figure 3).

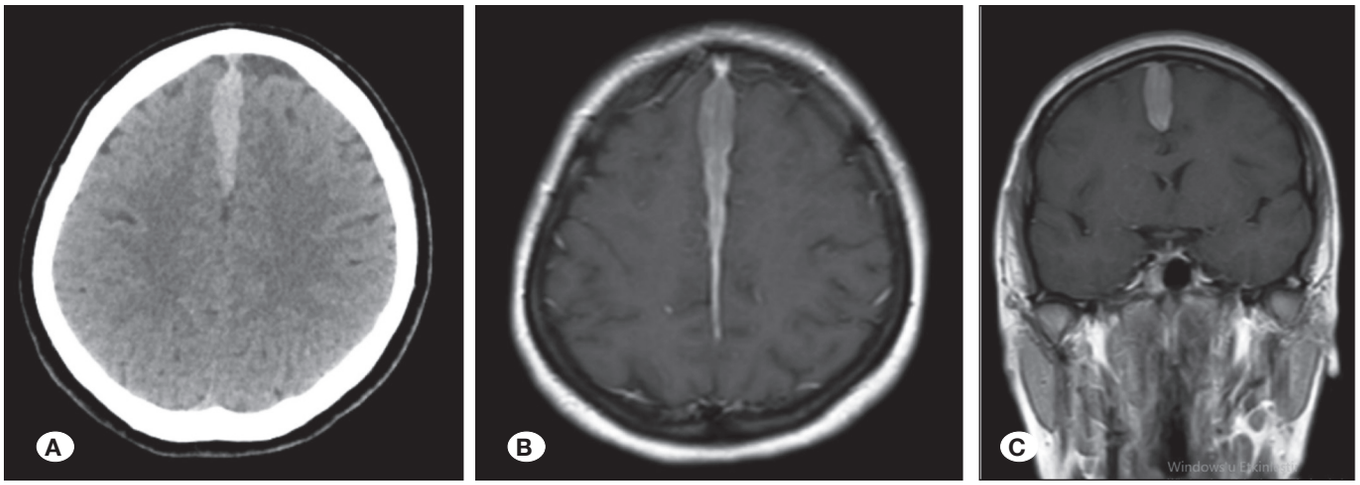

Figure 1: The patient's non-enhancing axial CT **(A)**, gadolinium-enhanced axial **(B)**, coronal **(C)** T1W MR images show a parafalcine extra-axial mass.

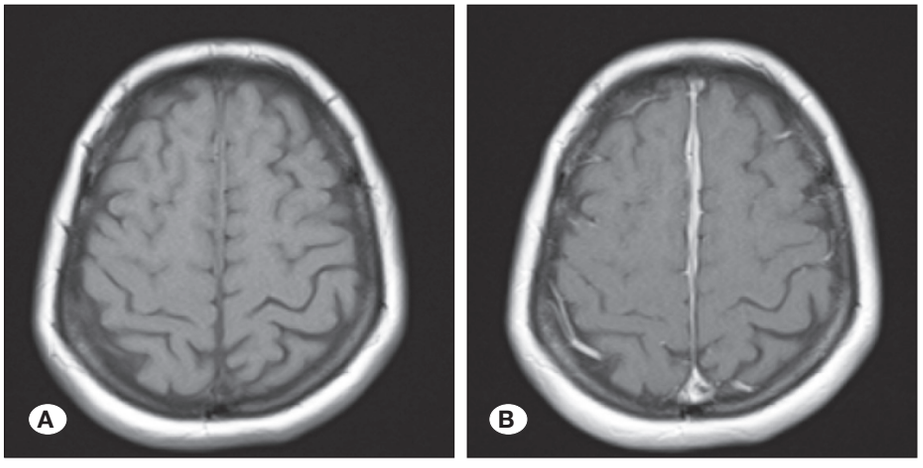

Figure 2: Post-operative third-month axial gadolinium-enhanced **(A)**, and non-enhanced **(B)** T1W MR images show that the tumour spontaneously regressed.

Spinal Dural Amyloidoma

A 70-year-old female patient presented with lower back pain, right-sided leg pain, left-sided leg numbness, and left foot paresis lasting for a month. Her medical history and blood tests were normal. Lumbar spinal MRI showed spinal stenosis at the L3-4 level, with a suspected space-occupying lesion on the posterior wall of the spinal canal and the interspinous area. Gadolinium-enhanced MRI showed a contrast-enhancing lesion on the right side of the posterior wall of the spinal canal, possibly involving the dura (Figure 4). Surgery was performed using a classical posterior spinal approach. Bilateral L3 hemilaminectomies were performed, the ligamentum flavum was excised, and neural tissues were decompressed. During the surgery, the ligamentum flavum appeared normal except for hypertrophy and increased calcification. Following the flavectomy, the lesion was observed to be associated with the spinal dura. Tissue samples were obtained from the interspinous and supraspinous ligaments, and these, along with the excised ligamentum flavum, were sent for histopathological examination.

After the surgery, the patient's pain was relieved, and the paresis remained stable. Pathological examination revealed amyloidoma. Immunohistochemical analysis showed kappa light chain positivity, but amyloid-A and lambda were negative. Congo red and crystal violet histochemical stains were positive (Figure 5).

The patient was referred to the haematology department for systemic amyloidosis evaluation. No systemic amyloidosis was detected during follow-up, and no recurrence was noted on control imaging (Figure 6).

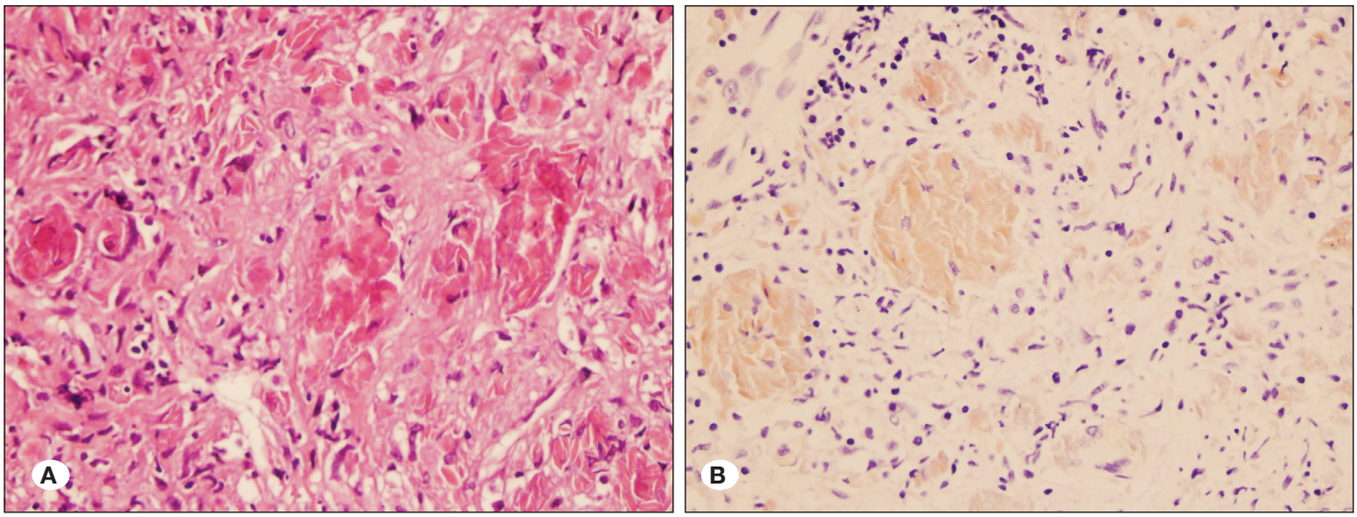

Figure 3: The accumulation of pink amorphous material in haematoxylin and eosin sections (200x) **(A)**. Positively stained areas in Congo red-based histochemical examination (200x) **(B)**.

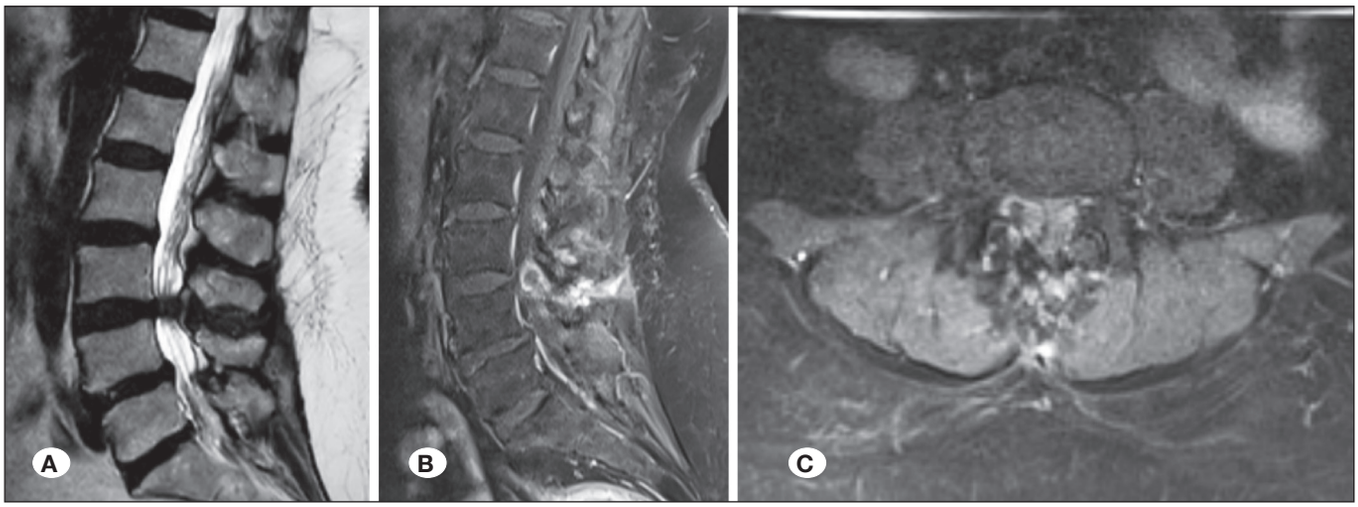

Figure 4: Preoperative T2W and gadolinium-enhanced T1W MR images show lumbar stenosis at the L3-4 level with contrast enhancement on the right side of the posterior wall of the spinal canal **(A, B, C)**.

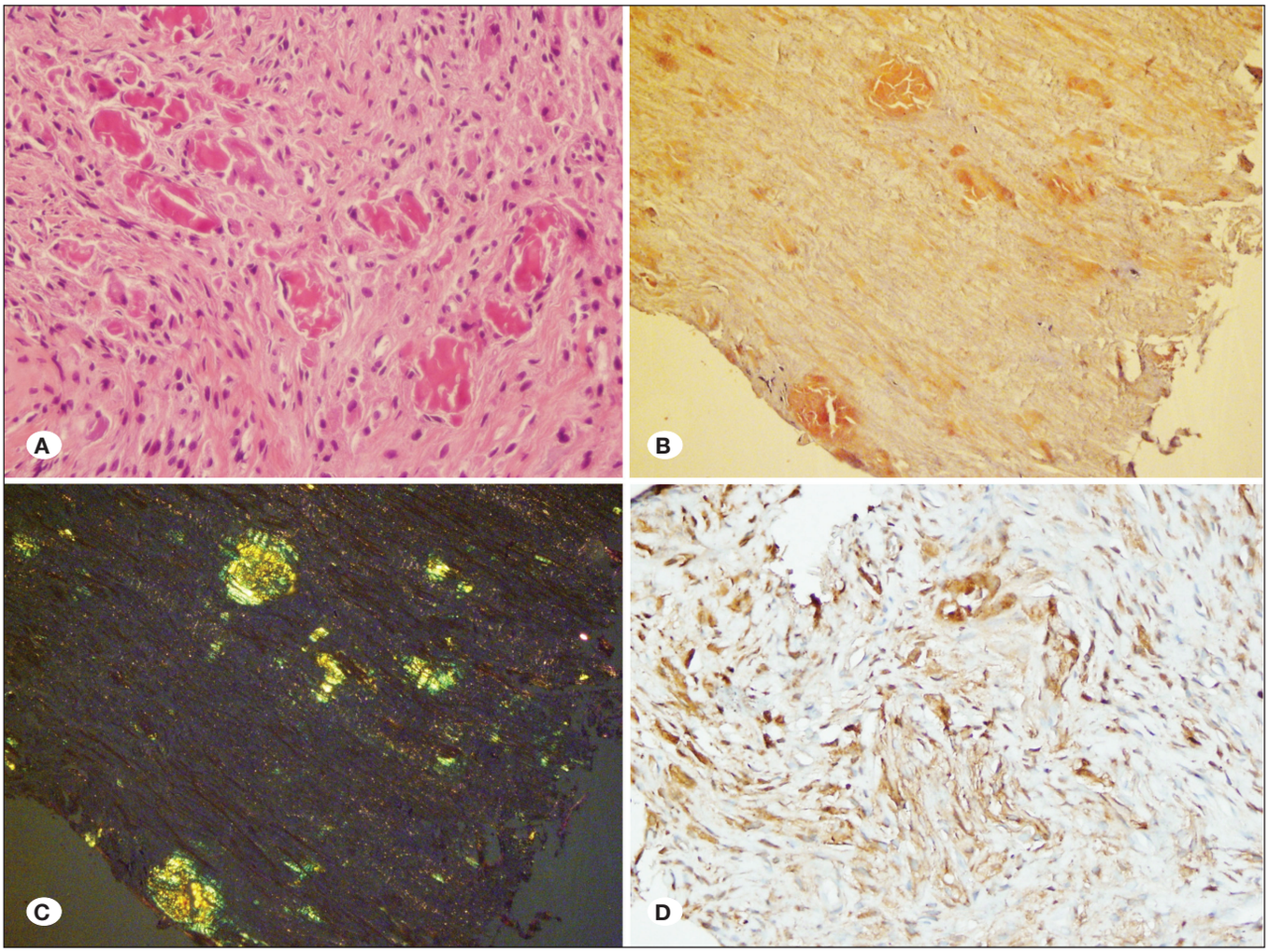

Figure 5: Accumulation of pink amorphous material in haematoxylin-eosin sections **(A)** (200x). Congo red-based histochemical examination shows positively stained areas **(B)** (100x), and an apple-green appearance under polarised light **(C)** (100x). Kappa light chain immunopositivity **(D)** (100x).

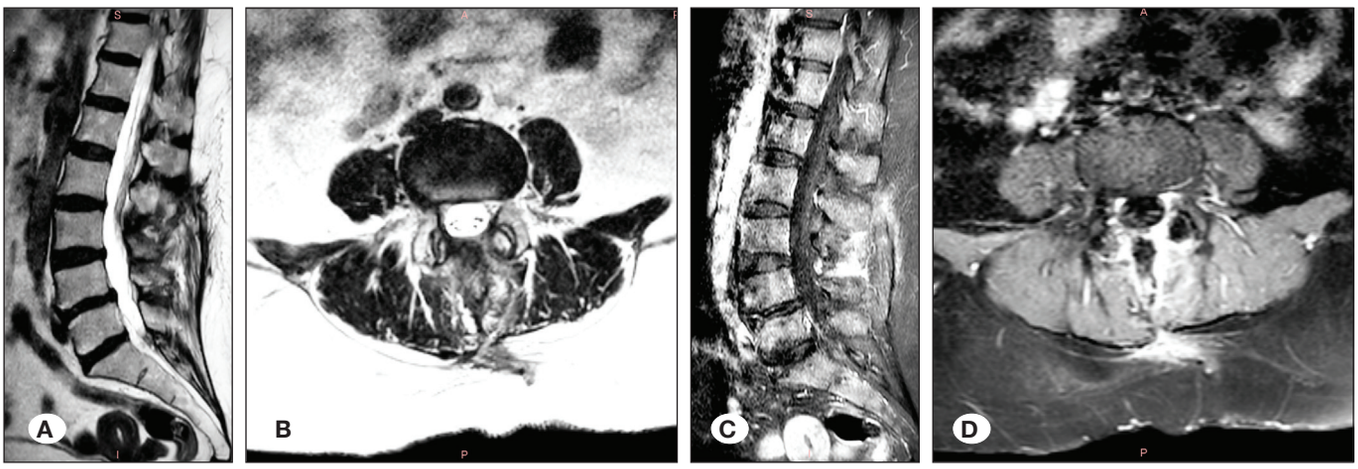

Figure 6: Postoperative T2W sagittal and axial **(A, B)**, and gadolinium-enhanced T1W MR images **(C, D)** show that the contrast-enhancing lesion disappeared and the neural tissues were decompressed.

DISCUSSION

The first patient presented with a homogeneously contrast-enhancing extra-axial mass on each side of the falx cerebri. Based on the radiological features, meningioma, lymphoma, plasmacytoma, and subdural hematoma, albeit less likely, were considered. Due to the lesion's location and elongated shape, a biopsy was recommended instead of total excision. Given the rare pathology, the patient was referred to the haematology department. Although cerebral amyloidoma is rare, it can be easily mistaken for more common space-occupying lesions. This case highlights the importance of considering biopsy rather than rushing into total excision when the pathology is uncertain.

The second patient presented with spinal stenosis caused by a contrast-enhancing lesion located in the spinal canal that initially appeared to be an extramedullary tumour due to its contrast-enhancing characteristics. Successful decompression was achieved. Pathological examination revealed amyloidoma, which had not been considered initially before the surgery. No systemic amyloidosis was detected during follow-up, and there was no recurrence.

CONCLUSION

Rare cases of amyloidoma located in structures covering the CNS, such as the falx cerebri and spinal dura, are presented and discussed. These lesions can easily be mistaken for other extra-axial and extramedullary space-occupying lesions of the CNS, such as meningiomas, high-grade gliomas, CNS lymphomas, or metastases. In these cases, the lesions appeared as contrast-enhancing masses and were initially considered tumours. Rare pathologies like amyloidoma should be considered, and decisions regarding surgical excision or biopsy should be made based on the patient's condition. A multidisciplinary approach is essential once the pathology is confirmed.

Declarations

Funding: The authors received no financial support for the research, authorship, and/or publication of this article.

Availability of data and materials: The datasets generated and/or analyzed during the current study are available from the corresponding author by reasonable request.

Disclosure: The authors declare no competing interests.

AUTHORSHIP CONTRIBUTION

Study conception and design: IA, ASK
Data collection: MG, ASK
Analysis and interpretation of results: ASK, GGU, MG
Draft manuscript preparation: SYKO, ASK
Critical revision of the article: IA, ASK, EE
Other (study supervision, fundings, materials, etc...): GGU
All authors (IA, ASK, MG, SYKO, GGU, EE) reviewed the results and approved the final version of the manuscript.

REFERENCES

1. Foreid H, Barroso C, Evangelista T, Campos A, Pimentel J: Intracerebral amyloidoma: Case report and review of the literature. Clin Neuropathol 29:217-222, 2010. https://doi.org/10.5414/NPP29217
2. Löhr M, Kessler AF, Monoranu CM, Grosche J, Linsenmann T, Ernestus RI, Härtig W: Primary brain amyloidoma, both a neoplastic and a neurodegenerative disease: A case report. BMC Neurology 19:59, 2019. https://doi.org/10.1186/s12883-019-1274-x
3. Merlini G, Bellotti V: Molecular mechanisms of amyloidosis. New England J Med 349:583-596, 2003. https://doi.org/10.1056/NEJMra023144
4. Moumouni AEK, Zolo DM, Kpelao E, Compaore P, Tabe DAT, Lawson L, Plante PR, Gueouguede EK, Souho B, Hamlat A: Brain amyloidoma: Case report and literature review. Open J Modern Neurosurgery 10:403-421, 2020. https://doi.org/10.4236/ojmn.2020.104043
5. Oruckaptan H, Karli Oguz K, Isikay I, Ruacan S: Amyloidoma of the temporal bone and upper cervical spine; presentation of a rare clinical entity with a brief literature review. Turk Neurosurg 19:159-162, 2009.
6. Shibao S, Dalprá FAR, Andrade CS, Leite CC: Dural amyloidoma. Neurology 86:1266-1267, 2016. https://doi.org/10.1212/WNL.0000000000002520

Turk Neurosurg 36(1):168-174, 2026
DOI: 10.5137/1019-5149.JTN.48237-24.2

Case Report

Received: 29.12.2024
Accepted: 16.03.2025
Published Online: 16.01.2026

Recurrent Glioblastoma with Turcot Syndrome

Zhuohua FU[1,2*], Gang DENG[2*], Jie ZHANG[1], Qibin SONG[1], Baohui LIU[2], Zhou XU[2], Huihua HE[3], Na ZHAN[3], Huangqing OUYANG[4], Qianxue CHEN[2], Weiguo HU[1]

[1]Renmin Hospital of Wuhan University, Cancer Center, Wuhan, 430060, China
[2]Renmin Hospital of Wuhan University, Department of Neurosurgery, Wuhan, 430060, China
[3]Renmin Hospital of Wuhan University, Department of Pathology, Wuhan, 430060, China
[4]Renmin Hospital of Wuhan University, Department of Radiology, Wuhan, 430060, China

*Contributed equally

Corresponding author: Qianxue CHEN, Weiguo HU ✉ chenqx666@whu.edu.cn, hwg74@163.com

ABSTRACT

Turcot syndrome (TS) is an extremely rare genetic disorder characterized by the concurrent occurrence of primary brain tumors and colorectal cancer. The prognosis for patients with TS is typically poor. A 57-year-old man with TS who developed recurrent glioblastoma and had a family history of colon cancer is reported. In 2022, the patient underwent robot-assisted stereotactic surgery for the resection of a central nervous system (CNS) tumor. Molecular genetic analysis identified microsatellite instability in the DNA mismatch repair (MMR) gene, confirming the diagnosis of TS. Additional mutations in the ATM and TP53 genes were also detected, which are rarely associated with TS. Despite treatment with the Stupp regimen, the patient experienced acute neurological deterioration, ultimately resulting in death 15 months after the onset of symptoms. Molecular diagnostics play a crucial role in guiding appropriate care and management for patients with TS. Early diagnosis, genetic testing, and preventive measures are essential for the effective management of this condition.

KEYWORDS: Turcot syndrome, Diffuse astrocytoma, Recurrent tumors of the central nervous system

INTRODUCTION

TS is a rare condition characterized by the co-occurrence of multiple gastrointestinal colon polyps and CNS neuroepithelial tumors (4). Brain tumors associated with TS vary in type, often presenting as single glioblastomas, medulloblastomas, or astrocytomas (6). The presence of multiple CNS tumors in TS is exceptionally rare, and the syndrome typically manifests in early adolescence. TS can be genetically classified into two subtypes: familial adenomatous polyposis (FAP) or hereditary nonpolyposis colorectal cancer (HNPCC) (12). Furthermore, TS is divided into Type I, characterized by glial tumors with fewer polyps and cancers, and Type II, characterized by extensive polyps and a higher risk of medulloblastoma (4).

Since the initial identification of TS, the literature has been limited to isolated case reports and small case series. TS Type I commonly involves glioblastomas associated with mutations in DNA MMR genes, particularly in the hMLH1 gene. Herein, we present a case of TS with a unique progression from wild-type diffuse astrocytoma to glioblastoma, resulting in rapid neurological decline and ultimately leading to the patient's death.

CASE REPORT

A 57-year-old male presented with episodes of involuntary head movement, left-sided facial numbness, and a skewed mouth in July 2021. Each episode lasted approximately one

Zhuohua FU : 0009-0008-8074-5315
Gang DENG : 0000-0003-1463-0508
Qibin SONG : 0000-0002-4350-0916
Baohui LIU : 0000-0002-4939-3605
Zhou XU : 0000-0003-3546-1520
Huihua HE : 0009-0009-7565-6980
Na ZHAN : 0000-0003-2247-3338
Huangqing OUYANG : 0009-0008-2371-6892
Qianxue CHEN : 0000-0002-9413-1030
Weiguo HU : 0000-0003-3808-234X

minute and resolved spontaneously. The patient's medical history included open surgery for colon cancer in 2003, with no recurrence noted during regular colonoscopies. He had a 40-year history of smoking and a family history of colorectal cancer affecting his grandfather, father, and sister.

Physical examination revealed a 12-cm surgical scar extending from below the umbilicus to the symphysis pubis and a café-au-lait spot on the skin (Figure 1). A brain MRI (Figure 1) performed upon admission showed long T1 and T2 patchy signals in the right frontal lobe-corona radiata, without enhancement on contrast imaging. MRS indicated a Cho/Cr peak ratio of 0.81–1.94 (Figure 1), suggesting a non-neoplastic lesion. However, 11C-methionine PET/CT (Figure 1) revealed a slightly hypodense lesion in the right frontal lobe, exhibiting increased methionine uptake, which was indicative of a neoplastic process. Due to the lesion's location in a functional area of the right frontal lobe and its diffuse nature, a stereotactic biopsy was performed after obtaining consent from the patient's family.

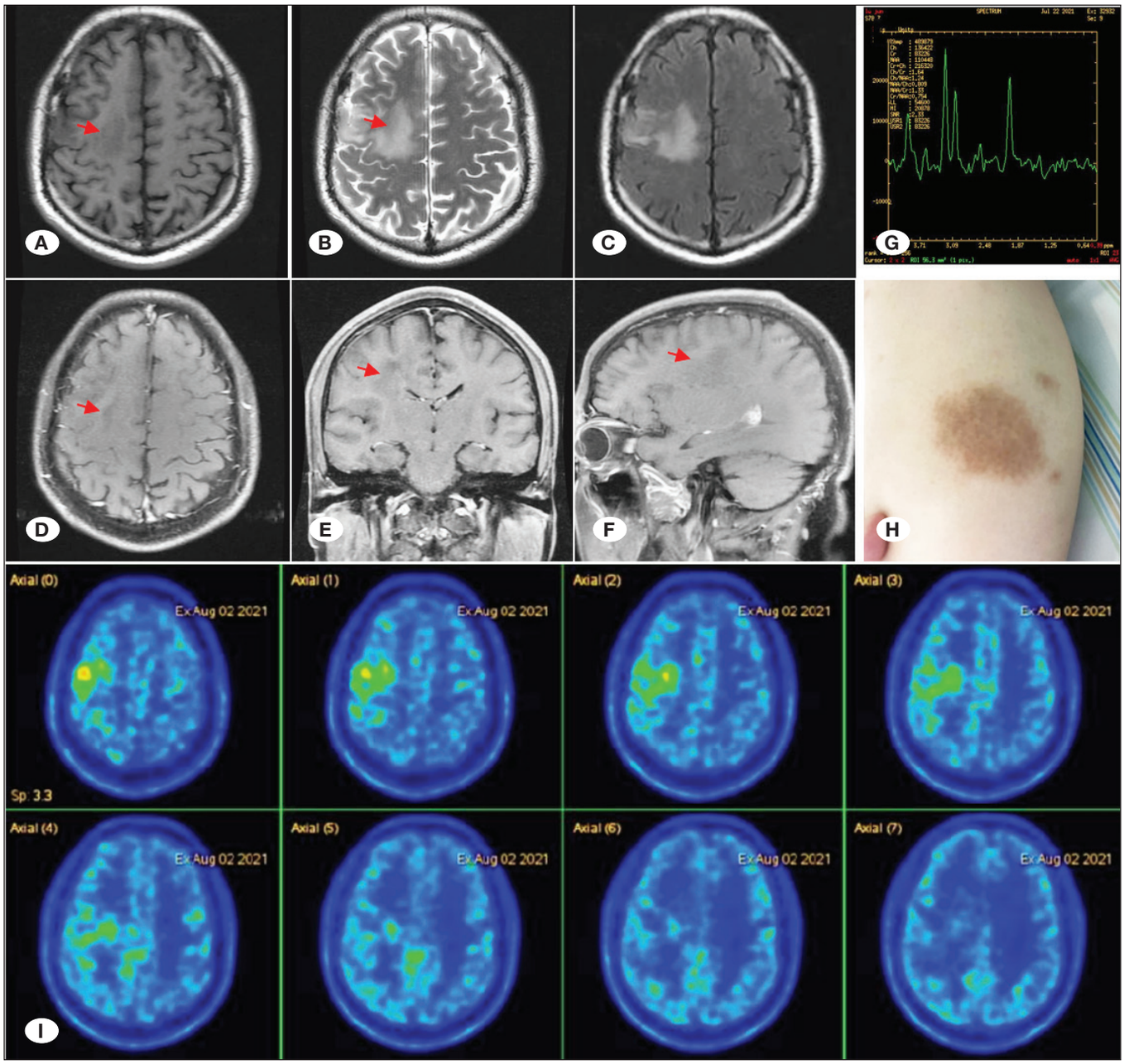

Figure 1: Axial **A)** T1W; **B)** T2W; **C)** fluid attenuated inversion recovery (FLAIR); and **D, E, F)** contrast enhanced T1W in axial, coronal, and sagittal positions. Brain MRI revealed long T1 and T2 patchy signals in the right frontal lobe-corona radiata. **G)** MR Spectroscopy indicated a Cho/Cr peak ratio of 0.81–1.94. **H)** Photograph of the patient skin caf´e-au-lait spot. **I)** 11C-methionine PET/CT showed enhance signal in right frontal lobe-corona region.

Fu Z. et al: Recurrent Glioblastoma with Turcot Syndrome

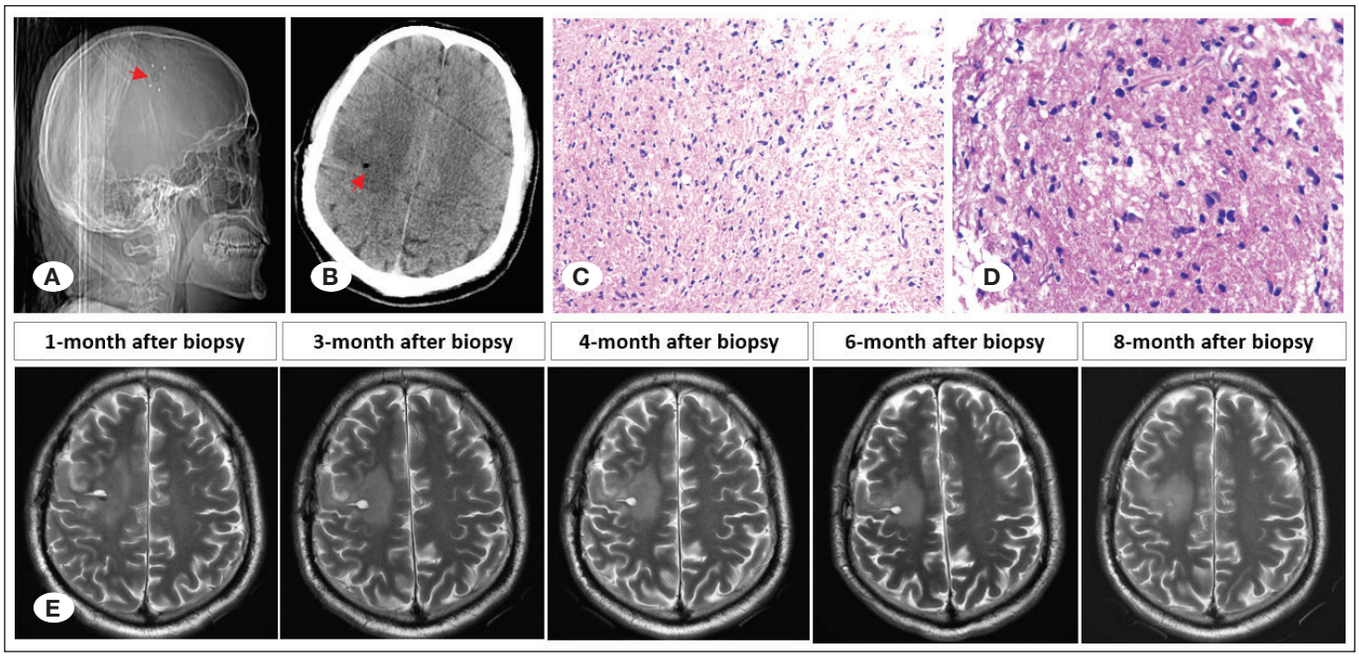

Figure 2: A, B) Postoperative X-ray images of the patient showing the surgical site. **C, D)** Hematoxylin and Eosin staining showed diffuse astrocytoma (WHO grade II) in the primary biopsy, magnification 100× and 200×, respectively. **E)** Brain MRI of patients 1 to 8 months after surgery.

The patient underwent a robot-assisted stereotactic lesion biopsy, and histopathology confirmed the presence of a WHO grade II diffuse astrocytoma (Figure 2). The immunohistochemistry results are summarized in Table I. Based on the 5th Edition WHO Classification of CNS Tumors, the morphology was consistent with a grade II IDH wild-type diffuse astrocytoma, which warranted consideration as a higher WHO grade. Subsequent gene sequencing (Table I) revealed high microsatellite instability (MSI-H) with a tumor mutation burden of 16.71. Furthermore, a frameshift mutation in the ATM gene (c.640del, p.Ser214Profs*16) with 24.8% abundance, along with an MSH2 mutation, confirmed the diagnosis of IDH wild-type astrocytoma and TS type I. The patient received treatment with the standard Stupp regimen, which included one month of concurrent chemoradiotherapy. The radiotherapy regimen consisted of GTV1: 2GY/30F/60GY and CTV1: 1.8GY/30F/54GY, while temozolomide was administered at a dose of 200 mg/m² on days 1–5, every 28 days for six cycles. Follow-up brain MRI demonstrated lesion shrinkage (Figure 2).

In June 2022, 10.5 months after the surgery and two months following the completion of chemotherapy, the patient presented with blurred vision. Upon examination, the patient exhibited clear consciousness, impaired cognition, slow movements, slurred speech, binocular papilledema, grade 2 muscle strength in the left limb, and grade 4 muscle strength in the right limb. MRI revealed the presence of multiple space-occupying lesions in the posterior third ventricle, right basal ganglia, and subependymal area, accompanied by obstructive hydrocephalus (Figure 3). To alleviate the hydrocephalus, the patient underwent a third ventriculostomy procedure under general anesthesia. Simultaneously, an endoscopic tumor biopsy was performed near the interventricular foramen, which revealed

Table I: The Summary of Immunohistochemical Results and Gene Detection Data

Protein	Result	Gene	Result
IDH1	(-)	IDH1	(-)
EMA	(-)	IDH2	(-)
ATRX	(-)	1p/19q	Non-codeletion
H3K27ME3	(+)	MGMT methylation	(-)
H3K27M	(-)	ATRX	(-)
BCL2	(+)	TERT	(-)
BCL6	(-)	BRAF	(-)
MUM1	(-)	EGFR	(-)
C-MYC	(-)	PTEN	(-)
Ki-67	(+, >5%)	PIK3CA	(-)
Olig-2	(+)	CDKN2A	(-)
S-100	(-)	CDKN2B	(-)
P53	(-)	ATM	Ser214Profs*16 24.8%
SYN	(-)	TP53	D41Ifs*2 36.5% R267W 33.3%
CD3	(-)	NF1	(-)
CD5	(-)	NF2	(-)
CD10	(-)	MEN1	(-)
CD19	(-)	TSC1	(-)
CD34	(+)	TSC2	(-)
D20	(-)	APC	(-)
		MMR	MSH2 deficiency

the presence of IDH wild-type glioblastoma (WHO grade IV) in the right basal ganglia (Figure 4). The molecular pathology results included IDH1(-), ATRX(+), H3K27M(-), H3K27Me3(+), and CDKN2A/B(-). Following the surgery, a marked improvement in postoperative hydrocephalus was observed. Three weeks after the surgical intervention, the patient reported im-

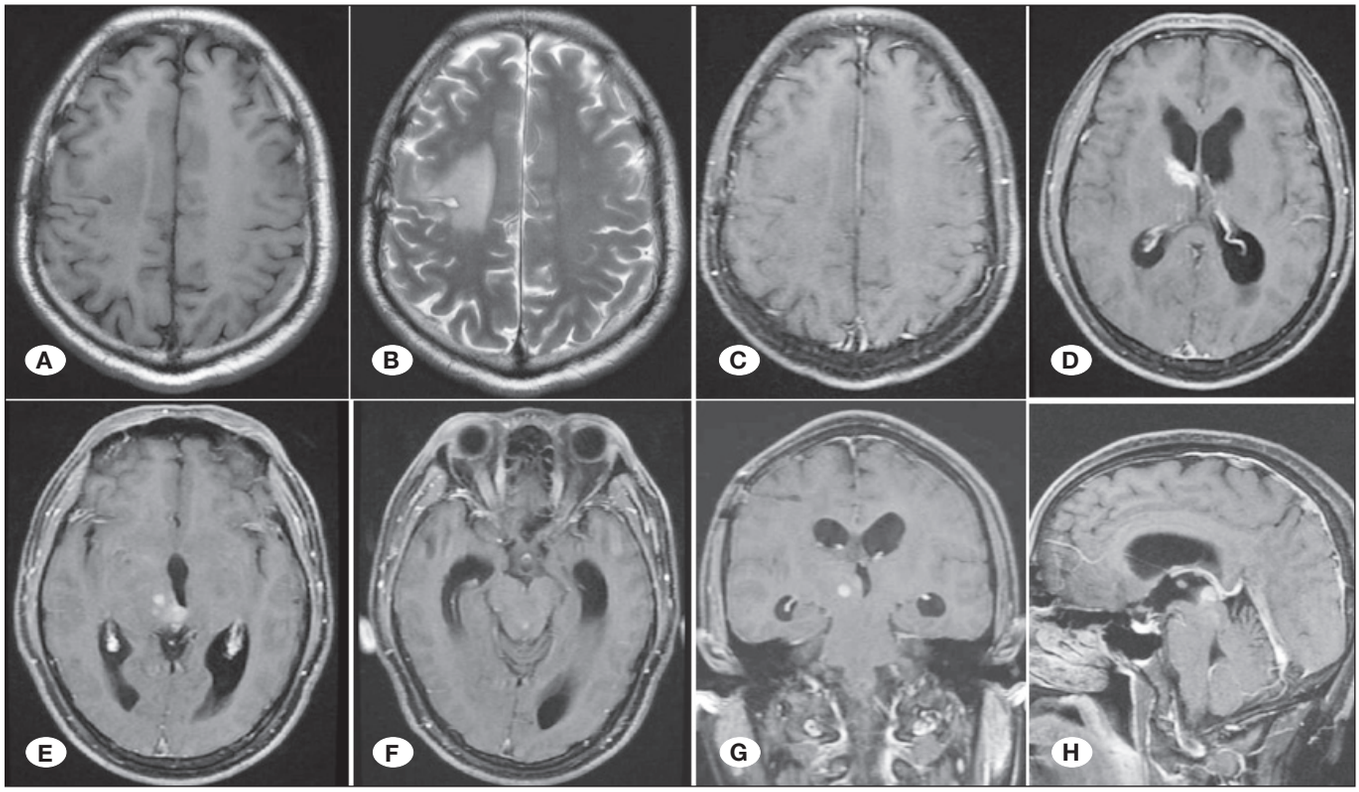

Figure 3: Axial **A)** T1W; **B)** T2W; and **C-H)** contrast enhanced T1W in axial, coranal and sagittal sections. There was no significant change in the original right-side lesions. MRI indicated multiple space-occupying lesions in the posterior third ventricle, right basal ganglia, and subependymal area, with obstructive hydrocephalus.

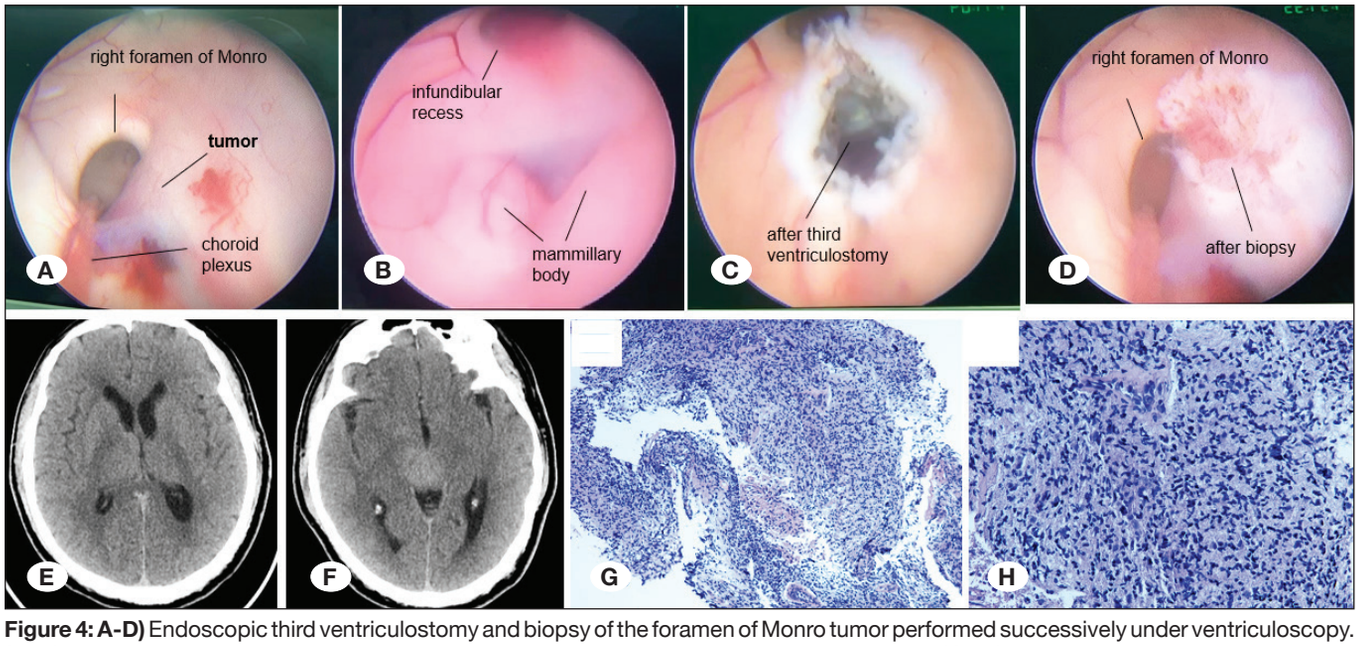

Figure 4: A-D) Endoscopic third ventriculostomy and biopsy of the foramen of Monro tumor performed successively under ventriculoscopy. **(E, F)** The postoperative hydrocephalus was significantly relieved. Histopathology revealed **(G, H)** Immunohistochemical staining for IDH-1 revealed IDH wild-type glioblastoma (WHO grade IV) in the right basal ganglia, magnification 40× and 200×, respectively.

proved vision and relief from headaches. Muscle strength was assessed as grade 4 in both the left and right limbs. The patient received treatment with temozolomide and bevacizumab and was subsequently discharged on August 1, 2022. However, the patient was readmitted on August 12, 2022, due to further alterations in consciousness. Repeat imaging revealed a significant enlargement of the right thalamus lesion, which compressed the brainstem (Figure 5). The patient experienced an acute deterioration and ultimately succumbed to his illness 15 months after the onset of neurological symptoms.

This case report was written in accordance with COPE guidelines and complies with the CARE statement. The manuscript adheres to the principles outlined in the 1964 WMA Declaration of Helsinki. All procedures performed and treatments received were part of routine care. The patient and his family kindly provided consent for the reporting of his case, which included imaging and histology. Anonymity is guaranteed in keeping with Information Governance stipulations of the National Health Service.

DISCUSSION

The present case report discusses TS, a rare and heterogeneous syndrome characterized by the association between primary brain tumors and colorectal polyposis, with only approximately 150 cases documented in the literature (2,9).

The onset of colonic polyposis during adolescence, which carries a high risk of malignancy and eventual CNS involvement, is a common feature of TS (11). In one notable family case, three siblings had colorectal adenocarcinoma, with two developing colonic adenomatosis and a 13-year-old relative presenting with TS. These observations suggest that TS may involve an autosomal gene with pleiotropic and variable expression (3). In the present case, a history of colorectal polyposis across three generations suggests a possible dominant inheritance pattern.

TS is considered a phenotypic variant of HNPCC and FAP. HNPCC is attributed to germline mutations in DNA MMR genes, including MLH1, PMS1, PMS2, MSH2, or MSH6 (5), with an MSH2 mutation confirmed in the patient presented here. Turcot syndrome is thought to develop from the loss of two alleles of the tumor suppressor gene and is classified into two main subtypes: Turcot syndrome 1 and Turcot syndrome 2, determined by the mutated genes. Turcot syndrome 1 is caused by the loss of two wild-type alleles of one or more genes involved in DNA MMR, while Turcot syndrome 2 is caused by the loss of two wild-type alleles of the APC gene (8). Characteristic skin manifestations, such as café-au-lait spots, melanocytic nevi, or aggressive fibromatosis, are exhibited by approximately 50% of TS patients. Café-au-lait spots are more frequently observed in TS type I patients, which was also noted in the case presented herein.

In the present case, the patient had a history of colorectal cancer and glioma, with café-au-lait spots observed on physical examination. Molecular analysis of the tumor specimen confirmed a deficiency in the MMR gene MSH2, leading to

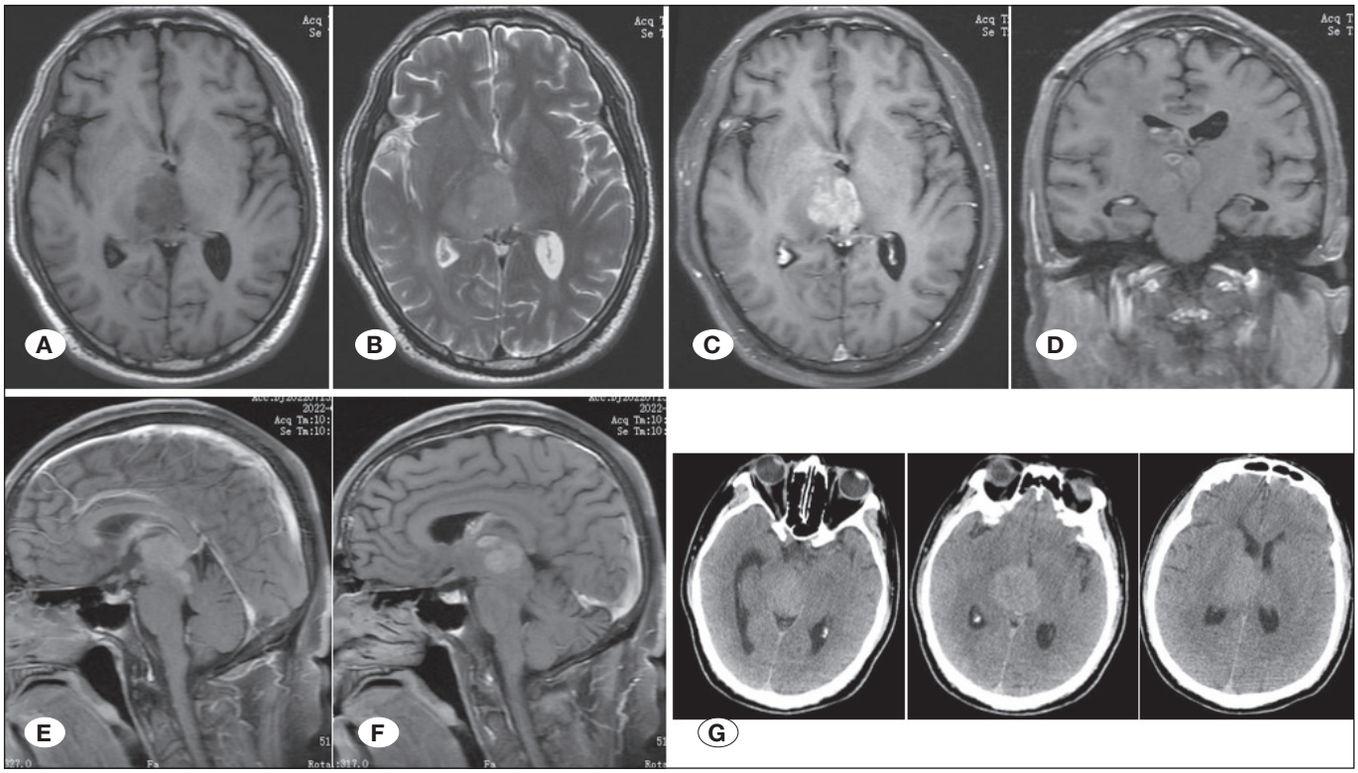

Figure 5: Axial **A)** T1W; **B)** T2W; **C-F)** contrast enhanced T1W images in axial, coronal and sagittal sections. **G)** CT images of the patient. Head CT was re-examined on August 12 **(G)**, and compared with brain MRI **(A-F)** on July 23, the lesions of the right thalamus were significantly enlarged and compressed the brain stem.

a diagnosis of TS type I. A stereotactic biopsy of the lesion revealed a WHO grade II diffuse astrocytoma with wild-type isocitrate dehydrogenase (IDH) status. Although molecular alterations such as EGFR amplification, gain of chromosome 7 with loss of chromosome 10 (+7/-10), or TERT promoter mutations could indicate a diagnosis of IDH-wildtype glioblastoma, none of these alterations were identified in this particular case. Given the prognostic implications associated with the IDH wild-type status, treatment was administered following a protocol typically used for higher WHO grade tumors, despite insufficient evidence to support a grade IV classification. Subsequent genetic sequencing confirmed the deficiency in MSH2, with no mutation detected in the adenomatous polyposis coli (APC) gene, and treatment was continued using the Stupp regimen.

Distinguishing TS from similar syndromes, such as neurofibromatosis type I (NF-1) or constitutional mismatch repair deficiency syndrome (CMMRDS), is crucial due to overlapping features, including café-au-lait spots and increased malignancy risks. NF-1 increases susceptibility to CNS tumors and gliomas, while CMMRDS predisposes patients to various malignancies (10). Genetic analysis plays a vital role in achieving an accurate diagnosis, underscoring the critical importance of molecular pathology in glioma diagnosis. Lynch syndrome, another genetic disease caused by mutations in MMR genes such as MLH1, MSH2, MSH6, and PMS2, results in defective DNA mismatch repair function, increasing the risk of colorectal, endometrial, ovarian, and other cancers. However, compared to Turcot syndrome type I, the risk of developing central nervous system tumors is relatively low in Lynch syndrome (1). Differential diagnosis between TS type I and Lynch syndrome should be based on clinical presentation, family history, and genetic testing results.

TS is associated with a poor prognosis, especially in patients presenting with both CNS tumors and colorectal cancer. Among the various tumor types, glioblastoma multiforme generally confers the worst outcomes, with an average survival of approximately 27 months (4). The management of TS primarily focuses on early diagnosis, genetic testing, and preventive care. Upon tumor development, treatment is supplemented by surgical resection, chemotherapy, and, in some cases, radiotherapy. In the present case, the patient underwent two biopsies and received concurrent chemoradiotherapy, adjuvant chemotherapy, dose-dense temozolomide, and bevacizumab. Although the initial treatment showed effectiveness, the patient ultimately succumbed to tumor recurrence and ventricular dissemination, resulting in a survival period of 14 months. In contrast, a case of CMMRD concurrent with glioblastoma has been reported, in which the patient exhibited good tolerance and efficacy following combined treatment with nivolumab and CCNU, leading to continuous tumor remission (7). This suggests the potential efficacy of immune checkpoint inhibitors in the treatment of hypermutated tumors.

CONCLUSION

In conclusion, TS results from germline defects in either the APC gene or DNA mismatch-repair genes. Molecular diagnostics play a crucial role in guiding appropriate care and management for patients with TS. Effective management of TS involves early diagnosis, genetic testing, and preventive measures.

Declarations

Funding: There is no funding for this case report.

Availability of data and materials: The datasets generated and/or analyzed during the current study are available from the corresponding author by reasonable request.

Disclosure: The authors declare no competing interests.

AUTHORSHIP CONTRIBUTION

Study conception and design: QC, WH

Data collection: GD, ZF

Analysis and interpretation of results: ZF, WH

Draft manuscript preparation: ZF, GD, JZ

Critical revision of the article: GD, QC, QS

All authors (ZF, GD, JZ, QS, BL, ZX, HH, NZ, HO, QC, WH) reviewed the results and approved the final version of the manuscript.

REFERENCES

1. Benusiglio PR, Elder F, Touat M, Perrier A, Sanson M, Colas C, Guerrini-Rousseau L, Thanh Tran D, Trabelsi N, Carpentier C, Marie Y, Adam C, Bernier M, Cazals-Hatem D, Mokhtari K, Tran S, Mathon B, Capelle L, Dhooge M, Idbaih A, Alentorn A, Houillier C, Dehais C, Hoang-Xuan K, Cuzzubbo S, Carpentier A, Duval A, Coulet F, Bielle F: Mismatch repair deficiency and lynch syndrome among adult patients with glioma. JCO Precis Oncol 7:e2200525, 2023. https://doi.org/10.1200/PO.22.00525
2. Corbera-Hincapie M, Beasley GL: A challenging treatment decision for a rare association: Case report of familial turcot syndrome with fistulizing crohn's disease. Front Pediatr 6:83, 2018. https://doi.org/10.3389/fped.2018.00083.
3. Costa OL, Silva DM, Colnago FA, Vieira MS, Musso C: Turcot syndrome. Autosomal dominant or recessive transmission? Dis Colon Rectum 30:391-394, 1987. https://doi.org/10.1007/BF02555461
4. Dipro S, Al-Otaibi F, Alzahrani A, Ulhaq A, Al Shail E: Turcot syndrome: A synchronous clinical presentation of glioblastoma multiforme and adenocarcinoma of the colon. Case Rep Oncol Med 2012:720273, 2012. https://doi.org/10.1155/2012/720273.
5. Jaffrelot M, Farés N, Brunac AC, Laurenty AP, Danjoux M, Grand D, Icher S, Meilleroux J, Mery E, Buscail E, Maulat C, Toulas C, Vande Perre P, Chipoulet E, Bonnet D, Staub A, Guimbaud R, Selves J: An unusual phenotype occurs in 15% of mismatch repair-deficient tumors and is associated with non-colorectal cancers and genetic syndromes. Mod Pathol 35:427-437, 2022. https://doi.org/10.1038/s41379-021-00918-3.
6. Julka M, Cherukuri M, Lameh R: Screening for cancerous and precancerous conditions of the colon. Prim Care 38:449-468, 2011. https://doi.org/10.1016/j.pop.2011.05.009.

7. Krugman J, Patel K, Cantor A, Snuderl M, Cooper B, Zan E, Radmanesh A, Hidalgo ET, Nicolaides T: Pediatric glioblastoma in the setting of constitutional mismatch-repair deficiency treated with upfront lomustine and nivolumab. Pediatr Blood Cancer 71:e30757, 2024. https://doi.org/10.1002/pbc.30757.
8. Mokhashi N, Cai LZ, Shields CL, Benson WE, Ho AC: Systemic considerations with pigmented fundus lesions and retinal pigment epithelium hamartomas in Turcot syndrome. Curr Opin Ophthalmol 32:567-573, 2021. https://doi.org/10.1097/ICU.0000000000000798.
9. Paraf F, Jothy S, Van Meir EG: Brain tumor-polyposis syndrome: Two genetic diseases? J Clin Oncol 15:2744-2758, 1997. https://doi.org/10.1200/JCO.1997.15.7.2744.
10. Sag E, Erkut M, Saygin I, Cebi AH, Bahadir A, Erduran E, Saruhan H, Cakir M: Constitutional mismatch repair gene defect syndrome presenting with adenomatous polyposis and cafe au lait spots: A case report. J Pediatr Hematol Oncol 42:e689-e691, 2020. https://doi.org/10.1097/MPH.0000000000001614.
11. Turcot J, Despres JP, ST Pierre F: Malignant tumors of the central nervous system associated with familial polyposis of the colon: Report of two cases. Dis Colon Rectum 2:465-468, 1959. https://doi.org/10.1007/BF02616938.
12. Umezawa K, Kumabe T, Shirane R, Yoshimoto T: Coexistence of intracranial arteriovenous malformation with Turcot's syndrome: A case report. Surg Neurol 52:397-399, 1999. https://doi.org/10.1016/s0090-3019(99)00099-3.

Turk Neurosurg 36(1):175-177, 2026
DOI: 10.5137/1019-5149.JTN.49202-25.0

Letter to Editor

Received: 04.06.2025
Accepted: 17.07.2025
Published Online: 16.01.2026

Perseus-The Protector of Mankind: Mesenchymal Stem Cell Transplantation may be a Promising Treatment for Neurological Diseases

Yanmin WANG[1]*, Bo HUANG[2]*, Huajiang DONG[2]

[1]Tianjin Beichen Hospital, Tianjin 300000, China
[2]Logistics University of Chinese People's Armed Police Forces, Tianjin 300309, China

*Equal to this work.

Corresponding author: Huajiang DONG ✉ donghj424@163.com

To the Editor;

We read with great interest that the article by Bozkaya et al. entitled "A New Hope in the Treatment of Intraventricular Haemorrhage in Preterm Infants: Mesenchymal Stem Cells" in Turkish Neurosurgery 32(2):344-346, 2022. https:// doi.org/ 10.5137/1019-5149.JTN.34850-21.2" (2). In this article, Bozkaya et al. drawed the conclusion that "Mesenchymal stem cell (MSC) transplantation may be a promising treatment for premature infants to reduce morbidity and mortality after intraventricular bleeding (IVH). However, a need exists for studies that evaluate the optimal application route, dose and time of administration, as well as its efffcacy and safety" .

MSCs are widely used in clinical applications (11,12). It could be envisioned that MSCs transplantation may be a promising treatment for Neurological diseases. Current research highlights MSCs applications in modulating neurogenesis, angiogenesis, and immune regulation, particularly through their capacity to promote progenitor cell differentiation. Notably, preclinical and clinical trials demonstrate therapeutic efficacy in premature infants with bronchopulmonary dysplasia (BPD) and hypoxic-ischemic encephalopathy (HIE). For instance, human umbilical cord blood-derived MSCs (UCB-MSCs) have shown marked neuroprotective effects in severe intraventricular hemorrhage (IVH) models, significantly reducing brain injury and post-hemorrhagic hydrocephalus (PHH) incidence in rodent studies (1-3). These findings underscore MSC therapy's potential to mitigate morbidity and mortality in IVH patients.

Stem cell therapy is another medical revolution after drug and surgical medication (11,12). Emerging evidence suggests MSCs transplantation holds significant promise for treating neurological diseases. MSCs are a class of cells with signiffcant self-renewal and multi-lineage differentiation properties and MSCs characterized by immune regulation, suppression of inffammation and promotion of angiogenesis. They are favorable for the treatment of various diseases and injuries (4-8,11). MSCs therapies were anticipated to repair the structure and function of diseased or damaged tissues via direct cell replacement and/or pretended by-stander effect (9). MSCs suppress T-lymphocyte proliferation and the infflammatory response, changing in the cytokine release of T cells (3,6). Due to, MSCs increase the production of anti-infflammatory cytokines, such as IL-10, while reducing the infflammatory cytokine release from dendritic cells, such as TNF-α, interleukin12 (IL-12) and interferon-γ, in IVH patients (1,10). It is indicated that the infflammatory reaction caused by Neurological injury disease is a crucial factor (6,11), MSCs can affect immune cells proliferation, differentiation, activation and infflammatory cytokine secretion by cells interaction and secretion of soluble immune regulatory factors and inhibit the proliferation of T cells and microglia, regulate dendritic cells, monocytes and macrophages and natural killer (NK) cells to Suppress the infflammatory response. MSCs secret a variety of cytokines and growth factors through paracrine, including vascular endothelial growth factor (VEGF), basic firoblast growth factor (BFGF), hepatocyte growth factor (HGF), that could stimulate peripheral mature endothelial cells proliferation and migration, improve the microenvironment of ischemic tissue to participate in angiogenesis (11,12).

Yanmin WANG : 0009-0007-9112-5691 Bo HUANG : 0009-0000-3725-8185 Huajiang DONG : 0000-0002-4141-3077

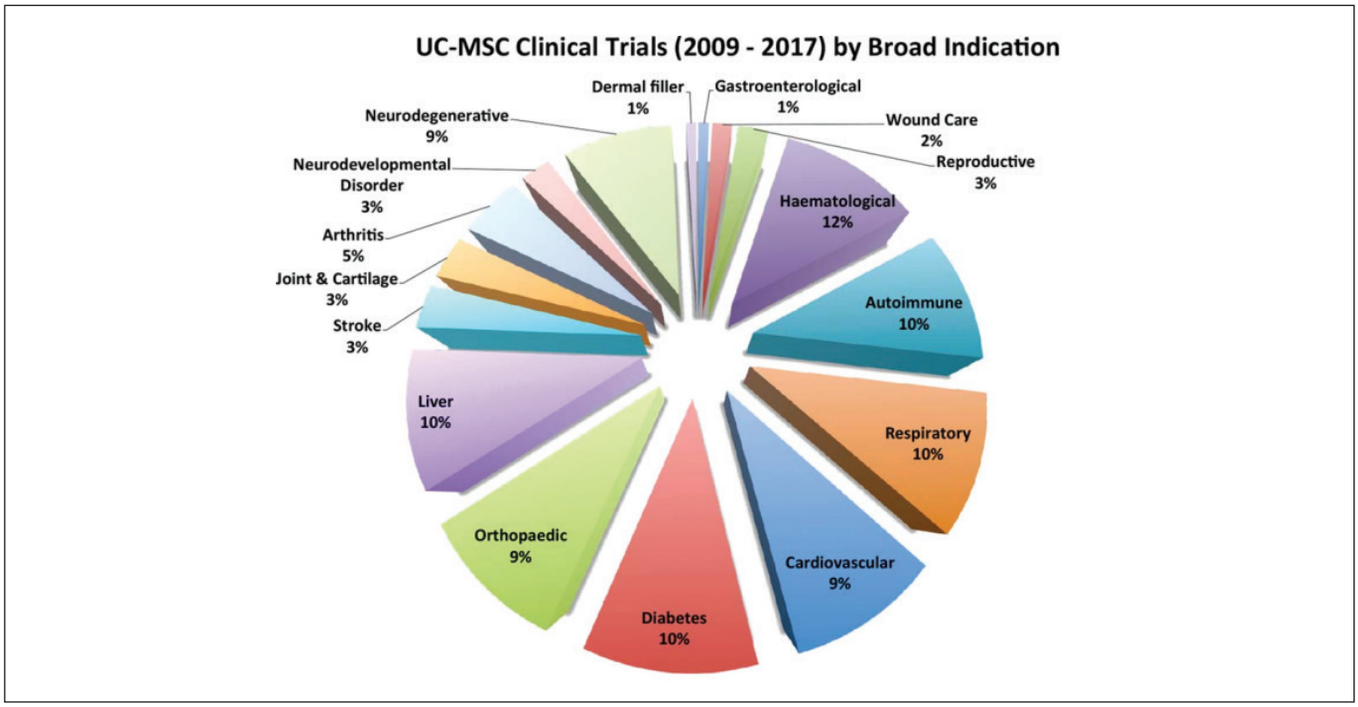

Figure 1: Representative applications of UCB-MSCs (Quoted from Reference #2).

We agree with the conclusions drawn from Bozkaya et al., and propose these questions to advance MSC research. Elucidating these aspects will facilitate protocol standardization and enhance therapeutic outcomes. Further investigation into dosage optimization, treatment timing, and mechanism validation remains imperative for clinical translation. Some challenges require resolution to standardize MSC therapeutics, such as administration optimization: Is intravenous infusion the optimal delivery route? Potential pulmonary sequestration may reduce therapeutic efficacy. Have recent studies explored alternative administration strategies? And the next question: what is the mechanism behind the therapeutic effect of MSCs? Cell replacement or paracrine-mediated microenvironment modulation? or something else? We look forward the reply. These questions awaiting to reply so as to better conduct relevant research and provide support for the application of MSCs. To solving these problems will benefit the further standardization of MSCs therapy and to improve MSCs therapy.

Despite the positive features of MSCs, there are many unanswered questions concerning IVH cases, such as the method of administration, dose and optimal timing, the mechanism of MSCs therapeutic effect, is cell replacement or something else? These all need to be studied in depth.

Declarations

Funding: This work was supported by the National Natural Science Foundation of China (81801240) and the High-level Scientific and Technological Innovation Talent Cultivation (ZZKY20222420).

Availability of data and materials: The datasets generated and/or analyzed during the current study are available from the corresponding author by reasonable request.

Disclosure: The authors declare no competing interests.

AUTHORSHIP CONTRIBUTION

Study conception and design: HD

Draft manuscript preparation: HD, YW, BH

Critical revision of the article: HD

Other (study supervision, fundings, materials, etc...): HD, YW

All authors (HD, YW, BH) reviewed the results and approved the final version of the manuscript.

REFERENCES

1. Ahn SY, Chang YS, Park WS: Mesenchymal stem cells transplantation for neuroprotection in preterm infants with severe intraventricular hemorrhage. Korean J Pediatr 57:251-256, 2014. https:// doi.org/ 10.3345/kjp.2014.57.6.251
2. Bozkaya D, Ceran B, Ozmen E, Okman E, Alyamac Dizdar E, Oguz SS, Ok Bozkaya I: A new hope in the treatment of intraventricular haemorrhage in preterm infants: Mesenchymal stem cells. Turk Neurosurg 32:344-346, 2022. https:// doi.org/ 10.5137/1019-5149.JTN.34850-21.2
3. Davies JE, Walker JT, Keating A: Concise review: Wharton's Jelly: The Rich, but enigmatic, source of mesenchymal stromal cells. Stem Cells Transl Med 6:1620-1630, 2017. https:// doi.org/ 10.1002/sctm.16-0492
4. Dong H, Li G, Ding H, Luo Y, Zhao M, Lin L: The potential value of adipose tissue-derived (rAT) mesenchymal stem cells (MSCs). Turk Neurosurg 28:849-850, 2018. https:// doi.org/10.5137/1019-5149.JTN.21566-17.0

5. Dong HJ, Shang CZ, Li G, Niu Q, Luo YC, Yang Y, Meng HP, Yin HJ, Zhang HX, Zhao ML, Lin L: The distribution of transplanted umbilical cord mesenchymal stem cells in large blood vessel of experimental design with traumatic brain injury. J Craniofac Surg 28:1615-1619, 2017. https:// doi.org/ 10.1097/SCS.0000000000003563
6. Dong HJ, Zhao MI, Li XH, Chen YS, Wang J, Chen MB, Wu S, Wang JJ, Liang HQ, Sun HT, Tu Y, Zhang S, Xiong J, Chen C: Hypothermia-modulating matrix elasticity of injured brain promoted neural lineage speciffcation of mesenchymal stem cells. Neuroscience 377:1-11, 2018. https:// doi.org/ 10.1016/j.neuroscience.2018.02.013
7. Gong W, Han Z, Zhao H, Wang Y, Wang J, Zhong J, Wang B, Wang S, Wang Y, Sun L, Han Z: Banking human umbilical cord-derived mesenchymal stromal cells for clinical use. Cell Transplant 21:207-216, 2012. https:// doi.org/ 10.3727/096368911X586756
8. Huajiang D, Dingwei P, Xiping Y, Yuetong H, Lei W, Chongzhi S, Keqiang W: Cell-free therapy may experience more rapid advancement - Pretended Bystander Effects" in cell-based therapy for treating diseases. Turk Neurosurg 30:315-316. https:// doi.org/ 10.5137/1019-5149.JTN.27196-19.2
9. Kean TJ, Lin P, Caplan AI, Dennis JE: MSCs: Delivery routes and engraftment, cell-targeting strategies, and immune modulation. Stem Cells International 2013:732742, 2013. https:// doi.org/ 10.1155/2013/732742
10. Kim ES, Chang YS, Choi SJ, Kim JK, Yoo HS, Ahn SY, Sung DK, Kim SY, Park YR, Park WS: Intratracheal transplantation of human umbilical cord blood-derived mesenchymal stem cells dose-dependently attenuates hyperoxia-induced lung injury in neonatal rats. Cell Transplant 20:1843-1854, 2011. https:// doi.org/ 10.3727/096368911X565038
11. Li G, Yang Y, Dong HJ, Lin L: The research progress of mesenchymal stem cells in the treatment of Traumatic brain injury. Turk Neurosurg 28:696-702, 2018. https://doi.org/10.5137/1019-5149.JTN.20829-17.1
12. Uccelli A, Moretta L, Pistoia V: Mesenchymal stem cells in health and disease. Nat Rev Immunol 8:726-736, 2008. https://doi.org/10.1038/nri2395
13. Wang Y, Peng D, Yang X, Huang P, Ye H, Hui Y, Wang X, Sun W, Wu H, Zhang S, Wang L, Sha H, Shang C, Dong H, Hu Q: Study on umbilical cord-matrix stem cells transplantation for treatment of acute trauma brain injury in rats. Turk Neurosurg 29:750-758, 2019. https://doi.org/10.5137/1019-5149.JTN.25463-18.2

Turk Neurosurg 36(1):178-179, 2026
DOI: 10.5137/1019-5149.JTN.47579-24.0

Letter to Editor

Received: 13.09.2025
Accepted: 25.10.2025
Published Online: 16.01.2026

Critique of the Case Report on Multiple Intracranial Aneurysms Concurrent with a Clinoid Meningioma

Muhammad IKRAMA, Muhammad USAMA, Shifa ISRAR

Services Institute of Medical Sciences, Lahore, Pakistan

Corresponding author: Muhammad IKRAMA ✉ dr.ikrama.md@gmail.com

Dear Editor,

I have been keenly interested in the case report entitled "Multiple Intracranial Aneurysms Simultaneously Presenting with a Clinoid Meningioma," authored by Zhou et al. published in your journal (1). Although this case report is quite unique and holds clinical relevance, I wish to present an elaborate critique considering the CARE guidelines for emphasizing areas of improvement that could be done in the report.

The introduction effectively portrays the rarity of the coexistence of intracranial aneurysms with a meningioma but could be strengthened by citing more recent literature to situate the report better within the current body of knowledge.

The report simply mentioned a 53-year-old male with hypertension for 20 years. There are no further insights into the demographic information of the patient—past medical history, medication use, family history, and environmental factors such as tobacco, alcohol use—all of which may result in serious implications for the pathogenesis of two aneurysms and meningiomas. This lack of specific information regarding the patient limits comprehensiveness with respect to understanding the case in its context and reduces the educational value of the report.

The report describes the clinical picture of sudden headache and vomiting, but it is not very clear on a timeline of events: it is vague when the patient first noticed symptoms, how rapidly they developed, and the time from onset of symptoms to admission to the hospital. A well-structured timeline, following the CARE guidelines, will enable readers to understand and appreciate the clinical course and the acuity of the situation.

All diagnostic work-up has been comprehensively documented regarding CT, CTA, and DSA findings. However, the report states that the meningioma of the left clinoid was not seen preoperatively, which makes one wonder how comprehensive the interpretation of the imaging study was. A critical evaluation of this diagnostic oversight is required. The report could have been enriched with the inclusion of a discussion on the differential diagnoses that were entertained while making the diagnosis and also the possibility of misinterpretation of radiological findings, especially when other pathologies coexist.

The surgical management has been well described with the technical details of the procedure. However, some of the negative aspects of the report are that it does not outline alternative therapeutic options, such as endovascular treatment, and it also does not justify why such an option was not chosen in this specific case. Greater transparency in decision-making is required, more so in complex cases where several treatment modalities can be adopted. It also does not address perioperative care or the complications that may occur, features considered by the CARE guidelines to be key.

The patient progressed well through the intervention without any neurological deficits in the follow-up period. No duration of follow-up was mentioned, though, and long-term results along with recurrence were not indicated. Long-term follow-up is necessary in such cases, especially with complex neurosurgical interventions, to evaluate the durability of the treatment in relation to quality of life. It would have been more enhanced if it were to record the treatment and recovery experience and perspective from the patient as per CARE recommendations.

The discussion section adequately reflects how unusual this case is but could have been more elaborate in the mechanisms of pathophysiology that may be coexistent between intracranial aneurysms and meningiomas. The authors only elaborate on the possibility of increased local blood flow or mechanical

Muhammad IKRAMA : 0000-0001-5818-5800 Muhammad USAMA : 0000-0001-6593-7089 Shifa ISRAR : 0000-0003-4511-3335

pressure from the meningioma, but they fail to go one step further in thinking about other hypotheses such as shared genetic or environmental risk factors. Moreover, an enriched discussion could be further enhanced with a critical appraisal of the literature, including possible biases and limitations in the cited studies.

The conclusion was very well done in bringing together the case but lacked the expression of the larger insights, including how this might impact or change clinical practice and recommendations. Considering that cases of multiple concurrent intracranial pathologies are very challenging, further detailed insights would be appropriate in the report for the sake of other clinicians who might come across this in the future.

Sincerely,

Declarations

Funding: This research did not receive any specific grant from funding agencies in the public, commercial, or not-for-profit sectors.

Availability of data and materials: The datasets generated and/or analyzed during the current study are available from the corresponding author by reasonable request.

Disclosure: The authors declare no competing interests.

Use of artificial intelligence (AI)-assisted technology for manuscript preparation: During the preparation of this work the authors used GPT 4.0 to improve the overall language and check for grammatical errors after writing the manuscript. After using this, the authors reviewed and edited the content as needed and take full responsibility for the content of the publication.

AUTHORSHIP CONTRIBUTION

Study conception and design: MI
Data collection: MI, MU, SI
Analysis and interpretation of results: MI
Draft manuscript preparation: MI, MU, SI
Critical revision of the article: MI, MU, SI
Other (study supervision, fundings, materials, etc...): MI, MU, SI
All authors (MI, MU, SI) reviewed the results and approved the final version of the manuscript.

REFERENCES

1. Xiangyang Z, Zhengbin D, Hong L, Yimin L: Multiple intracranial aneurysms concurrent with a clinoid meningioma: A case report. Turk Neurosurg 34:358-361, 2024. DOI: 10.5137/1019-5149.JTN.21084-17.1

Turk Neurosurg 36(1):180, 2026
DOI: 10.5137/1019-5149.JTN.47634-24.0

Letter to Editor

Received: 19.09.2024
Accepted: 31.10.2025
Published Online: 16.01.2026

Microvascular Decompression for Hemifacial Spasm without the Use of Neuromonitoring and Fix Retraction: A Single-Center Experience

Xu HAO*, Ding LEI*, Shao QIANG

General Hospital of the Yangtze River Shipping, Wuhan Brain Hospital, Department of Neurosurgery, Wuhan, China

*Xu Hao and Ding Lei contributed equally to this work.

Corresponding author: Shao QIANG ✉ s_q12345@qq.com

Dear Editor,

I have read with interest the article by Pusat et al. (2), which presents a single-center experience of microvascular decompression (MVD) for hemifacial spasm (HFS) without the use of neuromonitoring. While the authors assert that the disappearance of lateral spread response (LSR) during surgery does not correlate with postoperative symptom relief, our clinical experience contradicts this finding.

Our institution has a longstanding practice of utilizing intraoperative neuromonitoring for HFS surgeries. Our data, accumulated over years of meticulous monitoring, indicate that the elimination of LSR intraoperatively is closely associated with positive patient outcomes. Most of our patients experience significant symptom relief following surgery, aligning with the disappearance of LSR. This observation is supported by the systematic review and meta-analysis conducted by Thirumala et al. (3), which assigns a high negative predictive value, nearing 93% to 96%, to the absence of LSR in the operating room. The study concludes that persistent LSR is a significant risk factor for the continued presence of HFS, with a probability of symptom persistence ranging from 24.4% to 47.8% when LSR does not resolve (3). Pusat et al. believe that the disappearance of LSR may not be related to postoperative symptom relief, possibly because some HFS patients have a dual pathology involving both vascular compression and hyperexcitability of the facial nerve nucleus (1). However, this does not deny the importance of neurophysiological monitoring during surgery.

In conclusion, our experience and the literature support the continued use of LSR monitoring during MVD for HFS, as it is helpful to achieve better surgical outcomes and patient satisfaction. We are eager to engage in further discussions on surgical techniques and neurophysiological monitoring.

Declarations

Funding: This study has received funding from Scientific Research Fund of Wuhan Health Commission (WX21D68).

Availability of data and materials: The datasets generated and/or analyzed during the current study are available from the corresponding author by reasonable request.

Disclosure: The authors declare no competing interests.

AUTHORSHIP CONTRIBUTION

Study conception and design: XH
Data collection: DL
Analysis and interpretation of results: XH
Draft manuscript preparation: DL
Critical revision of the article: SQ
All authors (XH, DL, SQ) reviewed the results and approved the final version of the manuscript.

REFERENCES

1. Moller AR: Hemifacial spasm: Ephaptic transmission or hyperexcitability of the facial motor nucleus? Experimental Neurology 98:110-119, 1987. https://doi.org/10.1016/0014-4886(87)90076-8.
2. Pusat S, Erdogan E, Atar M, Erbas YC, Erdogan E: Microvascular decompression for hemifacial spasm without the use of neuromonitoring and fix retraction: A single-center experience. Turk Neurosurg 34:429-434, 2024. https://doi.org/10.5137/1019-5149.JTN.42249-22.3.
3. Thirumala PD, Altibi AM, Chang R, Saca EE, Iyengar P, Reddy R, Anetakis K, Crammond DJ, Balzer JR, Sekula RF: The utility of intraoperative lateral spread recording in microvascular decompression for hemifacial spasm: A systematic review and meta-analysis. Neurosurgery 87:E473-E484, 2020. https://doi.org/10.1093/neuros/nyaa069.

Xu HAO : 0000-0002-3002-5693 Ding LEI : 0009-0004-0370-4107 Shao QIANG : 0009-0008-5445-8849

Turk Neurosurg 36(1):181, 2026
DOI: 10.5137/1019-5149.JTN.49401-25.2

Corrigendum

Received: 07.07.2025
Accepted: 26.09.2025
Published Online: 16.01.2026

Corrigendum to: Anti-Inflammatory, Antioxidant and Neuroprotective Effects of Niacin on Mild Traumatic Brain Injury in Rats

Turk Neurosurg 33(6):1028-1037, 2023
DOI: 10.5137/1019-5149.JTN.42563-22.3

Dear Editor and Readers,

As the authors of the manuscript entitled “Anti-Inflammatory, Antioxidant and Neuroprotective Effects of Niacin on Mild Traumatic Brain Injury in Rats” (1), we noticed an error after a retrospective review and want to apologize for the inconvenience in Figure 4. We would like to replace the figure with the correct one as follows:

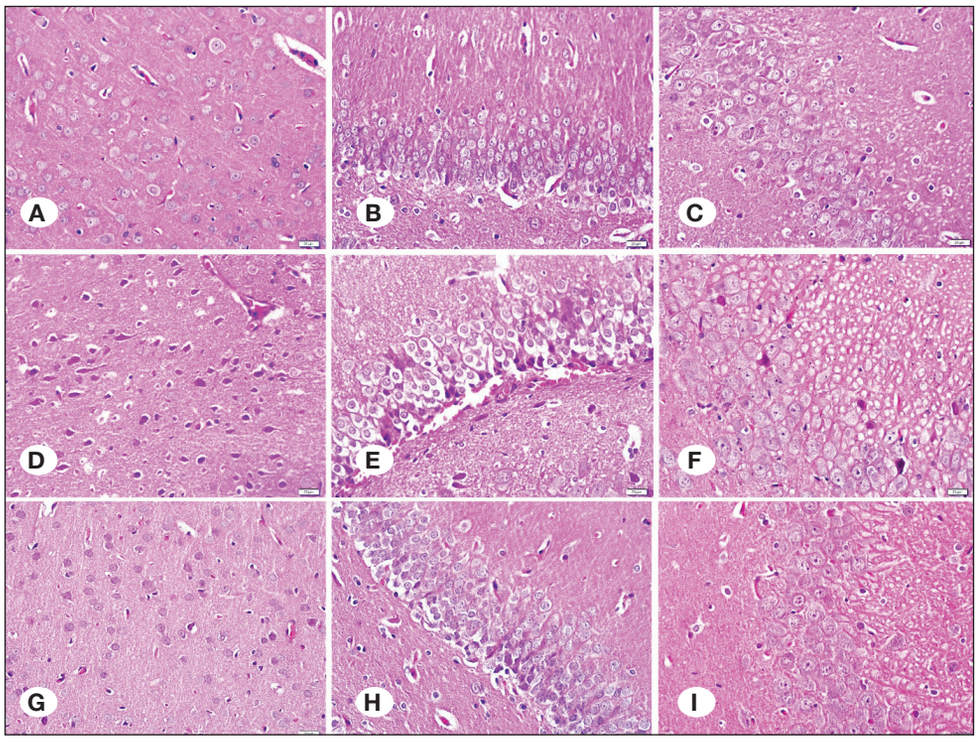

Figure 4: A-C) Representative sections of the cortex, hippocampal dentate gyrus (DG), and CA3 regions, in the control group.
D-F) Representative sections of the cortex, hippocampal DG, and CA3 regions in the TBI + placebo group.
G-I) Representative sections of the cortex, hippocampal DG, and CA3 regions in the niacin group. H&E stain. Scale bar: 50 µm.

The error relating to Figure 4.A-I in the published version did not affect any statistical data or the study outcome.

We hereby correct the mistake and present them as they should be in order not to misinform our colleagues who will read our study.

REFERENCES

1. Ozaydin D, Bektasoglu PK, Koyuncuoglu T, Ozkaya SC, Koroglu AK, Akakin D, Erzik C, Yuksel M, Yegen BC, Gurer B: Anti-inflammatory, antioxidant and neuroprotective effects of niacin on mild traumatic brain injury in rats. Turk Neurosurg 33:1028-1037, 2023. https://doi.org/10.5137/1019-5149.JTN.42563-22.3.